CHEMINFORMATIC AND MECHANISTIC STUDY OF DRUG SUBCELLULAR TRANSPORT/DISTRIBUTION

by

Nan Zheng

A dissertation submitted in partial fulfillment
of the requirements for the degree of
Doctor of Philosophy
(Pharmaceutical Sciences)
in The University of Michigan
2011

Doctoral Committee:

Associate Professor Gustavo Rosania, Chair
Professor Gordon L. Amidon
Associate Professor Kerby A. Shedden
Associate Research Professor Meihua Rose Feng

To Dad and Mom

With All My Love

ACKNOWLEDGEMENT

TABLE OF CONTENTS

LIST OF TABLES

LIST OF FIGURES

x

LIST OF APPENDICES

ABSTRACT

CHEMINFORMATIC AND MECHANISTIC STUDY OF
DRUG SUBCELLULAR TRANSPORT/DISTRIBUTION

The subcellular transport and distribution behavior determines both the pharmacological effect on the cellular level and the drug exposure at a tissue, organ and whole body level. Despite of the rapid evolution in experimental and computational approaches for studying the subcellular transport of small molecules, a thorough understanding and reliable experimental analysis of cellular pharmacokinetic behavior remain challenging. Mechanism-based computational models are promising tools for testing hypothesis, exploring mechanism and guiding experiment design and data analysis in pharmacokinetic and system biology studies. The primary goal of this work is to propose a hypothesis-driven, simulation-guided strategy for drug subcellular transport and distribution studies. The current knowledge of organelle targeting features of small molecules was analyzed in terms of its relevance to developing computational models for analyzing subcellular pharmacokinetic behavior. A non-invasive insert system was designed to characterize small molecules' intercellular transport kinetics, and a mechanism-based passive diffusion model was adapted to facilitate the design and analysis of subcellular distribution and intercellular transport experiments. This study pointed out many opportunities to advance effective screening for drug candidates with desirable distribution and

transport behavior at a subcellular and systemic level. These opportunities include: 1) the development of quantitative experimental platform for the real-time tracking and analysis of non-fluorescent molecules in multiple subcellular compartments; 2) the elaboration of hypothesis-driven, mechanistic modeling techniques emphasizing a better understanding of the non-steady-state intracellular accumulation behavior and limited intercellular diffusivity; 3) the promotion of simulation-guided experimental design strategy; and 4) the incorporation of synthetic biology concepts into pharmacokinetics studies.

Chapter I

Introduction

Abstract

The systemic pharmacokinetics and pharmacodynamics of small molecules are determined by subcellular transport phenomena. Although approaches used to study the subcellular distribution of small molecules have gradually evolved over the past several decades, experimental analysis and accurate prediction of cellular pharmacokinetics behavior remain a challenge. In this review, we surveyed the progress of subcellular distribution research since the 1960s, with a focus on the advantages, disadvantages and limitations of the various experimental techniques and computational predictive tools. Critical review of the existing body of knowledge pointed to many opportunities to advance the rational design of organelle-targeted chemical agents. These opportunities include: 1) development of quantitative, non-fluorescence-based, whole cell methods and techniques to measure the subcellular distribution of chemical agents in multiple compartments; 2) exploratory experimentation with non-specific transport probes that have not been enriched with putative, organelle-targeting features; 3) elaboration of hypothesis-driven, mechanistic and modeling-based approaches to guide experiments aimed at elucidating subcellular distribution and transport; and

4) introduction of revolutionary conceptual approaches borrowed from the field of synthetic biology combined with cutting edge experimental strategies. Specific aims were proposed for state-of-the-art subcellular transport studies which aimed at understanding the formation of new organelles in response to drug therapy, exploring the role of chemically-synthetic organelles as intracellular drug depots and developing subcellular pharmacokinetics models to guide the rationale design of organelle targeting super drugs.

Introduction

Despite of the rapid development in combinatorial chemistry and high content screening assays for synthesizing and testing of large numbers of new chemical agents, the discovery of drug candidates with favorable pharmacokinetics (PK) and pharmacodynamics (PD) properties has remained a challenge in drug discovery process. Nowadays, the pharmaceutical industry is facing the 'productivity crisis' featured by increasing R&D cost and decreasing number of marketing approvals [1], during which 75% of the cost of drug development turned out to be on failures in Phase II/III clinical trials and any attempted recoveries after regulatory rejection [2, 3]. Therefore, to meet the growing demand for more drugs [4, 5] and to increase rate of approval, the ability to accurately predict the absorption, distribution, metabolism, excretion, and toxicity (ADMET) profile of new chemical agents is highly desirable.

On the cellular level, the entire set of processes of absorption / uptake, distribution, metabolism and elimination within one single cell, as referred to as the subcellular transport and distribution, controls not only the benefit / toxic effect on a cellular level but also drug exposure at a tissue, organ and whole body level. This is because many drugs require entrance into specific subcellular organelles to reach their targets, or they have side effects associated with unwanted accumulation in non-target sites within cells. For example, although the concentration of many weak base anticancer agents remains high in drug-resistant cell lines, the efficacy of the drugs are often compromised due to sequestration of weak bases in acidic intracellular organelles rather than the

intracellular sites of action [6-10]. In osteoporosis therapy, the lysosomal cysteine protease inhibitor with physicochemical properties that facilitate lysosomal trapping also exhibit significantly higher in vitro and in vivo potencies than its derivatives with less preferable molecule properties [11].

On that ground, novel drug targeting strategies to improve compound efficiency in reaching specific organelles have been sought to increase a molecule's potency and decrease undesired side effects. For example, small molecules are being targeted to mitochondria by conjugating these molecules to cell-penetrating, lipophilic peptides, oligoguanidinium, or triphenylphosphonium moieties [12-17]. To fulfill this organelle targeting drug design strategy, there have been many efforts aiming at characterizing the physiological properties of the most important intracellular organelles and identifying key physicochemical features that determine the accumulation of exogenous chemical agents inside these organelles [18-21]. More importantly, the mechanisms driving the distribution kinetic of chemical agents within the cell and the dynamic cellular response to these chemical agents are being revealed with the aid of new experimental strategies and conceptual approaches.

To put the state-of-the-art of subcellular transport research in perspective, we reviewed the historical progress of subcellular biodistribution research, focusing on the evolution of experimental, theoretical and conceptual approaches used to analyze the organelle-targeting features of small molecule chemical agents. The advantages, disadvantages and limitations of the various experimental techniques and computational predictive tools were discussed.

Specific aims were proposed for pioneering subcellular transport studies which aimed at understanding cellular response to drug therapy, exploring the role of chemically-synthetic organelles as intracellular drug depots, and characterizing and analyzing the comprehensive pharmacokinetics behavior at a cellular level.

Pharmacological effects as evidence for specific organelle accumulation

Eukaryotic cells have highly organized subcellular compartments with distinct structural and functional features. Current knowledge of the physiological properties and general principles of target delivery into major subcellular organelles were summarized (Table 1.1). Pharmacological effects, i.e. changes in these features, especially changes in organelle morphology (swelling, rupture, shrinkage, etc.) upon drug treatment have been used in a large number of studies as the evidence for compound localization in specific organelles. Surveying the literature, a large number of subcellular localization reports were based on evidence that the chemicals induced changes in the structure or function of specific organelles [22].

Prior to the widespread adaption of cell-based uptake and transport assays in small molecule drug development, morphological changes were commonly used as evidence for organelle accumulation. From the 1960s to the 1980s, similar numbers of studies were based on observations with light microscopy, fluorescence microscopy and transmission electron microscopy [23-25]. Light microscopy was the preferred tool in detecting expansion in the endolysosomal compartment, visible as a massive, cytoplasmic vacuolation phenomenon. With

transmission electron microscopy, morphological changes of the major organelles could be observed directly, with or without the aid of specific organelle tracers. In the early 1980s, fluorescence microscopy became increasingly applied to the detection of organelle swelling and shrinkage using fluorescent probes. In the endolysosomal compartment, the observed morphological changes have been shown to reflect the accumulation of weakly basic compounds inside these organelles, or the inhibitory effects of cations on the activity of lysosomal proteins [26, 27].

Morphological changes in lysosomes and mitochondria often coincided with changes in membrane potential, pH gradients or membrane permeability [28-32]. Under some circumstances such changes resulted in the release of a resident, organelle-specific enzyme into the cytosol or into the extracellular compartment. Thus the detection of fluctuation in voltage or pH gradients, or the detection of released organelle components, was used as evidence for accumulation of exogenous small molecules in specific organelles, from the 1970s [33-36] and continuing to this day [37-40].

Also since the 1970s, analytical measurements using thin layer chromatography and HPLC to detect alterations in organelle composition, including changes in lipid content, protein concentrations and metabolic changes, have been used as evidence to infer accumulation of small molecules in specific organelles [41-43]. For example, significant increases of phospholipids in the renal cortex of gentamicin- or netilmicin-treated rats [44] were ascribed to impaired lysosomal degradation of phospholipids due to inhibition of lysosomal

6

phospholipase C by accumulation of said molecules in lysosomes. Ammonia, amiodarone and some other compounds that interfere with degradation of proteins or phospholipids in lysosomes [45-47] were also associated with inhibition of lysosomal proteases and phospholipases due to the accumulation of these weakly basic compounds in the lysosomes, resulting in intra-lysosomal pH changes with consequent effects on lysosomal enzyme activities [48-52].

Nevertheless, claims that a molecule "accumulates in" an organelle based on a change in organelle structure (or function) are circumstantial and prone to misinterpretation and experimental artifacts. For example, in the case of toxic compounds, inhibition of organelle function may not require direct interaction, or accumulation within a specific organelle. For instance, apoptosis signal transduction pathways lead to mitochondrial membrane permeabilization, loss of mitochondrial membrane potential and the release of cytochrome *c* from the mitochondria, as well as nonspecific effects on other organelles. Therefore, induced changes in mitochondrial volume, membrane potential, or permeability do not necessarily reflect a direct interaction with mitochondria. The same is true for other organelles [53].

Chemical analysis as evidence for specific organelle accumulation

Pharmacokinetics gradually became part of drug development from the 1960s through the 1980s. However, only since the 1990s, there has been an increasing recognition of the importance of cellular pharmacokinetics as a determinant of systemic pharmacokinetics. In the process, quantitative

7

measurement of chemical uptake *in vivo* or *in vitro* became increasingly important as direct evidence supporting the actual localization of a molecule in a specific subcellular compartment. Irrespective of the experimental strategy, analytical measurements were increasingly applied in cellular uptake or distribution studies, providing direct evidence for accumulation in specific organelles. However, only a relative small fraction of the molecules whose intracellular localization has been reported in the scientific literature is supported by such evidence [22].

In uptake experiments, researchers measure drug mass in intact cells or in isolated organelle after *in vitro* or *in vivo* administration of the compound. In some cases, a known, organelle-targeting compound was used to compete for the interaction or otherwise inhibit the organelle-specific accumulation mechanism. For instance, in a report of the subcellular localization sites of weakly basic molecules, the reduced cellular uptake after the disruption of trans-membrane pH gradients was used as evidence for endolysosomal accumulation [54, 55]. Less commonly, ion-selective electrodes have been used to study the uptake of positively charged, lipophilic compounds in isolated mitochondria [56-58]. Binding to resident organelle-specific components including protein, lipids or nucleic acids has also been measured as direct evidence to demonstrate organelle or cytosolic accumulation [59-62].

Starting in the 1990s, there was an increase in the number of investigations looking at the qualitative or semi-qualitative (relative) distribution of a compound in all subcellular compartments, simultaneously, featuring analytical

measurements following cell fractionation [22]. In cell fractionation studies, the basic experimental strategy has been to isolate the various organelles by differential centrifugation [63], followed by measurements of the absolute amount of a compound in each organelle fraction [64-66] and/or comparing that amount relative to the total accumulation of the compound in the cell [67-69]. Reliable separation of distinct subcellular organelles is critical to the evaluation of subcellular distribution profile. While enzyme activity of organelle specific marker proteins in each fraction can be readily determined, for effective separation of subcellular compartments requires little overlap in marker enzyme activities between the fractions. Then the fractions can be subjected to chemical analysis of organelle associated compound accumulation by means of spectrophotometry [70], HPLC [71-73], LC/MS [74], and most commonly, by scintillation counting of radiolabeled compounds [75-78].

Many significant advances in distribution studies were achieved through the development of cell fractionation techniques. Organelle separation and analysis techniques such as immunoisolation, fluorescence activated sorting and electromigration analysis was developed. However their use in subcellular distribution studies remains infrequent, possibly because they are technically demanding. For organelle immunoisolation, cell homogenates were exposed to organelle-specific antibodies attached to solid supports and the cell fractions of interest were concentrated by binding to antibody [79-81]. Fluorescent activated cell sorting was applied to separate multiple intracellular organelles stained with membrane dyes or labeled with fluorescent antibodies to organelle membrane

proteins [82-85]. Since around the early 2000s' electrophoresis has been used to separate different subcellular organelle fractions from cell homogenate [86-94]. Most recently, magnetic chromatography methods were developed to isolate and enrich lysosomes from cells that internalize iron-containing particles [95-97].

As a caveat, organelle isolation procedures are not necessarily free from experimental artifacts: organelle isolation procedures can disrupt such interactions [58]. During the lengthy procedures to attain higher purity and adequate amount for further analysis, organelle damage and compound leakage from one or more subcellular organelles are inevitable and difficult to control [63]. While whole cell fractionation analysis followed by analytical measurement has advantages over experiments that probe a specific compound-organelle interaction. However, fractionation analysis is very labor intensive.

Whole cell based microscopic imaging studies as evidence for intracellular localization.

Whole cell based microscopic imaging studies using intrinsically fluorescent or fluorescently-tagged molecules accounted the most number of scientific articles reporting a molecule's subcellular localization [22] and have been most common over the past decade. Less commonly, electron microscopy combined with immunocytochemical methods were used to obtain high resolution information of intracellular distribution of small molecular weight compounds that precipitated out at their sites of accumulation [98, 99] or that were tagged with a specific immune-epitope [22, 100, 101].

10

Compared to pharmacological and chemical analyses which are tedious and prone to artifacts, microscopic imaging has generally been preferred as an efficient and reliable method to obtain real-time intracellular distribution data. Microscopic visualization of fluorescent or fluorescently-tagged molecules provided the evidence for establishing subcellular localization, in the majority of published, subcellular localization studies [22]. While the intracellular accumulation sites of fluorescent compounds can be determined directly based on the characteristic morphology of stained compartments [102-108], the use of resident, reference fluorescent markers [109-113] has enabled determination of subcellular distribution by analysis of co-localization patterns. Following advances in location proteomics [114-118], machine vision-based quantitative image analysis has been used to establish the degree of co-localization between compounds of interest with an organelle-specific reference marker [119-121]. Furthermore, large combinatorial libraries of fluorescent probes and automated high content screening instruments have facilitated analysis of chemical motifs associated with specific intracellular distribution patterns [120-122]. For compounds with fluorescent property but interfered with cellular auto-fluorescence, the fluorescence resonance energy transfer-based approach has been designed to study the trafficking and distribution of xenobiotics with proper conjugation [123].

Fluorescence based imaging techniques offer many advantages over other detection methods, evidence for subcellular localization based on fluorescence-based studies is generally criticized due to well-known artifacts. For example,

environmental factors such as binding status [124], ionic strength [125], solvent polarity [126-128], pH [129-131] and temperature [132-134] can affect a molecule's fluorescence intensity, or peak excitation and emission wavelengths. If the fluorescence intensity is dependent on environmental factors, conclusions on subcellular distribution pattern might not be entirely accurate or complete as molecules may not be fluorescent in every compartment they localize to[135]. For non-fluorescent molecules to be detectable under fluorescent microscopy, a fluorescent tag needs to be conjugated to the compound. This tag can alter the distribution of the original compound. Thus, claims about the subcellular localization of a tagged compound are only valid in the context of the entire small molecule-fluorescent probe conjugate.

Over the past decade, more sensitive and general mass spectroscopy imaging methods, such as the confocal Raman microscopy and secondary ion mass spectroscopy, have also emerged to monitor the distribution of non-fluorescent compounds in cells [136]. To date, a few pioneering studies based on these techniques have been reported in intracellular mapping of xenobiotics [22, 137, 138]. Nevertheless, significant breakthroughs are being achieved in this area. For example, the major challenge in conventional Raman imaging is how to amplify and quantify the weak resonance signal in live cell environment. The application of coherent anti-stokes Raman scattering has led to improvement in signal detection and has been applied in tracking the intracellular distribution of endogenous lipids, virus RNA and organelle transport [139-141].

Yet another recent advance was the application of secondary ion mass spectrometry (SIMS) in analyzing subcellular localization sites of chemical agents. SIMS is the most sensitive analysis technique traditionally used in material sciences to analyze the elemental, isotopic or molecular composition of thin films [142-144]. Beginning the late 1990s' SIMS has seen new applications in quantifying the phospholipids composition in biological membranes [145] and mapping the distribution of isotope labeled chemical agents after *in vitro* or *in vivo* dosing [146-149]. Though still in its infancy, SIMS is garnering attention in subcellular distribution studies because of its high sensitivity and outstanding resolution.

Computational models to frame quantitative hypotheses and analyze subcellular distribution patterns.

Since the 2000s, cheminformatics and computational modeling-based approaches have become essential to drug discovery and development. In parallel, cheminformatics and computational approaches are increasingly being used to generate and test hypothesis about the intracellular distribution and transport behavior as well as the chemical-organelle interactions in particular subcellular organelles [18-20, 120, 150-152]. However, evaluation of computational models is inherently dependent on the quantity and quality of subcellular localization measurements. In the next few sections that follow, we will discuss the features and applications of common types of mathematical

models that have been developed to predict subcellular distribution and transport behavior.

Empirical and semi-empirical models

Computational models for predicting the subcellular PK/PD behaviors can be classified into two categories: the statistically-based, empirical or semi-empirical models and the mechanism-based physiological models. Typical statistical models use experimental observations of small molecule subcellular localization as a training dataset. With calculated physicochemical properties as input parameters, regression, multivariate statistical analysis or classification strategies can be applied to make qualitative (yes/no) or quantitative (how much) descriptions of the compound distribution pattern in the training set. If the fit between the model and the training set is acceptable, the model can be applied to a different test set of molecules with overlapping physicochemical properties, to make predictions about the molecules' localization. In cheminformatics research, this is referred to as a quantitative structural-activity relationship (QSAR) study [153].

QSAR models have been widely used in and seen commercialized products for the prediction of different ADMET properties, including the prediction of physicochemical and topological parameters [154-156], oral bioavailability [157-159] and toxicity, carcinogenicity, skin sensitization and so on [160-162]. In predicting the steady state subcellular distribution pattern, several published articles have been published to analyze compound intracellular accumulation

sites using decision trees and other regression based QSAR tools [18-20, 163-167]. QSAR models could also be combined with time exposure data to simulate the kinetics of distribution in different subcellular compartments [119, 152, 167-170]. In these models a multi-compartment model was built based on first order elimination and the time course, concentration or activity data from test compounds was used to optimize the adjustable parameters in the original model. The resultant model with optimized parameters could be applied in evaluation of efficacy and risk assessment for newly synthesized chemical agents.

The success of QSAR-based models depends largely on the accurate calculation of molecular properties and the quality of input data. Ideally the observations used for predictive QSAR models should be derived from the same experiments, based on the same mechanism of study, assessed with the same criteria, and performed with similar methods so as to avoid intra-laboratory variations in the manner the measurements are made and the way the observation is defined. QSAR models also benefit from large data sets of compounds. Therefore, QSAR models based on scant published data obtained with different methods and experimental approaches are more descriptive than predictive.

Mechanism-based physiologically-relevant models

Mechanism-based physiologically-relevant models for predicting subcellular localization take into account not only the molecular parameters of the chemical agents but also the physiological properties of subcellular organelles of interest.

The pH-partition theory and the ion-trapping mechanism have been proposed as basis of the earliest and simplest mechanism based model to estimate the steady state accumulation in single subcellular organelle type, as driven by trans-membrane electrical potentials and pH gradient across phospholipid bilayer. According to the pH-partition theory, lipophilic cations accumulate in the mitochondria due the negative mitochondria membrane potential, and the behavior could be predicted by the Nernst equation [171-173]. According to the ion-trapping theory [48], when a phospholipid bilayer separates two compartments of different pH levels or electrical potential, the basic membrane permeant lipophilic molecules become protonated and charged preferentially in the acidic compartment. Because of the lowered membrane permeability of the charged form of the molecule, the molecule becomes concentrated in the acidic compartment [174-176].

More recently, complex mathematical models have been developed to predict the subcellular distribution and transport behavior among all intracellular compartments. These models usually incorporate a number of general mechanisms including mass balance, Fick's law of diffusion, pH–partitioning theory and ion-trapping. For example, physiologically-based models were developed to calculate the uptake of electrolytes into plant cells [177], the intracellular accumulation and organelle distribution of molecules in cells suspended in homogeneous extracellular drug concentration [178], or in epithelial cells exposed to transcellular drug concentration gradient [179]. Using combinations of input values, simulations can be performed to mimic the kinetics

of small molecules distribution in lysosomes, mitochondria and cytosol of millions of virtual molecules differing in molecular properties [21]. To demonstrate the potential of this approach, a predictive, multi-scale, cell-based model was constructed to simulate the distribution properties of pulmonary drugs in different cell types and anatomical regions of the lung [180].

Translated to the *in vivo* realm, mechanism base models could be extend to incorporate some less general mechanisms involved in specific biological process (e.g. active transport, binding and metabolism) [181-185]. Unsurprisingly, the validation of more physiologically related models will require detailed experimental measurements and kinetic analysis of small molecule distribution at multiple scales, in a manner that exceeds the capabilities of state of the art experimental approaches by many orders of magnitude.

Conclusion

Thus far, we have presented a comprehensive survey of the past and present state of the art of subcellular transport knowledge, focused on the evolution of experimental approaches and methods. Our understanding of small molecule distribution inside cells has been shaped (and is being reshaped) by the application and limitations associated of each one of these approaches and methods, and the invention of new ones (Table 1.2). Analytical measurements following precise cell fractionation can be considered the most quantitative and convincing evidence for claims of preferential accumulation of chemical agents in specific subcellular compartments. However, fractionation studies are low

throughput and labor intensive. Accordingly, live cell-based imaging with fluorescence microscopes has become the most common method for documenting the subcellular distribution of small molecule chemical agents [22].

The application of fluorescence-based techniques in subcellular distribution studies has had two major consequences on the current state of knowledge in this field: 1) much of what is presently known about the subcellular localization properties of small molecules is biased towards fluorescent compounds, with either intrinsic fluorescence or fluorescent molecular tags; and 2) the majority of compounds with reported subcellular localizations are either highly specific, organelle-targeting transport probes or their subcellular distribution has been analyzed only in the context of a specific organelle. Thus, the development of methods to quantify the distribution pattern of non-fluorescent, non-targeted molecules at the whole cell level will be necessary to expand our current understanding of the subcellular distribution properties of small molecules.

For this reason, in addition to whole cell experimental analysis methods, physiologically-based modeling efforts aimed at predicting cellular pharmacokinetics are contributing positively towards formulating a hypothesis-driven framework for experimental, quantitative analysis of cellular biodistribution phenomena. Although still at its inception phase, whole-cell, mechanism-based computational modeling is a promising tool in terms of providing quantitative hypotheses for guiding the design of experiments aimed at furthering understanding of subcellular distribution and transport phenomena, without focusing on a particular location.

18

In the future, combinations of experimental methods will be used to study cells loaded with concentrated solutions of small molecules, which should facilitate analyses and provide new insights into the interaction of cells with exogenous chemical agents. For example, by combining computational modeling, Raman confocal microscopy, fluorescence microscopy, electron microscopy and chemical analysis [138], we found that incubating cells with concentrated chloroquine solutions (such as those found in the urine of patients undergoing chloroquine therapy) drives the formation of intralysosomal drug-membrane complexes that bind to other weakly basic molecules (Figure 1.1) [138]. With clofazimine, combining biochemical, microscopy and molecular imaging techniques, revealed that continuous exposure of cells to supersaturated drug solutions resulted in the synthesis of intracellular, autophagosome-like drug inclusions, new organelle-like cytoplasmic structures formed by condensed drug-membrane aggregates derived from mitochondria and possibly other organelles [186]. While such drug-membrane complexes may form and accumulate inside cells, such complexes may also form at the plasma membrane and can be shed by cells into the extracellular medium [187].

To conclude, continued investigation of subcellular transport phenomena will lead to fundamental insights into the chemistry of life, and the ability to predict and optimize the subcellular transport and biodistribution properties of small molecules at the cellular level is seen as a stepping stone towards predicting and optimizing systemic pharmacokinetics and pharmacodynamics. Although an accurate, quantitative assessment of the microscopic distribution of small

molecules inside cells remains a challenge, we envision that progress in this field with the development of an increasingly sophisticated combination of methods and analytical techniques will serve as a stepping stone towards developing new drug delivery strategies and therapeutic modalities.

Specific aims

As aforementioned, knowledge about the relationships between the molecular properties and subcellular distribution of exogenous chemical agents leads to greater understanding of their biological effects and serves as a basis for the rational design of "supertargeted" chemical agents to specific sites of action within cells [188]. While there have been many efforts in identifying specific molecular properties and physiological conditions that are associated with predictable subcellular distribution patterns and bioavailability [189-192], such efforts have been limited to a relatively small group of chemical agents. A comprehensive cheminformatic analysis of the physicochemical and subcellular distribution properties of a diverse set of small molecules would be valuable and may lead to more general insights that are important to prioritize future research efforts in this area.

Previously in our lab, a mechanism-based computational model of cell pharmacokinetics was developed to guide experimental design and analysis of the subcellular distribution and transport properties of small molecules across cell monolayer [193]. This model has seen successful application in predicting the transcellular permeability of small molecules across cell monolayer [194]. Using

the weakly dibasic drug chloroquine as a test compound, the model was capable of capturing the transcellular transport kinetics for the first four hours of drug treatment [194]. We envision that such physiologically based models would also be a useful tool in guiding experimental design for intracellular accumulation and intercellular transport studies.

The aim of this project is to assess the status of current knowledge of the subcellular pharmacokinetics of small molecules, and to develop a fast and cost effective computational tool to facilitate the experimental design and analysis of small molecules' subcellular distribution behavior, especially the intracellular distribution and intercellular transport. Four specific aims of this project are as follows:

1. To explore the extent to which current knowledge about the organelle-targeting features of small molecules may be applicable towards controlling the accumulation and distribution of exogenous chemical agents inside cells, and to evaluate the feasibility of developing a statistically based empirical model in predicting subcellular accumulation sites. In this study, molecules with known subcellular localization properties as reported in the scientific literature will be compiled into a single data set and compared to reference data sets from the DrugBank database or the PubChem database to identify potential physicochemical properties that are associated with subcellular targeting phenotype. Specific trends in the distribution of molecular properties as associated with reported subcellular localization sites will be

discussed in relation to the development of empirical structure-localization relationship models for predicting steady state subcellular distribution profile.

2. To evaluate the performance of a cell-based, physiologically relevant mathematic model in predicting subcellular distribution pattern by cheminformatic analysis of virtual libraries of small drug-like molecules. In this part of the study, mathematic models of single cells will be used to simulate the steady state intracellular distribution pattern of ninety-nine lysosomotropic small molecules in a leukocyte in homogeneous extracellular drug concentration or an epithelial cell facing an apical-to-basolateral drug concentration gradient. The simulated subcellular accumulation sites will be compared to literature reports and the relationship between the physicochemical properties and the associated cellular distribution profiles will be studied.

3. To demonstrate the flexibility and application of mechanism based models in hypothesis testing using chloroquine as a model compound. Chloroquine is a weak base drug with extensively intracellular accumulation which could not be explained by the traditional pH-portioning theory and ion trapping mechanisms. In this study, we proposed an alternative hypothesis to explain chloroquine accumulation: that drug-induced phospholipidosis corresponds to an inducible, weak base disposition system. We will perform detailed quantitative analysis of chloroquine cellular pharmacokinetics in epithelial cells and modify our cell-bases simulator to establish the impact of phospholipidosis on the cellular pharmacokinetics of chloroquine.

4. To apply the mechanism-based cell simulator to analyze the inter-cellular transport of small molecules within cell monolayers. In this study, a novel design featuring impermeable membrane support with geometric pore arrays will be proposed. The time course of inter-cellular transport of small molecules will be analyzed with a cell-based mathematic model. Fluorescence microscopy will be used to capture the kinetics of transport of different chemical compounds and to compare with simulation results.

References

1. A.D. Schachter and M.F. Ramoni. Clinical forecasting in drug development. *Nat Rev Drug Discov.* 6:107-108 (2007).

2. S.G. Peter Tollman, Michael Ringel. Rising to the Productivity Challenge: A Strategic Framework for Biopharma, Boston Consulting Group, 2004.

3. J.A. Dimasi. Risks in new drug development: approval success rates for investigational drugs. *Clin Pharmacol Ther.* 69:297-307 (2001).

4. S. Ekins, C.L. Waller, P.W. Swaan, G. Cruciani, S.A. Wrighton, and J.H. Wikel. Progress in predicting human ADME parameters in silico. *J Pharmacol Toxicol Methods.* 44:251-272 (2000).

5. Critical Path Opportunities Report - March 2006. In F.a.D. Administration (ed.), 2006.

6. V.Y. Chen and G.R. Rosania. The great multidrug-resistance paradox. *ACS Chem Biol.* 1:271-273 (2006).

7. M. Duvvuri, S. Konkar, K.H. Hong, B.S. Blagg, and J.P. Krise. A new approach for enhancing differential selectivity of drugs to cancer cells. *ACS Chem Biol.* 1:309-315 (2006).

8. M. Duvvuri and J.P. Krise. Intracellular drug sequestration events associated with the emergence of multidrug resistance: a mechanistic review. *Front Biosci.* 10:1499-1509 (2005).

9. V.Y. Chen, M.M. Posada, L.L. Blazer, T. Zhao, and G.R. Rosania. The Role of the VPS4A-Exosome Pathway in the Intrinsic Egress Route of a DNA-Binding Anticancer Drug. *Pharm Res* (2006).

10. V.Y. Chen, M.M. Posada, L. Zhao, and G.R. Rosania. Rapid doxorubicin efflux from the nucleus of drug-resistant cancer cells following extracellular drug clearance. *Pharm Res.* 24:2156-2167 (2007).

11. J.P. Falgueyret, S. Desmarais, R. Oballa, W.C. Black, W. Cromlish, K. Khougaz, S. Lamontagne, F. Masse, D. Riendeau, S. Toulmond, and M.D. Percival. Lysosomotropism of basic cathepsin K inhibitors contributes to increased cellular potencies against off-target cathepsins and reduced functional selectivity. *J Med Chem.* 48:7535-7543 (2005).

12. K. Zhao, G.M. Zhao, D. Wu, Y. Soong, A.V. Birk, P.W. Schiller, and H.H. Szeto. Cell-permeable peptide antioxidants targeted to inner mitochondrial membrane inhibit mitochondrial swelling, oxidative cell death, and reperfusion injury. *J Biol Chem.* 279:34682-34690 (2004).

13. J. Fernandez-Carneado, M. Van Gool, V. Martos, S. Castel, P. Prados, J. de Mendoza, and E. Giralt. Highly efficient, nonpeptidic oligoguanidinium vectors that selectively internalize into mitochondria. *J Am Chem Soc.* 127:869-874 (2005).

14. K.L. Horton, K.M. Stewart, S.B. Fonseca, Q. Guo, and S.O. Kelley. Mitochondria-penetrating peptides. *Chem Biol.* 15:375-382 (2008).

15. L.F. Yousif, K.M. Stewart, and S.O. Kelley. Targeting mitochondria with organelle-specific compounds: strategies and applications. *Chembiochem.* 10:1939-1950 (2009).

16. L. Rajendran, H.J. Knolker, and K. Simons. Subcellular targeting strategies for drug design and delivery. *Nat Rev Drug Discov.* 9:29-42 (2010).

17. S.B. Fonseca, M.P. Pereira, R. Mourtada, M. Gronda, K.L. Horton, R. Hurren, M.D. Minden, A.D. Schimmer, and S.O. Kelley. Rerouting chlorambucil to mitochondria combats drug deactivation and resistance in cancer cells. *Chem Biol.* 18:445-453 (2011).

18. J. Colston, R.W. Horobin, F. Rashid-Doubell, J. Pediani, and K.K. Johal. Why fluorescent probes for endoplasmic reticulum are selective: an experimental and QSAR-modelling study. *Biotech Histochem.* 78:323-332 (2003).

19. R.W. Horobin, J.C. Stockert, and F. Rashid-Doubell. Fluorescent cationic probes for nuclei of living cells: why are they selective? A quantitative structure-activity relations analysis. *Histochem Cell Biol.* 126:165-175 (2006).

20. R.W. Horobin, S. Trapp, and V. Weissig. Mitochondriotropics: a review of their mode of action, and their applications for drug and DNA delivery to mammalian mitochondria. *J Control Release.* 121:125-136 (2007).

21. X. Zhang, N. Zheng, and G.R. Rosania. Simulation-based cheminformatic analysis of organelle-targeted molecules: lysosomotropic monobasic amines. *J Comput Aided Mol Des.* 22:629-645 (2008).

22. N. Zheng, H.N. Tsai, X. Zhang, K. Shedden, and G.R. Rosania. The Subcellular Distribution of Small Molecules: A Meta-Analysis. *Mol Pharmaceutics.* DOI: 10.1021/mp200093z. (2011)

23. J. Lippincott-Schwartz, L.C. Yuan, J.S. Bonifacino, and R.D. Klausner. Rapid redistribution of Golgi proteins into the ER in cells treated with brefeldin A: evidence for membrane cycling from Golgi to ER. *Cell.* 56:801-813 (1989).

24. L.J. Journey and M.N. Goldstein. The effect of terramycin on the fine structure of HeLa cell mitochondria. *Cancer Res.* 23:551-554 (1963).

25. J. Lucocq, G. Warren, and J. Pryde. Okadaic acid induces Golgi apparatus fragmentation and arrest of intracellular transport. *J Cell Sci.* 100 (Pt 4):753-759 (1991).

26. M. Wibo and B. Poole. Protein degradation in cultured cells. II. The uptake of chloroquine by rat fibroblasts and the inhibition of cellular protein degradation and cathepsin B1. *J Cell Biol.* 63:430-440 (1974).

27. C.A. Homewood, D.C. Warhurst, W. Peters, and V.C. Baggaley. Lysosomes, pH and the anti-malarial action of chloroquine. *Nature.* 235:50-52 (1972).

28. P. Mitchell and J. Moyle. Estimation of membrane potential and pH difference across the cristae membrane of rat liver mitochondria. *Eur J Biochem.* 7:471-484 (1969).

29. M.A. Verity and W.J. Brown. Membrane permeability of hepatic mitochondria and lysosomes studied by structure-linked enzyme changes. *Exp Mol Pathol.* 19:1-14 (1973).

30. M.C. Beatrice, J.W. Palmer, and D.R. Pfeiffer. The relationship between mitochondrial membrane permeability, membrane potential, and the retention of Ca2+ by mitochondria. *J Biol Chem.* 255:8663-8671 (1980).

31. J.L. Scarlett, P.W. Sheard, G. Hughes, E.C. Ledgerwood, H.H. Ku, and M.P. Murphy. Changes in mitochondrial membrane potential during staurosporine-induced apoptosis in Jurkat cells. *FEBS Lett.* 475:267-272 (2000).

32. J. Kornhuber, A.W. Henkel, T.W. Groemer, S. Stadtler, O. Welzel, P. Tripal, A. Rotter, S. Bleich, and S. Trapp. Lipophilic cationic drugs increase the permeability of lysosomal membranes in a cell culture system. *J Cell Physiol.* 224:152-164 (2010).

33. S. Takayama and Y. Ojima. Photosensitizing Activity of Carcinogenic and Noncarciogenic Polycyclic Hydrocarbons on Cultured Cells. *Japan J Genetics.* 44:231-240 (1969).

34. A.J. Kowaltowski, J. Turin, G.L. Indig, and A.E. Vercesi. Mitochondrial effects of triarylmethane dyes. *J Bioenerg Biomembr.* 31:581-590 (1999).

35. A. Filipovska, G.F. Kelso, S.E. Brown, S.M. Beer, R.A. Smith, and M.P. Murphy. Synthesis and characterization of a triphenylphosphonium-conjugated peroxidase mimetic. Insights into the interaction of ebselen with mitochondria. *J Biol Chem.* 280:24113-24126 (2005).

36. E. Tian, T.H. Landowski, O.W. Stephens, S. Yaccoby, B. Barlogie, and J.D. Shaughnessy, Jr. Ellipticine derivative NSC 338258 represents a potential new antineoplastic agent for the treatment of multiple myeloma. *Mol Cancer Ther.* 7:500-509 (2008).

37. Z.M. Szulc, J. Bielawski, H. Gracz, M. Gustilo, N. Mayroo, Y.A. Hannun, L.M. Obeid, and A. Bielawska. Tailoring structure-function and targeting properties of ceramides by site-specific cationization. *Bioorg Med Chem.* 14:7083-7104 (2006).

38. D. Dindo, F. Dahm, Z. Szulc, A. Bielawska, L.M. Obeid, Y.A. Hannun, R. Graf, and P.A. Clavien. Cationic long-chain ceramide LCL-30 induces cell death by mitochondrial targeting in SW403 cells. *Mol Cancer Ther.* 5:1520-1529 (2006).

39. S.A. Novgorodov, Z.M. Szulc, C. Luberto, J.A. Jones, J. Bielawski, A. Bielawska, Y.A. Hannun, and L.M. Obeid. Positively charged ceramide is a potent inducer of mitochondrial permeabilization. *J Biol Chem.* 280:16096-16105 (2005).

40. A. Bielawska, J. Bielawski, Z.M. Szulc, N. Mayroo, X. Liu, A. Bai, S. Elojeimy, B. Rembiesa, J. Pierce, J.S. Norris, and Y.A. Hannun. Novel analogs of D-e-MAPP and B13. Part 2: signature effects on bioactive sphingolipids. *Bioorg Med Chem.* 16:1032-1045 (2008).

41. W.P. Doherty and T.C. Campbell. Aflatoxin inhibition of rat liver mitochondria. *Chem Biol Interact.* 7:63-77 (1973).

42. M. Kalina and J.J. Bubis. Myeloid bodies formation in triparanol treated cultured cells. *Virchows Arch B Cell Pathol.* 19:349-357 (1975).

43. J.Z. Byczkowski. The mode of action of p,p'=DDT on mammalian mitochondria. *Toxicology.* 6:309-314 (1976).

44. S. Feldman, M.Y. Wang, and G.J. Kaloyanides. Aminoglycosides induce a phospholipidosis in the renal cortex of the rat: an early manifestation of nephrotoxicity. *J Pharmacol Exp Ther.* 220:514-520 (1982).

45. P.O. Seglen. Protein degradation in isolated rat hepatocytes is inhibited by ammonia. *Biochemical and Biophysical Research Communications.* 6:42-52 (1975).

46. P.O. Seglen and P.B. Gordon. Effects of lysosomotropic monoamines, diamines, amino alcohols, and other amino compounds on protein degradation and protein synthesis in isolated rat hepatocytes. *Mol Pharm.* 18:468-475 (1980).

47. W.J. Martin, 2nd, D.L. Kachel, T. Vilen, and V. Natarajan. Mechanism of phospholipidosis in amiodarone pulmonary toxicity. *J Pharmacol Exp Ther.* 251:272-278 (1989).

48. C. de Duve, T. de Barsy, B. Poole, A. Trouet, P. Tulkens, and F. Van Hoof. Commentary. Lysosomotropic agents. *Biochem Pharmacol.* 23:2495-2531 (1974).

49. J.J. Luiken, J.M. Aerts, and A.J. Meijer. The role of the intralysosomal pH in the control of autophagic proteolytic flux in rat hepatocytes. *Eur J Biochem.* 235:564-573 (1996).

50. S.S. Huang, H.A. Koh, and J.S. Huang. Suramin enters and accumulates in low pH intracellular compartments of v-sis-transformed NIH 3T3 cells. *FEBS Lett.* 416:297-301 (1997).

51. F.G. Holz, F. Schutt, J. Kopitz, G.E. Eldred, F.E. Kruse, H.E. Volcker, and M. Cantz. Inhibition of lysosomal degradative functions in RPE cells by a retinoid component of lipofuscin. *Invest Ophthalmol Vis Sci.* 40:737-743 (1999).

52. F. Schutt, M. Bergmann, J. Kopitz, and F.G. Holz. [Mechanism of the inhibition of lysosomal functions in the retinal pigment epithelium by lipofuscin retinoid component A2-E]. *Ophthalmologe.* 98:721-724 (2001).

53. P. Boya, R.A. Gonzalez-Polo, D. Poncet, K. Andreau, H.L. Vieira, T. Roumier, J.L. Perfettini, and G. Kroemer. Mitochondrial membrane permeabilization is a critical step of lysosome-initiated apoptosis induced by hydroxychloroquine. *Oncogene.* 22:3927-3936 (2003).

54. J. Ishizaki, K. Yokogawa, F. Ichimura, and S. Ohkuma. Uptake of imipramine in rat liver lysosomes in vitro and its inhibition by basic drugs. *J Pharmacol Exp Ther.* 294:1088-1098 (2000).

55. W.A. Daniel, J. Wojcikowski, and A. Palucha. Intracellular distribution of psychotropic drugs in the grey and white matter of the brain: the role of lysosomal trapping. *Br J Pharmacol.* 134:807-814 (2001).

56. N. Kamo, M. Muratsugu, R. Hongoh, and Y. Kobatake. Membrane potential of mitochondria measured with an electrode sensitive to tetraphenyl phosphonium and relationship between proton electrochemical potential and phosphorylation potential in steady state. *J Membr Biol.* 49:105-121 (1979).

57. G.P. Davey, K.F. Tipton, and M.P. Murphy. Uptake and accumulation of 1-methyl-4-phenylpyridinium by rat liver mitochondria measured using an ion-selective electrode. *Biochem J.* 288 (Pt 2):439-443 (1992).

58. A.M. James, F.H. Blaikie, R.A. Smith, R.N. Lightowlers, P.M. Smith, and M.P. Murphy. Specific targeting of a DNA-alkylating reagent to mitochondria. Synthesis and characterization of [4-((11aS)-7-methoxy-1,2,3,11a-tetrahydro-5H-pyrrolo[2,1-c][1,4]benzodiaze pin-5-on-8-oxy)butyl]-triphenylphosphonium iodide. *Eur J Biochem.* 270:2827-2836 (2003).

59. A.R. Prasad, R.F. Luduena, and P.M. Horowitz. Detection of energy transfer between tryptophan residues in the tubulin molecule and bound bis(8-anilinonaphthalene-1-sulfonate), an inhibitor of microtubule assembly, that binds to a flexible region on tubulin. *Biochemistry.* 25:3536-3540 (1986).

60. E. Wagner, M. Cotten, K. Mechtler, H. Kirlappos, and M.L. Birnstiel. DNA-binding transferrin conjugates as functional gene-delivery agents: synthesis by linkage of polylysine or ethidium homodimer to the transferrin carbohydrate moiety. *Bioconjug Chem.* 2:226-231 (1991).

61. K. Schneider, A. Naujok, and H.W. Zimmermann. Influence of trans-membrane potential and of hydrophobic interactions on dye accumulation in mitochondria of living cells. Photoaffinity labelling of mitochondrial proteins, action of potential dissipating drugs, and competitive staining. *Histochemistry.* 101:455-461 (1994).

62. L.D. Ward and S.N. Timasheff. Cooperative multiple binding of bisANS and daunomycin to tubulin. *Biochemistry.* 33:11891-11899 (1994).

63. U. Michelsen and J. von Hagen. Isolation of subcellular organelles and structures. *Methods Enzymol.* 463:305-328 (2009).

64. L.B. Mellett and L.A. Woods. The intra cellular distribution of N-C14-methyl levorphanol in brain, liver and kidney tissue of the rat. *J Pharmacol Exp Ther.* 125:97-104 (1959).

65. P.P. Nair and C. Bucana. Intracellular distribution of vitamin D in rat liver. *Biochim Biophys Acta.* 124:254-259 (1966).

66. A.E. Albert and G.P. Warwick. The subcellular distribution of tritiated 4-dimethylaminoazobenzene and 2-methyl-4-dimethylaminoazobenzene in rat liver and spleen following a single oral administration. *Chem Biol Interact.* 5:65-68 (1972).

67. D.D. Choie, A.A. del Campo, and A.M. Guarino. Subcellular localization of cis-dichlorodiammineplatinum(II) in rat kidney and liver. *Toxicol Appl Pharmacol.* 55:245-252 (1980).

68. H. Yoshida, K. Okumura, and R. Hori. Subcellular distribution of basic drugs accumulated in the isolated perfused lung. *Pharm Res.* 4:50-53 (1987).

69. M. Miniati, A. Paci, F. Cocci, G. Ciarimboli, S. Monti, and M. Pistolesi. Mitochondria act as a reservoir for the basic amine HIPDM in the lung. *Eur Respir J.* 9:2306-2312 (1996).

70. A.E. Vickers, I.G. Sipes, and K. Brendel. Metabolism-related spectral characterization and subcellular distribution of polychlorinated biphenyl congeners in isolated rat hepatocytes. *Biochem Pharmacol.* 35:297-306 (1986).

71. W.J. Martin, 2nd and J.E. Standing. Amiodarone pulmonary toxicity: biochemical evidence for a cellular phospholipidosis in the bronchoalveolar lavage of human subjects. *J Pharmacol Exp Ther.* 244:774-779 (1988).

72. M. Duvvuri, W. Feng, A. Mathis, and J.P. Krise. A cell fractionation approach for the quantitative analysis of subcellular drug disposition. *Pharm Res.* 21:26-32 (2004).

73. Y. Saito, A. Fukuhara, K. Nishio, M. Hayakawa, Y. Ogawa, H. Sakamoto, K. Fujii, Y. Yoshida, and E. Niki. Characterization of cellular uptake and distribution of coenzyme Q10 and vitamin E in PC12 cells. *J Nutr Biochem.* 20:350-357 (2009).

74. A. Liu, N. Pajkovic, Y. Pang, D. Zhu, B. Calamini, A.L. Mesecar, and R.B. van Breemen. Absorption and subcellular localization of lycopene in human prostate cancer cells. *Mol Cancer Ther.* 5:2879-2885 (2006).

75. R.G. Bell and J.T. Matschiner. Intracellular distribution of vitamin K in the rat. *Biochim Biophys Acta.* 184:597-603 (1969).

76. Y. Woo, M.F. Argus, and J.C. Arcos. Tissue and subcellular distribution of 3H-dioxane in the rat and apparent lack of microsome-catalyzed covalent binding in the target tissue. *Life Sci.* 21:1447-1456 (1977).

77. L.D. Dial, D.K. Anestis, S.R. Kennedy, and G.O. Rankin. Tissue distribution, subcellular localization and covalent binding of 2-chloroaniline and 4-chloroaniline in Fischer 344 rats. *Toxicology.* 131:109-119 (1998).

78. M.F. Ross, T.A. Prime, I. Abakumova, A.M. James, C.M. Porteous, R.A. Smith, and M.P. Murphy. Rapid and extensive uptake and activation of hydrophobic triphenylphosphonium cations within cells. *Biochem J.* 411:633-645 (2008).

79. J.E. Gruenberg and K.E. Howell. Reconstitution of vesicle fusions occurring in endocytosis with a cell-free system. *EMBO J.* 5:3091-3101 (1986).

80. K.E. Howell, J. Gruenberg, A. Ito, and G.E. Palade. Immuno-isolation of subcellular components. *Prog Clin Biol Res.* 270:77-90 (1988).

81. C. Pasquali, I. Fialka, and L.A. Huber. Subcellular fractionation, electromigration analysis and mapping of organelles. *J Chromatogr B Biomed Sci Appl.* 722:89-102 (1999).

82. R.F. Murphy. Processing of Endocytosed Material *Advances in Molecular and Cell Biology.* 2:159-180 (1988).

83. G. Bock, P. Steinlein, and L.A. Huber. Cell biologists sort things out: Analysis and purification of intracellular organelles by flow cytometry. *Trends Cell Biol.* 7:499-503 (1997).

84. D. Rajotte, C.D. Stearns, and A.K. Kabcenell. Isolation of mast cell secretory lysosomes using flow cytometry. *Cytometry A.* 55:94-101 (2003).

85. A.M. Nasirudeen and K.S. Tan. Isolation and characterization of the mitochondrion-like organelle from Blastocystis hominis. *J Microbiol Methods.* 58:101-109 (2004).

86. I. Stefaner, H. Klapper, E. Sztul, and R. Fuchs. Free-flow electrophoretic analysis of endosome subpopulations of rat hepatocytes. *Electrophoresis.* 18:2516-2522 (1997).

87. A. Tulp, D. Verwoerd, A. Benham, and J. Neefjes. High-resolution density gradient electrophoresis of proteins and subcellular organelles. *Electrophoresis.* 18:2509-2515 (1997).

88. A. Tulp, M. Fernandez-Borja, D. Verwoerd, and J. Neefjes. High-resolution density gradient electrophoresis of subcellular organelles and proteins under nondenaturing conditions. *Electrophoresis.* 19:1288-1293 (1998).

89. P.J. Weber, G. Weber, and C. Eckerskorn. Isolation of organelles and prefractionation of protein extracts using free-flow electrophoresis. *Curr Protoc Protein Sci.* Chapter 22:Unit 22 25 (2004).

90. G. Xiong, Y. Chen, and E.A. Arriaga. Measuring the doxorubicin content of single nuclei by micellar electrokinetic capillary chromatography with laser-induced fluorescence detection. *Anal Chem.* 77:3488-3493 (2005).

91. Y. Chen and E.A. Arriaga. Individual acidic organelle pH measurements by capillary electrophoresis. *Anal Chem.* 78:820-826 (2006).

92. R.D. Johnson, M. Navratil, B.G. Poe, G. Xiong, K.J. Olson, H. Ahmadzadeh, D. Andreyev, C.F. Duffy, and E.A. Arriaga. Analysis of mitochondria isolated from single cells. *Anal Bioanal Chem.* 387:107-118 (2007).

93. V. Kostal and E.A. Arriaga. Recent advances in the analysis of biological particles by capillary electrophoresis. *Electrophoresis.* 29:2578-2586 (2008).

94. Y. Wang and E.A. Arriaga. Monitoring incorporation, transformation and subcellular distribution of N-l-leucyl-doxorubicin in uterine sarcoma cells using capillary electrophoretic techniques. *Cancer Lett.* 262:123-132 (2008).

95. O. Diettrich, K. Mills, A.W. Johnson, A. Hasilik, and B.G. Winchester. Application of magnetic chromatography to the isolation of lysosomes from fibroblasts of patients with lysosomal storage disorders. *FEBS Lett.* 441:369-372 (1998).

96. M. Duvvuri and J.P. Krise. A novel assay reveals that weakly basic model compounds concentrate in lysosomes to an extent greater than pH-partitioning theory would predict. *Mol Pharmaceutics.* 2:440-448 (2005).

97. A.M. Kaufmann, S.D. Goldman, and J.P. Krise. A fluorescence resonance energy transfer-based approach for investigating late endosome-lysosome retrograde fusion events. *Anal Biochem.* 386:91-97 (2009).

98. S.F. Hoff and A.J. MacInnis. Ultrastructural localization of phenothiazines and tetracycline: a new histochemical approach. *J Histochem Cytochem.* 31:613-625 (1983).

99. T. Muller. Electron microscopic demonstration of intracelluar promethazine accumulation sites by a precipitation technique: application to the cerebellar cortex of the mouse. *J Histochem Cytochem.* 44:531-535 (1996).

100. S. Ivanova, F. Batliwalla, J. Mocco, S. Kiss, J. Huang, W. Mack, A. Coon, J.W. Eaton, Y. Al-Abed, P.K. Gregersen, E. Shohami, E.S. Connolly, Jr., and K.J. Tracey. Neuroprotection in cerebral ischemia by neutralization of 3-aminopropanal. *Proc Natl Acad Sci U S A.* 99:5579-5584 (2002).

101. W. Li, X.M. Yuan, S. Ivanova, K.J. Tracey, J.W. Eaton, and U.T. Brunk. 3-Aminopropanal, formed during cerebral ischaemia, is a potent lysosomotropic neurotoxin. *Biochem J.* 371:429-436 (2003).

102. J.A. Bain and S.E. Mayer. The intracellular localization of fluorescent convulsants. *J Pharmacol Exp Ther.* 118:1-16 (1956).

103. M.J. Egorin, R.E. Clawson, L.A. Ross, N.M. Schlossberger, and N.R. Bachur. Cellular accumulation and disposition of aclacinomycin A. *Cancer Res.* 39:4396-4400 (1979).

104. M. Terasaki, J. Song, J.R. Wong, M.J. Weiss, and L.B. Chen. Localization of endoplasmic reticulum in living and glutaraldehyde-fixed cells with fluorescent dyes. *Cell.* 38:101-108 (1984).

105. C. Bucana, I. Saiki, and R. Nayar. Uptake and accumulation of the vital dye hydroethidine in neoplastic cells. *J Histochem Cytochem.* 34:1109-1115 (1986).

106. S.F. Steinberg, J.P. Bilezikian, and Q. Al-Awqati. Fura-2 fluorescence is localized to mitochondria in endothelial cells. *Am J Physiol.* 253:C744-747 (1987).

107. C.J. Jeon and R.H. Masland. Selective accumulation of diamidino yellow and chromomycin A3 by retinal glial cells. *J Histochem Cytochem.* 41:1651-1658 (1993).

108. Y. Deng, J.R. Bennink, H.C. Kang, R.P. Haugland, and J.W. Yewdell. Fluorescent conjugates of brefeldin A selectively stain the endoplasmic reticulum and Golgi complex of living cells. *J Histochem Cytochem.* 43:907-915 (1995).

109. M. Chalfie, Y. Tu, G. Euskirchen, W.W. Ward, and D.C. Prasher. Green fluorescent protein as a marker for gene expression. *Science.* 263:802-805 (1994).

110. R. Heim, D.C. Prasher, and R.Y. Tsien. Wavelength mutations and posttranslational autoxidation of green fluorescent protein. *Proc Natl Acad Sci U S A.* 91:12501-12504 (1994).

111. M. Huang and M. Chalfie. Gene interactions affecting mechanosensory transduction in Caenorhabditis elegans. *Nature.* 367:467-470 (1994).

112. R. Rizzuto, M. Brini, P. Pizzo, M. Murgia, and T. Pozzan. Chimeric green fluorescent protein as a tool for visualizing subcellular organelles in living cells. *Curr Biol.* 5:635-642 (1995).

113. R. Heim and R.Y. Tsien. Engineering green fluorescent protein for improved brightness, longer wavelengths and fluorescence resonance energy transfer. *Curr Biol.* 6:178-182 (1996).

114. X. Chen and R.F. Murphy. Objective clustering of proteins based on subcellular location patterns. *J Biomed Biotechnol.* 2005:87-95 (2005).

115. X. Chen, M. Velliste, and R.F. Murphy. Automated interpretation of subcellular patterns in fluorescence microscope images for location proteomics. *Cytometry A.* 69:631-640 (2006).

116. S.C. Chen, T. Zhao, G.J. Gordon, and R.F. Murphy. Automated image analysis of protein localization in budding yeast. *Bioinformatics.* 23:i66-71 (2007).

117. E. Garcia Osuna and R.F. Murphy. Automated, systematic determination of protein subcellular location using fluorescence microscopy. *Subcell Biochem.* 43:263-276 (2007).

118. J. Newberg, J. Hua, and R.F. Murphy. Location proteomics: systematic determination of protein subcellular location. *Methods Mol Biol.* 500:313-332 (2009).

119. V.Y. Chen, S.M. Khersonsky, K. Shedden, Y.T. Chang, and G.R. Rosania. System dynamics of subcellular transport. *Mol Pharmaceutics.* 1:414-425 (2004).

120. K. Shedden, Q. Li, F. Liu, Y.T. Chang, and G.R. Rosania. Machine vision-assisted analysis of structure-localization relationships in a combinatorial library of prospective bioimaging probes. *Cytometry A.* 75:482-493 (2009).

121. K. Shedden and G.R. Rosania. Chemical address tags of fluorescent bioimaging probes. *Cytometry A.* 77A:429-438 (2010).

122. G.R. Rosania, G. Crippen, P. Woolf, D. States, and K. Shedden. A cheminformatic toolkit for mining biomedical knowledge. *Pharm Res.* 24:1791-1802 (2007).

123. M.A. Phelps, A.B. Foraker, W. Gao, J.T. Dalton, and P.W. Swaan. A novel rhodamine-riboflavin conjugate probe exhibits distinct fluorescence resonance energy transfer that enables riboflavin trafficking and subcellular localization studies. *Mol Pharm.* 1:257-266 (2004).

124. R.E. Pagano, O.C. Martin, H.C. Kang, and R.P. Haugland. A novel fluorescent ceramide analogue for studying membrane traffic in animal cells: accumulation at the Golgi apparatus results in altered spectral properties of the sphingolipid precursor. *J Cell Biol.* 113:1267-1279 (1991).

125. D.F. Baxter, M. Kirk, A.F. Garcia, A. Raimondi, M.H. Holmqvist, K.K. Flint, D. Bojanic, P.S. Distefano, R. Curtis, and Y. Xie. A novel membrane potential-sensitive fluorescent dye improves cell-based assays for ion channels. *J Biomol Screen.* 7:79-85 (2002).

126. A. Kotaki and K. Yagi. Fluorescence properties of flavins in various solvents. *J Biochem.* 68:509-516 (1970).

127. M.A. Haidekker, T.P. Brady, D. Lichlyter, and E.A. Theodorakis. Effects of solvent polarity and solvent viscosity on the fluorescent properties of molecular rotors and related probes. *Bioorg Chem.* 33:415-425 (2005).

128. T. Gustavsson, N. Sarkar, A. Banyasz, D. Markovitsi, and R. Improta. Solvent effects on the steady-state absorption and fluorescence spectra of uracil, thymine and 5-fluorouracil. *Photochem Photobiol.* 83:595-599 (2007).

129. A. White. Effect of pH on fluorescence of tryosine, tryptophan and related compounds. *Biochem J.* 71:217-220 (1959).

130. I.D. Weiner and L.L. Hamm. Use of fluorescent dye BCECF to measure intracellular pH in cortical collecting tubule. *Am J Physiol.* 256:F957-964 (1989).

131. X.J. Jiang, P.C. Lo, S.L. Yeung, W.P. Fong, and D.K. Ng. A pH-responsive fluorescence probe and photosensitiser based on a tetraamino silicon(IV) phthalocyanine. *Chem Commun (Camb).* 46:3188-3190 (2010).

132. E. Sundbom, M. Strand, and J.E. Hallgren. Temperature-induced fluorescence changes : a screening method for frost tolerance of potato (solanum sp.). *Plant Physiol.* 70:1299-1302 (1982).

133. H. Ogawa, S. Inouye, F.I. Tsuji, K. Yasuda, and K. Umesono. Localization, trafficking, and temperature-dependence of the Aequorea green fluorescent protein in cultured vertebrate cells. *Proc Natl Acad Sci U S A.* 92:11899-11903 (1995).

134. C. Gota, K. Okabe, T. Funatsu, Y. Harada, and S. Uchiyama. Hydrophilic fluorescent nanogel thermometer for intracellular thermometry. *J Am Chem Soc.* 131:2766-2767 (2009).

135. T.Y. Ohulchanskyy, H.E. Pudavar, S.M. Yarmoluk, V.M. Yashchuk, E.J. Bergey, and P.N. Prasad. A monomethine cyanine dye Cyan 40 for two-photon-excited fluorescence detection of nucleic acids and their visualization in live cells. *Photochem Photobiol.* 77:138-145 (2003).

136. K.J. Olson, H. Ahmadzadeh, and E.A. Arriaga. Within the cell: analytical techniques for subcellular analysis. *Anal Bioanal Chem.* 382:906-917 (2005).

137. J. Ling, S.D. Weitman, M.A. Miller, R.V. Moore, and A.C. Bovik. Direct Raman imaging techniques for study of the subcellular distribution of a drug. *Appl Opt.* 41:6006-6017 (2002).

138. N. Zheng, X. Zhang, and G.R. Rosania. Effect of phospholipidosis on the cellular pharmacokinetics of chloroquine. *J Pharmacol Exp Ther.* 336:661-671 (2011).

139. X. Nan, E.O. Potma, and X.S. Xie. Nonperturbative chemical imaging of organelle transport in living cells with coherent anti-stokes Raman scattering microscopy. *Biophys J.* 91:728-735 (2006).

140. X. Nan, A.M. Tonary, A. Stolow, X.S. Xie, and J.P. Pezacki. Intracellular imaging of HCV RNA and cellular lipids by using simultaneous two-photon

fluorescence and coherent anti-Stokes Raman scattering microscopies. *Chembiochem.* 7:1895-1897 (2006).

141. R.K. Lyn, D.C. Kennedy, S.M. Sagan, D.R. Blais, Y. Rouleau, A.F. Pegoraro, X.S. Xie, A. Stolow, and J.P. Pezacki. Direct imaging of the disruption of hepatitis C virus replication complexes by inhibitors of lipid metabolism. *Virology.* 394:130-142 (2009).

142. P. Galle. Tissue localization of stable and radioactive nuclides by secondary-ion microscopy. *J Nucl Med.* 23:52-57 (1982).

143. S.G. Boxer, M.L. Kraft, and P.K. Weber. Advances in imaging secondary ion mass spectrometry for biological samples. *Annu Rev Biophys.* 38:53-74 (2009).

144. M.R. Kilburn, D.L. Jones, P.L. Clode, J.B. Cliff, E.A. Stockdale, A.M. Herrmann, and D.V. Murphy. Application of nanoscale secondary ion mass spectrometry to plant cell research. *Plant Signal Behav.* 5:760-762 (2010).

145. M.L. Pacholski, D.M. Cannon, Jr., A.G. Ewing, and N. Winograd. Static time-of-flight secondary ion mass spectrometry imaging of freeze-fractured, frozen-hydrated biological membranes. *Rapid Commun Mass Spectrom.* 12:1232-1235 (1998).

146. K. Oba, H. Gong, T. Amemiya, K. Baba, and K. Takaya. Applying secondary ion mass spectrometry to the analysis of elements in goblet cells of conjunctiva. *J Electron Microsc (Tokyo).* 50:325-332 (2001).

147. S. Chandra, I.D. Lorey, and D.R. Smith. Quantitative subcellular secondary ion mass spectrometry (SIMS) imaging of boron-10 and boron-11 isotopes in the same cell delivered by two combined BNCT drugs: in vitro studies on human glioblastoma T98G cells. *Radiat Res.* 157:700-710 (2002).

148. F. Chehade, C. de Labriolle-Vaylet, N. Moins, M.F. Moreau, J. Papon, P. Labarre, P. Galle, A. Veyre, and E. Hindie. Secondary ion mass spectrometry as a tool for investigating radiopharmaceutical distribution at the cellular level: the example of I-BZA and (14)C-I-BZA. *J Nucl Med.* 46:1701-1706 (2005).

149. P.L. Clode, R.A. Stern, and A.T. Marshall. Subcellular imaging of isotopically labeled carbon compounds in a biological sample by ion microprobe (NanoSIMS). *Microsc Res Tech.* 70:220-229 (2007).

150. Q. Li, Y. Kim, J. Namm, A. Kulkarni, G.R. Rosania, Y.H. Ahn, and Y.T. Chang. RNA-selective, live cell imaging probes for studying nuclear structure and function. *Chem Biol.* 13:615-623 (2006).

151. S. Trapp, G.R. Rosania, R.W. Horobin, and J. Kornhuber. Quantitative modeling of selective lysosomal targeting for drug design. *Eur Biophys J.* 37:1317-1328 (2008).

152. S. Balaz. Modeling kinetics of subcellular disposition of chemicals. *Chem Rev.* 109:1793-1899 (2009).

153. C.D. Selassie. History of Quantitative Structure-Activity Relationships. In *Burger's Medicinal Chemistry and Drug Discovery*, 6th ed.; Abraham, D. J., Ed.; John Wiley & Sons, Inc.: New York, 2003; pp 1_48.

154. A. Boobis, U. Gundert-Remy, P. Kremers, P. Macheras, and O. Pelkonen. In silico prediction of ADME and pharmacokinetics - Report of an expert meeting organised by COST B15. *European Journal of Pharmaceutical Sciences.* 17:183-193 (2002).

155. J.S. Delaney. Predicting aqueous solubility from structure. *Drug Discov Today.* 10:289-295 (2005).

156. A.H. Goller, M. Hennemann, J. Keldenich, and T. Clark. In silico prediction of buffer solubility based on quantum-mechanical and HQSAR- and topology-based descriptors. *J Chem Inf Model.* 46:648-658 (2006).

157. K. Brendel, E. Comets, C. Laffont, C. Laveille, and F. Mentre. Metrics for external model evaluation with an application to the population pharmacokinetics of gliclazide. *Pharm Res.* 23:2036-2049 (2006).

158. N. Parrott and T. Lave. Prediction of intestinal absorption: comparative assessment of GASTROPLUS and IDEA. *Eur J Pharm Sci.* 17:51-61 (2002).

159. S. Ekins and J. Rose. In silico ADME/Tox: the state of the art. *J Mol Graph Model.* 20:305-309 (2002).

160. A.M. Richard. Commercial toxicology prediction systems: a regulatory perspective. *Toxicol Lett.* 102-103:611-616 (1998).

161. R.D. Snyder, G.S. Pearl, G. Mandakas, W.N. Choy, F. Goodsaid, and I.Y. Rosenblum. Assessment of the sensitivity of the computational programs DEREK, TOPKAT, and MCASE in the prediction of the genotoxicity of pharmaceutical molecules. *Environ Mol Mutagen.* 43:143-158 (2004).

162. N.N. Ovanes Mekenyan, Stoyan Karabunarliev, Steven P. Bradbury, Gerald T. Ankley, Bjorn Hansen. New developments in a hazard identification algorithm for hormone receptor ligands. *Quantitative Structure-Activity Relationships.* 18:139-153 (1999).

163. R.W. Horobin and F. Rashid. Interactions of molecular probes with living cells and tissues. Part 1. Some general mechanistic proposals, making use of a simplistic Chinese box model. *Histochemistry.* 94:205-209 (1990).

164. S. Balaz, E. Sturdik, and J. Augustin. Subcellular distribution of compounds in biosystems. *Bull Math Biol.* 50:367-378 (1988).

165. F. Rashid and R.W. Horobin. Interaction of molecular probes with living cells and tissues. Part 2. A structure-activity analysis of mitochondrial staining by cationic probes, and a discussion of the synergistic nature of

image-based and biochemical approaches. *Histochemistry.* 94:303-308 (1990).

166. F. Rashid, R.W. Horobin, and M.A. Williams. Predicting the behaviour and selectivity of fluorescent probes for lysosomes and related structures by means of structure-activity models. *Histochem J.* 23:450-459 (1991).

167. R. Dvorsky, S. Balaz, and R.J. Sawchuk. Kinetics of subcellular distribution of compounds in simple biosystems and its use in QSAR. *J Theor Biol.* 185:213-222 (1997).

168. S. Balaz, E. Sturdik, M. Rosenberg, J. Augustin, and B. Skara. Kinetics of drug activities as influenced by their physico-chemical properties: antibacterial effects of alkylating 2-furylethylenes. *J Theor Biol.* 131:115-134 (1988).

169. S. Balaz, M. Wiese, and J.K. Seydel. A kinetic description of the fate of chemicals in biosystems. *Sci Total Environ.* 109-110:357-375 (1991).

170. S. Balaz. Model-based description of distribution of chemicals in biosystems for the continuous dose. *SAR QSAR Environ Res.* 4:177-187 (1995).

171. L.V. Johnson, M.L. Walsh, B.J. Bockus, and L.B. Chen. Monitoring of relative mitochondrial membrane potential in living cells by fluorescence microscopy. *J Cell Biol.* 88:526-535 (1981).

172. S.T. Smiley, M. Reers, C. Mottola-Hartshorn, M. Lin, A. Chen, T.W. Smith, G.D. Steele, Jr., and L.B. Chen. Intracellular heterogeneity in mitochondrial membrane potentials revealed by a J-aggregate-forming lipophilic cation JC-1. *Proc Natl Acad Sci U S A.* 88:3671-3675 (1991).

173. J.S. Modica-Napolitano and J.R. Aprille. Delocalized lipophilic cations selectively target the mitochondria of carcinoma cells. *Adv Drug Deliv Rev.* 49:63-70 (2001).

174. Y. Gong, Z. Zhao, D.J. McConn, B. Beaudet, M. Tallman, J.D. Speake, D.M. Ignar, and J.P. Krise. Lysosomes contribute to anomalous pharmacokinetic behavior of melanocortin-4 receptor agonists. *Pharm Res.* 24:1138-1144 (2007).

175. R. Hayeshi, C. Masimirembwa, S. Mukanganyama, and A.L. Ungell. Lysosomal trapping of amodiaquine: impact on transport across intestinal epithelia models. *Biopharm Drug Dispos.* 29:324-334 (2008).

176. M.T. Bawolak, G. Morissette, and F. Marceau. Vacuolar ATPase-mediated sequestration of local anesthetics in swollen macroautophagosomes. *Can J Anaesth* (2010).

177. S. Trapp. Plant uptake and transport models for neutral and ionic chemicals. *Environ Sci Pollut Res.* 11:33-39 (2004).

178. S. Trapp and R.W. Horobin. A predictive model for the selective accumulation of chemicals in tumor cells. *Eur Biophys J.* 34:959-966 (2005).

179. X. Zhang, K. Shedden, and G.R. Rosania. A cell-based molecular transport simulator for pharmacokinetic prediction and cheminformatic exploration. *Mol Pharmaceutics.* 3:704-716 (2006).

180. J.Y. Yu and G.R. Rosania. Cell-based multiscale computational modeling of small molecule absorption and retention in the lungs. *Pharm Res.* 27:457-467 (2010).

181. H.J. Kuh, S.H. Jang, M.G. Wientjes, and J.L. Au. Computational model of intracellular pharmacokinetics of paclitaxel. *J Pharmacol Exp Ther.* 293:761-770 (2000).

182. S.H. Jang, M.G. Wientjes, and J.L. Au. Kinetics of P-glycoprotein-mediated efflux of paclitaxel. *J Pharmacol Exp Ther.* 298:1236-1242 (2001).

183. C.A. Sarkar and D.A. Lauffenburger. Cell-level pharmacokinetic model of granulocyte colony-stimulating factor: implications for ligand lifetime and potency in vivo. *Mol Pharmacol.* 63:147-158 (2003).

184. D.L. Bourdet, G.M. Pollack, and D.R. Thakker. Intestinal absorptive transport of the hydrophilic cation ranitidine: a kinetic modeling approach to elucidate the role of uptake and efflux transporters and paracellular vs. transcellular transport in Caco-2 cells. *Pharm Res.* 23:1178-1187 (2006).

185. A. Poirier, T. Lave, R. Portmann, M.E. Brun, F. Senner, M. Kansy, H.P. Grimm, and C. Funk. Design, data analysis, and simulation of in vitro drug transport kinetic experiments using a mechanistic in vitro model. *Drug Metab Dispos.* 36:2434-2444 (2008).

186. J. Baik and G.R. Rosania. molecular Imaging of Intracellular Drug-Membrane Aggregate Formation. *Mol Pharmaceutics.* DOI: 10.1021/mp200101b. (2011)

187. K. Shedden, X.T. Xie, P. Chandaroy, Y.T. Chang, and G.R. Rosania. Expulsion of small molecules in vesicles shed by cancer cells: association with gene expression and chemosensitivity profiles. *Cancer Res.* 63:4331-4337 (2003).

188. G.R. Rosania. Supertargeted chemistry: identifying relationships between molecular structures and their sub-cellular distribution. *Curr Top Med Chem.* 3:659-685 (2003).

189. C.A. Lipinski, F. Lombardo, B.W. Dominy, and P.J. Feeney. Experimental and computational approaches to estimate solubility and permeability in drug discovery and development settings. *Adv Drug Deliv Rev.* 46:3-26 (2001).

190. M.R. Feng. Assessment of blood-brain barrier penetration: in silico, in vitro and in vivo. *Curr Drug Metab.* 3:647-657 (2002).

191. T. Rodgers, D. Leahy, and M. Rowland. Physiologically based pharmacokinetic modeling 1: predicting the tissue distribution of moderate-to-strong bases. *J Pharm Sci.* 94:1259-1276 (2005).

192. T. Rodgers and M. Rowland. Physiologically based pharmacokinetic modelling 2: predicting the tissue distribution of acids, very weak bases, neutrals and zwitterions. *J Pharm Sci.* 95:1238-1257 (2006).

193. X. Zhang, K. Shedden, and G.R. Rosania. A cell-based molecular transport simulator for pharmacokinetic prediction and cheminformatic exploration. *Mol Pharm.* 3:704-716 (2006).

194. X. Zhang, N. Zheng, P. Zou, H. Zhu, J.P. Hinestroza, and G.R. Rosania. Cells on Pores: A Simulation-Driven Analysis of Transcellular Small Molecule Transport. *Mol Pharm.* 7:456-467 (2010).

Tables

Table 1.1. Features of major subcellular compartments that affect the intracellular distribution pattern of small chemicals.

Major subcellular compartments	Major biological function	Morphological features	Physiological features	General mechanisms of accumulation
Lysosomes & endosomes	Degradation of excessive cellular proteins, lipids and organelles	Membrane-bound, vesicles	Acidic luminal environment (pH<6) Contain unique, lysosomal protease and hydrolyses.	Active transport; ion trapping; interaction with organelle resident proteins; receptor endocytosis; fluid phase pinocytosis; intracellular membrane trafficking.
Mitochondria	Energy conversion and storage of calcium ions	Membrane-bound, with internal membrane structure	Negative membrane potential. Weakly basic luminal pH (~8). Two membranes. Contain DNA.	Active transport; trapping by chem.-electrical potential; interaction with mtDNA and organelle resident proteins
Nucleus	Storage of genetic materials	Membrane-bound with large protein pores	Composed of phosphate-rich DNA, RNA, and a large variety of proteins	Active transport; partitioning to nuclear envelope; interaction with DNA, RNA (nucleoli) and organelle resident proteins
Plasma membrane	Separation of the cytosol form the outside environment	Membrane protein-rich phospholipid bilayer membrane	Fluid mosaic, lipid bilayer with selective permeability.	Lipophilic partitioning; absorption to phospholipids; interaction with membrane proteins
Endoplasm reticulum	Facilitation of protein folding and transport of synthesized proteins	Interconnected network of membrane tubules.		Intracellular membrane trafficking; interaction with phospholipids or organelle resident proteins
Golgi apparatus	Process and package of macromolecules	Stacks of semicircular or planar membrane-bound compartments		Intracellular membrane trafficking; interaction with phospholipids or organelle resident proteins
Cytosol		Intracellular solution-like matrix		Interaction with cytosolic components such as the cytoskeleton

Table 1.2. A summary of experimental methodologies.

Methods	Experimental systems	Instruments	Pros. & *Cons.*	
Pharmacological effect	Dead or living cells	LM; FM; TEM; analytical instruments such as HPLC, LCMS, and GE	*Does not provide sufficient evidence to ascertain localization* *Only provides indirect evidence for effect on a specific organelle.*	
Analytical measurements				
Uptake/binding experiments	Isolated organelles or cell culture	FM; FS; radiometer, or analytical instruments	Provide adequate evidence for localization to a specific organelle. *Cannot assess the accumulation in all subcellular organelles at one time*	
Distribution studies	Dead cells	Centrifuge, FACS, CC, CE, and analytical instruments	Depict the relative distribution pattern in all cellular organelles	*Separation of cellular organelles is difficult.* *Not suitable if compound undergoes rapid efflux*
Whole cell based imaging studies				
Immune-/ Histochemistry	Dead cells	TEM		*Sample processing steps may cause redistribution* *Detection of small amounts is challenging.*
Fluorescence microscopy	Live cells	FM		*May miss localization information if fluorescence intensity changes with environmental factors*
Raman imaging	Live cells	Raman microscopy		*Signals are weak and require amplification*
Secondary ion mass spectrometry	Dead cells	SIMS device		
Computational predictions	*in silico*	Computers		

Abreactions: LM - light microscopy; FM - fluorescence microscopy; FS - fluorescence spectrometer; FACS - Fluorescence-activated cell sorting; CC – column chromtography; CE - capillary electrophoresis TEM - transmission electron microscopy; HPLC - high performance liquid chromatography; LC/MS - Liquid chromatography-mass spectrometry ; GE - gel electrophoresis.

Figures

Figure 1.1. MDCK cells treated with 50 μM chloroquine concentration for 4 hours prior to staining with Lysotracker Green (yellow, lysosomes), Mitotracker Red (blue, mitochondria) and Hoechst (red, nuclei). Cells exposed to high concentrations of chloroquine undergo profound changes in endolysosomal membrane organization. Continuous accumulation of chloroquine leads to the formation of spherical, multilamellar drug-membrane complexes that visibly bind to Lysotracker Green within the lumen of the expanded lysosomes [138]. Scale bar: 5 μm.
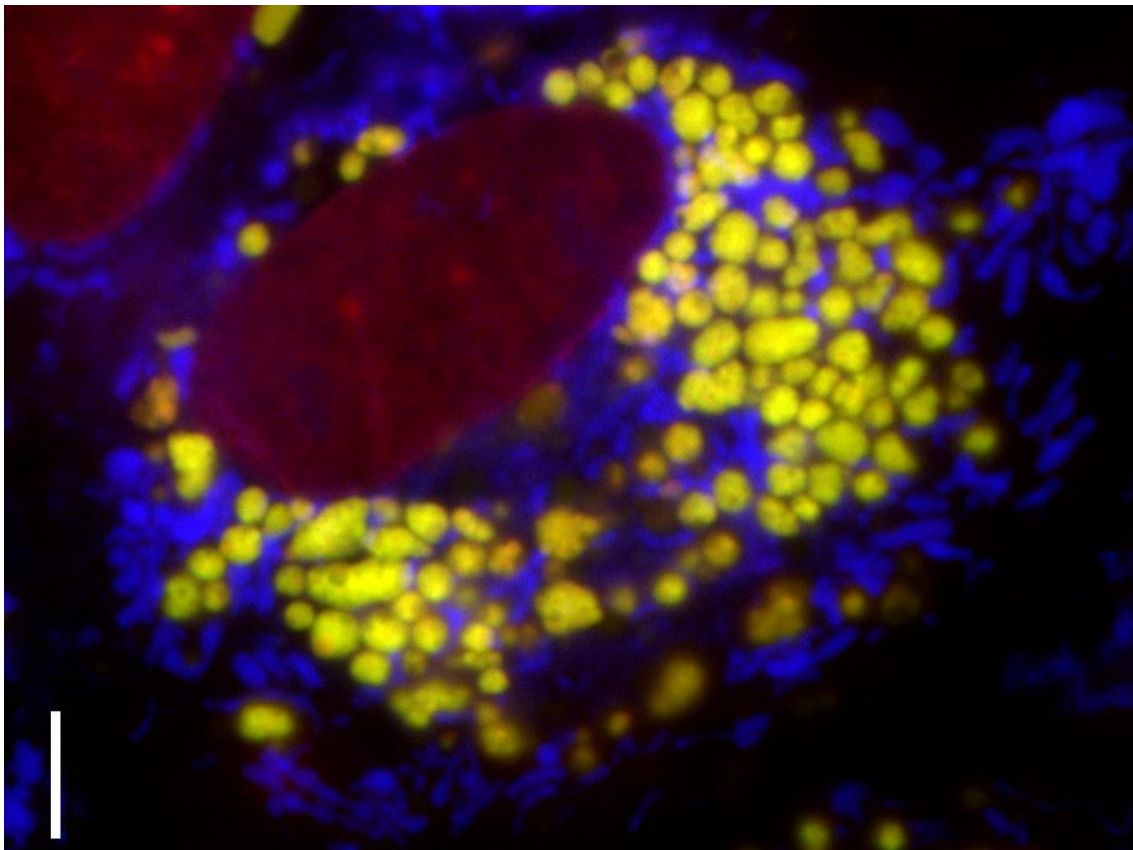
Chapter II

The Subcellular Distribution of Small Molecules:
A Meta-Analysis

Abstract

To explore the extent to which current knowledge about the organelle-targeting features of small molecules may be applicable towards controlling the accumulation and distribution of exogenous chemical agents inside cells, and to evaluate the feasibility of developing a statistically based empirical model in predicting subcellular accumulation sites, molecules with known subcellular localization properties (as reported in the scientific literature) were compiled into a single data set. This data set was compared to a reference data set of approved drug molecules derived from the DrugBank database, and to a reference data set of random organic molecules derived from the PubChem database. Cheminformatic analysis revealed that molecules with reported subcellular localizations were comparably diverse. However, the calculated physicochemical properties of molecules reported to accumulate in different organelles were markedly overlapping. In relation to the reference sets of Drug Bank and Pubchem molecules, molecules with reported subcellular localizations were biased towards larger, more complex chemical structures possessing

multiple ionizable functional groups and higher lipophilicity. Stratifying molecules based on molecular weight revealed that many physicochemical properties trends associated with specific organelles were reversed in smaller vs. larger molecules. Most likely, these reversed trends are due to the different transport mechanisms determining the subcellular localization of molecules of different sizes. Molecular weight can be dramatically altered by tagging molecules with fluorophores or by incorporating organelle targeting motifs. Generally, current body of knowledge in compounds with subcellular distribution information is not suitable for developing predictive empirical models. In order to better explore structure-localization relationships, subcellular targeting strategies would benefit from analysis of the biodistribution effects resulting from variations in the size of the molecules.

Keywords: drug transport; pharmacokinetics; biodistribution; drug targeting; databases; mathematical modeling; drug delivery; cheminformatics.

Introduction

To develop small molecule chemical agents that accumulate at specific sites within cells, one would need to address not only bioavailability and tissue distribution issues at a systemic level, but also focus on delivery and targeting strategies at the subcellular level. In this context, knowledge about the relationships between the physicochemical properties and subcellular distribution of exogenous chemical agents could lead to greater understanding of their biological effects and could serve as a basis for the rational design of chemical agents "supertargeted" to specific sites of action within cells [1]. As such, supertargeted collections of chemical agents could serve as a starting point for developing more potent and less toxic drug leads, focusing on molecules that concentrate at intended sites of action while avoiding unwanted interactions with unintended targets.

The scientific literature supports the notion that many small molecule chemical agents tend to accumulate in specific organelles. The localization is usually supported by evidence including physical interaction with organelle components, resulting changes in organelle structure and function, or it may be visualized microscopically when a molecule has a specific optical signature. At a microscopic level, tissue distribution profiles depend on drug molecules crossing cellular membranes. During this process, drug molecules may also accumulate in various subcellular organelles, or bind to components such as lipids, proteins, DNA, RNA that localize to different intracellular or extracellular compartments. Specific properties of small molecules (pK_a, $\log P$, molecular size, formal charges,

hydrogen bond forming capacity, etc.) have been associated with predictable differences in systemic bioavailability and tissue distribution [2-5]. Indeed, a comprehensive cheminformatic meta-analysis of the physicochemical and subcellular distribution properties of small molecules as reported in the scientific literature could lead to interesting insights and would be important to prioritize future research efforts in this area.

Here, to help assess the status of current knowledge about the distribution of small molecules inside cells and its application to develop predictive empirical models for subcellular drug targeting and delivery, we compiled a data set of small molecules with reported subcellular localization features. In turn, a meta-analysis was performed to reveal how chemical structure and physicochemical properties are associated with the subcellular transport and biodistribution properties of exogenous chemical agents inside cells.

Methods

Data collection. Manual, text-based searches were undertaken using PubMed, Web of Sciences, MEDLINE and a commercial catalogue of fluorescent probes (Molecular Probes Catalog, Invitrogen Inc) using standard MESH terms (i.e., lysosome, mitochondria, nucleus, cell membrane / plasma membrane / cytoplasmic membrane, endoplasmic reticulum, Golgi apparatus / Golgi complex, subcellular, intracellular, accumulation, distribution) to identify small molecules exhibiting organelle-specific intracellular localization patterns. This initial pool of references was expanded by searching for articles written by the same authors,

articles citing or cited by these articles, as well as articles describing studies perforomed on related compounds as identified by searching chemical substance names (e.g. styryls, amines, etc.). For molecules that were found in review articles or catalogues, the chemical name (and synonyms) were used as key words to search PubMed and Google Scholar for original research articles describing experimental evidence documenting their subcellular localization.

Database construction. Each molecule was incorporated into a database of 967 unique compounds with subcellular localization information about their chemical structure and distribution profile (Table 2.1, Appendix A-H). Claims for a specific subcellular distribution pattern were established based on the authors' interpretation of the data. For example: "*compound X* targets *organelle Y*"; "*compound X* (strongly / mainly / predominantly / selectively) localized in *organelle Y*" [6-10]; "*compound X* exhibited a *organelle Y* localization" [8, 11]; "*compound X* mostly concentrating in *organelle Y*" [12, 13]; "*method Z* showed significant enrichment of *compound X* in *organelle Y*" [14]; "strong *organelle Y* accumulation was observed for *compound X*" [15]; "*compound X* (preferentially) accumulated in *organelle Y*" [16-18]; "*Z* percentage of *compound X* was associated with *organelle Y*" [19]; "subcellular distribution of *compound X1* was almost identical with the distribution of *compound X2*" [20]; "*organelle Y* accounted for approximately *Z* percentage of the total distribution" [21-23]. The experimental methods used to support the claims were documented (Table 2.2). Each entry was linked to the main reference source about the compound's subcellular localization. Compound chemical structures were sketched in MOE

47

(Molecular Operating Environment, Chemical Computing Group Inc., Montreal, Canada) using the Molecule Builder, then reduced to single connected components (i.e., without counter-ions) with MOE Wash algorithm, and then converted to Simplified Molecular Input Line Entry Specification (SMILES) strings.

Localization categories. For integrative analysis, we manually grouped the chemical agents into one of seven major categories, based on their reported site of accumulation (Appendix A-H). Functional considerations led us to consider lysosomes and endosomes as a single endolysosomal compartment because the molecular components of endosomes and lysosomes generally overlap in different cell lines, possessing an acidic lumen pH and readily exchanging contents. Molecules accumulating in the endoplasmic membrane (ER) and Golgi apparatus were also grouped together since these two organelles share similar protein markers and exchange content (localization to the Golgi and ER is generally reported together, because these two organelles are also difficult to distinguish using fluorescence microscopy).

Database comparisons. For comparison purposes, a random sample of 1000 compounds was downloaded from DrugBank [24, 25] which represents a collection of drugs that have been approved by the FDA (Appendix I). Similarly, a random sample of 982 compounds was downloaded from PubChem which represents an arbitrary sample of small organic compounds (Appendix J). The two reference datasets did not have overlapping molecules. ChemAxon and MOE were used to calculate molecular descriptors of the major micro-species at pH 7.4 for each compound in the subcellular localization dataset, or the

PubChem and DrugBank reference sets. Z-score was computed to compare the mean descriptor value of molecules in the database to PubChem or DrugBank samples, according to the equation: Z-score $= (X_1 - X_0) \div \sqrt{\frac{s_1^2}{n_1} + \frac{s_0^2}{n_0}}$, where X_1 and X_0 are the mean descriptor value of two subgroups (i.e. the subcellular localization dataset vs PubChem or DrugBank datasets; the lower vs. higher molecular weight compounds; or, the targeting vs non-targeting compounds); s_1^2 and s_0^2 are the sample variances of the corresponding populations; and, n_1 and n_0 are the number of molecules in the corresponding populations. A positive or negative Z-score with an absolute value greater than 3.1 indicates X_1 is significantly greater or less then X_0 (p-value < 0.001). The histograms of molecular descriptors of the compounds in both datasets were plotted and overlaid for visual comparison. Statistical analyses were performed with Python 2.5 (www.python.org).

Discriminant analysis. Linear discriminant analysis (LDA) was used to elucidate how the seven molecular descriptors that showed greatest association with individual subcellular localization categories (molecular weight, a_don, b_rotR, dipole, glob, logP_ow, and formal charge at pH7.4) were related to the reported localization of compounds at the four major sites (lysosomes, mitochondria, nuclei and plasma membrane). The LDA was restricted to those compounds with complete property data and that localized exclusively to one of these four sites. Five of the seven properties (weight, a_don, b_rotR, dipole, glob) were non-negative and skewed, so they were logarithmically transformed using the function $\log_2(x+1)$. LDA was applied separately to compounds < 500 Daltons

(n = 437) and > 500 Daltons (n = 332). Scatter plots of the points according to the first two discriminant directions were constructed and the points were labeled according to each subcellular localization category.

Chemical diversity analysis. The chemical structures were input into MOE to generate a Simplified Molecular Input Line Entry Specification (SMILES) strings. Next, the MACCS Structure Keys (Molecular ACCess System, a library of 166 generic chemical substructure features) was used to generate a binary fingerprint of each molecule, based on which MACCS substructure feature is present or absent in each molecule (as captured by the SMILES strings). To calculate the Tanimoto coefficient for each pair of compounds, the total number of features shared by each pair of molecules and the number of common, overlapping features present in both molecules are used, according to the equation: $= \frac{C}{N1+N2-C}$, where *N1 + N2* represent the total number of unique features (bits) in the pair of molecules and *C* represents the number of unique features (bits) shared in common by the fingerprints of both molecules. Two molecules were considered as structurally similar if the *Tc* value was greater than 0.85. Average *Tc* of each sub-group of the subcellular localization dataset was calculated as the average of *Tc* values between all possible pairs of molecules present in each localization category.

Results

The physicochemical properties of compounds with reported subcellular localization features were compared with the corresponding properties of

50

reference compounds obtained from two public repositories of small molecule information (PubChem and DrugBank databases [24, 25]; Figure 2.1 and Figure 2.2). Relative to a random PubChem data set (Figure 2.1, line), compounds with reported localization properties (Figure 2.1, grey) were larger (e.g. higher molecular weight), possessed a broader charge distribution at physiological pH 7.4, and were more lipophilic (higher *logP_ow*). Compounds with reported localization properties also contained more hydrogen bond donors (*a_don*), more rotatable bonds (*b_rotR*, fraction of rotatable bonds) and were flatter (*glob*, or globularity, with a value of 1 indicating a perfect sphere and 0 indicating a one- or two- dimensional object) (Figure 2.1). Values for atom count, bond count, shape, volume and surface area-related descriptors of all localization categories were also greater than those of the reference PubChem compounds (histograms not shown).

Chemical agents with reported subcellular localization were also larger, more hydrophobic and contained more positive charges at physiological pH as compared to small molecule drugs currently on the market, represented by the DrugBank data set (Figure 2.2). When compared with DrugBank compounds [24, 25], compounds with reported subcellular localization possessed a more positive charge distribution at pH 7.4, higher *logP* values and higher molecular weight (Figure 2.2), although hydrogen donor count (*a_don*), rotatable bond fraction (*b_rotR*) and globularity (*glob*) were similar. Interestingly, while 84.7% and 71.6% DrugBank compounds conformed to Lipinski's Rule of Five or Oprea's Rule of Lead-likelihood, only 52.8% and 41.4% of compounds with known subcellular

localization features conformed to the Rule of 5 [2] and the Rule of Lead-likelihood [26] (Table 2.3). Most of the violations of drug-likeliness or lead-likeliness tests were due to higher molecular weight and higher *logP_ow* of compounds with reported localization (data not shown). The majority of violations observed for compounds reported to localize at the plasma membrane, ER/Golgi, and cytosol.

Many compounds with reported subcellular localization were conjugated to a specific targeting motif or fluorophore, to enhance organelle-specific accumulation or to facilitate the detection of the compounds inside cells [9, 18]. Such conjugation is accompanied by an increase in molecular weight, which could impact the mechanisms of transport and accumulation inside cells. Therefore, to assess the effect of molecular weight on localization, compounds with subcellular localization information were stratified into lower and higher molecular weight groups using a molecular weight of 500 Dalton as a threshold. Compounds < 500 Daltons are more "drug-like" or "lead-like" based on Lipinski's Rule of 5 or Oprea's Rule of Lead-likeness, and generally lack extraneous fluorophore tags or delivery vectors. Molecules with lower molecular weight (Figure 2.3, grey filled line) contained less hydrogen bond donors, smaller dipole moments, lower fractions of rotatable bonds, and were less lipophilic and less globular than molecules with higher molecular weight (Figure 2.3, solid line).

Exploring the pH-dependent ionization states of molecules with reported subcellular localization, the overall formal charge increased from negative to positive as pH decreased, as expected from the protonation of the ionizing

52

centers within each molecule. This trend was apparent in both low (Figure 2.4, grey filled line) and high (Figure 2.4, solid line) molecular weight compounds. Nevertheless, in most cases and especially under extreme pH conditions, higher molecular weight molecules showed a much broader distribution of formal charges than lower molecular weight compounds, reflecting the prevalence of multiple ionization centers in higher molecular weight compounds.

Other molecular properties of low and high molecular weight compounds were different, depending on the reported subcellular localizations (Table 2.4). Compared to larger compounds >500 Daltons, smaller compounds with reported endo-lysosomal localization were more positively charged at physiological pH, were smaller (lower *molecular weight*) and more spherical (higher *glob*). The smaller compounds with reported mitochondrial localization contained lower dipole moment (*dipole*). The smaller compounds with reported nuclear localization contained a lower fraction of rotatable bonds (*b_rotR*) and were flatter (lower *glob*). The smaller compounds with reported plasma membrane localizations were larger than non-localizing compounds but contained fewer hydrogen bond donors and were less spherical in shape.

Remarkably, for larger compounds within a given localization class, many trends observed between physicochemical properties and subcellular localizations appear reversed, when compared to the trends observed for smaller compounds (Table 2.4). This was especially striking in the case of molecular weight: lower molecular weight was associated with lysosomal localization for compounds <500 Daltons, while larger molecular weight was associated with

lysosomal localization for compounds >500 Daltons. In addition, higher molecular weight was associated with mitochondrial, nuclear and plasma membrane localization for compounds <500 Daltons, while lower molecular weight was associated with mitochondrial and plasma membrane localization for compounds >500 Daltons. Similar molecular weight-dependent trend reversals were observed for other physicochemical properties in every localization category (Table 2.4).

Linear discriminant analysis was applied to find linear combinations of features which separate compounds with different reported subcellular localization sites in the endo-lysosomes, mitochondria, nucleus and plasma membrane, amongst the lower and higher molecular weight subsets (Figure 2.5). For compounds <500 Daltons (Figure 2.5, left plot), only a small portion of molecules with reported endo-lysosomal localization could be distinguished from the rest by the first and second combination of molecular properties (LDA 1 and LDA 2). These endo-lysosomal compounds possessed lower molecular weight and lower lipophilicity (data not shown). However, these compounds were all derived from a single experimental report focusing on the pharmacological effects of closely related alkylamines [27]. For compounds >500 Daltons (Figure 2.5, right plot), molecules reported to localize to different subcellular compartments exhibited highly overlapping physicochemical properties.

Lastly, we confirmed that based on their chemical structure, molecules with reported subcellular localization features were reasonably diverse, irrespective of their organelle-targeting properties. The average Tanimoto coefficient (*Tc)* value

is 0.350 for molecules with reported localization, which was close to the average *Tc* values of random PubChem (0.282) and DrugBank (0.292) datasets. The group of molecules with reported lysosomal localization had the lowest average *Tc* of 0.325 while the group of reported ER/Golgi localization had the highest average *Tc* of 0.438. No molecule in the database was similar to more than 24 (2.5%) molecules in the entire dataset for *Tc> 0.85*. Within each category, there were variations in terms of the similarity of the molecules to each other (Figure 2.6), with molecules localizing to mitochondria and lysosomes being most diverse, and molecules localizing to the ER/Golgi and plasma membrane being least diverse. This trend could reflect an intrinsic tendency for molecules possessing specific structural features to accumulate in the ER/Golgi and plasma membrane compartments, although it was also possible that this reported localization may also be biased by systematic chemical synthesis efforts of molecules incorporating specific organelle-targeting motifs.

Discussion

Knowing the bioaccumulation and biodistribution patterns of exogenous chemical agents inside cells could be useful to develop subcellular drug targeting and delivery approaches for increasing drug efficacy and decreasing toxicity. In this study, we have evaluated the relationship between the chemical structure of small molecules and the subcellular distribution patterns, based on published reports compiled from the scientific literature. In an accompanying review article, we have reviewed the evolution of the methods that have been used for

performing subcellular distribution studies. Our major conclusion is that understanding of small molecule distribution inside cells has been biased by the experimental strategies that have been used for studying subcellular distribution, which have largely ignored the effect of molecular weight on the observed structure-localization relationships.

Today, fluorescence imaging constitutes the most common method used to establish the subcellular distribution of organelle-targeted small molecules. For this purpose, molecules are tagged with fluorescent probes and are studied because of their specific, organelle-targeting properties. Perhaps for this reason, molecules with known subcellular localization properties appeared to be more complex, larger, possessed many ionizable centers, and were more lipophilic as compared with references sets of molecules representing drugs currently on the market, or random samples of PubChem compounds without subcellular localization information.

As presented in the accompanying review article, there are many more reports of molecules that localize to a single organelle, as compared to reports of molecules that localize to multiple organelles. Perhaps this is because it is easier to focus analysis on localization to single organelles, but it could also be because most molecules that have been studied in terms of their localization are analyzed because of their specific targeting property. To target a single organelle, complex chemical structures with multiple functional groups may allow for strong and specific interactions with resident organelle components. Our results indicate that multiple ionizing centers are associated with larger compounds reported to

accumulate in specific organelles. While multiple ionization centers may underlie highly specific, organelle-targeting properties, high lipophilicity would be a necessary prerequisite for these molecules to penetrate inside cells. Our results also confirm that higher lipophilicity is a characteristic of compounds that have been reported to accumulate in specific organelles.

Molecular weight is an important parameter affecting transport properties and drug-likelihood [2, 26, 28] because of its direct inverse effect on diffusivity and plasma membrane permeability [29]. Using 500 Daltons as a threshold, molecular properties associated with specific subcellular compartments were identified and different trends of molecular properties distribution were observed for molecules lesser or greater than 500 Daltons. The differences in the observed trends emphasize the importance of molecular weight as a key property determining the transport mechanisms and molecular interactions affecting subcellular distribution.

In retrospect, the effect of molecular weight on the other physicochemical properties affecting localization may have been expected based on what is known about the molecular and cellular mechanisms responsible for organelle targeting and retention. For example, in the case of endolysosomal localization, the smallest molecules enter the cells and accumulate in lysosomes by passive diffusion while being retained by pH-dependent ion trapping. However, large, charged molecules enter the cells and accumulate in endolysosomes by pinocytosis or endocytosis, while being retained there by virtue of being intrinsically membrane impermeant. Similarly, flat, rigid, hydrophobic, small

molecules accumulate in the nucleus by directly traversing the membranes of the nuclear envelope while being retained there by intercalating between the bases of DNA. However, larger, more globular, less membrane-permeant molecules possessing multiple positive charges may preferentially accumulate in the nucleus by entering through the nuclear pores while being retained there by forming electrostatic ion complexes with the phosphate backbone of DNA. Only in the case of the plasma membrane were our results consistent with a single common mechanism affecting localization: lipophilic partitioning of hydrophobic molecules possessing lipid-like characteristics.

Based on this meta-analysis, the ability to derive chemical-structure localization relationships of small molecules could benefit from more focused, quantitative structure-localization relationship studies performed on molecules possessing closely-related chemical structures, taking into account how transport mechanisms are molecular size-dependent. In addition, experimental analysis of nonspecific subcellular distribution patterns of compounds lacking targeting motifs should be a priority. High throughput chemical analytical techniques including chemical imaging modalities that do not rely on a fluorescence signal, such as Raman confocal microscopy, could improve understanding of the subcellular transport and distribution properties without the need of fluorescent tags for detection. Today, physiologically-based models consider $\log P$, pK_a and charge as key input parameters to formulate quantitative pharmacokinetic hypothesis. Our results argue for the importance of research aimed at elucidating

the effect of molecular weight (and related molecular size-dependent properties)

in predictive pharmacokinetic models.

References

1.	G.R. Rosania. Supertargeted chemistry: identifying relationships between molecular structures and their sub-cellular distribution. *Curr Top Med Chem.* 3:659-685 (2003).

2.	C.A. Lipinski, F. Lombardo, B.W. Dominy, and P.J. Feeney. Experimental and computational approaches to estimate solubility and permeability in drug discovery and development settings. *Adv Drug Deliv Rev.* 46:3-26 (2001).

3.	M.R. Feng. Assessment of blood-brain barrier penetration: in silico, in vitro and in vivo. *Curr Drug Metab.* 3:647-657 (2002).

4.	T. Rodgers, D. Leahy, and M. Rowland. Physiologically based pharmacokinetic modeling 1: predicting the tissue distribution of moderate-to-strong bases. *J Pharm Sci.* 94:1259-1276 (2005).

5.	T. Rodgers and M. Rowland. Physiologically based pharmacokinetic modelling 2: predicting the tissue distribution of acids, very weak bases, neutrals and zwitterions. *J Pharm Sci.* 95:1238-1257 (2006).

6.	J.P. Berry, G. Lespinats, F. Escaig, P. Boumati, S. Tlouzeau, and J.F. Cavellier. Intracellular localization of drugs in cultured tumor cells by ion microscopy and image processing. *Histochemistry.* 93:397-400 (1990).

7.	T.P. Best, B.S. Edelson, N.G. Nickols, and P.B. Dervan. Nuclear localization of pyrrole-imidazole polyamide-fluorescein conjugates in cell culture. *Proc Natl Acad Sci U S A.* 100:12063-12068 (2003).

8.	A.C. Croce, G. Bottiroli, R. Supino, E. Favini, V. Zuco, and F. Zunino. Subcellular localization of the camptothecin analogues, topotecan and gimatecan. *Biochem Pharmacol.* 67:1035-1045 (2004).

9.	J. Fernandez-Carneado, M. Van Gool, V. Martos, S. Castel, P. Prados, J. de Mendoza, and E. Giralt. Highly efficient, nonpeptidic oligoguanidinium vectors that selectively internalize into mitochondria. *J Am Chem Soc.* 127:869-874 (2005).

10.	M.F. Ross, T.A. Prime, I. Abakumova, A.M. James, C.M. Porteous, R.A. Smith, and M.P. Murphy. Rapid and extensive uptake and activation of hydrophobic triphenylphosphonium cations within cells. *Biochem J.* 411:633-645 (2008).

11.	K.L. Horton, K.M. Stewart, S.B. Fonseca, Q. Guo, and S.O. Kelley. Mitochondria-penetrating peptides. *Chem Biol.* 15:375-382 (2008).

12.	P. Villa, D. Sassella, M. Corada, and I. Bartosek. Toxicity, uptake, and subcellular distribution in rat hepatocytes of roxithromycin, a new semisynthetic macrolide, and erythromycin base. *Antimicrob Agents Chemother.* 32:1541-1546 (1988).

13. W. Li, X.M. Yuan, S. Ivanova, K.J. Tracey, J.W. Eaton, and U.T. Brunk. 3-Aminopropanal, formed during cerebral ischaemia, is a potent lysosomotropic neurotoxin. *Biochem J.* 371:429-436 (2003).

14. H. Glaumann, A.M. Motakefi, and H. Jansson. Intracellular distribution and effect of the antimalarial drug mefloquine on lysosomes of rat liver. *Liver.* 12:183-190 (1992).

15. R.B. Lichtner, A. Rotgeri, T. Bunte, B. Buchmann, J. Hoffmann, W. Schwede, W. Skuballa, and U. Klar. Subcellular distribution of epothilones in human tumor cells. *Proc Natl Acad Sci U S A.* 98:11743-11748 (2001).

16. G. Cramb. Selective lysosomal uptake and accumulation of the beta-adrenergic antagonist propranolol in cultured and isolated cell systems. *Biochem Pharmacol.* 35:1365-1372 (1986).

17. A. Lansiaux, F. Tanious, Z. Mishal, L. Dassonneville, A. Kumar, C.E. Stephens, Q. Hu, W.D. Wilson, D.W. Boykin, and C. Bailly. Distribution of furamidine analogues in tumor cells: targeting of the nucleus or mitochondria depending on the amidine substitution. *Cancer Res.* 62:7219-7229 (2002).

18. R.J. Burns, R.A. Smith, and M.P. Murphy. Synthesis and characterization of thiobutyltriphenylphosphonium bromide, a novel thiol reagent targeted to the mitochondrial matrix. *Arch Biochem Biophys.* 322:60-68 (1995).

19. P.J. Houghton, J. Sosinski, J.H. Thakar, G.B. Boder, and G.B. Grindey. Characterization of the intracellular distribution and binding in human adenocarcinoma cells of N-(4-azidophenylsulfonyl)-N'-(4-chlorophenyl)urea (LY219703), a photoaffinity analogue of the antitumor diarylsulfonylurea sulofenur. *Biochem Pharmacol.* 49:661-668 (1995).

20. J.E. Pettersen and M. Aas. Subcellular localization of hexadecanedioic acid activation in human liver. *J Lipid Res.* 15:551-556 (1974).

21. K. Yokogawa, E. Nakashima, J. Ishizaki, H. Maeda, T. Nagano, and F. Ichimura. Relationships in the structure-tissue distribution of basic drugs in the rabbit. *Pharm Res.* 7:691-696 (1990).

22. K. Yokogawa, E. Nakashima, J. Ishizaki, M. Hasegawa, H. Kido, and F. Ichimura. Brain regional pharmacokinetics of biperiden in rats. *Biopharm Drug Dispos.* 13:131-140 (1992).

23. J. Ishizaki, K. Yokogawa, F. Ichimura, and S. Ohkuma. Uptake of imipramine in rat liver lysosomes in vitro and its inhibition by basic drugs. *J Pharmacol Exp Ther.* 294:1088-1098 (2000).

24. D.S. Wishart, C. Knox, A.C. Guo, S. Shrivastava, M. Hassanali, P. Stothard, Z. Chang, and J. Woolsey. DrugBank: a comprehensive resource for in silico drug discovery and exploration. *Nucleic Acids Res.* 34:D668-672 (2006).

25. D.S. Wishart, C. Knox, A.C. Guo, D. Cheng, S. Shrivastava, D. Tzur, B. Gautam, and M. Hassanali. DrugBank: a knowledgebase for drugs, drug actions and drug targets. *Nucleic Acids Res.* 36:D901-906 (2008).

26. T.I. Oprea. Property distribution of drug-related chemical databases. *J Comput Aided Mol Des.* 14:251-264 (2000).

27. P.O. Seglen and P.B. Gordon. Effects of lysosomotropic monoamines, diamines, amino alcohols, and other amino compounds on protein degradation and protein synthesis in isolated rat hepatocytes. *Mol Pharm.* 18:468-475 (1980).

28. O. Ursu and T.I. Oprea. Model-free drug-likeness from fragments. *J Chem Inf Model.* 50:1387-1394 (2010).

29. S. Balaz. Modeling kinetics of subcellular disposition of chemicals. *Chem Rev.* 109:1793-1899 (2009).

Tables

Table 2.1. Summary of the subcellular localization data set.

Reported subcellular localization site	No. of molecules	%	No. of references
Endo-lysosomes	226	23.37	96
Mitochondria	259	26.78	136
Nucleus	123	12.72	67
Plasma membrane	162	16.75	75
ER/Galgi	37	3.83	26
Cytosol	59	6.10	59
Multiple localizations	101	10.44	71
Total	967	100	

Table 2.2. Summary of experimental methods.

Experimental Methods		Count	Percentage (%)
Pharmacological effects		171	17.68
Chemical analysis	Uptake/binding experiments	67	6.93
	Cell fractionation	54	5.58
Microscopic imaging	Fluorescence	633	65.46
	Histochemistry	9	0.93
	Others	6	0.62
Not mentioned		25	2.59
Mixed		2	0.21

Table 2.3. Drug-likeness based on Lipinski's Rule of Five and lead-likeness based on Oprea's Rules of compounds with reported subcellular localizations. The number of drug-likely or lead-likely compounds in each location was calculated with MOE and divided by the total number of molecules in each location to calculate the percentage pass rate. The reference set of DrugBank compounds was used for comparison.

	Drug-likely		Lead-likely	
	Count	Percentage	Count	Percentage
Endo-lysosomes	149	65.93	134	59.29
Mitochondria	170	66.15	134	51.74
Nuclei	68	55.28	47	38.52
Plasma membrane	40	24.69	31	19.14
ER/Gogli	9	24.32	3	8.11
Cytosol	19	32.20	16	27.12
Multiple	49	48.51	35	34.65
Total	528	52.80	400	41.37
DrugBank	847	84.70	716	71.60

Table 2.4. Physicochemical property trends of small molecules stratified into lower (<500 Daltons) and higher (>500 Daltons) molecular weight categories, and associated with various subcellular localizations. Z-scores were used to compare differences in molecular properties of localizing vs. non-localizing molecules. Z-scores with an absolute value greater than 3.1 were highlighted in bold, indicating a significant trend associated with a specific localization. Z-scores with absolutes value greater than 3.1 and with a different sign from the Z-score of molecular weight were underscored. Z-scores for molecular descriptors that exhibited consistent (same sign) and significant differences between localizing vs. non-localizing compounds in both lower and higher MW groups were shaded in grey. Chemicals with reported ER/Golgi and Cyto localization were excluded from this analysis due to the small number of chemicals.

Lower MW molecules	Number (%)	difference of targeting from non-targeting small molecules (Z-scores)						
		weight	*a_don*	*b_rotR*	*charge*	*dipole*	*glob*	*logP_ow*
Endo-lysosomes	148 (65.5)	**-8.8**	-2.1	2.2	<u>**5.3**</u>	-1.4	<u>**5.3**</u>	**-8.4**
Mitochondria	164 (63.3)	**3.6**	-0.8	-2.6	**-3.1**	<u>**-3.7**</u>	-0.2	**3.1**
Nuclei	64 (52.0)	**4.6**	**4.7**	<u>**-3.9**</u>	**3.8**	-0.9	<u>**-4.7**</u>	-1.6
Plasma membrane	61 (37.7)	**6.2**	<u>**-6.9**</u>	**4.6**	-2.7	**7.0**	<u>**-8.8**</u>	**10.4**

Higher MW molecules	Number (%)	difference of targeting from non-targeting large molecules (Z-scores)						
		weight	*a_don*	*b_rotR*	*charge*	*dipole*	*glob*	*logP_ow*
Endo-lysosomes	78 (34.5)	**4.6**	**3.9**	<u>**-3.5**</u>	2.6	**3.4**	2.9	0.6
Mitochondria	95 (36.7)	**-3.8**	-0.9	-1.2	1.3	**-4.5**	-0.9	-1.6
Nuclei	59 (48)	0.4	1.9	<u>**-4.0**</u>	0.4	-0.7	-0.4	<u>**-5.7**</u>
Plasma membrane	101 (62.3)	**-7.0**	**-9.6**	<u>**8.4**</u>	**-3.9**	1.6	**-3.2**	<u>**8.0**</u>

Figures

Figure 2.1. Descriptor distributions of molecules with reported subcellular localization (filled gray area) and a random PubChem sample (solid line). Z-scores with an asterisk indicate a significant difference between the mean values of a descriptor in the group of compounds with reported localization and the reference PubChem dataset (p-value < 0.001). *a_don*: Hydrogen bond donor count. *b_rotR*: The fraction of rotatable bonds. *glob*: Globularity, a value of 1 indicates a perfect sphere while a value of 0 indicates a two- or one-dimensional object. *logP_ow*: Log of the octanol/water partition coefficient. *weight*: Molecular weight (including implicit hydrogens) in atomic mass units.
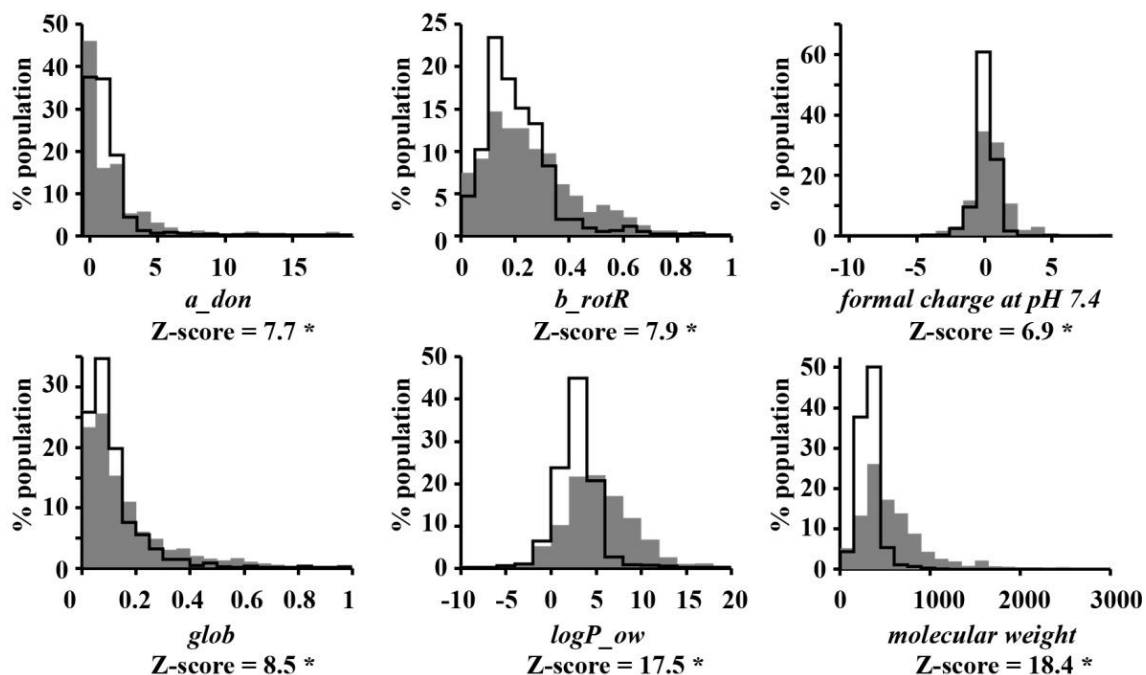
Figure 2.2. Descriptor distributions of molecules with reported subcellular localization (filled gray area) and random DrugBank dataset (solid line). Z-scores with an asterisk indicate a significant difference between the mean values of a descriptor in the group of compounds with reported localization and the reference DrugBank sample (p-value < 0.001). *a_don*: Hydrogen bond donor count. *b_rotR*: The fraction of rotatable bonds. *glob*: Globularity, with a value of 1 indicating a perfect sphere and a value of 0 indicating a two- or one-dimensional object. *logP_ow*: Log of the octanol/water partition coefficient. *weight*: Molecular weight (including implicit hydrogens) in atomic mass units.
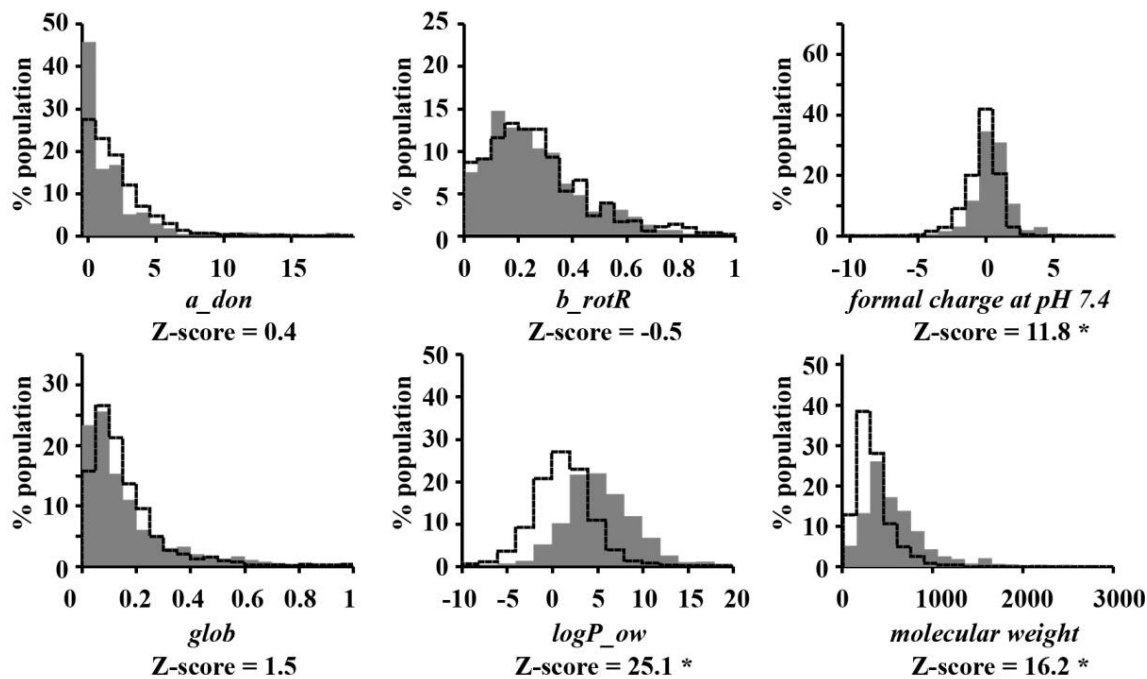
Figure 2.3. Descriptor distributions of lower molecular weight (filled gray area; <500 Daltons) and higher molecular weight (solid line; > 500 Daltons) molecules with reported subcellular localization. Z-scores with an asterisk indicate a significant difference between the mean values of the descriptor in the lower and higher molecular weight groups (p-value < 0.001). *a_don*: Hydrogen bond donor count. *b_rotR*: The fraction of rotatable bonds. *dipole moment*: Dipole moment calculated from the partial charges of the molecule. *glob*: Globularity, with value of 1 indicating a perfect sphere and a value of 0 indicating a two- or one-dimensional object. *logP_ow*: Log of the octanol/water partition coefficient.
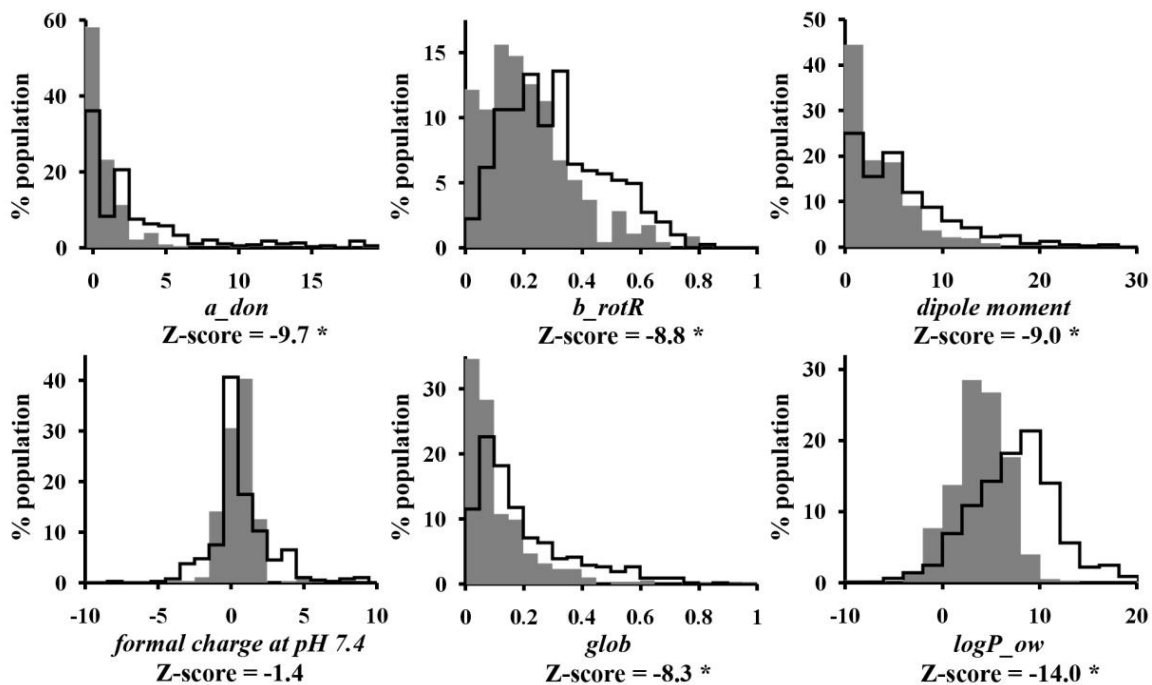
Figure 2.4. Calculated, formal charge distributions of lower molecular weight (filled gray area; <500 Daltons) and higher molecular weight (solid line; >500 Daltons) compounds with reported subcellular localization, at three different pH values.
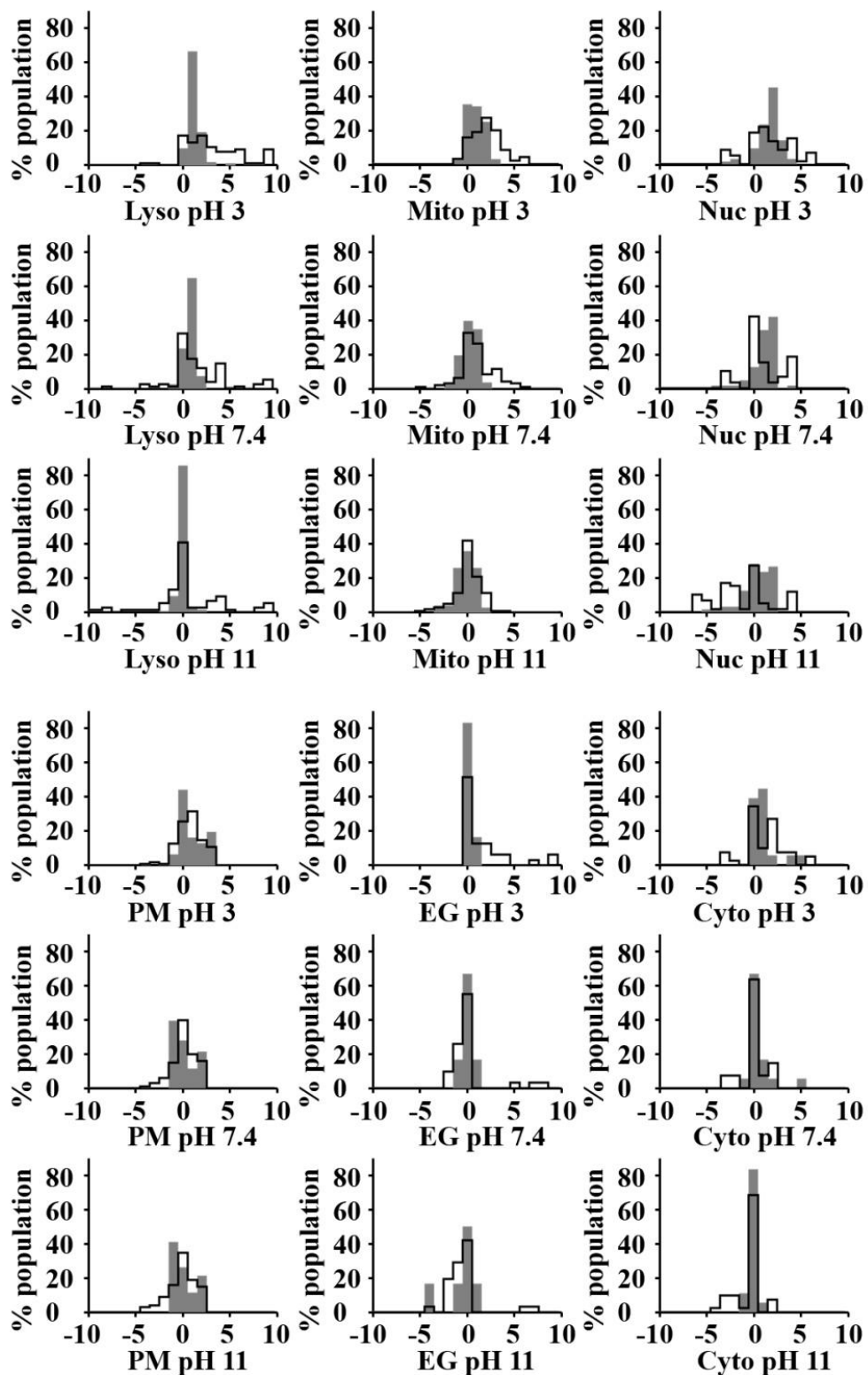
Figure 2.5. Linear discriminant analysis of low (<500 Daltons) and high (>500 Daltons) molecular weight compounds with reported subcellular localizations. The axes of the plot represent linear combinations of seven molecular properties, identified using linear discriminant analysis to maximize the separation amongst the localization classes. LDA1 and LDA2 corresponded to the two, dominant linear combinations, with the "between class" variance accounting for 37% and 11% of the total variance, respectively. Additional discriminant factors (not shown) explained less than 3% of the total variance. The units on the two axes are relative and arbitrary.
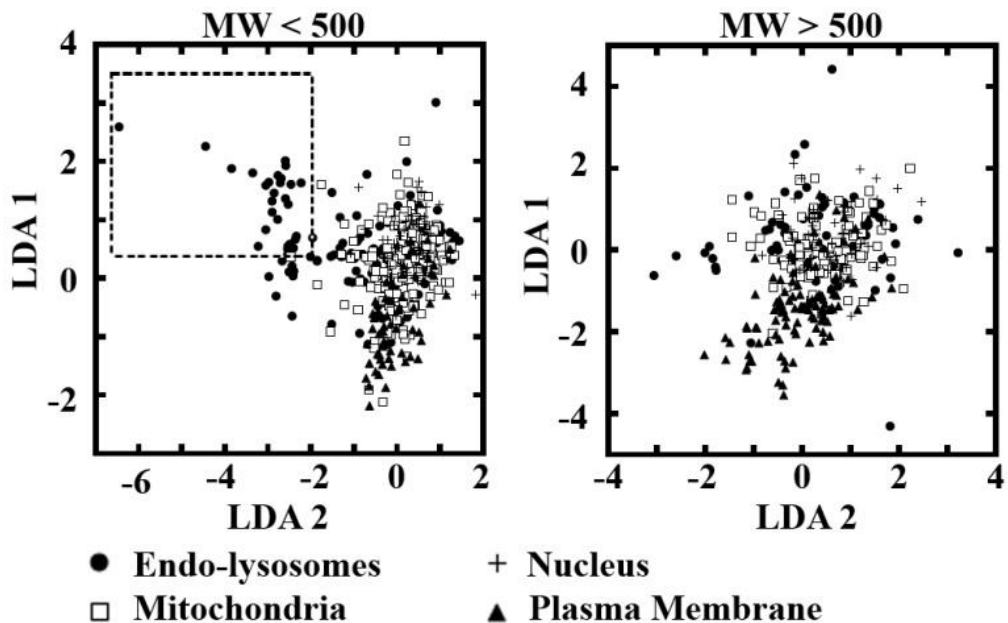
Figure 2.6. The major subcellular localization categories are represented by diverse subsets of molecules. In the plot, the x-axis indicates the percentage similarity threshold and the y-axis indicates the percentage of population in the group that falls between the similarity thresholds. With a *Tc* threshold of 0.85, above 65% percent of the compounds in each localization category were similar to no more than 2.5% of the subset, indicating highly diverse compounds representing each category. The relatively high percentage (21%) of PM molecules that are similar to 2.5% to 5% other molecules in PM group indicates that PM molecules are least diverse (Key: Lyso = lysosomes; Mito = Mitochondria; Nuc = nuclei; PM = plasma membrane; EG = Endoplasmic reticulum/Golgi body; Cyto = cytosolic; Multi = multiple localizations).
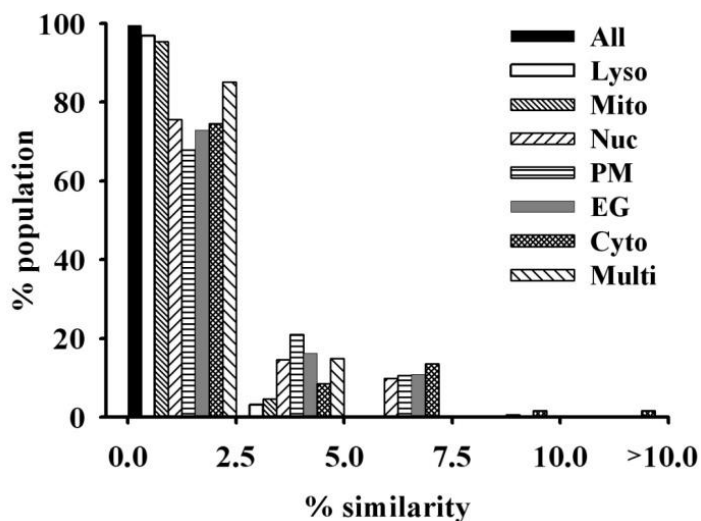
Chapter III

Simulation-based Analysis of Organelle-Targeted Molecules: Lysosomotropic Monobasic Amines

Abstract

To facilitate exploratory cheminformatic analysis of virtual libraries of small drug-like molecules, mathematical models of single cells were built from equations capturing the transport of small molecules across membranes. Physicochemical properties of small molecules were used as input to calculate the kinetics of intracellular drug distribution. Here, with mathematical equations and biological parameters adjusted so as to mimic a leukocyte in the blood, simulations were performed to calculate steady-state accumulation of small molecules in lysosomes, mitochondria, and cytosol of this target cell, in the presence of a homogenous extracellular drug concentration. Similarly, with equations and parameters set to mimic an intestinal epithelial cell, simulations were also performed to calculate steady state concentrations and transcellular permeability in this non-target cell, in the presence of an apical-to-basolateral drug concentration gradient. With a reference set of ninety-nine lysosomotropic small molecules, simulation results help map out relationships between the chemical diversity of the molecules, their calculated intracellular distributions and their associated cellular phenotypes.

Introduction

Weakly basic molecules possessing one or more amine groups have been reported to highly accumulate in lysosomes and other membrane-bound acidic organelles because of the proposed ion trapping mechanism [1-3]. Amines generally have a pKa value in the physiological pH range. Accordingly, they exist as a combination of ionized (protonated) and neutral (unprotonated) species. Because the pH of lysosomes is one or more units lower than the pH of the cytosol, the thermodynamic equilibrium between neutral and ionized species shifts towards the protonated, ionized state. Conversely, because the pH of the cytosol is higher, the thermodynamic equilibrium between neutral and ionized species shifts towards the neutral, unprotonated state. Since charged molecules are less membrane-permeant, the protonated species becomes trapped inside the membrane bound compartments, relative to the neutral species. Within an acidic lysosome, the concentration of the neutral, membrane-permeant species is less than its concentration in the more basic cytosol. This leads to a concentration gradient of the neutral form of the molecule across the lysosomal membrane, further driving the uptake of the neutral species of the molecule into the acidic organelle.

In medicinal chemistry, the ability to modify the chemical structure of small molecules so as to tailor lysosomotropic behavior may be important for decreasing unwanted side effects, as much as it may be important for increasing efficacy. For many monobasic amines that target extracellular domains of cell surface receptors and ion channels, lysosomal accumulation can be considered

a secondary effect of the physicochemical properties of the molecule [4-8]. Previously, many monobasic amines have been experimentally analyzed in cell-based assays, in terms of their ability to accumulate in lysosomes [6, 9-12]. In response to ion trapping, cells exposed to monobasic amines swell and become replete with large vacuoles [6, 9, 10, 13-15]. With a phase contrast microscope, swollen lysosomes can be easily discerned and scored. Furthermore, as monobasic amines accumulate in lysosomes, they can increase the pH of the organelle through a buffering effect, or by shuttling protons out of the lysosome, across the lysosomal membranes [16]. Therefore, such molecules "compete" with each other for lysosomal accumulation, providing another way to assay for lysosomotropic behavior [16, 17]. A third way to assay lysosomotropic behavior is by labeling lysosomes of cells with fluorescent probes (e.g. Lysotracker® dyes) [17]. As lysosomes expand in response to accumulation of lysosomotropic agents, they accumulate increasing amounts of the Lysotracker® dye and the cells become brightly labeled. By virtue of these effects on live cells, many monobasic amines have been positively identified as "lysosomotropic".

Nevertheless, different studies analyzing lysosomotropic monobasic amines have also identified molecules that deviate from the norm. Furthermore, there is a broad range of concentrations at which vacuolation becomes apparent, spanning several orders of magnitude [10, 18-20]. In addition, there are monobasic amines that do not exhibit any vacuolation-inducing behavior [6, 9, 10, 13, 14, 21], and do not compete with the lysosomal uptake of other lysosomotropic probes [6, 16], or that are cytotoxic [21]. Most importantly, some

lysosomotropic molecules have been reported to accumulate in other organelles, such as mitochondria [22]. Alprenolol, chlorpromazine, fluoxetine, propranolol, and diltiazem are just but some of the FDA approved drugs in this category [6, 16, 22, 23], that have been classified as being both lysosomotropic and mitochondriotropic by different investigators. In addition, certain monobasic amines may accumulate in lysosomes to a much greater extent than ion trapping mechanisms would predict [20].

These apparent discrepancies in terms of the lysosomotropic behavior prompted us to begin exploring the relationship between the phenotypic effects of monobasic amines, and their subcellular distribution in lysosomes vs. other organelles. We decided to use a cell-based molecular transport simulator [24, 25] to begin exploring the different possible behaviors of monobasic amines inside cells based on the ion trapping mechanism, paying special attention to their accumulation in lysosomes, cytosol and mitochondria. In this manner, the simulations are not meant to "predict" the actual concentration and distribution of the molecules inside the cells, but rather to assess the possible variations in intracellular transport behaviors, based solely on the biophysical principles underlying the ion trapping mechanism. Because the ability to optimize the subcellular transport of small molecules could have practical applications in drug development, we also deemed it important to calculate the distribution of molecules inside non-target cells mediating drug transport in the presence of a transcellular concentration gradient. In fact, although direct experimental measurement of subcellular concentration in the presence of a transcellular

concentration gradient would be difficult, this may be the condition that is most relevant for drug uptake and transport throughout the different tissues of the body.

Methods

Modeling the cellular pharmacokinetics of target cells in suspension: The T-Model. For subcellular compartments delimited by membranes, passive transport of small molecules in and out of these compartments is determined by the interaction of the molecules with the membrane, the concentration gradient of molecules across the membrane, the local microenvironment on either side of the membrane, and the transmembrane electrical potential [24, 25]. Drug-membrane interactions are largely dependent on the physicochemical properties of small molecules (such as pK_a and lipophilicity) and the environmental condition (such as local pH values and membrane potentials). Based on the biophysics of membrane transport, mass transfer of drug molecules between different organelles in a cell surrounded by a homogeneous extracellular drug concentration has been modeled mathematically [25] (Figure 3.1 A). Accordingly, three coupled ordinary differential equations describe the concentration change with time in each subcellular / cellular compartment:

$$\frac{dC_c}{dt} = \frac{A_c}{V_c} \times J_{o,c} - \frac{A_m}{V_c} \times J_{c,m} - \frac{A_l}{V_c} \times J_{c,l} \quad (1)$$

$$\frac{dC_m}{dt} = \frac{A_m}{V_m} \times J_{c,m} \quad (2)$$

$$\frac{dC_l}{dt} = \frac{A_l}{V_l} \times J_{c,l} \quad (3)$$

where *C* indicates the *concentration*, *J* indicates the *fluxes*, *A* and *V* indicate *membrane surface* and *volume* respectively. The subscripts *o,c,l,* and *m* indicate

79

extracellular compartment, cytosol, lysosomes, and *mitochondria* respectively.

The directions of fluxes are the orders of the subscripts, e.g. $J_{c,m}$ indicates the flux from cytosol to mitochondria. Calculations for fluxes between each pair of compartments were similar as described before [25]. The ordinary differential equations were numerically solved (Appendix K) [24].

An important feature of this model is that at steady state, the drug concentration in the cytosol is only dependent on the drug concentration outside the cell, the plasma membrane permeability properties, and the ionic conditions of the cytosol and the extracellular medium. Similarly, the drug concentration inside any given organelle is only dependent on the drug concentration in the cytosol, the permeability properties of the membrane delimiting the organelle, the ionic conditions of the cytosol, and the inner lumen of the organelle. Consequently, one can use the same equations to calculate steady state concentration or mass of drugs in lysosomes or mitochondria (and other organelles) simply by adjusting the pH of the organelle, the transmembrane electrical potential, and the organelle volume, surface area, and lipid fraction. For mitochondria, the inner lumen pH was set at 8 [25] and the membrane potential was set at -150 mV [26]. Mitochondria were considered as spheres with 1 µm radius. For lysosomes, the inner lumen pH was set at 5 [1, 27-29] and the membrane potential was set at +10 mV [30]. Leukocytes were modeled as spherical objects of 10 µm diameter. Plasma membrane potential was set at -60 mV [31] . Extracellular pH was set at 7.4 (blood). Cytosolic pH was set at 7.0 [32]. Since we are more interested in the drug aqueous concentration in cytosol

the lipid fraction equal to 0 was used in calculation. Other models parameters were adapted from the literature [25]. Hereafter, this cellular pharmacokinetic model applicable to free floating cells in suspension (e.g. leukocytes in the circulation) will be dubbed Trapp's Model or 'T-Model'.

Modeling cellular pharmacokinetics of non-target, polarized epithelial cells: The R-Model. For modeling drug transport across polarized epithelial cells [24], the cell surface area is divided into apical and basolateral membrane domains (Figure 3.1 B). Similarly, the extracellular space is divided into apical and basolateral extracellular compartments. Accordingly, drug uptake into the cell is represented by mass transfer of drug molecules from the apical extracellular medium into the cytosol, across the apical membrane. Drug efflux from the cells is represented by mass transfer from the cytosol to the basolateral medium, across the basolateral membrane. Because the apical membrane is normally covered with microvilli, the apical membrane surface area (A_a) can be adjusted independently from the basolateral membrane (A_b). Similarly, the extracellular pH of the apical (pH_a) and basolateral compartments (pH_b), and transmembrane electrical potentials across apical and basolateral membranes (E_a and E_b) can be independently adjusted, so as to mimic the local microenvironment of the epithelial cells.

A cellular pharmacokinetic model for intracellular concentration and passive transcellular permeability calculation was developed as described previously [24, 33]. Mass transport across the boundary of each compartment can be described by equations 4 to 7:

$$\frac{dC_c}{dt} = \frac{A_a}{V_c} \times J_{a,c} - \frac{A_m}{V_c} \times J_{c,m} - \frac{A_l}{V_c} \times J_{c,l} - \frac{A_b}{V_c} \times J_{c,b} \quad (4)$$

$$\frac{dC_m}{dt} = \frac{A_m}{V_m} \times J_{c,m} \quad (5)$$

$$\frac{dC_l}{dt} = \frac{A_l}{V_l} \times J_{c,l} \quad (6)$$

$$\frac{dC_b}{dt} = \frac{A_b}{V_b} \times J_{c,b} \quad (7)$$

The subscripts *a* and *b* indicate '*apical*' and '*basolateral*' respectively. Other symbols and subscripts mean the same as in the T-model. As in the T-model, the inner lumen pH of mitochondria was set at 8 [25] and the mitochondrial membrane potential was set at -150 mV [26]. For lysosomes, the inner lumen pH was set at 5 [1, 27-29] and the membrane potential was set at +10 mV [30]. Epithelial cells were modeled as cuboidal objects of 10 μm length. Again since we are more interested in the drug aqueous concentration in cytosol the lipid fraction was set to 0. All other model parameters used in calculation were obtained from the literature [24], and can be found in Appendix K. To maintain sink condition in the basolateral compartment, we set the volume of the basolateral compartment (V_b) equal to the human blood volume (4.7 L).

From simulating cytosol to basolateral flux of molecules in an intestinal epithelial cell, the membrane permeability of the intestinal epithelial cell monolayer can be calculated with the following equation [24]:

$$P_{eff} = \frac{dm_b}{C_a \times A_{aa} \times dt} \quad (8)$$

where P_{eff} is the effective permeability, C_a is the initial concentration in the apical compartment and is considered to be constant, dm$_b$/dt is the change in drug mass in the basolateral compartment per unit time, and A_{aa} is the apparent cross

sectional area of the cell, which would approximately correspond to the total area of the surface over which drug transport is occurring divided by the number of cells that are effectively transporting drug. Henceforth, this cellular pharmacokinetic model that applies in non-target epithelial cells will be dubbed Rosania's Model or 'R-Model'.

Simulating organelle-targeting and transcellular permeability with R- and T-models. To simulate the intracellular distribution of monovalent weakly basic molecules possessing amine functionality, all different combinations of octanol : water partition coefficients of the neutral form of the molecule ($\log P_n$); octanol : water partition coefficients of the ionized form of the molecule ($\log P_d$); and pK_a were used as input. $\log P_n$ and $\log P_d$ spanned a range from -5 to +5, with $\log P_d$ constrained to a value less than or equal to $\log P_n$. pK_a spanned a range from 0 to 14. pK_a, $\log P_n$, and $\log P_d$ were varied in 0.2 unit increments [24]. The molecular charge (z) was set equal to 1, which means the simulated whole physicochemical space is specific for monovalent amine-containing molecules. With R- and T-Model, drug concentrations in different compartments were calculated over time, until concentrations reached steady state (normally, at 10^6 seconds after beginning of the simulation). For R-Model simulations, initial apical drug concentration was set at 1 mM, and basolateral drug concentration was set at 0 mM. For T-model simulations, extracellular drug concentration was set at 1 mM, and kept constant. Accordingly, for each combination of pK_a, $\log P_n$, and $\log P_d$ used as input, there are seven calculated results: $C_{cyto}R$, $C_{mito}R$, $C_{lyso}R$ (the steady-state cytosolic, mitochondrial and lysosomal concentration calculated with

the R-model); P_{eff} (the steady-state effective permeability calculated with the R-Model); and $C_{cyto}T$, $C_{mito}T$, and $C_{lyso}T$ (the steady-state cytosolic, mitochondrial and lysosomal concentrations calculated with the T-Model) .

A reference set of monobasic amines with associated lysosomotropic behaviors. Focusing on lysosomal targeting, ninety-nine monobasic amines (Table 1) were found by searching PubMed abstracts and titles for articles containing the word "lysosome", "lysosomal", or "lysosomotropic"; from other articles referenced by these articles; and from current review articles describing the lysosomal accumulation of weakly basic molecules [1]. There are more lysosomotropic amine-conating molecules besides molecules included in our table (for example, zwitterions or dibasic amines). However since R- and T-Models have been validated mostlywith molecules possessing one ionizable functional grouop, lysosomotropic amines with more than one ionizable functionality were not included. To calculate the pK_a (at 310.15K), logP_n and logP_d for each molecule, we used ChemAxon (http://www.chemaxon.com). A liposomal approximation [24, 34] was applied for logP_n and logP_d based on the values obtained from ChemAxon. Intracellular concentrations were calculated for those ninety-nine molecules at steady state with the T-model and R-model. Transcellular permeability was calculated for the ninety-nine molecules at steady state with the R-model.

Interactive visualization of simulation results. Visualization of simulation results was performed with the Miner3D software package (Dimension 5, Ltd., Slovakia, EU). Simulation results were graphed as 3D scatter plots, with logP_n,

logP_d and pK_a plotted on the three coordinate axes, and the calculated steady state concentration or permeability determining the color and intensity of the points. For linking simulation results with the reference set of lysosomotropic molecules, we used the pK_a, logP_n and logP_d values obtained after liposomal approximations [24].

To plot different chemical spaces we set a threshold concentration value to define accumulation in a specific subcellular compartment. For intracellular concentration, the threshold lysosomal accumulation for lysosomotropic molecules was $C_{lyso}T$ ≥ 2 mM (i.e. tw0-fold greater than extracellular concentration). The thresholds for selective lysosomal accumulation were $C_{lyso}T$ ≥ 2 mM; $C_{lyso}T$ /$C_{mito}T$ ≥ 2 ; and $C_{lyso}T$ /$C_{cyto}T$ ≥ 2. The threshold for mitochondrial accumulation was $C_{mito}T$ ≥ 2 mM. The thresholds for selective mitochondrial accumulation were $C_{mito}T$ ≥ 2 mM; $C_{mito}T$ /$C_{lyso}T$ ≥2; and $C_{mito}T$ /$C_{cyto}T$ ≥2. The threshold for cytosolic accumulation was $C_{cyto}T$ ≥ 2 mM. The thresholds for selective cytosolic accumulation were $C_{cyto}T$ ≥ 2 mM; $C_{cyto}T$ /$C_{mito}T$ ≥ 2; and $C_{cyto}T$ /$C_{mito}T$ ≥ 2. The reason for using the 2-fold concentration value as a threshold is because it gave the highest percentage of correct classification and low false positive prediction for the reference set of lysosomotropic molecules (as detailed in the Results section).

As recommended by the FDA, the permeability value of metoprolol was used as a threshold to distinguish high vs. low permeability molecules [24]. Previously we calculated permeability for metoprolol , using the pKa and logP_n obtained from experimental measurements , to be equal to 35 ×10^{-6} cm/sec [24].

In the present study, we used this value as a threshold to distinguish high vs. low permeability molecules. In addition, we arbitrarily set a value of 1×10^{-6} cm/sec as a cut-off number to distinguish low from negligible permeability molecules. Accordingly, three permeability classes were defined as: negligible ($P_{eff} < 1 \times 10^{-6}$ cm/sec); low ($1 \leq P_{eff} < 35 \times 10^{-6}$ cm/sec); and high ($P_{eff} \geq 35 \times 10^{-6}$ cm/sec).

Results

Defining a lysosomal accumulation threshold for lysosomotropic molecules. We began by exploring the physicochemical property space occupied by monobasic amines, in relation to the reference set of molecules obtained from published research articles (Table 3.1). Three different lysosomal concentration values (2 mM, 4 mM and 8 mM) were tested in terms of their ability to discriminate lysosomotropic vs. non-lysosomotropic compounds (Figure 3.2). For compounds with ≥ 2 mM accumulation in lysosomes (Figure 3.2 A-D), eight of the reference compounds were below the accumulation threshold (Figure 3.2 A and B), while 91 were above the threshold (Figure 3.2 C and D). For compounds with ≥ 4 mM accumulation in lysosomes (Figure 3.2 E-H), twelve of the reference compounds were below the accumulation threshold (Figure 3.2 E, F), while 87 were above the threshold (Figure 3.2 G, H). For compounds with a ≥ 8 mM accumulation in lysosomes (Figure 3.2 I-L), 56 lie below the accumulation threshold (Figure 3.2 I, J) while 43 are above (Figure 3.2 K, L).

We established that a lysosomal accumulation threshold of 2 mM is best suited to distinguishing lysosomotropic from non-lysosomotropic molecules, since

it gave the highest correct classification and lowest false positive error in terms of matching simulation results with the experimentally-observed, lysosomotropic behaviors. Accordingly, for a lysosomal accumulation threshold of 2mM, of the eight molecules that were below the accumulation threshold, five (62.5%) have been positively identified as non-lysosomotropic. Conversely, of the 91 above the threshold, 8 (8.8%) non-lysosomotropic molecules have been false positively classified as lysosomotropic. For a lysosomal accumulation threshold of 4 mM, of the twelve below the threshold, five (41.7%) have been identified as non-lysosomotropic. Conversely, of the 87 above threshold, 8 (9.2%) non-lysosomotropic molecules have been false positively classified as lysosomotropic. For a lysosomal accumulation threshold of 8 mM, of the 56 below the threshold, 9 have been positively identified as non-lysosomotropic (16.1%). Conversely, of the 43 above the threshold, 4 (9.3%) non-lysosomotropic molecules have been false positively classified as lysosomotropic.

The reference set appears highly clustered in relation to the available lysosomotropic, physicochemical property space. Exploring the relationship between the physicochemical properties of the reference set of molecules obtained from the literature, with that of the theoretical physicochemical property space occupied by molecules that accumulate in lysosomes at the different threshold values, we observed that most of the reference molecules tend to be clustered in very specific region of "lysosomotropic space". In fact, physicochemical property space occupied by molecules that accumulate in lysosomes at ≥ 2 mM (Figure 3.2 B) appears largely similar to the space of

molecules that accumulate at ≥ 4 mM (Figure 3.2 F) and at ≥ 8 mM (Figure 3.2 J). It was surprising that most lysosomotropic molecules in the reference set were calculated to have a lysosomal accumulation between 2 and 8-fold over the extracellular medium, although the largest portion of the calculated physicochemical property space that can be occupied by monobasic amines corresponds to > 8-fold lysosomal accumulation.

Using simulation results to define the expected transport classes for monovalent weak bases. Using a 2-fold or greater concentration of drug over the extracellular medium to distinguish high vs. low lysosomal, mitochondrial and cytosolic concentration, and by incorporating high vs. low permeability classification obtained with the R-model, a total of 16 classes of molecules can be defined *a priori* (Table 3.1). By mapping the reference set of molecules to these 16 different classes, we find that some classes of molecules are well-represented by a number of molecules, while other classes of molecules are not represented at all (Table 3.1). However, according the simulation results, several of these *a priori* classifications are deemed to be "non-existent" by virtue of our being unable to find a combination of physicochemical properties consistent with the corresponding class of molecules in simulations.

Simulation results point to general trends in lysosomotropic behaviors. For the reference set of molecules, we observed that the calculated intracellular accumulation in non-target cells (R-Model) is much lower than the corresponding accumulation in target cells (T-model) (Table 3.1). We also observed lysosomal accumulation occurring for a broad range of transcellular permeability values

(Table 3.1). Unexpectedly, for most lysosomotropic molecules, we also observed mitochondrial concentration tending to be much greater than lysosomal or cytosolic concentration, suggesting that lysosomotropic behavior is not exclusively related to selective accumulation in lysosomes. Lastly, we observed that none of the lysosomotropic molecules in the reference set are able to accumulate in cytosol to a greater extent than they accumulate in mitochondria or in lysosomes (Table 3.1). In fact, plotting the physicochemical property space of such molecules yielded an empty space (data not shown), indicating that the lack of such type of molecules in the reference set is not because of sampling biases, but rather it is expected based on the calculated cellular pharmacokinetic properties of monovalent weak bases.

Calculating the physicochemical space occupied by selectively lysosomotropic molecules. Selectively lysosomotropic molecules were defined as those that accumulate in lysosomes to a 2-fold (or greater) level over the extracellular medium, cytosol, and mitochondria. Out of the 91 reference lysosomotropic molecules (Figure 3.3 A, out of circle), only seventeen (Figure 3.3B, D green circle) appear to be selective in terms of lysosomal accumulation. These 17 molecules (Figure 3.3 B) appear clustered at the middle pK_a value of the reference set of molecules comparing with non-lysosomotropic molecules (Figure 3.3 A, in green circle) and non-selectively lysosomotropic molecules. Plotting the theoretical physicochemical property space occupied by selectively lysosomotropic molecules related to the reference molecules reveals that the reference molecules that accumulate in lysosomes are highly clustered (Figure

3.3 C) in the middle pK_a and high logP_d values. This can also be observed in the corresponding plot of non-selectively lysosomotropic and non-lysosomotropic physicochemical property space (Figure 3.3 D).

Analyzing the effect of transcellular permeability on selective lysosomal accumulation. Next, we analyzed the relationship between selective lysosomal accumulation in target cells, and transcellular permeability in non-target cells, to determine if the ability to develop selective lysosomotropic agents may be constrained by desirably high transcellular permeability characteristics important for intestinal drug absorption and systemic tissue penetration (Figure 3.4). As a reference, the permeability of metoprolol (P_{eff} = 35×10^{-6} cm/sec) was used to distinguish high permeability from low permeability drugs. Accordingly, three permeability categories were defined: Negligible Permeability (P_{eff} < 1×10^{-6} cm/sec; Figure 3.4 A and B); Low Permeability (1 ≤ P_{eff} < 35×10^{-6} cm/sec; Figure 3.4 C and D); and High Permeability (P_{eff} ≥35×10^{-6} cm/sec, Figure 3.4 E and F).

With increasing permeability, the simulation results indicate that physicochemical space occupied by selective lysosomotropic molecules shifts towards lower pK_a values and higher logP_d values. The position of selective lysosomotropic chemical space in relation to the reference set of non-selective lysosomotropic or non- lysosomotropic molecules can be clearly seen, for molecules with P_{eff} < 1×10^{-6} cm/sec (Figure 3.4 A); 1 ≤ P_{eff} < 35×10^{-6} cm/sec (Figure 3.4 B); and P_{eff} ≥ 35×10^{-6} cm/sec (Figure 3.4 C). Accordingly, there is only one selectively-lysosomotropic reference molecule with P_{eff} < 1×10^{-6} cm/sec (Figure 3.4 B; green arrow); five with 1≤ Peff<35×10^{-6} cm/sec (Figure 3.4 D;

green arrow); and eleven with $P_{eff} \geq 35 \times 10^{-6}$ cm/sec (Figure 3.4 F; green arrow). Thus, high permeability and selective lysosomal accumulation are not mutually exclusive. Nevertheless, we observed that the selective lysosomotropic reference molecules with neglibile low and high permeability are tightly clustered in a small region of chemical space, at mid pK_a and high $logP_d$ values.

Demarcating the physicochemical property space of extracellular targeted molecules. Extracellular-targeted molecules can be defined as those whose intracellular accumulation at steady state is less than the extracellular concentration [24]. For drug development, such a class of molecules is important as many drug targets are extracellular. Accordingly, we analyzed simulation results to determine if there were molecules with low intracellular accumulation and high permeability, which would be desirable for the pharmaceutical design of orally absorbed drugs (Figure 3.5). By maximizing permeability and minimizing intracellular accumulation, (using $P_{eff} \geq 35 \times 10^{-6}$ cm/sec, $C_{cyto} < 1$mM, $C_{mito} < 1$mM, and $C_{lyso} < 1$mM as thresholds in both in the R and T models), we find five molecules falling into this class (Figure 3.5 A-C; green circle): pyrimidine, benzocaine, β-naphthylamine, 8-aminoquinoline, and the anti-epileptic drug candidate AF-CX1325XX. These are monobasic amines with $pK_a < 4.5$. Molecules with $pK_a > 4.5$ (the physicochemical property space shown in Figure 3.5 C) exhibit intracellular accumulation in lysosomes, cytosol or mitochondria to levels above those found in the extracellular medium. Figure 3.5 B shows the physicochemical space of molecules with high permeability and low intracellular accumulation. Figure 3.5C shows the physicochemical space of molecules with

91

high intracellular accumulation regardless of permeability. Again we can see that molecules with low intracellular accumulation have a pK_a < 4.5 and with high intracellular accumulation have a pK_a > 4.5.

Many reported lysosomotropic molecules are calculated to accumulate in mitochondria. For the majority of the reportedly lysosomotropic monobasic amines in the reference set, our calculations predict that they should accumulate in mitochondria more than they accumulate in lysosomes. In total, 56 of the 91 lysosomotropic molecules in the reference set accumulate in mitochondria at 2-fold or greater levels than they accumulate in lysosomes, cytosol, or the extracellular medium (Figure 3.6 A; Table 3.1, selectively mitochondrotropic compounds underlined). These molecules have a pK_a of 8.2 or greater, a $\log P_n$ of 1.5 or greater, and span a wide range of transcellular permeability values – from impermeant to very highly permeant. In addition, eighteen lysosomotropic molecules also exhibit mitochondrial and high cytosolic accumulation, at concentrations comparable to the concentrations at which they accumulate in lysosomes (Figure 3.6 B; Table 3.1). Again, these molecules span a broad range of transcellular permeability values, from impermeant to highly permeant. Plotting the theoretical physicochemical property space occupied by lysosomotropic molecules with selective mitochondrial accumulation reveals that the molecules in the reference set are clustered in this realm of physicochemical property space (Figure 3.6 C). Similarly, plotting the physicochemical property space occupied by lysosomotropic molecules that also accumulate in cytosol and

mitochondria reveals that the molecules are clustered in this realm of chemical space.

Calculated effect of pH in apical compartment on permeability and biodistribution. The accumulation of monobasic amines in lysosomes is largely dependent on the difference in pH of between lysosome and extracellular medium (data not shown). While the pH of the medium bathing the target cells is expected to be rather constant, the pH surrounding an intestinal epithelial cell is expected to vary along the intestinal tract [35]. To test if this variation would lead to major differences in the observed trends, we decided to test the extent to which the calculated chemical space occupied by selectively lysosomotropic molecules was affected by variation in the apical pH of non-target cells (Figure 3.7). We note that for selectively lysosomotropic molecules with negligible (Figure 3.7 A), low (Figure 3.7 B), and high (Figure 3.7 C) permeability, the theoretical physicochemical property space occupied by selectively lysosomotropic molecules is similar, and the reference molecules that fall into that region of chemical space tend to be the same. Similarly, other regions of physicochemical property space occupied with molecules of different permeability tend to be similar, with variations in the apical pH of the intestinal epithelial cell in a pH range of 4.5 to 6.8 (data not shown).

Discussion

Modeling the cellular pharmacokinetics of monobasic amines. Over the past few years, mathematical models of cellular pharmacokinetics have been

developed, based on coupled sets of differential equations capturing the transmembrane diffusion of small molecules. Previously, these models have been used to simulate the intracellular distribution of lipophilic cations in tumor cells [25], and the distribution and passage of small molecules across intestinal epithelial cells [24]. For a monovalent weakly acidic or weakly basic small molecule drug, three input physical-chemical properties are used to simulate cellular drug transport and distribution: the logarithms of the lipid/water partition coefficient of the neutral form of the molecule ($\log P_n$) and ionized form ($\log P_d$), and the negative logarithm of the dissociation constant of the ionizable group (pK_a). For monovalent weak bases, the transcellular permeability values calculated with this approach were comparable with measured human intestinal permeability and Caco-2 permeability, yielding good predictions [24]. Similarly, the corresponding mathematical models were able to predict mitochondrial accumulation of lipophilic cationic substances in tumor cells [22, 25].

For analyzing the lysosomotropic behavior of monovalent weak bases possessing an amine functionality, we adapted these two mathematical models to simulate the cellular pharmacokinetic behavior of target cells exposed to a homogeneous extracellular drug concentration, and non-target cells mediating drug absorption in the presence of an apical-to-basolateral concentration gradient. The results we obtained establish a baseline, expected concentration of small drug-like molecules in mitochondria, lysosomes and cytosol of target cells, as well as permeability in non-target cells. With a reference set of small molecules, the simulations permit exploration of the relationship between

94

physicochemical properties of the molecules, their calculated intracellular distributions and transport behavior, and the observed cellular phenotypes.

Simulation-based analysis and classification of lysosomotropic behavior. By analyzing the intracellular distribution and transcellular transport characteristics of a reference set of molecules, together with more general physicochemical space plots covering all possible combinations of pK_a, $logP_n$ and $logP_d$, sixteen *a priori* classes of lysosomotropic behavior for monobasic amines were defined (Table 3.1). However, we noted that several of these classes are deemed to be non-existent by the simulations –meaning that there is no combination of pK_a, $logP_n$ and $logP_d$ that will yield a molecule in such a class. For other classes, it was not possible to find a molecule in the reference set of lysosomotropic molecules whose calculated properties would lie within the physicochemical property space defining the hypothetical class of molecules. This is certainly the case for positively-identified, non-lysosomotropic molecules. These results argue for expanding the reference set of monovalent, weakly basic molecules, so as to represent all possible classes of intracellular transport behaviors.

An equally important observation from the simulation resides in the tight clustering of the reference molecules in constrained regions of physicochemical property space, in relation to the simulated physicochemical property space that is actually available for molecules in the different lysosomotropic and permeability categories.   Thus, the diversity of lysosomotropic behaviors represented by the reference set of molecules is rather limited. Indeed, the

simulations indicate that expanding the reference set of molecules to unexplored regions of physicochemical property space could be used to find molecules that better represent the different types of cellular pharmacokinetic behaviors. For example, in the case of low or high permeability molecules that are selectively lysosomotropic, most of the molecules in the reference set are clustered at the high levels of pKa and high log$P$, whereas the simulations indicate that it should be possible to find molecules with lower pKa and lower log$P$s. The reason for the limited chemical diversity of reported lysosomotropic molecules is related to the choice of molecules that have been tested experimentally and reported in the literature: the emphasis has not been on the probing the chemical diversity of lysosomotropic character, but rather, in analyzing the lysosomotropic character in a related series of compounds (for example, studies looking at mono, bi, and tri-substituted amines, functionalized with various aliphatic groups [9]). In other cases, the emphasis has been on studying the lysosomotropic character of a specific type of compound developed against a specific drug target [6] (for example, beta-adrenergic receptor antagonists such as propranolol, atenolol, practolol, etc), rather than on the full chemical space occupied by lysosomotropic, monvalent weakly basic amines.

Further experimental validation and testing of expected transport behaviors. Using lysosomal swelling, cell vacuolation and intralysosomal pH measurements as phenotypic read outs, it may be possible to test the model's quantitative prediction about the varying extent of lysosomal accumulation of monovalent weak bases as a function of the molecule's chemical structure or

96

physicochemical properties. For example, our model makes quantitative predictions about the lysosomal concentration of molecules of varying chemical structure. Previous studies looking at the lysosomotropic behavior of various molecules have reported differences in vacuolation induction for different probes, at extracellular drug concentrations ranging from high millimolar to micromolar range [10, 13, 16]. Also, for some molecules vacuolation occurs after less than an hour incubation, while for other probes vacuolation occurs after twenty-four hour incubation, or longer [6, 9, 10, 13, 14, 16]. Combinatorial libraries of fluorescent molecules are available today [36, 37], offering yet another way to test predictions about the intracellular accumulation and distribution of probes. Furthermore, with organelle-selective markers and kinetic microscopic imaging instruments, the rate and extent of swelling of lysosomes and other organelles could be monitored dynamically after exposure of cells to monovalent weakly basic molecules [37]. For such studies, cheminformatic analysis tools are being developed to relate the intracellular distribution of small molecules as apparent in image data, with chemical structure and physicochemical features of the molecules, and the predicted subcellular distribution [38, 39]. Lastly, more quantitative assessments of model predictions can be made by directly monitoring the total intracellular drug mass [40, 41], as well as drug mass associated with the lysosomal compartment [20, 42, 43]. Recently, methods are being developed to rapidly isolate the lysosomes and measure intralysosomal drug concentrations [43].

To test model predictions about the lysosomotropic behavior of small molecules in the presence of an apical-to-basolateral concentration gradient, various in vitro cell culture models have been developed to assess drug intestinal permeability and oral absorption [44]. These are Caco-2, MDCK, LLC-PK1, 2/4/A1, TC-7, HT-29, and IEC-18 cell models [44]. Among those models Caco-2 (human colon adenocarcinoma) cell monolayer is the most well-established cell model and has been widely accepted by pharmaceutical companies and academic research groups interested in studying drug permeability characteristics [44]. In addition to Caco-2 cells, MDCK (Madin-Darby canine kidney) is a dog renal epithelia cell line and is another widely used cell line in studying cell permeability characteristics [45].

Towards a computer-aided design of organelle-targeted molecules: implications for drug discovery and development. The ability to rationally tailor the transcellular permeability and subcellular distribution of monobasic amines can have important applications in medicinal chemistry efforts aimed at enhancing the efficacy of small molecules against specific targets, decreasing non-specific unwanted interactions with non-intended targets that lead to side effects and toxicity, as well as enhancing transcellular permeability for maximizing tissue penetration and oral bioavailability. For many FDA approved drugs, lysosomal accumulation of the molecules would appear to be a non-specific effect of the molecule's chemical structure. For example, in the case of the beta-adrenergic receptor antagonists like propranolol, the drug's target is a cell surface receptor located at the plasma membrane. Thus, lysosomal (and

98

any other intracellular) accumulation observed for this molecule is most likely an unintended consequence of its chemical structure [2, 6, 15, 16, 43, 46]. In general, due to the abundance of lysosomotropic drugs [6, 9, 10, 16], lysosomal accumulation seems to be tolerated, although it may not be a desirable property.

Nevertheless, there are certain classes of therapeutic agents were lysosomal accumulation may be highly desirable. For example, Toll-like receptor molecules are transmembrane proteins in the lysosomes of leukocytes (dendritic cells and macrophages). These receptors can be activated by endocytosed proteins, DNA and carbohydrates, and they generate inflammatory responses as part of the innate immune system [47, 48]. Small molecule agents that either block or activate Toll-like receptors are being sought to inhibit inflammatory reactions (associated with autoimmune diseases) or promote resistance against viral infections, respectively [49, 50]. A different class of molecules where lysosomal accumulation would be highly desirable involves agents that affect lysosomal enzymes involved in tissue remodeling [51]. Tissue remodeling is the basis of diseases like osteoporosis, which involves the loss of bone mass due to an imbalance in the rate of bone deposition and bone resorption.

From the simulations, mitochondria also appear as an important site of accumulation of monobasic amines – even for many molecules that have been previously classified as being "lysosomotropic". Our simulation results indicate that monovalent weak bases can selectively accumulate in mitochondria at very high levels –in fact, at much higher levels than they appear to be able to accumulate in lysosomes. From a drug toxicity standpoint, unintended

99

accumulation of small molecules in mitochondria can interfere with mitochondrial function, leading to cellular apoptosis [52-54]. Conversely, intentional targeting of small molecule therapeutic agents to mitochondria can be a desirable feature for certain classes of drugs: mitochondria dysfunction can cause a variety of diseases, so there is great interest in developing mitochondriotropic drugs [22, 55-57].

Nevertheless, perhaps the most important classes of subcellularly-targeted molecules are those that are aimed at extracellular domains of cell surface receptors [24]. Many 'blockbuster' drugs in the market today target cell surface receptors, ion channels, and other extracellular enzymes, making extracellular space one of the most valuable sites-of-action for drug development [58]. Extracellular-acting therapeutic agents include anticoagulants that interfere with clotting factors in the blood, agents that interfere with pro-hormone processing enzymes, ion channel blockers for treating heart conditions, GPCR antagonists for hypertension, inflammation and a variety of other different conditions, and many CNS-active agents that act on neurotransmitter receptors, transport and processing pathways. In order to target extracellular domains of blood proteins, cell surface receptors and ion channels, it is desirable that a molecule would have high transcellular permeability to facilitate absorption and tissue penetration. In addition, it would be desirable that the molecule would also have low intracellular accumulation so as to maximize extracellular concentration. The simulation results indicate that indeed, finding monovalent weak bases with high permeability and low intracellular accumulation in both target and non-target cells

is possible, with several molecules in the reference set residing in this realm of physicochemical property space.

To conclude, cell based molecular transport simulators constitute a promising cheminformatic analysis tool for analyzing the subcellular transport properties of small molecule drugs. The ability to combine results from different models, visualize simulations representing hundreds of thousands of different combinations of physicochemical properties, and relate these simulation results to the chemical structure and phenotypic effects of specific drugs and small drug-like molecules adds a new dimension to the existing mathematical models. As related to the specific class of lysosomotropic monobasic amines analyzed in this study, interactive visualization of simulation results point to a richness in subcellular transport and distribution behavior that is otherwise difficult to appreciate. We anticipate that the complexity of subcellular transport behaviors will ultimately be exploited in future generations of small molecule drug candidates "supertargeted" to their sites of action [59], be it in the extracellular space, the cytosol, mitochondria, lysosomes and potentially other intracellular organelles.

References

1. A.M. Kaufmann and J.P. Krise. Lysosomal sequestration of amine-containing drugs: analysis and therapeutic implications. *J Pharm Sci.* 96:729-746 (2007).

2. M. Duvvuri, Y.P. Gong, D. Chatterji, and J.P. Krise. Weak base permeability characteristics influence the intracellular sequestration site in the multidrug-resistant human leukemic cell line HL-60. *J Biol Chem.* 279:32367-32372 (2004).

3. C. de Duve, T. de Barsy, B. Poole, A. Trouet, P. Tulkens, and F. Van Hoof. Commentary. Lysosomotropic agents. *Biochem Pharmacol.* 23:2495-2531 (1974).

4. M.J. Reasor and S. Kacew. Drug-induced phospholipidosis: are there functional consequences? *Exp Biol Med (Maywood).* 226:825-830 (2001).

5. H. Fujimura, E. Dekura, M. Kurabe, N. Shimazu, M. Koitabashi, and W. Toriumi. Cell-based fluorescence assay for evaluation of new-drugs potential for phospholipidosis in an early stage of drug development. *Exp Toxicol Pathol.* 58:375-382 (2007).

6. G. Cramb. Selective lysosomal uptake and accumulation of the beta-adrenergic antagonist propranolol in cultured and isolated cell systems. *Biochem Pharmacol.* 35:1365-1372 (1986).

7. B. Styrt and M.S. Klempner. Lysosomotropic behavior of adrenergic antagonists in interactions with human neutrophils. *Biochem Pharmacol.* 37:435-441 (1988).

8. J.P. Ploemen, J. Kelder, T. Hafmans, H. van de Sandt, J.A. van Burgsteden, P.J. Saleminki, and E. van Esch. Use of physicochemical calculation of pKa and CLogP to predict phospholipidosis-inducing potential: a case study with structurally related piperazines. *Exp Toxicol Pathol.* 55:347-355 (2004).

9. P.O. Seglen and P.B. Gordon. Effects of lysosomotropic monoamines, diamines, amino alcohols, and other amino compounds on protein degradation and protein synthesis in isolated rat hepatocytes. *Mol Pharmacol.* 18:468-475 (1980).

10. S. Ohkuma and B. Poole. Cytoplasmic vacuolation of mouse peritoneal macrophages and the uptake into lysosomes of weakly basic substances. *J Cell Biol.* 90:656-664 (1981).

11. U.E. Honegger, G. Quack, and U.N. Wiesmann. Evidence for lysosomotropism of memantine in cultured human cells: cellular kinetics and effects of memantine on phospholipid content and composition, membrane fluidity and beta-adrenergic transmission. *Pharmacol Toxicol.* 73:202-208 (1993).

12. U.E. Honegger, A.A. Roscher, and U.N. Wiesmann. Evidence for lysosomotropic action of desipramine in cultured human fibroblasts. *J Pharmacol Exp Ther.* 225:436-441 (1983).

13. G. Morissette, E. Moreau, C.G. R, and F. Marceau. Massive cell vacuolization induced by organic amines such as procainamide. *J Pharmacol Exp Ther.* 310:395-406 (2004).

14. G. Morissette, E. Moreau, C.G. R, and F. Marceau. N-substituted 4-aminobenzamides (procainamide analogs): an assessment of multiple cellular effects concerning ion trapping. *Mol Pharmacol.* 68:1576-1589 (2005).

15. S.J. Hurwitz, M. Terashima, N. Mizunuma, and C.A. Slapak. Vesicular anthracycline accumulation in doxorubicin-selected U-937 cells: participation of lysosomes. *Blood.* 89:3745-3754 (1997).

16. J. Ishizaki, K. Yokogawa, F. Ichimura, and S. Ohkuma. Uptake of imipramine in rat liver lysosomes in vitro and its inhibition by basic drugs. *J Pharmacol Exp Ther.* 294:1088-1098 (2000).

17. B. Lemieux, M.D. Percival, and J.P. Falgueyret. Quantitation of the lysosomotropic character of cationic amphiphilic drugs using the fluorescent basic amine Red DND-99. *Anal Biochem.* 327:247-251 (2004).

18. W.C. Yang, F.F. Strasser, and C.M. Pomerat. Mechanism of Drug-Induced Vacuolization in Tissue Culture. *Exp Cell Res.* 38:495-506 (1965).

19. A. Bulychev, A. Trouet, and P. Tulkens. Uptake and intracellular distribution of neutral red in cultured fibroblasts. *Exp Cell Res.* 115:343-355 (1978).

20. M. Duvvuri and J.P. Krise. A novel assay reveals that weakly basic model compounds concentrate in lysosomes to an extent greater than pH-partitioning theory would predict. *Mol Pharm.* 2:440-448 (2005).

21. Z.I. Cabantchik, J. Silfen, R.A. Firestone, M. Krugliak, E. Nissani, and H. Ginsburg. Effects of lysosomotropic detergents on the human malarial parasite Plasmodium falciparum in in vitro culture. *Biochem Pharmacol.* 38:1271-1277 (1989).

22. R.W. Horobin, S. Trapp, and V. Weissig. Mitochondriotropics: a review of their mode of action, and their applications for drug and DNA delivery to mammalian mitochondria. *J Control Release.* 121:125-136 (2007).

23. R.J. Gonzalez-Rothi, D.S. Zander, and P.R. Ros. Fluoxetine hydrochloride (Prozac)-induced pulmonary disease. *Chest.* 107:1763-1765 (1995).

24. X. Zhang, K. Shedden, and G.R. Rosania. A cell-based molecular transport simulator for pharmacokinetic prediction and cheminformatic exploration. *Mol Pharm.* 3:704-716 (2006).

25. S. Trapp and R.W. Horobin. A predictive model for the selective accumulation of chemicals in tumor cells. *Eur Biophys J Biophys Lett.* 34:959-966 (2005).

26. L.M. Loew, R.A. Tuft, W. Carrington, and F.S. Fay. Imaging in five dimensions: time-dependent membrane potentials in individual mitochondria. *Biophys J.* 65:2396-2407 (1993).

27. S.L. Rybak and R.F. Murphy. Primary cell cultures from murine kidney and heart differ in endosomal pH. *J Cell Physiol.* 176:216-222 (1998).

28. C.C. Cain and R.F. Murphy. A chloroquine-resistant Swiss 3T3 cell line with a defect in late endocytic acidification. *J Cell Biol.* 106:269-277 (1988).

29. R.A. Preston, R.F. Murphy, and E.W. Jones. Assay of vacuolar pH in yeast and identification of acidification-defective mutants. *Proc Natl Acad Sci U S A.* 86:7027-7031 (1989).

30. R.W. Van Dyke. Proton pump-generated electrochemical gradients in rat liver multivesicular bodies. Quantitation and effects of chloride. *J Biol Chem.* 263:2603-2611 (1988).

31. S.M. Felber and M.D. Brand. Factors determining the plasma-membrane potential of lymphocytes. *Biochem J.* 204:577-585 (1982).

32. S. Simon, D. Roy, and M. Schindler. Intracellular pH and the control of multidrug resistance. *Proc Natl Acad Sci U S A.* 91:1128-1132 (1994).

33. X. Zhang and G.R. Rosania. A virtual cell-based simulator for pharmaceutical project management, risk assessment and decision making., *Proceedings of the 4th International Conference on Computer Science and its Applications*, San Diego, CA, 2006, pp. 58-65.

34. K. Balon, B.U. Riebesehl, and B.W. Muller. Drug liposome partitioning as a tool for the prediction of human passive intestinal absorption. *Pharm Res.* 16:882-888 (1999).

35. W.N. Charman, C.J. Porter, S. Mithani, and J.B. Dressman. Physiochemical and physiological mechanisms for the effects of food on drug absorption: the role of lipids and pH. *J Pharm Sci.* 86:269-282 (1997).

36. G.R. Rosania, J.W. Lee, L. Ding, H.S. Yoon, and Y.T. Chang. Combinatorial approach to organelle-targeted fluorescent library based on the styryl scaffold. *J Am Chem Soc.* 125:1130-1131 (2003).

37. V.Y. Chen, S.M. Khersonsky, K. Shedden, Y.T. Chang, and G.R. Rosania. System dynamics of subcellular transport. *Mol Pharm.* 1:414-425 (2004).

38. M.M. Posada, K. Shedden, Y.T. Chang, Q. Li, and G.R. Rosania. Prospecting for live cell bioimaging probes with cheminformatic assisted image arrays (CAIA), *Proceedings of the 4th IEEE International Symposium on Biomedical Imaging*, 2007.

39. K. Shedden, J. Brumer, Y.T. Chang, and G.R. Rosania. Chemoinformatic analysis of a supertargeted combinatorial library of styryl molecules. *J Chem Inf Comput Sci.* 43:2068-2080 (2003).

40. V.Y. Chen, M.M. Posada, L.L. Blazer, T. Zhao, and G.R. Rosania. The role of the VPS4A-exosome pathway in the intrinsic egress route of a DNA-binding anticancer drug. *Pharm Res.* 23:1687-1695 (2006).

41. V.Y. Chen, M.M. Posada, L. Zhao, and G.R. Rosania. Rapid Doxorubicin Efflux from the Nucleus of Drug-Resistant Cancer Cells Following Extracellular Drug Clearance. *Pharm Res* (2007).

42. M. Duvvuri, W. Feng, A. Mathis, and J.P. Krise. A cell fractionation approach for the quantitative analysis of subcellular drug disposition. *Pharm Res.* 21:26-32 (2004).

43. Y. Gong, Z. Zhao, D.J. McConn, B. Beaudet, M. Tallman, J.D. Speake, D.M. Ignar, and J.P. Krise. Lysosomes contribute to anomalous pharmacokinetic behavior of melanocortin-4 receptor agonists. *Pharm Res.* 24:1138-1144 (2007).

44. P.V. Balimane and S. Chong. Cell culture-based models for intestinal permeability: a critique. *Drug Discov Today.* 10:335-343 (2005).

45. J.D. Irvine, L. Takahashi, K. Lockhart, J. Cheong, J.W. Tolan, H.E. Selick, and J.R. Grove. MDCK (Madin-Darby canine kidney) cells: A tool for membrane permeability screening. *J Pharm Sci.* 88:28-33 (1999).

46. C.M. McCloud, T.L. Beard, S. Kacew, and M.J. Reasor. In vivo and in vitro reversibility of chlorphentermine-induced phospholipidosis in rat alveolar macrophages. *Exp Mol Pathol.* 62:12-21 (1995).

47. M. Matsumoto, K. Funami, M. Tanabe, H. Oshiumi, M. Shingai, Y. Seto, A. Yamamoto, and T. Seya. Subcellular localization of Toll-like receptor 3 in human dendritic cells. *J Immunol.* 171:3154-3162 (2003).

48. T. Kawai and S. Akira. TLR signaling. *Semin Immunol.* 19:24-32 (2007).

49. S. Fletcher, K. Steffy, and D. Averett. Masked oral prodrugs of toll-like receptor 7 agonists: a new approach for the treatment of infectious disease. *Curr Opin Investig Drugs.* 7:702-708 (2006).

50. P. Cristofaro and S.M. Opal. Role of Toll-like receptors in infection and immunity: clinical implications. *Drugs.* 66:15-29 (2006).

51. J.P. Falgueyret, S. Desmarais, R. Oballa, W.C. Black, W. Cromlish, K. Khougaz, S. Lamontagne, F. Masse, D. Riendeau, S. Toulmond, and M.D. Percival. Lysosomotropism of basic cathepsin K inhibitors contributes to increased cellular potencies against off-target cathepsins and reduced functional selectivity. *J Med Chem.* 48:7535-7543 (2005).

52. P.R. van Ginkel, D. Sareen, L. Subramanian, Q. Walker, S.R. Darjatmoko, M.J. Lindstrom, A. Kulkarni, D.M. Albert, and A.S. Polans. Resveratrol

inhibits tumor growth of human neuroblastoma and mediates apoptosis by directly targeting mitochondria. *Clin Cancer Res.* 13:5162-5169 (2007).

53. E. Jacotot, A. Deniaud, A. Borgne-Sanchez, Z. Touat, J.P. Briand, M. Le Bras, and C. Brenner. Therapeutic peptides: Targeting the mitochondrion to modulate apoptosis. *Biochim Biophys Acta.* 1757:1312-1323 (2006).

54. V.R. Fantin, M.J. Berardi, L. Scorrano, S.J. Korsmeyer, and P. Leder. A novel mitochondriotoxic small molecule that selectively inhibits tumor cell growth. *Cancer Cell.* 2:29-42 (2002).

55. G.G. D'Souza, S.V. Boddapati, and V. Weissig. Gene therapy of the other genome: the challenges of treating mitochondrial DNA defects. *Pharm Res.* 24:228-238 (2007).

56. V. Weissig and V.P. Torchilin. Mitochondriotropic cationic vesicles: a strategy towards mitochondrial gene therapy. *Curr Pharm Biotechnol.* 1:325-346 (2000).

57. G.G. D'Souza, R. Rammohan, S.M. Cheng, V.P. Torchilin, and V. Weissig. DQAsome-mediated delivery of plasmid DNA toward mitochondria in living cells. *J Control Release.* 92:189-197 (2003).

58. J.P. Overington, B. Al-Lazikani, and A.L. Hopkins. How many drug targets are there? *Nat Rev Drug Discov.* 5:993-996 (2006).

59. G.R. Rosania. Supertargeted chemistry: identifying relationships between molecular structures and their sub-cellular distribution. *Curr Top Med Chem.* 3:659-685 (2003).

60. M. Duvvuri, S. Konkar, K.H. Hong, B.S. Blagg, and J.P. Krise. A new approach for enhancing differential selectivity of drugs to cancer cells. *ACS Chem Biol.* 1:309-315 (2006).

61. W. Li, X.M. Yuan, S. Ivanova, K.J. Tracey, J.W. Eaton, and U.T. Brunk. 3-Aminopropanal, formed during cerebral ischaemia, is a potent lysosomotropic neurotoxin. *Biochem J.* 371:429-436 (2003).

62. P. Schneider. Drug-induced lysosomal disorders in laboratory animals: new substances acting on lysosomes. *Arch Toxicol.* 66:23-33 (1992).

63. B.P. Schmid, R.E. Hauser, and P. Donatsch. Effects of cyproheptadine on the rat yolk sac membrane and embryonic development in vitro. *Xenobiotica.* 15:695-699 (1985).

64. W.A. Daniel, J. Wojcikowski, and A. Palucha. Intracellular distribution of psychotropic drugs in the grey and white matter of the brain: the role of lysosomal trapping. *Br J Pharmacol.* 134:807-814 (2001).

65. J. Ishizaki, K. Yokogawa, M. Hirano, E. Nakashima, Y. Sai, S. Ohkuma, T. Ohshima, and F. Ichimura. Contribution of lysosomes to the subcellular distribution of basic drugs in the rat liver. *Pharm Res.* 13:902-906 (1996).

66. D. Drenckhahn, L. Kleine, and R. Lullmann-Rauch. Lysosomal alterations in cultured macrophages exposed to anorexigenic and psychotropic drugs. *Lab Invest.* 35:116-123 (1976).

67. M. Hetman, W. Danysz, and L. Kaczmarek. Increased expression of cathepsin D in retrosplenial cortex of MK-801-treated rats. *EXP NEUROL.* 147:229-237 (1997).

68. D. Pessayre, M. Bichara, C. Degott, F. Potet, J.P. Benhamou, and G. Feldmann. Perhexiline maleate-induced cirrhosis. *Gastroenterology.* 76:170-177 (1979).

Tables

Table 3.1.   The reference set of ninety-nine lysosomotropic monobasic amines. Based on simulation results, compounds were classified by permeability (P_{eff} calculated with the R-model) and subcellular concentrations (calculated with the T-model) as follows: **Low permeability**: P_{eff} < 35×10^{-6} cm/sec; **High permeability**: $P_{eff} \geq 35 \times 10^{-6}$ cm/sec; **Lyso**: $C_{lyso}T$ > 2 mM; **Mito**: $C_{mito}T$ > 2 mM; **Cyto**: $C_{cyto}T \geq 2mM$; **Non-lyso**: $C_{lyso}T$ < 2 mM; **Non-mito**: $C_{mito}T$ < 2 mM; **Non-cyto**: $C_{cyto}T$ < 2mM.   Compounds appear in gray background if they were reported as non-lysosomotropic in pubished research articles; in *italics* if they are calculated as selective lysosomotropic ($C_{lyso}T \geq 2mM$; $C_{lyso}T/C_{mito}T \geq 2mM$; $C_{lyso}T/C_{cyto}T \geq 2mM$), <u>underlined</u> if they are calculated as selectively mitochondriotropic ($C_{mito}T \geq 2mM$, $C_{mito}T/C_{lyso}T \geq 2$ mM, $C_{mito}T/C_{cyto}T \geq 2$ mM).

Category 1: Low Permeability, Non-lyso, Mito, Non-cyto — **Chemical space exists.**

Category 2: Low Permeability, Non-lyso, Non-mito, Non-cyto — **Chemical space exists.**

Category 3: Low Permeability, Non-lyso, Non-mito, Cyto — **Chemical space does not exist.**

Category 4: Low Permeability, Non-lyso, Mito, Cyto — **Chemical space exists.**

Category 5: Low Permeability, Lyso, Mito, Non-cyto — **Chemical space exists.**

Category 6: Low Permeability, Lyso, Non-mito, Non-cyto — **Chemical space exists.**

Name	pK_a	$\log P_n$	$\log P_d$	$C_{cyto}R$	$C_{mito}R$	$C_{lyso}R$	P_{eff}	$C_{cyto}T$	$C_{mito}T$	$C_{lyso}T$	Ref.
Lidocaine	7.2	2.71	1.16	0.15	0.06	1.74	26.67	1.87	0.81	22.26	[10]

Category 7: Low Permeability, Lyso, Non-mito, Cyto — **Chemical space exists.**

Name	pK_a	$\log P_n$	$\log P_d$	$C_{cyto}R$	$C_{mito}R$	$C_{lyso}R$	P_{eff}	$C_{cyto}T$	$C_{mito}T$	$C_{lyso}T$	
17-DMAG	7.31	2.46	0.87	0.15	0.06	1.69	13.01	2.05	0.81	22.73	[60]
β-dimethylaminoethylchloride	7.63	2.48	0.9	0.23	0.08	1.5	11.76	2.64	0.91	17.52	[21]
Diethylaminoethyl chloride	8.16	2.71	1.16	0.53	0.24	1.36	19.93	3.83	1.72	9.87	[21]
Triethanolamine	8.14	1.52	-0.18	0.4	0.14	1.39	0.91	3.57	1.25	12.35	[21]

Category 8: Low Permeability, Lyso, Mito, Cyto — **Chemical space exists.**

Name	pK_a	$\log P_n$	$\log P_d$	$C_{cyto}R$	$C_{mito}R$	$C_{lyso}R$	P_{eff}	$C_{cyto}T$	$C_{mito}T$	$C_{lyso}T$	
17-DMAP	8.3	2.47	0.89	0.62	0.31	1.35	10.79	4.17	2.08	9.07	[60]
2-amino-1-butanol	9.49	2.04	0.55	1.67	9.57	1.29	5.84	10.16	58.1	7.82	[21]
2-amino-2-methyl-1,3-propanediol	9.14	1.56	0	1.44	3.32	1.3	1.58	8.01	18.52	7.22	[21]
2-amino-2-methyl-1-propanol	9.68	1.92	0.41	1.73	14.32	1.29	4.27	10.85	89.76	8.06	[21]
2-aminoethanol(ethanolamine)	9.22	1.75	0.22	1.51	4.42	1.29	2.66	8.62	25.18	7.36	[21]
2-diethylaminoethanol	9.22	2.23	0.62	1.46	3.58	1.29	6.62	8.19	20.09	7.27	[21]
2-dimethylamino-2-methyl-1-propanol	9.25	2.17	0.55	1.47	3.76	1.29	5.65	8.31	21.23	7.3	[21]
2-dimethylaminoethanol	8.71	2.01	0.37	0.96	0.81	1.32	3.42	5.44	4.56	7.46	[21]
2-methylaminoethanol	9.46	1.89	0.32	1.63	7.29	1.29	3.41	9.67	43.34	7.66	[21]
3-amino-1-propanol	9.49	1.77	0.24	1.66	8.67	1.29	2.85	9.99	52.26	7.76	[21]

3-aminopropanal	9.14	1.77	0.24	1.46	3.6	1.29	2.76	8.17	20.17	7.25	[61]
3-dimethylamino-1-propanol	8.83	2.03	0.39	1.08	1.13	1.31	3.66	5.98	6.25	7.23	[21]
4-amino-1-butanol	9.55	1.92	0.41	1.69	10.52	1.29	4.24	10.34	64.43	7.88	[21]
Ammonia	8.55	1.81	0.41	1.05	1.08	1.31	3.8	5.67	5.82	7.08	[21]
Atenolol	9.32	2.29	0.76	1.57	5.7	1.29	9.32	9.15	33.13	7.5	[6]
Atropine	9.02	2.67	1.23	1.44	3.36	1.3	26.87	7.98	18.66	7.18	[10], [16]
Benzylamine	9.17	2.58	1.24	1.6	6.38	1.29	28.25	9.32	37.22	7.52	[10]
Butylamine	9.84	2.39	0.95	1.78	24.35	1.28	14.95	11.54	157.56	8.31	[21]
Diethylamine	10.2	2.36	0.84	1.82	45	1.28	11.68	12.09	298.98	8.53	[10], [21]
Dimethylamine	10.15	2.13	0.59	1.81	38.7	1.28	6.56	11.98	255.81	8.48	[21]
Ethylamine	9.86	2.11	0.62	1.78	22.73	1.28	6.99	11.46	146.61	8.28	[21]
Guanidine	12.09	1.82	0.39	1.86	461.27	1.28	4.17	12.78	3164.97	8.8	[10], [21]
Hexylamine	9.84	2.66	1.24	1.79	25.48	1.28	29.17	11.59	165.24	8.33	[21]
Isobutylamine	9.87	2.4	0.95	1.79	25.47	1.28	14.96	11.59	165.19	8.33	[21]
Isopropanolamine	9.26	1.89	0.38	1.55	5.16	1.29	3.87	8.94	29.72	7.44	[21]
Isopropylamine	10.06	2.25	0.78	1.81	37.09	1.28	10.16	11.95	244.64	8.47	[21]
Methylamine	9.72	2	0.5	1.74	16.1	1.29	5.27	11.02	101.71	8.12	[21]
Metoclopramide	8.73	2.56	0.99	1.05	1.06	1.31	14.48	5.81	5.82	7.22	[14], [13]
Morpholine	8.21	2.02	1.25	1.36	2.95	1.3	27.55	6.62	14.36	6.31	[10]
N-acetylprocainamide	8.73	2.51	0.93	1.04	1.02	1.31	12.59	5.76	5.66	7.25	[10],[13]
NAMA	8.72	2.38	0.79	1.02	0.97	1.31	9.09	5.68	5.36	7.29	[14]
N,N-Dimethyl-3-chloropropylamine	8.38	2.5	0.92	0.69	0.38	1.34	11.66	4.41	2.45	8.54	[21]
N,N-dimethyl-benzylamine	8.67	2.84	1.3	1.02	0.98	1.31	29.42	5.65	5.4	7.25	[10]
Pentylamine	9.84	2.53	1.09	1.78	24.35	1.28	20.64	11.54	157.56	8.31	[21]
Practolol	9.32	2.47	0.97	1.59	6.15	1.29	15.16	9.3	35.98	7.54	[6]
Propylamine	9.85	2.27	0.8	1.78	23.26	1.28	10.58	11.49	150.19	8.29	[21]
s-butylamine	10.07	2.4	0.95	1.81	39.59	1.28	15.03	12	261.77	8.49	[21]
t-butylamine	10.27	2.27	0.81	1.83	59.14	1.28	10.92	12.26	395.97	8.59	[21]
Triethylamine	9.84	2.59	1.02	1.76	18.05	1.29	17.49	11.18	114.96	8.18	[21]

| Trimethylamine | 9.23 | 2.25 | 0.64 | 1.47 | 3.67 | 1.29 | 6.94 | 8.25 | 20.66 | 7.28 | [10] |
| Tris(hydroxymethyl)methylamine | 8.64 | 1.2 | -0.4 | 0.93 | 0.75 | 1.32 | 0.58 | 5.29 | 4.25 | 7.51 | [10], [21] |

Category 9: High Permeability, Non-lyso, Mito, Cyto Chemical space does not exist.

Category 10: High Permeability, Non-lyso, Non-mito, Cyto Chemical space does not exist.

Category 11: High Permeability, Non-lyso, Mito, Non-cyto Chemical space exists.

Category 12: High Permeability, Non-lyso, Non-mito, Non-cyto Chemical space exists.

Name	pK_a	$\log P_n$	$\log P_d$	$C_{cyto}R$	$C_{mito}R$	$C_{lyso}R$	P_{eff}	$C_{cyto}T$	$C_{mito}T$	$C_{lyso}T$	
3-aminoquinoline	4.63	2.65	2.00	0.73	0.73	1.12	398.87	0.82	0.82	1.25	[1]
8-aminoquinoline	4.07	2.65	2.00	0.78	0.78	0.90	425.43	0.81	0.81	0.94	[1]
AF-CX1325XX	1.95	2.18	0.7	0.8	0.8	0.8	148	0.81	0.81	0.81	[62]
Aniline	4.5	2.62	1.2	0.73	0.73	1.1	372.35	0.82	0.81	1.22	[10]
Benzocaine	2.7	2.78	1.41	0.8	0.8	0.8	588.46	0.81	0.81	0.82	[13]
β-naphthylamine	4.12	2.95	1.57	0.77	0.77	0.93	838.56	0.81	0.81	0.98	[10]
Pyrimidine	1.55	2.17	1.4	0.8	0.8	0.8	144.65	0.81	0.81	0.81	[10]
Pyridine	4.95	2.44	1.88	0.69	0.69	1.3	229.69	0.82	0.82	1.56	[10]

Category 13: High Permeability, Lyso, Non-mito, Non-cyto Chemical space exists.

Name	pK_a	$\log P_n$	$\log P_d$	$C_{cyto}R$	$C_{mito}R$	$C_{lyso}R$	P_{eff}	$C_{cyto}T$	$C_{mito}T$	$C_{lyso}T$	
17-AEP	*6.59*	*2.56*	*0.99*	*0.14*	*0.09*	*2.43*	*37.31*	*1.17*	*0.80*	*20.89*	[60]
1-aminoisoquinoline	*6.88*	*2.74*	*1.94*	*0.36*	*0.30*	*1.45*	*123.44*	*1.53*	*1.28*	*6.16*	[1]
1-dodecylimidazole	6.56	3.65	3.3	0.64	0.81	1.36	2615.12	1.27	1.61	2.7	[21]
Eserine	*6.46*	*3.03*	*1.51*	*0.15*	*0.11*	*2.51*	*137.8*	*1.09*	*0.81*	*17.74*	[10]
Harmine	*5.95*	*2.81*	*2.06*	*0.38*	*0.36*	*1.82*	*265.16*	*0.91*	*0.88*	*4.40*	[1]
Imidazole	*6.73*	*2.12*	*1.59*	*0.51*	*0.56*	*1.39*	*52.47*	*1.41*	*1.53*	*3.81*	[21]
Papaverine	*6.07*	*3.1*	*2.39*	*0.37*	*0.35*	*1.72*	*489.43*	*0.94*	*0.91*	*4.42*	[1]
Pilocarpine	*6.39*	*2.38*	*1.89*	*0.48*	*0.51*	*1.44*	*109.54*	*1.1*	*1.18*	*3.32*	[10]
s-Collidine	*7.06*	*2.71*	*1.71*	*0.3*	*0.2*	*1.47*	*74.19*	*1.76*	*1.18*	*8.61*	[21]

Category 14: High Permeability, Lyso, Non-mito, Cyto Chemical space exists.

Name	pK_a	logP_n	logP_d	$C_{cyto}R$	$C_{mito}R$	$C_{lyso}R$	P_{eff}	$C_{cyto}T$	$C_{mito}T$	$C_{lyso}T$	
Cyproheptadine	*7.77*	*3.67*	*2.23*	*0.35*	*0.14*	*1.41*	*235.81*	*3.02*	*1.22*	*12.12*	[63]
Diltiazem	*7.89*	*3.08*	*1.57*	*0.37*	*0.14*	*1.4*	*51.38*	*3.23*	*1.25*	*12.07*	[16]
N-dodecylmorpholine	*7.5*	*3.58*	*2.14*	*0.24*	*0.1*	*1.49*	*203.16*	*2.44*	*0.98*	*15.24*	[21]

Category 15: High Permeability, Lyso, Mito, Non-cyto — Chemical space exists.

Category 16: High Permeability, Lyso, Mito, Cyto — Chemical space exists.

Name	pK_a	logP_n	logP_d	$C_{cyto}R$	$C_{mito}R$	$C_{lyso}R$	P_{eff}	$C_{cyto}T$	$C_{mito}T$	$C_{lyso}T$	
4-aminopyridine	8.63	2.18	1.59	1.71	11.8	1.29	64.2	9.96	68.73	7.5	[10]
4-aminoquinaldine	8.5	2.7	1.82	1.49	4.21	1.29	104.97	7.87	22.31	6.85	[10]
4-aminoquinoline	7.98	2.65	2.00	1.29	2.56	1.30	152.07	5.73	11.40	5.79	[1]
4-Dimethylaminopyridine	8.47	2.53	1.98	1.67	9.26	1.29	156.25	9.28	51.49	7.16	[10]
9-aminoacridine	8.97	3.11	2.4	1.76	18.6	1.28	419.24	10.96	115.66	7.99	[10]
Alprenolol	9.32	3.04	1.71	1.67	9.42	1.29	84.41	10.09	56.88	7.77	[6]
Amantadine	10.33	2.57	2.04	1.86	288.64	1.28	186.33	12.73	1973.95	8.77	[16]
Amiodarone	8.17	4.58	3.38	0.88	0.74	1.32	3439.62	4.69	3.96	7.07	[4]
Amitriptyline	9.41	3.7	2.27	1.67	9.14	1.29	306.28	10.07	55.23	7.78	[64]
Biperiden	8.97	3.25	1.76	1.36	2.57	1.3	89.81	7.43	14.07	7.1	[65] [66] ,
Chlorphentermine	10.24	3	1.62	1.84	65.54	1.28	70.54	12.32	439.85	8.61	[46]
Chlorpromazine	8.87	3.7	2.27	1.33	2.33	1.3	288.89	7.19	12.66	7.05	[16]
Desipramine	9.66	3.4	2.01	1.76	18.13	1.29	170.9	11.17	115.25	8.17	[12]
Dibutylamine	10.36	2.93	1.48	1.84	72.43	1.28	51.13	12.37	487.37	8.63	[21]
Dihydroalprenolol	9.32	3.11	1.69	1.63	7.53	1.29	80.09	9.69	44.73	7.65	[7]
Dizocilpine	8.3	3.29	1.89	0.80	0.55	1.33	110.20	4.61	3.18	7.70	[67]
Dodecylamine	9.84	3.44	2.12	1.8	31.89	1.28	221.84	11.8	208.84	8.41	[21]
Ephedrine	9.19	2.63	1.94	1.8	31.41	1.28	146.48	11.65	202.78	8.29	[10] [4],
Fluoxetine	9.45	3.58	3.01	1.84	69.46	1.28	1731.76	12.27	463.16	8.55	[23]
Imipramine	8.87	3.52	2.07	1.31	2.21	1.3	181.73	7.09	11.95	7.04	[4]
Iprindole	9.36	3.54	2.09	1.64	7.71	1.29	201.32	9.74	45.89	7.67	[66]
Mecamylamine	10.49	2.93	2.27	1.86	297.05	1.28	316.44	12.73	2032.53	8.77	[10]

Memantine	10.31	2.85	1.46	1.84	73.92	1.28	48.83	12.38	497.49	8.63	[11]
Octylamine	9.84	2.92	1.53	1.79	27.27	1.28	56.92	11.66	177.38	8.35	[21]
Perhexiline	10.2	3.83	3.28	1.86	244.79	1.28	3237.19	12.7	1671.65	8.76	[4], [68]
Phentermine	10.25	2.83	1.43	1.83	64.21	1.28	45.54	12.31	430.76	8.61	[66]
Piperidine	10.03	2.37	1.64	1.85	148.62	1.28	74.09	12.6	1009.79	8.71	[10]
Promazine	8.87	3.53	2.08	1.31	2.21	1.30	185.96	7.09	11.95	7.04	[64]
Propranolol	9.32	3.03	1.59	1.62	7.16	1.29	63.51	9.59	42.38	7.62	[10]
Sertraline	9.5	3.85	2.51	1.73	14.07	1.29	537.84	10.79	87.84	8.02	[64]
Thioridazine	8.61	4.01	2.61	1.11	1.27	1.31	608.81	5.96	6.80	7.02	[64]
Tributylamine	10.44	3.45	2.1	1.85	102.49	1.28	213.44	12.51	694.01	8.68	[10]
Verapamil	9.33	3.7	2.27	1.63	7.53	1.29	304.48	9.69	44.71	7.65	[16]

Figures

Figure 3.1. Diagrams showing the cellular pharmacokinetic phenomena captured by the two mathematical models used in this study: the T-Model of a leukocyte-like cell in suspension (A) and the R-Model an epithelial-like cell (B). Key: ap: apical compartment; bl: basolateral compartment; cyto: cytosol; mito: mitochondria; lyso: lysosome; R1: flux of the ionized/unionized form between the cytosol and the apical compartment; R2: flux of the ionized/unionized form between the cytosol and the basolateral compartment; R3: flux of the ionized/unionized form between the cytosol and the lysosome; R4: flux of the ionized/unionized form between the cytosol and the mitochondria; T1: flux of the ionized/unionized form between the cytosol and the extracellular compartment; T2: flux of the ionized/unionized form between the cytosol and lysosome; T3: flux of the ionized/unionized form between the cytosol and the extracellular compartment.
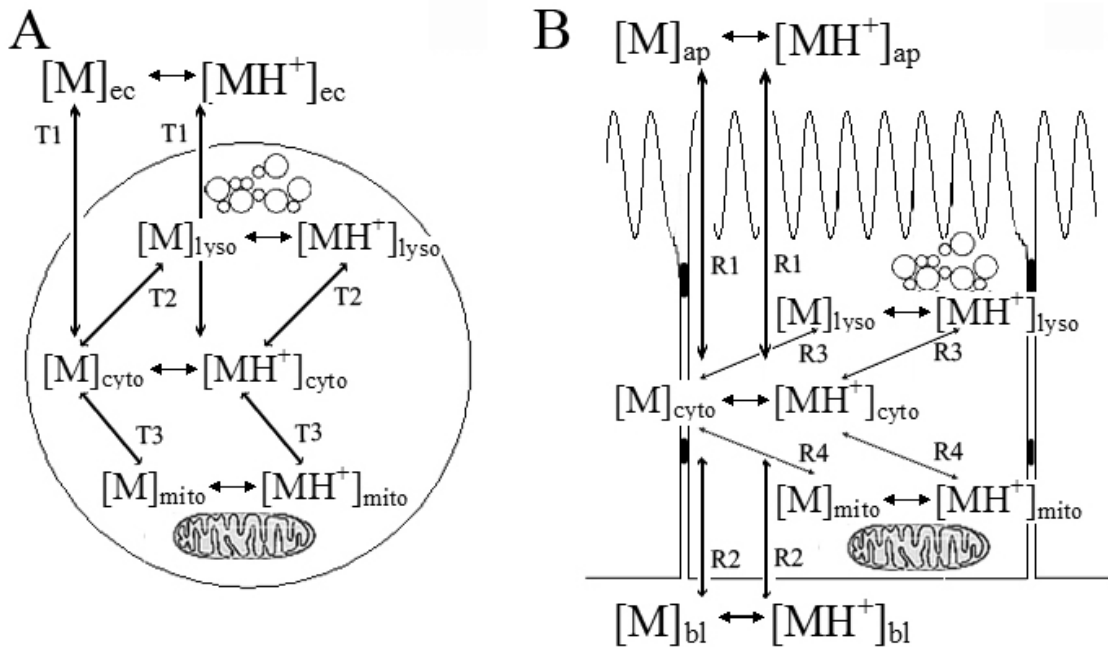
Figure 3.2. Visualizing the simulated physicochemical property space occupied by lysosomotropic monobasic amines. Individual molecules in the reference set are indicated by yellow dots. To discriminate between lysosomotropic vs. non-lysosomotropic molecules, three lysosomal concentration were explored as thresholds: 2 mM (A-D); 4 mM (E-H); and 8 mM (I-L). Columns show non-lysosomotropic molecules (A, E, I); non-lysosomotropic molecules plus lysosomotropic space (B, F, J); lysosomotropic molecules (C, G, K); and lysosomotropic molecules plus non-lysosomotropic space (D, H, L).
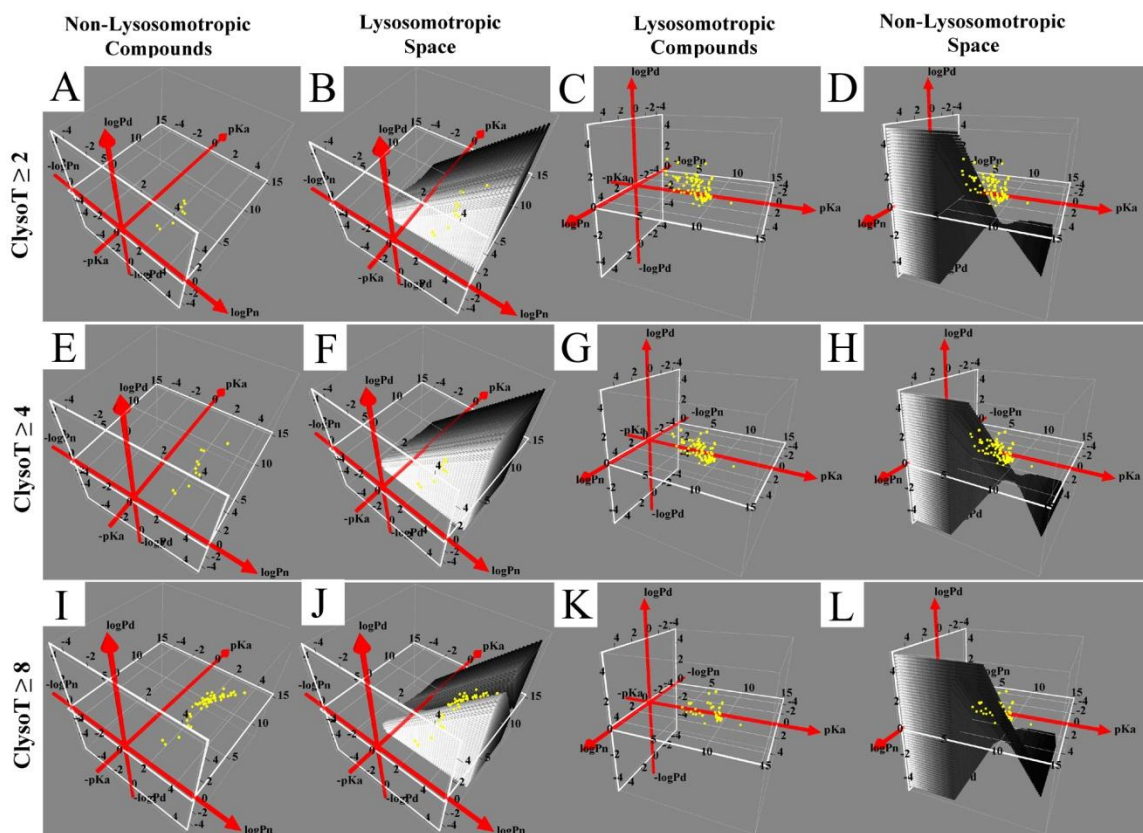
Figure 3.3. Visualizing the simulated physicochemical property space occupied by selectively lysosomotropic monobasic amines. Individual molecules in the reference set are indicated by yellow dots   The four graphs show: A) non-lysosomotropic molecules (inside blue circle) and non-selective lysosomotropic molecules (outside blue circle); B) selectively lysosomotropic molecules (inside green circle); C) physicochemical property space occupied by selectively lysosomotropic molecules, in relation to non-lysosomotropic molecules (inside blue circle) and non-selective lysosomotropic molecules (outside blue circle); D) selectively lysosomotropic molecules (yellow dots in green circle) in relation to the union of non-selective lysosomotropic and non-lysosomotropic physicochemical property space.
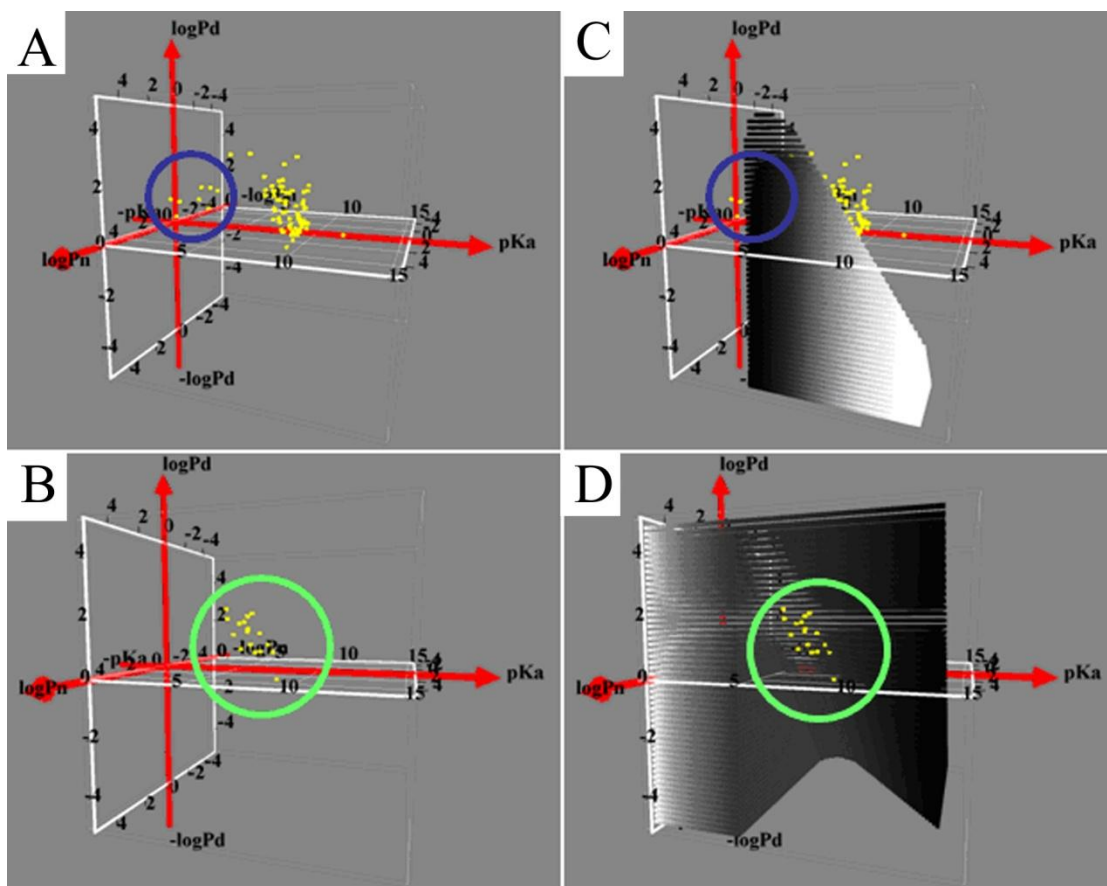
Figure 3.4. Visualizing the effect of transcellular permeability on selectively lysomotropic molecules. Individual molecules in the reference set are indicated by yellow dots   The six graphs show: A) physicochemical property space occupied by molecules with $P_{eff} < 1 \times 10^{-6}$ cm/s, in relation to non-selectively, lysosomotropic reference molecules; B) selectively lysosomotropic molecules with $P_{eff} < 1 \times 10^{-6}$ cm/s (yellow dots) in relation to the union of physicochemical property spaces occupied by non-selectively lysosomotropic, non-lysosomotropic, and selectively lysosomotropic molecules with $P_{eff} > 1 \times 10^{-6}$ cm/s; C) physicochemical property space occupied by molecules with 1×10^{-6} cm/s $< P_{eff} < 35 \times 10^{-6}$ cm/s, in relation to non-selectively lysosomotropic molecules; D) selectively lysosomotropic molecules with 1×10^{-6} cm/s $< P_{eff} < 35 \times 10^{-6}$ cm/s in relation to the union of physicochemical property spaces occupied by non-selectively lysosomotropic, non-lysosomotropic, and selectively lysosomotropic molecules excluding those with 1×10^{-6} cm/s $< P_{eff} < 35 \times 10^{-6}$ cm/s; E) physicochemical property space occupied by molecules with $P_{eff} > 35 \times 10^{-6}$ cm/s, in relation to non-selectively, lysosomotropic molecules;   F) selectively lysosomotropic molecules with $P_{eff} > 35 \times 10^{-6}$ cm/s in relation to the union of physicochemical property spaces occupied by non-selectively lysosomotropic, non-lysosomotropic, and selectively lysosomotropic molecules with $P_{eff} < 35 \times 10^{-6}$ cm/s; Green arrow point to the general region of physicochemical property space where the reference molecules are visibly clustered.
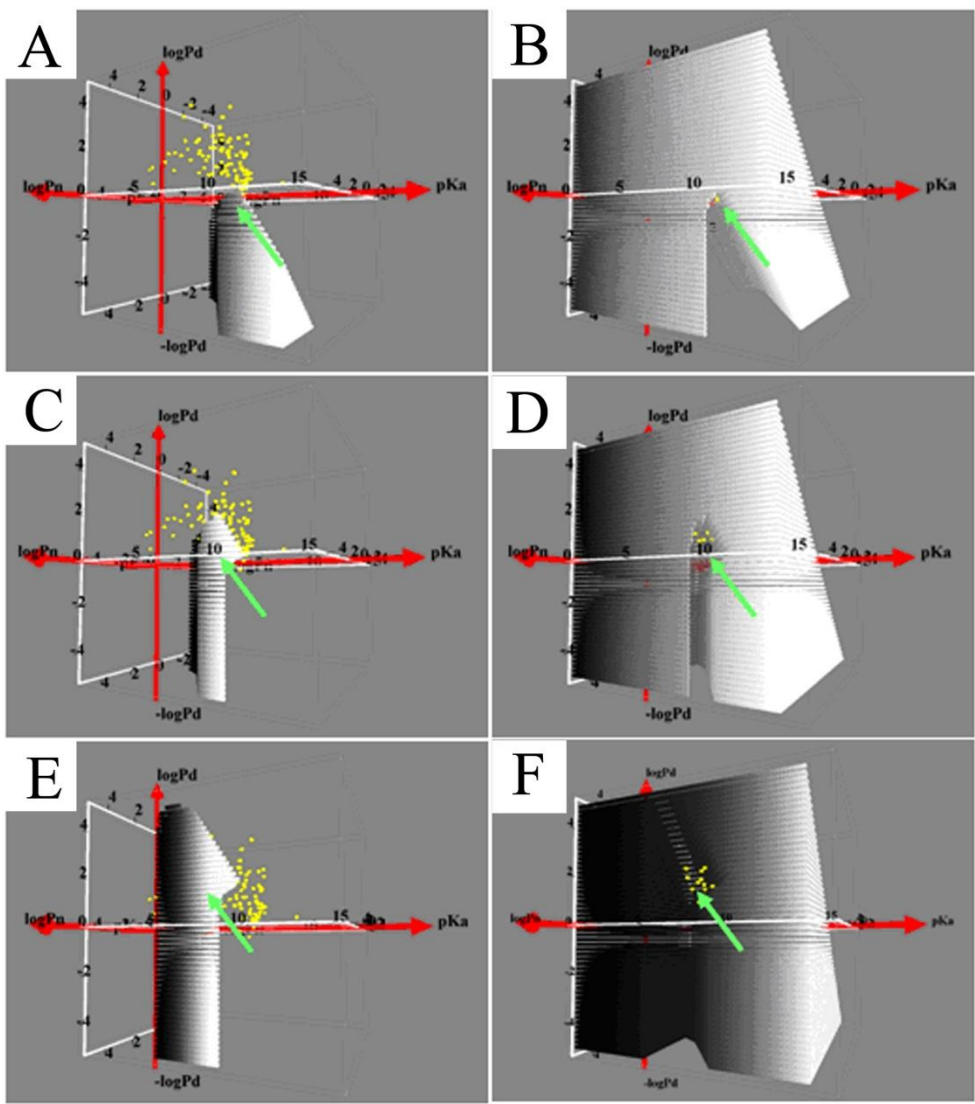
Figure 3.5. Visualizing the simulated physicochemical property space occupied by molecules with low intracellular accumulation and high permeability. Individual molecules in the reference set are indicated by yellow dots   The three graphs show: A) reference molecules with low intracellular accumulation and high permeability (inside green circle); B) physicochemical property space occupied by molecules with calculated low intracellular accumulation and high permeability (green circle same as in A); C) the simulated physicochemical property space occupied by molecules with high intracellular accumulation, regardless of permeability (green circle same as in A).
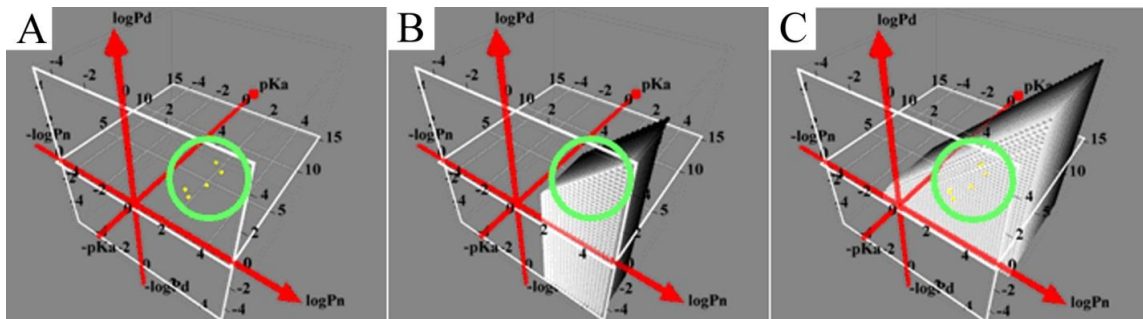
Figure 3.6. Visualizing the simulated physicochemical property space of various classes of non-selective, lysosomotropic molecules. Individual molecules in the reference set are indicated by yellow dots   The four graphs show: A) fifty six selectively mitochondriotropic reference molecules; B) seventeen lysosomotropic, reference molecules which are not selective in terms of lysosomal, mitochondrial or cytosolic accumulation; C) the simulated physicochemical property space occupied by lysosomotropic molecules that are also selectively mitochondriotropic; D) the simulated physicochemical property space of non-selective lysosomotropic, non-selective mitochondriotropic molecules.
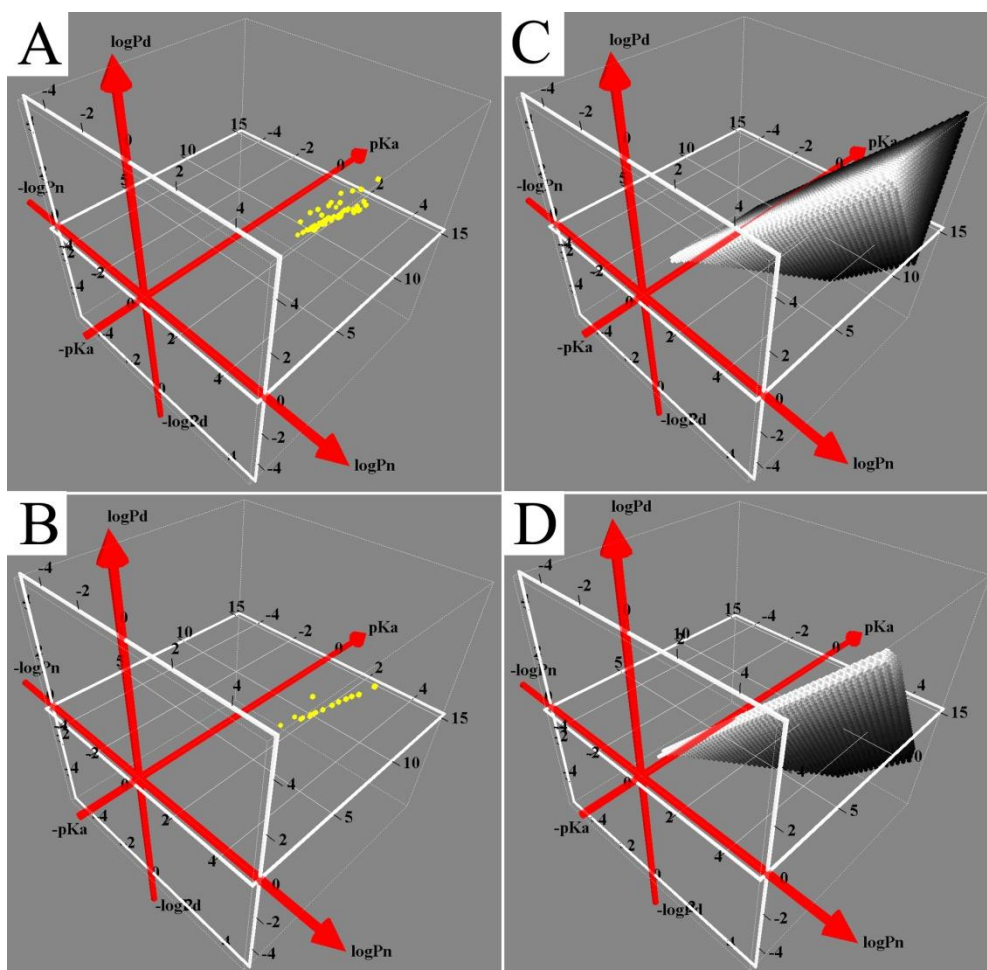
Figure 3.7. Visualizing the effect of extracellular pH on physicochemical property space occupied by selectively-lysosomotropic molecules. Simulations were carried out using an apical pH of 4.5 (A-C) and 6.8 (D-F) in the R-Model. Yellow dots indicate the individual molecules in the reference set. Each row shows the physicochemical property space occupied by molecules in different permeability classes, as follows: A and D) $P_{eff} < 1 \times 10^{-6}$ cm/s; B and E) 1×10^{-6} cm/s $< P_{eff} < 35 \times 10^{-6}$ cm/s, C and F) $P_{eff} > 35 \times 10^{-6}$ cm/s.
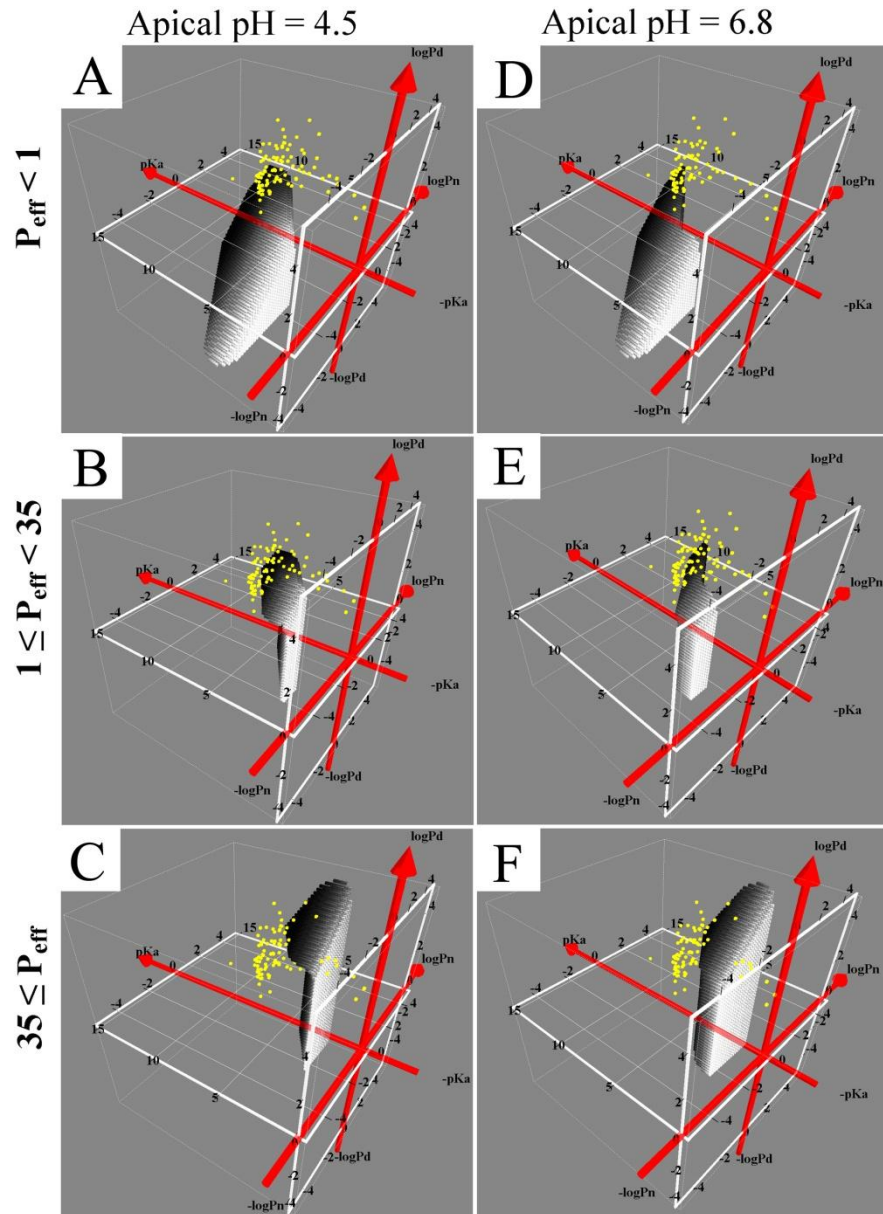
Chapter IV

The Intracellular Accumulation of Chloroquine:
Simulation-Based Analysis of the Phospholipidosis Effect

Abstract

In vivo, the weakly basic, lipophilic drug chloroquine (CQ) accumulates in the kidney to concentrations more than thousand-fold greater than in plasma. To study the cellular pharmacokinetics of chloroquine in cells derived from the distal tubule, Madin-Darby Canine Kidney (MDCK) cells were incubated with CQ under various conditions. CQ progressively accumulated without exhibiting steady state behavior. Experiments failed to yield evidence that known active transport mechanisms mediated CQ uptake at the plasma membrane. CQ induced a phospholipidosis-like phenotype, characterized by the appearance of numerous multivesicular and multilamellar bodies (MLB/MVBs) within the lumen of expanded cytoplasmic vesicles. Other induced phenotypic changes including changes in the volume and pH of acidic organelles were measured, and the integrated effects of all these changes were computationally modeled with a cell based pharmacokinetics simulator, to establish their impact on intracellular CQ mass accumulation. Based on CQ's passive transport behavior, the measured phenotypic changes fully accounted for the continuous, non-steady state CQ accumulation kinetics. Consistent with the simulation results, Raman confocal

microscopy of live cells confirmed that CQ became highly concentrated within induced, expanded cytoplasmic vesicles that contained multiple MLB/MVBs. Progressive CQ accumulation was increased by sucrose, a compound that stimulated the phospholipidosis-like phenotype, and was decreased by bafilomycin A1, a compound that inhibited this phenotype. Accordingly, phospholipidosis-associated changes in organelle structure and intracellular membrane content can exert a major influence on the local bioaccumulation and biodistribution of drugs.

Introduction

Xenobiotics can accumulate and reach very high concentrations in specific sites of the body due to active transport across cellular membranes, binding and partitioning into cellular components, or sequestration within organelles driven by pH gradients and trans-membrane electrical potentials present across phospholipid bilayers. For example, more than thirty years ago, DeDuve discovered that weakly basic molecules would accumulate within lysosomes by an ion trapping mechanism [1]. Ion trapping arises when a phospholipid bilayer separates two compartments of different pH levels. Under these conditions, basic membrane permeant lipophilic molecules become protonated and charged preferentially in the acidic compartment. Because of the lowered membrane permeability of the charged form of the molecule, the molecule becomes concentrated in the acidic compartment. Since then, many weakly basic, lipophilic small molecules have been reported to be sequestered within lysosomes or other acidic, membrane-bound intracellular compartments, through passive ion trapping [2-4].

However, detailed mass measurements have revealed that DeDuve's classical ion trapping mechanism often underestimates the extent of sequestration of many weakly basic compounds within acidic endolysosomal organelles [5, 6]. In fact, intracellular accumulation of weak bases may also be explained by active transport mechanisms or by the many concomitant changes in endolysosomal organelle structure and function, including alterations in pH and changes in membrane traffic leading to the formation of endolysosomal

124

organelles with unique membrane characteristics [7, 8]. In some cell types, exposure to lipophilic weak bases induces a peculiar phenotype, "phospholipidosis" [9], characterized by the formation of numerous, phospholipids- and cholesterol-rich multivesicular and multilamellar bodies (MLB/MVBs). Physiologically, MLB/MVBs are late endosomal compartments that normally form as a result of the activation of the ubiquitin-dependent membrane protein sorting and degradation pathway [10-12].

Previously, we developed a computational model of cell pharmacokinetics to predict the intracellular accumulation and transcellular transport properties of small molecules across cell monolayer [6, 13]. Using the weakly dibasic, high solubility drug chloroquine (CQ, pKa_1 = 9.96 and pKa_2 = 7.47) as a test compound, the model was capable of capturing the transcellular transport kinetics for the first four hours of drug treatment but underestimated the intracellular accumulation beyond the first five minutes of incubation [6]. Experimentally, the initial rate of transport of CQ across cell monolayer was directly proportional to initial concentrations in donor compartment. Also transport of CQ across MDCK monolayer in the presence of a transcellular concentration gradient was similar in both apical-to-basolateral and basolateral-to-apical directions. No saturation or nonlinear kinetics were observed at CQ concentrations < 500 μM, as expected from a passive transport mechanism [6].

Here, we present an alternative hypothesis to explain CQ accumulation: that drug-induced phospholipidosis corresponds to an inducible, weak base disposition system – a mechanism promoting CQ sequestration within cells. We

performed a detailed quantitative analysis of CQ pharmacokinetics in Madin-Darby Canine Kidney (MDCK) cells, a cell line that stably expresses the differentiated properties of distal tubular epithelial cells [14], extensively accumulates CQ and exhibits a marked phospholipidosis-like response [15] corresponding to the phospholipidosis phenotype reported in the kidney cells of CQ-treated patients [16]. The potential involvement of active transporters and plasma membrane mediated uptake mechanisms was evaluated in the presence of extracellular pH changes, sodium-free medium, and organic cation transporter inhibitors.

Although CQ concentration in plasma ranges between 10 to 250 nM [17, 18], cells lining the distal tubules are exposed to 10 to 300 μM CQ corresponding to the concentrations measured in the urine of human subjects [17]. Therefore clinically relevant urine concentrations (0-200 μM) of CQ were used to mimic the physiological conditions of the distal tubule, and used as input parameters in the cellular PK model of CQ's transport behavior. Simulation results were compared to experimental measurements of intracellular CQ mass in dose-response and time-course experiments, under condition that enhances phospholipidosis effect (co-treatment with sucrose [19, 20]) or inhibits vacuolation (co-treatment with bafilomycin A1 [21]).

Materials and Methods

Cell Culture. Madin-Darby canine kidney (MDCK) cells were purchased from ATCC (CCL-34[TM]) and grown in Dulbecco's modified Eagle's medium

(DMEM, Gibco® 11995) containing 10% FBS (Gibco® 10082), 1X non-essential amino acids (Gibco® 11140) and 1% penicillin/streptomycin (Gibco® 15140), at 37ºC in a humidified atmosphere with 5% CO_2. MDCK cells were seeded at a density between 1×10^5-2×10^5 cells per square centimeter and were grown until cell monolayer was formed as suggested by visual inspection.

Drugs and chemicals. Chloroquine diphosphate (CQ), cimetidine (Cim), guanidine (Gua) and tetraethylammonium (TEA) were obtained from Sigma-Aldrich (Catalog numbers C6628, C4522, G4505 and T2265) and dissolved in Dulbecco's Phosphate-Buffer Saline (DPBS, Gibco® 14190) at a concentration of 100mM for storage at 4 ℃. Bafilomycin A1 (Baf), hemicholinium-3 (HC3) and hydrocortisone (Sigma® B1793, H108 and H0888) were dissolved in DMSO (Sigma® D8418) to a final concentration of 5 μM (Baf) or 50 mM (HC3 and HCor) for storage at -20 ºC. 3-methyladenine (3MA, Sigma® M9281) was dissolved in warm DMEM at a concentration of 10 mg/ml immediately before use. FITC-dextran (FD, Sigma® FD150S) was dissolved in DPBS at a concentration of 10 mg/ml for storage at 4 ℃. Fluorescent dyes including BCECF-AM, LysoTracker® Green (LTG) and Hoechst 33342 (Molecular Probes® B1150, L7526 and H3570) were stored according to the manufacturer's instructions.

Measurement of LTG fluorescence intensity, distribution and LTG-labeled organelle volumes. MDCK cells were grown on optical bottom plate or chamber glass, subject to various CQ treatment, stained with 0.5 μM LTG for 30 min, and subject to microscopic analysis *in situ*. A Nikon TE2000S *epifluorescence microscope with* standard mercury bulb illumination, coupled to *a*

*CCD camera (*Roper Scientific, Tucson, AZ*), with a 20X objective ((Nikon Plan Fluor ELWD 20x) or a 100X oil immersion objective (Nikon CFI Plan Fluor 100xH oil),* and a triple-pass DAPI/FITC/TRITC filter set (Chroma Technology Corp. 86013v2) was used to image the LTG-labeled cells. The 12-bit grayscale images were acquired with the FITC channel, and background subtracted. The LTG-labeled expanded vesicles (or the MLB/MVBs contained within) were manually outlined with Circular Region tool in MetaMorph® software (Molecular Devices Corporation, Sunnyvale, CA). The volume and surface area of individual vesicles was calculated assuming a spherical shape. Fluorescence volume density was calculated as Integrated Intensity divided by vesicle volume. The total vesicular volume/surface area per cell under each treatment at each time point (0, 1, 2 or 4 hours) was determined using 10 cells. Contrast and brightness was adjusted to the same level for all figures.

Raman confocal microscopy of CQ distribution. MDCK cells were seeded on cover glass until confluent. CQ-treated cells were exposed 10 μM CQ for 12 hours, followed by 100 μM CQ for 2 hours, and briefly washed in DPBS buffer prior to mounting on microscope slides.. The induced Raman spectrum of solid CQ salt, 100 mM CQ solution in DPBS, and the vesicular/cytosolic regions of the cells under various treatment conditions was acquired with a Renishaw inVia confocal Raman microscope coupled with a Nikon CFI Plan Fluor 100xH oil immersion objective and a CCD detector. The excitation wavelength was 514 nm. The exposure time was 30 sec for each measurement, with spectral resolution set to 1.5 cm^{-1}, scanning from 400 cm^{-1} to 3200 cm^{-1}. All spectra were

128

smoothened, baseline subtracted and normalized to the highest peak with ACD/UV-IR Processor (ACD/Labs, Toronto, Canada). To determine the effect of pH on CQ's Raman spectra, spectra of 100 mM CQ solution in pH 7, 6 and 5 buffers were also acquired.

Measurement of lysosomal, cytosolic and extracellular pH. pH measurements were performed using published methods [22]. To measure lysosomal pH, MDCK cells were incubated with 0.2 mg/ml FD in DMEM for 24 hours in dark prior to drug treatments. FD-loaded cells were washed twice with warm DPBS buffer, incubated in CQ-DMEM with or without Suc or Baf for 1, 2, 3 or 4 hours. To measure cytosolic pH, BCECF-AM was added to a final concentration of 2 μg/ml during the last 30 min of drug treatment, in the dark. At the end of treatments, cells on plate were washed twice with cold buffer prior to ratiometric analysis of the pH-sensitive FD or BCECF-AM fluorescence signal. Fluorescence data was acquired with a BioTek Synergy^{TM} 2 Microplate Reader using Ex.485/20-Em.528/20 filter set and Ex.450/50-Em.528/20 filter set. Background fluorescence was acquired with dye-free untreated cells. Standard curves were obtained by first preloading untreated cells with 0.2 mg/ml FD for 24 hrs or 2 μg/ml BCECF-AM for 30 min, then equilibrating with 10 μg/ml nigericin in different pH buffer, and finally scanning with the same filter sets as mentioned above. The fluorescence ratio (FR) was calculated as: $FR = \dfrac{F485_i - F485_{bg}}{F450_i - F450_{bg}}$,

where $F485_i$ and $F450_i$ standard for integrated fluorescent intensity from the ith well of cells under Ex.485 nm and Ex.450 nm, respectively, and the subscript *bg* indicates background fluorescence. FR values were plotted against known pH

values to create a standard curve, or compared with the standard curve to calculate pH. Extracellular pH was measured with a Corning pH meter 430 at designated time points. The average vesicular pH, cytosolic pH and extracellular pH were reported as the mean ± S.D. over a 4-hour incubation period with each time point measured from 3 independent experiments.

Measurement of cell volume. Cells were detached from the tissue culture plates after drug treatment by incubating them with 0.25% trypisin-EDTA (Gibco® 25200) for 15 min. The rounded, detached cells were imaged with Nikon TE2000S inverted *microscope under brightfield illumination with* a 20X objective (*Nikon CFI Plan Fluor 20x)*. In the images, the perimeters of the cells were manually outlined with Circular Region Tool in MetaMorph® and cell volume was calculated from the radius of the outlined perimeter, assuming spherical shape. For each treatment, 10 bright field images (more than 100 cells) were collected after 1, 2, 3 or 4 hours. The average cell volume was reported as the mean ± S.D. over 4 hour treatment.

Measurement of the cellular partition coefficient of CQ. MDCK cells were grown on tissue culture dishes, treated with 50 μM CQ for 4 hours to induce vacuolar expansion and MLB/MVBs. After this induction period, the cells were permeabilized with 0.1% saponin in DPBS buffer for 30 min to extract soluble cellular components while leaving lipids, DNA, and associated, insoluble cytoskeletal components. Permeabilized cells were then incubated with 100 μM CQ for 1 hour, washed twice and centrifuged. Cellular lipids and associated molecules were extracted from the pellet with 1% Triton X-100 in DPBS for 1

130

hour. Nuclei and other insoluble debris were spun down, and the amount of extracted CQ in the supernatants was determined by measuring absorbance at 343 nm using Microplate Reader. Based on electron micrographs, we estimated a Triton-extractable, 5% lipid volume fraction in the cell. CQ concentration partitioned into the cellular lipid structures was calculated as bound CQ amount divided by the estimated lipid volume for the cells. The lipid partition coefficient was calculated as the logarithm of the lipid:buffer CQ concentration ratio.

Probing the mechanism of CQ uptake with transport inhibitors. To study the effect of active cation transporters on CQ uptake, MDCK cells on 24-well tissue culture plates (Costar® 3526 or Nunc™ 165305) were incubated with 50 μM CQ in 0.5 mL bicarbonate-free transport buffer (sodium chloride 140 mM, potassium chloride 5.4 mM, calcium chloride 1.8 mM, magnesium chloride 0.8 mM, d-glucose 25 mM, HEPES 10 mM, pH 5.5, 6.5, 7.4 and 8.5) or sodium-free, choline-based transport buffer (substitute sodium chloride with choline chloride in the above transport buffer), at 37 ℃. To study the effect of autophagy, energy supply, vacuolar-ATPase, organic cation transporters (OCTs) and pre-expanded lysosomal volume on CQ uptake, MDCK cells were incubated in 0.5 mL DMEM containing 50 μM CQ in the presence or the absence of 10 mg/ml 3MA (autophagy inhibitor); 5 μM FCCP (mitochondrial uncoupling agent that disrupts ATP synthesis and cellular metabolism); 10 nM Baf (vacuolar H+/ATPase inhibitor that disrupts endolysosomal pH gradients); 500 μM Cim (OCT inhibitor); 500 μM Gua (OCT inhibitor); 500 μM HC3 (OCT inhibitor); 500 μM TEA (OCT substrate/inhibitor); 20 μM HCor (a hormone that stimulates OCT expression); or,

0.1 M Suc (a treatment that enhances the phospholipidosis phenotype without competing with CQ uptake). Cells co-treated with CQ and sucrose (Suc) or hydrocortisone (HCor) were pre-incubated with 0.1 M sucrose or 20 μM hydrocortisone in DMEM for 24 hours or 48 hours, respectively, before the experiments. CQ uptake was measured 0.5, 5, 15, 30, 60, 120, 180 or 240 min after beginning of incubation with CQ, with or without Suc or Baf. CQ uptake was measured 30 min and 240 min after the beginning of incubation. For CQ uptake measurements, three of the four replicates under the same treatment were briefly washed with cold buffer and lyzed in 1% Triton X-100 for 1 hour. The lysates were centrifuged at 15,000 rpm for 10 minutes and the supernatant was collected for CQ measurement by reading absorbance at 343 nm using Microplate Reader. Intracellular CQ mass was normalized by the number of cells per well as evaluated by counting cells in the fourth replicate well. Background signal from 0 μM CQ treatment was subtracted and CQ mass was calculated with the aid of a standard curve. The results were expressed as mean ± S.E.M from 3 independent experiments for each time point.

Measurement of MLB/MVB morphology. For transmission electron microscopy, MDCK cells were grown on tissue culture dish (BD Falcon^{TM} 353003), incubated with 50 $\square$M CQ for 4 hours, washed twice with serum-free DMEM, fixed with 2.5% glutaraldehyde in 0.1 M Sorensen's buffer at pH 7.4 at 37 ℃, and washed with 0.1 M Sorensen's buffer three times, 5 min each. Cells were fixed with 1% osmium tetroxide in 0.1 Sorensen's buffer for 15 min at room temperature and washed three times with double-distilled water. Cells were

incubated with 8% uranyl acetate in double-distilled water for 1 hour at room temperature, dehydrated in a graded ethanol:water series (50, 70, 90 and 100%, 5 min each), infiltrated in Epon resin and polymerized at 60 ℃ overnight. Cells were sectioned and photographed with a Phillips CM-100 transmission electron microscope at magnifications from 2,600 to 96,000X. More than 5 cells were photographed for control and treated cells under each condition. Quantitative morphological analysis of EM images was performed with MetaMorph® software (Molecular Devices, Inc.)

Mathematical Modeling of CQ Uptake. A multi-compartment, constant-field, fixed-parameter mathematical model [23] was adapted to predict the passive, membrane potential and pH-dependent ion trapping behavior of CQ in MDCK cells. The original model was modified to incorporate the gradual volume expansion of the endolysosomal compartment induced by CQ, coupled to changes in extracellular concentration accompanying pronounced, intracellular CQ sequestration. Briefly, the total change in CQ mass with time in each compartment was expressed by equations 1-4:

$$\frac{dM_e}{dt} = -A_c \times J_{e,c} \tag{1}$$

$$\frac{dM_c}{dt} = A_c \times J_{e,c} - A_m \times J_{c,m} - A_l \times J_{c,l} \tag{2}$$

$$\frac{dM_m}{dt} = A_m \times J_{c,m} \tag{3}$$

$$\frac{dM_l}{dt} = A_l \times J_{c,l} \tag{4}$$

where, *M* stands for the *total mass*, *J* indicates the *flux*, *A* and *V* indicate the *membrane surface area* and *volume*, respectively, of the specific subcellular

133

compartments as indicated by the subscripts *e, c, m,* and *l: extracellular compartment, cytosol, mitochondria* and (acidic) *lysosomes compartment. A_c* indicates the cell's plasma membrane area. The comma between two subscripts means "*to*" (e.g. "$J_{c,m}$" represents the flux from cytosol to mitochondria). With extracellular volume, cell volume and mitochondria volume constant and lysosomal volume change, the concentration change in each compartment was expressed by equations 5-8:

$$\frac{dC_e}{dt} = -\frac{A_c}{V_e} \times J_{e,c} \tag{5}$$

$$\frac{dC_c}{dt} = \frac{A_c}{V_c} \times J_{e,c} - \frac{A_m}{V_c} \times J_{c,m} - \frac{A_l}{V_c} \times J_{c,l} \tag{6}$$

$$\frac{dC_m}{dt} = \frac{A_m}{V_m} \times J_{c,m} \tag{7}$$

$$\frac{dC_l}{dt} = \frac{A_l}{V_l} \times J_{c,l} - \frac{dV_l}{dt} \times \frac{C_l}{V_l} \tag{8}$$

For CQ, the total flux is contributed by a neutral form and two ionized forms with one or two positive charges [6]. The total flux across membrane as contributed by three species can be calculated with Fick's equation and Nernst-Planck equation:

$$J_{o,i} = P_n(f_{n,o}C_o - f_{n,i}C_i) + P_{d1}\frac{N_{d1}}{e^{N_{d1}}-1}(f_{d1,o}C_o - f_{d1,i}C_i e^{N_{d1}}) + P_{d2}\frac{N_{d2}}{e^{N_{d2}}-1}(f_{d2,o}C_o -$$

$$f_{d2,i}C_i e^{N_{d2}}) \tag{9}$$

where, subscripts *o* and *i* indicate *outer-* and *inner-*compartment, *n, d1,* and *d2* indicate *neutral form, ionized form with one charge,* and *ionized form with two charges*, respectively. *P* is the *permeability across the bilayer membranes* and it was estimated based on the logarithm of CQ's octanol/water partition coefficient ($\log P_{o/w}$) calculated with ChemAxon® MarvinSkecth 5.1.4

(http://www.chemaxon.com) as $\log P_{n,d1,d2} = \log P_{o/w} - 6.7$ [23]. *f* represents the *ratio of the activities (a_n, a_{d1} and a_{d2}) and the total concentration*. It can be calculated from lipid fraction and ionic strength in each compartment and the sorption coefficient for each species as estimated from $\log P_{o/w}$ [13, 23] or the measured cellular partition coefficient [6]. In equation 4, $N = zEF/(RT)$, where $z = +1$ for N_{d1} (ionized base with one charge), and $z = +2$ for N_{d2} (ionized base with two charges); *E, F, R,* and *T* are *membrane potential, Faraday constant, universal gas constant,* and *absolute temperature*, respectively. The rate of change in vesicular volume was derived by fitting volume measurement at each time point with a linear model. When simulating CQ binding to MLB/MVBs, the measured cellular partition coefficient of CQ was used to estimate *f*. The ordinary differential equations were numerically solved with MATLAB® ODE15s solver using the average value of each parameter to plot a kinetic curve of CQ intracellular accumulation. Model validation/consistency check was performed by summing CQ mass in all compartments during the simulation, confirming that total CQ mass in the system stays constant (mass balance).

Parameter Sensitivity and Error Propagation Analysis. To determine whether variations in individual parameters would lead to a large variation in prediction, sensitivity analysis was performed by systemically changing one parameter at a time and plotting predictions against parameter values. In addition, Monte Carlo simulations were performed to assess the distribution CQ accumulation values that would be consistent with uncertainties or experimental error of the input parameters. Parameter ranges were obtained based on the

error of experimental measurements or variations in the published literature reports. MATLAB$^{®}$ ODE15s solver was employed to run 10,000 simulations during which simulation parameters were randomly sampled from uniform distributions within the range of parameter values (Table 4.2 and Appendix L). Histograms of simulation results were plotted with R program (http://www.r-project.org).

Results

CQ-treated MDCK cells undergo marked changes in organelle structure and membrane organization. Electron microscopy was performed to study the effects of CQ on the membrane and organelle structure of MDCK cells during the course of a 4 hour incubation period. Most strikingly, CQ induced the formation of numerous MLB/MVBs within the lumen of expanded cytoplasmic vesicles (Figure 4.1). The expanded vesicles were approximately 1.50 ± 0.34 μm (n = 20) in diameter. Within these expanded vesicles there were often many MLBs of 0.42 ± 0.025 μm (n = 10) in diameter and MVBs of 0.39 ± 0.03 μm (n = 10) in diameter. For MLBs, the spacing between membrane layers ranged from 24.0 to 29.2 nm (25.7 ± 2.2 nm) and the apparent thickness of each layer varied from 22.5 to 24.0 nm (23.2 ± 0.7 nm). For MVBs, the internal vesicles varied in size between 50 to 100 nm in diameter. It was generally the case that in the presence of CQ, each expanded vesicle contained several MLB/MVBs. Without CQ treatment, control cells completely lacked these features (data not shown).

136

Induced MLB/MVBs sequester weakly basic lipophilic molecules. LTG is a weakly basic fluorescent probe that labels acidic organelles within cells by the ion trapping mechanism. Fluorescence micrographs of CQ-treated cells incubated with LTG showed LTG fluorescence accumulation in enlarged vesicles ranging 1-2 μm in diameter. Most remarkably, at high magnification, LTG distribution within each one of the expanded vesicles was clearly associated with intralumenal MLB/MVBs (Figure 4.2A). In many of these vesicles, LTG was clearly localized to multiple internal vesicles of about 0.34 ± 0.06 μm (n=20) in diameter, consistent with the numbers and diameters of the MLB/MVBs previously observed by electron microscopy. Based on quantitative image analysis, we calculated accumulation of LTG fluorescence bound to the MLB/MVBs was at least 4.7 ± 0.5 (n=20) –fold greater than its accumulation in the lumen of the expanded vesicle. LTG-labeled MLB/MVBs appeared to move by Brownian motion, within the confines of the outer membrane bounding the expanded vesicles (Figure 4.2A, *a-f*). Increasing CQ concentrations did not inhibit LTG fluorescence accumulation. Instead, the accumulation of LTG fluorescence in the vacuoles was directly dependent on the concentration of CQ used for treatment showing no evidence of competition or saturation (Figure 4.2B).

CQ accumulates within induced, expanded vesicles. The MLB/MVB containing, LTG-labeled vesicles induced by CQ corresponded to large, clear vacuoles apparent by brightfield transmitted light microscopy (Figure 4.3A). Confocal Raman microscopic imaging was performed in CQ-treated (Figure 4.3B, *a*) and -untreated (Figure 4.3B, *b*) cells. The signature Raman signal of CQ

137

(Figure 4.3B, spectrum 1, arrows, 1370 and 1560 cm^{-1}) was present in the vacuoles observed by brightfield transmitted light microscopy (Figure 4.3B, spectrum 2), yet CQ signal was mostly undetectable in the vesicle-free regions of the same cells (Figure 4.3B, spectrum 3). In control experiments, the signal intensity of the Raman vibrational peaks of CQ at 1370 and 1560 cm^{-1} were constant between pH 7 and 5 (data not shown), so differences in the pH of intracellular compartments cannot explain the observed, spectral differences in Raman signal. Furthermore, CQ signal was completely absent from untreated cells (Figure 4.3B, 4 and 5). Given their small volume, the presence of Raman signal within the vacuoles of CQ-treated cells confirmed that CQ is highly concentrated within these vesicles.

CQ uptake is coupled to induction of phospholipidosis-like phenotype and cannot be inhibited by OCT inhibitors. Consistent with the neutral, membrane-permeant form of CQ being mostly responsible for its passive cellular uptake, CQ uptake within the first 30 minutes was significantly reduced in by lowering extracellular pH (Figure 4.4A) but not significantly affected by the presence of OCT inhibitors and a stimulator (Cim, Gua, HC3, TEA or HCor) nor by the substitution of sodium with chloride in the transport buffer (Figure 4.4B). Incubation at 4 ℃ reduced CQ uptake in the first 30 min, consistent with inhibited passive diffusion at low temperature, while pre-incubation with 0.1 M sucrose-DMEM, a treatment that induced lysosomal volume expansion, stimulated CQ uptake by 32% during this time (Figure 4.4B). Bafilomycin A1, a vesicular-ATPase inhibitor which hampers the acidification of lysosomes, reduced CQ

138

uptake by 21% within the first 30 min of CQ incubation, while the autophagy inhibitor 3MA did not (Figure 4.4B). After 4h treatment, a close correlation between CQ uptake (Figure 4.4C) and lysosomal volume expansion (Figure 4.4D) was observed: in cells treated with Baf and FCCP, CQ-induced vesicular expansion was significantly suppressed, and so was the cellular uptake; in cells treated with transporter inhibitors, sucrose or 3MA, no significant reduction in vesicular expansion nor cellular uptake were observed, as compared with CQ treatment alone. In the presence of Suc, 3MA, or other OCT inhibitors we also observed LTG fluorescence accumulated in association with the MLB/MVBs present within the induced, expanded vacuoles, as was observed in cells treated with CQ alone.

CQ affected organelle volume and pH. LTG-positive (acidic) organelle volume and pH, as well as cell volume and cytosolic pH, were measured at various time points, during a 4 hour CQ incubation period (Table 4.1). Experiments were also performed in the presence of 0.1 M Suc, a treatment that perturbs endolysosomal membrane traffic and promotes a phospholipidosis-like phenotype [20]. CQ uptake measurements were also performed in the presence of 10 nM Baf, a treatment that inhibits the phospholipidosis effect. CQ-induced vacuolation was greater in the presence of sucrose compared to cells treated with CQ alone, and was inhibited by Baf (Table 4.1). Total cell volume significantly expanded in Suc but not in CQ or CQ/Baf. (Table 4.1). CQ (with or without Suc or Baf) increased vesicular pH during 4-hour incubation period, but cytosolic pH was not significantly perturbed (Table 4.1). The extent of CQ

induced vesicular pH increase was highest in the presence of Suc, intermediate with Baf and least with CQ alone. At 200 µM CQ, CQ toxicity became apparent, with several of the observed trends becoming reversed (Table 4.1). Consistent with the large buffering capacity of the extracellular medium, measurements confirmed that CQ treatments with or without Suc or Baf did not alter the extracellular pH (Table 4.1).

Organelle volume and pH also affect CQ uptake. The effects of Suc and Baf on the pharmacokinetics of CQ were measured in dose-response and time-course experiments. Upon prolonged incubation, CQ exhibited a time-dependent, gradual accumulation over the 4h incubation period (Figure 4.5). Suc treatment prior to CQ incubation led to the most pronounced intracellular accumulation of CQ (Figure 4.5A). Baf inhibited the gradual accumulation of CQ, with cells showing a rapid uptake during the first five minutes, followed by a low, steady state level during the next four hours (Figure 4.5A). At 50 and 100 µM CQ, CQ accumulation over the 4h period appears almost linear in Suc-treated cells as well as in cells that were incubated with CQ alone (Figure 4.5A).

Simulations of CQ cellular pharmacokinetics. Computational simulations of CQ uptake with a mathematical model that incorporates volume expansion of acidic organelles, protonated CQ binding to MLB/MVBs, and using the measured parameter values as input yielded CQ dose-response and time-course traces that were consistent with the experimentally measured values (Figure 4.5A) and well within the simulated margins of error based on physiologically-relevant ranges of input parameters (Figure 4.5B). The effects of Suc and Baf on CQ

140

uptake paralleled the experimental measurements (Figure 4.5A) for 25, 50 and 100 μM CQ treatments. Simulation results for 200 μM treatments tended to over-predict CQ uptake (Figure 4.5A), which we ascribe to the toxic effects that were apparent at this higher dose. Overall, the accuracy of predicted cellular uptake was good for a wide range of different CQ concentrations, in the presence or absence of Suc or Baf at 8 time points, with 70% of the predicted values within a factor of 2 or 86% within a factor of 3 of the measured cellular uptake values (Figure 4.6). Except for 200 μM treatments during which cellular uptake were possibly reduced by toxic effect, most other discrepancies were observed between predictions and measurements for the first time points when the amount of cellular CQ uptake was close to the detection limit of the instrument.

For comparison, the simulated intracellular CQ mass at the end of a 4-hour incubation period was calculated under three different conditions (1) in the presence of ion trapping but without expanding organelle volumes nor binding of protonated CQ species to MLB/MVBs (Figure 4.5B, green); (2) in the presence of ion trapping within expanding acidic organelles but without binding of protonated CQ species to MLB/MVBs (Figure 4.5B, blue); and (3) in the presence of ion trapping in expanding acidic organelles, with binding of protonated CQ species to MLB/MVBs (Figure 4.5B, black). Parameter sensitivity analysis [24] showed that molecular properties including pK_a and log$P$ for the neutral forms or ionized forms, pH and volume in the extracellular compartment, volume in the cytosol, pH, volume, membrane potential, ionic strength and lipid fraction in the lysosomes were important factors (caused a >20% change with parameters randomly

141

sampled from physiologically-relevant ranges) for CQ uptake. Consequently, Monte Carlo simulations were performed to calculate a distribution of predicted CQ accumulation values based on a range of these input parameters, in cells incubated with CQ alone, or in combination with Suc or Baf.

The impact of CQ induced phenotypic effects on the predicted cellular accumulation of CQ was consistent with most of the intracellular CQ accumulation occurring within the expanding acidic (LTG-positive) vesicles. Based on the simulations, the volume increase of acidic organelles led to a > 5 fold increase in the predicted intracellular mass (Figure 4.5B, green vs. blue), while adding an MLB/MVB binding component led to an additional 2-fold increase in intracellular CQ mass (Figure 4.5B, blue vs. black). Simulation results incorporating vesicular expansion and CQ binding to MLB/MVBs corresponded to the range of measured values (Figure 4.5B, black vs. red lines).

The greatest discrepancy between simulation results and experimental measurements was observed in Baf-treated cells. This discrepancy can be ascribed to measurement errors: In Baf, LTG uptake is much reduced and the diameter of acidic vesicles was close to the optical resolution limit of the microscope, so the organelle volume measurements were less precise as compared to the other conditions. Also, the accuracy and precision of CQ mass measurement in the presence of Baf was considerably lower than in the other experimental conditions, because the CQ signal in Baf was almost undetectable.

Discussion

In this study, we used MDCK cells exposed to 0 to 200 μM CQ as a physiologically-relevant *in vitro* experimental model to analyze CQ pharmacokinetics in cells of the distal renal tubule. We present quantitative evidence that the phospholipidosis-like phenotypic effect induced by CQ may be responsible for the observed, non-steady state intracellular accumulation of CQ. In the process, we elaborated a computational *in silico* model for simulating how phospholipidosis affects the cellular pharmacokinetics of small molecule drugs. As a physiologically-relevant transport probe, CQ is a weak base drug for treatments of malaria, arthritis, viral infection and cancer [25, 26]. Despite of its high solubility, CQ has slow clearance, accumulates in kidney (and other organs) >1000-fold relative to plasma concentrations, and has highly variable pharmacokinetics with the elimination half-life ranging from 20-60 days [27]. Significant variability in CQ pharmacokinetics have been ascribed to differences in protein binding, but functional differences in renal filtration could also be involved as the drug is mostly cleared by the kidney [28].

Previous studies have established that CQ reached high concentrations inside cells with particularly high levels in the lysosomes [29], presumably by the action of a carrier-mediated active transport mechanism. However, while CQ may be a substrate of multiple drug resistance 1 protein [30] and organic cation transporter-like 2 protein [31], both of these are involved in the excretion of drugs from cytosol to the extracellular medium. No active transporter mechanisms have been found to play a role in CQ cellular uptake. The organic cation

transporter 2 (OCT2) plays important roles in the uptake of cationic compounds in the kidney, but chloroquine does not appear to interact with OCT2 [32]. In fact, unlike other organic cations which are substrates of an active transporter (i.e., plasma membrane monoamine transporter or PMAT) [33], the cellular uptake of CQ did not depend on sodium concentration in the extracellular medium (Figure 4B and 4C). Also, while low pH in the extracellular medium has been found to stimulate the uptake of PMAT substrates, we found it significantly inhibited CQ uptake. Lastly, PMAT and OCTs are not extensively expressed in normal, distal tubular cells [34, 35]. Therefore, all available evidence supports the role of passive diffusion in CQ crossing biological membranes of MDCK cells (Figure 4A). We found that many pharmacological OCTs inhibitors did not affect cellular uptake of CQ (Figure 4A, 4B and 4C), while all treatments that directly affected the cellular vacuolation response did affect CQ uptake.

Microscopically, the appearance of MLB/MVBs in MDCK cells treated with CQ corresponds to the morphology of kidney cells of CQ-treated patients, as well as that of other cells following exposure to weakly basic, lipophilic drugs [16, 36, 37]. The sizes of the expanded vesicles and the internal vesicles as measured by fluorescence microscopy and TEM were comparable (Figure 1 and 2). The discrepancy between the absolute values of these two measurements can be ascribed to differences in sample preparation as well as the resolution of these two instruments. In fluorescence microscopy the samples are fresh and immersed in living cell environment, while in EM the samples are dehydrated. Secondly, for TEM sample preparation, cells are sliced with a ultramicrotome so

144

the diameter of the vesicles in TEM micrographs might not be the actual equatorial diameter. As a result, the measured size of the expanded vesicles in TEM images seemed smaller than measurements from fluorescent images. When comparing the measured sized of internal vesicles in MLB/MVB, the discrepancy in measured sizes was not significant considering the relatively low resolution of the fluorescence microscopy (1 pixel = 0.047 μm in this study).

Meanwhile a close relation between CQ-induced volume expansion of LTG-positive vesicles and CQ uptake was observed (Figure 4B and 4C). Accordingly, we sought to measure the cellular pharmacokinetics of CQ in dose-response and time-course experiments. In turn, these measurements were compared to simulation results obtained by modeling intracellular CQ mass accumulation under three different scenarios: (1) in the absence of CQ-induced phenotypic effects; (2) in the presence of expanding acidic organelles; and (3) in the presence of expanding acidic organelles coupled to binding to intralumenal MLB/MVBs. We found that the latter condition yielded results that were largely consistent with the measured absolute CQ levels as well as the relative changes of intracellular CQ mass under several different conditions.

Supporting a role for MLB/MVBs in the sequestration of CQ, LTG (a weakly basic fluorescent probe that accumulates in acidic organelles due to ion trapping) was visibly concentrated within MLB/MVBs in the lumen of expanded cytoplasmic vesicles induced by CQ. The inability of 3MA to inhibit the phenotypic effects induced by CQ suggests that the phospholipidosis effects of CQ are not due to an induced, autophagocytic mechanism. Experiments and simulations of CQ

uptake in combination with Suc provided evidence that stimulating the phospholipidosis-like phenotype facilitates CQ accumulation. Experiments and simulations of CQ uptake in combination with Baf provided evidence that inhibiting the phospholipidosis-like phenotype decreases CQ accumulation. Lastly, Raman confocal microscopy confirms that intracellular CQ accumulates within the expanded, CQ-induced cytoplasmic vesicles with intralumenal MLB/MVBs, as predicted by the model. Phospholipids such as phosphatidylcholine have very high affinity for protonated CQ [38], consistent with most of the protonated CQ within the expanded vesicles being bound to the membranes of intralumenal MLB/MVBs.

It is also noteworthy that intracellular transformation into a less membrane permeant CQ metabolite cannot account for the continuous chloroquine accumulation in MDCK cells. With MDCK cell monolayers on porous membrane supports, we have previously demonstrated that intracellular CQ in MDCK cells is mostly present in intact form. While passive diffusion coupled to ion trapping and phospholipid binding can explain the observed transport behaviors, we also searched for evidence that CQ accumulated by an active transport mechanism. However, the effects of bafilomycin and sucrose, the lack of effect of active transport inhibitors, and the good correlation between vacuolar expansion and the level of CQ, the insensitivity to extracellular sodium, the pH sensitivity of CQ uptake, and the linear concentration dependence of CQ uptake all made it very difficult to relate CQ's behavior to candidate active transport mechanisms.

To conclude, our results indicate that the phospholipidosis effects of CQ may underlie an inducible, highly effective, intracellular weak base sequestration system. To our knowledge, this is the first study to evaluate the potential effects of phospholipidosis on the cellular pharmacokinetic behavior of a weakly basic molecule. Our simulations and experimental results converge to provide evidence those changes in organelle structure and membrane organization induced by CQ can profoundly alter the intracellular bioaccumulation and distribution of CQ according to its passive transport properties, leading to the non-steady state accumulation behavior. Considering that these morphological changes have been reported in other weak base drugs that accumulate intracellularly such as procainamide and amiodarone [21], our results indicate that phenotypic changes associated phospholipidosis warrant consideration as candidate, mechanistic determinants of the local (and systemic) distribution and disposition of weakly basic lipophilic molecules in the tissues and organs of the body, especially in cells exposed to high local concentrations of the drug. Passive transport models have been successfully used for developing predictive physiologically-based pharmacokinetic models of bioaccumulation and biodistribution of neutral or ionized organic compounds in tissues and organs [39-41]. For weakly basic molecules, incorporating the cellular pharmacokinetic effects of phospholipidosis may considerably improve physiologically-based pharmacokinetic and biodistribution predictions.

References

1. C. de Duve, T. de Barsy, B. Poole, A. Trouet, P. Tulkens, and F. Van Hoof. Commentary. Lysosomotropic agents. *Biochem Pharmacol.* 23:2495-2531 (1974).

2. R. Hayeshi, C. Masimirembwa, S. Mukanganyama, and A.L. Ungell. Lysosomal trapping of amodiaquine: impact on transport across intestinal epithelia models. *Biopharm Drug Dispos.* 29:324-334 (2008).

3. Y. Gong, Z. Zhao, D.J. McConn, B. Beaudet, M. Tallman, J.D. Speake, D.M. Ignar, and J.P. Krise. Lysosomes contribute to anomalous pharmacokinetic behavior of melanocortin-4 receptor agonists. *Pharm Res.* 24:1138-1144 (2007).

4. M.T. Bawolak, G. Morissette, and F. Marceau. Vacuolar ATPase-mediated sequestration of local anesthetics in swollen macroautophagosomes. *Can J Anaesth* (2010).

5. M. Duvvuri and J.P. Krise. A novel assay reveals that weakly basic model compounds concentrate in lysosomes to an extent greater than pH-partitioning theory would predict. *Mol Pharm.* 2:440-448 (2005).

6. X. Zhang, N. Zheng, P. Zou, H. Zhu, J.P. Hinestroza, and G.R. Rosania. Cells on Pores: A Simulation-Driven Analysis of Transcellular Small Molecule Transport. *Mol Pharm.* 7:456-467 (2010).

7. J. Heuser. Changes in lysosome shape and distribution correlated with changes in cytoplasmic pH. *J Cell Biol.* 108:855-864 (1989).

8. U.E. Honegger, G. Quack, and U.N. Wiesmann. Evidence for lysosomotropism of memantine in cultured human cells: cellular kinetics and effects of memantine on phospholipid content and composition, membrane fluidity and beta-adrenergic transmission. *Pharmacol Toxicol.* 73:202-208 (1993).

9. M.J. Reasor and S. Kacew. Drug-induced phospholipidosis: are there functional consequences? *Exp Biol Med (Maywood).* 226:825-830 (2001).

10. J. Gruenberg and H. Stenmark. The biogenesis of multivesicular endosomes. *Nat Rev Mol Cell Biol.* 5:317-323 (2004).

11. P. Saftig and J. Klumperman. Lysosome biogenesis and lysosomal membrane proteins: trafficking meets function. *Nat Rev Mol Cell Biol.* 10:623-635 (2009).

12. R.C. Piper and D.J. Katzmann. Biogenesis and function of multivesicular bodies. *Annu Rev Cell Dev Biol.* 23:519-547 (2007).

13. X. Zhang, K. Shedden, and G.R. Rosania. A cell-based molecular transport simulator for pharmacokinetic prediction and cheminformatic exploration. *Mol Pharm.* 3:704-716 (2006).

14. M.J. Rindler, L.M. Chuman, L. Shaffer, and M.H. Saier, Jr. Retention of differentiated properties in an established dog kidney epithelial cell line (MDCK). *J Cell Biol.* 81:635-648 (1979).

15. K.Y. Hostetler and D.D. Richman. Studies on the mechanism of phospholipid storage induced by amantadine and chloroquine in Madin Darby canine kidney cells. *Biochem Pharmacol.* 31:3795-3799 (1982).

16. J. Muller-Hocker, H. Schmid, M. Weiss, U. Dendorfer, and G.S. Braun. Chloroquine-induced phospholipidosis of the kidney mimicking Fabry's disease: case report and review of the literature. *Hum Pathol.* 34:285-289 (2003).

17. Y. Bergqvist, C. Hed, L. Funding, and A. Suther. Determination of chloroquine and its metabolites in urine: a field method based on ion-pair extraction. *Bull World Health Organ.* 63:893-898 (1985).

18. O. Walker, A.H. Dawodu, A.A. Adeyokunnu, L.A. Salako, and G. Alvan. Plasma chloroquine and desethylchloroquine concentrations in children during and after chloroquine treatment for malaria. *Br J Clin Pharmacol.* 16:701-705 (1983).

19. P.D. Wilson, R.A. Firestone, and J. Lenard. The Role of Lysosomal-Enzymes in Killing of Mammalian-Cells by the Lysosomotropic Detergent N-Dodecylimidazole. *Journal of Cell Biology.* 104:1223-1229 (1987).

20. A. Helip-Wooley and J.G. Thoene. Sucrose-induced vacuolation results in increased expression of cholesterol biosynthesis and lysosomal genes. *Experimental Cell Research.* 292:89-100 (2004).

21. G. Morissette, A. Ammoury, D. Rusu, M.C. Marguery, R. Lodge, P.E. Poubelle, and F. Marceau. Intracellular sequestration of amiodarone: role of vacuolar ATPase and macroautophagic transition of the resulting vacuolar cytopathology. *Br J Pharmacol.* 157:1531-1540 (2009).

22. C. Nilsson, K. Kagedal, U. Johansson, and K. Ollinger. Analysis of cytosolic and lysosomal pH in apoptotic cells by flow cytometry. *Methods Cell Sci.* 25:185-194 (2003).

23. S. Trapp and R.W. Horobin. A predictive model for the selective accumulation of chemicals in tumor cells. *Eur Biophys J.* 34:959-966 (2005).

24. N. Zheng, X. Zhang, and G.R. Rosania. The Effect of Phospholipidosis on the Cellular Pharmacokinetics of Chloroquine. *J Pharmacol Exp Ther* (2011).

25. B. Djordevic, C.S. Lange, and M. Rotman. Potentiation of radiation lethality in mouse melanoma cells by mild hyperthermia and chloroquine. *Melanoma Res.* 2:321-326 (1992).

26. W.M. Pardridge, J. Yang, and A. Diagne. Chloroquine inhibits HIV-1 replication in human peripheral blood lymphocytes. *Immunol Lett.* 64:45-47 (1998).

27. J. Ducharme and R. Farinotti. Clinical pharmacokinetics and metabolism of chloroquine. Focus on recent advancements. *Clin Pharmacokinet.* 31:257-274 (1996).

28. S. Krishna and N.J. White. Pharmacokinetics of quinine, chloroquine and amodiaquine. Clinical implications. *Clin Pharmacokinet.* 30:263-299 (1996).

29. K.Y. Hostetler, M. Reasor, and P.J. Yazaki. Chloroquine-induced phospholipid fatty liver. Measurement of drug and lipid concentrations in rat liver lysosomes. *J Biol Chem.* 260:215-219 (1985).

30. J.W. Polli, S.A. Wring, J.E. Humphreys, L. Huang, J.B. Morgan, L.O. Webster, and C.S. Serabjit-Singh. Rational use of in vitro P-glycoprotein assays in drug discovery. *J Pharmacol Exp Ther.* 299:620-628 (2001).

31. M. Reece, D. Prawitt, J. Landers, C. Kast, P. Gros, D. Housman, B.U. Zabel, and J. Pelletier. Functional characterization of ORCTL2--an organic cation transporter expressed in the renal proximal tubules. *FEBS Lett.* 433:245-250 (1998).

32. O. Zolk, T.F. Solbach, J. Konig, and M.F. Fromm. Structural determinants of inhibitor interaction with the human organic cation transporter OCT2 (SLC22A2). *Naunyn Schmiedebergs Arch Pharmacol.* 379:337-348 (2009).

33. K. Engel and J. Wang. Interaction of organic cations with a newly identified plasma membrane monoamine transporter. *Mol Pharmacol.* 68:1397-1407 (2005).

34. L. Xia, M. Zhou, T.F. Kalhorn, H.T. Ho, and J. Wang. Podocyte-specific expression of organic cation transporter PMAT: implication in puromycin aminonucleoside nephrotoxicity. *Am J Physiol Renal Physiol.* 296:F1307-1313 (2009).

35. U. Karbach, J. Kricke, F. Meyer-Wentrup, V. Gorboulev, C. Volk, D. Loffing-Cueni, B. Kaissling, S. Bachmann, and H. Koepsell. Localization of organic cation transporters OCT1 and OCT2 in rat kidney. *Am J Physiol Renal Physiol.* 279:F679-687 (2000).

36. A. Hallberg, P. Naeser, and A. Andersson. Effects of long-term chloroquine exposure on the phospholipid metabolism in retina and pigment epithelium of the mouse. *Acta Ophthalmol (Copenh).* 68:125-130 (1990).

37. F. Marceau, M.T. Bawolak, J. Bouthillier, and G. Morissette. Vacuolar ATPase-mediated cellular concentration and retention of quinacrine: a model for the distribution of lipophilic cationic drugs to autophagic vacuoles. *Drug Metab Dispos.* 37:2271-2274 (2009).

38.   Y. Kuroda and M. Saito. Prediction of phospholipidosis-inducing potential of drugs by in vitro biochemical and physicochemical assays followed by multivariate analysis. *Toxicol In Vitro* (2009).

39.   W. Fu, A. Franco, and S. Trapp. Methods for estimating the bioconcentration factor of ionizable organic chemicals. *Environ Toxicol Chem.* 28:1372-1379 (2009).

40.   J.Y. Yu and G.R. Rosania. Cell-based multiscale computational modeling of small molecule absorption and retention in the lungs. *Pharm Res.* 27:457-467 (2010).

41.   S. Trapp, A. Franco, and D. Mackay. Activity-based concept for transport and partitioning of ionizing organics. *Environ Sci Technol.* 44:6123-6129 (2010).

42.   R.J. Barry and J. Eggenton. Membrane potentials of epithelial cells in rat small intestine. *J Physiol.* 227:201-216 (1972).

Tables

Table 4.1. Cellular parameters obtained during 4-hour incubation with different concentrations of CQ. pH measurements and cell volume correspond to the average over the 4-hour incubation period; data was presented as mean ± S.D., n = 4. Vesicle volume corresponds to the volume at the end of the fourth hour treatment; data was presented as mean ± S.D., n = 10. Values in bold indicate a statistically significant difference from the untreated cells using Tukey's test ($p < 0.05$).

		vesicular pH	vesicle volume / cell (μm^3)	vesicle surface area / cell (μm^2)	cytosolic pH	cell volume ($10^3 \mu m^3$)	extracellular pH
Untreated		5.03±0.15	21±8	219±74	7.4±0.2	1.64±0.41	7.45±0.04
25 μM CQ	Suc	**5.91±0.23**	**602±145**	**2130±349**	7.37±0.02	**3.00±0.14**	7.48±0.03
	/	5.36±0.28	304±76	1159±47	7.36±0.04	1.66±0.12	7.48±0.03
	Baf	5.55±0.17	18±5	189±55	7.38±0.03	1.74±0.14	7.47±0.03
50 μM CQ	Suc	**6.08±0.20**	**843±176**	**2795±491**	7.36±0.01	**3.05±0.28**	7.47±0.03
	/	5.51±0.34	**587±126**	**2207±1050**	7.36±0.01	1.84±0.05	7.47±0.03
	Baf	5.69±0.37	19±4	204±24	7.35±0.02	1.70±0.15	7.47±0.03
100 μM CQ	Suc	**6.45±0.21**	**1121±343**	**2995±385**	7.37±0.02	**2.95±0.33**	7.50±0.02
	/	**5.81±0.21**	294±53	**1219±234**	7.35±0.04	1.83±0.12	7.50±0.02
	Baf	**5.88±0.14**	17±3	178±28	**7.34±0.03**	1.77±0.14	7.50±0.02
200 μM CQ	Suc	**6.73±0.28**	565±140	1468±351	7.37±0.02	**3.27±0.37**	7.50±0.02
	/	**5.98±0.45**	204±47	785±193	**7.30±0.02**	1.62±0.17	7.50±0.02
	Baf	**6.26±0.45**	17±4	186±32	**7.17±0.04**	1.78±0.09	7.50±0.02

Table 4.2. Parameter ranges for Monte Carlo simulations. pH, E, A, V, L and Is indicate *pH*, *membrane potential relative to the cytosol*, *surface area*, *volume*, *lipid fraction* and *ionic strength* in each compartment, while the subscripts a, c, l, and m indicate the *apical/extracellular*, *cytosolic*, *lysosomal* and *mitochondrial compartment*. pH_a, pH_l, V_l, V_c, A_l, rate of change in surface area or volume and cellular partition coefficient ($\log P_{n,d1,d2\_cell}$) were measurement as described in the manuscript. pK_{a1}, pK_{a2}, $\log P_n$, $\log P_{d1}$ and $\log P_{d2}$ were calculated by ChemAxon® based on weighted method prediction with 0.5 log units variant. Temperature (T) is set to 310.15 K during uptake experiment. Ionic strength and membrane potential values were based on literature report [13, 23, 42].

		CQ				CQ/Suc.				CQ/Baf.			
		25	50	100	200	25	50	100	200	25	50	100	200
pH_c [2, 4]	a	7.29	7.34	7.28	7.27	7.34	7.34	7.34	7.32	7.33	7.32	7.29	7.10
	b	7.43	7.38	7.42	7.33	7.40	7.38	7.40	7.38	7.43	7.38	7.39	7.24
pH_l [2]	a	4.88	5.22	5.45	5.20	5.51	6.03	6.09	6.25	5.26	5.05	5.64	5.48
	b	5.84	5.80	6.17	6.76	6.31	6.73	6.81	7.21	5.84	6.33	6.12	7.04
V_c (μm^3) [2]	a	1452	1752	1616	1314	2761	2572	2391	2630	1491	1437	1512	1608
	b	1874	1922	2042	1916	3250	3535	3516	3904	1989	1961	2022	1945
V_l_initial [2] (μm^3)	a	8.8	8.8	8.8	8.8	54.9	54.9	54.9	54.9	8.8	8.8	8.8	8.8
	b	32.4	32.4	32.4	32.4	128.0	128.0	128.0	128.0	32.4	32.4	32.4	32.4
A_l_initial [2, 4]	a	111.5	111.5	111.5	111.5	517.5	517.5	517.5	517.5	111.5	111.5	111.5	111.5
	b	335.0	335.0	335.0	335.0	899.7	899.7	899.7	899.7	335.0	335.0	335.0	335.0
rate of change A: μm^2/hr [3, 4]	A	239.3	466.3	247.9	163.0	339.0	549.9	624.2	206.2	0.0	0.0	0.0	0.0
V: μm^3/hr [3]	V	68.7	106.9	66.0	45.1	121.4	227.2	266.3	127.3	0.0	0.0	0.0	0.0
T (K)		310.15											
$\log P_n$		(3.68, 4.18)											
$\log P_{d1}$		(0.18, 0.68)											
$\log P_{d2}$		(-1.16, -0.66)											
$\log P_{n,d1,d2\_cell}$		(1.70, 1.83)											
pK_{a1}		(9.71, 10.21)											
pK_{a2}		(7.22, 7.72)											
E_a (mV) [4]		-10											

E_l (mV)	(5, 15)
E_m (mV)	-160
pH_a	(7.4, 7.5)
pH_m [4]	8
cellNo (/well)	$(50, 70) \times 10^4$
V_a (μm^3)	0.5×10^{12}/cellNo
V_m (μm^3)	16.35
A_a (μm^2) [4]	100
A_m (μm^2) [4]	196.35
L_c [4]	0.05
L_l	(0.025, 0.075)
L_m [4]	0.05
ls_c [4]	0.3
ls_l	(0.2, 0.4)
ls_m [4]	0.3

[1] The center points for each range were used to simulate the typical kinetic curves under specific each treatment, as shown in Figure 3.6.

[2] The upper (b) and lower (a) boundaries of uniform distribution were calculated from the following equations based on measurements: $mean = \frac{1}{2}(a+b)$, (S1) and $variance = \frac{1}{12}(b-a)^2$, (S2) where the mean values were reported in the above table, and the variance was calculated as the squared s.d..

[3] Rate of changes of vesicular volume and surface area were obtained by fitting measurements at 1-4 hour time points with a linear model using the initial values as intercepts. The slope of vesicular volume and surface area under CQ treatments with bafilomycin A1 were essentially 0 after statistical analysis.

[4] These parameters do not significantly affect intracellular mass of CQ as suggested by sensitivity studies.

Figures

Figure 4.1. CQ induces a phospholipidosis-like phenotype characterized by the formation of many MLB/MVBs in MDCK cells. MDCK cells were treated with 50 μM CQ for 4 hours followed by transmission electron microscopy analysis. A. (Magnification 7900X), B. and C. (Magnification 34000X), and D. (Magnification 13600X) illustrate MDCK cells with enlarged vesicular compartments, or MLB/MVBs, comprised of intralumenal MLBs (single arrows) or MVBs (double arrows). The nucleus is noted by N.
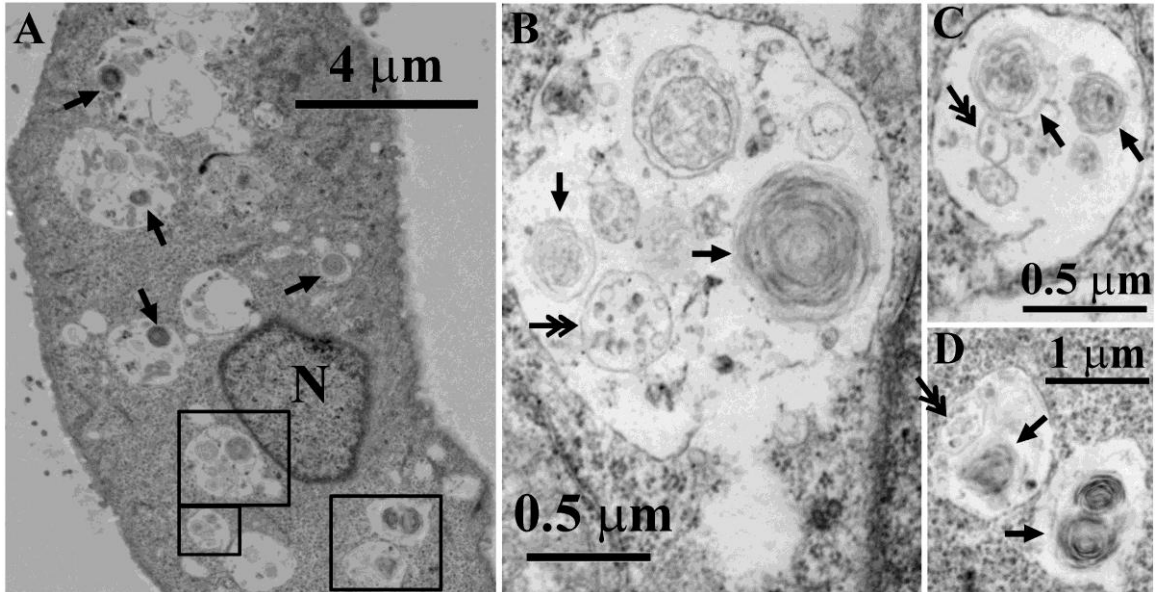
Figure 4.2. CQ-induced non-uniform distribution (A) and dose-dependent accumulation (B) of LTG within the LTG-positive vesicles in MDCK cells. A. At the end of 4-hour incubation with 50 μM CQ, LTG fluorescence within individual vesicles was concentrated within small particles of 0.3 – 0.4 μm in diameter, which underwent Brownian motion within the confines of the enlarged vesicles. These particles corresponded in shape and size to MLB/MVBs observed by EM (see Figure 4.1). Image *a* to *f* was taken at 4 second intervals to show the Brownian movement of the bright MLB/MVB particles within the lumen of the expanded vesicles. Scale bar: 2 μm. B. After 4-hour incubation with different amount of CQ, the fluorescence volume intensity per vesicle increased as CQ treatment. 5 cells (more than 300 vesicles) were measured under the same treatment.
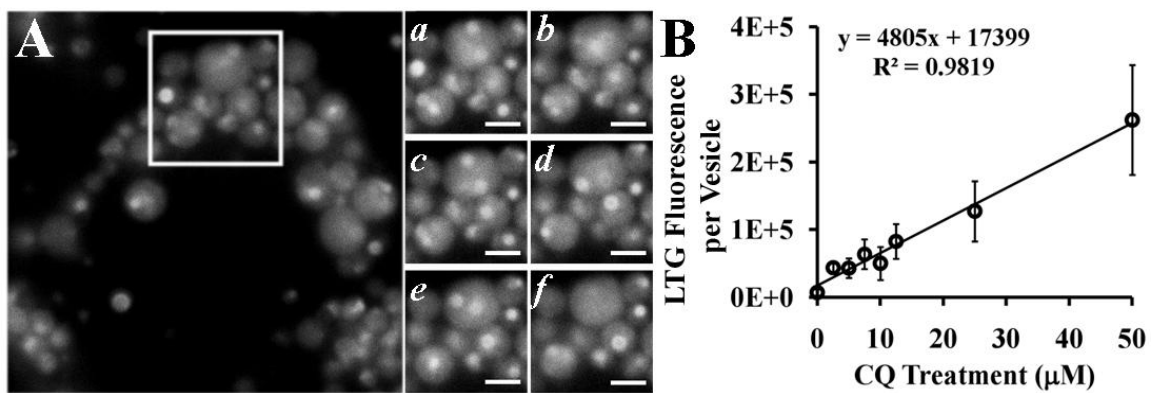
Figure 4.3. CQ accumulates within enlarged MLB/MVB-positive vesicles.
MDCK cells were treated with 10 μM CQ for 12 hours, which primes them for vacuolar expansion and MLB/MVB formation, followed by 100 μM CQ for 2 hours prior to imaging. For fluorescence microscopy, cells were incubated with 0.5 μM LTG for 30 min immediately prior to imaging. A. LTG fluorescence (top) and the corresponding brightfield image (middle) of a representative CQ-treated cell was merged (bottom) showing the highly heterogenous LTG fluorescence associated with MLB/MVBs within the expanded cytoplasmic vesicles. Scale bar: 4 μm. B. Analysis of intracellular CQ distribution by confocal Raman microscopy. (upper) Brightfield image showing a 100 μM CQ-treated (***a***) and untreated (***b***) cells from which spectra were acquired. Scale bar: 5 μm. (lower) Spectrum 1 was acquired from 100 mM CQ solution in buffer, as reference. Spectrum 2 and 3 were acquired from the vesicles and cytosol of treated cells, respectively; spectrum 4 and 5 were acquired from the vesicles and cytosol of untreated cells. In these spectra, CQ-specific Raman vibrational peaks (around wavenumbers 1370 and 1560) were identified based on Spectrum 1. CQ-specific Raman signal was mostly localized within the expanded vesicles of CQ treated cells.
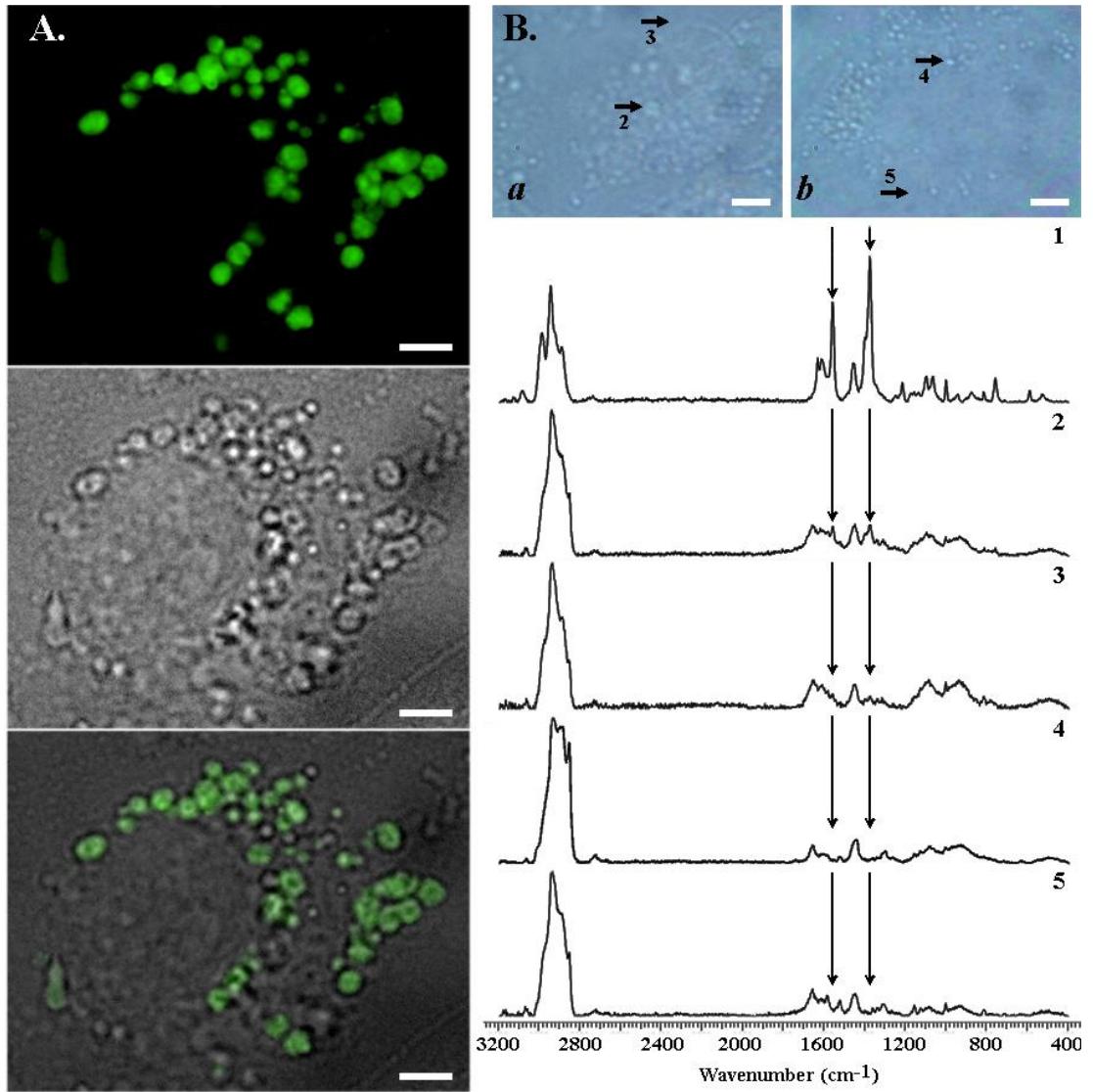
Figure 4.4. Temperature- and pH-dependent CQ uptake parallels the induced phospholipidosis effect, and is insensitive to pharmacological inhibitors of organic cation transport. (A) Within 30 min CQ uptake (50 μM) into MDCK cells was significantly reduced by lowering extracellular pH and lowering the temperature. Uptake experiments were performed in transport buffer. Control experiments were performed at pH 7.4 and 37 ℃. (B) Within 30 min of incubation, CQ uptake (50 μM) and cellular vacuolation were not significantly perturbed by inhibitors of autophagy or active transport. Pre-incubation with 0.1 M sucrose in DMEM increased CQ uptake within 30 min, while co-treatment with bafilomycin A1 inhibited CQ uptake, but the difference was not significant. Uptake experiments were performed in choline-based transport buffer (Cho) and DMEM (all the other conditions). (C) and (D) At the end of 4-hour incubation, CQ uptake and LTG-positive vesicular expansion was partially inhibited by FCCP, significantly suppressed by bafilomycin A1 but not reduced by OCT inhibitor/stimulator, the autophagy inhibitor 3MA or the sodium-free extracellular buffer.. Con.: control, 50 μM CQ only; Cho: 50 μM CQ in choline-based transport buffer; Cim: 500 μM cimetidine; HC3, 500 μM hemicholinium-3; Gua: 500 μM guanidine; TEA: 500 μM tetraethylammonium; HCor: 20 μM hydrocortisone; FCCP: 5 μM FCCP; 3MA: 10 mg/mL 3-methyladenine; Suc: 0.1 M sucrose; Baf: 10 nM bafilomycin A1. Data were presented as mean ± S.E.M from 3 experiments. Asterisks indicate significant difference from control using unpaired Student's t-test ($p < 0.05$). The nucleus is indicated by N. Scale bar: 10 μm.
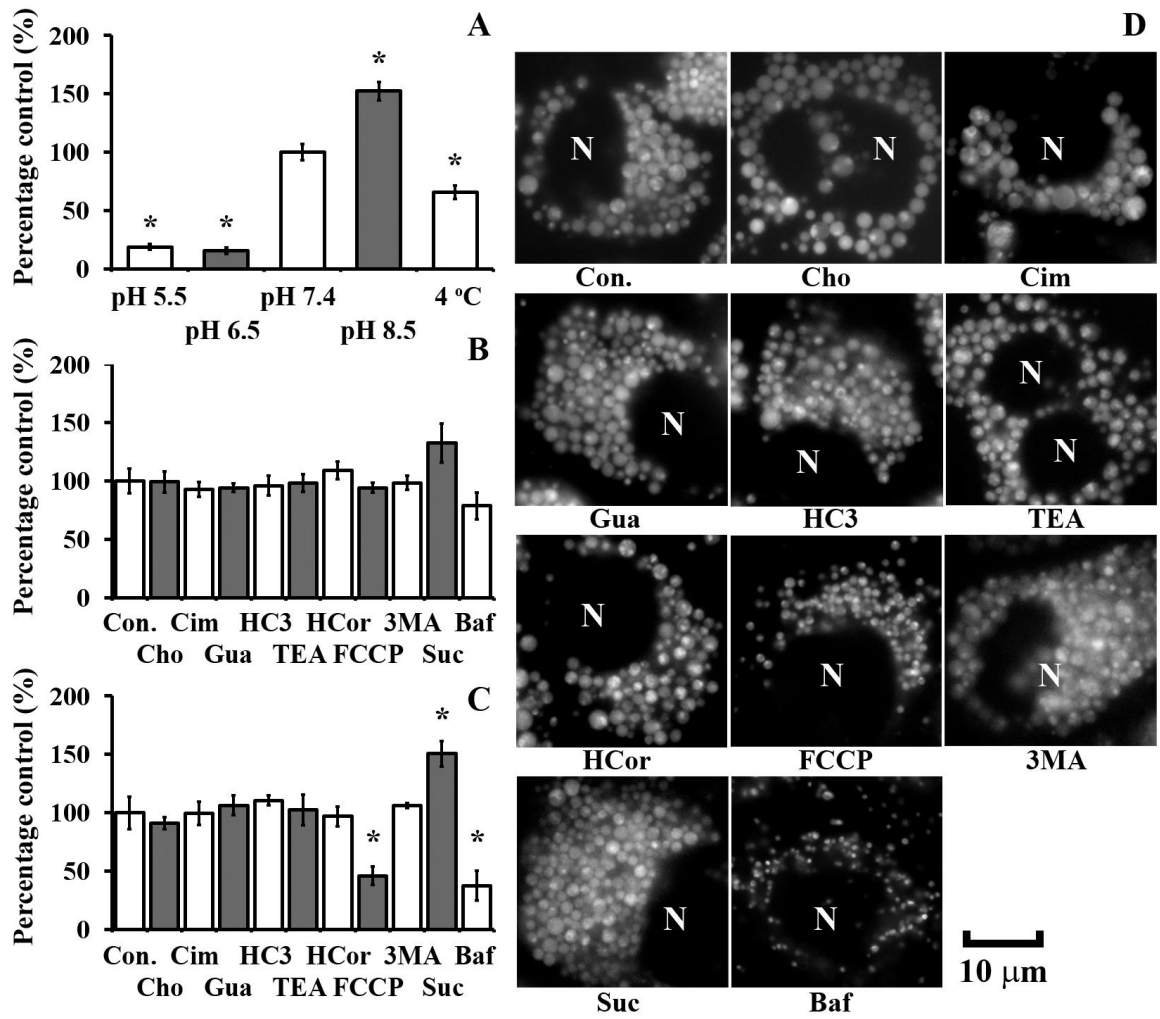
Figure 4.5. Quantitative analysis and mechanism-based, predictive pharmacokinetic modeling of CQ uptake in MDCK cells. A. Measured uptake kinetics during 1) 25, 50, 100 and 200 μM CQ treatments, in previously untreated cells (CQ/); 2) Suc pre-treated cells during co-treatment with CQ and sucrose (CQ/Suc); and 3) co-treatment with CQ and Baf in previously untreated cells (CQ/Baf). Data points correspond to mean ± S.E.M. (n = 3). B. Histograms of Monte Carlo simulations of intracellular CQ accumulation in relation to experimental CQ mass accumulation. A total of 10,000 simulations were performed with parameters randomly selected from a range (Table 4.2). Red solid lines correspond to the measured, average CQ mass per cell at the end of a 4-hour incubation with 25, 50, 100 and 200 μM CQ (red dashed lines represent ± S.E.M). Green: simulation results in the absence of phenotypic changes. Blue: simulation results incorporating volume changes of organelles but without partitioning to MLB/MVBs. Black: simulation results incorporating volume changes in acidic organelles, as well as CQ partitioning to MLB/MVBs.
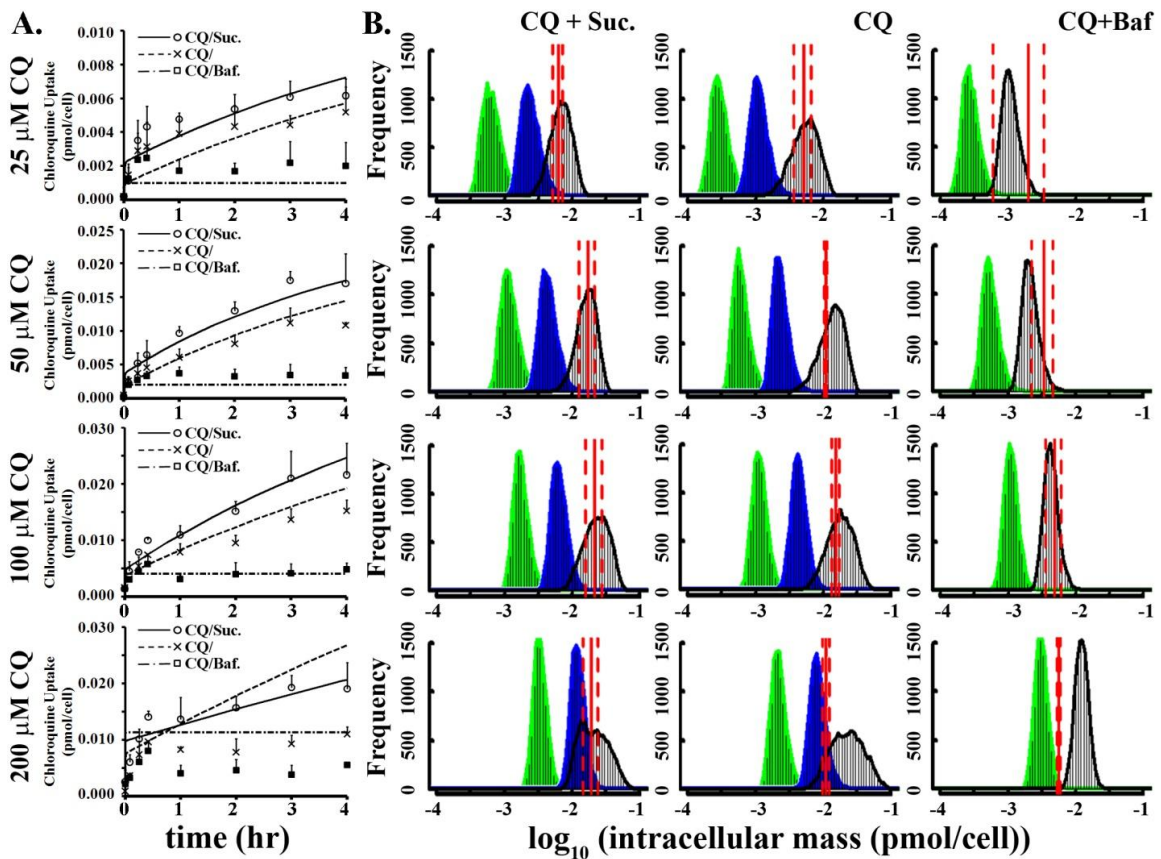
Figure 4.6. Assessing the performance of the cellular pharmacokinetic model. The predicted intracellular mass was plotted against the measured values at 8 time points for 4 levels of CQ treatment with (or without) sucrose or bafilomycin A1. The solid line represents the unity line and the dashed lines represent a factor of 2 on both side of the unity. The dotted line represents the best fit with the equation displayed. (A) All the 96 data points were plotted. The solid circles represent data from 25, 50 and 100 μM CQ treatments; the open circles represent data from 200 μM CQ treatments. (B) The fitted line for data without 200 μM treatments.
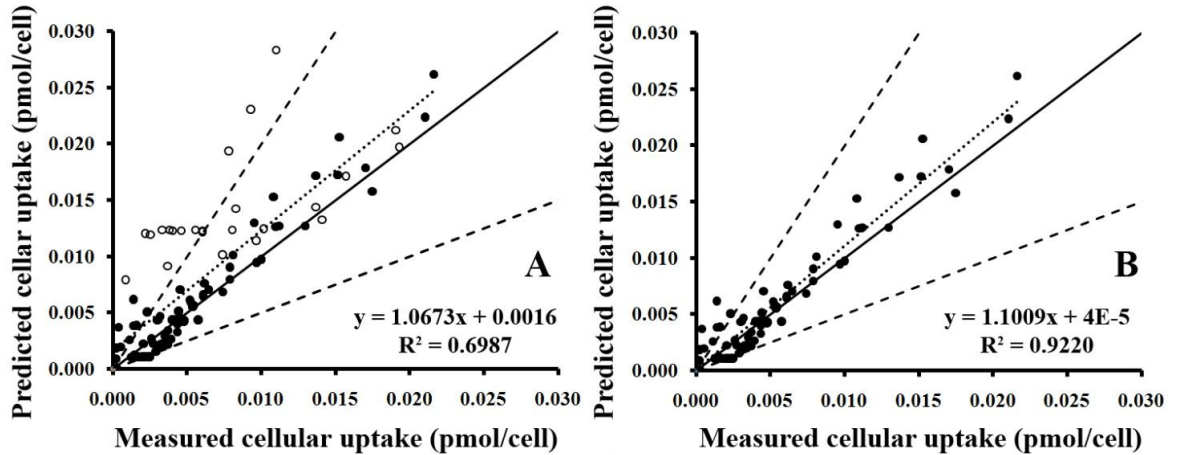
Chapter V

Simulation-Driven Analysis for Assessing the
Lateral Inter-Cellular Transport of Small Molecules
on Micro-Fabricated Pore Arrays

Abstract

Studies on the inter-cellular transport between cells in a monolayer have been limited to small amounts of hydrophilic fluorescent molecules microinjected into single cells. Here, we proposed a novel design, utilizing impermeable polyester membranes perforated by single 3 μm diameter pore or geometric pore arrays, to probe the intracellular and intercellular transport pathways of small hydrophobic molecules within and between cells in a monolayer. In experimental demonstrations, Madin-Darby Canine Kidney epithelial cells were inoculated into inserts holders with patterned, transparent polyester membrane supports. The small, cell permeant dyes, Hoechst 33342, MitoTracker Red and BCECF-AM were added into the basolateral compartment of the transwell system. Lateral transport of the dye within cell monolayer was tracked by fluorescence microscopy. The time course of probe uptake and the distribution of probe within individual cells were analyzed with quantitative imaging software. We observed that single pores feed only into cells in the immediate vicinity and lateral diffusion between cells was highly constrained and occurred slowly, leading to geometric labeling patterns controlled by the area and pattern of the pores and the transport

properties of the cells. A cell-based mathematic model was developed to guide the analysis of observed standing gradient in between neighboring cells. Despite of its simplicity, geometrically patterned, micro-fabricated pore arrays provide an experimental system to quantitatively studying the cellular transport pathways of various hydrophobic small compounds.

Keywords: transwell system; later diffusion; inter-cellular transport; pore arrays; simulation; pharmacokinetics.

Introduction

Lateral transport between neighboring cells is critical to the maintaining of spatial and functional organizations in different tissue and organs. Depending on cell types, the lateral transport of xenobiotic and/or endoergic signaling molecules plays pivotal roles ranging from maintaining the cell homeostasis, to establishing the electrical propagation, and to conducting regulating the differential and developmental fates in adjacent cells [1-4]. It can be generated by many local stimuli including but not limiting to neuronal cell transmission, calcium waves in myocytes or liver endothelial cell monolayers, coupled cellular contraction in cardiac muscle and signal transduction during developmental processes. Improper regulation of lateral intercellular transport has been associated with a series of disease progressions including cardiac arrythmia, epileptic seizures, and anticancer drug resistance phenomenon [5-8].

For small molecules there are two major routes for lateral intercellular transport: the gap-junction mediated lateral transport and the passive diffusion across plasma membranes. The concept of gap junctions, clusters of connexin protein channels that connect adjacent cells, was introduced more than fifty years ago, as the fundamentals of impulse transmission and metabolite exchange between neighboring cells [9-11]. By coupling immune-histology with electro-physiological studies or fluorescence-based imaging techniques, researchers have revealed an urgent need to screening for biological and genetic factors (e.g. the structure, distribution, and composition of connexin proteins) on the selectivity and permeability of gap junctions to hydrophilic compounds or

charged ions [12]. Nevertheless, traditional fluorescence-based methods, which initiate with the microinjection and scrape loading of fluorescent dyes into a single cell within a cell monolayer or cluster, are very time consuming and could not be escalated for high throughput screening assays in lateral diffusion studies [13]. Fluorescence recovery after photobleaching (FRAP) assays have also been developed in monitoring the diffusion of fluorescent dyes, but similar to the traditional loading methods, FRAP is intrusive to cell viability [14].

For hydrophobic compounds that get transported across cell boundaries mainly by passive diffusion, even less knowledge has been collected on their lateral transport properties. One of the reasons is that the loading of hydrophobic compounds in the source cell requires higher efficiency as these compounds might escape from the apical membrane to the extracellular environment even before the monitoring starts. Thus a design that provides constant source to the center cell would be highly desirable in the lateral transport studies of hydrophobic compounds.

In this paper we presented a trans-well insert system that could provide a constant supply of small compounds to the cell in a non-intrusive manner as well as a mechanism-based computational model that simulate the lateral diffusion properties of small molecules. By seeding Madin-Darby Canine Kidney (MDCK) epithelial cells (a cell lines that does not have functional gap junctions at confluency [15, 16]) on non-permeant polyester membrane supports with patterned pore arrays and adding hydrophobic fluorescent compounds in the basolateral side of cell monolayer, the time course dye uptake in the cells sitting

above the pores and the kinetics of lateral transport between neighboring cells of could be visualized spontaneously with a fluorescence microscopy. Furthermore, when a hydrophobic pro-drug of a hydrophilic gap junction substrate was administered, gap junction mediated dye transfer could also be analyzed for the quantitatively evaluation of gap junction functions. We demonstrated that this insert system serves as a platform for comprehensive studies on the lateral transport phenomenon through both passive diffusing route and gap junction mediated route.

Materials and Methods.

Design of point-source insert system. We designed an insert system with fabricated polyester membranes to support cell growth and to provide point source for compound administration (Figure 5.1). Non-porous, transparent, polyester membranes were perforated with focused-ion-beam techniques to create patterned pore arrays. These arrays features 3 μm pore size, arranged 20 μm apart in a 5-by-5 array, or 40, 80 and 160 μm apart in 3-by-3 arrays. The patterned membranes were glued (Krazy® Glue) to the bottom of hollow Transwell® holder (Costar 3462 or 3460) to create permeable support for cell growth.

Cell culture. Madin-Darby canine kidney (MDCK) cells were purchased from ATCC (CCL-34[TM]) and grown in Dulbecco's modified Eagle's medium (DMEM, Gibco 11995) containing 10% FBS (Gibco 10082), 1X non-essential amino acids (Gibco 11140) and 1% penicillin/streptomycin (Gibco 15140), at 37ºC in a

humidified atmosphere with 5% CO_2. MDCK cells were seeded at a density between 1×10^5-2×10^5 cells per square centimeter and were grown until cell monolayer was formed.

Chemicals. Organelle targeting fluorescent dyes, Hoechst 33342 (Hoe) (Molecular Probes H3570) was stored by manufacturer instruction. Fluorescent dye BCECF-AM and MitoTracker Red (MTR) (Molecular Probes® B1170 and M7512) were stored according to the manufacturer's instructions and was dissolved in DMSO to final concentrations of 2 mg/ml before use. Trypan Blue (Sigma T6146) was dissolved in HBSS buffer (Gibco 14025) to a final concentration of 5 mM and stored in room temperature.

Characterization of the insert system. The integrity of insert system was tested by adding 5 mM Trypan Blue into the insert wells. The inserts was considered intact if there will be no sign of Trypan Blue leakage from the edge of the insert membranes. In this situation, the transport of test chemicals from the basolateral to the apical compartment only occurred through the pore arrays. To evaluate the effect of pore arrays on cell growth, MDCK cells were washed and incubated in transport buffer (HBSS buffer supplemented with 25 mM D-glucose, pH 7.4) for 30 min, and subjected to transepithelial electrical resistance (TEER) measurement using Millipore Millicell ERS. Cell monolayers were considered intact if the background subtracted TEER values were higher than 100 $\Omega\cdot cm^2$.

Fluorescence imaging and image analysis. Fluorescent dyes were added into the basolateral compartment of the transwell system at time 0. A Nikon TE2000S epifluorescence microscope with standard mercury bulb illumination,

coupled to a CCD camera (Roper Scientific, Tucson, AZ), with a 10X objective ((Nikon Plan Fluor ELWD 10x) or a 20X objective ((Nikon Plan Fluor ELWD 20x). A triple-pass DAPI/FITC/TRITC filter set (Chroma Technology Corp. 86013v2) was used to image the dynamic staining pattern in the cells. The 12-bit grayscale images were acquired and background subtracted. Individual cells or nucleus were manually outlined with Region tool in MetaMorph software (Molecular Devices Corporation, Sunnyvale, CA). The average and standard deviation of cellular or nucleus fluorescence intensity was captured with MetaMorph. The rate of staining of Hoe in the nucleus was measured as the slope of fluorescence increase normalized by the slope of increase in the first nucleus (closest to the pore).

Estimation of intercellular diffusivity of cell permeant hydrophobic dyes. The distance (L) between the pore and the furthest stained object (the nucleus or the mitochondria) in between 2 to 3 hours were measured with MetaMorph. The equivalent lateral diffusion coefficient (D) assuming free diffusion was calculated according to the equation: $D = L^2/(4*t)$, where t is the time lapse after the addition of the dye into the basolateral compartment. The theoretical lateral diffusion coefficient assuming free diffusion in solution was estimated using the Einstein–Stokes equation: $D = \frac{k_B \times T}{6\pi\eta r}$, where k_B is the Boltzmann's constant, T is the absolute temperature, η is the viscosity of the solution, and r is the Radius of the particle could be calculated with MarvinSketch at www.chemaxon.com.

Mathematical Modeling of the Intercellular gradient of Hoe. A multi-compartment, constant-field, fixed-parameter mathematical model [17] was adapted to predict the passive diffusion of Hoe from the first cell on top of a single pore to its neighboring cells within MDCK cell monolayer (Figure 5.2). Briefly, the cell monolayer was modeled as five layers of hexagon cells. Only the nucleus compartment was included in the model. The total change in Hoe mass with time in each compartment was expressed by equations 1-5:

$$\frac{dM_b}{dt} = -A_b \times J_{b,c1} \tag{1}$$

$$\frac{dM_{cx}}{dt} = A_{i(x-1)} \times J_{i(x-1),cx} - A_{nx} \times J_{cx,nx} - A_{ix,x} \times J_{cx,ix} - A_{ax} \times J_{cx,a} \tag{2}$$

$$\frac{dM_{nx}}{dt} = A_{nx} \times J_{cx,nx} \tag{3}$$

$$\frac{dM_{ix}}{dt} = A_{ix,x} \times J_{cx,ix} - A_{ix,x+1} \times J_{c(x+1),ix} \tag{4}$$

$$\frac{dM_a}{dt} = \sum_{x=1}^{x=5} A_{cx} \times J_{cx,a} \tag{5}$$

where, *M* stands for the *total mass*, *J* indicates the *flux*, *A* and *V* indicate the *membrane surface area* and *volume*, respectively, of the specific subcellular compartments as indicated by the subscripts *a, b, c, n,* and *i*: *apical, basolateral compartment, cytosol, nucleus* and *intercellular space between two neighboring layers of cells*. *x* indicates the *cell layer number,* ranging from 1 to 5 for the cytosol and nucleus compartment and 1 to 4 for the intercellular space. $A_{ix,x}$ is the surface area facing the xth layer and $A_{ix,x+1}$ is facing the x+1th layer of cells. A_{i0} and $J_{i0,c1}$ (when *x* = 1) are the same as A_b and $J_{b,c1}$. When x = 5, the terms regarding the 5th intercellular space are removed. The comma between two subscripts in the flux means *"to"* (e.g. "$J_{c,m}$" represents the flux from cytosol to

mitochondria). With all and surface area terms constant, the concentration change in each compartment was expressed by equations 6-10:

$$\frac{dC_b}{dt} = -\frac{A_b}{V_b} \times J_{b,c1} \tag{6}$$

$$\frac{dC_{cx}}{dt} = \frac{A_{c(x-1)}}{V_{cx}} \times J_{i(x-1),cx} - \frac{A_{nx}}{V_{cx}} \times J_{cx,nx} - \frac{A_{ix,x}}{V_{cx}} \times J_{cx,ix} - \frac{A_{ax}}{V_{cx}} \times J_{cx,a} \tag{7}$$

$$\frac{dC_{nx}}{dt} = \frac{A_{nx}}{V_{nx}} \times J_{cx,nx} \tag{8}$$

$$\frac{dC_{ix}}{dt} = \frac{A_{ix,x}}{V_{ix}} \times J_{cx,ix} - \frac{A_{ix,x+1}}{V_{ix}} \times J_{c(x+1),ix} \tag{9}$$

$$\frac{dC_a}{dt} = \sum_{x=1}^{x=5} \frac{A_{ax}}{V_{ax}} \times J_{cx,a} \tag{10}$$

For Hoe, the total flux is contributed by a neutral form and three ionized forms with one to three positive charges. The total flux across membrane as contributed by three species can be calculated with Fick's equation and Nernst-Planck equation [18] :

$$J_{o,i} = \boldsymbol{P}_n(\boldsymbol{f}_{n,o}C_o - \boldsymbol{f}_{n,i}C_i) + \boldsymbol{P}_{d1}\frac{N_{d1}}{e^{N_{d1}}-1}(\boldsymbol{f}_{d1,o}C_o - \boldsymbol{f}_{d1,i}C_ie^{N_{d1}}) + \boldsymbol{P}_{d2}\frac{N_{d2}}{e^{N_{d2}}-1}(\boldsymbol{f}_{d2,o}C_o - \boldsymbol{f}_{d2,i}C_ie^{N_{d2}}) + \boldsymbol{P}_{d3}\frac{N_{d3}}{e^{N_{d3}}-1}(\boldsymbol{f}_{d3,o}C_o - \boldsymbol{f}_{d3,i}C_ie^{N_{d3}}) \tag{11}$$

where, subscripts *o* and *i* indicate *outer-* and *inner*-compartment, *n, d1,* and *d2* indicate *neutral form, ionized form with one charge,* and *ionized form with two charges*, respectively. **P** is the *permeability across the bilayer membranes* and it was estimated based on the logarithm of Hoe's octanol/water partition coefficient (log$P_{o/w}$) calculated with ChemAxon® MarvinSkecth 5.1.4 (http://www.chemaxon.com) as $\log P_{n,d1,d2} = \log P_{o/w} - 6.7$ [17]. **f** represents the *ratio of the activities (a_n, a_{d1} and a_{d2}) and the total concentration*. It can be calculated from lipid fraction and ionic strength in each compartment and the sorption coefficient for each species as estimated from log$P_{o/w}$ [17, 19]. When

estimating Hoe binding to DNA in the nucleus, sorption coefficient in the nucleus was estimated by $2*10^{-14}$ M of binding sites / Hoe in 5 μm^3 radius sphere-shape nucleus in the presence of 10 μM Hoe in the extracellular medium [20]. In equation 4, $N = zEF/(RT)$, where z = +1, +2 and +3 for N_{d1}, N_{d2} and N_{d3} (ionized base with one, two and three charges); $E, F, R,$ and T are *membrane potential, Faraday constant, universal gas constant,* and *absolute temperature*, respectively. The ordinary differential equations were numerically solved with MATLAB® ODE15s solver to plot a kinetic curve of nucleus concentration of Hoe. Model validation/consistency check was performed by summing Hoe mass in all compartments during the simulation, confirming that total Hoe mass in the system stays constant (mass balance).

The intercellular gradient between neighboring cells was modeled as the difference in the rate of staining over a 2 hour period. Monte Carlo simulations were performed to assess the distribution of staining rate in neighboring layers of cells. MATLAB® ODE15s solver was employed to run 1,000 simulations during which simulation parameters were randomly sampled from uniform distributions within the range of parameter values.

Results

The design of membrane support insert system of pattern pore arrays.
The inserts with impermeable polyester membranes (with fabricated pore arrays) were placed in a 12-well plate (Figure 5.1A). MDCK cells were inoculated in the insert and let grown to confluence (Figure 5.1B) in 0.5 ml fully supplemented

DMEM medium. Before transport experiments, cells were washed and incubated in 0.5 ml dye-free transport buffer for 30 min. After equilibrium, 1.5 ml transport buffer containing appropriate dyes were added into the basolateral compartment. Fluorescence microscopy could be applied to capture the staining of MDCK cell monolayer at designated time points.

The effect of pore arrays on cell growth. The morphology of cell monolayer exhibited no visual differences between membranes with various pore array patterns (Figure 5.1B). No cell migration through the pores was observed for all membrane types. The TEER values of MDCK cell monolayer and the number of cells per insert well were similar regardless of different membrane types (Table 5.1). Cell counts on patterned membranes were comparable to previous reports on commercialized, porous insert with 0.4 μm pores and similar cell supporting membrane area [21]. The TEER value was significantly higher on the patterned membranes than the porous membrane, indicating the formation of tighter intercellular junctions in the presence of less scattered pore area [21].

Lateral transport of small hydrophobic dye occurred at limited rate around the pores. Using Hoechst 33342 as a fluorescent probe, the kinetics of dye staining within MDCK cell monolayer was tracked with fluorescence microscopy at room temperature (Figure 5.3). Within 3 hrs, only cells that lied within close vicinity was stained (Figure 5.3), indicating that the cells formed a tight seal with the pores such that each pore fed almost exclusively into cells that were in immediate contact with the pores. A geometric labeling pattern was observed as controlled by the area and pattern of the pores and the transport

properties of the cells (Figure 5.4). These results suggested that the pores served as point sources of sustained dye supply to the adjacent cells. Therefore, for cells grown on membranes with 3×3, 80 μm or 160 μm-apart pore arrays, each pore could be considered as the single point source of dye molecules.

Also consistent with this limited lateral diffusion rate statement, while each nucleus accumulated more dye with time, Hoe staining was not saturated over 3-hour period (Figure 5.5). Similar geometric label patterns were also observed for other small hydrophobic, cell permeant dyes MitoTracker Red (Figure 5.6) and LysoTracker Green (data not shown).

The application of fabricated insert system to study different lateral transport behavior of small molecules. Within MDCK cell monolayer stained with Hoe, a standing gradient was observed in neighboring cells with various distant to the pore (Figure 5.5 and 5.6). Fluorescence intensity decreases dramatically as the number of layers to the pore increases (Figure 5.5). The same staining gradient was observed for other cell permeant dyes including MTR (Figure 5.6). After 2-hours staining from the basolateral compartment, the normalized fluorescence intensity in the third layer of cell from the pore was significantly higher for MTR than Hoe (Figure 5.6D). Not surprisingly, the measured equivalent lateral diffusivity assuming free diffusion within live cell monolayer was higher for MTR than for Hoe (5.88 ± 1.33 E-14 m^2/sec for MTR and 3.12 ± 1.12 E-14 m^2/sec for Hoe, n = 6). In a separate study, MDCK cells were pre-treated with 1% Triton 100 for 10 min before the addition of Hoe in the basolateral compartment. The number of cells stained within 2 hours was

174

significantly larger than under the live cell condition (Figure 5.7). The measured intercellular lateral diffusivity assuming free diffusion in the membrane extracted environment was 1.18 ± 0.434 E-13 m^2/sec.

When stained with BCECF-AM from the basolateral compartment with BCECF-AM, green fluorescence of the hydrophobic hydrolysis product, BCECF, was only observed in the first layers of cells that are in direct contact with the pores (Figure 5.8).

Simulation of the gradient in neighboring cells from single point source. The rate of change in the average fluorescence intensity against time was measured and normalized to the closest cell to the pore on a 3-by-3, 160 μm apart pore array (Figure 5.9A). The rate of change in nucleus concentration against time was also simulated and normalized with MatLab® for 1000 cells using randomly selected cellular parameters within reasonable range (Figure 5.9B). In both the measurement and the simulation results, a gradient in the rate of staining (the measured slope of fluorescence increment and the calculated rate of change of Hoe) was observed in neighboring cell layers. The difference in the rate of staining in neighboring cells could be described with exponential decay $y = Ae^{-x}$. The measured exponent was significantly less than that derived from model simulations (0.966 ± 0.313, n = 9 *vs.* 2.043 ± 0.294, n = 957), and the higher variation in measured exponents reflected a huge heterogeneity in the intercellular diffusion pathways within the same cell monolayer.

Discussion

175

In this study we presented a practical method to trace the real time lateral transport of various chemical agents with distinguished properties. The insert system with patterned pore arrays provides the flexibility to study the rapid flux of molecules to different regions under various experimental conditions. It takes common materials to build this insert system. Once coupled with appropriate imaging instrument, this system could be easily adjusted for high content screening purposes in search for molecules with specific diffusion properties.

The choice of the cell lines in this experiment is the wild type MDCK cells, a cell line that stably expresses the differentiated properties of distal tubular epithelial cells [22], forms intact cell monolayer quickly in vitro and not extensively expresses active transporters [23-25]. Therefore, although Hoe is a substrate of many multidrug resistance transporters, the transport behavior of Hoe in wild type MDCK cell should be driven by passive diffusion [26]. It has also been well established that MDCK does not form functional gap junctions when reaching confluency [15, 16], thus, it can be used a negative control in selecting molecules that are restrict gap junction substrate.

With this design, we studied the lateral transport behavior of Hoe, a hydrophobic cell permeant fluorescent dye. We found that lateral transport of Hoe occurred at limited rate around the pores. For a spherical particle with a similar molecular weight as Hoe, the Einstein–Stokes equation predicts the diffusion coefficient in water and blood to be around 1E-10 m^2/sec. The measured lateral intercellular diffusivities in live cells was less than one third of that in membrane extracted, dead cells, and the later was barely comparable to

diffusivities measured from FRAP studies for similar molecular weight fluorescent compounds (<5E-13 m^2/sec) [27, 28]. We consider this low, measured diffusion coefficient of Hoe was due to DNA binding that attenuate chemical potential at cell boundaries and the crowding effect as present in the cellular environment, the latter of which is known to slow the diffusion of solutes [29]. When cell membrane was removed, the crowding effect as introduced by the cytoplasmic organelles and membrane structures were reduced [29], but the DNA binding effect still remains to hamper the free diffusion of Hoe. It also comes to our notice that, the basolateral staining of Hoe in cell monolayer sitting on top of commercialized membrane support (with more densely and randomly distributed 3 μm pores) would reach steady state within 3 hours (data not shown). This implies that the pattern of point sources has impact on way the dye interacts with its molecular target.

The application of mathematic modeling has seen general success in quantitative prediction of intercellular concentration gradient. However, the model predicted a more homogeneous distribution in the second and third layers of cells. These discrepancies between the simulation and observation indicates alternative hypothesis (in addition to the passive diffusion, instantaneous intracellular mixing and instant binding to DNA) in Hoe staining in the MDCK cells.

One disadvantage of the current design system is the limited resolution in acquired images. Unlike the optical glass based chip designs [28, 30, 31], the polyester membrane support is not suitable for high resolution confocal analysis. In the PARTCELL system as proposed by Takayama et al., subpopulations of the

177

cells that grow on cover glasses could be selectively labeled with fluorescent dyes as delivered by multiple laminar fluid streams [31]. The cells could be analyzed with high resolution and high precision confocal microscopy to visualize the 3D distribution of xenobiotic agents. The spatial distribution of xenobiotic agents will provide valuable information in understanding the intracellular diffusion and mixing process.

Conclusions.

In this study we presented a simple geometrically patterned pore arrays as a useful tool for quantitatively studying small molecule transport between epithelial cells within a monolayer, at a single cell level. Compared with traditional fluorescence based methods, e.g. microinjection, scalpel loading and FRAP, this insert system represent a cell-friendlier, faster, more flexible and more quantitative alternative that is suitable for a more diverse group of chemical agents. Future efforts in improving current design with micro-fabricated pore arrays will be focused on elucidating the spatial distribution and intracellular diffusion process with more desirable membrane materials which are suitable for cell growth and high resolution imaging techniques.

References

1.   L. Ghitescu and M. Bendayan. Transendothelial transport of serum albumin: a quantitative immunocytochemical study. *J Cell Biol.* 117:745-755 (1992).

2.   S. Rohr. Role of gap junctions in the propagation of the cardiac action potential. *Cardiovasc Res.* 62:309-322 (2004).

3.   P.R. Brink, K. Cronin, and S.V. Ramanan. Gap junctions in excitable cells. *J Bioenerg Biomembr.* 28:351-358 (1996).

4.   G.H. Kalimi and C.W. Lo. Gap junctional communication in the extraembryonic tissues of the gastrulating mouse embryo. *J Cell Biol.* 109:3015-3026 (1989).

5.   M. Noguchi, K. Nomata, J. Watanabe, H. Kanetake, and Y. Saito. Changes in the gap junctional intercellular communication in renal tubular epithelial cells in vitro treated with renal carcinogens. *Cancer Lett.* 122:77-84 (1998).

6.   G. Gakhar, D.H. Hua, and T.A. Nguyen. Combinational treatment of gap junctional activator and tamoxifen in breast cancer cells. *Anticancer Drugs.* 21:77-88 (2010).

7.   H. Sato, H. Iwata, Y. Takano, R. Yamada, H. Okuzawa, Y. Nagashima, K. Yamaura, K. Ueno, and T. Yano. Enhanced effect of connexin 43 on cisplatin-induced cytotoxicity in mesothelioma cells. *J Pharmacol Sci.* 110:466-475 (2009).

8.   Y. Wang, J.V. Denisova, K.S. Kang, J.D. Fontes, B.T. Zhu, and A.B. Belousov. Neuronal gap junctions are required for NMDA receptor-mediated excitotoxicity: implications in ischemic stroke. *J Neurophysiol.* 104:3551-3556 (2010).

9.   J.L. Madara and K. Dharmsathaphorn. Occluding junction structure-function relationships in a cultured epithelial monolayer. *J Cell Biol.* 101:2124-2133 (1985).

10.   W.R. Loewenstein and Y. Kanno. Studies on an Epithelial (Gland) Cell Junction. I. Modifications of Surface Membrane Permeability. *J Cell Biol.* 22:565-586 (1964).

11.   J. Wiener, D. Spiro, and W.R. Loewenstein. Studies on an Epithelial (Gland) Cell Junction. Ii. Surface Structure. *J Cell Biol.* 22:587-598 (1964).

12.   G. Kanaporis, P.R. Brink, and V. Valiunas. Gap junction permeability: selectivity for anionic and cationic probes. *Am J Physiol Cell Physiol.* 300:C600-609 (2011).

13.   M. Abbaci, M. Barberi-Heyob, W. Blondel, F. Guillemin, and J. Didelon. Advantages and limitations of commonly used methods to assay the

molecular permeability of gap junctional intercellular communication. *Biotechniques.* 45:33-52, 56-62 (2008).

14. J.S. Goodwin and A.K. Kenworthy. Photobleaching approaches to investigate diffusional mobility and trafficking of Ras in living cells. *Methods.* 37:154-164 (2005).

15. G. Morgan, J.D. Pearson, and F.V. Sepulveda. Absence of gap junctional complexes in two established renal epithelial cell lines (LLC-PK1 and MDCK). *Cell Biol Int Rep.* 8:917-922 (1984).

16. M. Cereijido, E. Robbins, D.D. Sabatini, and E. Stefani. Cell-to-cell communication in monolayers of epithelioid cells (MDCK) as a function of the age of the monolayer. *J Membr Biol.* 81:41-48 (1984).

17. S. Trapp and R.W. Horobin. A predictive model for the selective accumulation of chemicals in tumor cells. *Eur Biophys J.* 34:959-966 (2005).

18. X. Zhang, N. Zheng, P. Zou, H. Zhu, J.P. Hinestroza, and G.R. Rosania. Cells on Pores: A Simulation-Driven Analysis of Transcellular Small Molecule Transport. *Mol Pharm.* 7:456-467 (2010).

19. X. Zhang, K. Shedden, and G.R. Rosania. A cell-based molecular transport simulator for pharmacokinetic prediction and cheminformatic exploration. *Mol Pharm.* 3:704-716 (2006).

20. M.V. Filatov and E.Y. Varfolomeeva. Active dissociation of Hoechst 33342 from DNA in living mammalian cells. *Mutat Res.* 327:209-215 (1995).

21. X.Y. Zhang, N. Zheng, P. Zou, H.N. Zhu, J.P. Hinestroza, and G.R. Rosania. Cells on Pores: A Simulation-Driven Analysis of Transcellular Small Molecule Transport. *Molecular Pharmaceutics.* 7:456-467 (2010).

22. M.J. Rindler, L.M. Chuman, L. Shaffer, and M.H. Saier, Jr. Retention of differentiated properties in an established dog kidney epithelial cell line (MDCK). *J Cell Biol.* 81:635-648 (1979).

23. L. Xia, M. Zhou, T.F. Kalhorn, H.T. Ho, and J. Wang. Podocyte-specific expression of organic cation transporter PMAT: implication in puromycin aminonucleoside nephrotoxicity. *Am J Physiol Renal Physiol.* 296:F1307-1313 (2009).

24. U. Karbach, J. Kricke, F. Meyer-Wentrup, V. Gorboulev, C. Volk, D. Loffing-Cueni, B. Kaissling, S. Bachmann, and H. Koepsell. Localization of organic cation transporters OCT1 and OCT2 in rat kidney. *Am J Physiol Renal Physiol.* 279:F679-687 (2000).

25. C.S. Karyekar, N.D. Eddington, T.S. Garimella, P.O. Gubbins, and T.C. Dowling. Evaluation of P-glycoprotein-mediated renal drug interactions in an MDR1-MDCK model. *Pharmacotherapy.* 23:436-442 (2003).

26. H.B. van den Berg van Saparoea, J. Lubelski, R. van Merkerk, P.S. Mazurkiewicz, and A.J. Driessen. Proton motive force-dependent Hoechst

33342 transport by the ABC transporter LmrA of Lactococcus lactis. *Biochemistry.* 44:16931-16938 (2005).

27.   C.W. Cunningham, A. Mukhopadhyay, G.H. Lushington, B.S. Blagg, T.E. Prisinzano, and J.P. Krise. Uptake, distribution and diffusivity of reactive fluorophores in cells: implications toward target identification. *Mol Pharm.* 7:1301-1310 (2010).

28.   S. Chen and L.P. Lee. Non-invasive microfluidic gap junction assay. *Integr Biol (Camb).* 2:130-138 (2010).

29.   J.A. Dix and A.S. Verkman. Crowding effects on diffusion in solutions and cells. *Annu Rev Biophys.* 37:247-263 (2008).

30.   N. Ye, C. Bathany, and S.Z. Hua. Assay for molecular transport across gap junction channels in one-dimensional cell arrays. *Lab Chip.* 11:1096-1101 (2011).

31.   S. Takayama, E. Ostuni, P. LeDuc, K. Naruse, D.E. Ingber, and G.M. Whitesides. Selective chemical treatment of cellular microdomains using multiple laminar streams. *Chem Biol.* 10:123-130 (2003).

Tables

Table 5.1. Properties of MDCK cell monolayers on patterned membranes.

	TEER values $\Omega \cdot cm^2$	Cell count ($\times 10^5$ / well)
Patterned membrane 5 × 5, 20 μm	458 ± 69	4.9 ± 0.5
Patterned membrane 3 × 3, 40 μm	379 ± 76	5.2 ± 0.4
Patterned membrane 3 × 3, 80 μm	388 ± 106	5.2 ± 0.3
Patterned membrane 3 × 3, 160 μm	429 ± 45	4.9 ± 0.2

Figures

Figure 5.1. The design of insert system with patterned pore arrays on membrane support. (A) Insert design and imaging strategy. (B) Light scattering images of a 5×5, 20 μm apart pore array. (C) MDCK cell monolayer above a membrane support with 3×3, 40 μm apart pore array. Scale bar: 40 μm.
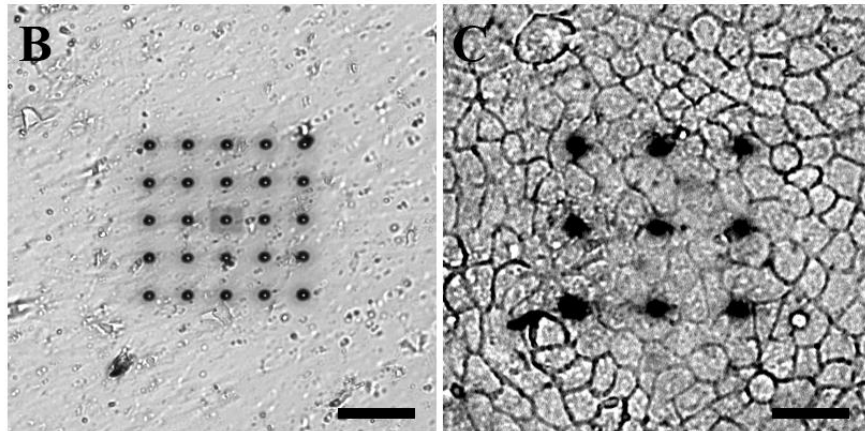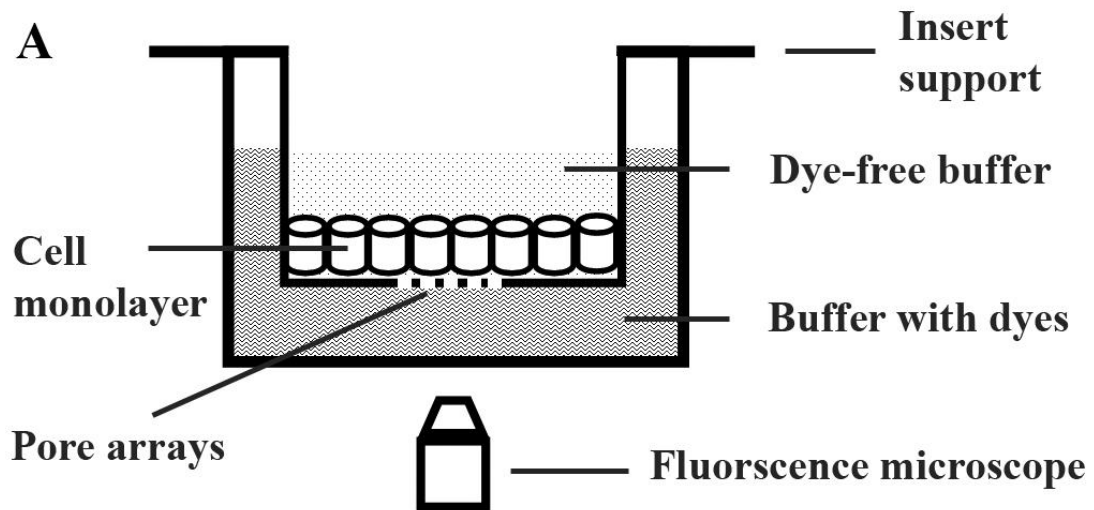
Figure 5.2. Diagrams showing the intercellular pharmacokinetic.
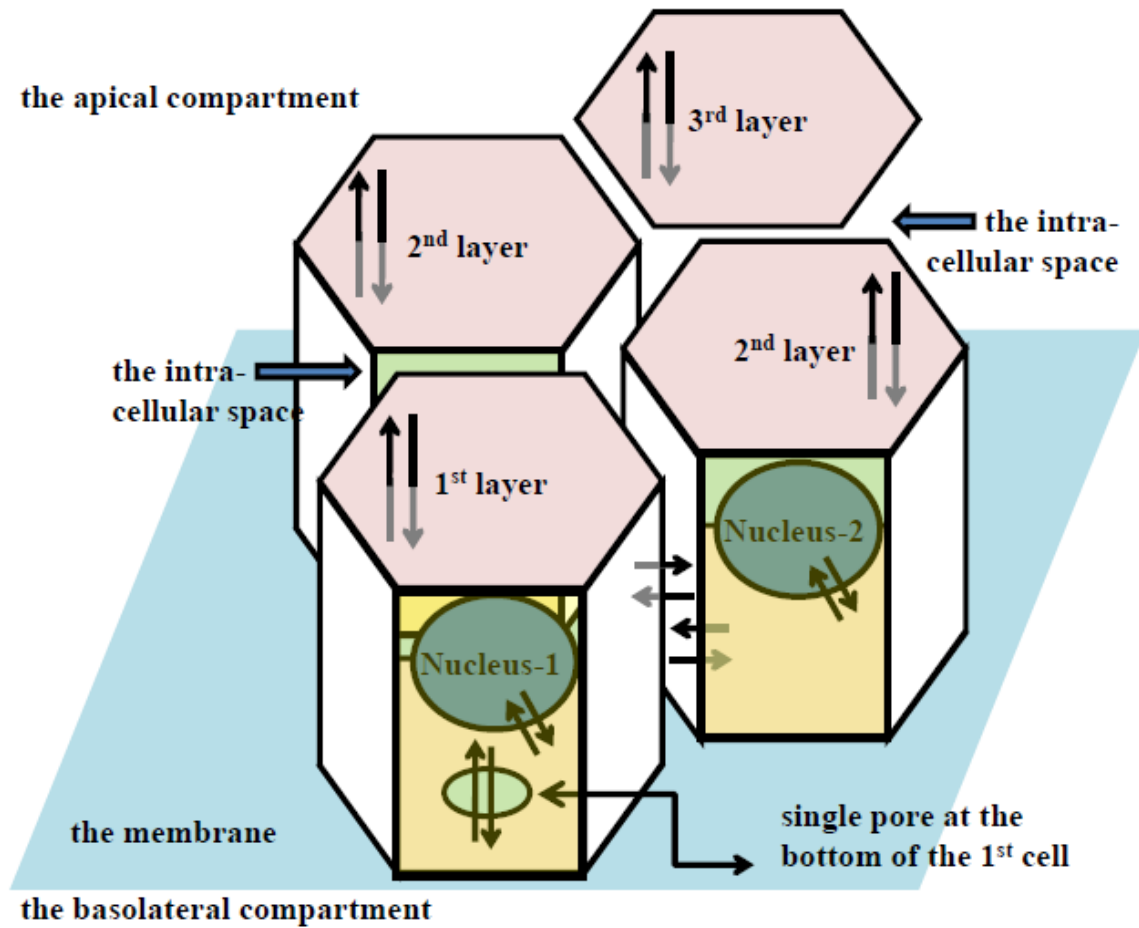
Figure 5.3. Time course and differential uptake of Hoechst 33342 in cell monolayer on 5×5, 20 μm apart pore arrays. Images (A-F) were taken 25, 45, 55, 70, 85 and 115 min after the addition of Hoe in the basolateral compartment. Red circles indicate pore locations. Scale bar: 40 μm.
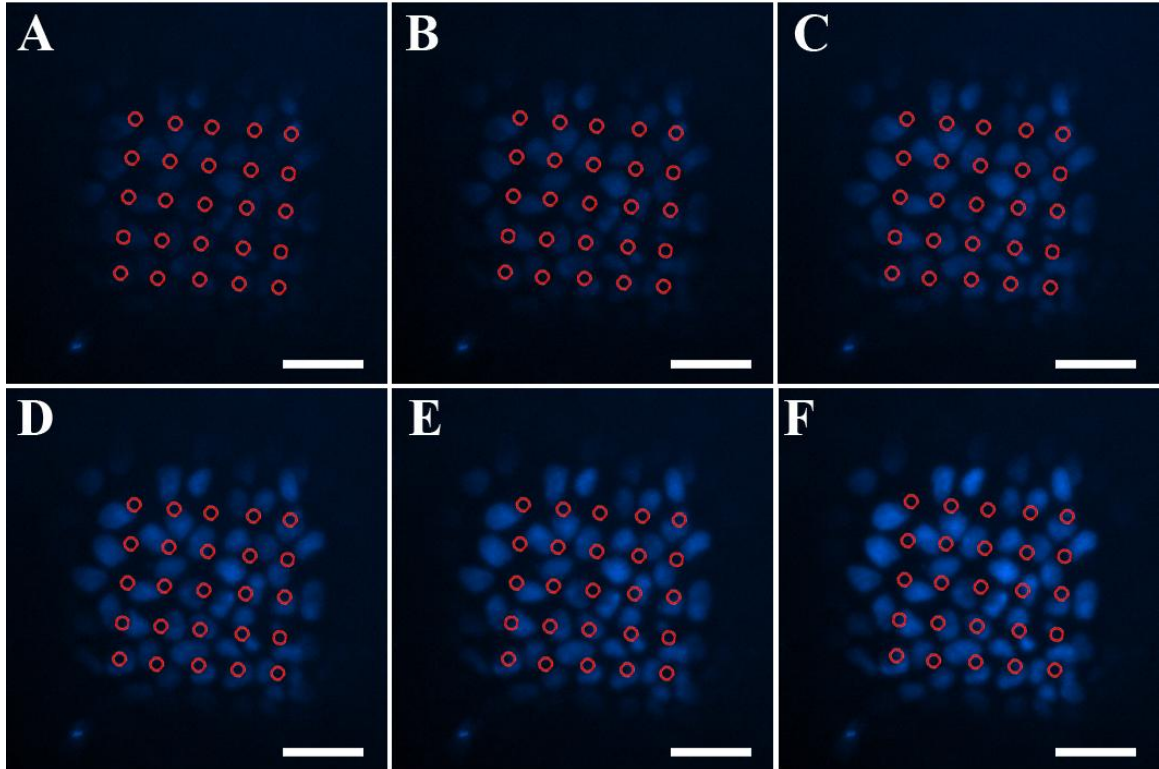
Figure 5.4. Fluorescent images of cell monolayer stained between 2.5-3 hours after the addition of Hoechst 33342 in the basolateral compartment. Cells were grown and imaged on a (A) 5×5, 20 μm apart, (B) a 3×3, 40 μm apart, (C) 3×3, 80 μm apart and (D) 3×3, 160 μm apart pore array membranes. Red spots indicate the location of pores. Scale bar: 80 μm.
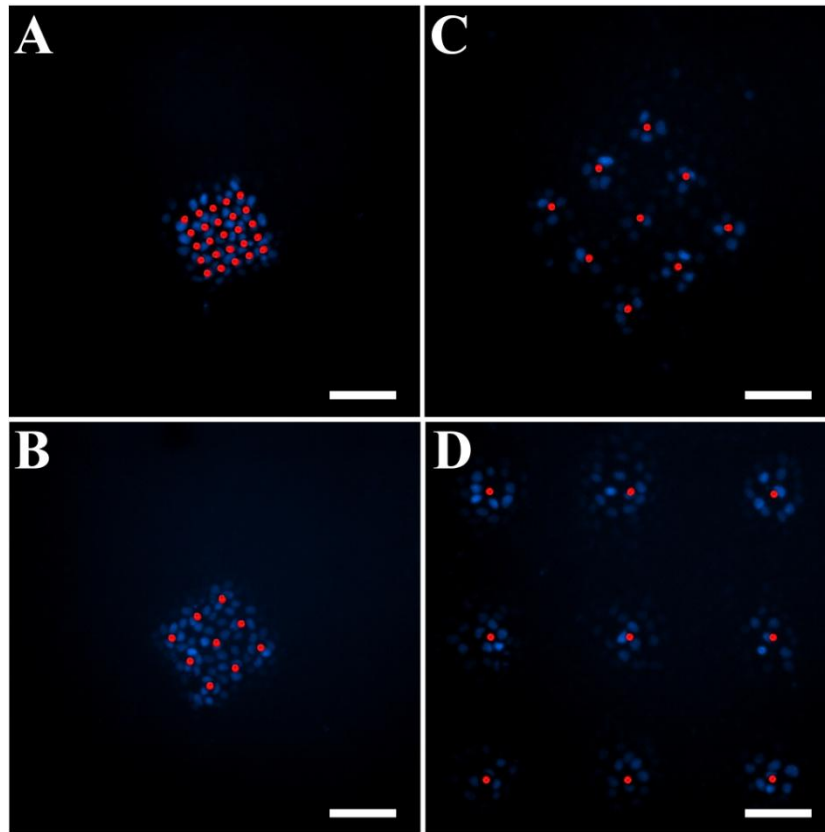
Figure 5.5. Fluorescent images of cell monolayer stained 3 hours after the addition of Hoechst 33342 in the basolateral compartment (A) and the kinetics of differential fluorescence intensity incensement in neighboring cells (B). MDCK cells were grown on a 3×3, 160 μm apart pore array membranes. Cell numbers indicates vicinity to the closet pore. Red spots indicate the location of pores. Normalized fluorescence intensity was presented in mean ± s.d. of 6 sets of cells. Scale bar: 20 μm.
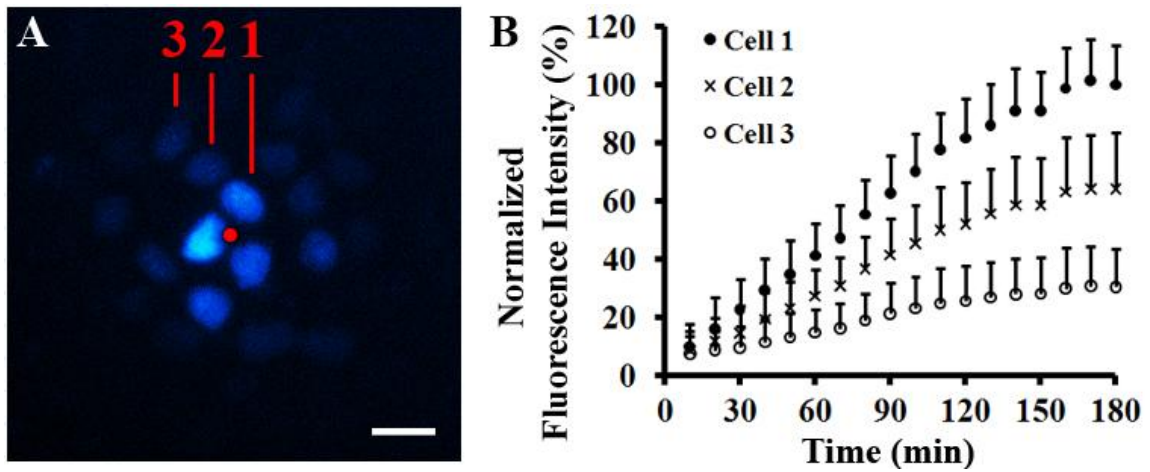
Figure 5.6. Fluorescent images of cell monolayer stained 2 hours after the addition of Hoechst 33342 and MitoTracker Red in the basolateral compartment and the gradient of staining in neighboring cells. MDCK cells were grown on a 3×3, 160 μm apart pore array membranes. Cell numbers indicates vicinity to the closet pore. (A) The staining of the nucleus with Hoechst 33342; (B) the staining of mitochondria with MitoTracker Red; (C) Overlay image of cells stained with both dyes. White spots indicate the location of pores. Normalized fluorescence intensity was presented in mean ± s.d. of 6 sets of cells. Asterisk indicates significant difference using Student's T-test (p<0.05). Scale bar: 20 μm.
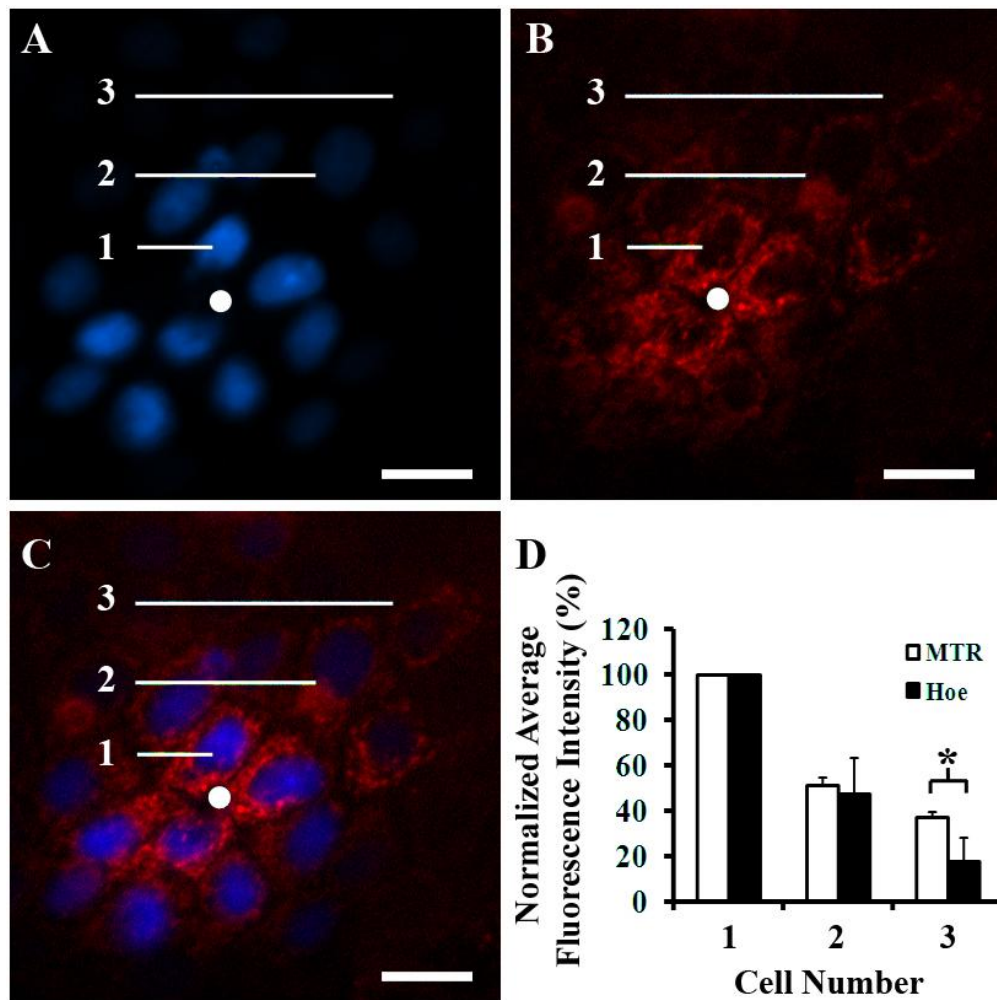
Figure 5.7. Fluorescent images of live cell monolayer (A) and Triton extracted cell monolayer (B) between 2.5-3 hours after the addition of Hoechst 33342 in the basolateral compartment. Cells were grown and imaged on 3×3, 80 μm apart pore array membranes. Red spots indicate the location of pores. Scale bar: 80 μm.
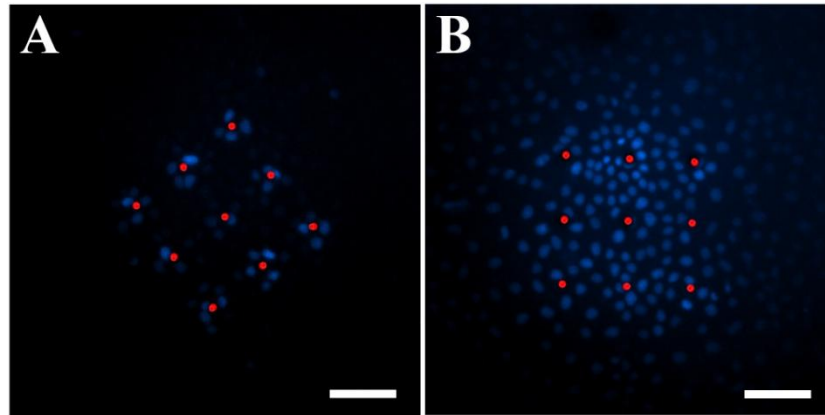
Figure 5.8. Fluorescent images of cell monolayer stained 2 hours after the addition of Hoechst 33342 and BCECF-AM in the basolateral compartment. MDCK cells were grown on a 3×3, 40 μm apart pore array membranes. (A) The staining of the nucleus with Hoechst 33342; (B) the staining of cytosol with BCECF-AM; (C) Overlay image of cells stained with both dyes. Red spots indicate the location of pores. Scale bar: 20 μm.
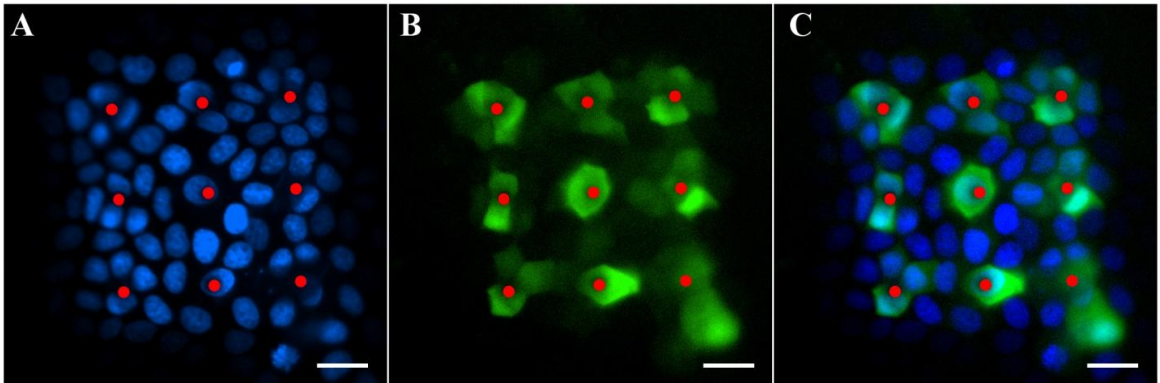
Figure 5.9. Normalized rate of change of Hoechst concentration. (A) The rate of change in the average fluorescence intensity against time was measured for individual nucleus on a 3-by-3, 160 μm apart pore array. This number was divided by the maximum rate of all nucleuses and plotted against the distance as the xth nucleus to the pore. (B) The rate of change in nucleus concentration against time was simulated with MatLab® for 1000 cells using randomly selected cellular parameters within reasonable range. This number was divided by the medium rate of all nucleuses and those equal or smaller than the medium was plotted against distance as the xth nucleus to the pore.
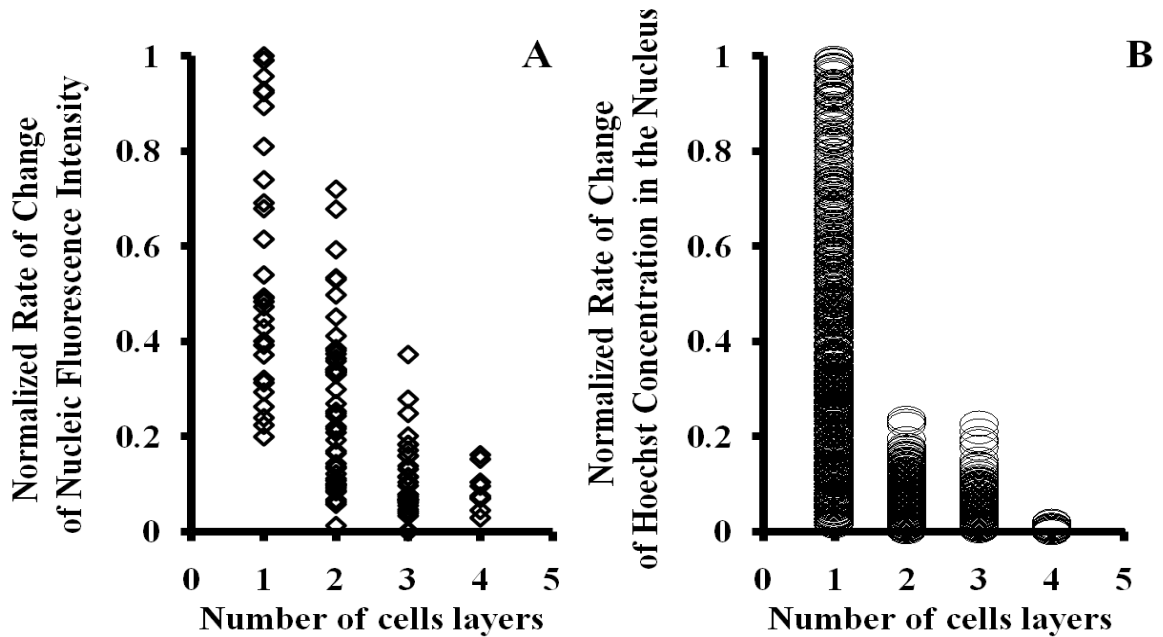
Chapter VI

Summary

In this project the current knowledge of organelle targeting features of small molecules were evaluated in terms of its relevance to developing computational tool for subcellular pharmacokinetics behavior. A mechanism-based computational model [1] that has been successful in predicting the trans-cellular permeability of highly permeable molecules [2] was further applied to study 1) the relationship between the physicochemical properties and the associated cellular distribution profiles of small molecules; 2) the effect of drug-induced cellular response on non-steady state, continuous subcellular transport and accumulation; and 3) the slower-than-expected intercellular lateral diffusion rate of small hydrophobic cell permeant fluorescent dyes. These studies exemplify the usefulness of a mechanistic cell-based model to advance subcellular transport knowledge of passively diffusing molecules, guide experiments aiming at elucidating subcellular pharmacokinetics, and to serve as a step stone toward building a physiologically-based pharmacokinetic model to facilitate the analysis of drug distribution and efficacy in human bodies.

This study also pointed out many opportunities to advance effective screening for drug candidates with desirable distribution and transport behavior at a subcellular and systemic level. In the following sections we will be discussing

several opportunities that the cheminformatic and mechanistic study of drug distribution / transport could benefit from.

The development of quantitative experimental platform for the real time tracking and analysis of non-fluorescent molecules in multiple subcellular compartments

The advantages and limitations of experimental methods used in subcellular pharmacokinetics studies have been shaping and re-shaping our understanding of small molecule distribution / transport behavior and generating evidences that would affect our judgment on emerging approaches in the field. In Chapter I, we have reviewed the progress of subcellular distribution research in the past half century. We realized that current knowledge of small molecule subcellular distribution and intracellular transport is biased towards fluorescent compounds, with either intrinsic fluorescence or fluorescent molecular tags. Therefore, the development of experimental platform that are applicable to non-fluorescent, non-targeted molecules will be very beneficial to expand our current understanding of the subcellular distribution properties of small molecules.

In Chapter V we have proposed an insert system with geometrically patterned pore arrays for quantitative, real time tracking of the intracellular and intercellular transport of small fluorescent molecules. Similar with the multiple laminar fluid streams design as proposed by Takayama et al. [3], this system could be used to track the pharmacological effect of non-fluorescent molecules

within cell monolayer. We envision this novel insert design would be a useful tool in testing hypothesis of drug subcellular transport behavior.

Elaboration of hypothesis-driven, mechanistic modeling technique

The success of mechanism-based modeling replied on a thorough understanding of the biological phenomenon of the interest. When discrepancies between model estimation and observation are observed, the researcher is encouraged to search for mechanisms that are left out in the model. For example, the earliest cell-based transport simulator [1] was build based upon mass balance, Fick's law of diffusion, Nernst–Planck equation. The input parameters of the models, including the physiological properties of the cellular environment were considered constant throughout drug treatment. While this basic model well predicted the lysosomotropic phenomenon [4] and the trans-cellular permeability of highly permeable molecules [2], its performance in analyzing the intracellular accumulation of chloroquine was compromised   [2]. In Chapter IV, because chloroquine is observed to induce phospholipidosis like response, the modified model was proposed to incorporate the lysosomal swelling mechanism as modeled by increasing volume in the acidic compartment, and the binding mechanism as represented by higher sorption efficient. This updated model well captured the kinetics of chloroquine inside cells [5]. More mechanisms that are often encountered during subcellular distribution and transport studies include the metabolism, active transport and reverse binding to cellular components [6].

Other factors that may contribute to improved model performances include the better estimation of molecule diffusivity in the cellular environment. In Chapter V we have shown that measured intercellular diffusivities of Hoechst 33342, a fluorescent nucleus stain, are different in live and dead cellular environment, both of which were significantly lower than the theoretical estimate based on the Einstein-Stoke equation. This discrepancy in the measured and theoretically predicted diffusivities was observed for similar molecular weight compounds [7, 8]. The crowding effect has been proposed to account for this slow diffusion of solutes in the cellular environment, possibly due to the electrostatic interaction between ionic species and charged cellular components (e.g. negatively charged DNA and phospholipids, mitochondria with negative membrane potentials) [9, 10]. A quantitative characterization of the molecular size effect and the crowding effect in the model should be able to facilitate model-guided experimental design and analysis.

Promotion of simulation-guided experimental design

The application of mechanism-based computational models function as a cost-effective '*in silico* laboratory' in which every aspect of knowledge about molecules can be applied, sorted and analyzed according to their relevance to the desired property [11-13]. This strategy cuts down the number of candidates for detailed studies by focusing on the most promising candidate molecules as well as the key parameters for experiment control. The cell-based passive transport model has been successfully used to develop predictive physiologically-

based pharmacokinetic models for absorption, distribution and clearance in tissues and organs [14-19]. However, the development and application of these physiologically-based models have been restricted to a much smaller number of scientific research groups than it could have been potentially useful. The adaption of these Matlab® or Perl based models to window-based, programming-free and more user-friendly software would be highly desirable to promote the application of simulation-guided experimental design.

Incorporation of synthetic biology concepts into pharmacokinetics studies

In Chapter IV, we found that chloroquine continuously accumulated inside cells, by forming complexes with multilamellar bodies that appeared de novo within the lysosomes [5]. Similarly, in our laboratory, we found that chronic administration of clofazimine, a very lipophilic antibiotic, resulted in the formation of autophagosome-like drug inclusions ("aldis"), a new organelle that is derived from mitochondria ([20], under review in Molecular Pharmaceutics). These synthetic organelles may play an important role in determining the pharmacokinetics behavior and subcellular delivery pathways. In the future, we envision that the development of new drug delivery strategies and therapeutic modalities will greatly benefit from a better understanding the formation of new organelles in response to drug therapy, deeper insights into the role of chemically-synthetic organelles as intracellular drug depots, and the capability of synthesizing new organelles with extraordinary physical and chemical properties.

References

1. X. Zhang, K. Shedden, and G.R. Rosania. A cell-based molecular transport simulator for pharmacokinetic prediction and cheminformatic exploration. *Mol Pharmaceutics.* 3:704-716 (2006).

2. X. Zhang, N. Zheng, P. Zou, H. Zhu, J.P. Hinestroza, and G.R. Rosania. Cells on Pores: A Simulation-Driven Analysis of Transcellular Small Molecule Transport. *Mol Pharm.* 7:456-467 (2010).

3. S. Takayama, E. Ostuni, P. LeDuc, K. Naruse, D.E. Ingber, and G.M. Whitesides. Selective chemical treatment of cellular microdomains using multiple laminar streams. *Chem Biol.* 10:123-130 (2003).

4. X. Zhang, N. Zheng, and G.R. Rosania. Simulation-based cheminformatic analysis of organelle-targeted molecules: lysosomotropic monobasic amines. *J Comput Aided Mol Des.* 22:629-645 (2008).

5. N. Zheng, X. Zhang, and G.R. Rosania. The Effect of Phospholipidosis on the Cellular Pharmacokinetics of Chloroquine. *J Pharmacol Exp Ther* (2011).

6. T. Watanabe, H. Kusuhara, K. Maeda, Y. Shitara, and Y. Sugiyama. Physiologically based pharmacokinetic modeling to predict transporter-mediated clearance and distribution of pravastatin in humans. *J Pharmacol Exp Ther.* 328:652-662 (2009).

7. C.W. Cunningham, A. Mukhopadhyay, G.H. Lushington, B.S. Blagg, T.E. Prisinzano, and J.P. Krise. Uptake, distribution and diffusivity of reactive fluorophores in cells: implications toward target identification. *Mol Pharm.* 7:1301-1310 (2010).

8. S. Chen and L.P. Lee. Non-invasive microfluidic gap junction assay. *Integr Biol (Camb).* 2:130-138 (2010).

9. J.A. Dix and A.S. Verkman. Crowding effects on diffusion in solutions and cells. *Annu Rev Biophys.* 37:247-263 (2008).

10. H.M. Jones, N. Parrott, K. Jorga, and T. Lave. A novel strategy for physiologically based predictions of human pharmacokinetics. *Clin Pharmacokinet.* 45:511-542 (2006).

11. C. Lipinski and A. Hopkins. Navigating chemical space for biology and medicine. *Nature.* 432:855-861 (2004).

12. C.M. Dobson. Chemical space and biology. *Nature.* 432:824-828 (2004).

13. A.C. Anderson. The process of structure-based drug design. *Chem Biol.* 10:787-797 (2003).

14. K.S. Pang. Modeling of intestinal drug absorption: roles of transporters and metabolic enzymes (for the Gillette Review Series). *Drug Metab Dispos.* 31:1507-1519 (2003).

15. D. Tam, H. Sun, and K.S. Pang. Influence of P-glycoprotein, transfer clearances, and drug binding on intestinal metabolism in Caco-2 cell monolayers or membrane preparations: a theoretical analysis. *Drug Metab Dispos.* 31:1214-1226 (2003).

16. L. Yan, S. Sheihk-Bahaei, S. Park, G.E. Ropella, and C.A. Hunt. Predictions of hepatic disposition properties using a mechanistically realistic, physiologically based model. *Drug Metab Dispos.* 36:759-768 (2008).

17. W. Fu, A. Franco, and S. Trapp. Methods for estimating the bioconcentration factor of ionizable organic chemicals. *Environ Toxicol Chem.* 28:1372-1379 (2009).

18. J.Y. Yu and G.R. Rosania. Cell-based multiscale computational modeling of small molecule absorption and retention in the lungs. *Pharm Res.* 27:457-467 (2010).

19. S. Trapp, A. Franco, and D. Mackay. Activity-based concept for transport and partitioning of ionizing organics. *Environ Sci Technol.* 44:6123-6129 (2010).

20. J. Baik and G.R. Rosania. molecular Imaging of Intracellular Drug-Membrane Aggregate Formation. *Mol Pharmaceutics*.

APPENDICES

Appendix A

The chemical compounds with reported subcellular localization site in the endo-lysosomes. References information is available in Appendix H. Structure is presented as the Simplified Molecular Input Line Entry Specification string of the major microspecies at pH 7.4, as calculated by ChemAxon.

Name:	Ammonia
Method:	Pharmacological Effect
References:	1
Structure:	[NH4+]

Name:	Methylamine
Method:	Pharmacological Effect
References:	1
Structure:	C[NH3+]

Name:	Dimethylamine
Method:	Pharmacological Effect
References:	1
Structure:	C[NH2+]C

Name:	Ethylamine
Method:	Pharmacological Effect
References:	1
Structure:	CC[NH3+]

Name:	Isopropylamine
Method:	Pharmacological Effect
References:	1
Structure:	CC(C)[NH3+]

Name:	Propylamine
Method:	Pharmacological Effect
References:	1
Structure:	CCC[NH3+]

Name:	Trimethylamine
Method:	Pharmacological Effect
References:	1
Structure:	C[NH+](C)C

Name:	Ethylenediamine
Method:	Pharmacological Effect

References:	1
Structure:	NCC[NH3+]

Name:	Ethanolamine; 2-aminoethanol
Method:	Pharmacological Effect
References:	1
Structure:	[NH3+]CCO

Name:	Imidazole
Method:	Pharmacological Effect
References:	1, 229
Structure:	c1c[nH]cn1

Name:	Butylamine
Method:	Pharmacological Effect
References:	1
Structure:	CCCC[NH3+]

Name:	Diethylamine
Method:	Pharmacological Effect
References:	1
Structure:	CC[NH2+]CC

Name:	Isobutylamine
Method:	Pharmacological Effect
References:	1
Structure:	CC(C)C[NH3+]

Name:	S-butylamine
Method:	Pharmacological Effect
References:	1
Structure:	CCC(C)[NH3+]

Name:	T-butylamine
Method:	Pharmacological Effect
References:	1

Structure:	CC(C)(C)[NH3+]
Name:	1,2-Diaminopropane
Method:	Pharmacological Effect
References:	1
Structure:	CC([NH3+])CN
Name:	2-Methylaminoethanol
Method:	Pharmacological Effect
References:	1
Structure:	C[NH2+]CCO
Name:	Isopropanolamine
Method:	Pharmacological Effect
References:	1
Structure:	CC(O)C[NH3+]
Name:	Pentylamine
Method:	Pharmacological Effect
References:	1
Structure:	CCCCC[NH3+]
Name:	N,N-Dimethylethylenediamine
Method:	Pharmacological Effect
References:	1
Structure:	CNCC[NH2+]C
Name:	2-amino-1-butanol
Method:	Pharmacological Effect
References:	1
Structure:	CCC([NH3+])CO
Name:	2-amino-2-methyl-1-propanol
Method:	Pharmacological Effect
References:	1
Structure:	CC(C)([NH3+])CO
Name:	2-Dimethylaminoethanol
Method:	Pharmacological Effect
References:	1
Structure:	C[NH+](C)CCO
Name:	4-amino-1-butanol
Method:	Pharmacological Effect
References:	1
Structure:	[NH3+]CCCCO
Name:	Hexylamine
Method:	Pharmacological Effect
References:	1
Structure:	CCCCCC[NH3+]
Name:	Triethylamine
Method:	Pharmacological Effect

References:	1
Structure:	CC[NH+](CC)CC
Name:	3-Dimethylamino-1-propylamine
Method:	Pharmacological Effect
References:	1
Structure:	C[NH+](C)CCC[NH3+]
Name:	3-Dimethylamino-1-propanol
Method:	Pharmacological Effect
References:	1
Structure:	C[NH+](C)CCCO
Name:	2-Amino-2-methyl-1,3-propanediol
Method:	Pharmacological Effect
References:	1
Structure:	CC([NH3+])(CO)CO
Name:	beta-Dimethylaminoethylchloride
Method:	Pharmacological Effect
References:	1
Structure:	C[NH+](C)CCCl
Name:	N,N-Diethylaminoethylamine
Method:	Pharmacological Effect
References:	1
Structure:	CC[NH+](CC)CCN
Name:	2-(diethylamino)ethanol
Method:	Pharmacological Effect
References:	1
Structure:	CC[NH+](CC)CCO
Name:	2-Dimethylamino-2-methyl-1-propanol
Method:	Pharmacological Effect
References:	1
Structure:	C[NH+](C)C(C)(C)CO
Name:	N,N-Dimethyl-3-chloropropylamine
Method:	Pharmacological Effect
References:	1
Structure:	C[NH+](C)CCCCl
Name:	Dibutylamine
Method:	Pharmacological Effect
References:	1
Structure:	CCCC[NH2+]CCCC
Name:	Triethanolamine

Method:	Pharmacological Effect
References:	1
Structure:	OCC[NH+](CCO)CCO
Name:	Phentermine
Method:	Pharmacological Effect
References:	6, 512
Structure:	CC(C)([NH3+])Cc1ccccc1
Name:	Chlorphentermine
Method:	Pharmacological Effect
References:	6, 512
Structure:	CC(C)([NH3+])Cc1ccc(Cl)cc1
Name:	Fenfluramine
Method:	Pharmacological Effect
References:	6, 516
Structure:	CCC(C)([NH3+])Cc1ccc(cc1)C(F)(F)F
Name:	Alprenolol
Method:	Uptake/Binding
References:	3
Structure:	CC(C)[NH2+]CC(O)COc1ccccc1CC=C
Name:	Propranolol
Method:	Uptake/Binding
References:	3, 4, 6
Structure:	CC(C)[NH2+]CC(O)COc1cccc2ccccc12
Name:	Nortriptyline
Method:	Pharmacological Effect
References:	6, 522
Structure:	C[NH2+]CCC=C1c2ccccc2CCc2ccccc12
Name:	Mianserin
Method:	Pharmacological Effect
References:	6, 510
Structure:	C[NH+]1CCN2C(C1)c1ccccc1Cc1ccccc21
Name:	Amitriptyline
Method:	Pharmacological Effect
References:	6, 512
Structure:	C[NH+](C)CCC=C1c2ccccc2CCc2ccccc12
Name:	Maprotiline
Method:	Pharmacological Effect
References:	6, 523
Structure:	C[NH2+]CCCC12CCC(c3cccc

	c13)c1ccccc21
Name:	Perhexiline
Method:	Pharmacological Effect
References:	2, 6, 510
Structure:	C1CCC(CC1)C(CC1CCCC[NH2+]1)C1CCCCC1
Name:	Promazine
Method:	Uptake/Binding
References:	6, 175
Structure:	C[NH+](C)CCCN1c2ccccc2Sc2ccccc12
Name:	Iprindole
Method:	Pharmacological Effect
References:	6, 512
Structure:	C[NH+](C)CCCn1c2CCCCCCc2c2ccccc12
Name:	Cyanopindolol
Method:	Uptake/Binding
References:	3
Structure:	CC(C)(C)[NH2+]CC(O)COc1cccc2[nH]c(cc12)C#N
Name:	N3246; Neutral red
Method:	Fluorescence Microscopy
References:	583
Structure:	CN(C)c1ccc2nc3cc(C)c(N)cc3nc2c1
Name:	Noxiptiline
Method:	Pharmacological Effect
References:	6, 512
Structure:	C[NH+](C)CCON=C1c2ccccc2CCc2ccccc12
Name:	Chlorcyclizine
Method:	Pharmacological Effect
References:	2, 6, 718
Structure:	C[NH+]1CCN(CC1)C(c1ccccc1)c1ccc(Cl)cc1
Name:	Biperiden
Method:	Uptake/Binding
References:	5
Structure:	OC(CC[NH+]1CCCCC1)(C1CC2CC1C=C2)c1ccccc1
Name:	Clomipramine
Method:	Fluorescence Microscopy
References:	6, 522
Structure:	C[NH+](C)CCCN1c2ccccc2C

	Cc2ccc(Cl)cc12

Name:	Chloroquine
Method:	Pharmacological Effect
References:	673
Structure:	CC[NH+](CC)CCCC(C)Nc1cc[nH+]c2cc(Cl)ccc12

Name:	D113; 5-dimethylaminonaphthalene-1-(N-(5-aminopentyl))sulfonamide (dansyl cadaverine)
Method:	Fluorescence Microscopy
References:	51
Structure:	CN(C)c1cccc2c(cccc12)S(=O)(=O)NCCCCC[NH3+]

Name:	Hydroxychloroquine
Method:	Fluorescence Microscopy
References:	45
Structure:	CC[NH+](CCO)CCCC(C)Nc1cc[nH+]c2cc(Cl)ccc12

Name:	L7534; LysoTracker® Green DND-153
Method:	Fluorescence Microscopy
References:	663
Structure:	C[NH+](C)CCNc1ccc2-c3nc4ccccc4n3C(=O)c3cccc1c23

Name:	Indomethacin
Method:	Fluorescence Microscopy
References:	127
Structure:	COc1ccc2n(C(=O)c3ccc(Cl)cc3)c(C)c(CC([O-])=O)c2c1

Name:	11
Method:	Uptake/Binding
References:	7
Structure:	CC(C)C(C(=O)[N-]C#N)c1cccc(c1)-c1ccc(cc1)N1CC[NH2+]CC1

Name:	L7545; LysoTracker® Yellow/Blue DND-160
Method:	Fluorescence Microscopy
References:	654
Structure:	C[NH+](C)CCNC(=O)COc1ccc(cc1)-c1cnc(o1)-c1ccncc1

Name:	Thioridazine
Method:	Uptake/Binding
References:	6, 175, 510

Structure:	CSc1ccc2Sc3ccccc3N(CCC3CCCC[NH+]3C)c2c1

Name:	Tamoxifen
Method:	Pharmacological Effect
References:	2, 6, 510
Structure:	CC\C(c1ccccc1)=C(/c1ccccc1)c1ccc(OCC[NH+](C)C)cc1

Name:	L7533; LysoTracker® Blue DND-167
Method:	Fluorescence Microscopy
References:	655
Structure:	C1C[NH+](CCO1)Cc1c2ccccc2c(C[NH+]2CCOCC2)c2ccccc12

Name:	Mefloquine
Method:	Fluorescence Microscopy
References:	529, 530
Structure:	OC(C1CCCC[NH2+]1)c1cc(nc2c(cccc12)C(F)(F)F)C(F)(F)F

Name:	D1552; N-(3-((2,4-dinitrophenyl)amino)propyl)-N-(3-aminopropyl)methylamine, dihydrochloride DAMP
Method:	histo
References:	598
Structure:	C[NH+](CCC[NH3+])CCCNc1ccc(cc1N(=O)=O)N(=O)=O

Name:	D10460; Dapoxyl® (2-aminoethyl)sulfonamide
Method:	Fluorescence Microscopy
References:	682
Structure:	CN(C)c1ccc(cc1)-c1cnc(o1)-c1ccc(cc1)S(=O)(=O)NCC[NH3+]

Name:	L7535; LysoTracker® Green DND-189
Method:	Fluorescence Microscopy
References:	352
Structure:	O=C1c2cccc3c(NCCN4CCOCC4)ccc(-c4nc5ccccc5n14)c23

Name:	L7526; LysoTracker® Green DND-26
Method:	Fluorescence Microscopy
References:	500, 584
Structure:	C[NH+](C)CCNC(=O)CCC1=[N+]2C(C=C1)=Cc1c(C)cc(C)n1[B-]2(F)F

Name:	L7528; LysoTracker® Red DND-99			1)C(=O)[N-]C#N
Method:	Fluorescence Microscopy		Name:	Verapamil
References:	584		Method:	Uptake/Binding
Structure:	C[NH+](C)CCNC(=O)CCC1=[N+]2C(C=C1)=Cc1ccc(-c3ccc[nH]3)n1[B-]2(F)F		References:	5
			Structure:	COc1ccc(CC[NH+](C)CCCC(C#N)(C(C)C)c2ccc(OC)c(OC)c2)cc1OC
Name:	Mepacrine; Quinacrine			
Method:	Fluorescence Microscopy		Name:	10
References:	6, 127, 510		Method:	Uptake/Binding
Structure:	CC[NH+](CC)CCCC(C)Nc1c2ccc(Cl)cc2[nH+]c2ccc(OC)cc12		References:	7
			Structure:	CCC[NH+]1CCN(CC1)c1nc(cs1)-c1ccc(cc1)C(=O)NC1(CCCCC1)C(=O)[N-]C#N
Name:	Trifluoperazine			
Method:	Uptake/Binding		Name:	F7030; FUN® 1
References:	5		Method:	Fluorescence Microscopy
Structure:	CN1CC[NH+](CCCN2c3ccccc3Sc3ccc(cc23)C(F)(F)F)CC1		References:	606
			Structure:	C[n+]1c(sc2cccccc12)\C=C1/C=C(Cl)N(c2ccccc2)c2ccccc12
Name:	Disobutamide			
Method:	Cell Fractionation		Name:	T3166; N-(3-triethylammoniumpropyl)-4-(6-(4-(diethylamino)phenyl)hexatrienyl)pyridinium dibromide FM® 4-64
References:	6, 513		
Structure:	CC(C)[NH+](CCC(CC[NH+]1CCCCC1)(C(N)=O)c1ccccc1Cl)C(C)C		
			Method:	NA
Name:	Tilorone; [2,7-bis-[2-(diethylamino)ethoxy]fluoren-9		References:	Invi
Method:	Fluorescence Microscopy		Structure:	CCN(CC)c1ccc(cc1)\C=C\C=C\C=C\c1cc[n+](CCC[N+](CC)(CC)CC)cc1
References:	6, 517, 518		
Structure:	CC[NH+](CC)CCOc1ccc-2c(c1)C(=O)c1cc(OCC[NH+](CC)CC)ccc-21		
			Name:	Desethylamiodarone
Name:	Diltiazem		Method:	Cell Fractionation
Method:	Uptake/Binding		References:	6, 24, 521
References:	5		Structure:	CCCCc1oc2ccccc2c1C(=O)c1cc(I)c(OCC[NH2+]CC)c(I)c1
Structure:	COc1ccc(cc1)C1Sc2ccccc2N(CC[NH+](C)C)C(=O)C1OC(C)=O		
			Name:	Amiodarone
Name:	Triparanol		Method:	Pharmacological Effect
Method:	Pharmacological Effect		References:	2, 6, 24, 42, 510
References:	6, 520		Structure:	CCCCc1oc2ccccc2c1C(=O)c1cc(I)c(OCC[NH+](CC)CC)c(I)c1
Structure:	CC[NH+](CC)CCOc1ccc(cc1)C(O)(Cc1ccc(Cl)cc1)c1ccc(C)cc1		
			Name:	N3524; 6-((N-(7-nitrobenz-2-oxa-1,3- diazol-4-yl)amino)hexanoyl)sphingosyl phosphocholineNBD C6-sphingomyelin
Name:	1		
Method:	Fluorescence Microscopy		
References:	7		
Structure:	CN1CCN(CC1)c1nc(cs1)-c1ccc(cc1)C(=O)NC1(CCCCC		Method:	Fluorescence Microscopy
			References:	636

Structure:	CCCCCCCCCCCCC\C=C\C(O)C(COP([O-])(=O)OCC[N+](C)(C)C)NC(=O)CCCCNc1ccc(c2nonc12)N(=O)=O
Name:	Azithromycin
Method:	Cell Fractionation
References:	162
Structure:	CCC1OC(=O)C(C)C(OC2CC(C)(OC)C(O)C(C)O2)C(C)C(OC2OC(C)CC(C2O)[NH+](C)C)C(C)(O)CC(C)C[NH+](C)C(C)C(O)C1(C)O
Name:	Netilmicin
Method:	Pharmacological Effect
References:	23
Structure:	CC[NH2+]C1CC([NH3+])C(OC2OC(C[NH3+])=CCC2[NH3+])C(O)C1OC1OCC(C)(O)C([NH2+]C)C1O
Name:	3-Aminopropanal
Method:	Fluorescence Microscopy
References:	11
Structure:	[NH3+]CCC=O
Name:	Stilbamidine
Method:	Fluorescence Microscopy
References:	127
Structure:	NC(=[NH2+])c1ccc(cc1)\C=C\c1ccc(cc1)C(N)=[NH2+]
Name:	Hydroxystilbamide
Method:	Fluorescence Microscopy
References:	127
Structure:	NC(=[NH2+])C1=CC(=O)C(/C=C1)=C/C=C1C=CC(C=C1)=C(N)N
Name:	Antrycide
Method:	Fluorescence Microscopy
References:	127
Structure:	CN1C(C)=CC(=[NH2+])c2cc(Nc3cc(C)[n+](C)c(N)n3)ccc12
Name:	Dexamethasone
Method:	Fluorescence Microscopy
References:	127
Structure:	CC1CC2C3CCC4=CC(=O)C=CC4(C)C3(F)C(O)CC2(C)C1(O)C(=O)CO
Name:	Eosin

Method:	Fluorescence Microscopy
References:	127
Structure:	[O-]C(=O)c1ccccc1C1=C2C=C(Br)C(=O)C(Br)=C2Oc2c(Br)c([O-])c(Br)cc12
Name:	Anthracene
Method:	Fluorescence Microscopy
References:	127
Structure:	C1=CC2=CC3=C(C=CC=C3)C=C2C=C1
Name:	Vitamin A
Method:	Fluorescence Microscopy
References:	127
Structure:	CC(\C=C\C=C(C)\C=C\C1=C(C)CCCC1(C)C)=C/CO
Name:	Uroporphyrin I
Method:	Fluorescence Microscopy
References:	127
Structure:	[O-]C(=O)CCc1c(CC([O-])=O)c2cc3[nH]c(cc4[nH]c(cc5nc(cc1n2)c(CC([O-])=O)c5CCC([O-])=O)c(CC([O-])=O)c4CCC([O-])=O)c(CC([O-])=O)c3CCC([O-])=O
Name:	Amantadine
Method:	Pharmacological Effect
References:	5, 229
Structure:	[NH3+]C12CC3CC(CC(C3)C1)C2
Name:	Atropine
Method:	Pharmacological Effect
References:	5, 229
Structure:	C[NH+]1C2CCC1CC(C2)OC(=O)C(CO)c1ccccc1
Name:	LCL284
Method:	Pharmacological Effect
References:	13
Structure:	CCCCCCCCCCCCCC[NH2+]C(C)C(O)c1ccccc1
Name:	LCL204
Method:	Pharmacological Effect
References:	13
Structure:	CCCCCCCCCCCCCC[NH2+]C(CO)C(O)c1ccc(cc1)N(=O)=O

Name:	MSDH; O-methyl-serine dodecylamine hydrochloride
Method:	Pharmacological Effect
References:	44, 46
Structure:	CCCCCCCCCCCCNC(=O)C([NH3+])COC

Name:	Serine Dodecylamide; SDA
Method:	Pharmacological Effect
References:	46
Structure:	CCCCCCCCCCCCNC(=O)C([NH3+])CO

Name:	N-dodecylimidazole
Method:	Pharmacological Effect
References:	46
Structure:	CCCCCCCCCCCCn1ccnc1

Name:	Dansylamylamine; MDH
Method:	Fluorescence Microscopy
References:	62
Structure:	CCCCCNS(=O)(=O)c1cccc2c(cccc12)N(C)C

Name:	D-tubocurarine
Method:	Cell Fractionation
References:	73
Structure:	COc1cc2CC[NH+](C)C3Cc4ccc(Oc5c(O)c(OC)cc6CC[N+](C)(C)C(Cc7ccc(O)c(Oc1cc23)c7)c56)cc4

Name:	PPC; Pyridinium Zn (II) phthalocyanine
Method:	Fluorescence Microscopy
References:	87
Structure:	C(c1ccc2c3nc(nc4n5[Zn]n6c(nc7nc(nc5c5cc(C[n+]8ccccc8)ccc45)c4ccc(C[n+]5ccccc5)cc74)c4ccc(C[n+]5ccccc5)cc4c6n3)c2c1)[n+]1ccccc1

Name:	TSPC; Tetrasulfonated Zn(II) phthalocyanine
Method:	Fluorescence Microscopy
References:	87
Structure:	[O-]S(=O)(=O)c1ccc2c3nc(nc4n5[Zn]n6c(nc7nc(nc5c5cc(ccc45)S([O-])(=O)=O)c4ccc(cc74)S([O-])(=O)=O)c4ccc(cc4c6n3)S([O-])(=O)=O)c2c1

Name:	Hypericin
Method:	Fluorescence Microscopy
References:	90
Structure:	Cc1cc(O)c2C(=O)c3c(O)cc([O-])c4c5c([O-])cc(O)c6C(=O)c7c(O)cc(C)c8c1c2c(c34)c(c78)c56

Name:	EtNBS; 5-ethylamino-9-diethyl-aminobenzo[a]phenothiazinium chloride
Method:	Fluorescence Microscopy
References:	96
Structure:	CC\N=C1/C=C2Sc3cc(ccc3N=C2c2ccccc12)N(CC)CC

Name:	Ofloxacin
Method:	Fluorescence Microscopy
References:	97
Structure:	CC1COc2c(N3CCN(C)CC3)c(F)cc3C(=O)C(=CN1c23)C([O-])=O

Name:	Norfloxacin
Method:	Fluorescence Microscopy
References:	97
Structure:	CCN1C=C(C([O-])=O)C(=O)c2cc(F)c(cc12)N1CC[NH2+]CC1

Name:	Lomefloxacin
Method:	Fluorescence Microscopy
References:	97
Structure:	CCN1C=C(C([O-])=O)C(=O)c2cc(F)c(N3CC[NH2+]C(C)C3)c(F)c12

Name:	BAYy3118
Method:	Fluorescence Microscopy
References:	97
Structure:	[O-]C(=O)C1=CN(C2CC2)c2c(Cl)c(N3CC4CCC[NH2+]C4C3)c(F)cc2C1=O

Name:	Cyamemazine; CMZ
Method:	Fluorescence Microscopy
References:	101
Structure:	CC(CN1c2ccccc2Sc2ccc(cc12)C#N)C[NH+](C)C

Name:	PCI-0123; Lutetium Texapyrin
Method:	Fluorescence Microscopy
References:	110

Structure:	CCC1=C(CC)/C2=C/C3=N/C(=C\N=C4\C=C(OCCOCCOCCOC)C(OCCOCCOCCOC)=C\C\4=N\C=C4/N=C(/C=C\1N2[Lu])C(CCCO)=C/4C)/C(C)=C3CCCO
Name:	NBA
Method:	Fluorescence Microscopy
References:	112
Structure:	CCN(CC)c1ccc2N=C3C(Oc2c1)=CC(=N)c1ccccc31
Name:	NBA-6I
Method:	Fluorescence Microscopy
References:	112
Structure:	CCN(CC)c1ccc2N=C3c4ccccc4C(=N)C(I)=C3Oc2c1
Name:	NBS
Method:	Fluorescence Microscopy
References:	112
Structure:	CCN(CC)c1ccc2N=C3C(Sc2c1)=CC(=[NH2+])c1ccccc31
Name:	NBS-6I
Method:	Fluorescence Microscopy
References:	112
Structure:	CCN(CC)c1ccc2N=C3c4ccccc4C(=N)C(I)=C3Sc2c1
Name:	Sat-NBS
Method:	Fluorescence Microscopy
References:	112
Structure:	CCN(CC)c1ccc2N=C3C(Sc2c1)=CC(=[NH2+])C1=C3CCCC1
Name:	Sat-NBS-6I
Method:	Fluorescence Microscopy
References:	112
Structure:	CCN(CC)c1ccc2N=C3C4=C(CCCC4)C(=N)C(I)=C3Sc2c1
Name:	AlPcS2a
Method:	Fluorescence Microscopy
References:	125
Structure:	O[Al-]1(O)n2c3cc4nc(cc5n1c(cc1nc(cc2c2ccccc32)c2cccc(c12)S([O-])(=O)=O)c1cccc(c51)S([O-])(=O)=O)c1ccccc41
Name:	Gimatecan
Method:	Fluorescence Microscopy

References:	130
Structure:	CCC1(O)C(=O)OCC2=C1C=C1N(Cc3c1nc1ccccc1c3\C=N\OC(C)(C)C)C2=O
Name:	DADP-o; 5,15-di[4-(N-trimethylaminophenyl)-10,20-diphenylporphyrin
Method:	Fluorescence Microscopy
References:	138
Structure:	C[N+](C)(C)c1ccc(cc1)-c1c2ccc(n2)c(-c2ccccc2)c2ccc([nH]2)c(-c2ccc(cc2)[N+](C)(C)C)c2ccc(n2)c(-c2ccccc2)c2ccc1[nH]2
Name:	Tilmicosin
Method:	Cell Fractionation
References:	145
Structure:	CCC1OC(=O)CC(O)C(C)C(OC2OC(C)C(O)C(C2O)[NH+](C)C)C(CC[NH+]2CC(C)CC(C)C2)CC(C)C(=O)\C=C\C(C)=C\C1COC1OC(C)C(O)C(OC)C1OC
Name:	Roxithromycin
Method:	Cell Fractionation
References:	160
Structure:	CCC1OC(=O)C(C)C(OC2CC(C)(OC)C(O)C(C)O2)C(C)C(OC2OC(C)CC(C2O)[NH+](C)C)C(C)(O)CC(C)\C(=N\OCOCCOC)C(C)C(O)C1(C)O
Name:	Erythromycin
Method:	Cell Fractionation
References:	160
Structure:	CCC1OC(=O)C(C)C(OC2CC(C)(OC)C(O)C(C)O2)C(C)C(OC2OC(C)CC(C2O)[NH+](C)C)C(C)(O)CC(C)C(=O)C(C)C(O)C1(C)O
Name:	Sertraline
Method:	Uptake/Binding
References:	175
Structure:	C[NH2+]C1CCC(c2ccc(Cl)c(Cl)c2)c2ccccc12
Name:	Perazine
Method:	Uptake/Binding
References:	175
Structure:	CN1CC[NH+](CCCN2c3ccccc3Sc3ccccc23)CC1

Name:	IR-1
Method:	Fluorescence Microscopy
References:	193
Structure:	CC1(C)\C(=C/C=C2CCCC(/C=C/C3=[N+](CCCCS([O-])(=O)=O)c4ccccc4C3(C)C)=C\2Oc2ccc(CCC(=O)NCC3OC(O)C([NH3+])C(O)C3O)cc2)N(CCCCS([O-])(=O)=O)c2ccccc12

Name:	IR-2
Method:	Fluorescence Microscopy
References:	193, 506
Structure:	CC1(C)\C(=C/C=C2CCCC(/C=C/C3=[N+](CCCCS([O-])(=O)=O)c4ccccc4C3(C)C)=C\2Oc2cccc(OCCCC[NH2+]CC3OC(O)C([NH3+])C(O)C3O)c2)N(CCCCS([O-])(=O)=O)c2ccccc12

Name:	AR-L 115 BS; Sulmazole
Method:	Pharmacological Effect
References:	196
Structure:	COc1cc(ccc1-c1nc2ncccc2[nH]1)S(C)=O

Name:	HX-CH 44 BS
Method:	Pharmacological Effect
References:	196
Structure:	COc1ccc2N=C(N(C)C(=O)c2c1)c1ccc(OCC(O)C[NH2+]C(C)(C)C)cc1

Name:	SX-AB 1316 SE
Method:	Pharmacological Effect
References:	196
Structure:	[O-]C(=O)Cc1ccc2CC(Cc2c1)NS(=O)(=O)c1ccc(Cl)cc1

Name:	AF-CX 1325 XX
Method:	Pharmacological Effect
References:	196
Structure:	N\C(c1ccccc1)=C1/C(=O)c2ccccc2S1=O

Name:	Oritavancin
Method:	Pharmacological Effect
References:	201
Structure:	C[NH2+]C(CC(C)C)C(=O)NC1C(O)c2ccc(Oc3cc4cc(Oc5ccc(cc5Cl)C(OC5CC(C)([NH3+])C(O)C(C)O5)C5NC(=O)C(NC(=O)C4NC(=O)C(CC(N)=O)NC1=O)c1ccc(O)c(c1)-c1c(O)cc(O)cc1C(NC5=O)C([O-])=O)c3OC1OC(CO)C(O)C(O)C1OC1CC(C)([NH2+]Cc3ccc(cc3)-c3ccc(Cl)cc3)C(O)C(C)O1)c(Cl)c2

Name:	Tobramycin
Method:	histo
References:	208
Structure:	[NH3+]CC1OC(OC2C([NH3+])CC([NH3+])C(OC3OC(CO)C(O)C([NH3+])C3O)C2O)C([NH3+])CC1O

Name:	Vancomycin
Method:	histo
References:	208
Structure:	C[NH2+]C(CC(C)C)C(=O)NC1C(O)c2ccc(Oc3cc4cc(Oc5ccc(cc5Cl)C(O)C5NC(=O)C(NC(=O)C4NC(=O)C(CC(N)=O)NC1=O)c1ccc(O)c(c1)-c1c(O)cc(O)cc1C(NC5=O)C([O-])=O)c3OC1OC(CO)C(O)C(O)C1OC1CC(C)([NH3+])C(O)C(C)O1)c(Cl)c2

Name:	ABP; N-(3-dimethylaminopropyl)benzylpenicillinamide
Method:	Cell Fractionation
References:	209
Structure:	C[NH+](C)CCCNC(=O)C1N2C(SC1(C)C)C(NC(=O)Cc1ccccc1)C2=O

Name:	Bacteriopurpurinimide Derivative 7
Method:	Fluorescence Microscopy
References:	212
Structure:	CCCCCCN1C(=O)C2=C(C)\C3=C\C4=N\C(=C/C5[NH2+]C(\C=C6/N=C(C(CCC(=O)OCCC)C6C)C(C1=O)=C2N3)C(C)=C5C(C)OC)C(C)C4CC

Name:	CPT1
Method:	Fluorescence Microscopy
References:	215

Structure:	CCCOc1ccc(cc1)-c1c2ccc(n2)c(-c2ccc(OCCCCCCCCCCC[N+](C)(C)C)cc2)c2ccc([nH]2)c(-c2ccc(OCCCCCCCCCCC[N+](C)(C)C)cc2)c2ccc(n2)c(-c2ccc(OCCCCCCCCCCC[N+](C)(C)C)cc2)c2ccc1[nH]2

Name:	Benz(a)anthracene
Method:	Pharmacological Effect
References:	221
Structure:	c1ccc2cc3c(ccc4ccccc34)cc2c1

Name:	Benzo(a)pyrene
Method:	Pharmacological Effect
References:	221
Structure:	c1ccc2c(c1)cc1ccc3cccc4ccc2c1c34

Name:	7,9-Dimethylbenz(c)acridine
Method:	Pharmacological Effect
References:	221
Structure:	Cc1ccc2nc3c(ccc4ccccc34)c(C)c2c1

Name:	7,12-Dimethylbenz(a)anthracene
Method:	Pharmacological Effect
References:	221
Structure:	Cc1c2ccccc2c(C)c2c1ccc1ccccc21

Name:	3-Methylcholanthrene
Method:	Pharmacological Effect
References:	221
Structure:	Cc1ccc2cc3c(ccc4ccccc34)c3CCc1c23

Name:	Porphyrin-MLS
Method:	Fluorescence Microscopy
References:	211
Structure:	CCC(C)C(NC(=O)C(CCCC[NH3+])NC(=O)C(C)NC(=O)C(CCCNC(N)=[NH2+])NC(=O)C1CCCN1C(=O)C(NC(=O)C1CCCN1C(=O)C(CC(C)C)NC(=O)C(CCCNC(N)=[NH2+])NC(=O)C(CCCNC(N)=[NH2+])NC(=O)C(C)NC(=O)C(CO)NC(=O)CNC(=O)C(NC(=O)C(CC(C)C)NC(=O)CNC(=O)C(CCCNC(N)=[NH2+])NC(=O)C(CC(C)C)NC(=O)C(CC(C)C)NC(=O)C(

Structure:	CC(C)C)NC(=O)C1CCCN1C(=O)C(NC(=O)C(CC(C)C)NC(=O)C(NC(=O)C(CO)NC(=O)C(CCSC)NC(=O)OCCOCCOCCOCCOCCOCCNC(=O)COCC(=O)Nc1ccc(cc1)C1=C2\C=CC(=N\2)/C(c2ccccc2)=C2/C=CC(=N/2)\C(c2ccccc2)=C2\C=CC(=N\2)/C(c2ccccc2)=C2/C=CC\1=N/2)C(C)C)C(C)O)C(C)O)C(C)C)C(=O)NC(Cc1c[nH]cn1)C(=O)NC(CO)C(=O)NC(CC(C)C)C([O-])=O

Name:	Methotrexate Polyglutamate
Method:	Cell Fractionation
References:	195
Structure:	CN(Cc1cnc2nc(N)nc(N)c2n1)c1ccc(cc1)C(=C)[NH2+]C(CCC(=O)NC(CCC(=O)NC(CCC([O-])=O)C([O-])=O)C([O-])=O)C([O-])=O

Name:	TPC-Ahx-ATWLPPR
Method:	Fluorescence Microscopy
References:	220
Structure:	CC(C)CC(NC(=O)C(Cc1c[nH]c2ccccc12)NC(=O)C(NC(=O)C(C)NC(=O)CCCCNC(=O)c1ccc(cc1)-c1c2ccc(n2)c(-c2ccccc2)c2ccc([nH]2)c(-c2ccccc2)c2ccc(n2)c(-c2ccccc2)c2ccc1[nH]2)C(C)O)C(=O)N1CCCC1C(=O)N1CCCC1C(=O)NC(CCCNC(N)=[NH2+])C([O-])=O

Name:	Sparfloxacin
Method:	Fluorescence Microscopy
References:	223
Structure:	CC1CN(CC(C)[NH2+]1)c1c(F)c(N)c2C(=O)C(=CN(C3CC3)c2c1F)C([O-])=O

Name:	ATMPn; 9,-Acetoxy-2,7,12,17-tetrakis-(ß-methoxyethyl)-porphycene
Method:	Fluorescence Microscopy
References:	255
Structure:	COCCc1cc2nc1ccc1[nH]c(cc1CCOC)c1cc(CCOC)c(n1)c(OC(C)=O)cc1[nH]c2cc1CCOC

Name:	Telavancin

Method:	Cell Fractionation
References:	286
Structure:	CCCCCCCCC[NH2+]CC[NH2+]C1(C)CC(OC(C)C1O)OC1C(O)C(O)C(CO)OC1Oc1c2Oc3ccc(cc3Cl)C(O)C(NC(=O)C(CC(C)C)[NH2+]C)C(=O)NC(CC(N)=O)C(=O)NC3C(=O)[N-]C4C(=O)NC(C(O)c5ccc(Oc1cc3c2)c(Cl)c5)C(=O)NC(C([O-])=O)c1cc(O)c(C[NH2+]CP(O)([O-])=O)c(O)c1-c1cc4ccc1O
Name:	ZnPcOCH3
Method:	Fluorescence Microscopy
References:	303
Structure:	COc1ccc2c3nc(nc4n5[Zn]n6c(nc7nc(nc5c5cc(OC)ccc45)c4ccc(OC)cc74)c4ccc(OC)cc4c6n3)c2c1
Name:	EB1089
Method:	Fluorescence Microscopy
References:	308
Structure:	CCC(O)(CC)\C=C\C=C\C(C)C1CCC2\C(CCCC12C)=C/C=C1/CC(O)CC(O)C1=C
Name:	HexoTMPn
Method:	Fluorescence Microscopy
References:	323
Structure:	CCCCCCC(=O)Oc1cc2[nH]c(cc2CCOC)c2cc(CCOC)c(ccc3[nH]c(cc3CCOC)c3cc(CCOC)c1n3)n2
Name:	PeloTMPn
Method:	Fluorescence Microscopy
References:	323
Structure:	CCCCCCCCC(=O)Oc1cc2[nH]c(cc2CCOC)c2cc(CCOC)c(cc3[nH]c(cc3CCOC)c3cc(CCOC)c1n3)n2
Name:	CpoTMPn
Method:	Fluorescence Microscopy
References:	323
Structure:	CCCCCC(=O)Oc1cc2[nH]c(cc2CCOC)c2cc(CCOC)c(ccc3[nH]c(cc3CCOC)c3cc(CCOC)c1n3)n2
Name:	EBC
Method:	Fluorescence Microscopy
References:	332

Structure:	CCc1c(C)c2cc3[nH]c(c(C)c3CC)c3cc(cc4c3nc(cc3[nH]c(cc1n2)c(C)c3CC)C4(C)CC)S([O-])(=O)=O
Name:	Porphyrin-Retinamide Derivative 2
Method:	Fluorescence Microscopy
References:	352
Structure:	CC(\C=C\C1=C(C)CCCC1(C)C)=C/C=C/C(C)=C/C(=O)Nc1ccc(cc1)C1=C2\C=CC(=N\2)/C(c2ccccc2)=C2NC(/C=C\2)=C(c2ccccc2)\C2=N\C(/C=C2)=C(/C2[NH2+]C\1C=C2)c1ccccc1
Name:	Porphyrin-Retinamide Derivative 3
Method:	Fluorescence Microscopy
References:	352
Structure:	CC(\C=C\C1=C(C)CCCC1(C)C)=C\C=C/C(C)=C/C(=O)Nc1ccc(cc1)C1=C2\C=CC(=N\2)/C(c2ccccc2)=C2NC(/C=C\2)=C(c2ccccc2)\C2=N\C(/C=C2)=C(/C2[NH2+]C\1C=C2)c1ccccc1
Name:	Cationic Water-Soluble Phthalocyanine Derivative 10
Method:	Fluorescence Microscopy
References:	353
Structure:	C[n+]1cccc(Oc2cc3c4cc5n6[Zn]n7c(cc(n4)c3cc2Oc2ccc[n+](C)c2)c2cc(Oc3ccc[n+](C)c3)c(Oc3ccc[n+](C)c3)cc2c7cc2nc(cc6c3cc(Oc4ccc[n+](C)c4)c(Oc4ccc[n+](C)c4)cc53)c3cc(Oc4ccc[n+](C)c4)c(Oc4ccc[n+](C)c4)cc23)c1
Name:	Cationic Water-Soluble Phthalocyanine Derivative 11
Method:	Fluorescence Microscopy
References:	353
Structure:	COCCOCCOCC[n+]1cccc(Oc2cc3c4cc5n6[Zn]n7c(cc(n4)c3cc2Oc2ccc[n+](CCOCCOCCOC)c2)c2cc(Oc3ccc[n+](CCOCCOCCOC)c3)c(Oc3ccc[n+](CCOCCOCCOC)c3)cc2c7cc2nc(cc6c3cc(Oc4ccc[n+](CCOCCOCCOC)c4)c(Oc4ccc[n+](CCOCCOCCOC)c4)cc53)c3c

	c(Oc4ccc[n+](CCOCCOCCOC)c4)c(Oc4ccc[n+](CCOCCOCCOC)c4)cc23)c1
Name:	Cationic Water-Soluble Phthalocyanine Derivative 12
Method:	Fluorescence Microscopy
References:	353
Structure:	CCC[Si](CCC)(CCC)[Si]1(N2C3=CC4=N\C(=C/C5[NH+]1C(\C=C1/N=C(C=C2c2cc(Oc6ccc[n+](C)c6)c(Oc6ccc[n+](C)c6)cc32)c2cc(Oc3ccc[n+](C)c3)c(Oc3ccc[n+](C)c3)cc12)c1cc(Oc2ccc[n+](C)c2)c(Oc2ccc[n+](C)c2)cc51)c1cc(Oc2ccc[n+](C)c2)c(Oc2ccc[n+](C)c2)cc41)[Si](CCC)(CCC)CCC
Name:	Cationic Water-Soluble Phthalocyanine Derivative 13
Method:	Fluorescence Microscopy
References:	353
Structure:	CCC(CC)[Si](C(CC)CC)(C(CC)CC)[Si]1([NH+]2C3C=C4N=C(C=C5[NH+]1C(=CC1=N\C(=C/C2c2cc(Oc6ccc[n+](C)c6)c(Oc6ccc[n+](C)c6)cc32)c2cc(Oc3ccc[n+](C)c3)c(Oc3ccc[n+](C)c3)cc12)c1cc(Oc2ccc[n+](C)c2)c(Oc2ccc[n+](C)c2)cc51)c1cc(Oc2ccc[n+](C)c2)c(Oc2ccc[n+](C)c2)cc41)[Si](C(CC)CC)(C(CC)CC)C(CC)CC
Name:	Cationic Water-Soluble Phthalocyanine Derivative 14
Method:	Fluorescence Microscopy
References:	353
Structure:	C[n+]1cccc(Oc2cc3C4\C=C5/N=C(/C=C6\[NH+]7C(=CC8=N\C(=C/C([NH+]4[Si]7([Si](c4ccccc4)(c4ccccc4)C(C)(C)C)[Si](c4ccccc4)(c4ccccc4)C(C)(C)C)c3cc2Oc2ccc[n+](C)c2)c2cc(Oc3ccc[n+](C)c3)c(Oc3ccc[n+](C)c3)cc82)c2cc(Oc3ccc[n+](C)c3)c(Oc3ccc[n+](C)c3)cc62)c2cc(Oc3ccc[n+](C)c3)c(Oc3ccc[n+](C)c3)cc52)c1
Name:	Cationic Water-Soluble Phthalocyanine Derivative 15
Method:	Fluorescence Microscopy
References:	353

	COCCOCCOCC[n+]1cccc(Oc2cc3C4\C=C5/N=C(/C=C6\[NH+]7\C(=C/C8=N/C(=C\C([NH+]4[Si]7([Si](c4ccccc4)(c4ccccc4)C(C)(C)C)[Si](c4ccccc4)(c4ccccc4)C(C)(C)C)c3cc2Oc2ccc[n+](CCOCCOCCOC)c2)c2cc(Oc3ccc[n+](CCOCCOCCOC)c3)c(Oc3ccc[n+](CCOCCOCCOC)c3)cc82)c2cc(Oc3ccc[n+](CCOCCOCCOC)c3)c(Oc3ccc[n+](CCOCCOCCOC)c3)cc62)c2cc(Oc3ccc[n+](CCOCCOCCOC)c3)c(Oc3ccc[n+](CCOCCOCCOC)c3)cc52)c1
Name:	Porphyrin Conjugate Derivative 10
Method:	Fluorescence Microscopy
References:	354
Structure:	CC(C)C(NC(=O)C(CCCC[NH3+])NC(=O)C(CCCNC(N)=[NH2+])NC(=O)C(CCCC[NH3+])NC(=O)C(CCCC[NH3+])NC(=O)C(CCCC[NH3+])NC(=O)C1CCCN1C(=O)COCC(=O)NCCOCCOCCOCCOCCOCCOCCOCCNC(=O)COc1ccc(cc1)-c1c2ccc(n2)c(-c2ccc(OCC([O-])=O)cc2)c2ccc([nH]2)c(-c2ccc(OCC([O-])=O)cc2)c2ccc(n2)c(-c2ccc(OCC([O-])=O)cc2)c2ccc1[nH]2)C(N)=O
Name:	Porphyrin Conjugate Derivative 11
Method:	Fluorescence Microscopy
References:	354
Structure:	NC(=[NH2+])NCCCC(NC(=O)CNC(=O)COCC(=O)NCCOCCOCCOCCOCCOCCOCCNC(=O)COc1ccc(cc1)-c1c2ccc(n2)c(-c2ccc(OCC([O-])=O)cc2)c2ccc([nH]2)c(-c2ccc(OCC([O-])=O)cc2)c2ccc(n2)c(-c2ccc(OCC([O-])=O)cc2)c2ccc1[nH]2)C(=O)NC(CCCC[NH3+])C(=O)NC(CCCC[NH3+])C(=O)NC(CCCNC(N)=[NH2+])C(=O)NC(CCCNC(N)=[NH2+])C(=O)NC(CCCN C(N)=[NH2+])C(=O)NC(CCC(N)=O)C(=O)NC(CCCNC(N)=[

NH2+])C(=O)NC(CCCNC(N)=[NH2+])C(=O)NC(CCCNC(N)=[NH2+])C(=O)N1CCCC1C(=O)N1CCCC1C(=O)NC(CCC(N)=O)C(N)=O

Name:	Porphyrin-Peptide Conjugate 3
Method:	Fluorescence Microscopy
References:	378
Structure:	CSCCC(NC(=O)COCCOCCOCCOCCOCCOCCNC(=O)COCC(=O)Nc1ccc(cc1)-c1c2ccc(n2)c(-c2ccccc2)c2ccc([nH]2)c(-c2ccccc2)c2ccc(n2)c(-c2ccccc2)c2ccc1[nH]2)C(=O)NCC(=O)NC(CC(C)C)C(=O)NCC(=O)NC(CC(C)C)C(=O)NC(Cc1c[nH]cn1)C(=O)NC(CC(C)C)C(=O)NC(CC(C)C)C(=O)NC(C(C)C)C(=O)NC(CC(C)C)C(=O)NC(C)C(=O)NC(C)C(=O)NC(C)C(=O)NC(CC(C)C)C(=O)NC(CCC(N)=O)C(=O)NCC(=O)NC(C)C(=O)NC(Cc1c[nH]c2ccccc12)C(=O)NC(CO)C(=O)NC(CCC(N)=O)C(=O)NC(C)C(=O)N1CCCC1C(=O)N1CCCC1C(=O)NC(CCCC[NH3+])C(=O)NC(CCCC[NH3+])C(=O)NC(CCCC[NH3+])C(=O)NC(CCCNC(N)=[NH2+])C(=O)NC(CCCC[NH3+])C(=O)NC(C(C)C)C(=O)NCC([O-])=O

Name:	Porphyrin-Peptide Conjugate 4
Method:	Fluorescence Microscopy
References:	378
Structure:	CCC(C)C(NC(=O)C(CCC(N)=O)NC(=O)C(CCCNC(N)=[NH2+])NC(=O)COCCOCCOCCOCCOCCOCCNC(=O)COCC(=O)Nc1ccc(cc1)-c1c2ccc(n2)c(-c2ccccc2)c2ccc([nH]2)c(-c2ccccc2)c2ccc(n2)c(-c2ccccc2)c2ccc1[nH]2)C(=O)NC(CCCC[NH3+])C(=O)NC(C(C)CC)C(=O)NC(Cc1c[nH]c2ccccc12)C(=O)NC(Cc1ccccc1)C(=O)NC(CCC(N)=O)C(=O)NC(CC(N)=O)C(=O)NC(CCCNC(N)=[NH2+])C(=O)NC(CCCNC(N)=[NH2+])C(=O)N[C@H]

(CCSC)C(=O)NC(CCCC[NH3+])C(=O)NC(Cc1c[nH]c2ccccc12)C(=O)NC(CCCC[NH3+])C(=O)NC(CCCC[NH3+])C(=O)NC(C)C(=O)N1CCCC1C(=O)N1CCCC1C(=O)NC(CCCC[NH3+])C(=O)NC(CCCC[NH3+])C(=O)NC(CCCC[NH3+])C(=O)NC(CCCNC(N)=[NH2+])C(=O)NC(CCCC[NH3+])C(=O)NC(C(C)C)C(=O)NCC([O-])=O

Name:	Porphyrin-Peptide Conjugate 5
Method:	Fluorescence Microscopy
References:	378
Structure:	CC(C)CC(NC(=O)C(CCCC[NH3+])NC(=O)C(CCCC[NH3+])NC(=O)C(CCCC[NH3+])NC(=O)C(C)NC(=O)C(CCC(N)=O)NC(=O)CNC(=O)C(C)NC(=O)C(CCCC[NH3+])NC(=O)C(CCC[NH3+])NC(=O)C(NC(=O)C(C)NC(=O)C(C)NC(=O)C1CCCN1C(=O)C(CCCNC(N)=[NH2+])NC(=O)C(CCCC[NH3+])NC(=O)COCCOCCOCCOCCOCCNC(=O)COCC(=O)Nc1ccc(cc1)-c1c2ccc(n2)c(-c2ccccc2)c2ccc([nH]2)c(-c2ccccc2)c2ccc(n2)c(-c2ccccc2)c2ccc1[nH]2)C(C)O)C(=O)NC(CCC([O-])=O)C(=O)NC(CC([O-])=O)C(=O)N1CCCC1C(=O)NC(CCCNC(N)=[NH2+])C(=O)NC(CCCC[NH3+])C(=O)NC(CCC[NH3+])C(=O)NC(CCCNC(N)=[NH2+])C(=O)NC(CCCNC(N)=[NH2+])C(=O)NC(CCC(N)=O)C(=O)NC(CCCNC(N)=[NH2+])C(=O)NC(CCCNC(N)=[NH2+])C(=O)NC(CCCNC(N)=[NH2+])C(=O)N1CCCC1C(=O)N1CCCC1C(=O)NC(CCC(N)=O)C(=O)NCC([O-])=O

Name:	Nonaggregated Water-Soluble Phthalocyanine Derivative 5a
Method:	Fluorescence Microscopy
References:	380
Structure:	[O-]C(=O)c1cc(Oc2cc3c4nc(nc5n6[Zn]n7c(n4)c4cc(Oc8cc(cc(c8)C([O-])=O)C([O-

	])=O)c(Oc8cc(cc(c8)C([O-])=O)C([O-])=O)cc4c7nc4nc(nc6c6cc(Oc7cc(cc(c7)C([O-])=O)C([O-])=O)c(Oc7cc(cc(c7)C([O-])=O)C([O-])=O)cc56)c5cc(Oc6cc(cc(c6)C([O-])=O)C([O-])=O)c(Oc6cc(cc(c6)C([O-])=O)C([O-])=O)cc45)c3cc2Oc2cc(cc(c2)C([O-])=O)C([O-])=O)cc(c1)C([O-])=O

Name:	Porphyrin-Peptide Conjugate 1A
Method:	Fluorescence Microscopy
References:	387
Structure:	Nc1ccc(cc1)-c1c2ccc(n2)c(-c2ccccc2)c2ccc([nH]2)c(-c2ccccc2)c2ccc(n2)c(-c2ccccc2)c2ccc1[nH]2

Name:	Porphyrin-Peptide Conjugate 5A
Method:	Fluorescence Microscopy
References:	387
Structure:	S=C=Nc1ccc(cc1)-c1c2ccc(n2)c(-c2ccccc2)c2ccc([nH]2)c(-c2ccccc2)c2ccc(n2)c(-c2ccccc2)c2ccc1[nH]2

Name:	Porphyrin-Peptide Conjugate 13A
Method:	Fluorescence Microscopy
References:	387
Structure:	[NH3+]CCCCC(NC(=S)Nc1ccc(cc1)-c1c2ccc(n2)c(-c2ccccc2)c2ccc([nH]2)c(-c2ccccc2)c2ccc(n2)c(-c2ccccc2)c2ccc1[nH]2)C([O-])=O

Name:	Porphyrin-Peptide Conjugate 14A
Method:	Fluorescence Microscopy
References:	387
Structure:	[NH3+]CCCCC(NC(=O)C(CCCC[NH3+])NC(=S)Nc1ccc(cc1)-c1c2ccc(n2)c(-c2ccccc2)c2ccc([nH]2)c(-c2ccccc2)c2ccc(n2)c(-c2ccccc2)c2ccc1[nH]2)C([O-])=O

Name:	Porphyrin-Peptide Conjugate 15A
Method:	Fluorescence Microscopy
References:	387
Structure:	[NH3+]CCCCC(NC(=O)C(CCCC[NH3+])NC(=O)C(CCCC[NH3+])NC(=S)Nc1ccc(cc1)-c1c2ccc(n2)c(-c2ccccc2)c2ccc([nH]2)c(-c2ccccc2)c2ccc(n2)c(-c2ccccc2)c2ccc1[nH]2)C([O-])=O

Name:	Porphyrin-Peptide Conjugate 16A
Method:	Fluorescence Microscopy
References:	387
Structure:	[NH3+]CCCCC(NC(=O)CCCC(=O)Nc1ccc(cc1)-c1c2ccc(n2)c(-c2ccccc2)c2ccc([nH]2)c(-c2ccccc2)c2ccc(n2)c(-c2ccccc2)c2ccc1[nH]2)C([O-])=O

Name:	Porphyrin-Peptide Conjugate 17A
Method:	Fluorescence Microscopy
References:	387
Structure:	[NH3+]CCCCC(NC(=O)C(CCCC[NH3+])NC(=O)CCCC(=O)Nc1ccc(cc1)-c1c2ccc(n2)c(-c2ccccc2)c2ccc([nH]2)c(-c2ccccc2)c2ccc(n2)c(-c2ccccc2)c2ccc1[nH]2)C([O-])=O

Name:	Porphyrin-Peptide Conjugate 18A
Method:	Fluorescence Microscopy
References:	387
Structure:	[NH3+]CCCCC(NC(=O)C(CCCC[NH3+])NC(=O)C(CCCC[NH3+])NC(=O)CCCC(=O)Nc1ccc(cc1)-c1c2ccc(n2)c(-c2ccccc2)c2ccc([nH]2)c(-c2ccccc2)c2ccc(n2)c(-c2ccccc2)c2ccc1[nH]2)C([O-])=O

Name:	Porphyrin-Peptide Conjugate 19A
Method:	Fluorescence Microscopy
References:	387

Structure:	[NH3+]CCCCC(NC(=O)C(CCCC[NH3+])NC(=O)C(CCCC[NH3+])NC(=O)CCCC(=O)Nc1ccc(cc1)-c1c2ccc(n2)c(-c2ccccc2)c2ccc3c(-c4ccccc4)c4ccc(n4)c(-c4ccccc4)c4ccc1n4[Zn]n23)C([O-])=O

Name:	Porphyrin-Peptide Conjugate 20A
Method:	Fluorescence Microscopy
References:	387
Structure:	[NH3+]CCCCC(NC(=O)C(CCCC[NH3+])NC(=O)C(CCCC[NH3+])NC(=O)CCCC(=O)Nc1ccc3c(-c4ccccc4)c4ccc5c(-c6ccccc6)c6ccc7c(-c8ccccc8)c8ccc1[n+]8[Sn@@](n67)(n23)[n+]45)C([O-])=O

Name:	Porphyrin-Peptide Conjugate 21A
Method:	Fluorescence Microscopy
References:	387
Structure:	NC(=[NH2+])NCCCC(NC(=O)C(CCCC[NH3+])NC(=O)C(CCCNC(N)=[NH2+])NC(=O)C(CCCNC(N)=[NH2+])NC(=S)Nc1ccc(cc1)-c1c2ccc(n2)c(-c2ccccc2)c2ccc([nH]2)c(-c2ccccc2)c2ccc(n2)c(-c2ccccc2)c2ccc1[nH]2)C(N)=O

Name:	Porphyrin-Peptide Conjugate 22A
Method:	Fluorescence Microscopy
References:	387
Structure:	NC(=O)C(CCCC[NH3+])NC(=O)C(CCCC[NH3+])NC(=O)C(CCCC[NH3+])NC(=O)CCCC(=O)Nc1ccc(cc1)-c1c2ccc(n2)c(-c2ccccc2)c2ccc([nH]2)c(-c2ccccc2)c2ccc(n2)c(-c2ccccc2)c2ccc1[nH]2

Name:	Porphyrin-Peptide Conjugate 23A
Method:	Fluorescence Microscopy
References:	387
Structure:	NC(=[NH2+])NCCCC(NC(=O)C(CCCNC(N)=[NH2+])NC(=O

	)C(CCCNC(N)=[NH2+])NC(=O)CCCC(=O)Nc1ccc(cc1)-c1c2ccc(n2)c(-c2ccccc2)c2ccc([nH]2)c(-c2ccccc2)c2ccc(n2)c(-c2ccccc2)c2ccc1[nH]2)C(N)=O

Name:	Porphyrin-Peptide Conjugate 24A
Method:	Fluorescence Microscopy
References:	387
Structure:	NC(=[NH2+])NCCCC(NC(=O)C(CCCNC(N)=[NH2+])NC(=O)C(CCCNC(N)=[NH2+])NC(=O)C(CCCC[NH3+])NC(=O)CCCC(=O)Nc1ccc(cc1)-c1c2ccc(n2)c(-c2ccccc2)c2ccc([nH]2)c(-c2ccccc2)c2ccc(n2)c(-c2ccccc2)c2ccc1[nH]2)C(N)=O

Name:	Porphyrin-Peptide Conjugate 25A
Method:	Fluorescence Microscopy
References:	387
Structure:	NC(=[NH2+])NCCCC(NC(=O)C(CCCC[NH3+])NC(=O)C(CCCNC(N)=[NH2+])NC(=O)C(CCCNC(N)=[NH2+])NC(=O)CCCC(=O)Nc1ccc(cc1)-c1c2ccc(n2)c(-c2ccccc2)c2ccc([nH]2)c(-c2ccccc2)c2ccc(n2)c(-c2ccccc2)c2ccc1[nH]2)C(N)=O

Name:	Saponin Derivative 1a
Method:	Fluorescence Microscopy
References:	421
Structure:	CC1CCC2(OC1)OC1CC3C4CCC5CC(CCC5(C)C4CCC3(C)C1C2C)OC1OC(CO)C(OC2OC(C)C(OCCNS(=C)(=C)c3cccc4c(cccc34)N(C)C)C(O)C2O)C(O)C1OC1OC(C)C(O)C(O)C1O

Name:	Saponin Derivative 1b
Method:	Fluorescence Microscopy
References:	421
Structure:	CC1CCC2(OC1)OC1CC3C4CCC5CC(CCC5(C)C4CCC3(C)C1C2C)OC1OC(CO)C(OC2O

	C(C)C(OCCNC(=S)Nc3ccc4c(c3)C(=O)OC43c4ccc(C)cc4Oc4cc(C)ccc34)C(O)C2O)C(O)C1OC1OC(C)C(O)C(O)C1O

Name:	Saponin Derivative 2
Method:	Fluorescence Microscopy
References:	421
Structure:	CC1CCC2(OC1)OC1CC3C4CCC5CC(CCC5(C)C4CCC3(C)C1C2C)OC1OC(C)C(OC2OC(C)C(ONS(=C)(=C)c3cccc4c(cccc34)N(C)C)C(O)C2O)C(O)C1OC1OC(C)C(O)C(O)C1O

Name:	Saponin Derivative 3
Method:	Fluorescence Microscopy
References:	421
Structure:	CC(C)CCCC(C)C1CCC2C3CC4CC(CCC4(C)C3CCC12C)OC1OC(CO)C(OC2OC(C)C(OCCNS(=C)(=C)c3cccc4c(cccc34)N(C)C)C(O)C2O)C(O)C1OC1OC(C)C(O)C(O)C1O

Name:	Iejimalide Derivative 8
Method:	Fluorescence Microscopy
References:	423
Structure:	CCN(CC)c1ccc2C=C(NC(=O)Oc3ccccc3)C(=O)Oc2c1

Name:	Glucosylated Si(IV) Phthalocyanine Derivative 3
Method:	Fluorescence Microscopy
References:	427
Structure:	CC1(C)OCC(O1)C1OC2OC(C)(C)OC2C1OCCOCCOCCOCCO[Si]1(OCCOCCOCCOCCOC2C(OC3OC(C)(C)OC23)C2COC(C)(C)O2)n2c3cc4nc(cc5n1c(cc1nc(cc2c2ccccc32)c2ccccc12)c1ccccc51)c1ccccc41

Name:	Subphthalocyanine Derivative 2
Method:	Fluorescence Microscopy
References:	428
Structure:	OCCOCCOCCOB1N2C3\N=C4/N=C(/N=C5\N1C(N=C2c1ccccc31)c1ccccc51)c1ccccc41

Name:	Subphthalocyanine Derivative 3
Method:	Fluorescence Microscopy
References:	428

Structure:	OCCOCCOCCOCCOB1N2C3\N=C4/N=C(/N=C5\N1C(N=C2c1ccccc31)c1ccccc51)c1ccccc41

Name:	Subphthalocyanine Derivative 4
Method:	Fluorescence Microscopy
References:	428
Structure:	COCCOCCOCCOc1ccc(OB2N3C4\N=C5/N=C(/N=C6\N2C(N=C3c2ccccc42)c2ccccc62)c2ccccc52)cc1

Name:	Subphthalocyanine Derivative 5
Method:	Fluorescence Microscopy
References:	428
Structure:	COCCOCCOCCOCCOc1ccc(OB2N3C4\N=C5/N=C(/N=C6\N2C(N=C3c2ccccc42)c2ccccc62)c2ccccc52)cc1

Name:	Porphyrin-Bile Acid Conjugate 1
Method:	Fluorescence Microscopy
References:	439
Structure:	CC(CCC(=O)NCC[N+](C)(C)c1ccc(cc1)-c1c2ccc(n2)c(-c2ccc(cc2)[N+](C)(C)CCNC(=O)CCC(C)C2CCC3C4C(O)CC5CC(O)CCC5(C)C4CC(O)C23C)c2ccc([nH]2)c(-c2ccc(cc2)[N+](C)(C)CCNC(=O)CCC(C)C2CCC3C4C(O)CC5CC(O)CCC5(C)C4CC(O)C23C)c2ccc(n2)c(-c2ccc(cc2)[N+](C)(C)CCNC(=O)CCC(C)C2CCC3C4C(O)CC5CC(O)CCC5(C)C4CC(O)C23C)c2ccc1[nH]2)C1CCC2C3C(O)CC4CC(O)CCC4(C)C3CC(O)C12C

Name:	Porphyrin-Bile Acid Conjugate 2
Method:	Fluorescence Microscopy
References:	439
Structure:	CC(CCC(=O)NCC[N+](C)(C)c1cccc(c1)-c1c2ccc(n2)c(-c2cccc(c2)[N+](C)(C)CCNC(=O)CCC(C)C2CCC3C4C(O)CC5CC(O)CCC5(C)C4CC(O)C23C)c2ccc([nH]2)c(-c2cccc(c2)[N+](C)(C)CCNC(=

	O)CCC(C)C2CCC3C4C(O)C C5CC(O)CCC5(C)C4CC(O)C 23C)c2ccc(n2)c(- c2cccc(c2)[N+](C)(C)CCNC(= O)CCC(C)C2CCC3C4C(O)C C5CC(O)CCC5(C)C4CC(O)C 23C)c2ccc1[nH]2)C1CCC2C3 C(O)CC4CC(O)CCC4(C)C3C C(O)C12C

Name:	Porphyrin-Bile Acid Conjugate 3
Method:	Fluorescence Microscopy
References:	439
Structure:	CC(CCC(=O)NCCC[N+](C)(C) c1ccc(cc1)-c1c2ccc(n2)c(- c2ccc(cc2)[N+](C)(C)CCCNC(=O)CCC(C)C2CCC3C4C(O)C C5CC(O)CCC5(C)C4CC(O)C 23C)c2ccc([nH]2)c(- c2ccc(cc2)[N+](C)(C)CCCNC(=O)CCC(C)C2CCC3C4C(O)C C5CC(O)CCC5(C)C4CC(O)C 23C)c2ccc(n2)c(- c2ccc(cc2)[N+](C)(C)CCCNC(=O)CCC(C)C2CCC3C4C(O)C C5CC(O)CCC5(C)C4CC(O)C 23C)c2ccc1[nH]2)C1CCC2C3 C(O)CC4CC(O)CCC4(C)C3C C(O)C12C

Name:	Porphyrin-Bile Acid Conjugate 4
Method:	Fluorescence Microscopy
References:	439
Structure:	CC(CCC(=O)NCCC[N+](C)(C) c1cccc(c1)-c1c2ccc(n2)c(- c2cccc(c2)[N+](C)(C)CCCNC(=O)CCC(C)C2CCC3C4C(O)C C5CC(O)CCC5(C)C4CC(O)C 23C)c2ccc([nH]2)c(- c2cccc(c2)[N+](C)(C)CCCNC(=O)CCC(C)C2CCC3C4C(O)C C5CC(O)CCC5(C)C4CC(O)C 23C)c2ccc(n2)c(- c2cccc(c2)[N+](C)(C)CCCNC(=O)CCC(C)C2CCC3C4C(O)C C5CC(O)CCC5(C)C4CC(O)C 23C)c2ccc1[nH]2)C1CCC2C3 C(O)CC4CC(O)CCC4(C)C3C C(O)C12C

Name:	Si(IV) Phthalocyanine analogue 1
Method:	Fluorescence Microscopy

References:	538
Structure:	Clc1cc2c3nc(nc4n5c(nc6nc(n c7n(c(n3)c3cc(Cl)c(Cl)cc73)[S i]5(Cl)Cl)c3cc(Cl)c(Cl)cc63)c3 cc(Cl)c(Cl)cc43)c2cc1Cl

Name:	Oregon-Green-RNase A Conjugate
Method:	Fluorescence Microscopy
References:	449
Structure:	CC(=O)Oc1cc(C)cc(C)c1C(C) (C)CC(=O)Nc1ccc2c(Oc3cc(N C(=O)NCCCN4C(=O)C=CC4 =O)ccc3C22OC(=O)c3ccccc2 3)c1

Name:	Rhodamine-Riboflavin
Method:	Fluorescence Microscopy
References:	539
Structure:	CN(C)c1ccc2c(OC3=CC(C=C C3=C2c2ccc(N)cc2C([O-])=O)=[N+](C)C)c1

Name:	FG-H503
Method:	Fluorescence Microscopy
References:	500
Structure:	CC(C)C1[NH2+]CC2=C3C=C C=CC3=C(C[NH2+]C(C(C)C) C(=O)NCCCNC1=O)C1=C2C =CC=C1

Name:	Chlorpromazine
Method:	Pharmacological Effect
References:	512
Structure:	C[NH+](C)CCCN1C2=CC=CC =C2SC2=C1C=C(Cl)C=C2

Name:	Lidocaine
Method:	Pharmacological Effect
References:	229
Structure:	CNC(=O)OC1=CC=C2N(C)[C @H]3N(C)CC[C@@]3(C)C2= C1

Name:	Eserine
Method:	Pharmacological Effect
References:	229
Structure:	C[NH+](C)CC1=CC=CC=C1

Name:	Procaine
Method:	Pharmacological Effect
References:	229
Structure:	CC[NH+](CC)CCOC(=O)C1= CC=C(N)C=C1

Name:	N,N-dimethyl-benzylamine
Method:	Pharmacological Effect
References:	229
Structure:	CNC(=O)OC1=CC2=C(C=C1)N(C)C1N(C)CCC21C
Name:	4-Aminopyridine
Method:	Pharmacological Effect
References:	229
Structure:	NC1=CC=[NH+]C=C1
Name:	4-Aminoquinaldine
Method:	Pharmacological Effect
References:	229
Structure:	CC1=[NH+]C2=C(C=CC=C2)C(N)=C1
Name:	Ephedrine
Method:	Pharmacological Effect
References:	229
Structure:	C[NH2+]C(C)C(O)C1=CC=CC=C1
Name:	4-Dimethylaminopyridine
Method:	Pharmacological Effect
References:	229
Structure:	CN(C)C1=CC=[NH+]C=C1
Name:	Atropine
Method:	Pharmacological Effect
References:	229
Structure:	C[NH+]1C2CCC1CC(C2)OC(=O)C(CO)C1=CC=CC=C1
Name:	Mecamylamine
Method:	Pharmacological Effect
References:	229
Structure:	C[NH2+]C1(C)C2CCC(C2)C1(C)C
Name:	Pilocarpine
Method:	Pharmacological Effect
References:	229
Structure:	CCC1C(COC1=O)CC1=CN=CN1C
Name:	Nicotine
Method:	Pharmacological Effect
References:	229
Structure:	C[NH+]1CCCC1C1=CN=CC=C1
Name:	Morpholine
Method:	Pharmacological Effect

References:	229
Structure:	C1COCC[NH2+]1
Name:	Tetramethylethylenediamine
Method:	Pharmacological Effect
References:	229
Structure:	CN(C)CC[NH+](C)C
Name:	Piperazine
Method:	Pharmacological Effect
References:	229
Structure:	C1C[NH2+]CCN1
Name:	Putrescine
Method:	Pharmacological Effect
References:	229
Structure:	[NH3+]CCCC[NH3+]
Name:	Piperidine
Method:	Pharmacological Effect
References:	229
Structure:	C1CC[NH2+]CC1
Name:	Desipramine
Method:	Uptake/Binding
References:	705
Structure:	C[NH2+]CCCN1C2=CC=CC=C2CCC2=CC=CC=C12
Name:	Ciprofloxacin
Method:	Fluorescence Microscopy
References:	97
Structure:	[O-]C(=O)C1=CN(C2CC2)C2=C(C=C(F)C(=C2)N2CC[NH2+]CC2)C1=O
Name:	6'-O-lissamine-rhodamine B-glucosamine
Method:	Fluorescence Microscopy
References:	713
Structure:	CCN(CC)C1=CC2=C(C=C1)C(C1=CC(=CC(=C1)[S-](=O)=O)S(=O)(=O)OCC1OC(O)C([NH3+])C(O)C1O)=C1C=C/C(/C=C1O2)=[N+](/CC)CC
Name:	Suramin
Method:	Pharmacological Effect
References:	730
Structure:	CC1=C(NC(=O)C2=CC(NC(=O)NC3=CC=CC(=C3)C(=O)NC3=C(C)C=CC(=C3)C(=O)NC3=C4C(=CC(=CC4=C(C=C3)

S(O)(=O)=O)S(O)(=O)=O)S(O
)(=O)=O)=CC=C2)C=C(C=C1
)C(=O)NC1=C2C(=CC(=CC2=
C(C=C1)S(O)(=O)=O)S(O)(=
O)=O)S(O)(=O)=O

The chemical compounds with reported subcellular localization site in the mitochondrion. References information is available in Appendix H. Structure is presented as the Simplified Molecular Input Line Entry Specification string of the major microspecies at pH 7.4, as calculated by ChemAxon.

Name:	Valproic acid
Method:	Uptake/Binding
References:	4, 714
Structure:	CCCC(CCC)C([O-])=O

Name:	Menadione
Method:	Pharmacological Effect
References:	4, 715
Structure:	CC1=CC(=O)c2ccccc2C1=O

Name:	Aspirin
Method:	Pharmacological Effect
References:	4
Structure:	CC(=O)Oc1ccccc1C([O-])=O

Name:	Paraquat
Method:	Pharmacological Effect
References:	4
Structure:	C[n+]1ccc(cc1)-c1cc[n+](C)cc1

Name:	CCCP
Method:	Pharmacological Effect
References:	4, 717
Structure:	Clc1cccc(NN=C(C#N)C#N)c1

Name:	Clofibric acid
Method:	Pharmacological Effect
References:	4
Structure:	CC(C)(Oc1ccc(Cl)cc1)C([O-])=O

Name:	Nonylphenol
Method:	Pharmacological Effect
References:	4
Structure:	CCCCCCCCCc1ccccc1O

Name:	2-methylharmine
Method:	Pharmacological Effect
References:	4
Structure:	COC1=CC2=NC3=C(C)N(C)C=CC3=C2C=C1

Name:	Nalidixic acid
Method:	Pharmacological Effect
References:	4

Structure:	CCN1C=C(C([O-])=O)C(=O)c2ccc(C)nc12

Name:	Ellipticine
Method:	Pharmacological Effect
References:	4
Structure:	Cc1c2ccncc2c(C)c2c3ccccc3[nH]c12

Name:	Meperidine
Method:	Pharmacological Effect
References:	4
Structure:	CCOC(=O)C1(CC[NH+](C)CC1)c1ccccc1

Name:	Amytal
Method:	Pharmacological Effect
References:	4
Structure:	CCC1(CCC(C)C)C(=O)NC(=O)NC1=O

Name:	DASPEI; (2-(4-(dimethylamino)styryl)-1-methyl pyridinium
Method:	Fluorescence Microscopy
References:	4, 75
Structure:	CC[n+]1ccccc1\C=C\c1ccc(cc1)N(C)C

Name:	FCCP
Method:	Uptake/Binding
References:	4, 716
Structure:	FC(F)(F)Oc1ccc(NN=C(C#N)C#N)cc1

Name:	Trichlorophenoxyacetic acid
Method:	Pharmacological Effect
References:	4
Structure:	[O-]C(=O)COc1c(Cl)cc(Cl)cc1Cl

Name:	Zidovudine
Method:	Uptake/Binding
References:	4, 230
Structure:	CC1=CN(C2CC(N=[N+]=[N-])C(CO)O2)C(=O)NC1=O

Name:	Diethylstilbestrol		Name:	Pyronine; Pyronin Y
Method:	Pharmacological Effect		Method:	Fluorescence Microscopy
References:	4		References:	4, 185, 708
Structure:	CC\C(c1ccc(O)cc1)=C(/CC)c1ccc(O)cc1		Structure:	CN(C)c1ccc2C=C3C=CC(C=C3Oc2c1)=[N+](C)C
Name:	Vacor		Name:	Nimesulide
Method:	Pharmacological Effect		Method:	Pharmacological Effect
References:	4		References:	4
Structure:	O=C(NCc1cccnc1)Nc1ccc(cc1)N(=O)=O		Structure:	CS([O-])(=O)=Nc1ccc(cc1Oc1ccccc1)N(=O)=O
Name:	Methyltriphenylphosphonium		Name:	TBTP (Thiobutyltriphenylphosphonium bromide)
Method:	Cell Fractionation			
References:	4, 25, 26		Method:	Uptake/Binding
Structure:	C[P+](c1ccccc1)(c1ccccc1)c1ccccc1		References:	4, 37
			Structure:	SCCCC[P+](c1ccccc1)(c1ccccc1)c1ccccc1
Name:	Imipramine			
Method:	Cell Fractionation		Name:	Amquinate
References:	264		Method:	Pharmacological Effect
Structure:	C[NH+](C)CCCN1c2ccccc2CCc2ccccc12		References:	4
			Structure:	CCCc1cc2C(=O)C(=C[N-]c2cc1N(CC)CC)C(=O)OC
Name:	Rhein			
Method:	Pharmacological Effect		Name:	Safranin O
References:	4		Method:	Pharmacological Effect
Structure:	Oc1cccc2C(=O)c3cc(cc(O)c3C(=O)c12)C([O-])=O		References:	4
			Structure:	Cc1cc2nc3cc(C)c(N)cc3[n+](-c3ccccc3)c2cc1N
Name:	Diazepam			
Method:	Pharmacological Effect		Name:	Chlorpromazine
References:	4, 6		Method:	histo
Structure:	CN1C(=O)CN=C(c2ccccc2)c2cc(Cl)ccc12		References:	4, 5, 6, 8, 58, 510
			Structure:	C[NH+](C)CCCN1c2ccccc2Sc2ccc(Cl)cc12
Name:	Ciprofibrate			
Method:	Pharmacological Effect		Name:	Dichlorodiphenyldichloroethane (DDD)
References:	4			
Structure:	CC(C)(Oc1ccc(cc1)C1CC1(Cl)Cl)C([O-])=O		Method:	Pharmacological Effect
			References:	4
Name:	Nitroxinil; Nitroxynil		Structure:	ClC(Cl)C(c1ccc(Cl)cc1)c1ccccc1Cl
Method:	Pharmacological Effect			
References:	4		Name:	Lonidamine
Structure:	[O-]c1c(I)cc(cc1N(=O)=O)C#N		Method:	Pharmacological Effect
			References:	4
Name:	Diclofenac		Structure:	[O-]C(=O)c1nn(Cc2ccc(Cl)cc2Cl)c2ccccc12
Method:	Pharmacological Effect			
References:	4		Name:	MPCU
Structure:	[O-]C(=O)Cc1ccccc1Nc1c(Cl)cccc1Cl			

Method:	Uptake/Binding
References:	4, 106
Structure:	Cc1ccc(cc1)S([O-])(=O)=NC(=O)Nc1ccc(Cl)cc1

Name:	Tebufenpyrad
Method:	Pharmacological Effect
References:	4, 527
Structure:	CCc1nn(C)c(C(=O)NCc2ccc(cc2)C(C)(C)C)c1Cl

Name:	UHDBT
Method:	Pharmacological Effect
References:	4
Structure:	CCCCCCCCCCCC1=C([O-])c2ncsc2C(=O)C1=O

Name:	Tetraphenylphosphonium
Method:	Pharmacological Effect
References:	4
Structure:	c1ccc(cc1)[P+](c1ccccc1)(c1ccccc1)c1ccccc1

Name:	Pentamidine
Method:	Pharmacological Effect
References:	4
Structure:	NC(=[NH2+])c1ccc(OCCCCCOc2ccc(cc2)C(N)=[NH2+])cc1

Name:	D632; dihydrorhodamine 123
Method:	Fluorescence Microscopy
References:	594, 601
Structure:	COC(=O)c1ccccc1C1c2ccc(N)cc2Oc2cc(N)ccc12

Name:	Phosphate diethylstilbesterol
Method:	Pharmacological Effect
References:	4
Structure:	CC\C(c1ccc(O)cc1)=C(/CC)c1ccc(OP([O-])([O-])=O)cc1

Name:	Sulofenur
Method:	Pharmacological Effect
References:	4
Structure:	[O-]S(=O)(=NC(=O)Nc1ccc(Cl)cc1)c1ccc2CCCc2c1

Name:	Buquinolate
Method:	Pharmacological Effect
References:	4
Structure:	CCOC(=O)C1=C[N-]c2cc(OCC(C)C)c(OCC(C)C)cc2C1=O

Name:	Malachite green
Method:	Uptake/Binding
References:	4, 41
Structure:	CN(C)c1ccc(cc1)C(c1ccccc1)=C1C=CC(C=C1)=[N+](C)C

Name:	Pyridaben
Method:	Pharmacological Effect
References:	4
Structure:	CC(C)(C)N1N=CC(SCc2ccc(cc2)C(C)(C)C)=C(Cl)C1=O

Name:	Methylbenzoquate
Method:	Pharmacological Effect
References:	4
Structure:	CCCCc1cc2C(=O)C(=C[N-]c2cc1OCc1ccccc1)C(=O)OC

Name:	D288; 4-(4-(dimethylamino)styryl)-N-methylpyridinium iodide4-Di-1-ASP
Method:	Fluorescence Microscopy
References:	244
Structure:	CN(C)c1ccc(cc1)\C=C\c1cc[n+](C)cc1

Name:	Menoctone
Method:	Pharmacological Effect
References:	4
Structure:	[O-]C1=C(CCCCCCCC2CCCC2)C(=O)C(=O)c2ccccc12

Name:	Cinnarizine
Method:	Pharmacological Effect
References:	4
Structure:	C1C[NH+](CCN1C\C=C\c1ccccc1)C(c1ccccc1)c1ccccc1

Name:	Crystal violet
Method:	Uptake/Binding
References:	4, 41
Structure:	CN(C)c1ccc(cc1)C(c1ccc(cc1)N(C)C)=C1C=CC(C=C1)=[N+](C)C

Name:	Haloperidol
Method:	Pharmacological Effect
References:	4, 6
Structure:	OC1(CC[NH+](CCCC(=O)c2ccc(F)cc2)CC1)c1ccc(Cl)cc1

Name:	T639; Tetramethylrosamine

	chlorid
Method:	Fluorescence Microscopy
References:	577
Structure:	CN(C)c1ccc2c(OC3=CC(C=CC3=C2c2ccccc2)=[N+](C)C)c1
Name:	M7511; MitoTracker® Orange CM-H2TMRos
Method:	Fluorescence Microscopy
References:	306, 578
Structure:	CN(C)c1ccc2C(c3ccc(CCl)cc3)c3ccc(cc3Oc2c1)N(C)C
Name:	Tioxaprofen
Method:	Pharmacological Effect
References:	4
Structure:	CC(Sc1nc(-c2ccc(Cl)cc2)c(o1)-c1ccc(Cl)cc1)C([O-])=O
Name:	Rotenone
Method:	Pharmacological Effect
References:	4
Structure:	COc1cc2OCC3Oc4c5CC(Oc5ccc4C(=O)C3c2cc1OC)C(C)=C
Name:	Hexachlorophene
Method:	Pharmacological Effect
References:	4
Structure:	[O-]c1c(Cl)cc(Cl)c(Cl)c1Cc1c([O-])c(Cl)cc(Cl)c1Cl
Name:	Perfluorooctanoic acid
Method:	Pharmacological Effect
References:	4
Structure:	[O-]C(=O)C(F)(F)C(F)(F)C(F)(F)C(F)(F)C(F)(F)C(F)(F)C(F)(F)F
Name:	Decoquinate
Method:	Pharmacological Effect
References:	4
Structure:	CCCCCCCCCCOc1cc2C(=O)C(=C[N-]c2cc1OCC)C(=O)OCC
Name:	M7510; MitoTracker® Orange CMTMRos; Tetramethylrosamine
Method:	Fluorescence Microscopy
References:	579
Structure:	CN(C)c1ccc2c(OC3=CC(C=C

	C3=C2c2ccc(CCl)cc2)=[N+](C)C)c1
Name:	Ranolazine
Method:	Pharmacological Effect
References:	4
Structure:	COc1ccccc1OC[C@H](O)CN1CCN(CC1)CC(=O)Nc1c(C)cccc1C
Name:	MKT-077
Method:	Fluorescence Microscopy
References:	4, 190
Structure:	CCN1C(=O)\C(S\C1=C/c1cccc[n+]1CC)=C1\Sc2ccccc2N1C
Name:	R14060; RedoxSensor™ Red CC-1
Method:	Fluorescence Microscopy
References:	306
Structure:	CN(C)c1ccc2C(c3ccc(cc3Oc2c1)N(C)C)c1c(F)c(F)c(F)c(F)c1F
Name:	Fluphenazine
Method:	Pharmacological Effect
References:	4, 58
Structure:	OCCN1CC[NH+](CCCN2c3ccccc3Sc3ccc(cc23)C(F)(F)F)CC1
Name:	Rhodamine 6G
Method:	Fluorescence Microscopy
References:	4, 76
Structure:	CCNc1cc2OC3=C\C(=N\CC)\C(C)=CC3=C(c2cc1C)c1ccccc1C(=O)OCC
Name:	D633; Dihydrorhodamine 6G
Method:	Fluorescence Microscopy
References:	601, 710
Structure:	CCNc1cc2Oc3cc(NCC)c(C)cc3C(c2cc1C)c1ccccc1C(=O)OCC
Name:	Cyhalothrine; Cyhalothrin
Method:	Pharmacological Effect
References:	4
Structure:	CC1(C)C(\C=C(/Cl)C(F)(F)F)C1C(=O)OC(C#N)c1cccc(Oc2ccccc2)c1
Name:	P243; 1-pyrenehexadecanoic acid
Method:	Fluorescence Microscopy

221

References:	672			[N+](C)C
Structure:	[O-]C(=O)CCCCCCCCCCCCCCCc1ccc2ccc3cccc4ccc1c2c34			
			Name:	L6868; Bis-N-methylacridinium nitrate; Lucigenin
Name:	Dequalinium		Method:	Uptake/Binding
Method:	Fluorescence Microscopy		References:	580
References:	4, 27		Structure:	C[n+]1c2ccccc2c(-c2c3ccccc3[n+](C)c3ccccc23)c2ccccc12
Structure:	Cc1cc(N)c2ccccc2[n+]1CCCCCCCCCC[n+]1c(C)cc(N)c2ccccc12			
			Name:	Janus green B
Name:	Betulinic acid		Method:	Cell Fractionation
Method:	Pharmacological Effect		References:	712
References:	4		Structure:	CCN(CC)c1ccc2nc3ccc(cc3[n+](-c3ccccc3)c2c1)\N=N\c1ccc(cc1)N(C)C
Structure:	CC(=C)C1CCC2(CCC3(C)C(CCC4C5(C)CCC(O)C(C)(C)C5CCC34C)C12)C([O-])=O			
			Name:	Perfluorodecanoic acid
Name:	Victoria blue		Method:	Pharmacological Effect
Method:	Pharmacological Effect		References:	4
References:	4		Structure:	[O-]C(=O)C(F)(F)C(F)(F)C(F)(F)C(F)(F)C(F)(F)C(F)(F)C(F)(F)C(F)(F)F
Structure:	CN(C)c1ccc(cc1)C(c1ccc(cc1)N(C)C)=C1C=C/C(=N/c2ccccc2)c2ccccc12			
			Name:	T669; Tetramethylrhodamine, ethyl ester, perchlorate; TMRE
Name:	Rhodamine B		Method:	Fluorescence Microscopy
Method:	Fluorescence Microscopy		References:	463
References:	677, 711		Structure:	CCOC(=O)c1ccccc1C1=C2C=CC(C=C2Oc2cc(ccc12)N(C)C)=[N+](C)C
Structure:	CCN(CC)c1ccc2c(OC3=CC(C=CC3=C2c2ccccc2C([O-])=O)=[N+](CC)CC)c1			
			Name:	M7512; MitoTracker® Red CMXRos
Name:	Myxothiazol		Method:	Fluorescence Microscopy
Method:	Pharmacological Effect		References:	50, 582
References:	4		Structure:	ClCc1ccc(cc1)C1=C2C=C3CCC[N+]4=C3C(CCC4)=C2Oc2c3CCCN4CCCc(cc12)c34
Structure:	COC(\C=C\c1csc(n1)-c1csc(n1)C(C)\C=C\C=C\C(C)C)C(C)C(\OC)=C/C(N)=O			
			Name:	M22426; MitoTracker® Deep Red 633
Name:	M7513; MitoTracker® Red CM-H2XRos		Method:	Fluorescence Microscopy
Method:	Fluorescence Microscopy		References:	607
References:	50		Structure:	C[N+]1=C(/C=C\C=C\C=C2/N(Cc3ccc(CCl)cc3)c3ccccc3C2(C)C)C(C)(C)c2ccccc12
Structure:	ClCc1ccc(cc1)C1c2cc3CCCN4CCCc(c2Oc2c1cc1CCCN5CCCc2c15)c34			
			Name:	Protoporphyrin IX
Name:	T668; Tetramethylrhodamine, methyl ester, perchlorate; TMRM		Method:	Uptake/Binding
			References:	4, 118
Method:	Fluorescence Microscopy			
References:	463			
Structure:	COC(=O)c1ccccc1C1=C2C=CC(C=C2Oc2cc(ccc12)N(C)C)=			

222

Structure:	Cc1c(CCC([O-])=O)c2cc3nc(cc4[nH]c(cc5[nH]c(cc1n2)c(C)c5C=C)c(C)c4C=C)c(C)c3CCC([O-])=O
Name:	Xanthomegnin
Method:	Pharmacological Effect
References:	4
Structure:	COC1=C(C(=O)c2c(O)c3C(=O)OC(C)Cc3cc2C1=O)C1=C(OC)C(=O)c2cc3CC(C)OC(=O)c3c(O)c2C1=O
Name:	Bromophenophos
Method:	Pharmacological Effect
References:	4
Structure:	Oc1cc(Br)cc(Br)c1-c1c(Br)cc(Br)cc1OP([O-])([O-])=O
Name:	D378; 3,3'-diheptyloxacarbocyanine iodide; DiOC7(3)
Method:	Fluorescence Microscopy
References:	582
Structure:	CCCCCCCN1\C(Oc2ccccc12)=C\C=C\c1oc2ccccc2[n+]1CCCCCCC
Name:	T3168; 5,5',6,6'-tetrachloro-1,1',3,3'-tetraethylbenzimidazolylcarbocyanine iodide; JC-1; CBIC2(3)
Method:	Fluorescence Microscopy
References:	52
Structure:	CCN1C(=C\C=C\c2n(CC)c3cc(Cl)c(Cl)cc3[n+]2CC)N(CC)c2cc(Cl)c(Cl)cc12
Name:	M7514; MitoTracker® Green FM
Method:	Fluorescence Microscopy
References:	154
Structure:	CN1\C(Oc2ccccc12)=C/C=C/c1n(Cc2ccc(CCl)cc2)c2cc(Cl)c(Cl)cc2[n+]1Cc1ccc(CCl)cc1
Name:	Verteporfin
Method:	Pharmacological Effect
References:	4
Structure:	COC(=O)CCc1c(C)c2cc3nc(cc4[nH]c(cc5nc(cc1[nH]2)c(CCC([O-])=O)c5C)c(C=C)c4C)C1=CC

	=C([C@@H](C(=O)OC)[C@@]31C)C(=O)OC
Name:	Ditercalinium
Method:	Pharmacological Effect
References:	4
Structure:	COc1ccc2[nH]c3ccc4cc[n+](CCN5CCC(CC5)C5CCN(CC5)CC[n+]5ccc6ccc7[nH]c8ccc(OC)cc8c7c6c5)cc4c3c2c1
Name:	M22425; MitoTracker® Red 580
Method:	Fluorescence Microscopy
References:	576
Structure:	CN1c2ccccc2C(C)(C)\C1=C/C=C/C=C/c1n(Cc2ccc(CCl)cc2)c2cc(Cl)c(Cl)cc2[n+]1Cc1ccc(CCl)cc1
Name:	Rhodopinal glucoside; RPA
Method:	Pharmacological Effect
References:	4
Structure:	C\C(C)=C\C=C\C(C)=C\C=C\C(C)=C\C=C\C(CO)=C\C=C\C=C(C)\C=C\C=C(C)\C=C\C=C(/C)CCCC(C)(C)OC1OC(CO)C(O)C(O)C1O
Name:	Rhod-2
Method:	Pharmacological Effect
References:	4
Structure:	CN(C)c1ccc2c(Oc3cc(ccc3C2=C2C=CC(C(OCCOc3cc(C)ccc3N(CC([O-])=O)CC([O-])=O)=C2)=[N+](CC([O-])=O)CC([O-])=O)N(C)C)c1
Name:	Rhodamine 123
Method:	Fluorescence Microscopy
References:	4
Structure:	COC(=O)c1ccccc1C1=C2C=CC(=[NH2+])C=C2Oc2cc(N)ccc12
Name:	Methylene Blue
Method:	Pharmacological Effect
References:	12
Structure:	CN(C)c1ccc2nc3ccc(cc3[s+]c2c1)N(C)C
Name:	Nefazodone
Method:	Pharmacological Effect
References:	14
Structure:	CCC1=NN(CCCN2CCN(CC2)

	c2cccc(Cl)c2)C(=O)N1CCOc1ccccc1

Name:	IBTP; 4-iodobutyl-tri(phenyl)phosphanium iodide
Method:	Cell Fractionation
References:	25
Structure:	ICCCC[P+](c1ccccc1)(c1ccccc1)c1ccccc1

Name:	IDTP
Method:	Cell Fractionation
References:	26
Structure:	ICCCCCCCCCC[P+](c1ccccc1)(c1ccccc1)c1ccccc1

Name:	DecylTPP
Method:	Cell Fractionation
References:	26
Structure:	CCCCCCCCCC[P+](c1ccccc1)(c1ccccc1)c1ccccc1

Name:	MitoQ; [10-(4,5-dimethoxy-2-methyl-3,6-dioxo-1,4-cyclohexadien-1-yl)decyl]triphenylphosphonium bromide; Mitoquinone
Method:	Cell Fractionation
References:	25, 26
Structure:	COC1=C(OC)C(=O)C(CCCCCCCCCC[P+](c2ccccc2)(c2ccccc2)c2ccccc2)=C(C)C1=O

Name:	MitoVit E; [2-(3,4-dihydro-6-hydroxy-2,5,7,8-tetramethyl-2H-1-benzopyran-2-yl)ethyl]triphenylphosphonium bromide
Method:	Cell Fractionation
References:	25, 26
Structure:	Cc1c(C)c2OC(C)(CCc2c(C)c1O)CC[P+](c1ccccc1)(c1ccccc1)c1ccccc1

Name:	Chlortetracycline
Method:	Fluorescence Microscopy
References:	127
Structure:	C[NH+](C)C1C2CC3C(C(=O)C2(O)C(=O)\C(=C(/N)[O-])C1=O)=C([O-])c1c(O)ccc(Cl)c1C3(C)O

Name:	LCL120
Method:	Pharmacological Effect
References:	13

Structure:	CC(NC(=O)CCCCCCCCCCCCCC[n+]1ccccc1)C(O)c1ccccc1

Name:	LCL85
Method:	Pharmacological Effect
References:	13
Structure:	OCC(NC(=O)CCCCCCCCCCCCC[n+]1ccccc1)C(O)c1ccc(cc1)N(=O)=O

Name:	1a
Method:	Fluorescence Microscopy
References:	19
Structure:	CN1\C(Sc2ccccc12)=C\c1cc[n+](CCCCCC(=O)NC(CC2CCCCC2)C(=O)NC(CCC\[NH+]=C(\N)N)C(=O)NC(CC2CCCCC2)C(=O)NC(CCCC[NH3+])C(=O)NC(CC2CCCCC2)C(=O)NC(CCC\[NH+]=C(\N)N)C(=O)NC(CC2CCCCC2)C(=O)NC(CCCC[NH3+])C(N)=O)c2ccccc12

Name:	1b
Method:	Fluorescence Microscopy
References:	19
Structure:	CN1\C(Sc2ccccc12)=C\c1cc[n+](CCCCCC(=O)NC(Cc2ccccc2)C(=O)NC(CCC\[NH+]=C(\N)N)C(=O)NC(Cc2ccccc2)C(=O)NC(CCCC[NH3+])C(=O)NC(Cc2ccccc2)C(=O)NC(CCC\[NH+]=C(\N)N)C(=O)NC(Cc2ccccc2)C(=O)NC(CCCC[NH3+])C(N)=O)c2ccccc12

Name:	2a
Method:	Fluorescence Microscopy
References:	19
Structure:	CN1\C(Sc2ccccc12)=C\c1cc[n+](CCCCCC(=O)NC(CC2CCCCC2)C(=O)NC(CCC\[NH+]=C(\N)N)C(=O)NC(CC2CCCCC2)C(=O)NC(CCCC[NH3+])C(N)=O)c2ccccc12

Name:	2b
Method:	Fluorescence Microscopy
References:	19, 251
Structure:	CN1\C(Sc2ccccc12)=C\c1cc[n+](CCCCCC(=O)NC(Cc2ccccc2)C(=O)NC(CCC\[NH+]=C(\N)N)C(=O)NC(Cc2ccccc2)C(=O)NC(CCCC[NH3+])C(N)=O)

	c2ccccc12
Name:	2c
Method:	Fluorescence Microscopy
References:	19
Structure:	CN1\C(Sc2ccccc12)=C\c1cc[n+](CCCCCC(=O)NC(Cc2ccccc2)C(=O)NC(CCC\[NH+]=C(\N)N)C(=O)NC(CC2CCCCC2)C(=O)NC(CCCC[NH3+])C(N)=O)c2ccccc12
Name:	2d
Method:	Fluorescence Microscopy
References:	19
Structure:	CN1\C(Sc2ccccc12)=C\c1cc[n+](CCCCCC(=O)NC(Cc2ccccc2)C(=O)NC(CCC\[NH+]=C(\N)N)C(=O)NC(C(c2ccccc2)c2ccccc2)C(=O)NC(CCCC[NH3+])C(N)=O)c2ccccc12
Name:	2e
Method:	Fluorescence Microscopy
References:	19
Structure:	CN1\C(Sc2ccccc12)=C\c1cc[n+](CCCCCC(=O)NC(Cc2ccccc2)C(=O)NC(CCC\[NH+]=C(\N)N)C(=O)NC(Cc2cccc3ccccc23)C(=O)NC(CCCC[NH3+])C(N)=O)c2ccccc12
Name:	2f
Method:	Fluorescence Microscopy
References:	19
Structure:	CCCCCCC(NC(=O)C(CCC\[NH+]=C(\N)N)NC(=O)C(Cc1ccccc1)NC(=O)CCCCC[n+]1ccc(\C=C2/Sc3ccccc3N2C)c2ccccc12)C(=O)NC(CCCC[NH3+])C(N)=O
Name:	2g
Method:	Fluorescence Microscopy
References:	19
Structure:	COc1ccc(CC(NC(=O)C(CCC\[NH+]=C(\N)N)NC(=O)C(Cc2ccccc2)NC(=O)CCCCC[n+]2ccc(\C=C3/Sc4ccccc4N3C)c3ccccc23)C(=O)NC(CCCC[NH3+])C([O-])=O)cc1
Name:	MitoQH2
Method:	Cell Fractionation
References:	26

Structure:	COc1c(O)c(C)c(CCCCCCCCCC[P+](c2ccccc2)(c2ccccc2)c2ccccc2)c(O)c1OC
Name:	F16
Method:	Fluorescence Microscopy
References:	29
Structure:	C[n+]1ccc(cc1)\C=C\c1c[nH]c2ccccc12
Name:	Ethyl Violet; EV+
Method:	Uptake/Binding
References:	41
Structure:	CCN(CC)c1ccc(cc1)C(c1ccc(cc1)N(CC)CC)=C1C=CC(C=C1)=[N+](CC)CC
Name:	Victoria Blue R; VBR+
Method:	Uptake/Binding
References:	41
Structure:	CCN(CC)c1ccc(C(c2ccc(cc2)N(C)C)=C2C=CC(C=C2)=[N+](C)C)c2ccccc12
Name:	Victoria Blue B; VBB+
Method:	Uptake/Binding
References:	41
Structure:	CN(C)c1ccc(cc1)C(=C1C=CC(C=C1)=[N+](C)C)c1ccc(Nc2ccccc2)c2ccccc12
Name:	Victoria Pure Blue BO; VPBBO+
Method:	Uptake/Binding
References:	41
Structure:	CCNc1ccc(C(c2ccc(cc2)N(CC)CC)=C2C=CC(C=C2)=[N+](CC)CC)c2ccccc12
Name:	MitoPeroxidase; 2-[4-(4-triphenylphosphoniobutoxy)phenyl]-1,2-benzisoselenazol)-3(2H)-one iodide
Method:	Uptake/Binding
References:	38
Structure:	O=C1N([Se]c2ccccc12)c1ccc(OCCCC[P+](c2ccccc2)(c2ccccc2)c2ccccc2)cc1
Name:	Ebselen
Method:	Uptake/Binding
References:	38
Structure:	O=C1N([Se]c2ccccc12)c1ccccc1

Name:	HMP 1c; 3,3'-[ω, ω'-alkanediylbis(oxy)[2-(hydroxylimino)methyl]-1-methylpyridinium
Method:	Uptake/Binding
References:	47
Structure:	C[n+]1cccc(OCCCCOc2ccc[n+](C)c2\C=N\[O-])c1\C=N\[O-]

Name:	HMP 1d; 3,3'-[ω, ω'-alkanediylbis(oxy)[2-(hydroxylimino)methyl]-1-methylpyridinium
Method:	Uptake/Binding
References:	47
Structure:	C[n+]1cccc(OCCCCCOc2ccc[n+](C)c2\C=N\[O-])c1\C=N\[O-]

Name:	HMP 1e; 3,3'-[ω, ω'-alkanediylbis(oxy)[2-(hydroxylimino)methyl]-1-methylpyridinium
Method:	Uptake/Binding
References:	47
Structure:	C[n+]1cccc(OCCCCCCOc2ccc[n+](C)c2\C=N\[O-])c1\C=N\[O-]

Name:	MPP+; 1-methyl-4-phenylpyridinium
Method:	Uptake/Binding
References:	49
Structure:	c1ccc(cc1)-c1ccncc1

Name:	Rhodamine 110; Rh 110
Method:	Fluorescence Microscopy
References:	64
Structure:	Nc1ccc2c(OC3=CC(=[NH2+])C=CC3=C2c2ccccc2C([O-])=O)c1

Name:	HAO; 3,6-Bis(dimethylamino)-10-hexylacridinium; acridine orange 10-hexyl bromide
Method:	Fluorescence Microscopy
References:	72
Structure:	CCCCCC[n+]1c2cc(ccc2cc2cc(cc12)N(C)C)N(C)C

Name:	MAO; 3,6-Bis(dimethylamino)-10-methylacridinium Iodide; acridine orange 10-methyl iodide
Method:	Fluorescence Microscopy

References:	72
Structure:	CN(C)c1ccc2cc3ccc(cc3[n+](C)c2c1)N(C)C

Name:	NAO; 3,6-Bis(dimethylamino)-10-nonylacridinium bromide; acridine orange 10-nonyl bromide
Method:	Fluorescence Microscopy
References:	72
Structure:	CCCCCCCCC[n+]1c2cc(ccc2cc2ccc(cc12)N(C)C)N(C)C

Name:	Oxytetracycline; Terramycin
Method:	histo
References:	74
Structure:	C[NH+](C)C1C2C(O)C3C(C(=O)C2(O)C(=O)\C(=C(/N)[O-])C1=O)=C([O-])c1c(O)cccc1C3(C)O

Name:	Rhodamine 3B; R3B
Method:	Fluorescence Microscopy
References:	76
Structure:	CCOC(=O)c1ccccc1C1=C2C=CC(C=C2Oc2cc(ccc12)N(CC)CC)=[N+](CC)CC

Name:	DiOC2(3)
Method:	Fluorescence Microscopy
References:	76
Structure:	CCN1\C(Oc2ccccc12)=C\C=C\c1oc2ccccc2[n+]1CC

Name:	APMC (azopentylmethylindocarbocyanine)
Method:	Fluorescence Microscopy
References:	77
Structure:	CN1c2ccccc2C(C)(C)\C1=C/C=C/C1=[N+](CCCC2(C)N=N2)c2ccccc2C1(C)C

Name:	PhoCy
Method:	Fluorescence Microscopy
References:	78
Structure:	CN1c2ccc(CNc3ccc(cc3N(=O)=O)N=[N+]=[N-])cc2C(C)(C)\C1=C\C=C\C1=[N+](C)c2ccc(CNc3ccc(cc3N(=O)=O)N=[N+]=[N-])cc2C1(C)C

Name:	mTHPC (meso-tetrahydroxyphenylchlorin); Foscan; Temoporfin

Method:	Fluorescence Microscopy
References:	83
Structure:	Oc1cccc(c1)-c1c2CCc(n2)c(-c2cccc(O)c2)c2ccc([nH]2)c(-c2cccc(O)c2)c2ccc(n2)c(-c2cccc(O)c2)c2ccc1[nH]2
Name:	Photofrin
Method:	Fluorescence Microscopy
References:	95
Structure:	CCc1c(C)c2cc3nc(cc4nc(cc5[nH]c(cc1[nH]2)c(C)c5C(C)O)c(C)c4CCC([O-])=O)c(CCC([O-])=O)c3C
Name:	Aminolevulinic Acid
Method:	Fluorescence Microscopy
References:	95
Structure:	[NH3+]CC(=O)CCC([O-])=O
Name:	CPO
Method:	Fluorescence Microscopy
References:	99
Structure:	CC(CCO)CC(O)N(O)CCCC(NC(C)=O)C(=O)OCC\C=C\C(O)N(O)\C=C\CC1NC(=O)C(NC1=O)\C=C\CN(O)C(O)CC(C)CCO
Name:	Mesochlorin; Mce6
Method:	Fluorescence Microscopy
References:	100
Structure:	CCc1c(C)c2cc3[nH]c(cc4nc(c(CCC([O-])=O)c4C)c(CC(=O)NCC[NH3+])c4[nH]c(cc1n2)c(C)c4C([O-])=O)c(C)c3CC
Name:	EDKC; N,N'-bis(2-ethyl-1,3-dioxolane)kryptocyanine
Method:	Fluorescence Microscopy
References:	109
Structure:	C1COC(CCN2C=C/C(=C/C=C/c3cc[n+](CCC4OCCO4)c4ccccc34)c3ccccc23)O1
Name:	MBMG; Methylglyoxal-bis(guanylhydrazone)]
Method:	Pharmacological Effect
References:	126
Structure:	CC(\C=N\N=C(N)N)=N/N=C(N)N
Name:	Topotecan
Method:	Fluorescence Microscopy

References:	130
Structure:	CCC1(O)C(=O)OCC2=C1C=C1N(Cc3cc4c(C[NH+](C)C)c(O)ccc4nc13)C2=O
Name:	Demethylchlortetracycline; Demeclocycline
Method:	Fluorescence Microscopy
References:	127
Structure:	C[NH+](C)C1C2CC3C(O)c4c(Cl)ccc(O)c4C([O-])=C3C(=O)C2(O)C(=O)\C(=C(/N)[O-])C1=O
Name:	Porphyrin Derivative 4
Method:	Fluorescence Microscopy
References:	132
Structure:	CCc1c(C)c2nc1cc1[nH]c(cc3nc(cc4[nH]c(c(C)c4CC)c2-c2cc(OCc4cc(cc(c4)C(F)(F)F)C(F)(F)F)cc(OCc4cc(cc(c4)C(F)(F)F)C(F)(F)F)c2)c(C)c3CCC(=O)OCc(CCC(=O)OC)c1C
Name:	Chlorin 30
Method:	Fluorescence Microscopy
References:	132
Structure:	CCc1c(C)c2[nH]c1cc1nc(cc3[nH]c(cc4nc(c2-c2cc(OCc5cc(cc(c5)C(F)(F)F)C(F)(F)F)cc(OCc5cc(cc(c5)C(F)(F)F)C(F)(F)F)c2)C(C)(O)C4(O)CC)c(C)c3CCC(=O)OC)c(CCC(=O)OC)c1C
Name:	Bacteriochlorin 31
Method:	Fluorescence Microscopy
References:	132
Structure:	CCc1c(C)c2[nH]c1cc1nc(cc3[nH]c(cc4nc(c2-c2cc(OCc5cc(cc(c5)C(F)(F)F)C(F)(F)F)cc(OCc5cc(cc(c5)C(F)(F)F)C(F)(F)F)c2)C(C)(O)C4(O)CC)c(C)c3CCC(=O)OC)C(O)(CCC(=O)OC)C1(C)O
Name:	6-Aminoquinoline Derivative 2
Method:	Fluorescence Microscopy
References:	137
Structure:	Cc1c(N2CCc3ccccc3C2)c(N)cc2C(=O)C(=CN(C3CC3)c12)C([O-])=O
Name:	6-Aminoquinoline Derivative 3
Method:	Fluorescence Microscopy

References:	137
Structure:	CN1C=C(C([O-])=O)C(=O)c2cc(N)c(cc12)N1CCN(CC1)c1ccccn1
Name:	DADP-a; 5,10-di[4-(N-trimethylaminophenyl)-15,20-diphenylporphyrin
Method:	Fluorescence Microscopy
References:	138
Structure:	C[N+](C)(C)c1ccc(cc1)-c1c2ccc(n2)c(-c2ccc(cc2)[N+](C)(C)C)c2ccc([nH]2)c(-c2ccccc2)c2ccc(n2)c(-c2ccccc2)c2ccc1[nH]2
Name:	99mTc-sestamibi
Method:	Cell Fractionation
References:	144
Structure:	COC(C)(C)C[N+]#C
Name:	Fura-2
Method:	Fluorescence Microscopy
References:	168
Structure:	Cc1ccc(N(CC([O-])=O)CC([O-])=O)c(OCCOc2cc3cc(oc3cc2N(CC([O-])=O)CC([O-])=O)-c2ncc(o2)C([O-])=O)c1
Name:	Pancratistatin
Method:	Pharmacological Effect
References:	169
Structure:	OC1C(O)C(O)C2C(NC(=O)c3c(O)c4OCOc4cc23)C1O
Name:	Anthralin
Method:	Fluorescence Microscopy
References:	178
Structure:	Oc1cccc2Cc3cccc(O)c3C(=O)c12
Name:	Paclitaxel
Method:	Pharmacological Effect
References:	188
Structure:	CC(=O)OC1C(=O)C2(C)C(O)CC3OCC3(OC(C)=O)C2C(OC(=O)c2ccccc2)C2(O)CC(OC(=O)C(O)C(NC(=O)c3ccccc3)c3ccccc3)C(C)=C1C2(C)C
Name:	Gossypol
Method:	Pharmacological Effect
References:	189
Structure:	CC(C)c1c(O)c(O)c(C=O)c2c(

	O)c(c(C)cc12)-c1c(C)cc2c(C(C)C)c(O)c(O)c(C=O)c2c1O
Name:	Mahanine
Method:	Pharmacological Effect
References:	192
Structure:	C\C(C)=C\CCC1(C)Oc2ccc3c4ccc(O)cc4[nH]c3c2C=C1
Name:	Bacteriopurpurinimide Derivative 8
Method:	Fluorescence Microscopy
References:	212
Structure:	CCCCCCN1C(=O)C2=C(C)\C3=C\C4=N\C(=C/C5[NH2+]C(\C=C6/N=C(C(CCC(=O)OCCC)C6C)C(C1=O)=C2N3C(C)=C5C(C)OCCC)C(C)C4CC
Name:	Bacteriopurpurinimide Derivative 9
Method:	Fluorescence Microscopy
References:	212
Structure:	CCCCCCCOC(C)C1=C(C)C2[NH2+]C1\C=C1/N=C(/C=C3NC4=C(C(=O)N(CCCCCC)C(=O)C4=C\3C)C3=N/C(=C\2)C(C)C3CCC(=O)OCCC)C(CC)C1C
Name:	Bacteriopurpurinimide Derivative 10
Method:	Fluorescence Microscopy
References:	212
Structure:	CCCCCCCCCCOC(C)C1=C(C)C2[NH2+]C1\C=C1/N=C(/C=C3NC4=C(C(=O)N(CCCCC)C(=O)C4=C\3C)C3=N/C(=C\2)C(C)C3CCC(=O)OCCC)C(CC)C1C
Name:	XF 70
Method:	Fluorescence Microscopy
References:	215
Structure:	C[N+](C)(C)CCCOc1cccc(c1)-c1c2ccc(cc3ccc([nH]3)c(-c3cccc(OCCC[N+](C)(C)C)c3)c3ccc(cc4ccc1[nH]4)n3)n2
Name:	XF 73
Method:	Fluorescence Microscopy
References:	215
Structure:	C[N+](C)(C)CCCOc1ccc(cc1)-c1c2ccc(cc3ccc([nH]3)c(-

	c3ccc(OCCC[N+](C)(C)C)cc3)c3ccc(cc4ccc1[nH]4)n3)n2
Name:	Silicon (IV) Phthalocyanine; SIPc[C3H5(NMe2)2O](OMe)
Method:	Fluorescence Microscopy
References:	217, 427
Structure:	CO[Si]1(OC(CN(C)C)C[NH+](C)C)n2c3cc4nc(cc5n1c(cc1nc(cc2c2ccccc32)c2ccccc12)c1ccccc51)c1ccccc41
Name:	SS-02; Dmt-D-Arg-Phe-Lys-NH2; (Dmt^1)-DALDA
Method:	Fluorescence Microscopy
References:	31, 156
Structure:	Cc1cc(O)cc(C)c1CC([NH3+])C(=O)NC(CCCNC(N)=[NH2+])C(=O)NC(Cc1ccccc1)C(=O)NC(CCCC[NH3+])C(N)=O
Name:	SS-19; Dmt-D-Arg-Phe-atnDap-NH2; (Dmt^1,atnDap^4)-DALDA
Method:	Fluorescence Microscopy
References:	31, 156
Structure:	Cc1cc(O)cc(C)c1CC([NH3+])C(=O)NC(CCCNC(N)=[NH2+])C(=O)NC(Cc1ccccc1)C(=O)NC(C(N)C(=O)c1ccccc1N)C(N)=O
Name:	SS-31; D-Arg-Dmt-Lys-Phe-NH2
Method:	Fluorescence Microscopy
References:	31
Structure:	Cc1cc(O)cc(C)c1CC(NC(=O)C([NH3+])CCCNC(N)=[NH2+])C(=O)NC(CCCC[NH3+])C(=O)NC(Cc1ccccc1)C(N)=O
Name:	MitoDC-81; [4-((11aS)-7-methoxy-1,2,3,11a-tetrahydro-5H-pyrrolo[2,1-c][1,4]benzodiazepin-5-on-8-oxy)butyl] triphenylphosphonium iodide
Method:	Fluorescence Microscopy
References:	39
Structure:	COc1cc2C(=O)N3CCCC3C=Nc2cc1OCCCC[P+](c1ccccc1)(c1ccccc1)c1ccccc1
Name:	Isometamidium
Method:	Cell Fractionation

References:	205
Structure:	CC[n+]1c(-c2ccccc2)c2cc(ccc2c2ccc(N)cc12)\N=N\Nc1cccc(c1)C(N)=[NH2+]
Name:	5(6)Carboxyfluorescein-Containing Tetragunidinium Vector
Method:	Fluorescence Microscopy
References:	33
Structure:	CCCC[Si](OCC1CCN2CCC(CSCC3CCN4CCC(CSCC5CCN6CCC(CSCC7CCN8CCC(CSCCNC(=O)c9ccc%10C(=O)OC%11(c%12ccc(O)cc%12Oc%12cc(O)ccc%11%12)c%10c9)NC8=[NH+]7)NC6=[NH+]5)NC4=[NH+]3)NC2=[NH+]1)(c1ccccc1)c1ccccc1
Name:	Pyropheophorbide-a Derivative 5
Method:	Fluorescence Microscopy
References:	92
Structure:	CCCCCOC(C)C1=C(C)/C2=C/C3=N/C(C(C(CCC([O-])=O)C3C)=C3CC(=O)C4=C/3NC(/C=C3\N=C(\C=C\1N2)C(C)=C\3CC)=C4C
Name:	Pyropheophorbide-a Derivative 6
Method:	Fluorescence Microscopy
References:	92
Structure:	CCCCCCOC(C)C1=C(C)/C2=C/C3=N/C(C(C(CCC([O-])=O)C3C)=C3CC(=O)C4=C/3NC(/C=C3\N=C(\C=C\1N2)C(C)=C\3CC)=C4C
Name:	LY 219703; N-(4-azidophenylsulfonyl)-N'-(4-chlorophenyl)urea
Method:	Cell Fractionation
References:	533
Structure:	[O-]S(=O)(=NC(=O)Nc1ccc(Cl)cc1)c1ccc(cc1)N=[N+]=[N-]
Name:	LCL-30
Method:	Pharmacological Effect
References:	206
Structure:	CCCCCCCCCCCCCCCC(=O)NC(CO)C(O)\C=C\CCCCC

	CCCCCCC

Name:	Bacteriochlorin Derivative 16
Method:	Fluorescence Microscopy
References:	532
Structure:	CCc1c(C)c2cc3nc(C(CCC(=O)OC)C3C)c3CC(=O)c4c(C)c(cc5nc(cc1[nH]2)C1(C)C(C(=O)OC)C(=CC=C51)C(=O)OC)[nH]c34

Name:	Bacteriochlorin Derivative 17
Method:	Fluorescence Microscopy
References:	532
Structure:	CCc1c(C)c2cc3nc(C(CCC(=O)OC)C3C)c(CC(=O)OC)c3[nH]c(cc4nc(cc1[nH]2)C1(C)C(C(=O)OC)C(=CC=C41)C(=O)OC)c(C)c3C(=O)OC

Name:	Bacteriochlorin Derivative 18
Method:	Fluorescence Microscopy
References:	532
Structure:	CCc1c(C)c2cc3nc(C(CCC(=O)OC)C3C)c(C(=O)OC)c3[nH]c(cc4nc(cc1[nH]2)C1(C)C(C(=O)OC)C(=CC=C41)C(=O)OC)c(C)c3C(=O)OC

Name:	Bacteriochlorin Derivative 19
Method:	Fluorescence Microscopy
References:	532
Structure:	CCCCCCN1C(=O)c2c3nc(cc4[nH]c(cc5nc(cc6[nH]c2c(C1=O)c6C)C1=CC=C(C(C(=O)OC)C51C)C(=O)OC)c(CC)c4C)[C@@H](C)C3CCC(=O)OC

Name:	Bacteriochlorin Derivative 20
Method:	Fluorescence Microscopy
References:	532
Structure:	CCc1c(C)c2cc3nc(C(CCC(=O)OC)C3C)c3C(=O)N(Cc4cc(cc4)C(F)(F)F)C(F)(F)F)C(=O)c4c(C)c(cc5nc(cc1[nH]2)C1(C)C(C(=O)OC)C(=CC=C51)C(=O)OC)[nH]c34

Name:	POR10; 5,10,15,20-tetrakis(1-decylpyridinium-4-yl)-21H.23H-porphyrin tetrabromide
Method:	Pharmacological Effect
References:	231
Structure:	CCCCCCCCCC[n+]1ccc(cc1)-c1c2ccc(n2)c(-c2cc[n+](CCCCCCCCCC)cc2)c2ccc([nH]2)c(-c2cc[n+](CCCCCCCCCC)cc2)c2ccc(n2)c(-c2cc[n+](CCCCCCCCCC)cc2)c2ccc1[nH]2

Name:	Pyridoxal 5'-Phosphate
Method:	Uptake/Binding
References:	243
Structure:	Cc1ncc(COP([O-])([O-])=O)c(C=O)c1O

Name:	DASPMI; Dimethylaminostyrylmethylpyridinium Iodine
Method:	Fluorescence Microscopy
References:	244
Structure:	CN(C)c1ccc(cc1)\C=C\c1cccc[n+]1C

Name:	Tetramethylethidium Bromide
Method:	Uptake/Binding
References:	246
Structure:	CC[n+]1c(-c2ccccc2)c2cc(N)ccc2c2c(C)c(C)c(cc12)N(C)C

Name:	Betaine B
Method:	Uptake/Binding
References:	246
Structure:	CCO[n+]1c(-c2ccccc2)c2cc(N)ccc2c2ccc(O)cc12

Name:	PTP1; 2-amino-5H-pyrido[3',2;5,6]thiopyrano[4,3-d]pyrimidine
Method:	Pharmacological Effect
References:	250
Structure:	Nc1ncc2CSc3ncccc3-c2n1

Name:	Cyanine Dye Conjugate 4b
Method:	Fluorescence Microscopy
References:	251
Structure:	COC(=O)CCCCC[n+]1ccc(cc1)\C=C1\Sc2ccccc2N1C

Name:	Cyanine Dye Conjugate 6b
Method:	Fluorescence Microscopy
References:	251
Structure:	COC(=O)CCCCC[n+]1ccc(cc1)\C=C/C=C1\Sc2ccccc2N1C

Name:	Cyanine Dye Conjugate 7b
Method:	Fluorescence Microscopy
References:	251
Structure:	COC(=O)CCCCC[n+]1ccc(\C=C/C=C2\Sc3ccccc3N2C)c2cccc12

Name:	Cyanine Dye Conjugate 4c
Method:	Fluorescence Microscopy
References:	251
Structure:	CN1\C(Sc2ccccc12)=C/c1cc[n+](CCCCCC(=O)NC(Cc2ccccc2)C(=O)NC(CCCNC(N)=[NH2+])C(=O)NC(Cc2ccccc2)C(=O)NC(CCCC[NH3+])C(N)=O)cc1

Name:	Cyanine Dye Conjugate 6c
Method:	Fluorescence Microscopy
References:	251
Structure:	CN1c2ccccc2S\C1=C/C=C\c1cc[n+](CCCCCC(=O)NC(Cc2ccccc2)C(=O)NC(CCCNC(N)=[NH2+])C(=O)NC(Cc2ccccc2)C(=O)NC(CCCC[NH3+])C(N)=O)cc1

Name:	Cyanine Dye Conjugate 7c
Method:	Fluorescence Microscopy
References:	251
Structure:	CN1\C(Sc2ccccc12)=C/C=C\c1cc[n+](CCCCCC(=O)NC(Cc2ccccc2)C(=O)NC(CCCNC(N)=[NH2+])C(=O)NC(Cc2ccccc2)C(=O)NC(CCCC[NH3+])C(N)=O)c2ccccc12

Name:	DNCTT
Method:	Pharmacological Effect
References:	252
Structure:	FC(F)(F)c1cc(c(Cl)c(c1)N(=O)=O)N(=O)=O

Name:	DDT
Method:	Pharmacological Effect
References:	253
Structure:	Clc1ccc(cc1)C(c1ccc(Cl)cc1)C(Cl)(Cl)Cl

Name:	Fusaric Acid
Method:	Pharmacological Effect
References:	254
Structure:	CCCCc1ccc(nc1)C([O-])=O

Name:	MIBG (Meta-Iodobenzylguanidine)
Method:	Pharmacological Effect
References:	262
Structure:	NC(=[NH2+])NCc1cccc(I)c1

Name:	Metoclopramide
Method:	Cell Fractionation
References:	264
Structure:	CC[NH+](CC)CCNC(=O)c1cc(Cl)c(N)cc1OC

Name:	HIPDM
Method:	Cell Fractionation
References:	265
Structure:	CN(CCC[NH+](C)C)Cc1cc(I)cc(C)c1O

Name:	Ditercalinium
Method:	Fluorescence Microscopy
References:	266
Structure:	COc1ccc2[nH]c3ccc4cc[n+](CCC[NH+]5CCC(CC5)C5CC[NH+](CCC[n+]6ccc7ccc8[nH]c9ccc(OC)cc9c8c7c6)CC5)cc4c3c2c1

Name:	Genistein
Method:	Pharmacological Effect
References:	267
Structure:	Oc1ccc(cc1)C1=COc2cc([O-])cc(O)c2C1=O

Name:	Aflatoxin B1
Method:	Pharmacological Effect
References:	268
Structure:	COc1cc2OC3OC=CC3c2c2OC(=O)C3=C(CCC3=O)c12

Name:	Rubratoxin B
Method:	Pharmacological Effect
References:	269
Structure:	CCCCCCC(O)C1C(O)C2=C(CC(CC3=C1C(=O)OC3=O)C(O)C1CC=CC(=O)O1)C(=O)OC2=O

Name:	FUdRFloxuridine
Method:	Distr.others
References:	260
Structure:	OCC1OC(CC1O)N1C=C(F)C(=O)NC1=O

Name:	Pyrrolo(2,3-h)quinolone Compound 10

Method:	Fluorescence Microscopy
References:	275
Structure:	Cc1cc2C3=C(CCc2n1-c1ccccc1)C=C(C(=O)N3)S(=O)(=O)c1ccccc1
Name:	Pyrrolo(2,3-h)quinolone Compound 11
Method:	Fluorescence Microscopy
References:	275
Structure:	Cc1cc2C3=C(CCc2n1-c1ccccc1)C=C(C(=O)N3)C(=O)c1ccccc1
Name:	Pyrrolo(2,3-h)quinolone Compound 12
Method:	Fluorescence Microscopy
References:	275
Structure:	Cc1cc2C3=C(CCc2n1-c1ccccc1)C=C(C#N)C(=O)[N-]3
Name:	Pyrrolo(2,3-h)quinolone Compound 13
Method:	Fluorescence Microscopy
References:	275
Structure:	CCOC(=O)C1=CC2=C(NC1=O)c1cc(C)n(c1CC2)-c1ccccc1
Name:	Pyrrolo(2,3-h)quinolone Compound 14
Method:	Fluorescence Microscopy
References:	275
Structure:	Cc1cc2C3=C(CCc2n1C)C=C(C(=O)N3)S(=O)(=O)c1ccccc1
Name:	Pyrrolo(2,3-h)quinolone Compound 15
Method:	Fluorescence Microscopy
References:	275
Structure:	Cc1cc2C3=C(CCc2n1C)C=C(C(=O)N3)C(=O)c1ccccc1
Name:	Pyrrolo(2,3-h)quinolone Compound 16
Method:	Fluorescence Microscopy
References:	275
Structure:	Cc1cc2C3=C(CCc2n1Cc1ccccc1)C=C(C(=O)N3)S(=O)(=O)c1ccccc1
Name:	Pyrrolo(2,3-h)quinolone Compound 17
Method:	Fluorescence Microscopy
References:	275

Structure:	Cc1cc2C3=C(CCc2n1Cc1ccccc1)C=C(C(=O)N3)C(=O)c1ccccc1
Name:	EPED3
Method:	Pharmacological Effect
References:	277
Structure:	C[NH+](C)CCOc1ccc2[nH]c3c(C)c4ccncc4c(C)c3c2c1
Name:	Methylene Blue Derivative
Method:	Fluorescence Microscopy
References:	283
Structure:	CCON1c2cc3[s+]c4cc5N(OC)C)C(C)(C)CC(C)c5cc4nc3cc2C(C)CC1(C)C
Name:	Rhodamine 800
Method:	Uptake/Binding
References:	293
Structure:	N#CC1=C2C=C3CCC[N+]4=C3C(CCC4)=C2Oc2c3CCCN4CCCc(cc12)c34
Name:	Fluorinated Tetrapyridylporphyrin Analogue 8
Method:	Fluorescence Microscopy
References:	302
Structure:	C[n+]1cccc(c1F)-c1c2ccc(n2)c(-c2ccc[n+](C)c2F)c2ccc([nH]2)c(-c2ccc[n+](C)c2F)c2ccc(n2)c(-c2ccc[n+](C)c2F)c2ccc1[nH]2
Name:	MitP
Method:	Fluorescence Microscopy
References:	309
Structure:	CCC(C)C([NH3+])C(=O)NC(CC(N)=O)C(=O)NC(CC(C)C)C(=O)NC(CCCC[NH3+])C(=O)NC(CCCC[NH3+])C(=O)NC(CC(C)C)C(=O)NC(C)C(=O)NC(CCC[NH3+])C(=O)NC(CC(C)C)C(=O)NC(C)(C)C(=O)NC(CCC[NH3+])C(=O)NC(CCCC[NH3+])C(=O)NC(C(C)CC)C(=O)NC(CC(C)C)C(N)=O
Name:	Z-Gly-RGD-f-mitP
Method:	Fluorescence Microscopy
References:	309
Structure:	CCC(C)C(NC(=O)C(Cc1ccccc1)NC(=O)C(CC([O-

	])=O)NC(=O)CNC(=O)C(CCC NC(N)=[NH2+])NC(=O)CNC(= O)OCc1ccccc1)C(=O)NC(CC(N)=O)C(=O)NC(CC(C)C)C(= O)NC(CCCC[NH3+])C(=O)NC (CCCC[NH3+])C(=O)NC(CC(C)C)C(=O)NC(C)C(=O)NC(C CCC[NH3+])C(=O)NC(CC(C) C)C(=O)NC(C)(C)C(=O)NC(C CCC[NH3+])C(=O)NC(CCCC[NH3+])C(=O)NC(CC(C)C)C(N)=O

Name:	Coenzyme Q9
Method:	Cell Fractionation
References:	319
Structure:	COC1=C(OC)C(=O)C(C\C=C(/C)CC\C=C(/C)CC\C=C(/C)C C\C=C(/C)CC\C=C(/C)CC\C= C(/C)CC\C=C(/C)CC\C=C(/C) CCC=C(C)C)=C(C)C1=O

Name:	Conenzyme Q10
Method:	Cell Fractionation
References:	319
Structure:	COC1=C(OC)C(=O)C(C\C=C(/C)CC\C=C(/C)CC\C=C(/C)C C\C=C(/C)CC\C=C(/C)CC\C= C(/C)CC\C=C(/C)CC\C=C(/C) CC\C=C(/C)CCC=C(C)C)=C(C)C1=O

Name:	(1''-pyrene butyl)-2-rhodamine ester
Method:	Fluorescence Microscopy
References:	324
Structure:	Nc1ccc2c(OC3=CC(=[NH2+]) C=CC3=C2c2cccc(c2)C(=O)O CCCCc2ccc3ccc4cccc5ccc2c 3c45)c1

Name:	Pyocyanin
Method:	Fluorescence Microscopy
References:	325
Structure:	CN1C2=CC=CC(=O)C2=Nc2c cccc12

Name:	TEMPO
Method:	Fluorescence Microscopy
References:	348
Structure:	CC(=C)c1cc(N\C(SCc2ccc(C[P+](c3ccccc3)(c3ccccc3)c3cc cccc3)cc2)=N/C2CC(C)(C)N(O) C(C)(C)C2)ccc1C1=C2C=CC(=O)C=C2Oc2cc(O)ccc12

Name:	5-Aminofluorescein conjugated 9-Hydroxystearic Acid
Method:	Fluorescence Microscopy
References:	329
Structure:	CCCCCCCCC(O)CCCCCC CC(=O)Nc1ccc2c(c1)C(=O)O C21c2ccc(O)cc2Oc2cc(O)ccc 12

Name:	CDS1
Method:	Fluorescence Microscopy
References:	332
Structure:	CCc1c(CC)c2cc3c(CC)c(CC)c 4n3[Cu]n3c(cc1n2)c(CC)c(CC)c3c(\C=[N+](\C)C)c1nc2c(ccc c42)C1(CC)CC

Name:	MTT; 3-(4,5-dimethylthiazol-2-yl)-2,5-diphenyltetrazolium bromide
Method:	Pharmacological Effect
References:	333
Structure:	Cc1nc(sc1C)-n1nc(n[n+]1-c1ccccc1)-c1ccccc1

Name:	2-methyl-4-dimethylaminoazobenzene
Method:	Cell Fractionation
References:	534
Structure:	CN(C)c1ccc(\N=N\c2ccccc2)c (C)c1

Name:	DMSP-Coumarin Derivative 4
Method:	Fluorescence Microscopy
References:	351
Structure:	CCCCCCCCCCCCCC\C=C\C(OC(=O)C1Cc2ccc(cc2OC1=O)N(CC)CC)C(CO)[NH+](C)C

Name:	DMSP-Coumarin Derivative 5
Method:	Fluorescence Microscopy
References:	351
Structure:	CCCCCCCCCCCCCC\C=C\C(O)C(COC(=O)C1Cc2ccc(cc2 OC1=O)N(CC)CC)[NH+](C)C

Name:	MitoPY1
Method:	Fluorescence Microscopy
References:	355
Structure:	CC1(C)OB(OC1(C)C)c1ccc2c (Oc3cc(ccc3C22OC(=O)c3ccc cc23)N2CC[NH+](CCCC[P+](c3ccccc3)(c3ccccc3)c3ccccc3

	)CC2)c1

Name:	2-Quinolinecarboxamide Derivative 6a
Method:	Uptake/Binding
References:	358
Structure:	CN(Cc1ccccc1)C(=O)c1nc2ccccc2c(-c2ccccc2)c1CN1CC[NH2+]CC1

Name:	2-Quinolinecarboxamide Derivative 6b
Method:	Uptake/Binding
References:	358
Structure:	CN(Cc1ccccc1)C(=O)c1nc2ccccc2c(-c2ccccc2)c1CN1CC[NH+](CC1)Cc1c(nc2ccccc2c1-c1ccccc1)C(=O)N(C)Cc1ccccc1

Name:	2-Quinolinecarboxamide Derivative 6c
Method:	Uptake/Binding
References:	358
Structure:	CN(Cc1ccccc1)C(=O)c1nc2ccccc2c(-c2ccccc2)c1CN1CCN(CC1)C(=O)Nc1ccccc1

Name:	2-Quinolinecarboxamide Derivative 6d
Method:	Uptake/Binding
References:	358
Structure:	CN(Cc1ccccc1)C(=O)c1nc2ccccc2c(-c2ccccc2)c1C[NH+]1CCN(CCN2C(=O)c3ccccc3C2=O)CC1

Name:	2-Quinolinecarboxamide Derivative 6e
Method:	Uptake/Binding
References:	358
Structure:	CN(Cc1ccccc1)C(=O)c1nc2ccccc2c(-c2ccccc2)c1C[NH+]1CCN(CCN2C(=O)c3ccccc3C2=O)CC1

Name:	2-Quinolinecarboxamide Derivative 6f
Method:	Uptake/Binding
References:	358
Structure:	CN(Cc1ccccc1)C(=O)c1nc2cc

	ccc2c(-c2ccccc2)c1CN1CC[NH+](CCCN2C(=O)c3ccccc3C2=O)CC1

Name:	2-Quinolinecarboxamide Derivative 6j
Method:	Uptake/Binding
References:	358
Structure:	CN(Cc1ccccc1)C(=O)c1nc2ccccc2c(-c2ccccc2)c1C[NH+]1CCN(CCC[N+]23CCS[Re--]22(O)SCCN2C(=O)C3)CC1

Name:	2-Quinolinecarboxamide Derivative 6m
Method:	Uptake/Binding
References:	358
Structure:	CN(Cc1ccccc1)C(=O)c1nc2ccccc2c(-c2ccccc2)c1CN1CCN(CC1)C(=O)C[N+]12CCS[Re--]11(O)SCCN1C(=O)C2

Name:	N-methylated imidazopyridine-acetamide Derivative 7
Method:	Uptake/Binding
References:	359
Structure:	CN(C(=C)Cc1c(nc2c(Cl)cc(Cl)cn12)-c1ccc(Cl)cc1)c1ccccc1

Name:	SSR180575
Method:	Uptake/Binding
References:	362
Structure:	CN(C)C(=O)CC1=NN(C(=O)c2c1c1ccc(Cl)cc1n2C)c1ccccc1

Name:	Alpidem
Method:	Pharmacological Effect
References:	535
Structure:	CCCN(CCC)C(=O)Cc1c(nc2cc(Cl)cn12)-c1ccc(Cl)cc1

Name:	DAA1097
Method:	Uptake/Binding
References:	365
Structure:	CC(C)Oc1ccccc1CN(C(C)=O)c1ccc(Cl)cc1Oc1ccccc1

Name:	DAA1106
Method:	Uptake/Binding
References:	365
Structure:	COc1ccc(OC)c(CN(C(C)=O)c

	2cc(F)ccc2Oc2ccccc2)c1

Name:	Pyrrolobenzoxazepine Derivative 17f
Method:	Uptake/Binding
References:	366
Structure:	CCON(OCC)C(=O)OC1=C(Oc2ccccc2-n2cccc12)c1ccccc1

Name:	Pyrrolobenzoxazepine Derivative 17j
Method:	Uptake/Binding
References:	366
Structure:	CCON(OCC)C(=O)OC1=C(Oc2ccccc2-n2cccc12)c1ccc(C)cc1

Name:	Dipyridamole
Method:	Uptake/Binding
References:	368
Structure:	CC(=O)OCCN(CCO)c1nc(N2CCCCC2)c2nc(nc(N3CCCCC3)c2n1)N(CCO)CCO

Name:	RA-25
Method:	Uptake/Binding
References:	368
Structure:	CNc1nc(NC)c2nc(NC)nc(NC)c2n1

Name:	GBLD470
Method:	Uptake/Binding
References:	370
Structure:	ClC1Nn2c(C=C1)nc(-c1ccc(cc1)-c1ccccc1)c2CNC(=O)c1ccccc1

Name:	GBLD471
Method:	Uptake/Binding
References:	370
Structure:	CC(=O)NCc1c(nc2C=CC(Cl)Nn12)-c1ccc(cc1)-c1ccccc1

Name:	GBLD696
Method:	Uptake/Binding
References:	370
Structure:	ClC1Nn2c(C=C1)nc(\C=C\c1ccccc1)c2CNC(=O)c1ccccc1

Name:	GBLD700
Method:	Uptake/Binding
References:	370
Structure:	CC(C)(C)c1ccc(cc1)-c1nc2C=CC(Cl)Nn2c1CNC(=

	O)c1ccccc1

Name:	GBLD703
Method:	Uptake/Binding
References:	370
Structure:	CC(C)(C)c1ccc(cc1)-c1nc2C=CC(Cl)Nn2c1CNC(=O)c1ccc(F)cc1

Name:	Imidazopyridine-7-nitrofurazan Conjugate 10
Method:	Fluorescence Microscopy
References:	373
Structure:	Clc1ccc(cc1)-c1nc2c(Cl)cc(Cl)cn2c1CC(=O)N(CCCCCCNc1ccc(c2nonc12)N(=O)=O)Cc1ccccc1

Name:	Glucoconjugated Chlorin Derivative 7
Method:	Fluorescence Microscopy
References:	405
Structure:	OC[C@H]1O[C@@H](Oc2ccc(c2)-c2c3CCc([nH]3)c(-c3cccc(O[C@@H]4O[C@H](CO)[C@@H](O)[C@@H](O)[C@H]4O)c3)c3ccc(n3)c(-c3cccc(O[C@@H]4O[C@H](CO)[C@@H](O)[C@@H](O)[C@H]4O)c3)c3ccc([nH]3)c(-c3cccc(O[C@@H]4O[C@H](CO)[C@@H](O)[C@@H](O)[C@H]4O)c3)c3ccc2n3)[C@H](O)[C@H](O)[C@@H]1O

Name:	Glucoconjugated Chlorin Derivative 9
Method:	Fluorescence Microscopy
References:	405
Structure:	OC[C@H]1O[C@@H](Oc2ccc(c2)-c2c3ccc(n3)c(-c3cccc(O[C@@H]4O[C@H](CO)[C@@H](O)[C@@H](O)[C@H]4O)c3)c3ccc([nH]3)c(-c3cccc(O[C@@H]4O[C@H](CO)[C@@H](O)[C@@H](O)[C@H]4O)c3)c3ccc(n3)c(-c3ccccc3)c3ccc2[nH]3)[C@H](O)[C@H](O)[C@@H]1O

Name:	Porphyrazine 16[0]
Method:	Fluorescence Microscopy
References:	403
Structure:	CC(C)Oc1ccc(OC(C)C)c2c3nc4nc(nc5[nH]c(nc6nc(nc([nH]3

	)c12)c(SCCOCCOCCO)c6SCCOCCOCCO)c1c(OC(C)C)ccc(OC(C)C)c51)c(SCCOCCOCCO)c4SCCOCCOCCO
Name:	FCp6
Method:	Fluorescence Microscopy
References:	429
Structure:	CCC1=C(C)C2=NC1=CC1=C(C)C(C([O-])=O)=C(N1)C(C([O-])=O)=C1N=C(C=C3NC(=C2)C(C=O)=C3C)C(C)=C1CCC([O-])=O
Name:	Biotinylated Glyfoline
Method:	histo
References:	431
Structure:	COC1=C(OC)C(OC)=C(OC)C2C1N(C)c1c(OC)c(OCCCCNC(=O)CCCNC(=O)CCCCC3SCC4(C)NC(=O)NC34C)ccc1C2=O
Name:	Methyl Pyropheophorbide-a Derivative 7
Method:	Fluorescence Microscopy
References:	537
Structure:	CCCCCCOC(C)C1=C(C)/C2=C/C3=N/C(C(CCC(=O)OC)C3C)=C3CC(=O)C4=C/3NC(/C=C3\N=C(\C=C\1N2)C(C)=C\3CC)=C4C
Name:	Methyl Pyropheophorbide-a Derivative 8
Method:	Fluorescence Microscopy
References:	537
Structure:	CCC1=C(C)C2=N\C\1=C/C1=C(C)C3=C4N1[In](Cl)N1C(=C/C5=N/C(C(CCC(=O)OC)C5C)=C\4CC3=O)\C(C)=C(C(C)OCCOCCOCCOC)/C1=C/2
Name:	CP
Method:	Fluorescence Microscopy
References:	443
Structure:	COc1cc(OC)c(c(OC)c1)-c1c2CCc([nH]2)c(-c2ccc(cc2)[N+](C)(C)C)c2ccc(

	n2)c(-c2c(OC)cc(OC)cc2OC)c2ccc([nH]2)c(-c2c(OC)cc(OC)cc2OC)c2ccc1n2
Name:	Fluorinated Bacteriopurpurinimide Derivative 3
Method:	Fluorescence Microscopy
References:	444
Structure:	CCC1C(C)C2=C/C3NC(/C=C4\N=C(C(CCC(=O)OC)C4C)C4=C5NC(=C\C1=N\2)/C(C)=C5C(=O)N(Cc1cc(cc(c1)C(F)(F)F)C(F)(F)F)C4=O)C(C)=C3C(C)[NH2+]Cc1cc(cc(c1)C(F)(F)F)C(F)(F)F
Name:	Hexadecanedioic Acid
Method:	Pharmacological Effect
References:	455
Structure:	[O-]C(=O)CCCCCCCCCCCCCCC([O-])=O
Name:	PBR Fluorescent Derivative 4
Method:	Fluorescence Microscopy
References:	471
Structure:	O=C(Cc1c([nH]c2cccccc12)-c1ccccc1)NCCCCCCNc1ccc(c2nonc12)N(=O)=O
Name:	Pi-Extended Squaraines Derivative 1b
Method:	Fluorescence Microscopy
References:	507
Structure:	COCCOCCOCn1c(ccc1C1=C([O-])\C(C1=O)=C1/C=CC(\C=N\N(C)C)=[N+]/1COCCOCCOC)\C=N\N(C)C
Name:	Toluidine blue O
Method:	Distr.others
References:	185
Structure:	CC1=CC2=C(SC3=C/C(/C=C C3=N2)=[N+](/C)C)C=C1N

Appendix C

The chemical compounds with reported subcellular localization site in the nucleus. References information is available in Appendix H. Structure is presented as the Simplified Molecular Input Line Entry Specification string of the major microspecies at pH 7.4, as calculated by ChemAxon.

Name:	DAPI
Method:	Fluorescence Microscopy
References:	4
Structure:	NC(=[NH2+])c1ccc(cc1)-c1cc2ccc(cc2[nH]1)C(N)=[NH2+]

Name:	Ethidium bromide
Method:	Fluorescence Microscopy
References:	4, 163
Structure:	CC[n+]1c(-c2ccccc2)c2cc(N)ccc2c2ccc(N)cc12

Name:	E1374; Ethidium monoazide bromide; EMA
Method:	Fluorescence Microscopy
References:	600
Structure:	CC[n+]1c(-c2ccccc2)c2cc(ccc2c2ccc(N)cc12)N=[N+]=[N-]

Name:	L7595; LDS 751
Method:	Fluorescence Microscopy
References:	602
Structure:	CC[n+]1c(\C=C\C=C/c2ccc(cc2)N(C)C)ccc2cc(ccc12)N(C)C

Name:	H22845; hydroxystilbamidine, methanesulfonate
Method:	Fluorescence Microscopy
References:	603
Structure:	NC(=[NH2+])c1ccc(cc1)\C=C\c1ccc(cc1O)C(N)=[NH2+]

Name:	H1398; Pentahydrate (bis-benzimide); Hoechst 33258
Method:	Fluorescence Microscopy
References:	147
Structure:	C[NH+]1CCN(CC1)c1ccc2nc([nH]c2c1)-c1ccc2[nH]c(nc2c1)-c1ccc(O)cc1

Name:	H21486; Hoechst 34580
Method:	Fluorescence Microscopy

References:	658
Structure:	CN(C)c1ccc(cc1)-c1nc2cc(ccc2[nH]1)-c1nc2ccc(cc2[nH]1)N1CC[NH+](C)CC1

Name:	H1399; trihydrochloride, trihydrate; Hoechst 33342
Method:	Fluorescence Microscopy
References:	630
Structure:	CCOc1ccc(cc1)-c1nc2cc(ccc2[nH]1)-c1nc2ccc(cc2[nH]1)N1CC[NH+](C)CC1

Name:	P3581; PO-PRO™ 1 iodide (435/455)
Method:	Fluorescence Microscopy
References:	631
Structure:	C[n+]1c(C=C2C=CN(CCC[N+](C)(C)C)C=C2)oc2ccccc12

Name:	N21485; Hoechst S769121, trihydrochloride, trihydrate; Nuclear yellow
Method:	Fluorescence Microscopy
References:	670
Structure:	C[NH+]1CCN(CC1)c1ccc2nc([nH]c2c1)-c1ccc2[nH]c(nc2c1)-c1ccc(cc1)S(N)(=O)=O

Name:	P3585; PO-PRO™-3 iodide (539/567)
Method:	NA
References:	Invi
Structure:	C[n+]1c(\C=C\C=C2C=CN(CCC[N+](C)(C)C)C=C2)oc2ccccc12

Name:	Y3603; YO-PRO®-1 iodide (491/509)
Method:	Fluorescence Microscopy
References:	71
Structure:	C[n+]1c(oc2ccccc12)\C=C1\C=CN(CCC[N+](C)(C)C)c2ccccc1

Name:	T3602; TO-PRO®-1 iodide (515/531)
Method:	Fluorescence Microscopy
References:	684
Structure:	C[n+]1c(sc2ccccc12)\C=C1/C=CN(CCC[N+](C)(C)C)c2ccccc12

Name:	Y3607; YO-PRO®-3 iodide (612/631)
Method:	Fluorescence Microscopy
References:	608
Structure:	C[n+]1c(\C=C/C=C2/C=CN(CCC[N+](C)(C)C)c3ccccc23)oc2cccc12

Name:	P1304MP; Propidium Iodide
Method:	Fluorescence Microscopy
References:	71
Structure:	CC[N+](C)(CC)CCC[n+]1c(-c2ccccc2)c2cc(N)ccc2c2ccc(N)cc12

Name:	T3605; TO-PRO®-3 iodide (642/661)
Method:	Fluorescence Microscopy
References:	71
Structure:	C[n+]1c(\C=C\C=C2/C=CN(CCC[N+](C)(C)C)c3ccccc23)sc2ccccc12

Name:	A666; Bis-(6-chloro-2-methoxy-9-acridinyl) spermine; Acridine homodimer
Method:	Fluorescence Microscopy
References:	723
Structure:	COc1ccc2[nH+]c3cc(Cl)ccc3c(NCCC[NH2+]CCCC[NH2+]CCCNc3c4ccc(Cl)cc4[nH+]c4ccc(OC)cc34)c2c1

Name:	T7596; TO-PRO®-5 iodide (745/770)
Method:	Uptake/Binding
References:	635
Structure:	C[n+]1c(\C=C\C=C/C=C2\C=CN(CCC[N+](C)(C)C)c3ccccc23)sc2ccccc12

Name:	E1169; Ethidium homodimer-1; EthD-1
Method:	Fluorescence Microscopy
References:	613

Structure:	Nc1ccc2c(c1)c(-c1ccccc1)[n+](CCCNCC[NH2+]CCC[n+]1c(-c3ccccc3)c3cc(N)ccc3c3ccc(N)cc13)c1cc(N)ccc21

Name:	P3580; POPO™ 1 iodide (434/456)
Method:	Uptake/Binding
References:	650
Structure:	C[n+]1c(C=C2C=CN(CCC[N+](C)(C)CCC[N+](C)(C)CCCN3C=CC(C=C3)=Cc3oc4ccccc4[n+]3C)C=C2)oc2ccccc12

Name:	B3586; BOBO™3 iodide (570/602)
Method:	Fluorescence Microscopy
References:	651
Structure:	C[n+]1c(\C=C\C=C2C=CN(CCC[N+](C)(C)CCC[N+](C)(C)CCCN3C=CC(C=C3)=C/C=C\c3sc4ccccc4[n+]3C)C=C2)sc2ccccc12

Name:	A7592; Actinomycin D
Method:	Distr.others
References:	620
Structure:	CC(C)C1NC(=O)C(NC(=O)c2ccc(C)c3OC4=C(C)C(=O)C(N)=C(C(=O)NC5C(C)OC(=O)C(C(C)C)N(C)C(=O)CN(C)C(=O)C6CCCN6C(=O)C(NC5=O)C(C)C)C4=Nc23)C(C)OC(=O)C(C(C)C)N(C)C(=O)CN(C)C(=O)C2CCCN2C1=O

Name:	A1310; 7-aminoactinomycin D; 7-AAD
Method:	Uptake/Binding
References:	621
Structure:	CC(C)C1NC(=O)C(NC(=O)c2cc(N)c(C)c3OC4=C(C)C(=O)C(N)=C(C(=O)NC5C(C)OC(=O)C(C(C)C)N(C)C(=O)CN(C)C(=O)C6CCCN6C(=O)C(NC5=O)C(C)C)C4=Nc23)C(C)OC(=O)C(C(C)C)N(C)C(=O)CN(C)C(=O)C2CCCN2C1=O

Name:	Y3601; YOYO®-1 iodide (491/509)
Method:	Fluorescence Microscopy
References:	608
Structure:	C[n+]1c(oc2ccccc12)\C=C1\C=

	CN(CCC[N+](C)(C)CCC[N+](C)(C)CCCN2C=C/C(=C\c3oc4ccccc4[n+]3C)c3ccccc23)c2ccccc12
Name:	E3599; Ethidium homodimer-2; EthD-2
Method:	Fluorescence Microscopy
References:	680
Structure:	C[N+](C)(CCC[n+]1c(-c2ccccc2)c2cc(N)ccc2c2ccc(N)cc12)CCC[N+](C)(C)CCC[n+]1c(-c2ccccc2)c2cc(N)ccc2c2ccc(N)cc12
Name:	T3600; TOTO®-1 iodide (514/533)
Method:	Fluorescence Microscopy
References:	681
Structure:	C[n+]1c(sc2ccccc12)\C=C1\C=CN(CCC[N+](C)(C)CCC[N+](C)(C)CCCN2C=C/C(=C\c3sc4ccccc4[n+]3C)c3ccccc23)c2ccccc12
Name:	Y3606; YOYO®-3 iodide (612/631)
Method:	Uptake/Binding
References:	622
Structure:	C[n+]1c(\C=C/C=C2/C=CN(CCC[N+](C)(C)CCC[N+](C)(C)CCCN3C=C/C(=C/C=C\c4oc5ccccc5[n+]4C)c4ccccc34)c3ccccc23)oc2ccccc12
Name:	T3604; TOTO®-3 iodide (642/660)
Method:	Fluorescence Microscopy
References:	71
Structure:	C[n+]1c(\C=C/C=C2/C=CN(CCC[N+](C)(C)CCC[N+](C)(C)CCCN3C=C/C(=C\C=C/c4sc5ccccc5[n+]4C)c4ccccc34)c3ccccc23)sc2ccccc12
Name:	Adriamycin; Doxorubicin
Method:	Fluorescence Microscopy/Cell Fractionation
References:	17, 729
Structure:	COc1cccc2C(=O)c3c(O)c4CC(O)(CC(OC5CC([NH3+])C(O)C(C)O5)c4c(O)c3C(=O)c12)C(=O)CO

Name:	Acriflavine
Method:	Fluorescence Microscopy
References:	127
Structure:	C[n+]1c2cc(N)ccc2cc2ccc(N)cc12
Name:	Hydroethidine
Method:	Fluorescence Microscopy
References:	57
Structure:	CCC1C(c2ccccc2)c2cc(N)ccc2-c2cncc(N)c12
Name:	Tetracycline
Method:	histo
References:	58
Structure:	C[NH+](C)C1C2CC3C(C(=O)C2(O)C(=O)\C(C1=O)=C(\N)[O-])=C([O-])c1c(O)cccc1C3(C)O
Name:	Chromomycin A3
Method:	Fluorescence Microscopy
References:	69
Structure:	COC1C(O)CC(OC1C)OC1CC(OC(C)C1OC(C)=O)Oc1cc2cc3CC(C(OC)C(=O)C(O)C(C)O)C(OC4CC(OC5CC(OC6CC(C)(O)C(OC(C)=O)C(C)O6)C(O)C(C)O5)C(O)C(C)O4)C(=O)c3c(O)c2c(O)c1C
Name:	SYBR Green I
Method:	Fluorescence Microscopy
References:	71
Structure:	CCCN(CCC[NH+](C)C)C1=C/C(=C/c2sc3ccccc3[n+]2C)c2ccccc2N1c1ccccc1
Name:	Cyan 40; 4-((1-methylbenzothiazolyliliden-2)methyl)-1,2,6-trimethylpyridinium perchlorate
Method:	Fluorescence Microscopy
References:	81
Structure:	CN1C(C)=CC(C=C1C)=Cc1sc2ccccc2[n+]1C
Name:	AN-152; Lys(6)-LHRH-doxorubicin
Method:	Fluorescence Microscopy
References:	104
Structure:	COc1cccc2C(=O)c3c(O)c4CC(O)(CC(OC5CC(NC(=O)CCCC(=O)NCCCCC(NC(=O)C(Cc6ccc(O)cc6)NC(=O)C(CO)NC(=O)C(Cc6c[nH]c7ccccc67)NC(=O)

	C(Cc6ncc[nH]6)NC(=O)C6CCC(=O)N6)C(=O)NC(CC(C)C)C(=O)NC(CCCNC(N)=[NH2+])C(=O)N6CCCC6C(=O)NCC(N)=O)C(O)C(C)O5)c4c(O)c3C(=O)c12)C(=O)CO

Name:	E36
Method:	Fluorescence Microscopy
References:	115
Structure:	C[n+]1c(\C=C\c2c[nH]c3ccccc23)ccc2ccccc12

Name:	E144
Method:	Fluorescence Microscopy
References:	115
Structure:	COc1cc(OC)c(\C=C\c2ccc3ccccc3[n+]2C)c(OC)c1

Name:	F22
Method:	Fluorescence Microscopy
References:	115
Structure:	COc1ccc2[n+](C)c(\C=C\c3ccc(cc3)N(C)C)ccc2c1

Name:	2'-O-Methyl
Method:	Fluorescence Microscopy
References:	128
Structure:	BC1OC(COC)C(OP([O-])(=O)OCC2OC(B)C(OC)C2OP(C)([O-])=O)C1OC

Name:	PBD Derivative 11; 7-Diethylaminocoumarin pyrrolobenzodiazepine derivative 11
Method:	Fluorescence Microscopy
References:	136
Structure:	CCN(CC)c1ccc2C=C(C(=O)NCCCOc3cc4N=CC5CCCN5C(=O)c4cc3OC)C(=O)Oc2c1

Name:	DRAQ5
Method:	Fluorescence Microscopy
References:	147
Structure:	C[NH+](C)CCNc1ccc(O)c2C(=O)c3c(NCC[NH+](C)C)ccc(O)c3C(=O)c12

Name:	Morin; 3,5,7,2',4'-pentahydroxyflavanol
Method:	Fluorescence Microscopy
References:	148
Structure:	Oc1cc(O)cc(c1)C1=C([O-])C(=O)c2c(O)cc(O)cc2O1

Name:	Mithramycin
Method:	Fluorescence Microscopy
References:	149
Structure:	COC(C1Cc2cc3cc(OC4CC(OC5CC(O)C(O)C(C)O5)C(O)C(C)O4)c(C)c(O)c3c(O)c2C(=O)C1OC1CC(OC2CC(OC3CC(C)(O)C(O)C(C)O3)C(O)C(C)O2)C(O)C(C)O1)C(=O)C(O)C(C)O

Name:	Polyamide 1
Method:	Fluorescence Microscopy
References:	159
Structure:	C[NH+](CCCNC(=O)CCNC(=O)c1cc(NC(=O)c2cc(NC(=O)c3cc(NC(=O)c4cc(NC(=O)CCCNC(=O)c5cc(NC(=O)c6cc(NC(=O)c7nc(NC(=O)c8nccn8C)cn7C)cn6C)cn5C)cn4C)cn3C)cn2C)c[nH]1)CCCNC(=S)Nc1ccc(c(c1)C([O-])=O)C1=C2C=CC(=O)C=C2Oc2cc(O)ccc12

Name:	Polyamide 3
Method:	Fluorescence Microscopy
References:	159
Structure:	C[NH+](CCCNC(=S)Nc1ccc(c(c1)C([O-])=O)C1=C2C=CC(=O)C=C2Oc2cc(O)ccc12)CCCNC(=O)c1cc(NC(=O)c2cc(NC(=O)c3cc(NC(=O)c4nc(NC(=O)CCCNC(=O)c5cc(NC(=O)c6cc(NC(=O)c7nc(NC(=O)c8nccn8C)cn7C)cn6C)cn5C)cn4C)cn3C)cn2C)cn1C

Name:	Polyamide 5
Method:	Fluorescence Microscopy
References:	159
Structure:	C[NH+](CCCNC(=S)Nc1ccc(c(c1)C([O-])=O)C1=C2C=CC(=O)C=C2Oc2cc(O)ccc12)CCCNC(=O)c1cc(NC(=O)c2cc(NC(=O)c3cc(NC(=O)c4cc(NC(=O)CCCNC(=O)c5cc(NC(=O)c6cc(NC(=O)c7nc(NC(=O)c8nccn8C)cn7C)cn6C)cn5C)cn4C)cn3C)cn2C)cn1C

Name:	Polyamide 6
Method:	Fluorescence Microscopy

References:	159

Structure:	C[NH+](CCCNC(=S)Nc1ccc(c(c1)C([O-])=O)C1=C2C=CC(=O)C=C2Oc2cc(O)ccc12)CCCNC(=O)c1cc(NC(=O)c2cc(NC(=O)c3cc(NC(=O)c4cc(NC(=O)CCCNC(=O)c5nc(NC(=O)c6cc(NC(=O)c7cc(NC(=O)c8nccn8C)cn7C)cn6C)cn5C)cn4C)cn3C)cn2C)cn1C

Name:	Polyamide 11
Method:	Fluorescence Microscopy
References:	159

Structure:	C[NH+](CCCNC(=S)Nc1ccc(c(c1)C([O-])=O)C1=C2C=CC(=O)C=C2Oc2cc(O)ccc12)CCCNC(=O)c1cc(NC(=O)c2cc(NC(=O)c3cc(NC(=O)c4nc(NC(=O)C([NH3+])CCNC(=O)c5cc(NC(=O)c6cc(NC(=O)c7nc(NC(=O)c8nccn8C)cn7C)cn6C)cn5C)cn4C)cn3C)cn2C)cn1C

Name:	Polyamide 12
Method:	Fluorescence Microscopy
References:	159

Structure:	C[NH+](CCCNC(=S)Nc1ccc(c(c1)C([O-])=O)C1=C2C=CC(=O)C=C2Oc2cc(O)ccc12)CCCNC(=O)c1cc(NC(=O)c2cc(NC(=O)c3cc(NC(=O)c4nc(NC(=O)[C@H](CCNC(=O)c5cc(NC(=O)c6cc(NC(=O)c7nc(NC(=O)c8nccn8C)cn7C)cn6C)cn5C)NC(C)=O)cn4C)cn3C)cn2C)cn1C

Name:	Polyamide 13
Method:	Fluorescence Microscopy
References:	159

Structure:	C[NH+](CCCNC(=S)Nc1ccc(c(c1)C([O-])=O)C1=C2C=CC(=O)C=C2Oc2cc(O)ccc12)CCCNC(=O)c1cc(NC(=O)c2cc(NC(=O)c3nc(NC(=O)c4cc(NC(=O)[C@H](CCNC(=O)c5cc(NC(=O)c6cc(NC(=O)c7cc(NC(=O)c8nccn8C)cn7C)cn6C)cn5C)NC(C)=O)cn4C)cn3C)cn2C)cn1C

Name:	Polyamide 14

Method:	Fluorescence Microscopy
References:	159

Structure:	C[NH+](CCCNC(=S)Nc1ccc(c(c1)C([O-])=O)C1=C2C=CC(=O)C=C2Oc2cc(O)ccc12)CCCNC(=O)c1cc(NC(=O)c2cc(NC(=O)c3nc(NC(=O)c4cc(NC(=O)C(CCNC(=O)c5cc(NC(=O)c6cc(NC(=O)c7nc(NC(=O)c8nccn8C)cn7C)cn6C)cn5C)NC(C)=O)cn4C)cn3C)cn2C)cn1C

Name:	Polyamide 22
Method:	Fluorescence Microscopy
References:	159

Structure:	C[NH+](CCCNC(=S)Nc1ccc(c(c1)C([O-])=O)C1=C2C=CC(=O)C=C2Oc2cc(O)ccc12)CCCNC(=O)c1cc(NC(=O)c2cc(NC(=O)c3cc(NC(=O)CCCNC(=O)c4cc(NC(=O)c5cc(NC(=O)c6nccn6C)cn5C)cn4C)cn3C)cn2C)cn1C

Name:	Olivomycin
Method:	Fluorescence Microscopy
References:	164

Structure:	COC1C(O)CC(OC1C)OC1CC(OC(C)C1OC(C)=O)Oc1cc(O)c2c(O)c3C(=O)C(OC4CC(OC5CC(OC6CC(C)(O)C(OC(=O)C(C)C)C(C)O6)C(O)C(C)O5)C(O)C(C)O4)C(Cc3cc2c1)C(OC)C(=O)C(O)C(C)O

Name:	Flunitrazepam
Method:	Fluorescence Microscopy
References:	172
Structure:	CN1C(=O)CN=C(c2ccccc2F)c2cc(ccc12)N(=O)=O

Name:	BODIPY-labeled Polyamide 2
Method:	Fluorescence Microscopy
References:	176

Structure:	C[NH+](CCCNC(=O)CCNC(=O)c1cc(NC(=O)c2cc(NC(=O)c3cc(NC(=O)c4cc(NC(=O)CCCNC(=O)c5cc(NC(=O)c6cc(NC(=O)c7nc(NC(=O)c8nccn8C)cn7C)cn6C)cn5C)cn4C)cn3C)cn2C)cn1C)CCCNC(=S)Nc1ccc(C2c3cc(O)cc3Oc3cc(O)ccc23)c(c1)C([O-])=O

Name:	Uracil Mustard
Method:	Cell Fractionation
References:	180
Structure:	ClCCN(CCCl)C1=CNC(=O)NC1=O

Name:	M-223; 10(2-diethylaminoethyl)-9-acridone
Method:	Fluorescence Microscopy
References:	173
Structure:	CC[NH+](CC)CCN1c2ccccc2C(=O)c2ccccc12

Name:	RB2Z; Dibenzo[h,j]dipyrido[3,2-a2',3'-c]phenazine)bis(2,2'-bipyridine)ruthenium(II) dication
Method:	Fluorescence Microscopy
References:	82
Structure:	c1ccc(nc1)-c1ccccn1

Name:	PicoGreen; [2-[N-bis-(3-dimethylaminopropyl)-amino]-4-[2,3-dihydro-3-methyl-(benzo-1,3-thiazol-2-yl)-methylidene]-1-phenyl-quinolinium]+
Method:	Fluorescence Microscopy
References:	542
Structure:	C[NH+](C)CCCN(CCC[NH+](C)C)C1=C/C(=C/c2sc3ccccc3[n+]2C)c2ccccc2N1c1ccccc1

Name:	Mitoxantrone
Method:	Fluorescence Microscopy
References:	235
Structure:	OCC[NH2+]CCNc1ccc(NCC[NH2+]CCO)c2C(=O)c3c(O)ccc(O)c3C(=O)c12

Name:	Pirarubicin
Method:	Fluorescence Microscopy
References:	236
Structure:	COc1cccc2C(=O)c3c(O)c4CC(O)(CC(OC5CC([NH3+])C(OC6CCCCO6)C(C)O5)c4c(O)c3C(=O)c12)C(=O)CO

Name:	Cascade Blue Derivative 2
Method:	Fluorescence Microscopy
References:	272
Structure:	[O-]C(=O)COc1cc(c2CC=C3C(C=C(c4ccc1c2c34)S([O-])=O)S([O-])=O)S([O-])=O

Name:	Cascade Blue Derivative 3
Method:	Fluorescence Microscopy
References:	272
Structure:	[NH3+]CCNC(=O)COc1cc(c2CC=C3C(C=C(c4ccc1c2c34)S([O-])=O)S([O-])=O)S([O-])=O

Name:	Cascade Blue Derivative 4
Method:	Fluorescence Microscopy
References:	272
Structure:	[NH3+]CCCCCCNC(=O)COc1cc(c2CC=C3C(C=C(c4ccc1c2c34)S([O-])=O)S([O-])=O)S([O-])=O

Name:	Cascade Blue Derivative 10
Method:	Fluorescence Microscopy
References:	272
Structure:	OCCNC(=O)COc1cc(c2CC=C3C(C=C(c4ccc1c2c34)S([O-])=O)S([O-])=O)S([O-])=O

Name:	Cascade Blue Derivative 11
Method:	Fluorescence Microscopy
References:	272
Structure:	NNC(=O)COc1cc(c2CC=C3C(C=C(c4ccc1c2c34)S([O-])=O)S([O-])=O)S([O-])=O

Name:	Cascade Blue Derivative 14
Method:	Fluorescence Microscopy
References:	272
Structure:	CC(C)(C)OC(=O)N1CCCC1C(=O)NCCNC(=O)COc1cc(c2CC=C3C(C=C(c4ccc1c2c34)S([O-])=O)S([O-])=O)S([O-])=O

Name:	Cascade Blue Derivative 15
Method:	Fluorescence Microscopy
References:	272
Structure:	CC(C)(C)OC(=O)N1CCCC1C(=O)NCCCCCCNC(=O)COc1cc(c2CC=C3C(C=C(c4ccc1c2c34)S([O-])=O)S([O-])=O)S([O-])=O

Name:	Cascade Blue Derivative 16
Method:	Fluorescence Microscopy
References:	272
Structure:	[O-]S(=O)C1C=C(c2ccc3c(OCC(=O)NCCCCCCC#N)cc(c4CC=C1c2c34)S([O-])=O)S([O-])=O

Name:	Cascade Blue Derivative 19
Method:	Fluorescence Microscopy
References:	272
Structure:	[O-]S(=O)C1C=C(c2ccc3c(OCC(=O)NCCCCCCNC(=O)C=C)cc(c4CC=C1c2c34)S([O-])=O)S([O-])=O

Name:	Cascade Blue Derivative 20
Method:	Fluorescence Microscopy
References:	272
Structure:	[O-]S(=O)C1C=C(c2ccc3c(OCC(=O)NCCCCCCNC(=O)c4ccc(cc4)N=[N+]=[N-])cc(c4CC=C1c2c34)S([O-])=O)S([O-])=O

Name:	BUdR; Broxuridine; 5-Bromo-2'-deoxyuridine
Method:	Distr.others
References:	260
Structure:	OCC1OC(CC1O)N1C=C(Br)C(=O)NC1=O

Name:	F3TdR; Trifluridine; 5-trifluorothymidine
Method:	Distr.others
References:	260
Structure:	OCC1OC(CC1O)N1C=C(C(=O)NC1=O)C(F)(F)F

Name:	Daunorubicin Analogue 1
Method:	Fluorescence Microscopy
References:	261
Structure:	COc1cccc2C(=O)c3c(O)c4CC(O)(CC(OC5CC([NH2+]CC(C)=O)C(O)C(C)O5)c4c(O)c3C(=O)c12)C(C)=O

Name:	Lycopene
Method:	Cell Fractionation
References:	278
Structure:	CC(C)=CCC\C(C)=C\C=C\C(C)=C\C=C\C(C)=C\C=C\C=C(C)\C=C\C=C(C)\C=C\C=C(/C)CCC=C(C)C

Name:	BBR 3422
Method:	Cell Fractionation
References:	312
Structure:	C[NH2+]CCNc1ccc2n(CC[NH3+])nc3-c4cnccc4C(=O)c1c23

Name:	Cisplatin
Method:	Cell Fractionation
References:	316
Structure:	Cl[Pt++]Cl

Name:	DB75; Furamidine
Method:	Fluorescence Microscopy
References:	327
Structure:	N[C+](N)c1ccc(cc1)-c1ccc(o1)-c1ccc(cc1)[C+](N)N

Name:	DB181
Method:	Fluorescence Microscopy
References:	327
Structure:	CC(C)N[C+](N)c1ccc(cc1)-c1ccc(o1)-c1ccc(cc1)[C+](N)NC(C)C

Name:	DB226
Method:	Fluorescence Microscopy
References:	327
Structure:	CCC(CC)N[C+](N)c1ccc(cc1)-c1ccc(o1)-c1ccc(cc1)[C+](N)NC(CC)CC

Name:	DB244
Method:	Fluorescence Microscopy
References:	327
Structure:	N[C+](NC1CCCC1)c1ccc(cc1)-c1ccc(o1)-c1ccc(cc1)[C+](N)NC1CCCC1

Name:	DB249
Method:	Fluorescence Microscopy
References:	327
Structure:	N[C+](NC1CCCCC1)c1ccc(cc1)-c1ccc(o1)-c1ccc(cc1)[C+](N)NC1CCCCC1

Name:	DB417
Method:	Fluorescence Microscopy
References:	327
Structure:	CN[C+](N)c1ccc(cc1)-c1ccc(o1)-c1ccc(cc1)[C+](N)NC

Name:	DB569
Method:	Fluorescence Microscopy
References:	327
Structure:	NC(=[NH+]c1ccccc1)c1ccc(cc1)-c1ccc(o1)-c1ccc(cc1)C(N)=[NH+]c1ccccc1

Name:	DB673
Method:	Fluorescence Microscopy
References:	327
Structure:	NC(N)=[NH+]c1ccc(cc1)-c1ccc(o1)-c1ccc(cc1)[NH+]=C(N)N
Name:	NT2
Method:	Fluorescence Microscopy
References:	332
Structure:	CCCOC(=O)C1=Cc2c3nc(cc4[nH]c(cc5nc(cc6[nH]c2c(CC)c6CC)c(CC)c5CC)c(CC)c4CC)C(CC)C13CC
Name:	4-dimethylaminoazobenzene
Method:	Cell Fractionation
References:	534
Structure:	CN(C)c1ccc(cc1)\N=N\c1ccccc1
Name:	Zinc Benzochlorin
Method:	Fluorescence Microscopy
References:	357
Structure:	CCC1=C(CC)C2N3[Zn]N4C(=C\C5=N\C(=C/C13)\C(CC)=C5CC)/C(CC)=C(CC)\C4=C1/C=CC=C3C/1=N\C(=C2\C=[N+](\C)C)C3(CC)CC
Name:	Porphyrin-Ruthenium
Method:	Fluorescence Microscopy
References:	372
Structure:	COc1cc(ccc1O)-c1c2ccc(n2)c(-c2cc[n+](cc2)[Ru-5]234(Cl)[n+]5ccccc5-c5cccc[n+]25)c2ccc([nH]2)c(-c2ccc(O)c(OC)c2)c2ccc(n2)c(-c2ccc(O)c(OC)c2)c2ccc1[nH]2.c1cc[n+]3c(c1)-c1cccc[n+]41
Name:	ZnPcBr8
Method:	Fluorescence Microscopy
References:	376
Structure:	BrCc1cc2c3nc4[n+]5c(nc6n7c(nc8[n+]9c(nc(n3[Zn--]579)c2cc1CBr)c1cc(CBr)c(CBr)cc81)c1cc(CBr)c(CBr)cc61)c1cc(CBr)c(CBr)cc41
Name:	ß-Carboline Derivative A
Method:	Fluorescence Microscopy
References:	424
Structure:	CCn1c2ccccc2c2cc(nc(C)c12)C(=O)NCC[NH3+]

Name:	ß-Carboline Derivative B
Method:	Fluorescence Microscopy
References:	424
Structure:	CCCCn1c2ccccc2c2cc(nc(C)c12)C(=O)NCC[NH3+]
Name:	ß-Carboline Derivative C
Method:	Fluorescence Microscopy
References:	424
Structure:	Cc1nc(cc2c3ccccc3n(Cc3ccccc3)c12)C(=O)NCC[NH3+]
Name:	ß-Carboline Derivative D
Method:	Fluorescence Microscopy
References:	424
Structure:	CCn1c2ccccc2c2cc(nc(C)c12)C(=O)NCCCCCCNC(=O)c1cc2c3ccccc3n(CC)c2c(C)n1
Name:	ß-Carboline Derivative E
Method:	Fluorescence Microscopy
References:	424
Structure:	Cc1nc(cc2c3ccccc3n(Cc3ccccc3)c12)C(=O)NCCNC(=O)c1cc2c3ccccc3n(Cc3ccccc3)c2c(C)n1
Name:	Sanguinarine
Method:	Fluorescence Microscopy
References:	437
Structure:	C[n+]1cc2c(OO)c(OO)ccc2c2cc3cc(OCO)c(OCO)cc3c12
Name:	Chelerythrine
Method:	Fluorescence Microscopy
References:	437
Structure:	COc1ccc2c(c[n+](C)c3c4cc(OCO)c(OCO)cc4ccc23)c1OC
Name:	Sanguirubine
Method:	Fluorescence Microscopy
References:	437
Structure:	COc1cc2ccc3c4c(OC)cc(OO)c(OO)c4c[n+](C)c3c2cc1OC
Name:	Chelirubine
Method:	Fluorescence Microscopy
References:	437
Structure:	COc1cc(OO)c(OO)c2c[n+](C)c3c4cc(OCO)c(OCO)cc4ccc3c12
Name:	Macarpine

Method:	Fluorescence Microscopy
References:	437
Structure:	COc1cc2c3c(OC)cc(OO)c(OO)c3c[n+](C)c2c2cc(OCO)c(OCO)cc12
Name:	DB293
Method:	Fluorescence Microscopy
References:	472
Structure:	NC(=[NH2+])c1ccc(cc1)-c1ccc(o1)-c1nc2ccc(cc2[nH]1)C(N)=[NH2+]
Name:	DB60
Method:	Fluorescence Microscopy
References:	472
Structure:	C1C[NH+]=C(N1)c1ccc(cc1)-c1ccc(o1)-c1ccc(cc1)C1=[NH+]CCN1
Name:	DB302
Method:	Fluorescence Microscopy
References:	472
Structure:	C1C[NH+]=C(N1)c1ccc(cc1)-c1ccc(o1)-c1nc2ccc(cc2[nH]1)C1=[NH+]CCN1
Name:	DB501
Method:	Fluorescence Microscopy
References:	472
Structure:	Nc1ccc(cc1)-c1ccc(o1)-c1nc2ccc(cc2[nH]1)C(N)=[NH2+]
Name:	DB182
Method:	Fluorescence Microscopy
References:	472
Structure:	C[NH+](C)CCCNC(=[NH2+])c1ccc(cc1)-c1ccc(o1)-c1ccc(cc1)C(=[NH2+])NCCC[NH+](C)C
Name:	DB340
Method:	Fluorescence Microscopy
References:	472
Structure:	C[NH+](C)CCCNC(=[NH2+])c1ccc(cc1)-c1ccc(o1)-c1nc2ccc(cc2[nH]1)C(=[NH2+])NCCC[NH+](C)C
Name:	Hoechst 33377 (H1)
Method:	Fluorescence Microscopy
References:	475

Structure:	CN1CC[NH+](CC1)C1CCC2[NH+]=C(NC2C1)c1ccc2NC(Nc2c1)c1ccc(Oc2ccccc2)cc1
Name:	Hoechst 33342 (H20)
Method:	Fluorescence Microscopy
References:	475
Structure:	CCOc1ccc(cc1)C1Nc2ccc(cc2N1)C1=[NH+]C2CCC(CC2N1)[NH+]1CCN(C)CC1
Name:	pEB
Method:	Cell Fractionation
References:	477
Structure:	CCCC1C(O)C(C)CCCC2(C)OC2CC(OC(=O)CC(O)C(C)(C)C1=O)C(\C)=C\c1csc(C)n1
Name:	pED
Method:	Cell Fractionation
References:	477
Structure:	CCCC1C(O)C(C)CCC\C(C)=C/CC(OC(=O)CC(O)C(C)(C)C1=O)C(\C)=C\c1csc(C)n1
Name:	BNIPSpd
Method:	Fluorescence Microscopy
References:	479
Structure:	O=C1N(CCC[NH2+]CCCC[NH2+]CCC[NH2+]CCCN2C(=O)c3cccc4cccc(C2=O)c34)C(=O)c2cccc3cccc1c23
Name:	BNIPSpm
Method:	Fluorescence Microscopy
References:	479
Structure:	O=C1N(CCC[NH2+]CCC[NH2+]CCCC[NH2+]CCC[NH2+]CCCN2C(=O)c3cccc4cccc(C2=O)c34)C(=O)c2cccc3cccc1c23
Name:	BNIPOSpm
Method:	Fluorescence Microscopy
References:	479
Structure:	O=C1N(OCCC[NH2+]CCC[NH2+]CCCC[NH2+]CCC[NH2+]CCCON2C(=O)c3cccc4cccc(C2=O)c34)C(=O)c2cccc3cccc1c23
Name:	Pyrrolobenzodiazepine-Poly(N-methylpyrrole) Conjugate 50a
Method:	Fluorescence Microscopy
References:	481

Structure:	COC(=O)c1cc(NC(=O)CCCOc2cc3N=CC4CCCN4C(=O)c3cc2OC)cn1C
Name:	Pyrrolobenzodiazepine-Poly(N-methylpyrrole) Conjugate 50b
Method:	Fluorescence Microscopy
References:	481
Structure:	COC(=O)c1cc(NC(=O)c2cc(NC(=O)CCCOc3cc4N=CC5CCCN5C(=O)c4cc3OC)cn2C)cn1C
Name:	Pyrrolobenzodiazepine-Poly(N-methylpyrrole) Conjugate 50c
Method:	Fluorescence Microscopy
References:	481
Structure:	COC(=O)c1cc(NC(=O)c2cc(NC(=O)c3cc(NC(=O)CCCOc4cc5N=CC6CCCN6C(=O)c5cc4OC)cn3C)cn2C)cn1C
Name:	Polyamide-FITC Conjugate 1
Method:	Fluorescence Microscopy
References:	486
Structure:	C[NH+](CCCNC(=S)Nc1ccc(c(c1)C([O-])=O)C1=C2C=CC(=O)C=C2Oc2cc(O)ccc12)CCCNC(=O)c1cc(NC(=O)c2cc(NC(=O)c3nc(NC(=O)c4cc(NC(=O)C([NH3+])CCNC(=O)c5nc(NC(=O)c6cc(NC(=O)c7cc(NC(=O)c8sccc8Cl)cn7C)cn6C)cn5C)cn4C)cn3C)cn2C)cn1C
Name:	Polyamide-FITC Conjugate 2
Method:	Fluorescence Microscopy
References:	486
Structure:	C[NH+](CCCNC(=S)Nc1ccc(c(

	c1)C([O-])=O)C1=C2C=CC(=O)C=C2Oc2cc(O)ccc12)CCCNC(=O)c1cc(NC(=O)c2cc(NC(=O)c3cc(NC(=O)c4nc(NC(=O)C([NH3+])CCNC(=O)c5nc(NC(=O)c6cc(NC(=O)c7nc(NC(=O)c8nccn8C)cn7C)cn6C)cn5C)cn4C)cn3C)cn2C)cn1C
Name:	TP-2py
Method:	Fluorescence Microscopy
References:	503
Structure:	C[n+]1ccc(\C=C\c2ccc(cc2)N(c2ccccc2)c2ccc(cc2)\C=C\c2cc[n+](C)cc2)cc1
Name:	TP-3py
Method:	Fluorescence Microscopy
References:	503
Structure:	C[n+]1ccc(cc1)\C=C\c1ccc(cc1)N(c1ccc(cc1)\C=C\c1cc[n+](C)cc1)c1ccc(cc1)\C=C\c1cc[n+](C)cc1
Name:	Daunorubicin
Method:	Fluorescence Microscopy
References:	261
Structure:	COc1cccc2C(=O)c3c(O)c4CC(O)(CC(OC5CC([NH3+])C(O)C(C)O5)c4c(O)c3C(=O)c12)C(C)=O
Name:	Levofloxacin
Method:	Cell Fractionation
References:	241
Structure:	C[C@H]1COC2=C3N1C=C(C([O-])=O)C(=O)C3=CC(F)=C2N1CCN(C)CC1

246

Appendix D

The chemical compounds with reported subcellular localization site in the plasma membrane. References information is available in Appendix H. Structure is presented as the Simplified Molecular Input Line Entry Specification string of the major microspecies at pH 7.4, as calculated by ChemAxon.

Name:	D202; 1,6-diphenyl-1,3,5-hexatrieneDPH
Method:	Fluorescence Microscopy
References:	589, 700, 701
Structure:	c1ccc(cc1)\C=C\C=C\C=C\c1ccccc1

Name:	D3921; 4,4-difluoro-1,3,5,7-tetramethyl-4-bora-3a,4a-diaza-s-indacene; BODIPY® 505/515
Method:	Fluorescence Microscopy
References:	590
Structure:	CC1=CC(C)=[N+]2C1=Cc1c(C)cc(C)n1[B-]2(F)F

Name:	D3923; 4-(dicyanovinyl)julolidine; DCVJ
Method:	Fluorescence Microscopy
References:	591
Structure:	N#CC(=Cc1cc2CCCN3CCCc(c1)c23)C#N

Name:	P36005; Cis-parinaric acid
Method:	Fluorescence Microscopy
References:	592, 702
Structure:	CC\C=C\C=C\C=C\C=C/CCCCCCCC([O-])=O

Name:	A47; 1-anilinonaphthalene-8-sulfonic acid1,8-ANS
Method:	Uptake/Binding
References:	662
Structure:	[O-]S(=O)(=O)c1cccc2cccc(Nc3ccccc3)c12

Name:	A50; 2-anilinonaphthalene-6-sulfonic acid; 2,6-ANS
Method:	Uptake/Binding
References:	662
Structure:	[O-]S(=O)(=O)c1ccc2cc(Nc3ccccc3)ccc2c1

Name:	D383; 4,4-difluoro-5,7-dimethyl-4-bora-3a,4a- diaza-s-indacene-3-pentanoic acid; BODIPY® FL C5
Method:	Fluorescence Microscopy
References:	668
Structure:	Cc1cc(C)n2c1C=C1C=CC(CCCCC([O-])=O)=[N+]1[B-]2(F)F

Name:	T53; 2-(p-toluidinyl)naphthalene-6-sulfonic acid, sodium salt; 2,6-TNS
Method:	Fluorescence Microscopy
References:	623
Structure:	Cc1ccc(Nc2ccc3cc(ccc3c2)S([O-])(=O)=O)cc1

Name:	D250; 6-dodecanoyl-2-dimethylaminonaphthalene; Laurdan
Method:	Fluorescence Microscopy
References:	595
Structure:	CCCCCCCCCCCC(=O)c1ccc2cc(ccc2c1)N(C)C

Name:	P31; 1-pyrenedecanoic acid
Method:	NA
References:	Invi
Structure:	[O-]C(=O)CCCCCCCCCc1ccc2ccc3cccc4ccc1c2c34

Name:	N678; 12-(N-(7-nitrobenz-2-oxa-1,3- diazol-4-yl)amino)dodecanoic acid
Method:	NA
References:	Invi
Structure:	[O-]C(=O)CCCCCCCCCCCNc1ccc(c2nonc12)N(=O)=O

Name:	P96;1-pyrenedodecanoic acid

Method:	Fluorescence Microscopy
References:	653
Structure:	[O-]C(=O)CCCCCCCCCCCc1ccc2ccc3cccc4ccc1c2c34
Name:	H22730; 4-heptadecyl-7-hydroxycoumarin
Method:	Fluorescence Microscopy
References:	626
Structure:	CCCCCCCCCCCCCCCCCC1=CC(=O)Oc2cc(O)ccc12
Name:	B3824; 5-butyl-4,4-difluoro-4-bora-3a,4a- diaza-s-indacene-3-nonanoic acid; BODIPY® 500/510 C4, C9
Method:	Fluorescence Microscopy
References:	627, 721
Structure:	CCCCc1ccc2C=C3C=CC(CCCCCCCC([O-])=O)=[N+]3[B-](F)(F)n12
Name:	D3823; 4,4-difluoro-5-methyl-4-bora-3a,4a- diaza-s-indacene-3-dodecanoic acid; BODIPY® 500/510 C1, C12
Method:	Fluorescence Microscopy
References:	628
Structure:	Cc1ccc2C=C3C=CC(CCCCCCCCCCC([O-])=O)=[N+]3[B-](F)(F)n12
Name:	D3825; 4,4-difluoro-5-octyl-4-bora-3a,4a-diaza- s-indacene-3-pentanoic acid; BODIPY® 500/510 C8, C5
Method:	Fluorescence Microscopy
References:	627
Structure:	CCCCCCCCc1ccc2C=C3C=CC(CCCCC([O-])=O)=[N+]3[B-](F)(F)n12
Name:	D3862; 4,4-difluoro-5,7-dimethyl-4-bora-3a,4a- diaza-s-indacene-3-undecanoic acid; BODIPY® FL C11
Method:	Cell Fractionation
References:	605
Structure:	Cc1cc(C)n2c1C=C1C=CC(CCCCCCCCCC([O-])=O)=[N+]1[B-]2(F)F
Name:	B3932; (E,E)-3,5-bis-(4-phenyl-1, 3-butadienyl)-4,4-difluoro-4-
	bora-3a,4a- diaza-s-indacene; BODIPY® 665/676
Method:	NA
References:	Invi
Structure:	F[B-]1(F)n2c(\C=C\C=C\c3ccccc3)cc2C=C2C=CC(/C=C/C=C\c3ccccc3)=[N+]12
Name:	D3835; 4,4-difluoro-5-(2-thienyl)-4-bora-3a,4a- diaza-s-indacene-3-dodecanoic acid; BODIPY® 558/568 C12
Method:	NA
References:	Invi
Structure:	[O-]C(=O)CCCCCCCCCCCC1=[N+]2C(C=C1)=Cc1ccc(-c3cccs3)n1[B-]2(F)F
Name:	D3821; 4,4-difluoro-5,7-dimethyl-4-bora-3a,4a- diaza-s-indacene-3-hexadecanoic acid; BODIPY® FL C16
Method:	Fluorescence Microscopy
References:	604
Structure:	Cc1cc(C)n2c1C=C1C=CC(CCCCCCCCCCCCCC([O-])=O)=[N+]1[B-]2(F)F
Name:	N1148; NBD cholesterol; (22-(N-(7-nitrobenz-2-oxa-1,3-diazol-4-yl)amino)-23,24-bisnor-5- cholen-3beta-ol)
Method:	Fluorescence Microscopy
References:	683
Structure:	CC(CNc1ccc(c2nonc12)N(=O)=O)C1CCC2C3CC=C4CC(O)CC4(C)C3CCC12C
Name:	D3861; 4,4-difluoro-5-(4-phenyl-1,3-butadienyl) -4-bora-3a,4a-diaza-s-indacene-3-undecanoic acid; BODIPY® 581/591 C11
Method:	Fluorescence Microscopy
References:	605
Structure:	[O-]C(=O)CCCCCCCCCCC1=[N+]2C(C=C1)=Cc1ccc(\C=C\C=C\c3ccccc3)n1[B-]2(F)F
Name:	D109; 5-dodecanoylaminofluorescein
Method:	NA

References:	Invi

Structure:	CCCCCCCCCCCC(=O)Nc1ccc(c(c1)C([O-])=O)C1=C2C=CC(=O)C=C2Oc2cc(O)ccc12

Name:	F3857; Fluorescein octadecyl ester
Method:	Uptake/Binding
References:	623
Structure:	CCCCCCCCCCCCCCCCCCOC(=O)c1ccccc1C1=C2C=CC(=O)C=C2Oc2cc(O)ccc12

Name:	H110; 5-hexadecanoylaminofluorescein
Method:	Fluorescence Microscopy
References:	675
Structure:	CCCCCCCCCCCCCCCC(=O)Nc1ccc(c(c1)C([O-])=O)C1=C2C=CC(=O)C=C2Oc2cc(O)ccc12

Name:	D291; 4-(4-(didecylamino)styryl)-N-methylpyridinium iodide; 4-Di-10-ASP
Method:	Fluorescence Microscopy
References:	676
Structure:	CCCCCCCCCCN(CCCCCCCCCC)c1ccc(cc1)\C=C\c1cc[n+](C)cc1

Name:	O246; Octadecyl rhodamine B chloride; R18
Method:	Uptake/Binding
References:	678
Structure:	CCCCCCCCCCCCCCCCCCOC(=O)c1ccccc1C1=C2C=CC(C=C2Oc2cc(ccc12)N(CC)CC)=[N+](CC)CC

Name:	D3805; 2-(4,4-difluoro-5,7-dimethyl-4-bora-3a, 4a-diaza-s-indacene-3-pentanoyl)- 1-hexadecanoyl-sn-glycero-3-phosphate, diammonium salt; Beta-BODIPY® FL C5-HPA
Method:	NA
References:	Invi
Structure:	CCCCCCCCCCCCCCCC(=O)OCC(COP([O-])([O-])=O)OC(=O)CCCCC1=[N+]2C(C=C1)=Cc1c(C)cc(C)n1[B-]2(F)F

Name:	D383; 1,1'-didodecyl-3,3,3',3'-tetramethylindocarbocyanine perchlorate; DilC12(3)
Method:	Fluorescence Microscopy
References:	611
Structure:	CCCCCCCCCCCCN1c2ccccc2C(C)(C)\C1=C\C=C\C1=[N+](CCCCCCCCCCCC)c2ccccc2C1(C)C

Name:	N3786; 2-(6-(7-nitrobenz-2-oxa-1,3-diazol-4-yl) amino)hexanoyl-1-hexadecanoyl-sn- glycero-3-phosphocholine; NBD C6-HPC
Method:	Fluorescence Microscopy
References:	724
Structure:	CCCCCCCCCCCCCCCC(=O)OCC(COP([O-])(=O)OCC[N+](C)(C)C)OC(=O)CCCCCNc1ccc(c2nonc12)N(=O)=O

Name:	D476; 2-(3-(diphenylhexatrienyl)propanoyl)-1- hexadecanoyl-sn-glycero-3-phosphocholine; Beta-DPH HPC
Method:	Fluorescence Microscopy
References:	657
Structure:	CCCCCCCCCCCCCCCC(=O)OCC(COP([O-])(=O)OCC[N+](C)(C)C)OC(=O)CCc1ccc(\C=C/C=C/C=C\c2ccccc2)cc1

Name:	C3927MP; Cholesteryl 4,4-difluoro-5,7-dimethyl-4-bora-3a,4a- diaza-s-indacene-3-dodecanoate; Cholesteryl BODIPY® FL C12
Method:	Fluorescence Microscopy
References:	659
Structure:	CC(C)CCCC(C)C1CCC2C3CC=C4CC(CCC4(C)C3CCC12C)OC(=O)CCCCCCCCCCC1=[N+]2C(C=C1)=Cc1c(C)cc(C)n1[B-]2(F)F

Name:	D3883; 4-Di-16-ASP (4-(4-(dihexadecylamino)styryl)- N-methylpyridinium iodide; DiA
Method:	Fluorescence Microscopy
References:	612

Structure:	CCCCCCCCCCCCCCCCCN(CCCCCCCCCCCCCCCCC)c1ccc(cc1)\C=C\c1cc[n+](C)cc1
Name:	D3803; 2-(4,4-difluoro-5,7-dimethyl-4-bora-3a, 4a-diaza-s-indacene-3-pentanoyl)- 1-hexadecanoyl-sn-glycero-3-phosphocholine; Beta-BODIPY® FL C5-HPC
Method:	Fluorescence Microscopy
References:	660
Structure:	CCCCCCCCCCCCCCCC(=O)OCC(COP([O-])(=O)OCC[N+](C)(C)C)OC(=O)CCCCC1=[N+]2C(C=C1)=Cc1c(C)cc(C)n1[B-]2(F)F
Name:	D11253,3'-dihexadecyloxacarbocyanine perchlorate; DiOC16(3)
Method:	Fluorescence Microscopy
References:	639
Structure:	CCCCCCCCCCCCCCCCCN1\C(Oc2ccccc12)=C/C=C/c1oc2ccccc2[n+]1CCCCCCCCCCCCCCCC
Name:	H361; 1-hexadecanoyl-2-(1-pyrenedecanoyl)- sn-glycero-3-phosphocholine; Beta-py-C10-HPC
Method:	Pharmacological Effect
References:	666
Structure:	CCCCCCCCCCCCCCCC(=O)OCC(COP([O-])(=O)OCC[N+](C)(C)C)OC(=O)CCCCCCCCCc1cc2ccc3cccc4ccc(c1)c2c34
Name:	D3771; 2-decanoyl-1-(O-(11-(4,4- difluoro-5,7-dimethyl-4-bora-3a,4a- diaza-s-indacene-3-propionyl) amino)undecyl)-sn-glycero-3-phosphocholine
Method:	NA
References:	Invi
Structure:	CCCCCCCCCC(=O)OC(COCCCCCCCCCCNC(=O)CCC1=[N+]2C(C=C1)=Cc1c(C)cc(C)n1[B-]2(F)F)COP([O-])(=O)OCC[N+](C)(C)C
Name:	N3787; 2-(12-(7-nitrobenz-2-oxa-1,3-diazol-4-

	yl)amino)dodecanoyl-1-hexadecanoyl- sn-glycero-3-phosphocholine; NBD C12-HPC
Method:	Fluorescence Microscopy
References:	725
Structure:	CCCCCCCCCCCCCCCC(=O)OCC(COP([O-])(=O)OCC[N+](C)(C)C)OC(=O)CCCCCCCCCCCCNc1ccc(c2nonc12)N(=O)=O
Name:	H3809; 1-hexadecanoyl-2-(1-pyrenedecanoyl)-sn-glycero-3-phosphoglycerol, ammonium salt; Beta-py-C10-PG
Method:	NA
References:	Invi
Structure:	CCCCCCCCCCCCCCCC(=O)OCC(COP([O-])(=O)OCC(O)CO)OC(=O)CCCCCCCCCc1cc2ccc3cccc4ccc(c1)c2c34
Name:	D7711; N-(4,4-difluoro-5,7-dimethyl-4- bora-3a,4a-diaza-s-indacene-3-dodecanoyl)sphingosyl phosphocholine ; BODIPY® FL C12-sphingomyelin
Method:	Fluorescence Microscopy
References:	611
Structure:	CCCCCCCCCCCCC\C=C/C(O)C(COP([O-])(=O)OCC[N+](C)(C)C)NC(=O)CCCCCCCCCCCC1=[N+]2C(C=C1)=Cc1c(C)cc(C)n1[B-]2(F)F
Name:	D3898; 3,3'-dilinoleyloxacarbocyanine perchlorate; FAST DiO™ solid; DiODelta9,12- C18(3), ClO4
Method:	NA
References:	Invi
Structure:	CCCCC\C=C\C\C=C\CCCCCCCCN1\C(Oc2ccccc12)=C/C=C/c1oc2ccccc2[n+]1CCCCCCCC\C=C\C\C=C\CCCCC
Name:	D384; 1,1'-dihexadecyl-3,3,3',3'-tetramethylindocarbocyanine perchlorate; DiIC16(3)
Method:	Fluorescence Microscopy

References:	615
Structure:	CCCCCCCCCCCCCCCCCN1c2ccccc2C(C)(C)\C1=C/C=C/C1=[N+](CCCCCCCCCCCCCCCC)c2ccccc2C1(C)C
Name:	D275; 3,3'-dioctadecyloxacarbocyanine perchlorate
Method:	Fluorescence Microscopy
References:	641
Structure:	CCCCCCCCCCCCCCCCCCN1\C(Oc2ccccc12)=C/C=C/c1oc2ccccc2[n+]1CCCCCCCCCCCCCCCCCC
Name:	D3793; 2-(4,4-difluoro-5-methyl-4-bora-3a,4a- diaza-s-indacene-3-dodecanoyl)-1-hexadecanoyl-sn-glycero-3-phosphocholine; Beta-BODIPY® 500/510 C12-HPC
Method:	Fluorescence Microscopy
References:	642
Structure:	CCCCCCCCCCCCCCCC(=O)OCC(COP([O-])(=O)OCC[N+](C)(C)C)OC(=O)CCCCCCCCCCCC1=[N+]2C(C=C1)=Cc1ccc(C)n1[B-]2(F)F
Name:	D3792; 2-(4,4-difluoro-5,7-dimethyl-4-bora-3a, 4a-diaza-s-indacene-3-dodecanoyl) -1-hexadecanoyl-sn-glycero-3-phosphocholine; Beta-BODIPY® FL C12-HPC
Method:	Fluorescence Microscopy
References:	611
Structure:	CCCCCCCCCCCCCCCC(=O)OCC(COP([O-])(=O)OCC[N+](C)(C)C)OC(=O)CCCCCCCCCCCC1=[N+]2C(C=C1)=Cc1c(C)cc(C)n1[B-]2(F)F
Name:	D7758; 4-(4-(dilinoleylamino)styryl)-N-methylpyridinium 4-chlorobenzenesulfonate; FAST DiA™ solid; DiDelta9,12-C18ASP, CBS
Method:	Fluorescence Microscopy
References:	616
Structure:	CCCCC\C=C\C\C=C\CCCCCCCCN(CCCCCCCC\C=C\C\C=C/CCCCC)c1ccc(cc1)\C=C\c1cc[n+](C)cc1
Name:	D3815; 2-(4,4-difluoro-5,7-diphenyl-4-bora-3a, 4a-diaza-s-indacene-3-pentanoyl)- 1-hexadecanoyl-sn-glycero-3-phosphocholine; Beta-BODIPY® 530/550 C5-HPC
Method:	Fluorescence Microscopy
References:	642
Structure:	CCCCCCCCCCCCCCCC(=O)OCC(COP([O-])(=O)OCC[N+](C)(C)C)OC(=O)CCCCC1=[N+]2C(C=C1)=Cc1c(cc(-c3ccccc3)n1[B-]2(F)F)-c1ccccc1
Name:	D3886; 1,1'-dioleyl-3,3,3',3'-tetramethylindocarbocyanine methanesulfonate; Delta9-DiI
Method:	NA
References:	Invi
Structure:	CCCCCCCC\C=C\CCCCCCCCN1c2ccccc2C(C)(C)\C1=C\C=C/C1=[N+](CCCCCCCC\C=C\CCCCCCCC)c2ccccc2C1(C)C
Name:	D3899; 1,1'-dilinoleyl-3,3,3',3'-tetramethylindocarbocyanine perchlorate; FAST DiI™ oil; DiIDelta9,12- C18(3), ClO4
Method:	Fluorescence Microscopy
References:	611
Structure:	CCCCC\C=C\C\C=C\CCCCCCCCN1c2ccccc2C(C)(C)\C1=C\C=C/C1=[N+](CCCCCCCC\C=C\C\C=C\CCCCC)c2ccccc2C1(C)C
Name:	D282; 1,1'-dioctadecyl-3,3,3',3'-tetramethylindocarbocyanine perchlorate; DiI'; DiIC18(3)
Method:	Fluorescence Microscopy
References:	641, 645
Structure:	CCCCCCCCCCCCCCCCCCN1c2ccccc2C(C)(C)\C1=C/C=C/C1=[N+](CCCCCCCCCCCCCCCCCC)c2ccccc2C1(C)C
Name:	M12652; Marina Blue® 1,2-dihexadecanoyl-sn-glycero-3-phosphoethanolamine; Marina Blue® DHPE
Method:	NA

References:	Invi
Structure:	CCCCCCCCCCCCCCCC(=O)OCC(COP([O-])(=O)OCCNC(=O)CC1=C(C)c2cc(F)c([O-])c(F)c2OC1=O)OC(=O)CCCCCCCCCCCC
Name:	N360; N-(7-nitrobenz-2-oxa-1,3-diazol- 4-yl)-1,2- dihexadecanoyl-sn- glycero-3-phosphoethanolamine, triethylammonium salt; NBD-PE
Method:	Fluorescence Microscopy
References:	8, 617
Structure:	CCCCCCCCCCCCCCC(=O)OCC(COP([O-])(=O)OCCNc1ccc(c2nonc12)N(=O)=O)OC(=O)CCCCCCCCCCCCCC
Name:	D307; 1,1'-dioctadecyl-3,3,3',3'-tetramethylindodicarbocyanine perchlorate; DiD' oil; DiIC18(5) oil
Method:	Fluorescence Microscopy
References:	685
Structure:	CCCCCCCCCCCCCCCCCCN1c2ccccc2C(C)(C)\C1=C\C=C\C=C\C1=[N+](CCCCCCCCCCCCCCCCCC)c2ccccc2C1(C)C
Name:	P22652; Pacific Blue™ 1,2-ditetradecanoyl-sn-glycero-3-phosphoethanolamine, triethylammonium salt; Pacific Blue™ DMPE
Method:	NA
References:	Invi
Structure:	CCCCCCCCCCCCCC(=O)OCC(COP([O-])(=O)OCCNC(=O)C1=Cc2cc(F)c([O-])c(F)c2OC1=O)OC(=O)CCCCCCCCCCCC
Name:	D7776; 1,1'-dioctadecyl-3,3,3',3'-tetramethylindocarbocyanine-5,5'- disulfonic acid; DiIC18(3)-DS
Method:	NA
References:	Invi
Structure:	CCCCCCCCCCCCCCCCCCN 1c2ccc(cc2C(C)(C)\C1=C/C=C/C1=[N+](CCCCCCCCCCCCCC CCCCC)c2ccc(cc2C1(C)C)S([O-])(=O)=O)S([O-])(=O)=O
Name:	D6562; 1,2-dioleoyl-3-(1-pyrenedodecanoyl)- rac-glycerol
Method:	NA
References:	Invi
Structure:	CCCCCCCC\C=C\CCCCCCCC(=O)OCC(COC(=O)CCCCCC CCCCCc1ccc2ccc3cccc4ccc1c2c34)OC(=O)CCCCCCCC\C=C/CCCCCCCC
Name:	D12731; 1,1'-dioctadecyl-3,3,3',3'-tetramethylindotricarbocyanine iodid; DiR; DiIC18(7)
Method:	Fluorescence Microscopy
References:	664
Structure:	CCCCCCCCCCCCCCCCCCN1c2ccccc2C(C)(C)\C1=C\C=C/C=C/C=C\C1=[N+](CCCCCCCCCCCCCCCCCC)c2ccccc2C1(C)C
Name:	B1550; N-(biotinoyl)-1,2-dihexadecanoyl-sn-glycero-3-phosphoethanolamine, triethylammonium salt; Biotin DHPE
Method:	NA
References:	Invi
Structure:	CCCCCCCCCCCCCCCC(=O)OCC(COP([O-])(=O)OCCNC(=O)CCCCC1SCC2NC(=O)NC12)OC(=O)CCCCCCCCCCCCCC
Name:	D57; N-(5-dimethylaminonaphthalene-1-sulfonyl)-1,2-dihexadecanoyl-sn- glycero-3-phosphoethanolamine, triethylammonium salt; Dansyl DHPE
Method:	NA
References:	Invi
Structure:	CCCCCCCCCCCCCCCC(=O)OCC(COP([O-])(=O)OCCNS(=O)(=O)c1cccc2c(cccc12)N(C)C)OC(=O)CCCCCCCCCCCCCC

Name:	B7701; 1,2-bis-(4,4-difluoro-5,7-dimethyl-4- bora-3a,4a-diaza-s-indacene-3-undecanoyl)-sn-glycero-3-phosphocholine; Bis-BODIPY® FL C11-PC
Method:	Fluorescence Microscopy
References:	648
Structure:	Cc1cc(C)n2c1C=C1C=CC(CCCCCCCCCC(=O)OCC(COP([O-])(=O)OCC[N+](C)(C)C)OC(=O)CCCCCCCCCC3=[N+]4C(C=C3)=Cc3c(C)cc(C)n3[B-]4(F)F)=[N+]1[B-]2(F)F
Name:	C7000; CellTracker™ CM-DiI
Method:	Fluorescence Microscopy
References:	618
Structure:	CCCCCCCCCCCCCCCCCCN1c2ccccc2C(C)(C)\C1=C\C=C\C1=[N+](CCCCCCCCCCCCCCCCCC)c2ccc(CNC(=O)c3ccc(CCl)cc3)cc2C1(C)C
Name:	O12650; Oregon Green® 488 1,2-dihexadecanoyl-sn-glycero-3- phosphoethanolamine; Oregon Green® 488 DHPE
Method:	NA
References:	Invi
Structure:	CCCCCCCCCCCCCCCC(=O)OCC(COP([O-])(=O)OCCNC(=O)c1ccc(c(c1)C([O-])=O)C1=C2C=C(F)C(=O)C=C2Oc2cc(O)c(F)cc12)OC(=O)CCCCCCCCCCCCCCC
Name:	D7778; 3,3'-dioctadecyl-5,5'-di(4-sulfophenyl) oxacarbocyanine, sodium salt; SP-DiOC18(3)
Method:	Fluorescence Microscopy
References:	727
Structure:	CCCCCCCCCCCCCCCCCCN1\C(Oc2ccc(cc12)-c1ccc(cc1)S([O-])(=O)=O)=C/C=C/c1oc2ccc(cc2[n+]1CCCCCCCCCCCCCCCCCC)-c1ccc(cc1)S([O-])(=O)=O
Name:	B1616; N-((6-

	(biotinoyl)amino)hexanoyl)-1,2-dihexadecanoyl-sn-glycero-3-phosphoethanolamine, triethylammonium salt; Biotin-X DHPE
Method:	NA
References:	Invi
Structure:	CCCCCCCCCCCCCCCC(=O)OCC(COP([O-])(=O)OCCNC(=O)CCCCCNC(=O)CCCCC1SCC2NC(=O)NC12)OC(=O)CCCCCCCCCCCCCCC
Name:	D7777; 1,1'-dioctadecyl-6,6'-di(4-sulfophenyl)- 3,3,3',3'-tetramethylindocarbocyanine; SP-DiIC18(3)
Method:	Fluorescence Microscopy
References:	649
Structure:	CCCCCCCCCCCCCCCCCCN1c2cc(ccc2C(C)(C)\C1=C\C=C\C1=[N+](CCCCCCCCCCCCCCCCCC)c2cc(ccc2C1(C)C)-c1ccc(cc1)S([O-])(=O)=O)-c1ccc(cc1)S([O-])(=O)=O
Name:	F362; N-(fluorescein-5-thiocarbamoyl)- 1,2-dihexadecanoyl-sn-glycero-3-phosphoethanolamine, triethylammonium salt; Fluorescein DHPE
Method:	NA
References:	Invi
Structure:	CCCCCCCCCCCCCCCC(=O)OCC(COP([O-])(=O)OCCNC(=S)Nc1ccc(c(c1)C([O-])=O)C1=C2C=CC(=O)C=C2Oc2cc(O)ccc12)OC(=O)CCCCCCCCCCCCCCC
Name:	T1391; N-(6-tetramethylrhodaminethiocarbamoyl)-1,2- dihexadecanoyl-sn-glycero-3-phosphoethanolamine, triethylammonium salt; TRITC DHPE
Method:	Fluorescence Microscopy
References:	679
Structure:	CCCCCCCCCCCCCCCC(=O)OCC(COP([O-])(=O)OCCNC(=S)Nc1ccc(C([O

	-])=O)c(c1)C1=C2C=C/C(/C=C2 Oc2cc(ccc12)N(C)C)=[N+](\C) C)OC(=O)CCCCCCCCCCCCC CC

Name:	Hostalux SN
Method:	Fluorescence Microscopy
References:	55
Structure:	CC(C)COCCS(=O)(=O)c1ccc(c1)N1CCC(=N1)c1ccc(Cl)cc1

Name:	Uvitex EBF
Method:	Fluorescence Microscopy
References:	55
Structure:	c1ccc2oc(nc2c1)-c1csc(c1)-c1nc2ccccc2o1

Name:	Blancophor DCR
Method:	Fluorescence Microscopy
References:	55
Structure:	CS(=O)(=O)c1ccc(cc1)N1CCC(=N1)c1ccc(Cl)cc1

Name:	MPPT
Method:	Fluorescence Microscopy
References:	55
Structure:	Cn1c(nc2ccccc12)-c1ccc(s1)C1=NN(CC1)c1ccccc1

Name:	3-Cyanoperylene
Method:	Fluorescence Microscopy
References:	55
Structure:	N#Cc1ccc2c3cccc4cccc(c5cccc1c25)c34

Name:	ZnPcS3C6
Method:	Fluorescence Microscopy
References:	88
Structure:	CCCCC#Cc1ccc2c3nc4nc(nc5n6[Zn]n3c(nc3nc(nc6c6ccc(cc56)S([O-])(=O)=O)c5cc(ccc35)S([O-])(=O)=O)c2c1)c1ccc(cc41)S([O-])(=O)=O

Name:	ZnPcS3C9
Method:	Fluorescence Microscopy
References:	88
Structure:	CCCCCCCC#Cc1ccc2c3nc4nc(nc5n6[Zn]n3c(nc3nc(nc6c6ccc(cc56)S([O-])(=O)=O)c5cc(ccc35)S([O-])(=O)=O)c2c1)c1ccc(cc41)S([

	O-])(=O)=O

Name:	Rhodac
Method:	Fluorescence Microscopy
References:	102
Structure:	CCOC(=C\C=C1\SC(\C=C2\SC(c3ccccc3)=C(N2CC)c2ccccc2)=[N+](CC)C1=O)\C=C1\Sc2ccc(C)cc2N1CC

Name:	3-THPP; tetra(3-hydroxyphenyl)porphine
Method:	Fluorescence Microscopy
References:	111
Structure:	Oc1cccc(c1)-c1c2ccc(n2)c(-c2cccc(O)c2)c2ccc([nH]2)c(-c2cccc(O)c2)c2ccc(n2)c(-c2cccc(O)c2)c2ccc1[nH]2

Name:	Cytochalasin D
Method:	Cell Fractionation
References:	143
Structure:	CC1C\C=C\C2C(O)C(=C)C(C)C3C(Cc4ccccc4)NC(=O)C23C(OC(C)=O)\C=C\C(C)(O)C1=O

Name:	HBDP-R1; 2,-(N,N-dimethylamino)-propylamine-HB
Method:	Fluorescence Microscopy
References:	186
Structure:	COC1=CC(=O)c2c(NCCC[NH+](C)C)c(OC)c3CC(C)=C(C(C)=O)c4c(OC)c(NCCC[NH+](C)C)c5C(=O)C=C(OC)c6c1c2c3c4c56

Name:	CIBC Derivative 2
Method:	Fluorescence Microscopy
References:	227
Structure:	CCC1C(C)c2cc3[nH]c(cc4nc(C(CCC([O-])=O)C4C)c4C(=O)N(OC)C(=O)c5c(C)c(cc1n2)[nH]c45)c(C)c3C(C)O

Name:	CICD Derivative 5; 13,15-N-cycloimide Derivatives of Chlorin p10
Method:	Fluorescence Microscopy
References:	86
Structure:	CCc1c(C)c2cc3[nH]c(cc4nc(C(CCC(=O)OC)C4C)c4C(=O)N(OC)C(=O)c5c(C)c(cc1n2)[nH]c45)c(C)c3C=C

Name:	di-4-ANEPPDHQ
Method:	Fluorescence Microscopy
References:	291
Structure:	CCCCN(CCCC)c1ccc2cc(CCc3cc[n+](CC(O)C[N+](C)(C)CCO)cc3)ccc2c1

Name:	Evans Blue
Method:	Fluorescence Microscopy
References:	294
Structure:	Cc1cc(ccc1N\N=C1/C=Cc2c(cc(c(N)c2C1=O)S([O-])(=O)=O)S([O-])(=O)=O)-c1ccc(N\N=C2/C=Cc3c(cc(c(N)c3C2=O)S([O-])(=O)=O)S([O-])(=O)=O)c(C)c1

Name:	SnNT2H2 (Cl2)
Method:	Fluorescence Microscopy
References:	332
Structure:	CCCOC(=O)C1Cc2c3[n+]4c(cc5c(CC)c(CC)c6cc7c(CC)c(CC)c8cc9c(CC)c(CC)c2n9[Sn]4(n56)[n+]78)C(CC)C13CC

Name:	EBCS
Method:	Fluorescence Microscopy
References:	332
Structure:	CCc1c(C)c2cc3[nH]c(c(C)c3CC)c3cccc4c3nc(cc3[nH]c(cc1n2)c(C)c3CC)C4(C)CC

Name:	SnEBCS
Method:	Fluorescence Microscopy
References:	332
Structure:	CCc1c(C)c2cc3c(CC)c(C)c4cc5c(CC)c(C)c6n5[Sn]5(n2c1cc1[n+]5c2c(cc(cc62)S([O-])(=O)=O)C1(C)CC)[n+]34

Name:	JPW-3028; Di-1-ANEPEQ
Method:	Fluorescence Microscopy
References:	383
Structure:	CN(C)c1ccc2cc(ccc2c1)\C=C\c1cc[n+](CC[N+](C)(C)C)cc1

Name:	JPW-3080; Di-1-APEFEQPQ
Method:	Fluorescence Microscopy
References:	383
Structure:	CN(C)c1ccc(\C=C\c2ccc(\C=C\c3cc[n+](CCC[N+](C)(C)C)c4ccccc34)o2)cc1

Name:	JPW-600; Di-4-ANBDQPQ

Method:	Fluorescence Microscopy
References:	383
Structure:	CCCCN(CCCC)c1ccc2cc(\C=C\C=C\c3cc[n+](CCC[N+](C)(C)C)c4ccccc34)ccc2c1

Name:	JPW-4090; Di-2-ANBDQPQ
Method:	Fluorescence Microscopy
References:	383
Structure:	CCN(CC)c1ccc2cc(\C=C\C=C\c3cc[n+](CCC[N+](C)(C)C)c4ccccc34)ccc2c1

Name:	PY-1261; Di-2-BTEPPTEA
Method:	Fluorescence Microscopy
References:	383
Structure:	CCN(CC)c1ccc(s1)-c1ccc(\C=C\c2cc[n+](CCC[N+](CC)(CC)CC)cc2)s1

Name:	PY-1268; Di-2-TTEPPTEA
Method:	Fluorescence Microscopy
References:	383
Structure:	CCN(CC)c1ccc(s1)-c1ccc(s1)-c1ccc(\C=C\c2cc[n+](CCC[N+](CC)(CC)CC)cc2)s1

Name:	PY-1286; Di-3-BTEPPTEA
Method:	Fluorescence Microscopy
References:	383
Structure:	CCCN(CCC)c1ccc(s1)-c1ccc(\C=C\c2cc[n+](CCC[N+](CC)(CC)CC)cc2)s1

Name:	PY-1266; Di-4-BTEPPTEA
Method:	Fluorescence Microscopy
References:	383
Structure:	CCCCN(CCCC)c1ccc(s1)-c1ccc(\C=C\c2cc[n+](CCC[N+](CC)(CC)CC)cc2)s1

Name:	JPW-3067
Method:	Fluorescence Microscopy
References:	384
Structure:	CN(C)c1ccc(\C=C\c2ccc(\C=C\C3=[N+](CCC[N+](C)(C)C)c4ccccc4C3(C)C)s2)cc1

Name:	JPW-5034
Method:	Fluorescence Microscopy
References:	384
Structure:	CCCCN(CCCC)c1ccc(\C=C\c2ccc(\C=C\C3=[N+](CCC[N+](C)(C)C)c4ccccc4C3(C)C)s2)cc1

Name:	JPW-5020
Method:	Fluorescence Microscopy
References:	384
Structure:	CCCCCCCCN(CCCCCCCC)c1ccc(\C=C\c2ccc(\C=C\C3=[N+](CCC[N+](C)(C)C)c4ccccc4C3(C)C)s2)cc1
Name:	di-4-ANEPPS
Method:	Fluorescence Microscopy
References:	384
Structure:	CCCCN(CCCC)c1ccc2cc(ccc2c1)\C=C\c1cc[n+](CCCS([O-])(=O)=O)cc1
Name:	JPW-3012
Method:	Fluorescence Microscopy
References:	385
Structure:	C[N+](C)(C)CCC[n+]1ccc(\C=C\c2cc3CCCN4CCCc(c2)c34)c2ccccc12
Name:	KDH-160
Method:	Fluorescence Microscopy
References:	385
Structure:	CCN1CCCc2ccc(\C=C\c3cc[n+](CCCS([O-])(=O)=O)c4ccccc34)cc12
Name:	JPW-3066
Method:	Fluorescence Microscopy
References:	385
Structure:	CN(C)c1ccc(\C=C\c2ccc(\C=C\c3cc[n+](CCC[N+](C)(C)C)c4ccccc34)s2)cc1
Name:	JPW-4012
Method:	Fluorescence Microscopy
References:	385
Structure:	CCCCN(CCCC)c1ccc(\C=C\c2ccc(\C=C\c3cc[n+](CCC[N+](C)(C)C)c4ccccc34)o2)cc1
Name:	JPW-4023
Method:	Fluorescence Microscopy
References:	385
Structure:	CCN(CC)c1ccc(\C=C\c2ccc(\C=C\c3cc[n+](CCC[N+](C)(C)C)c4ccccc34)o2)cc1
Name:	RE-66
Method:	Fluorescence Microscopy
References:	385
Structure:	CCCCN(CCCC)c1ccc(cc1)\C=C\c1c2ccccc2[n+](CCCCS([O-

	])(=O)=O)c2ccccc12
Name:	RE-136
Method:	Fluorescence Microscopy
References:	385
Structure:	CCCCN(CCCC)c1ccc(cc1)\C=C\C=C\c1c2ccccc2[n+](CCCS([O-])(=O)=O)c2ccccc12
Name:	RK-57
Method:	Fluorescence Microscopy
References:	385
Structure:	CCCCOC1CN2CC(Cc3cc(\C=C\c4c5ccccc5[n+](CCCS([O-])(=O)=O)c5ccccc45)cc(C1)c23)OCCCC
Name:	JPW-5019
Method:	Fluorescence Microscopy
References:	385
Structure:	CCCCCCCCN(CCCCCCCC)c1ccc(\C=C\c2ccc(\C=C\c3cc[n+](CCC[N+](C)(C)C)c4ccccc34)s2)cc1
Name:	JPW-5021
Method:	Fluorescence Microscopy
References:	385
Structure:	CCCCCCCCN(CCCCCCCC)c1ccc(\C=C\c2ccc(\C=C\c3cc[n+](CCC[N+](C)(C)C)c4ccccc34)o2)cc1
Name:	JPW-5026
Method:	Fluorescence Microscopy
References:	385
Structure:	CCCCCCCCCCCCN(CCCCCCCCCCC)c1ccc(\C=C\c2ccc(\C=C\c3cc[n+](CCC[N+](C)(C)C)c4ccccc34)s2)cc1
Name:	JPW-5028
Method:	Fluorescence Microscopy
References:	385
Structure:	CCCCCCCCCCCCN(CCCCCCCCCCC)c1ccc(\C=C\c2ccc(\C=C\c3cc[n+](CCC[N+](C)(C)C)c4ccccc34)o2)cc1
Name:	DB1-195
Method:	Fluorescence Microscopy
References:	385
Structure:	CCCCN(CCCC)c1ccc(cc1)\C=C\c1c2ccccc2[n+](CCCS([O-])(=O)=O)c2ccccc12

Name:	JPW-5031
Method:	Fluorescence Microscopy
References:	385
Structure:	CCN(CC)c1ccc2cc(\C=C\C=C\C3=[N+](CCC[N+](C)(C)C)c4ccccc4C3(C)C)ccc2c1
Name:	DB2-039
Method:	Fluorescence Microscopy
References:	385
Structure:	CCCCCC1C(CCCC)Cc2cc(\C=C\c3cc[n+](CCC[N+](C)(C)C)c4ccccc34)cc3CCCN1c23
Name:	JPW1114
Method:	Fluorescence Microscopy
References:	411
Structure:	CCN(CC)c1ccc2cc(ccc2c1)\C=C\c1cc[n+](CC[N+](C)(C)C)cc1
Name:	RH795
Method:	Fluorescence Microscopy
References:	413
Structure:	CCCCN(CCCC)c1ccc(CCCCc2cc[n+](CC(O)CC(C)(C)CCO)c2)cc1
Name:	JPW3039
Method:	Fluorescence Microscopy
References:	413
Structure:	CCN(CC)c1ccc2cc(ccc2c1)\C=C\c1cc[n+](CC(O)CC(C)(C)CCO)cc1
Name:	JPW2081
Method:	Fluorescence Microscopy
References:	413
Structure:	CCCCN(CCCC)c1ccc2cc(ccc2c1)\C=C\c1cc[n+](CC(O)CC(C)(C)CCO)cc1
Name:	JPW3031
Method:	Fluorescence Microscopy
References:	413
Structure:	CCCCCCN(CCCCCC)c1ccc2cc(\C=C\c3cc[n+](CC(O)CC(C)(C)CCO)cc3)ccc2c1
Name:	JPW5037; di-8-ANEPPS
Method:	Fluorescence Microscopy
References:	412, 413
Structure:	CCCCCCCCN(CCCCCCCC)c1ccc2cc(\C=C\c3cc[n+](CCCS([O-])(=O)=O)cc3)ccc2c1

Name:	ANNINE-6plus
Method:	Fluorescence Microscopy
References:	414
Structure:	CCCCN(CCCC)c1ccc2c(ccc3c2ccc2c4ccc5c[n+](CCC[N+](C)(C)C)ccc5c4ccc32)c1
Name:	RH160
Method:	Fluorescence Microscopy
References:	415
Structure:	CCCCN(CCCC)c1ccc(cc1)\C=C\C=C\c1cc[n+](CCCCS([O-])(=O)=O)cc1
Name:	di-4-ANEPBS
Method:	Fluorescence Microscopy
References:	415
Structure:	CCCCN(CCCC)c1ccc2cc(ccc2c1)\C=C\c1cc[n+](CCCCS([O-])(=O)=O)cc1
Name:	BNBIQ
Method:	Fluorescence Microscopy
References:	415
Structure:	CCCCN(CCCC)c1ccc2cc(ccc2c1)-c1ccc2c[n+](CCCCS([O-])(=O)=O)ccc2c1
Name:	ANNINE-5
Method:	Fluorescence Microscopy
References:	415
Structure:	CCCCN(CCCC)c1ccc2c(ccc3c2ccc2c4cc[n+](CCCCS([O-])(=O)=O)cc4ccc32)c1
Name:	ANNINE-6
Method:	Fluorescence Microscopy
References:	415
Structure:	CCCCN(CCCC)c1ccc2c(ccc3c2ccc2c4ccc5c[n+](CCCCS([O-])(=O)=O)ccc5c4ccc32)c1
Name:	WW375
Method:	Fluorescence Microscopy
References:	417
Structure:	CCN1C(=S)S\C(=C/C=C\C=C2/C=CN(CCCS([O-])(=O)=O)c3ccccc23)C1=O
Name:	RH155
Method:	Fluorescence Microscopy
References:	417
Structure:	CC1=NN(c2ccc(cc2)S([O-])(=O)=O)C(=O)C\1=C\C=C(\C

	=C\c1c(C)nn(-c2ccc(cc2)S([O-])(=O)=O)c1O)c1ccccc1

Name:	WW781
Method:	Fluorescence Microscopy
References:	417
Structure:	CCCCN1C(=O)N(CCCC)C(O)=C(\C=C\C=C\C=C2\C(C)=NN(C2=O)c2ccc(cc2)S([O-])(=O)=O)C1=O

Name:	C4A-FL
Method:	Fluorescence Microscopy
References:	448
Structure:	[O-]C(=O)CCCc1ccc-2c(Cc3ccccc-23)c1

Name:	C4A-FL-C4
Method:	Fluorescence Microscopy
References:	448
Structure:	CCCCc1ccc-2c(Cc3cc(CCCC([O-])=O)ccc-23)c1

Name:	C8A-FL
Method:	Fluorescence Microscopy
References:	448
Structure:	[O-]C(=O)CCCCCCCc1ccc-2c(Cc3ccccc-23)c1

Name:	C8A-FL-C4
Method:	Fluorescence Microscopy
References:	448
Structure:	CCCCc1ccc-2c(Cc3cc(CCCCCCCC([O-])=O)ccc-23)c1

Name:	C6A-FL
Method:	Fluorescence Microscopy
References:	448
Structure:	[O-]C(=O)CCCCCc1ccc-2c(Cc3ccccc-23)c1

Name:	C6A-FL-C2
Method:	Fluorescence Microscopy
References:	448
Structure:	CCc1ccc-2c(Cc3cc(CCCCCC([O-])=O)ccc-23)c1

Name:	C6A-FL-C4
Method:	Fluorescence Microscopy
References:	448
Structure:	CCCCc1ccc-2c(Cc3cc(CCCCCC([O-]

	])=O)ccc-23)c1

Name:	C6A-FL-C6
Method:	Fluorescence Microscopy
References:	448
Structure:	CCCCCCc1ccc-2c(Cc3cc(CCCCCC([O-])=O)ccc-23)c1

Name:	C6ABz PC
Method:	Fluorescence Microscopy
References:	448
Structure:	CCCCCCCCCCCCC(=O)OCC(COP([O-])(=O)OCC[N+](C)(C)C)OC(=O)CCCCCc1ccc(cc1)C(=O)c1ccccc1

Name:	C6ABzC6
Method:	Fluorescence Microscopy
References:	448
Structure:	CCCCCCCCCCCCC(=O)OCC(COP([O-])(=O)OCC[N+](C)(C)C)OC(=O)CCCCCc1ccc(cc1)C(=O)c1ccc(CCCCCC)cc1

Name:	C8ABz PC
Method:	Fluorescence Microscopy
References:	448
Structure:	CCCCCCCCCCCCC(=O)OCC(COP([O-])(=O)OCC[N+](C)(C)C)OC(=O)CCCCCCCc1ccc(cc1)C(=O)c1ccccc1

Name:	C8ABzC4 PC
Method:	Fluorescence Microscopy
References:	448
Structure:	CCCCCCCCCCCCC(=O)OCC(COP([O-])(=O)OCC[N+](C)(C)C)OC(=O)CCCCCCCc1ccc(cc1)C(=O)c1ccc(CCCC)cc1

Name:	1-Pyrene Butyric Acid; PBA
Method:	Fluorescence Microscopy
References:	456
Structure:	[O-]C(=O)CCCC1=CCC2=C3C4C(C=C2)=CC=CC4=CC=C13

Name:	Lepidine Dye
Method:	Fluorescence Microscopy
References:	462

Structure:	CCCCN(CCCC)c1ccc(\C=C\c2ccc(\C=C\c3cc[n+](CCCCS([O-])(=O)=O)c4ccccc34)s2)cc1

Name:	Indolenine Dye
Method:	Fluorescence Microscopy
References:	462
Structure:	CCCCN(CCCC)c1ccc(\C=C\c2ccc(\C=C\C3=[N+](CCCCS([O-])(=O)=O)c4ccccc4C3(C)C)s2)cc1

Name:	Benzthiazole Dye
Method:	Fluorescence Microscopy
References:	462
Structure:	CCCCN(CCCC)c1ccc(\C=C\c2ccc(\C=C\c3sc4ccccc4[n+]3CCCCS([O-])(=O)=O)s2)cc1

Name:	Sulfindolenine Dye
Method:	Fluorescence Microscopy
References:	462
Structure:	CCCCN(CCCC)c1ccc(\C=C\c2ccc(\C=C\C3=[N+](CCCCS([O-])(=O)=O)c4ccc(cc4C3(C)C)S([O-])(=O)=O)s2)cc1

Name:	Benzoxazole Dye
Method:	Fluorescence Microscopy
References:	462
Structure:	CCCCN(CCCC)c1ccc(\C=C\c2ccc(\C=C\c3oc4ccccc4[n+]3CCCCS([O-])(=O)=O)s2)cc1

Name:	Sulfoindolenme Dye
Method:	Fluorescence Microscopy
References:	462
Structure:	CCCCN(CCCC)c1ccc(\C=C\c2ccc(\C=C\C3=[N+](CC)c4cc(CS([O-])(=O)=O)ccc4C3(C)C)s2)cc1

Name:	Methoxyquinaldine Dye
Method:	Fluorescence Microscopy
References:	462
Structure:	CCCCN(CCCC)c1ccc(\C=C\c2ccc(C=Cc3ccc4cc(OC)ccc4[n+]3CCCCS([O-])(=O)=O)s2)cc1

Name:	Methoxylepidine Dye
Method:	Fluorescence Microscopy
References:	462
Structure:	CCCCN(CCCC)c1ccc(\C=C\c2ccc(\C=C\c3cc[n+](CCCCS([O-])(=O)=O)c4ccc(OC)cc34)s2)cc

	1

Name:	Amethyst Violet
Method:	Fluorescence Microscopy
References:	463
Structure:	CCN(CC)c1ccc2nc3ccc(cc3[n+](-c3ccccc3)c2c1)N(CC)CC

Name:	DiOC1(3)
Method:	Fluorescence Microscopy
References:	463
Structure:	CN1\C(Oc2ccccc12)=C/C=C/c1oc2ccccc2[n+]1C

Name:	RH355
Method:	Fluorescence Microscopy
References:	464
Structure:	CN(C)c1ccc(cc1)\C=C\C=C\c1cc[n+](CCC[N+](C)(C)C)cc1

Name:	RH461
Method:	Fluorescence Microscopy
References:	464
Structure:	CCN(CC)c1ccc(cc1)\C=C\C=C\c1cc[n+](CCC[N+](C)(C)C)cc1

Name:	RH437
Method:	Fluorescence Microscopy
References:	464
Structure:	CCCN(CCC)c1ccc(cc1)\C=C\C=C\c1cc[n+](CCC[N+](C)(C)C)cc1

Name:	JPW1234
Method:	Fluorescence Microscopy
References:	465
Structure:	CCCCN(CCCC)c1ccc2cc(ccc2c1)\C=C\c1cc[n+](CC(C)CO)cc1

Name:	JPW1259
Method:	Fluorescence Microscopy
References:	465
Structure:	CCCCN(CCCC)c1ccc2cc(\C=C\c3cc[n+](CC4OC(OC)C(O)C4O)cc3)ccc2c1

Name:	JPW1290
Method:	Fluorescence Microscopy
References:	465
Structure:	CCN(CC)c1ccc2cc(ccc2c1)\C=C\c1cc[n+](CC(C)CO)cc1

Name:	F8N1S

Method:	Fluorescence Microscopy
References:	466
Structure:	CCCCCCCCN(CCCCCCCC)c1ccc(cc1)C1=C([O-])C(=O)c2cc(C[N+](C)(C)CCCS([O-])(=O)=O)ccc2O1

Name:	PPZ8
Method:	Fluorescence Microscopy
References:	466
Structure:	CCCCCCCCCOc1ccc2OC(=C([O-])C(=O)c2c1)c1ccc(cc1)N1CCN(CC1)c1cc[n+](CCCS([O-])(=O)=O)cc1

Name:	RH237
Method:	Fluorescence Microscopy
References:	492
Structure:	CCCCN(CCCC)c1ccc(cc1)\C=C\C=C\C=C\c1cc[n+](CCCCS([O-])(=O)=O)cc1

Name:	O^6-Benzylguanine-Pennsylvania Green
Method:	Fluorescence Microscopy

References:	495
Structure:	Cc1cc(ccc1C1=C2C=C(F)C(=O)C=C2Oc2cc(O)c(F)cc12)C(=O)NCc1ccc(COc2nc(N)nc3[nH]cnc23)cc1

Name:	Pennsylvania Green Fluorophore Derivative 22
Method:	Fluorescence Microscopy
References:	498
Structure:	CC(C)CCCC(C)C1CCC2C3CC=C4CC(CCC4(C)C3CCC12C)[NH2+]CCCNC(=O)CCNC(=O)CCNC(=O)c1ccc(c(C)c1)C1=C2C=C(F)C(=O)C=C2Oc2cc(O)c(F)cc12

Name:	::Pennsylvania Green Fluorophore Derivative 23::::::
Method:	Fluorescence Microscopy
References:	498
Structure:	CC(C)CCCC(C)C1CCC2C3CC=C4CC(CCC4(C)C3CCC12C)[NH2+]CCCNC(=O)CCNC(=O)CCNC(=O)c1ccc(c(C)c1)C1=C2C=CC(=O)C=C2Oc2cc(O)ccc12

Appendix E

The chemical compounds with reported subcellular localization site in the endoplasmic reticulum and Golgi apparatus. References information is available in Appendix H. Structure is presented as the Simplified Molecular Input Line Entry Specification string of the major microspecies at pH 7.4, as calculated by ChemAxon.

Name:	B7450; Brefeldin A
Method:	Fluorescence Microscopy
References:	54, 593
Structure:	CC1CCC\C=C/C2CC(O)CC2 C(O)\C=C/C(=O)O1

Name:	D272; 3,3'- dipentyloxacarbocyanine iodideDiOC5(3)
Method:	Fluorescence Microscopy
References:	28
Structure:	CCCCCN1\C(Oc2ccccc12)=C \C=C\c1oc2ccccc2[n+]1CCCC C

Name:	B7447; Brefeldin A, BODIPY® FL conjugate; gBFA I
Method:	Fluorescence Microscopy
References:	54
Structure:	CC1CCC\C=C\C2CC(O)CC2 C(OC(=O)CCC2=[N+]3C(C=C 2)=Cc2c(C)cc(C)n2[B-]3(F)F)\C=C\C(=O)O1

Name:	N1154; 6-((N-(7-nitrobenz-2- oxa-1,3- diazol-4- yl)amino)hexanoyl)sphingosin e; NBD C6-ceramide
Method:	Fluorescence Microscopy
References:	146
Structure:	CCCCCCCCCCCCC\C=C\C(O)C(CO)NC(=O)CCCCCNc1c cc(c2nonc12)N(=O)=O

Name:	E12353; ER-Tracker™ Blue- White DPX
Method:	Fluorescence Microscopy
References:	586
Structure:	CN(C)c1ccc(cc1)-c1cnc(o1)- c1ccc(cc1)S(=O)(=O)NCCNC(=O)c1c(F)c(F)c(F)c(F)c1F

Name:	D3521; N-(4,4-difluoro-5,7- dimethyl-4- bora-3a,4a-diaza- s-indacene-3- pentanoyl)sphingosine; BODIPY® FL C5-ceramide
Method:	Fluorescence Microscopy
References:	131
Structure:	CCCCCCCCCCCCC\C=C/C(O)C(CO)NC(=O)CCCCC1=[N +]2C(C=C1)=Cc1c(C)cc(C)n1[B-]2(F)F

Name:	B7449; Brefeldin A, BODIPY® 558/568 conjugate; rBFA
Method:	Fluorescence Microscopy
References:	54
Structure:	CC1CCC\C=C\C2CC(O)CC2 C(OC(=O)CCC2=[N+]3C(C=C 2)=Cc2ccc(-c4cccs4)n2[B-]3(F)F)\C=C\C(=O)O1

Name:	D7540; N-((4-(4,4-difluoro-5- (2-thienyl)-4-bora-3a,4a- diaza-s-indacene-3- yl)phenoxy)acetyl)sphingosine ; BODIPY® TR ceramide
Method:	Fluorescence Microscopy
References:	719
Structure:	CCCCCCCCCCCCC\C=C/C(O)C(CO)NC(=O)COc1ccc(cc1)- c1ccc2C=C3C=CC(c4cccs4)= [N+]3[B-](F)(F)n12

Name:	D3522; N-(4,4-difluoro-5,7- dimethyl-4- bora-3a,4a-diaza- s-indacene-3- pentanoyl)sphingosyl phosphocholine ; BODIPY® FL C5-sphingomyelin
Method:	Fluorescence Microscopy
References:	588

Structure:	CCCCCCCCCCCCC\C=C/C(O)C(COP([O-])(=O)OCC[N+](C)(C)C)NC(=O)CCCCC1=[N+]2C(C=C1)=Cc1c(C)cc(C)n1[B-]2(F)F
Name:	E34251; ER-Tracker™ Green; BODIPY® FL glibenclamide
Method:	NA
References:	Invi
Structure:	COc1c(NC(=O)CCC2=[N+]3C(C=C2)=Cc2c(C)cc(C)n2[B-]3(F)F)cc(Cl)cc1C(=O)NCCc1ccc(cc1)S([O-])(=O)=NC(=O)NC1CCCCC1
Name:	D7519; N-(4,4-difluoro-5,7-dimethyl-4- bora-3a,4a-diaza-s-indacene-3-dodecanoyl)sphingosyl 1-beta-D-galactopyranoside; BODIPY® FL C12-galactocerebroside
Method:	Fluorescence Microscopy
References:	661
Structure:	CCCCCCCCCCCCC\C=C\C(O)C(COC1OC(CO)C(O)C(O)C1O)NC(=O)CCCCCCCCCCC1=[N+]2C(C=C1)=Cc1c(C)cc(C)n1[B-]2(F)F
Name:	E34250; ER-Tracker™ Red; BODIPY® TR glibenclamide
Method:	Fluorescence Microscopy
References:	644
Structure:	COc1c(NC(=O)COc2ccc(cc2)C2=[N+]3C(C=C2)=Cc2ccc(-c4cccs4)n2[B-]3(F)F)cc(Cl)cc1C(=O)NCCc1ccc(cc1)S([O-])(=O)=NC(=O)NC1CCCCC1
Name:	TDEPC; Tetradiethanolamine Zn(II) phthalocyanine
Method:	Fluorescence Microscopy
References:	87
Structure:	OCCN(CCO)S(=O)(=O)c1ccc2c3nc(nc4n5[Zn]n6c(nc7nc(nc5c5cc(ccc45)S(=O)(=O)N(CCO)CCO)c4cccc(c74)S(=O)(=O)N(CCO)CCO)c4ccc(cc4c6n3)S(=O)(=O)N(CCO)CCO)c2c1
Name:	Tolyporphin
Method:	Fluorescence Microscopy

References:	117
Structure:	CC1CC(OC(C)=O)C(OC(C)=O)C(O1)C1(C)C(=O)c2cc3cc(C)c(cc4nc(cc5[nH]c(cc5C)cc1n2)C(=O)C4(C)C1OC(C)C(CC1OC(C)=O)OC(C)=O)[nH]3
Name:	KRN5500
Method:	Fluorescence Microscopy
References:	120
Structure:	CCCCCCCC\C=C\C=C\C(=O)NCC(=O)NC1C(O)C(O)C(Nc2ncnc3nc[nH]c23)OC1C(O)CO
Name:	gBFA II
Method:	Fluorescence Microscopy
References:	54
Structure:	CC1CCC\C=C\C2CC(CC2C(O)\C=C\C(=O)O1)OC(O)CCC1CCC2CC3C(C)CC(C)N3[B-](F)(F)[NH+]12
Name:	13-Oxo-methyl Pyropheophorbide-a Derivative 10
Method:	Fluorescence Microscopy
References:	218
Structure:	CCCCCCCCCCCCOC(C)c1c(C)c2cc3nc(C(CCC(=O)OC)C3C)c3C(=O)C(=O)c4c(C)c(cc5nc(cc1[nH]2)C(C)C5CC)[nH]c34
Name:	13-Oxo-methyl Pyropheophorbide-a Derivative 14
Method:	Fluorescence Microscopy
References:	218
Structure:	CCCCCCCCCCCCOC(C)C1=C(C)C2\C=C3/N=C(C(CCC(=O)OC)C3C)C3=C4N5[In](Cl)N2C1\C=C1/N=C(/C=C5/C(C)=C4C(=O)C3=O)C(CC)C1C
Name:	CIBC Derivative 1
Method:	Fluorescence Microscopy
References:	227
Structure:	CCC1C(C)c2cc3[nH]c(cc4nc(C(CCC([O-])=O)C4C)c4C(=O)OC(=O)c5c(C)c(cc1n2)[nH]c45)c(C)c3C(C)=O
Name:	CIBC Derivative 5

Method:	Fluorescence Microscopy
References:	227
Structure:	CCC1C(C)c2cc3[nH]c(cc4nc(C(CCC([O-])=O)C4C)c4C(=O)N(OC)C(=O)c5c(C)c(cc1n2)[nH]c45)c(C)c3C(C)OCC(O)CO
Name:	CIBC Derivative 10
Method:	Fluorescence Microscopy
References:	227
Structure:	CCC1C(C)c2cc3[nH]c(cc4nc(C(CCC([O-])=O)C4C)c4C(=O)N(NC(=O)c5ccncc5)C(=O)c5c(C)c(cc1n2)[nH]c45)c(C)c3C(C)=O
Name:	2-BA-2-DMHB2-butylamino-2-demethoxy-hypocrellin B
Method:	Fluorescence Microscopy
References:	245
Structure:	CCCCNc1c(O)c2C(=O)C=C(OC)c3c4C(OC)=CC(=O)c5c(O)c(OC)c6C(C(C)=O)=C(C)Cc1c(c23)c6c45
Name:	Monensin
Method:	Pharmacological Effect
References:	249
Structure:	CCC1(CCC(O1)C1(C)CCC2(CC(O)C(C)C(O2)C(C)C(OC)C(C)C([O-])=O)O1)C1OC(CC1C)C1OC(O)(CO)C(C)CC1C
Name:	Okadaic Acid
Method:	Pharmacological Effect
References:	249
Structure:	CC1CCC2(CCCCO2)OC1C(C)CC(O)C1OC2CCC3(CCC(O3)\C=C\C(C)C3CC(C)=CC4(OC(CCC4O)CC(C)(O)C([O-])=O)O3)OC2C(O)C1=C
Name:	Purpurinimide Carbohydrate Conjugate 13
Method:	Fluorescence Microscopy
References:	263
Structure:	CCCCCCN1C(=O)c2c(C)c3cc4nc(cc5[nH]c(cc6nc(C(CCC(=O)OC)C6C)c(C1=O)c2[nH]3)c(C)c5CO)c(C)c4CC
Name:	Vitamin K
Method:	Cell Fractionation
References:	337
Structure:	CC(C)CCCC(C)CCCC(C)CCCC(C)\C=C\C1=C(C)C(=O)c2ccccc2C1=O
Name:	Porphyrin Conjugate Derivative 4
Method:	Fluorescence Microscopy
References:	354
Structure:	CC(C)C(NC(=O)C(CCCC[NH3+])NC(=O)C(CCCNC(N)=[NH2+])NC(=O)C(CCCC[NH3+])NC(=O)C(CCCC[NH3+])NC(=O)C(CCCC[NH3+])NC(=O)C1CCCN1C(=O)CNC(=O)COCCOCCOCCOCCOCCNC(=O)COCC(=O)Nc1ccc(cc1)-c1c2ccc(n2)c(-c2ccccc2)c2ccc([nH]2)c(-c2ccccc2)c2ccc(n2)c(-c2ccccc2)c2ccc1[nH]2)C(N)=O
Name:	Porphyrin Conjugate Derivative 5
Method:	Fluorescence Microscopy
References:	354
Structure:	NC(=[NH2+])NCCCC(NC(=O)C(CCCNC(N)=[NH2+])NC(=O)C(CCCNC(N)=[NH2+])NC(=O)C(CCCNC(N)=[NH2+])NC(=O)C(CCCNC(N)=[NH2+])NC(=O)C(CCCNC(N)=[NH2+])NC(=O)C(CCCNC(N)=[NH2+])NC(=O)CNC(=O)COCCOCCOCCOCCOCCNC(=O)COCC(=O)Nc1ccc(cc1)-c1c2ccc(n2)c(-c2ccccc2)c2ccc([nH]2)c(-c2ccccc2)c2ccc(n2)c(-c2ccccc2)c2ccc1[nH]2)C([O-])=O
Name:	Porphyrin Conjugate Derivative 6
Method:	Fluorescence Microscopy
References:	354
Structure:	CN(CCCCC(=O)N1CCCC1C(=O)NC(CCC(N)=O)C(N)=O)C(=O)C(CCCNC(N)=[NH2+])NC(=O)C(CCCNC(N)=[NH2+])NC(=O)C(CCCNC(N)=[NH2+])NC(=O)C(CCC(N)=O)NC(=O)C(CCCNC(N)=[NH2+])NC(=

	O)C(CCCNC(N)=[NH2+])NC(=O)C(CCCC[NH3+])NC(=O)C(CCCC[NH3+])NC(=O)C(CCCNC(N)=[NH2+])NC(=O)CNC(=O)COCCOCCOCCOCCOCCOCCNC(=O)COCC(=O)Nc1ccc(cc1)-c1c2ccc(n2)c(-c2ccccc2)c2ccc([nH]2)c(-c2ccccc2)c2ccc(n2)c(-c2ccccc2)c2ccc1[nH]2
Name:	SNAFR-6
Method:	Fluorescence Microscopy
References:	388
Structure:	Oc1ccc2cc3c(OC4=CC(=O)C=CC4=C3c3ccccc3)cc2c1
Name:	ADPM01
Method:	Fluorescence Microscopy
References:	407
Structure:	F[B-]1(F)n2c(cc(-c3ccccc3)c2N=C2C(=CC(c3ccccc3)=[N+]12)c1ccccc1)-c1ccccc1
Name:	Hypericin Derivatives 2
Method:	Fluorescence Microscopy
References:	418
Structure:	Cc1ccc2C(=O)c3c(O)cc([O-])c4c3c(-c2c1)c1-c2cc(C)ccc2C(=O)c2c(O)cc([O-])c4c12
Name:	Hypericin Derivatives 3
Method:	Fluorescence Microscopy
References:	418
Structure:	COc1cc(OC)c2c3c1C(=O)c1ccc(C)cc1-c3c1-

	c3cc(C)ccc3C(=O)c3c(OC)cc(OC)c2c13
Name:	Hypericin Derivatives 4
Method:	Fluorescence Microscopy
References:	418
Structure:	Cc1ccc2C(=O)c3c(O)c(Br)c([O-])c4c3c(-c2c1)c1-c2cc(C)ccc2C(=O)c2c(O)c(Br)c([O-])c4c12
Name:	Hypericin Derivatives 5
Method:	Fluorescence Microscopy
References:	418
Structure:	CCCCNc1cc(O)c2c3c1C(=O)c1ccc(C)cc1-c3c1-c3cc(C)ccc3C(=O)c3c(NCCCC)cc(O)c2c13
Name:	Zinpyr-1
Method:	Fluorescence Microscopy
References:	458, 706
Structure:	[O-]C(=O)c1ccccc1C1=C2C=C(Cl)C(=O)C(CN(Cc3ccccn3)Cc3ccccn3)=C2Oc2c(CN(Cc3ccccn3)Cc3ccccn3)c([O-])c(Cl)cc12
Name:	Zinpyr-2
Method:	Fluorescence Microscopy
References:	458, 706
Structure:	Oc1ccc2c(OC3=C(CN(Cc4ccccn4)Cc4ccccn4)C(=O)C=CC3=C2c2ccccc2C([O-])=O)c1CN(Cc1ccccn1)Cc1ccccn1

Appendix F

The chemical compounds with reported subcellular localization site in the cytosol. References information is available in Appendix H. Structure is presented as the Simplified Molecular Input Line Entry Specification string of the major microspecies at pH 7.4, as calculated by ChemAxon.

Name:	Gentamicin
Method:	Cell Fractionation
References:	2, 23, 161
Structure:	C[NH2+]C(C)C1CCC([NH3+])C(O1)OC1C([NH3+])CC([NH3+])C(OC2OCC(C)(O)C([NH2+]C)C2O)C1O

Name:	L7525; LysoTracker® Blue DND-22
Method:	Fluorescence Microscopy
References:	585
Structure:	CN(C)CC[NH2+]Cc1c2ccccc2c(C[NH2+]CCN(C)C)c2ccccc12

Name:	B153; 4,4'-dianilino-1,1'-binaphthyl-5,5'- disulfonic acid, dipotassium salt; Bis-ANS
Method:	Uptake/Binding
References:	609
Structure:	[O-]S(=O)(=O)c1cccc2c(ccc(Nc3ccccc3)c12)-c1ccc(Nc2ccccc2)c2c(cccc12)S([O-])(=O)=O

Name:	PBD Derivative 5; 7-Diethylaminocoumarin pyrrolobenzodiazepine derivative 5
Method:	Fluorescence Microscopy
References:	136
Structure:	CCOC(=O)C1=Cc2ccc(cc2OC1=O)N(CC)CC

Name:	PBD Derivative 17; 7-Diethylaminocoumarin pyrrolobenzodiazepine derivative 17
Method:	Fluorescence Microscopy
References:	136
Structure:	CCN(CC)c1ccc2C=C(C(=O)N

	CCCCCCCCCOc3cc4N=CC5CCCN5C(=O)c4cc3OC)C(=O)Oc2c1

Name:	PBD Derivative 20; 7-Diethylaminocoumarin pyrrolobenzodiazepine derivative 20
Method:	Fluorescence Microscopy
References:	136
Structure:	CCN(CC)c1ccc2C=C(C(=O)NCCCNC(=O)COc3cc4N=CC5CCCN5C(=O)c4cc3OC)C(=O)Oc2c1

Name:	6-Aminoquinoline Derivative 1
Method:	Fluorescence Microscopy
References:	137
Structure:	Cc1c(N2CCCCC2)c(N)cc2C(=O)C(=CN(C3CC3)c12)C([O-])=O

Name:	Triflupromazine
Method:	Fluorescence Microscopy
References:	172
Structure:	C[NH+](C)CCCN1c2ccccc2Sc2ccc(cc12)C(F)(F)F

Name:	PCI-2000
Method:	Fluorescence Microscopy
References:	219
Structure:	CCC1=C(CC)C2=CC3=NC(=Cc4[nH]c(c(CC)c4CC)-c4[nH]c(C=C5N=C(C=C1N2)C(CCCO)=C5C)c(CC)c4CC)C(C)=C3CCCO

Name:	(Dmt[1],dnsDap[4])-DALDA; Dmt-D-Arg-Phe-dnsDap-NH2
Method:	Fluorescence Microscopy
References:	156
Structure:	CN(C)c1cccc2c(cccc12)S(=O)(=O)C(N)C(NC(=O)C(Cc1ccccc1)NC(=O)C(CCCNC(N)=[NH

	2+])NC(=O)C([NH3+])Cc1c(C)cc(O)cc1C)C(N)=O
Name:	Aclacinomycin A
Method:	Fluorescence Microscopy
References:	282
Structure:	CCC1(O)CC(OC2CC(C(OC3CC(O)C(OC4CCC(=O)C(C)O4)C(C)O3)C(C)O2)[NH+](C)C)c2c(O)c3C(=O)c4c(O)cccc4C(=O)c3cc2C1C(=O)OC
Name:	Rose Bengal Acetate
Method:	Fluorescence Microscopy
References:	298
Structure:	[O-]c1c(I)cc2c(Oc3c(I)c([O-])c(I)cc3C22OC(=O)c3c(Cl)c(Cl)c(Cl)c(Cl)c23)c1I
Name:	P-H; tri-cationic 5-(4-carboxyphenyl)-10,15,20-tris(4-methylpyridinium-4-yl)porphyrin tri-iodide
Method:	Fluorescence Microscopy
References:	301
Structure:	C[n+]1ccc(cc1)-c1c2ccc(n2)c(C([O-])=O)c2ccc([nH]2)c(-c2cc[n+](C)cc2)c2ccc([nH]2)c(-c2cc[n+](C)cc2)c2ccc1n2
Name:	Photolabeled BBR 3422
Method:	Cell Fractionation
References:	312
Structure:	C[NH2+]CCNc1ccc2n(CCNC(=O)c3ccc(cc3O)N=[N+]=[N-])nc3-c4cnccc4C(=O)c1c23
Name:	4-DCB; 4,4'-dichlorobiphenyl
Method:	Cell Fractionation
References:	312
Structure:	Clc1ccc(cc1)-c1ccc(Cl)cc1
Name:	236-HCB; 2,2',3,3',6,6'-Hexachlorobiphenyl
Method:	Cell Fractionation
References:	312
Structure:	Clc1ccc(Cl)c(c1Cl)-c1c(Cl)ccc(Cl)c1Cl
Name:	245-HCB; 2,2',4,4',5,5'-hexachlorobiphenyl
Method:	Cell Fractionation
References:	312
Structure:	Cc1cc(Cl)c(Cl)cc1-

	c1cc(Cl)c(Cl)cc1Cl
Name:	2-Chloroaniline
Method:	Cell Fractionation
References:	315
Structure:	Nc1ccccc1Cl
Name:	4-Chloroaniline
Method:	Cell Fractionation
References:	315
Structure:	Nc1ccc(Cl)cc1
Name:	Dioxane
Method:	Cell Fractionation
References:	317
Structure:	C1COCCO1
Name:	ZnPcS3C2
Method:	Fluorescence Microscopy
References:	328
Structure:	[O-]S(=O)(=O)c1ccc2c3nc(nc4n5[Zn]n6c(nc7nc(nc5c5cc(ccc45)S([O-])(=O)=O)c4ccc(cc74)S([O-])(=O)=O)c4ccc(cc4c6n3)C#C)c2c1
Name:	ZnPcS3C12
Method:	Fluorescence Microscopy
References:	328
Structure:	CCCCCCCCCC#Cc1ccc2c3nc4nc(nc5n6[Zn]n3c(nc3nc(nc6c6ccc(cc56)S([O-])(=O)=O)c5cc(ccc35)S([O-])(=O)=O)c2c1)c1ccc(cc41)S([O-])(=O)=O
Name:	ZnPcS3C16
Method:	Fluorescence Microscopy
References:	328
Structure:	CCCCCCCCCCCCCC#Cc1ccc2c3nc4nc(nc5n6[Zn]n3c(nc3nc(nc6c6ccc(cc56)S([O-])(=O)=O)c5cc(ccc35)S([O-])(=O)=O)c2c1)c1ccc(cc41)S([O-])(=O)=O
Name:	Dansyl-TPA
Method:	Fluorescence Microscopy
References:	330
Structure:	CC1C(OC(=O)CCCCCCCCCCNS(=O)(=O)c2cccc3c(cccc23)N(C)C)C2(OC(C)=O)C(C3C=C(CO)CC4(O)C(C=C(C)C4

	=O)C13O)C2(C)C

Name:	Ergocalciferol; Vitamin D2
Method:	Cell Fractionation
References:	343
Structure:	CC(C)C(C)\C=C\C(C)C1CCC2C1(C)CCC\C2=C/C=C1\CC(O)CCC1=C

Name:	Cholecalciferol; Vitamin D3
Method:	Cell Fractionation
References:	343
Structure:	CC(C)CCCC(C)C1CCC2C1(C)CCC\C2=C/C=C1\CC(O)CCC1=C

Name:	Oxyethylene-rich Zn(II)-Phthalocyanine Derivative 4
Method:	Fluorescence Microscopy
References:	382
Structure:	COCCOCCOCCOc1cc(COc2cccc3c4nc5nc(nc6n7[Zn]n4c(nc4nc(nc7c7ccccc67)c6ccccc46)c23)c2ccccc52)cc(OCCOCCOCCOC)c1OCCOCCOCCOC

Name:	Oxyethylene-rich Zn(II)-Phthalocyanine Derivative 5
Method:	Fluorescence Microscopy
References:	382
Structure:	COCCOCCOCCOc1cc(COc2ccc3c4nc5nc(nc6n7[Zn]n4c(nc4nc(nc7c7ccccc67)c6ccccc46)c3c2)c2ccccc52)cc(OCCOCCOCCOC)c1OCCOCCOCCOC

Name:	Oxyethylene-rich Zn(II)-Phthalocyanine Derivative 8
Method:	Fluorescence Microscopy
References:	382
Structure:	COCCOCCOCCOc1cc(COc2ccc(OCc3cc(OCCOCCOCCOC)c(OCCOCCOCCOC)c(OCCOCCOCCOC)c3)c3c4nc5nc(nc6n7[Zn]n4c(nc4nc(nc7c7ccccc67)c6ccccc46)c23)c2ccccc52)cc(OCCOCCOCCOC)c1OCCOCCOCCOC

Name:	DCHQ Derivative 1
Method:	Fluorescence Microscopy
References:	452
Structure:	Oc1c(CN2CCOCCOCCN(CC

	OCCOCC2)Cc2ccc3cccnc3c2O)ccc2cccnc12

Name:	Porphyrazine A4 Derivative 5
Method:	Fluorescence Microscopy
References:	410
Structure:	COCCOCCOCCOCCSc1c(SCCOCCOCCOCCOC)c2nc1nc1[nH]c(nc3nc(nc4[nH]c(n2)c(SCCOCCOCCOCCOC)c4SCCOCCOCCOCCOC)c(SCCOCCOCCOCCOC)c3SCCOCCOCCOCCOC)c(SCCOCCOCCOCCOC)c1SCCOCCOCCOCCOC

Name:	Porphyrazine A4 Derivative 8
Method:	Fluorescence Microscopy
References:	410
Structure:	COCCOCCOCCOCCSc1c(SCCOCCOCCOCCOC)c2nc1nc1c(SCCOCCOCCOCCOC)c(SCCOCCOCCOCCOC)c3nc4nc(nc5c(SCCOCCOCCOCCOC)c(SCCOCCOCCOCCOC)c(n2)n5[Zn]n13)c(SCCOCCOCCOCCOC)c4SCCOCCOCCOCCOC

Name:	Porphyrazine A3B Derivative 6
Method:	Fluorescence Microscopy
References:	410
Structure:	COCCOCCOCCOCCSc1c(SCCOCCOCCOCCOC)c2nc1nc1[nH]c(nc3nc(nc4[nH]c(n2)c2c(OC(C)C)ccc(OC(C)C)c42)c(SCCOCCOCCOCCOC)c3SCCOCCOCCOCCOC)c(SCCOCCOCCOCCOC)c1SCCOCCOCCOCCOC

Name:	Porphyrazine A3B Derivative 9
Method:	Fluorescence Microscopy
References:	410
Structure:	COCCOCCOCCOCCSc1c(SCCOCCOCCOCCOC)c2nc1nc1c(SCCOCCOCCOCCOC)c(SCCOCCOCCOCCOC)c3nc4nc(nc5n([Zn]n13)c(n2)c1c(OC(C)C)ccc(OC(C)C)c51)c(SCCOCCOCCOCCOC)c4SCCOCCOCCOCCOC

Name:	Porphyrazine A2B2 Derivative 7
Method:	Fluorescence Microscopy
References:	410
Structure:	COCCOCCOCCOCCSc1c(SCCOCCOCCOCCOC)c2nc1nc1[nH]c(nc3nc(nc4[nH]c(n2)c2c(OC(C)C)ccc(OC(C)C)c42)c(SCCOCCOCCOCCOC)c3SCCOCCOCCOCCOC)c2c(OC(C)C)ccc(OC(C)C)c12
Name:	Porphyrazine A2B2 Derivative 10
Method:	Fluorescence Microscopy
References:	410
Structure:	COCCOCCOCCOCCSc1c(SCCOCCOCCOCCOC)c2nc1nc1n3[Zn]n4c(n2)c2c(OC(C)C)ccc(OC(C)C)c2c4nc2nc(nc3c3c(OC(C)C)ccc(OC(C)C)c13)c(SCCOCCOCCOCCOC)c2SCCOCCOCCOCCOC
Name:	Pentaphyrin Derivative 1; isopentaphyrin
Method:	Fluorescence Microscopy
References:	399
Structure:	CCC1=C(C)\C2=C\C3=N\C(\C=C3)=C(c3ccccc3)\c3ccc(\C=C4[NH2+]C(=C/c5[nH]c(/C=C/1[NH2+]2)c(CC)c5CC)\C(CC)=C/4C)[nH]3
Name:	Pentaphyrin Derivative 2; pentaphyrin
Method:	Fluorescence Microscopy
References:	399
Structure:	CCC1=C(C)C2=N\C\1=C\c1[nH]c(\C=C3/N=C(C=C4C=CC(=N4)C(c4ccccc4)=C4NC(C=C4)=C2)C(C)=C/3CC)c(CC)c1CC
Name:	TPP(p-Deg-OH)3
Method:	Fluorescence Microscopy
References:	409
Structure:	OCCOCCOc1ccc(cc1)-c1c2ccc(n2)c(-c2ccc(OCCOCCO)cc2)c2ccc([nH]2)c(-c2ccc(OCCOCCO)cc2)c2ccc(n2)c(-c2ccccc2)c2ccc1[nH]2
Name:	TPP(p-Deg-O-ß-GalOH)3

Method:	Fluorescence Microscopy
References:	409
Structure:	OC[C@@H]1O[C@@H](OCCOCCOc2ccc(cc2)-c2c3ccc(n3)c(-c3ccccc3)c3ccc([nH]3)c(-c3ccc(OCCOCCO[C@@H]4O[C@@H](CO)[C@@H](O)[C@H](O)[C@@H]4O)cc3)c3ccc(n3)c(-c3ccc(OCCOCCO[C@@H]4O[C@@H](CO)[C@@H](O)[C@H](O)[C@@H]4O)cc3)c3ccc2[nH]3)[C@@H](O)[C@@H](O)[C@@H]1O
Name:	m-1c
Method:	Fluorescence Microscopy
References:	422
Structure:	O[C@@H]1CO[C@@H](Oc2cccc(c2)-c2c3CCc([nH]3)c(-c3cccc(O[C@@H]4OC[C@@H](O)[C@H](O)[C@H]4O)c3)c3ccc(n3)c(-c3cccc(O[C@@H]4OC[C@@H](O)[C@H](O)[C@H]4O)c3)c3ccc([nH]3)c(-c3cccc(O[C@@H]4OC[C@@H](O)[C@H](O)[C@H]4O)c3)c3ccc2n3)[C@H](O)[C@@H]1O
Name:	Iejimalide Derivative 7b
Method:	Fluorescence Microscopy
References:	423
Structure:	CCN(CC)c1ccc2C=C(NC(=O)OCC(NC=O)C(=O)NC\C(C)=C\C=C(/C)C3OC(=O)\C(C)=C\C(C)\C=C\C(C)=C\C(C\C=C\C(C)=C/CCC(OC)\C=C\C=C\C3C)OC)C(=O)Oc2c1
Name:	Ruthenium-Porphyrin Derivative 2
Method:	Fluorescence Microscopy
References:	425
Structure:	Cl[Ru](Cl)(N1CC=C(C=C1)c1c2ccc(n2)c(C2=CCN(C=C2)[Ru](Cl)(Cl)c2ccc(cc2)-c2ccccc2)c2ccc([nH]2)c(C2=CCN(C=C2)[Ru](Cl)(Cl)c2ccc(cc2)-c2ccccc2)c2ccc(n2)c(C2=CCN(C=C2)[Ru](Cl)(Cl)c2ccc(cc2)-c2ccccc2)c2ccc1[nH]2)c1ccc(

268

	cc1)-c1ccccc1

Name:	SIM01
Method:	Fluorescence Microscopy
References:	426
Structure:	Oc1cc(O)cc(c1)-c1c2CCc(cc3ccc([nH]3)c(-c3cc(O)cc(O)c3)c3ccc(cc4ccc1[nH]4)n3)n2

Name:	Glycosylated Zn(II) Phthalocyanine Derivative 9
Method:	Fluorescence Microscopy
References:	536
Structure:	CC1(C)OC2OC(COc3cccc4c5nc(N=c6n7[Zn]n8c(=Nc9nc(N=c7c7c(OCC%10OC%11OC(C)(C)OC%11C%11OC(C)(C)OC%10%11)cccc67)c6cccc(OCC7OC%10OC(C)(C)OC%10C%10OC(C)(C)OC7%10)c96)c6cccc(OCC7OC9OC(C)(C)OC9C9OC(C)(C)OC79)c6c8=N5)c34)C3OC(C)(C)OC3C2O1

Name:	Glycosylated Zn(II) Phthalocyanine Derivative 17
Method:	Fluorescence Microscopy
References:	536
Structure:	CC1(C)OC2OC(COc3cccc4c5nc(N=c6n7[Zn]n8c(=Nc9nc(N=c7c7ccccc67)c6ccccc96)c6cccc6c8=N5)c34)C3OC(C)(C)OC3C2O1

Name:	Glycosylated Zn(II) Phthalocyanine Derivative 19
Method:	Fluorescence Microscopy
References:	536
Structure:	CC1(C)OC2OC(COc3ccc4c5nc(N=c6n7[Zn]n8c(=Nc9nc(N=c7c7ccccc67)c6ccccc96)c6cccc6c8=N5)c4c3)C3OC(C)(C)OC3C2O1

Name:	Mono-Substituted Amphiphilic Zn(II) Phthalocyanine Derivative 3
Method:	Fluorescence Microscopy
References:	442
Structure:	CN(C)CC(C[NH+](C)C)Oc1ccc2c3nc4nc(nc5n6[Zn]n3c(nc3nc(nc6c6ccccc56)c5ccccc35)c2c1)c1ccccc41

Name:	Mono-Substituted Amphiphilic Zn(II) Phthalocyanine Derivative 4
Method:	Fluorescence Microscopy
References:	442
Structure:	CN(C)CC(C[NH+](C)C)Oc1ccc2c3nc4nc(nc5n6[Zn]n3c(nc3nc(nc6c6ccccc56)c5ccccc35)c12)c1ccccc41

Name:	Mono-Substituted Amphiphilic Zn(II) Phthalocyanine Derivative 5
Method:	Fluorescence Microscopy
References:	442
Structure:	C[N+](C)(C)CC(C[N+](C)(C)C)Oc1ccc2c3nc4nc(nc5n6[Zn]n3c(nc3nc(nc6c6ccccc56)c5ccccc35)c2c1)c1ccccc41

Name:	Mono-Substituted Amphiphilic Zn(II) Phthalocyanine Derivative 6
Method:	Fluorescence Microscopy
References:	442
Structure:	C[N+](C)(C)CC(C[N+](C)(C)C)Oc1cccc2c3nc4nc(nc5n6[Zn]n3c(nc3nc(nc6c6ccccc56)c5ccccc35)c12)c1ccccc41

Name:	NiNc
Method:	Distr.others
References:	470
Structure:	CCCCOc1c2ccccc2c(OCCCC)c2c3nc4[n+]5c(nc6n7c(nc8[n+]9c(nc(n3[Ni--]579)c12)c1c(OCCCC)c2cccc2c(OCCCC)c81)c1c(OCCCC)c2ccccc2c(OCCCC)c61)c1c(OCCCC)c2ccccc2c(OCCCC)c41

Name:	DB607
Method:	Fluorescence Microscopy
References:	472
Structure:	COc1ccc(cc1)-c1ccc(o1)-c1ccc(cc1)C(N)=[NH2+]

Name:	4-Hydroxymethyl-3-aminoacridine Derivative 1
Method:	Fluorescence Microscopy
References:	478
Structure:	Nc1ccc2cc3ccccc3nc2c1CO

Name:	4-Hydroxymethyl-3-

	aminoacridine Derivative 2
Method:	Fluorescence Microscopy
References:	478
Structure:	CNc1ccc2cc3ccccc3nc2c1CO
Name:	4-Hydroxymethyl-3-aminoacridine Derivative 3
Method:	Fluorescence Microscopy
References:	478
Structure:	CN(C)c1ccc2cc3ccccc3nc2c1CO
Name:	O[6]-Benzylguanine-Oregon Green
Method:	Fluorescence Microscopy
References:	495
Structure:	Nc1nc(OCc2ccc(CNC(=O)c3cc(c(c3)C([O-])=O)C3=C4C=C(F)C(=O)C=C4Oc4cc(O)c(F)cc34)cc2)c2nc[nH]c2n1
Name:	Eu2(LC3)3
Method:	Fluorescence Microscopy

References:	499
Structure:	COCCOCCOCCn1c-2nc3cc(Cc4ccc5n(CCOCCOCCOC)c(nc5c4)-c4cccc(n4)C(=O)O[Eu]456(OC(=O)c7cccc-2n7)OC(=O)c2cccc(n2)-c2nc7cc(Cc8ccc9n(CCOCCOCCCOC)c(nc9c8)-c8cccc(n8)C(=O)O4)ccc7n2CCOCCOCCOC)ccc13.COCCOCCOCCn1c(nc2cc(Cc3ccc4n(CCOCCOCCCOC)c(nc4c3)-c3cccc(n3)C(=O)O5)ccc12)-c1cccc(n1)C(=O)O6
Name:	Pi-Extended Squaraines Derivative 2a
Method:	Fluorescence Microscopy
References:	507
Structure:	COCCOCCOCn1c(\C=C\c2ccncc2)ccc1C1=C([O-])\C(C1=O)=C1/C=CC(\C=C\c2ccncc2)=[N+]/1COCCOCCOC

The chemical compounds with multiple reported subcellular localization sites. Localization 1: endo-lysosomes; 2: mitochondria; 3: nucleus; 4: plasma membrane; 5: endoplasmic reticulum and Golgi apparatus; and 6: cytosol. References information is available in Appendix H. Structure is presented as the Simplified Molecular Input Line Entry Specification string of the major microspecies at pH 7.4, as calculated by ChemAxon.

Name:	A1301; Acridine orange
Localization:	1, 3
Method:	Fluorescence Microscopy
References:	Invi.
Structure:	CN(C)c1ccc2cc3ccc(cc3[nH+]c2c1)N(C)C
Name:	Fluoxetine
Localization:	1,2
Method:	Pharmacological Effect
References:	2, 4, 6
Structure:	C[NH2+]CCC(Oc1ccc(cc1)C(F)(F)F)c1ccccc1
Name:	D23107; dihydroethidium (hydroethidine)
Localization:	2, 3
Method:	Fluorescence Microscopy
References:	667
Structure:	CCN1C(c2ccccc2)c2cc(N)ccc2-c2ccc(N)cc12
Name:	N1142; Nile red
Localization:	1, 3, 4
Method:	Fluorescence Microscopy
References:	122
Structure:	CCN(CC)c1ccc2N=C3C(Oc2c1)=CC(=O)c1ccccc31
Name:	Quinine
Localization:	1, 2
Method:	Fluorescence Microscopy/Cell Fractionation
References:	5, 127; 264
Structure:	COc1ccc2nccc(C(O)C3CC4CC[NH+]3CC4C=C)c2c1
Name:	Trifluoperazine (TFP)
Localization:	1, 2
Method:	Pharmacological Effect

References:	4
Structure:	CN1C=CN(CCCN2c3ccccc3Sc3ccc(cc23)C(F)(F)F)C=C1
Name:	T204; 1-(4-trimethylammoniumphenyl)-6-phenyl- 1,3,5-hexatriene p-toluenesulfonate; TMA-DPH
Localization:	1, 4
Method:	Fluorescence Microscopy
References:	108
Structure:	C[N+](C)(C)c1ccc(cc1)\C=C\C=C\C=C\c1ccccc1
Name:	H7593; Hexidium iodide
Localization:	3, 6
Method:	NA
References:	Invi.
Structure:	CCCCCC[n+]1c(-c2ccccc2)c2cc(N)ccc2c2ccc(N)cc12
Name:	D273; 3,3'-dihexyloxacarbocyanine iodideDiOC6(3)
Localization:	2, 5
Method:	NA
References:	Invi.
Structure:	CCCCCCN1\C(Oc2ccccc12)=C\C=C\c1oc2ccccc2[n+]1CCCCCC
Name:	R648MP; rhodamine B, hexyl ester, perchlorate (R6)
Localization:	2, 6
Method:	Fluorescence Microscopy
References:	677
Structure:	CCCCCCOC(=O)c1ccccc1C1=C2C=CC(C=C2Oc2cc(ccc12)N(CC)CC)=[N+](CC)CC

Name:	D13951; N-(4,4-difluoro-5,7-dimethyl-4- bora-3a,4a-diaza-s-indacene-3-pentanoyl)sphingosyl 1-beta-D-lactoside; BODIPY® FL C5-lactosylceramide
Localization:	4, 5
Method:	NA
References:	Invi.
Structure:	CCCCCCCCCCCCC\C=C/C(O)C(COC1OC(CO)C(OC2OC(CO)C(O)C(O)C2O)C(O)C1O)NC(=O)CCCCc1ccc2C=C3C(C)=CC(C)=[N+]3[B-](F)(F)n12
Name:	Proflavine
Localization:	1, 3
Method:	Fluorescence Microscopy
References:	127
Structure:	Nc1ccc2cc3ccc(N)cc3[nH+]c2c1
Name:	Euchrysine
Localization:	1, 3
Method:	Fluorescence Microscopy
References:	127
Structure:	Cc1cc2c(C)c3cc(C)c(N)cc3[nH+]c2cc1N
Name:	Acridine orange R
Localization:	1, 3
Method:	Fluorescence Microscopy
References:	127
Structure:	CN(C)c1ccc2cc3cccc(N(C)C)c3nc2c1
Name:	BBDX
Localization:	2, 4
Method:	Fluorescence Microscopy
References:	55
Structure:	CN(C)c1ccc2c(Oc3cc(ccc3C2(O)c2cc(C)c(N(C)C)c(C)c2)N(C)C)c1
Name:	Promethazine
Localization:	2, 5, 6
Method:	histo
References:	66
Structure:	CC(CN1c2ccccc2Sc2ccccc12)[NH+](C)C
Name:	HDAO; 3,6-Bis(dimethylamino)-10-hexadecylacridinium bromide; acridine orange 10-hexadecyl

	bromide
Localization:	2, 6
Method:	Fluorescence Microscopy
References:	72
Structure:	CCCCCCCCCCCCCCCC[n+]1c2cc(ccc2cc2ccc(cc12)N(C)C)N(C)C
Name:	TPPS4; 5,10,15,20-tetra(4-sulfonatophenyl)porphine
Localization:	1, 3
Method:	Fluorescence Microscopy
References:	84
Structure:	[O-]S(=O)(=O)c1ccc(cc1)-c1c2ccc(n2)c(-c2ccc(cc2)S([O-])(=O)=O)c2ccc([nH]2)c(-c2ccc(cc2)S([O-])(=O)=O)c2ccc([nH]2)c(-c2ccc(cc2)S([O-])(=O)=O)c2ccc1n2
Name:	Merocyanine 540
Localization:	1, 2, 4
Method:	Fluorescence Microscopy
References:	93
Structure:	CCCCN1C(=O)N(CCCC)C(=O)C(=C\C=C\C=C2/Oc3ccccc3N2CCCS([O-])(=O)=O)C1=O
Name:	SnET2
Localization:	1, 2
Method:	Fluorescence Microscopy
References:	99
Structure:	CCOC(=O)C1=Cc2c3n4c(cc5nc(cc6c(CC)c(C)c(cc7nc2c(C)c7CC)n6[Sn]4(Cl)Cl)c(C)c5CC)C(C)C13CC
Name:	Curcurmin
Localization:	3, 4
Method:	Fluorescence Microscopy
References:	133
Structure:	COc1cc(ccc1O)\C=C\C(=O)CC(=O)\C=C\c1ccc(O)c(OC)c1
Name:	Edelfosine
Localization:	4, 5
Method:	Fluorescence Microscopy
References:	170
Structure:	CCCCCCCCCCCCCCCCCCOCC(COP([O-])(=O)OCC[N+](C)(C)C)OC
Name:	Toluidine Blue

Localization:	4, 5
Method:	Fluorescence Microscopy
References:	171
Structure:	Cc1cc2N=C3C=CC(C=C3Sc2cc1N)=[N+](C)C

Name:	Levorphanol
Localization:	2, 3
Method:	Cell Fractionation
References:	174
Structure:	C[NH+]1CCC23CCCCC2C1Cc1ccc(O)cc31

Name:	BODIPY-labeled Polyamide 1
Localization:	1, 5
Method:	Fluorescence Microscopy
References:	176
Structure:	C[NH+](CCCNC(=O)CCCCCNC(=O)CCC1=[N+]2C(C=C1)=Cc1c(C)cc(C)n1[B-]2(F)F)CCCNC(=O)CCNC(=O)c1cc(NC(=O)c2cc(NC(=O)c3cc(NC(=O)c4cc(NC(=O)CCCNC(=O)c5cc(NC(=O)c6cc(NC(=O)c7cc(NC(=O)c8nccn8C)cn7C)cn6C)cn5C)cn4C)cn3C)cn2C)cn1C

Name:	M-129
Localization:	3, 6
Method:	Fluorescence Microscopy
References:	173
Structure:	CC(CN1c2ccccc2C(=O)c2ccccc12)[NH+](C)C

Name:	Motexafin Gadolinium
Localization:	1, 2, 5
Method:	Fluorescence Microscopy
References:	184
Structure:	CCO.CCC1=C(CC)/C2=C/C3=N/C(=C\N=C4\C=C(OCCOCCOCCOC)C(OCCOCCOCCOC)=C\C\4=N\C=C4/N=C(/C=C\1N2[Gd]([O-])OC(C)=O)C(CCCO)=C/4C)/C(C)=C3CCCO

Name:	HB; Hypocrellin B
Localization:	1, 4
Method:	Fluorescence Microscopy
References:	186
Structure:	COC1=CC(=O)c2c(O)c(OC)c3CC(C)=C(C(C)=O)c4c(OC)c(O)c5C(=O)C=C(OC)c6c1c2c3c4c56

Name:	HBEA-R1; Ethanolaminated HB
Localization:	1, 4
Method:	Fluorescence Microscopy
References:	186
Structure:	COC1=CC(=O)c2c(NCCO)c(OC)c3CC(C)=C(C(C)=O)c4c(OC)c(NCCO)c5C(=O)C=C(OC)c6c1c2c3c4c56

Name:	HBBA-R2; Butylaminated HB
Localization:	4, 5
Method:	Fluorescence Microscopy
References:	186
Structure:	CCCCNc1cc(OC)c2c3c1C(=O)C(OC)=C1CC(C)=C(C(C)=O)C4=C(OC)C(=O)c5c(NCCCC)cc(OC)c2c5c4c31

Name:	BPD-MA
Localization:	2, 3
Method:	Fluorescence Microscopy
References:	210
Structure:	CCOC(=O)C1C(=CC=C2c3cc4[nH]c(cc5nc(cc6[nH]c(cc(n3)C12C)c(C=C)c6C)c(C)c5CCC([O-])=O)c(CCC([O-])=O)c4C)C(=O)OCC

Name:	Guanidine Porphyrin
Localization:	1, 2, 5
Method:	Fluorescence Microscopy
References:	211
Structure:	NC(N)=Nc1ccc(cc1)-c1c2ccc(n2)c(-c2ccccc2)c2ccc([nH]2)c(-c2ccccc2)c2ccc(n2)c(-c2ccccc2)c2ccc1[nH]2

Name:	Biguanidine Porphyrin
Localization:	1, 2
Method:	Fluorescence Microscopy
References:	211
Structure:	N[C+](N)\N=C(/N)Nc1ccc(cc1)-c1c2ccc(n2)c(-c2ccccc2)c2ccc([nH]2)c(-c2ccccc2)c2ccc(n2)c(-c2ccccc2)c2ccc1[nH]2

Name:	Pc4
Localization:	2, 5
Method:	Fluorescence Microscopy
References:	214
Structure:	NC1=NC(=O)N(C=C1)C1OC(

	COP([O-])(=O)OC2C(O)C(COP([O-])(=O)OC3C(O)C(COP([O-])(=O)OC4C(O)C(COP([O-])([O-])=O)OC4N4C=CC(N)=NC4=O)OC3N3C=CC(N)=NC3=O)OC2N2C=CC(N)=NC2=O)C(O)C1O

Name:	Zn-BC-AM
Localization:	2, 5
Method:	Fluorescence Microscopy
References:	216
Structure:	CCc1c(CC)c2cc3c(CC)c(CC)c4n3[Zn]n3c(cc5nc6c(cc(cc46)[C+](N)N)C5(CC)CC)c(CC)c(CC)c3cc1n2

Name:	PPME
Localization:	1, 5, 6
Method:	Fluorescence Microscopy
References:	222
Structure:	CCc1c(C)c2cc3[nH]c(cc4nc(C(CCC(=O)OC)C4C)c4CC(=O)C5C(C)c(cc1n2)[nH]c45)c(C)c3C=C

Name:	CIBC Derivative 3
Localization:	4, 5
Method:	Fluorescence Microscopy
References:	227
Structure:	CCC1C(C)c2cc3[nH]c(cc4nc(C(CCC([O-])=O)C4C)c4C(=O)N(OC)C(=O)c5c(C)c(cc1n2)[nH]c45)c(C)c3C(C)OCCOCCO

Name:	CIBC Derivative 4
Localization:	4, 5
Method:	Fluorescence Microscopy
References:	227
Structure:	CCC1C(C)c2cc3[nH]c(cc4nc(C(CCC([O-])=O)C4C)c4C(=O)N(OC)C(=O)c5c(C)c(cc1n2)[nH]c45)c(C)c3C(C)OCCOCCOCCO

Name:	CIBC Derivative 6
Localization:	4, 5
Method:	Fluorescence Microscopy
References:	227
Structure:	CCC1C(C)c2cc3[nH]c(cc4nc(C(CCC([O-])=O)C4C)c4C(=O)N(OC)C(=

	O)c5c(C)c(cc1n2)[nH]c45)c(C)c3C(C)OCCOC

Name:	CIBC Derivative 8
Localization:	4, 5
Method:	Fluorescence Microscopy
References:	227
Structure:	CCC1C(C)c2cc3[nH]c(cc4nc(C(CCC([O-])=O)C4C)c4C(=O)N(N(C)C)C(=O)c5c(C)c(cc1n2)[nH]c45)c(C)c3C(C)=O

Name:	CIBC Derivative 9
Localization:	4, 5
Method:	Fluorescence Microscopy
References:	227
Structure:	CCC1C(C)c2cc3[nH]c(cc4nc(C(CCC([O-])=O)C4C)c4C(=O)N(N)C(=O)c5c(C)c(cc1n2)[nH]c45)c(C)c3C(C)=O

Name:	CIBC Derivative 11
Localization:	4, 5
Method:	Fluorescence Microscopy
References:	227
Structure:	CCC1C(C)c2cc3[nH]c(cc4nc(C(CCC([O-])=O)C4C)c4C(=O)N(NC(=O)c5cc[n+](C)cc5)C(=O)c5c(C)c(cc1n2)[nH]c45)c(C)c3C(C)=O

Name:	CICD Derivative 1; 13,15-N-cycloimide Derivatives of Chlorin p6
Localization:	2, 5
Method:	Fluorescence Microscopy
References:	86
Structure:	CCc1c(C)c2cc3[nH]c(cc4nc(C(CCC([O-])=O)C4C)c4C(=O)N(CCCO)C(=O)c5c(C)c(cc1n2)[nH]c45)c(C)c3C=C

Name:	CICD Derivative 2; 13,15-N-cycloimide Derivatives of Chlorin p7
Localization:	2, 5
Method:	Fluorescence Microscopy
References:	86
Structure:	CCc1c(C)c2cc3[nH]c(cc4nc(C(CCC([O-])=O)C4C)c4C(=O)N(CCO)C(=O)c5c(C)c(cc1n2)[nH]c45)c(

	C)c3C=C

Name:	CICD Derivative 3; 13,15-N-cycloimide Derivatives of Chlorin p8
Localization:	2, 5
Method:	Fluorescence Microscopy
References:	86
Structure:	CCc1c(C)c2cc3[nH]c(cc4nc(C(CCC([O-])=O)C4C)c4C(=O)N(OC(C)=O)C(=O)c5c(C)c(cc1n2)[nH]c45)c(C)c3C=C

Name:	CICD Derivative 4; 13,15-N-cycloimide Derivatives of Chlorin p9
Localization:	2, 5
Method:	Fluorescence Microscopy
References:	86
Structure:	CCc1c(C)c2cc3[nH]c(cc4nc(C(CCC(=O)OC)C4C)c4C(=O)N([O-])C(=O)c5c(C)c(cc1n2)[nH]c45)c(C)c3C=C

Name:	Pyropheophorbide-a Derivative 8
Localization:	1, 2
Method:	Fluorescence Microscopy
References:	92
Structure:	CCCCCCCCOC(C)c1c(C)c2cc3nc(C(CCC([O-])=O)C3C)c3CC(=O)c4c(C)c(cc5nc(cc1[nH]2)c(C)c5CC)[nH]c34

Name:	Pyropheophorbide-a Derivative 10
Localization:	1, 2
Method:	Fluorescence Microscopy
References:	92
Structure:	CCCCCCCCCCOC(C)c1c(C)c2cc3nc(C(CCC([O-])=O)C3C)c3CC(=O)c4c(C)c(cc5nc(cc1[nH]2)c(C)c5CC)[nH]c34

Name:	Pyropheophorbide-a Derivative 12
Localization:	1, 2
Method:	Fluorescence Microscopy
References:	92
Structure:	CCCCCCCCCCCCOC(C)c1c(C)c2cc3nc(C(CCC([O-

	])=O)C3C)c3CC(=O)c4c(C)c(cc5nc(cc1[nH]2)c(C)c5CC)[nH]c34

Name:	MPPa; Pyropheophorbide-a methyl ester
Localization:	1, 2, 3, 5
Method:	Fluorescence Microscopy
References:	94
Structure:	CCc1c(C)c2cc3[nH]c(cc4nc(C(CCC(=O)OC)C4C)c4CC(=O)c5c(C)c(cc1n2)[nH]c45)c(C)c3C=C

Name:	CAME (Chlorin e6 triacetoxymethyl ester) (Lysosomes)
Localization:	1, 2
Method:	Fluorescence Microscopy
References:	98
Structure:	CCc1c(C)c2cc3[nH]c(cc4nc(C(CCC(=O)OCOC(C)=O)C4C)c(CC(=O)OCOC(C)=O)c4nc(cc1[nH]2)c(C)c4C(=O)OCOC(C)=O)c(C)c3C=C

Name:	Deuteroporphyrin
Localization:	4, 6
Method:	Fluorescence Microscopy
References:	125
Structure:	Cc1cc2cc3nc(cc4[nH]c(cc5[nH]c(cc5C)cc1n2)c(C)c4CCC([O-])=O)c(CCC([O-])=O)c3C

Name:	Thiamine
Localization:	1, 3
Method:	Fluorescence Microscopy
References:	238
Structure:	Cc1ncc(C[n+]2csc(CCO)c2C)c(N)n1

Name:	F-DDP
Localization:	1, 5
Method:	Fluorescence Microscopy
References:	240
Structure:	Oc1ccc2C(C3C=CC(=O)C=C3Oc2c1)c1ccc(cc1C([O-])=O)C(=O)NCC1C[NH2+][Pt--](Cl)(Cl)N1

Name:	Grepafloxacin
Localization:	3, 4
Method:	Fluorescence Microscopy
References:	242
Structure:	CC1CN(CC[NH2+]1)c1cc2N(

	C=C(C(C([O-])=O)C(=O)c2c(C)c1F)C1CC1
Name:	Distamycin Analogue 10
Localization:	2, 6
Method:	Fluorescence Microscopy
References:	258
Structure:	C[NH+](C)CCCNC(=O)c1cc(NC(=C)c2cc(NC(=O)c3cc(NC=O)cn3C)cn2CCNC(=O)OC2c3ccccc3-c3ccccc23)cn1C
Name:	Purpurinimide Carbohydrate Conjugate 3
Localization:	1, 5
Method:	Fluorescence Microscopy
References:	263
Structure:	CCCCCCN1C(=O)c2c(C)c3cc4nc(cc5[nH]c(cc6nc(C(CCC(=O)OC)C6C)c(C1=O)c2[nH]3)c(C)c5C)c(COC1OC(CO)C(OC2OC(CO)C(O)C(O)C2O)C(O)C1O)c4CC
Name:	Fluoromycin
Localization:	3, 6
Method:	Fluorescence Microscopy
References:	279
Structure:	CC(O)C(NC(=O)CC(O)C(C)NC(=O)C(NC(=O)c1nc(nc(N)c1C)C(CC(N)=O)NCC([NH3+])C(N)=O)C(OC1OC(CO)C(O)C(O)C1OC1OC(CO)C(O)C(OC(N)=O)C1O)c1c[nH]cn1)C(=O)NC(OC1OC(C)C([NH3+])C(O)C1O)C(O)c1nc(cs1)-c1nc(cs1)C(=O)NCCCCNC(=S)[N-]F
Name:	TMR-Se
Localization:	3, 6
Method:	Fluorescence Microscopy
References:	295
Structure:	CN(C)c1ccc2c([Se]C3=CC(C=CC3=C2c2ccccc2)=[N+](C)C)c1
Name:	8-oxoguanine
Localization:	2, 3
Method:	Fluorescence Microscopy
References:	296
Structure:	NC1=NC(=O)C2=NC(=O)N=C2N1
Name:	TMPyP; meso-tetra(4-N-

	methylpyridyl)porphyrin
Localization:	1, 3
Method:	Fluorescence Microscopy
References:	299
Structure:	C[n+]1ccc(cc1)-c1c2ccc(n2)c(-c2cc[n+](C)cc2)c2ccc([nH]2)c(-c2cc[n+](C)cc2)c2ccc([nH]2)c(-c2cc[n+](C)cc2)c2ccc1n2
Name:	PF-TMRos
Localization:	1, 2
Method:	Fluorescence Microscopy
References:	306
Structure:	CN(C)c1ccc2c(OC3=CC(C=CC3=C2c2c(F)c(F)c(F)c(F)c2F)=[N+](C)C)c1
Name:	PEG-HPPt; diammine{7,12-bis[1-(polyethyleneglycol-750-monomethylether-1-yl)ethyl]-3,8,13,17-2,18-dipropionato}platinum(II)tetramethylporphyrin-
Localization:	4, 5
Method:	Fluorescence Microscopy
References:	313
Structure:	COCCOCCOCCOCCOCCOCCOCCOCCOCCOCCOCCOCCOCCOCCOCCOCCOCCOCC(C)c1c(C)c2cc3[nH]c(cc4nc5cc6[nH]c(cc1n2)c(C)c6CCC(=O)O[Pt--](N)(N)OC(=O)Cc5c4C)c(C)c3C(C)OCCOCCOCCOCCOCCOCCOCCOCCOCCOCCOCCOCCOCCOCCOC
Name:	PEG-HP; 7,12-bis[1-(polyethyleneglycol-750-monomethylether-1-yl)ethyl]-3,8,13,17-tetramethylporphyrin-2,18-dipropionic acid
Localization:	4, 5
Method:	Fluorescence Microscopy
References:	313
Structure:	COCCOCCOCCOCCOCCOCCOCCOCCOCCOCCOCCOCCOCCOCCOCCOCC(C)c1c(C)c2cc3[nH]c(cc4nc(cc5[nH]c(cc1n2)c(C)c5CCC([O-])=O)c(CC([O-

	])=O)c4C)c(C)c3C(C)OCCOC COCCOCCOCCOCCOCCOC COCCOCCOCCOCCOCCOC COCCOCCOCCOC

Name:	DEHP
Localization:	2, 5
Method:	histo
References:	322
Structure:	CCCCC(CC)COC(=O)c1ccccc 1C(=O)OCC(CC)CCCC

Name:	C1311
Localization:	1, 3
Method:	Fluorescence Microscopy
References:	326
Structure:	CC[NH+](CC)CCNc1ccc2ncn 3-c4ccc(O)cc4C(=O)c1c23

Name:	RP 38422
Localization:	1, 3
Method:	Cell Fractionation
References:	331
Structure:	COC(=O)CSCC(=O)C1(O)CC (OC2CC([NH3+])C(O)C(C)O2)c2c(O)c3C(=O)c4c(OC)cccc4 C(=O)c3c(O)c2C1

Name:	RP 21080
Localization:	1, 3
Method:	Cell Fractionation
References:	331
Structure:	COc1cccc2C(=O)c3c(O)c4CC (O)(CC(OC5CCCC([NH3+])C 5)c4c(O)c3C(=O)c12)C(C)=O

Name:	SnEBC
Localization:	1, 4
Method:	Pharmacological Effect
References:	332
Structure:	CCc1c(C)c2cc3c(CC)c(C)c4n 3[SnH2]n3c(cc1n2)c(C)c(CC) c3cc1nc2c(cc(cc42)S([O-])(=O)=O)C1(C)CC

Name:	Porphyrin-Retinamide Derivative 4
Localization:	1, 5
Method:	Fluorescence Microscopy
References:	352
Structure:	CC(\C=C\C1=C(C)CCCC1(C) C)=C/C=C/C(C)=C/C(=O)NC COCCOCCOCCOCCOC COCCNC(=O)COCC(=O)Nc1 ccc(cc1)C1=C2\C=CC(=N\2)/

C(c2ccccc2)=C2NC(/C=C\2)= C(c2ccccc2)\C2=N\C(/C=C2)= C(/C2[NH2+]C\1C=C2)c1cccc c1

Name:	Porphyrin-Retinamide Derivative 5
Localization:	1, 5
Method:	Fluorescence Microscopy
References:	352
Structure:	CC(\C=C\C1=C(C)CCCC1(C) C)=C/C=C\C(C)=C/C(=O)NC COCCOCCOCCOCCOC COCCNC(=O)COCC(=O)Nc1 ccc(cc1)C1=C2\C=CC(=N\2)/ C(c2ccccc2)=C2NC(/C=C\2)= C(c2ccccc2)\C2=N\C(/C=C2)= C(/C2[NH2+]C\1C=C2)c1cccc c1

Name:	Porphyrin-Peptide Conjugate 2
Localization:	1, 5
Method:	Fluorescence Microscopy
References:	378
Structure:	CC(C)C(NC(=O)C(CCCC[NH 3+])NC(=O)C(CCCNC(N)=[N H2+])NC(=O)C(CCCC[NH3+]) NC(=O)C(CCCC[NH3+])NC(= O)C(CCCC[NH3+])NC(=O)C1 CCCN1C(=O)C1CCCN1C(=O)C(C)NC(=O)COCCOCCOCC OCCOCCOCCNC(=O)COCC(=O)Nc1ccc(cc1)-c1c2ccc(n2)c(-c2ccccc2)c2ccc([nH]2)c(-c2ccccc2)c2ccc(n2)c(-c2ccccc2)c2ccc1[nH]2)C(=O) NC(CCC([O-])=O)C(=O)NC(CC([O-])=O)C(=O)N1CCCC1C(=O)N C(CCCNC(N)=[NH2+])C(=O) NC(CCCC[NH3+])C(=O)NC(C CCC[NH3+])C(=O)NC(CCCN C(N)=[NH2+])C(=O)NC(CCC NC(N)=[NH2+])C(=O)NC(CC C(N)=O)C(=O)NC(CCCNC(N) =[NH2+])C(=O)NC(CCCNC(N)=[NH2+])C(=O)NC(CCCNC(N)=[NH2+])C(=O)N1CCCC1C (=O)N1CCCC1C(=O)NC(CCC (N)=O)C(=O)NCC([O-])=O

Name:	Si(sol)2PC
Localization:	4, 6

Method:	Fluorescence Microscopy
References:	379
Structure:	CC1(C)OCC(CO[Si]2(OCC3COC(C)(C)O3)N3C4\N=C5/N=C(/N=C6\N2\C(=N/C2=N/C(=N\C3c3ccccc43)c3ccccc23)c2ccccc62)c2ccccc52)O1
Name:	PS6A
Localization:	1, 2, 5
Method:	Fluorescence Microscopy
References:	400
Structure:	CCCc1cc2cc3[nH]c(cc4nc(cc4CCC)cc4[nH]c(cc4CCC)cc1n2)c(c3CCC)S(=O)(=O)N(C)CCCCCC[N+](C)(C)C
Name:	PEG-Functionalized meso-TPP Conjugate 6
Localization:	2, 5
Method:	Fluorescence Microscopy
References:	393
Structure:	[O-]C(=O)COCCOCCOCCOCCOCCOCCNC(=O)COCC(=O)Nc1ccc(cc1)-c1c2ccc(n2)c(-c2ccccc2)c2ccc([nH]2)c(-c2ccccc2)c2ccc(n2)c(-c2ccccc2)c2ccc1[nH]2
Name:	PEG-Functionalized meso-TPP Conjugate 7
Localization:	2, 5
Method:	Fluorescence Microscopy
References:	393
Structure:	[O-]C(=O)COCCOCCOCCOCCOCCOCCNC(=O)COCC(=O)Nc1ccc(cc1)-c1c2ccc(n2)c(-c2ccccc2)c2ccc([nH]2)c(-c2ccccc2)c2ccc(n2)c(-c2ccc(NC(=O)COCC(=O)NCCOCCOCCOCCOCCOCC([O-])=O)cc2)c2ccc1[nH]2
Name:	PEG-Functionalized meso-TPP Conjugate 8
Localization:	1, 2
Method:	Fluorescence Microscopy
References:	393
Structure:	[O-]C(=O)COCCOCCOCCOCCOCCOCCNC(=O)COCC(=O)Nc1ccc(cc1)-c1c2ccc(n2)c(-c2ccccc2)c2ccc([nH]2)c(-

	c2ccc(NC(=O)COCC(=O)NCCOCCOCCOCCOCCOCC([O-])=O)cc2)c2ccc(n2)c(-c2ccc(NC(=O)COCC(=O)NCCOCCOCCOCCOCCOCC([O-])=O)cc2)c2ccc1[nH]2
Name:	PEG-Functionalized meso-TPP Conjugate 9
Localization:	1, 2
Method:	Fluorescence Microscopy
References:	393
Structure:	[O-]C(=O)COCCOCCOCCOCCOCCOCCNC(=O)COCC(=O)Nc1ccc(cc1)-c1c2ccc(n2)c(-c2ccc(NC(=O)COCC(=O)NCCOCCOCCOCCOCCOCC([O-])=O)cc2)c2ccc([nH]2)c(-c2ccc(NC(=O)COCC(=O)NCCOCCOCCOCCOCCOCC([O-])=O)cc2)c2ccc(n2)c(-c2ccc(NC(=O)COCC(=O)NCCOCCOCCOCCOCCOCC([O-])=O)cc2)c2ccc1[nH]2
Name:	SNAFR-1
Localization:	2, 3, 5
Method:	Fluorescence Microscopy
References:	417
Structure:	Oc1ccc2c(OC3=CC=C4C(=O)C=CC=C4C3=C2c2ccccc2)c1
Name:	TPYR-PP
Localization:	4, 6
Method:	Fluorescence Microscopy
References:	436
Structure:	CCCCCCCCCCCCCCCCOc1ccc(cc1)-c1c2ccc(n2)c(-c2ccncc2)c2ccc([nH]2)c(-c2ccncc2)c2ccc(n2)c(-c2ccncc2)c2ccc1[nH]2
Name:	C16-TTP
Localization:	4, 6
Method:	Fluorescence Microscopy
References:	436
Structure:	CCCCCCCCCCCCCCCCOc1ccc(cc1)-c1c2ccc(n2)c(-c2ccc(C)cc2)c2ccc([nH]2)c(-c2ccc(C)cc2)c2ccc(n2)c(-c2ccc(C)cc2)c2ccc1[nH]2
Name:	Berberine
Localization:	2, 3, 6

Method:	Fluorescence Microscopy
References:	473
Structure:	COc1ccc2cc3-c4cc5OCOc5cc4CC[n+]3cc2c1OC
Name:	CO-1
Localization:	1, 3
Method:	Fluorescence Microscopy
References:	474
Structure:	CN1C(=O)C=C2c3ccccc3C(=O)c3c(NCC[NH+](C)C)ccc1c23
Name:	CO-3
Localization:	1, 4
Method:	Fluorescence Microscopy
References:	474
Structure:	CN1C(=O)C=C2c3ccccc3C(=O)c3c(NCCC[NH+](C)C)ccc1c23
Name:	CO-4
Localization:	1, 5
Method:	Fluorescence Microscopy
References:	474
Structure:	CC[NH2+]CCNc1ccc2N(C)C(=O)C=C3c4ccccc4C(=O)c1c23
Name:	CO-5
Localization:	1, 6
Method:	Fluorescence Microscopy
References:	474
Structure:	CC[NH+](CC)CCNc1ccc2N(C)C(=O)C=C3c4ccccc4C(=O)c1c23
Name:	CO-6
Localization:	1, 3
Method:	Fluorescence Microscopy
References:	474
Structure:	CN1C(=O)C=C2c3ccccc3C(=O)c3c(NCC[NH2+]CCO)ccc1c23
Name:	CO-7
Localization:	1, 3
Method:	Fluorescence Microscopy
References:	474
Structure:	CN1C(=O)C=C2c3ccccc3C(=O)c3c(NCC[NH3+])ccc1c23
Name:	4-Hydroxymethyl-3-

	aminoacridine Derivative 13
Localization:	3, 6
Method:	Fluorescence Microscopy
References:	478
Structure:	CCOC(=O)Nc1ccc2cc3ccc(N)c(CO)c3nc2c1
Name:	Polyamide-Bodipy FL Conjugate 1
Localization:	3, 6
Method:	Fluorescence Microscopy
References:	480
Structure:	C[NH+](C)CCCNC(=O)CCNC(=O)c1cc(NC(=O)c2cc(NC(=O)c3cc(NC(=O)c4cc(NC(=O)CCCNC(=O)c5cc(NC(=O)c6cc(NC(=O)c7cc(NC(=O)c8nccn8C)cn7CCCNC(=O)CCC7=[N+]8C(C=C7)=Cc7c(C)cc(C)n7[B-]8(F)F)cn6C)cn5C)cn4C)cn3C)cn2C)cn1C
Name:	Polyamide-Bodipy FL Conjugate 2
Localization:	3, 6
Method:	Fluorescence Microscopy
References:	480
Structure:	C[NH+](C)CCCNC(=O)CCNC(=O)c1cc(NC(=O)c2cc(NC(=O)c3cc(NC(=O)c4cc(NC(=O)CCCNC(=O)c5cc(NC(=O)c6cc(NC(=O)c7nc(NC(=O)c8nccn8C)cn7C)cn6CCCNC(=O)CCC6=[N+]7C(C=C6)=Cc6c(C)cc(C)n6[B-]7(F)F)cn5C)cn4C)cn3C)cn2C)cn1C
Name:	Polyamide-Bodipy FL Conjugate 3
Localization:	3, 6
Method:	Fluorescence Microscopy
References:	480
Structure:	C[NH+](C)CCCNC(=O)CCNC(=O)c1cc(NC(=O)c2nc(NC(=O)CCNC(=O)c3cc(NC(=O)c4nc(NC(=O)CCCNC(=O)c5cc(NC(=O)c6nc(NC(=O)CCNC(=O)c7cc(NC(=O)c8nccn8C)cn7CCCNC(=O)CCC7=[N+]8C(C=C7)=Cc7c(C)cc(C)n7[B-]8(F)F)cn6C)cn5C)cn4C)cn3C)cn2C)cn1C
Name:	Vecuronium

Localization:	2, 3
Method:	Cell Fractionation
References:	485
Structure:	CC(=O)OC1CC2CCC3C4CC(C(OC(C)=O)C4CCC3C2(C)CC1[NH+]1CCCCC1)[N+]1(C)CCCCC1
Name:	Org 6368
Localization:	2, 3
Method:	Cell Fractionation
References:	485
Structure:	CC(=O)OC1CC2CCC3C4CC(CC4CCC3C2(C)CC1[N+]1(C)CCCCC1)[N+]1(C)CCCCC1
Name:	Pancuronium
Localization:	1, 2
Method:	Cell Fractionation
References:	485
Structure:	CC(=O)OC1CC2CCC3C4CC(C(OC(C)=O)C4CCC3C2(C)CC1[N+]1(C)CCCCC1)[N+]1(C)CCCCC1
Name:	Ageladine A
Localization:	1, 4
Method:	Fluorescence Microscopy
References:	488
Structure:	Nc1[nH]c2cc(ncc2[nH+]1)-c1cc(Br)c(Br)[nH]1
Name:	Dimethyl-PEPEP
Localization:	2, 3
Method:	Fluorescence Microscopy
References:	502
Structure:	Cn1c(ccc1\C=C\c1cc[n+](C)cc1)\C=C\c1cc[n+](C)cc1

Name:	Chlorin 1
Localization:	1, 2, 5
Method:	Fluorescence Microscopy
References:	540
Structure:	OC1C(O)c2nc1c(-c1ccccc1)c1ccc([nH]1)c(-c1ccccc1)c1ccc(n1)c(-c1ccccc1)c1ccc([nH]1)c2-c1ccccc1
Name:	Chlorin 3
Localization:	1, 2
Method:	Fluorescence Microscopy
References:	540
Structure:	OC1C(O)c2nc1c(-c1cccc(O)c1)c1ccc([nH]1)c(-c1cccc(O)c1)c1ccc(n1)c(-c1cccc(O)c1)c1ccc([nH]1)c2-c1cccc(O)c1
Name:	Chlorin 4
Localization:	1, 2
Method:	Fluorescence Microscopy
References:	540
Structure:	COc1cccc(c1)-c1c2nc(C(O)C2O)c(-c2cccc(OC)c2)c2ccc([nH]2)c(-c2cccc(OC)c2)c2ccc(n2)c(-c2cccc(OC)c2)c2ccc1[nH]2
Name:	HDAO
Localization:	2, 6
Method:	Fluorescence Microscopy
References:	72
Structure:	CCCCCCCCCCCCCCCC[N+]1=C2C=C(C=CC2=CC2=C1C=C(C=C2)N(C)C)N(C)C

Appendix H

References to the dataset with subcellular localization information.

ID	References
1	Seglen PO, Gordon PB: **Effects of lysosomotropic monoamines, diamines, amino alcohols, and other amino compounds on protein degradation and protein synthesis in isolated rat hepatocytes**. *Mol Pharmacol* 1980, **18**(3):468-475.
2	Reasor MJ, Kacew S: **Drug-induced phospholipidosis: are there functional consequences?** *Exp Biol Med (Maywood)* 2001, **226**(9):825-830.
3	Cramb G: **Selective lysosomal uptake and accumulation of the beta-adrenergic antagonist propranolol in cultured and isolated cell systems**. *Biochem Pharmacol* 1986, **35**(8):1365-1372.
4	Horobin RW, Trapp S, Weissig V: **Mitochondriotropics: a review of their mode of action, and their applications for drug and DNA delivery to mammalian mitochondria**. *J Control Release* 2007, **121**(3):125-136.
5	Ishizaki J, Yokogawa K, Ichimura F, Ohkuma S: **Uptake of imipramine in rat liver lysosomes in vitro and its inhibition by basic drugs**. *J Pharmacol Exp Ther* 2000, **294**(3):1088-1098.
6	Ploemen JP, Kelder J, Hafmans T, van de Sandt H, van Burgsteden JA, Saleminki PJ, van Esch E: **Use of physicochemical calculation of pKa and CLogP to predict phospholipidosis-inducing potential: a case study with structurally related piperazines**. *Exp Toxicol Pathol* 2004, **55**(5):347-355.
7	Falgueyret JP, Desmarais S, Oballa R, Black WC, Cromlish W, Khougaz K, Lamontagne S, Masse F, Riendeau D, Toulmond S *et al*: **Lysosomotropism of basic cathepsin K inhibitors contributes to increased cellular potencies against off-target cathepsins and reduced functional selectivity**. *J Med Chem* 2005, **48**(24):7535-7543.
8	Fujimura H, Dekura E, Kurabe M, Shimazu N, Koitabashi M, Toriumi W: **Cell-based fluorescence assay for evaluation of new-drugs potential for phospholipidosis in an early stage of drug development**. *Exp Toxicol Pathol* 2007, **58**(6):375-382.
11	Li W, Yuan XM, Ivanova S, Tracey KJ, Eaton JW, Brunk UT: **3-Aminopropanal, formed during cerebral ischaemia, is a potent lysosomotropic neurotoxin**. *Biochem J* 2003, **371**(Pt 2):429-436.
12	Gabrielli D, Belisle E, Severino D, Kowaltowski AJ, Baptista MS: **Binding, aggregation and photochemical properties of methylene blue in mitochondrial suspensions**. *Photochem Photobiol* 2004, **79**(3):227-232.
13	Bielawska A, Bielawski J, Szulc ZM, Mayroo N, Liu X, Bai A, Elojeimy S, Rembiesa B, Pierce J, Norris JS *et al*: **Novel analogs of D-e-MAPP and B13. Part 2: signature effects on bioactive sphingolipids**. *Bioorg Med Chem* 2008, **16**(2):1032-1045.
14	Dykens JA, Jamieson JD, Marroquin LD, Nadanaciva S, Xu JJ, Dunn MC, Smith AR, Will Y: **In vitro assessment of mitochondrial dysfunction and cytotoxicity of nefazodone, trazodone, and buspirone**. *Toxicol Sci* 2008, **103**(2):335-345.

17 Chen VY, Posada MM, Zhao L, Rosania GR: **Rapid doxorubicin efflux from the nucleus of drug-resistant cancer cells following extracellular drug clearance**. *Pharm Res* 2007, **24**(11):2156-2167.

19 Horton KL, Stewart KM, Fonseca SB, Guo Q, Kelley SO: **Mitochondria-penetrating peptides**. *Chem Biol* 2008, **15**(4):375-382.

23 Feldman S, Wang MY, Kaloyanides GJ: **Aminoglycosides induce a phospholipidosis in the renal cortex of the rat: an early manifestation of nephrotoxicity**. *J Pharmacol Exp Ther* 1982, **220**(3):514-520.

24 Martin WJ, 2nd, Standing JE: **Amiodarone pulmonary toxicity: biochemical evidence for a cellular phospholipidosis in the bronchoalveolar lavage of human subjects**. *J Pharmacol Exp Ther* 1988, **244**(2):774-779.

25 Smith RA, Porteous CM, Gane AM, Murphy MP: **Delivery of bioactive molecules to mitochondria in vivo**. *Proc Natl Acad Sci U S A* 2003, **100**(9):5407-5412.

26 Ross MF, Prime TA, Abakumova I, James AM, Porteous CM, Smith RA, Murphy MP: **Rapid and extensive uptake and activation of hydrophobic triphenylphosphonium cations within cells**. *Biochem J* 2008, **411**(3):633-645.

27 Weiss MJ, Wong JR, Ha CS, Bleday R, Salem RR, Steele GD, Jr., Chen LB: **Dequalinium, a topical antimicrobial agent, displays anticarcinoma activity based on selective mitochondrial accumulation**. *Proc Natl Acad Sci U S A* 1987, **84**(15):5444-5448.

28 Terasaki M, Song J, Wong JR, Weiss MJ, Chen LB: **Localization of endoplasmic reticulum in living and glutaraldehyde-fixed cells with fluorescent dyes**. *Cell* 1984, **38**(1):101-108.

29 Fantin VR, Berardi MJ, Scorrano L, Korsmeyer SJ, Leder P: **A novel mitochondriotoxic small molecule that selectively inhibits tumor cell growth**. *Cancer Cell* 2002, **2**(1):29-42.

31 Zhao KS, Zhao GM, Wu DL, Soong Y, Birk AV, Schiller PW, Szeto HH: **Cell-permeable peptide antioxidants targeted to inner mitochondrial membrane inhibit mitochondrial swelling, oxidative cell death, and reperfusion injury**. *Journal of Biological Chemistry* 2004, **279**(33):34682-34690.

33 Fernandez-Carneado J, Van Gool M, Martos V, Castel S, Prados P, de Mendoza J, Giralt E: **Highly efficient, nonpeptidic oligoguanidinium vectors that selectively internalize into mitochondria**. *J Am Chem Soc* 2005, **127**(3):869-874.

37 Burns RJ, Smith RAJ, Murphy MP: **Synthesis and Characterization of Thiobutyltriphenylphosphonium Bromide, a Novel Thiol Reagent Targeted to the Mitochondrial Matrix**. *Archives of Biochemistry and Biophysics* 1995, **322**(1):60-68.

38 Filipovska A, Kelso GF, Brown SE, Beer SM, Smith RAJ, Murphy MP: **Synthesis and characterization of a triphenylphosphonium-conjugated peroxidase mimetic - Insights into the interaction of ebselen with mitochondria**. *Journal of Biological Chemistry* 2005, **280**(25):24113-24126.

39 James AM, Blaikie FH, Smith RAJ, Lightowlers RN, Smith PM, Murphy MP: **Specific targeting of a DNA-alkylating reagent to mitochondria - Synthesis and characterization of [4-((11aS)-7-methoxy-1,2,3,11a-tetrahydro-5H-pyrrolo[2,1-c][1,4]benzodiazepin-5-on-8-oxy)butyl]-triphenylphosphonium iodide**. *European Journal of Biochemistry* 2003, **270**(13):2827-2836.

41 Kowaltowski AJ, Turin J, Indig GL, Vercesi AE: **Mitochondrial effects of triarylmethane dyes**. *J Bioenerg Biomembr* 1999, **31**(6):581-590.

42 Martin WJ, Kachel DL, Vilen T, Natarajan V: **Mechanism of Phospholipidosis in Amiodarone Pulmonary Toxicity**. *Journal of Pharmacology and Experimental Therapeutics* 1989, **251**(1):272-278.

44 Li W, Yuan XM, Nordgren G, Dalen H, Dubowchik GM, Firestone RA, Brunk UT: **Induction of cell death by the lysosomotropic detergent MSDH**. *Febs Letters* 2000, **470**(1):35-39.

45 Boya P, Gonzalez-Polo RA, Poncet D, Andreau K, Vieira HLA, Roumier T, Perfettini JL, Kroemer G: **Mitochondrial membrane permeabilization is a critical step of lysosome-initiated apoptosis induced by hydroxychloroquine**. *Oncogene* 2003, **22**(25):3927-3936.

46 Dubowchik GM, Gawlak SL, Firestone RA: **The in vitro effects of three lysosomotropic detergents against three human tumor cell lines** *Bioorganic & Medicinal Chemistry Letters* 1995, **5**(8):893-898.

47 Dodin G, Averbeck D, Demerseman P, Nocentini S, Dupont J: **Mitochondrial Uptake of Bridged Bis-Methylpyridinium Aldoximes and Induction of the Petite Phenotype in Yeast**. *Biochemical and Biophysical Research Communications* 1991, **179**(2):992-999.

49 Davey GP, Tipton KF, Murphy MP: **Uptake and Accumulation of 1-Methyl-4-Phenylpyridinium by Rat-Liver Mitochondria Measured Using an Ion-Selective Electrode**. *Biochemical Journal* 1992, **288**:439-443.

50 Poot M, Zhang YZ, Kramer JA, Wells KS, Jones L, Hanzel DK, Lugade AG, Singer VL, Haughland RP: **Analysis of mitochondrial morphology and function with novel fixable fluorescent stains**. *Journal of Histochemistry & Cytochemistry* 1996, **44**(12):1363-1372.

51 Niemann A, Takatsuki A, Elsasser HP: **The lysosomotropic agent monodansylcadaverine also acts as a solvent polarity probe**. *Journal of Histochemistry & Cytochemistry* 2000, **48**(2):251-258.

52 Gravance CG, Garner DL, Miller MG, Berger T: **Flow cytometric assessment of changes in rat sperm mitochondrial function after treatment with pentachlorophenol**. *Toxicology in Vitro* 2003, **17**(3):253-257.

54 Deng YP, Bennink JR, Kang HC, Haugland RP, Yewdell JW: **Fluorescent Conjugates of Brefeldin-a Selectively Stain the Endoplasmic-Reticulum and Golgi-Complex of Living Cells**. *Journal of Histochemistry & Cytochemistry* 1995, **43**(9):907-915.

55 Simmons DM, Mercer AV, Hallas G, Dyson JE: **Characterization of six textile dyes as fluorescent stains for flow cytometry**. *J Histochem Cytochem* 1990, **38**(1):41-49.

57 Bucana C, Saiki I, Nayar R: **Uptake and Accumulation of the Vital Dye Hydroethidine in Neoplastic-Cells**. *Journal of Histochemistry & Cytochemistry* 1986, **34**(9):1109-1115.

58 Hoff SF, Macinnis AJ: **Ultrastructural-Localization of Phenothiazines and Tetracycline - a New Histochemical Approach**. *Journal of Histochemistry & Cytochemistry* 1983, **31**(5):613-625.

62 Niemann A, Baltes J, Elsasser HP: **Fluorescence properties and staining behavior of monodansylpentane, a structural homologue of the lysosomotropic agent monodansylcadaverine**. *Journal of Histochemistry & Cytochemistry* 2001, **49**(2):177-185.

64 Jeannot V, Salmon JM, Deumie M, Viallet P: **Intracellular accumulation of rhodamine 110 in single living cells**. *Journal of Histochemistry & Cytochemistry* 1997, **45**(3):403-412.

66 Muller T: **Electron microscopic demonstration of intracelluar promethazine**

accumulation sites by a precipitation technique: application to the cerebellar cortex of the mouse. *J Histochem Cytochem* 1996, **44**(5):531-535.

69   Jeon CJ, Masland RH: **Selective accumulation of diamidino yellow and chromomycin A3 by retinal glial cells**. *J Histochem Cytochem* 1993, **41**(11):1651-1658.

71   Suzuki T, Fujikura K, Higashiyama T, Takata K: **DNA staining for fluorescence and laser confocal microscopy**. *J Histochem Cytochem* 1997, **45**(1):49-53.

72   Rodriguez ME, Azizuddin K, Zhang P, Chiu SM, Lam M, Kenney ME, Burda C, Oleinick NL: **Targeting of mitochondria by 10-N-alkyl acridine orange analogues: role of alkyl chain length in determining cellular uptake and localization**. *Mitochondrion* 2008, **8**(3):237-246.

73   Weitering JG, Lammers W, Meijer DK, Mulder GJ: **Localization of d-tubocurarine in rat liver lysosomes. Lysosomal uptake, biliary excretion and displacement by quinacrine in vivo**. *Naunyn Schmiedebergs Arch Pharmacol* 1977, **299**(3):277-281.

74   Journey LJ, Goldstein MN: **The effect of terramycin on the fine structure of HeLa cell mitochondria**. *Cancer Res* 1963, **23**:551-554.

75   Rafael J, Nicholls DG: **Mitochondrial membrane potential monitored in situ within isolated guinea pig brown adipocytes by a styryl pyridinium fluorescent indicator**. *FEBS Lett* 1984, **170**(1):181-185.

76   Johnson LV, Walsh ML, Bockus BJ, Chen LB: **Monitoring of relative mitochondrial membrane potential in living cells by fluorescence microscopy**. *J Cell Biol* 1981, **88**(3):526-535.

77   Schneider K, Naujok A, Zimmermann HW: **Influence of trans-membrane potential and of hydrophobic interactions on dye accumulation in mitochondria of living cells. Photoaffinity labelling of mitochondrial proteins, action of potential dissipating drugs, and competitive staining**. *Histochemistry* 1994, **101**(6):455-461.

78   Hahn KM, Conrad PA, Chao JC, Taylor DL, Waggoner AS: **A photocross-linking fluorescent indicator of mitochondrial membrane potential**. *J Histochem Cytochem* 1993, **41**(4):631-634.

81   Ohulchanskyy TY, Pudavar HE, Yarmoluk SM, Yashchuk VM, Bergey EJ, Prasad PN: **A monomethine cyanine dye Cyan 40 for two-photon-excited fluorescence detection of nucleic acids and their visualization in live cells**. *Photochem Photobiol* 2003, **77**(2):138-145.

82   Jimenez-Hernandez ME, Orellana G, Montero F, Portoles MT: **A ruthenium probe for cell viability measurement using flow cytometry, confocal microscopy and time-resolved luminescence**. *Photochemistry and Photobiology* 2000, **72**(1):28-34.

83   Chen JY, Mak NK, Yow CMN, Fung MC, Chiu LC, Leung WN, Cheung NH: **The binding characteristics and intracellular localization of temoporfin (mTHPC) in myeloid leukemia cells: Phototoxicity and mitochondrial damage**. *Photochemistry and Photobiology* 2000, **72**(4):541-547.

84   Malik Z, Amit I, Rothmann C: **Subcellular localization of sulfonated tetraphenyl porphines in colon carcinoma cells by spectrally resolved imaging**. *Photochem Photobiol* 1997, **65**(3):389-396.

85   Konan YN, Chevallier J, Gurny R, Allemann E: **Encapsulation of p-THPP into nanoparticles: Cellular uptake, subcellular localization and effect of serum on photodynamic activity**. *Photochemistry and Photobiology* 2003, **77**(6):638-644.

86 Feofanov A, Sharonov G, Grichine A, Karmakova T, Pljutinskaya A, Lebedeva V, Ruziyev R, Yakubovskaya R, Mironov A, Refregier M *et al*: **Comparative study of photodynamic properties of 13,15-N-cycloimide derivatives of chlorin p6**. *Photochem Photobiol* 2004, **79**(2):172-188.

87 Wood SR, Holroyd JA, Brown SB: **The subcellular localization of Zn(II) phthalocyanines and their redistribution on exposure to light**. *Photochemistry and Photobiology* 1997, **65**(3):397-402.

88 Cauchon N, Nader M, Bkaily G, van Lier JE, Hunting D: **Photodynamic activity of substituted zinc trisulfophthalocyanines: Role of plasma membrane damage**. *Photochemistry and Photobiology* 2006, **82**(6):1712-1720.

90 Theodossiou T, Spiro MD, Jacobson J, Hothersall JS, MacRobert AJ: **Evidence for intracellular aggregation of hypericin and the impact on its photocytotoxicity in PAM 212 murine keratinocytes**. *Photochemistry and Photobiology* 2004, **80**(3):438-443.

92 MacDonald IJ, Morgan J, Bellnier DA, Paszkiewicz GM, Whitaker JE, Litchfield DJ, Dougherty TJ: **Subcellular localization patterns and their relationship to photodynamic activity of pyropheophorbide-a derivatives**. *Photochem Photobiol* 1999, **70**(5):789-797.

93 Chen JY, Cheung NH, Fung MC, Wen JM, Leung WN, Mak NK: **Subcellular localization of merocyanine 540 (MC540) and induction of apoptosis in murine myeloid leukemia cells**. *Photochemistry and Photobiology* 2000, **72**(1):114-120.

94 Sun X, Leung WN: **Photodynamic therapy with pyropheophorbide-a methyl ester in human lung carcinoma cancer cell: Efficacy, localization and apoptosis**. *Photochemistry and Photobiology* 2002, **75**(6):644-651.

95 Wilson BC, Olivo M, Singh G: **Subcellular localization of Photofrin(R) and aminolevulinic acid and photodynamic cross-resistance in vitro in radiation-induced fibrosarcoma cells sensitive or resistant to photofrin-mediated photodynamic therapy**. *Photochemistry and Photobiology* 1997, **65**(1):166-176.

96 Georgakoudi I, Foster TH: **Effects of the subcellular redistribution of two nile blue derivatives on photodynamic oxygen consumption**. *Photochemistry and Photobiology* 1998, **68**(1):115-122.

97 Ouedraogo G, Morliere P, Bazin N, Santus P, Kratzer B, Miranda MA, Castell JV: **Lysosomes are sites of fluoroquinolone photosensitization in human skin fibroblasts: A microspectrofluorometric approach**. *Photochemistry and Photobiology* 1999, **70**(2):123-129.

98 Kessel D, Poretz RD: **Sites of photodamage induced by photodynamic therapy with a chlorin e6 triacetoxymethyl ester (CAME)**. *Photochemistry and Photobiology* 2000, **71**(1):94-96.

99 Kessel D, Castelli M: **Evidence that bcl-2 is the target of three photosensitizers that induce a rapid apoptotic response**. *Photochemistry and Photobiology* 2001, **74**(2):318-322.

100 Kessel D, Reiners JJ, Jr.: **Apoptosis and autophagy after mitochondrial or endoplasmic reticulum photodamage**. *Photochem Photobiol* 2007, **83**(5):1024-1028.

101 Morliere P, Haigle J, Aissani K, Filipe P, Silva JN, Santus R: **An insight into the mechanisms of the phototoxic response induced by cyamemazine in cultured fibroblasts and keratinocytes**. *Photochemistry and Photobiology* 2004, **79**(2):163-171.

102 Delaey EM, Vantieghem AM, Derycke A, Agostinis PM, de Witte PAM: **In vitro**

photobiological evaluation of Rhodac, a new rhodacyanine photosensitizer. *Photochemistry and Photobiology* 2001, **74**(2):331-338.

104 Wang XP, Krebs LJ, Al-Nuri M, Pudavar HE, Ghosal S, Liebow C, Nagy AA, Schally AV, Prasad PN: **A chemically labeled cytotoxic agent: Two-photon fluorophore for optical tracking of cellular pathway in chemotherapy**. *Proceedings of the National Academy of Sciences of the United States of America* 1999, **96**(20):11081-11084.

106 Houghton PJ, Bailey FC, Houghton JA, Murti KG, Howbert JJ, Grindey GB: **Evidence for Mitochondrial Localization of N-(4-Methylphenylsulfonyl)-N'-(4-Chlorophenyl)Urea in Human Colon Adenocarcinoma Cells**. *Cancer Research* 1990, **50**(3):664-668.

108 Illinger D, Poindron P, Fonteneau P, Modollel M, Kuhry JG: **Internalization of the Lipophilic Fluorescent-Probe Trimethylamino-Diphenylhexatriene Follows the Endocytosis and Recycling of the Plasma-Membrane in Cells**. *Biochimica Et Biophysica Acta* 1990, **1030**(1):73-81.

109 Oseroff AR, Ohuoha D, Ara G, Mcauliffe D, Foley J, Cincotta L: **Intramitochondrial Dyes Allow Selective Invitro Photolysis of Carcinoma-Cells**. *Proceedings of the National Academy of Sciences of the United States of America* 1986, **83**(24):9729-9733.

110 Woodburn KW, Fan Q, Miles DR, Kessel D, Luo Y, Young SW: **Localization and efficacy analysis of the phototherapeutic lutetium texaphyrin (PCI-0123) in the murine EMT6 sarcoma model**. *Photochemistry and Photobiology* 1997, **65**(3):410-415.

111 Peng Q, Moan J, Farrants G, Danielsen HE, Rimington C: **Localization of Potent Photosensitizers in Human Tumor Lox by Means of Laser Scanning Microscopy**. *Cancer Letters* 1991, **58**(1-2):17-27.

112 Lin CW, Shulok JR, Kirley SD, Cincotta L, Foley JW: **Lysosomal Localization and Mechanism of Uptake of Nile Blue Photosensitizers in Tumor-Cells**. *Cancer Research* 1991, **51**(10):2710-2719.

115 Li Q, Kim Y, Namm J, Kulkarni A, Rosania GR, Ahn YH, Chang YT: **RNA-selective, live cell imaging probes for studying nuclear structure and function**. *Chemistry & Biology* 2006, **13**(6):615-623.

117 Morliere P, Maziere JC, Santus R, Smith CD, Prinsep MR, Stobbe CC, Fenning MC, Golberg JL, Chapman JD: **Tolyporphin: A natural product from cyanobacteria with potent photosensitizing activity against tumor cells in vitro and in vivo**. *Cancer Research* 1998, **58**(16):3571-3578.

118 Koller ME, Romslo I: **Uptake of Protoporphyrin-Ix by Isolated Rat-Liver Mitochondria**. *Biochemical Journal* 1980, **188**(2):329-335.

120 Kamishohara M, Kenney S, Domergue R, Vistica DT, Sausville EA: **Selective accumulation of the endoplasmic reticulum-Golgi intermediate compartment induced by the antitumor drug KRN5500**. *Exp Cell Res* 2000, **256**(2):468-479.

122 Sit KH, Bay BH, Paramanantham R, Tana HM, Wong KP: **Acidification-and-recovery induces nuclear accumulation of neutral red and DNA into human KB oral carcinoma cells**. *Cancer Letters* 1996, **104**(1):63-69.

125 Bonneau S, Morliere P, Brault D: **Dynamics of interactions of photosensitizers with lipoproteins and membrane-models: correlation with cellular incorporation and subcellular distribution**. *Biochemical Pharmacology* 2004, **68**(7):1443-1452.

126 Pleshkewych A, Maurer TC, Porter CW: **Ultrastructural-Changes in the Mitochondria of Intestinal Epithelium of Rodents Treated with**

Methylglyoxal-Bis(Guanylhydrazone). *Cancer Research* 1983, **43**(2):646-652.

127 Allison AC, Young MR: **Uptake of Dyes and Drugs by Living Cells in Culture**. *Life Sciences* 1964, **3**(12):1407-1414.

128 Dirks RW, Molenaar C, Tanke HJ: **Visualizing RNA molecules inside the nucleus of living cells**. *Methods* 2003, **29**(1):51-57.

130 Croce AC, Bottiroli G, Supino R, Favini E, Zuco V, Zunino F: **Subcellular localization of the camptothecin analogues, topotecan and gimatecan**. *Biochemical Pharmacology* 2004, **67**(6):1035-1045.

131 Pagano RE, Martin OC, Kang HC, Haugland RP: **A Novel Fluorescent Ceramide Analog for Studying Membrane Traffic in Animal-Cells - Accumulation at the Golgi-Apparatus Results in Altered Spectral Properties of the Sphingolipid Precursor**. *Journal of Cell Biology* 1991, **113**(6):1267-1279.

132 Pandey SK, Gryshuk AL, Graham A, Ohkubo K, Fukuzumi S, Dobhal MP, Zheng G, Ou ZP, Zhan RQ, Kadish KM *et al*: **Fluorinated photosensitizers: synthesis, photophysical, electrochemical, intracellular localization, in vitro photosensitizing efficacy and determination of tumor-uptake by F-19 in vivo NMR spectroscopy**. *Tetrahedron* 2003, **59**(50):10059-10073.

133 Kunwar A, Barik A, Mishra B, Rathinasamy K, Pandey R, Priyadarsini KI: **Quantitative cellular uptake, localization and cytotoxicity of curcumin in normal and tumor cells**. *Biochimica Et Biophysica Acta-General Subjects* 2008, **1780**(4):673-679.

136 Wells G, Suggitt M, Coffils M, Baig MAH, Howard PW, Loadman PM, Hartley JA, Jenkins TC, Thurston DE: **Fluorescent 7-diethylaminocoumarin pyrrolobenzodiazepine conjugates: Synthesis, DNA interaction, cytotoxicity and differential cellular localization**. *Bioorganic & Medicinal Chemistry Letters* 2008, **18**(6):2147-2151.

137 Viola G, Facciolo L, Dall'Acqua S, Di Lisa F, Canton M, Vedaldi D, Fravolini A, Tabarrini O, Cecchetti V: **6-Aminoquinolones: photostability, cellular distribution and phototoxicity**. *Toxicology in Vitro* 2004, **18**(5):581-592.

138 Kessel D, Luguya R, Vicente MGH: **Localization and photodynamic efficacy of two cationic porphyrins varying in charge distribution**. *Photochemistry and Photobiology* 2003, **78**(5):431-435.

143 Tannenbaum J, Tanenbaum SW, Lo LW, Godman GC, Miranda AF: **Binding and Subcellular-Localization of Tritiated Cytochalasin-D**. *Experimental Cell Research* 1975, **91**(1):47-56.

144 Hetrakul N, Civelek C, Stagg CA, Udelsman R: **In vitro accumulation of technetium-99m-sestamibi in human parathyroid mitochondria**. *Surgery* 2001, **130**(6):1011-1018.

145 Scorneaux B, Shryock TR: **Intracellular accumulation, subcellular distribution, and efflux of tilmicosin in bovine mammary, blood, and lung cells**. *Journal of Dairy Science* 1999, **82**(6):1202-1212.

146 Pagano RE, Sepanski MA, Martin OC: **Molecular trapping of a fluorescent ceramide analogue at the Golgi apparatus of fixed cells: interaction with endogenous lipids provides a trans-Golgi marker for both light and electron microscopy**. *J Cell Biol* 1989, **109**(5):2067-2079.

147 Martin RM, Leonhardt H, Cardoso MC: **DNA labeling in living cells**. *Cytometry A* 2005, **67**(1):45-52.

148 Malinin GI: **Permanent Fluorescent Staining of Nucleic-Acids in Isolated Cells**. *Journal of Histochemistry & Cytochemistry* 1978, **26**(11):1018-1020.

149 Johannisson E, Thorell B: **Mithramycin Fluorescence for Quantitative-Determination of Deoxyribonucleic-Acid in Single Cells**. *Journal of Histochemistry & Cytochemistry* 1977, **25**(2):122-128.

154 Claudia Piccoli DB, and Nazzareno Capitanio: **Comparative analysis of mitochondria selective dyes in different cell types detected by confocal laser scanning microscopy: methods and applications**. In: *Current Issues on Multidisciplinary Microscopy Research and Education.* Edited by L.Labajos-Broncano AM-Va. Badajoz, Spain; 2004: 130-139.

156 Szeto HH, Schiller PW, Zhao K, Luo G: **Fluorescent dyes alter intracellular targeting and function of cell-penetrating tetrapeptides**. *FASEB J* 2005, **19**(1):118-120.

159 Best TP, Edelson BS, Nickols NG, Dervan PB: **Nuclear localization of pyrrole-imidazole polyamide-fluorescein conjugates in cell culture**. *Proceedings of the National Academy of Sciences of the United States of America* 2003, **100**(21):12063-12068.

160 Villa P, Sassella D, Corada M, Bartosek I: **Toxicity, Uptake, and Subcellular-Distribution in Rat Hepatocytes of Roxithromycin, a New Semisynthetic Macrolide, and Erythromycin Base**. *Antimicrobial Agents and Chemotherapy* 1988, **32**(10):1541-1546.

161 Nassberger L, Bergstrand A, Depierre JW: **Intracellular-Distribution of Gentamicin within the Rat-Kidney Cortex - a Cell Fractionation Study**. *Experimental and Molecular Pathology* 1990, **52**(2):212-220.

162 Schwab JC, Cao Y, Slowik MR, Joiner KA: Localization of azithromycin in Toxoplasma gondii-infected cells. Antimicrob Agents Chemother 1994, 38(7):1620-1627.

163 van Zandvoort MAMJ, de Grauw CJ, Gerritsen HC, Broers JLV, Egbrink MGAO, Ramaekers FCS, Slaaf DW: **Discrimination of DNA and RNA in cells by a vital fluorescent probe: Lifetime Imaging of SYTO13 in healthy and apoptotic cells**. *Cytometry* 2002, **47**(4):226-235.

164 Crissman HA, Oka MS, Steinkamp JA: **Rapid staining methods for analysis of deoxyribonucleic acid and protein in mammalian cells**. *J Histochem Cytochem* 1976, **24**(1):64-71.

168 Steinberg SF, Bilezikian JP, Alawqati Q: **Fura-2 Fluorescence Is Localized to Mitochondria in Endothelial-Cells**. *American Journal of Physiology* 1987, **253**(5):C744-C747.

169 McLachlan A, Kekre N, McNulty J, Pandey S: **Pancratistatin: A natural anti-cancer compound that targets mitochondria specifically in cancer cells to induce apoptosis**. *Apoptosis* 2005, **10**(3):619-630.

170 Nieto-Miguel T, Gajate C, Mollinedo F: **Differential targets and subcellular localization of antitumor alkyl-lysophospholipid in leukemic versus solid tumor cells**. *Journal of Biological Chemistry* 2006, **281**(21):14833-14840.

171 Tremblay JF, Dussault S, Viau G, Gad F, Boushira M, Bissonnette R: **Photodynamic therapy with toluidine blue in Jurkat cells: cytotoxicity, subcellular localization and apoptosis induction**. *Photochemical & Photobiological Sciences* 2002, **1**(11):852-856.

172 Zhang LL, Tardy M, Berry JP, Escaig F, Galle P: **Subcellular localization of two neurotropic drugs in three varieties of central nervous system cells by secondary ion mass spectroscopy (SIMS) microscopy**. *Biol Cell* 1992, **74**(1):99-103.

173 Bain JA, Mayer SE: **The intracellular localization of fluorescent convulsants**. *J Pharmacol Exp Ther* 1956, **118**(1):1-16.

174 Mellett LB, Woods LA: **Intracellular Distribution of N-C-14-Methyl Levorphanol in Brain, Liver and Kidney Tissue of the Rat**. *Journal of Pharmacology and Experimental Therapeutics* 1959, **125**(2):97-104.

175 Daniel WA, Wojcikowski J, Palucha A: **Intracellular distribution of psychotropic drugs in the grey and white matter of the brain: the role of lysosomal trapping**. *British Journal of Pharmacology* 2001, **134**(4):807-814.

176 Crowley KS, Phillion DP, Woodard SS, Schweitzer BA, Singh M, Shabany H, Burnette B, Hippenmeyer P, Heitmeier M, Bashkin JK: **Controlling the intracellular localization of fluorescent polyamide analogues in cultured cells**. *Bioorganic & Medicinal Chemistry Letters* 2003, **13**(9):1565-1570.

178 McGill A, Frank A, Emmett N, Leech SN, Turnbull DM, Birch-Machin MA, Reynolds NJ: **The antipsoriatic drug anthralin accumulates in keratinocyte mitochondria, dissipates mitochondrial membrane potential, and induces apoptosis through a pathway dependent on respiratory competent mitochondria**. *Faseb Journal* 2005, **19**(3):1012-+.

180 Byvoet P, Busch H: **Intracellular Distribution of 5-Bis (2-Chloroethyl)Aminouracil-2-C14 in Tissues of Tumor-Bearing Rats**. *Cancer Research* 1962, **22**(2):249-&.

184 Woodburn KW: **Intracellular localization of the radiation enhancer motexafin gadolinium using interferometric Fourier fluorescence microscopy**. *Journal of Pharmacology and Experimental Therapeutics* 2001, **297**(3):888-894.

185 Darzynkiewicz Z, Carter SP: **Photosensitizing Effects of the Tricyclic Heteroaromatic Cationic Dyes Pyronin-Y and Toluidine Blue-O (Tolonium Chloride)**. *Cancer Research* 1988, **48**(5):1295-1299.

186 Miller GG, Brown K, Ballangrud AM, Barajas O, Xiao Z, Tulip J, Lown JW, Leithoff JM, AllalunisTurner MJ, Mehta RD *et al*: **Preclinical assessment of hypocrellin B and hypocrellin B derivatives as sensitizers for photodynamic therapy of cancer: Progress update**. *Photochemistry and Photobiology* 1997, **65**(4):714-722.

188 Andre N, Carre M, Brasseur G, Pourroy B, Kovacic H, Briand C, Braguer D: **Paclitaxel targets mitochondria upstream of caspase activation in intact human neuroblastoma cells**. *Febs Letters* 2002, **532**(1-2):256-260.

189 Benz CC, Keniry MA, Ford JM, Townsend AJ, Cox FW, Palayoor S, Matlin SA, Hait WN, Cowan KH: **Biochemical Correlates of the Antitumor and Antimitochondrial Properties of Gossypol Enantiomers**. *Molecular Pharmacology* 1990, **37**(6):840-847.

190 Koya K, Li Y, Wang H, Ukai T, Tatsuta N, Kawakami M, Shishido T, Chen LB: **MKT-077, a novel rhodacyanine dye in clinical trials, exhibits anticarcinoma activity in preclinical studies based on selective mitochondrial accumulation**. *Cancer Research* 1996, **56**(3):538-543.

192 Roy MK, Thalang VN, Trakoontivakorn G, Nakahara K: **Mahanine, a carbazole alkaloid from Micromelum minutum, inhibits cell growth and induces apoptosis in U937 cells through a mitochondrial dependent pathway**. *British Journal of Pharmacology* 2005, **145**(2):145-155.

193 Li C, Greenwood TR, Glunde K: **Glucosamine-bound near-infrared fluorescent probes with lysosomal specificity for breast tumor imaging**. *Neoplasia* 2008, **10**(4):389-398.

195 Marshall LA, Rhee MS, Hofmann L, Khodjakov A, Schneider E: **Increased lysosomal uptake of methotrexate-polyglutamates in two methotrexate-resistant cell lines with distinct mechanisms of resistance**. *Biochemical*

Pharmacology 2005, **71**(1-2):203-213.

196   Schneider P: **Drug-Induced Lysosomal Disorders in Laboratory-Animals - New Substances Acting on Lysosomes**. *Archives of Toxicology* 1992, **66**(1):23-33

201   Van Bambeke F, Carryn S, Seral C, Chanteux H, Tyteca D, Mingeot-Leclercq MP, Tulkens PM: **Cellular pharmacokinetics and pharmacodynamics of the glycopeptide antibiotic oritavancin (LY333328) in a model of J774 mouse macrophages**. *Antimicrob Agents Chemother* 2004, **48**(8):2853-2860.

205   Philips FS, Sternberg SS, Cronin AP, Sodergren JE, Vidal PM: Physiologic disposition and intracellular localization of isometamidium. Cancer Res 1967, 27(2):333-349.

206   Dindo D, Dahm F, Szulc Z, Bielawska A, Obeid LM, Hannun YA, Graf R, Clavien PA: **Cationic long-chain ceramide LCL-30 induces cell death by mitochondrial targeting in SW403 cells**. *Molecular Cancer Therapeutics* 2006, **5**(6):1520-1529.

208   Beauchamp D, Gourde P, Simard M, Bergeron MG: **Subcellular-Localization of Tobramycin and Vancomycin Given Alone and in Combination in Proximal Tubular Cells, Determined by Immunogold Labeling**. *Antimicrobial Agents and Chemotherapy* 1992, **36**(10):2204-2210.

209   Renard C, Vanderhaeghe HJ, Claes PJ, Zenebergh A, Tulkens PM: **Influence of Conversion of Penicillin-G into a Basic Derivative on Its Accumulation and Subcellular-Localization in Cultured Macrophages**. *Antimicrobial Agents and Chemotherapy* 1987, **31**(3):410-416.

210   Takeuchi Y, Ichikawa K, Yonezawa S, Kurohane K, Koishi T, Nango M, Namba Y, Oku N: **Intracellular target for photosensitization in cancer antiangiogenic photodynamic therapy mediated by polycation liposome**. *J Control Release* 2004, **97**(2):231-240.

211   Sibrian-Vazquez M, Nesterova IV, Jensen TJ, Vicente MGH: **Mitochondria targeting by guanidine-and biguanidine-porphyrin photosensitizers**. *Bioconjugate Chemistry* 2008, **19**(3):705-713.

212   Chen Y, Graham A, Potter W, Morgan J, Vaughan L, Bellnier DA, Henderson BW, Oseroff A, Dougherty TJ, Pandey RK: **Bacteriopurpurinimides: highly stable and potent photosensitizers for photodynamic therapy**. *J Med Chem* 2002, **45**(2):255-258

214   Trivedi NS, Wang HW, Nieminen AL, Oleinick NL, Izatt JA: **Quantitative analysis of Pc 4 localization in mouse lymphoma (LY-R) cells via double-label confocal fluorescence microscopy**. *Photochemistry and Photobiology* 2000, **71**(5):634-639.

215   Maisch T, Bosl C, Szeimies RM, Lehn N, Abels C: **Photodynamic effects of novel XF porphyrin derivatives on prokaryotic and eukaryotic cells**. *Antimicrob Agents Chemother* 2005, **49**(4):1542-1552.

216   Mak NK, Li KM, Leung WN, Wong RNS, Huang DP, Lung ML, Lau YK, Chang CK: **Involvement of both endoplasmic reticulum and mitochondria in photokilling of nasopharyngeal carcinoma cells by the photosensitizer Zn-BC-AM**. *Biochemical Pharmacology* 2004, **68**(12):2387-2396.

217   Lo PC, Huang JD, Cheng DYY, Chan EYM, Fong WP, Ko WH, Ng DKP: **New amphiphilic silicon(IV) phthalocyanines as efficient Photosensitizers for photodynamic therapy: Synthesis, photophysical properties, and in vitro photodynamic activities**. *Chemistry-a European Journal* 2004, **10**(19):4831-4838.

218   Rosenfeld A, Morgan J, Goswami LN, Hulchanskyy T, Zheng X, Prasad PN,

Seroff A, Pandey RK: **Photosensitizers derived from 13(2) oxo-methyl pyropheophorbide-a: Enhanced effect of indium(III) as a central metal in in vitro and in vivo photosensitizing efficacy**. *Photochemistry and Photobiology* 2006, **82**(3):626-634.

219   Naumovski L, Ramos J, Sirisawad M, Chen J, Thiemann P, Lecane P, Magda D, Wang Z, Cortez C, Boswell G *et al*: **Sapphyrins induce apoptosis in hematopoietic tumor-derived cell lines and show in vivo antitumor activity**. *Molecular Cancer Therapeutics* 2005, **4**(6):968-976.

220   Tirand L, Thomas N, Dodeller M, Dumas D, Frochot C, Maunit B, Guillemin F, Barberi-Heyob M: **Metabolic profile of a peptide-conjugated chlorin-type photosensitizer targeting neuropilin-1: An in vivo and in vitro study**. *Drug Metabolism and Disposition* 2007, **35**(5):806-813.

221   Takayama.S, Ojima Y: **Photosensitizing Activity of Carcinogenic and Noncarcinogenic Polycyclic Hydrocarbons on Cultured Cells**. *Japanese Journal of Genetics* 1969, **44**(4):231-&.

222   Matroule JY, Bonizzi G, Morliere P, Paillous N, Santus R, Bours V, Piette J: **Pyropheophorbide-a methyl ester-mediated photosensitization activates transcription factor NF-kappa B through the interleukin-1 receptor-dependent signaling pathway**. *Journal of Biological Chemistry* 1999, **274**(5):2988-3000.

223   Sayama K, Morishima A, Fujita H, Ito A, Nakamura K, Sasaki M: **Possible targets of sparfloxacine-photosensitization in human buccal mucosa cells as revealed by fluorescence microscopy and microspectrofluorometry**. *Journal of Photopolymer Science and Technology* 2003, **16**(5):655-660.

227   Sharonov GV, Karmakova TA, Kassies R, Pljutinskaya AD, Grin MA, Refregiers M, Yakubovskaya RI, Mironov AF, Maurizot JC, Vigny P *et al*: **Cycloimide bacteriochlorin p derivatives: Photodynamic properties and cellular and tissue distribution**. *Free Radical Biology and Medicine* 2006, **40**(3):407-419.

229   Ohkuma S, Poole B: **Cytoplasmic Vacuolation of Mouse Peritoneal-Macrophages and the Uptake into Lysosomes of Weakly Basic Substances**. *Journal of Cell Biology* 1981, **90**(3):656-664.

230   Barile M, Valenti D, Passarella S, Quagliariello E: **3'-Azido-3'-deoxythymidine uptake into isolated rat liver mitochondria and impairment of ADP/ATP translocator**. *Biochemical Pharmacology* 1997, **53**(7):913-920.

231   Cernay T, Zimmermann HW: **Selective photosensitization of mitochondria by the lipophilic cationic porphyrin POR10**. *Journal of Photochemistry and Photobiology B-Biology* 1996, **34**(2-3):191-196.

235   Feofanov A, Sharonov S, Fleury F, Kudelina I, Nabiev I: **Quantitative confocal spectral imaging analysis of mitoxantrone within living K562 cells: Intracellular accumulation and distribution of monomers, aggregates, naphthoquinoxaline metabolite, and drug-target complexes**. *Biophysical Journal* 1997, **73**(6):3328-3336.

236   Belhoussine R, Morjani H, Millot JM, Sharonov S, Manfait M: **Confocal scanning microspectrofluorometry reveals specific anthracyline accumulation in cytoplasmic organelles of multidrug-resistant cancer cells**. *Journal of Histochemistry & Cytochemistry* 1998, **46**(12):1369-1376.

238   Balaghi M, Pearson WN: **Tissue and Intracellular Distribution of Radioactive Thiamine in Normal and Thiamine-Deficient Rats**. *Journal of Nutrition* 1966, **89**(2):127-&.

240   Safaei R, Katano K, Larson BJ, Samimi G, Holzer AK, Naerdemann W, Tomioka M, Goodman M, Howell SB: **Intracellular localization and trafficking**

of fluorescein-labeled cisplatin in human ovarian carcinoma cells. *Clinical Cancer Research* 2005, **11**(2):756-767.

241 Vazifeh D, Bryskier A, Labro MT: **Mechanism underlying levofloxacin uptake by human polymorphonuclear neutrophils**. *Antimicrobial Agents and Chemotherapy* 1999, **43**(2):246-252.

242 Suzuki T, Kato Y, Sasabe H, Itose M, Miyamoto G, Sugiyama Y: **Mechanism for the tissue distribution of grepafloxacin, a fluoroquinolone antibiotic, in rats**. *Drug Metabolism and Disposition* 2002, **30**(12):1393-1399.

243 Lui A, Lumeng L, Li TK: **Transport of Pyridoxine and Pyridoxal 5'-Phosphate in Isolated Rat-Liver Mitochondria**. *Journal of Biological Chemistry* 1982, **257**(24):4903-4906.

244 Bereiter-Hahn J: **Dimethylaminostyrylmethylpyridiniumiodine (daspmi) as a fluorescent probe for mitochondria in situ**. *Biochim Biophys Acta* 1976, **423**(1):1-14.

245 Yang H, Wu T, Zhang M, Zhang Z: **A novel photosensitizer, 2-butylamino-2-demethoxy-hypocrellin B (2-BA-2-DMHB) - its photodynamic effects on HeLa cells: efficacy and apoptosis**. *Biochim Biophys Acta* 2001, **1540**(1):22-31.

246 Roding J, Naujok A, Zimmermann HW: **Effects of ethidium bromide, tetramethylethidium bromide and betaine B on the ultrastructure of HeLa cell mitochondria in situ. A comparative binding study**. *Histochemistry* 1986, **85**(3):215-222.

249 Lucocq J, Warren G, Pryde J: **Okadaic Acid Induces Golgi-Apparatus Fragmentation and Arrest of Intracellular-Transport**. *Journal of Cell Science* 1991, **100**:753-759.

250 Via LD, Marini AM, Salerno S, Toninello A: **Mitochondrial permeability transition induced by novel pyridothiopyranopyrimidine derivatives: Potential new antimitochondrial antitumour agents**. *Biochemical Pharmacology* 2006, **72**(12):1657-1667.

251 Carreon JR, Stewart KM, Mahon KP, Shin S, Kelley SO: **Cyanine dye conjugates as probes for live cell imaging**. *Bioorganic & Medicinal Chemistry Letters* 2007, **17**(18):5182-5185.

252 Schiller CM: **In vitro effects of substituted toluenes on mitochondria isolated from rat liver**. *Biochem Pharmacol* 1980, **29**(18):2485-2489.

253 Byczkowski JZ: **The mode of action of p,p'=DDT on mammalian mitochondria**. *Toxicology* 1976, **6**(3):309-314.

254 Telles-Pupulin AR, Salgueiro-Pagadigorria CL, Bracht A, Ishii-Iwamoto EL: **Effects of fusaric acid on rat liver mitochondria**. *Comp Biochem Physiol C Pharmacol Toxicol Endocrinol* 1998, **120**(1):43-51.

255 Fickweiler S, Abels C, Karrer S, Baumler W, Landthaler M, Hofstadter F, Szeimies RM: **Photosensitization of human skin cell lines by ATMPn (9-acetoxy-2,7,12,17-tetrakis-(beta-methoxyethyl)-porphycene) in vitro: mechanism of action**. *Journal of Photochemistry and Photobiology B-Biology* 1999, **48**(1):27-35.

258 Sharma SK, Morrissey AT, Miller GG, Gmeiner WH, Lown JW: **Design, synthesis, and intracellular localization of a fluorescently labeled DNA binding polyamide related to the antibiotic distamycin**. *Bioorganic & Medicinal Chemistry Letters* 2001, **11**(6):769-772.

260 Berry JP, Lespinats G, Escaig F, Boumati P, Tlouzeau S, Cavellier JF: **Intracellular localization of drugs in cultured tumor cells by ion microscopy and image processing**. *Histochemistry* 1990, **93**(4):397-400.

261 Duvvuri M, Konkar S, Funk RS, Krise JM, Krise JP: **A chemical strategy to manipulate the intracellular localization of drugs in resistant cancer cells**. *Biochemistry* 2005, **44**(48):15743-15749.

262 Loesberg C, Van Rooji H, Romijn JC, Smets LA: **Mitochondrial effects of the guanidino group-containing cytostatic drugs, m-iodobenzylguanidine and methylglyoxal bis (guanylhydrazone)**. *Biochem Pharmacol* 1991, **42**(4):793-798.

263 Pandey SK, Zheng X, Morgan J, Missert JR, Liu TH, Shibata M, Bellnier DA, Oseroff AR, Henderson BW, Dougherty TJ *et al*: **Purpurinimide carbohydrate conjugates: effect of the position of the carbohydrate moiety in photosensitizing efficacy**. *Mol Pharm* 2007, **4**(3):448-464.

264 Yoshida H, Okumura K, Hori R: **Subcellular distribution of basic drugs accumulated in the isolated perfused lung**. *Pharm Res* 1987, **4**(1):50-53.

265 Miniati M, Paci A, Cocci F, Ciarimboli G, Monti S, Pistolesi M: **Mitochondria act as a reservoir for the basic amine HIPDM in the lung**. *European Respiratory Journal* 1996, **9**(11):2306-2312.

266 Fellous R, Coulaud D, Elabed I, Roques BP, Lepecq JB, Delain E, Gouyette A: **Cytoplasmic Accumulation of Ditercalinium in Rat Hepatocytes and Induction of Mitochondrial Damage**. *Cancer Research* 1988, **48**(22):6542-6549.

267 Salvi M, Brunati AM, Clari G, Toninello A: **Interaction of genistein with the mitochondrial electron transport chain results in opening of the membrane transition pore**. *Biochimica Et Biophysica Acta-Bioenergetics* 2002, **1556**(2-3):187-196.

268 Doherty WP, Campbell TC: **Aflatoxin Inhibition of Rat-Liver Mitochondria**. *Chemico-Biological Interactions* 1973, **7**(2):63-77.

269 Hayes AW: **Action of Rubratoxin-B on Mouse-Liver Mitochondria**. *Toxicology* 1976, **6**(2):253-261.

272 Whitaker JE, Haugland RP, Moore PL, Hewitt PC, Reese M, Haugland RP: **Cascade Blue Derivatives - Water-Soluble, Reactive, Blue Emission Dyes Evaluated as Fluorescent Labels and Tracers**. *Analytical Biochemistry* 1991, **198**(1):119-130.

275 Barraja P, Diana P, Montalbano A, Dattolo G, Cirrincione G, Viola G, Vedaldi D, Dall'Acqua F: **Pyrrolo[2,3-h]quinolinones: A new ring system with potent photoantiproliferative activity**. *Bioorganic & Medicinal Chemistry* 2006, **14**(24):8712-8728.

277 Tian E, Landowski TH, Stephens OW, Yaccoby S, Barlogie B, Shaughnessy JD: **Ellipticine derivative NSC 338258 represents a potential new antineoplastic agent for the treatment of multiple myeloma**. *Molecular Cancer Therapeutics* 2008, **7**(3):500-509.

278 Liu A, Pajkovic N, Pang Y, Zhu DW, Calamini B, Mesecar AL, van Breemen RB: **Absorption and subcellular localization of lycopene in human prostate cancer cells**. *Molecular Cancer Therapeutics* 2006, **5**(11):2879-2885.

279 Mistry JS, Jani JP, Morris G, Mujumdar RB, Reynolds IJ, Sebti SM, Lazo JS: **Synthesis and Evaluation of Fluoromycin - a Novel Fluorescence-Labeled Derivative of Talisomycin S10b**. *Cancer Research* 1992, **52**(3):709-718.

282 Egorin MJ, Clawson RE, Ross LA, Schlossberger NM, Bachur NR: **Cellular Accumulation and Disposition of Aclacinomycin-A**. *Cancer Research* 1979, **39**(11):4396-4400.

283 Noodt BB, Rodal GH, Wainwright M, Peng Q, Horobin R, Nesland JM, Berg K: **Apoptosis induction by different pathways with methylene blue derivative**

and light from mitochondrial sites in V79 cells. *International Journal of Cancer* 1998, **75**(6):941-948.

Barcia-Macay M, Mouaden F, Mingeot-Leclercq MP, Tulkens PM, Van Bambeke F: **Cellular pharmacokinetics of telavancin, a novel lipoglycopeptide antibiotic, and analysis of lysosomal changes in cultured eukaryotic cells (J774 mouse macrophages and rat embryonic fibroblasts)**. *J Antimicrob Chemother* 2008, **61**(6):1288-1294.

Jin L, Millard AC, Wuskell JP, Dong XM, Wu DQ, Clark HA, Loew LM: **Characterization and application of a new optical probe for membrane lipid domains**. *Biophysical Journal* 2006, **90**(7):2563-2575.

Jilkina O, Kong HJ, Hwi L, Kuzio B, Xiang B, Manley D, Jackson M, Kupriyanov VV: **Interaction of a mitochondrial membrane potential-sensitive dye, rhodamine 800, with rat mitochondria, cells, and perfused hearts**. *Journal of Biomedical Optics* 2006, **11**(1):-.

Hed J, Dahlgren C, Rundquist I: **A Simple Fluorescence Technique to Stain the Plasma-Membrane of Human-Neutrophils**. *Histochemistry* 1983, **79**(1):105-110.

Detty MR, Prasad PN, Donnelly DJ, Ohulchanskyy T, Gibson SL, Hilf R: **Synthesis, properties, and photodynamic properties in vitro of heavy-chalcogen analogues of tetramethylrosamine**. *Bioorganic & Medicinal Chemistry* 2004, **12**(10):2537-2544.

Soultanakis RP, Melamede RJ, Bespalov IA, Wallace SS, Beckman KB, Ames BN, Taatjes DJ, Janssen-Heininger YMW: **Fluorescence detection of 8-oxoguanine in nuclear and mitochondrial DNA of cultured cells using a recombinant Fab and confocal scanning laser microscopy**. *Free Radical Biology and Medicine* 2000, **28**(6):987-998.

Croce AC, Supino R, Lanza KS, Locatelli D, Baglioni P, Bottiroli G: **Photosensitizer accumulation in spontaneous multidrug resistant cells: a comparative study with Rhodamine 123, Rose Bengal acetate and Photofrin (R)**. *Photochemical & Photobiological Sciences* 2002, **1**(1):71-78.

Patito IA, Rothmann C, Malik Z: **Nuclear transport of photosensitizers during photosensitization and oxidative stress**. *Biology of the Cell* 2001, **93**(5):285-291.

Nuno Silva J, Haigle J, Tome JP, Neves MG, Tome AC, Maziere JC, Maziere C, Santus R, Cavaleiro JA, Filipe P *et al*: **Enhancement of the photodynamic activity of tri-cationic porphyrins towards proliferating keratinocytes by conjugation to poly-S-lysine**. *Photochem Photobiol Sci* 2006, **5**(1):126-133.

Ko YJ, Yun KJ, Kang MS, Park J, Lee KT, Park SB, Shin JH: **Synthesis and in vitro photodynamic activities of water-soluble fluorinated tetrapyridylporphyrins as tumor photosensitizers**. *Bioorganic & Medicinal Chemistry Letters* 2007, **17**(10):2789-2794.

Yslas EI, Durantini EN, Rivarola VA: **Zinc-(II) 2,9,16,23-tetrakis (methoxy) phthalocyanine: Potential photosensitizer for use in photodynamic therapy in vitro**. *Bioorganic & Medicinal Chemistry* 2007, **15**(13):4651-4660.

Chen SR, Gee KR: **Redox-dependent trafficking of 2,3,4,5,6-pentafluorodihydrotetramethylrosaimine, a novel fluorogenic indicator of cellular oxidative activity**. *Free Radical Biology and Medicine* 2000, **28**(8):1266-1278.

Hoyer-Hansen M, Bastholm L, Mathiasen IS, Elling F, Jaattela M: **Vitamin D analog EB1089 triggers dramatic lysosomal changes and Beclin 1-mediated autophagic cell death**. *Cell Death and Differentiation* 2005,

12(10):1297-1309.

S. Jones CM, A. Belzacq-Casagrande, C. Brenner and J. Howl: **Mitoparans: mitochondriotoxic cell penetratinb peptides and novel inducer of apoptosis**. In: *the 4th International Peptide Symposium in conjunction with the 7th Australian Peptide Conference and the 2nd Asia-Pacific International Peptide Symposium, 2007: 2007*; 2007.

309

Vickers AEM, Sipes IG, Brendel K: **Metabolism-Related Spectral Characterization and Subcellular-Distribution of Polychlorinated Biphenyl Congeners in Isolated Rat Hepatocytes**. *Biochemical Pharmacology* 1986, **35**(2):297-306.

312

Lottner C, Knuechel R, Bernhardt G, Brunner H: **Distribution and subcellular localization of a water-soluble hematoporphyrin-platinum(II) complex in human bladder cancer cells**. *Cancer Letters* 2004, **215**(2):167-177.

313

Dial LD, Anestis DK, Kennedy SR, Rankin GO: **Tissue distribution, subcellular localization and covalent binding of 2-chloroaniline and 4-chloroaniline in Fischer 344 rats**. *Toxicology* 1998, **131**(2-3):109-119.

315

Choie DD, del Campo AA, Guarino AM: **Subcellular localization of cis-dichlorodiammineplatinum(II) in rat kidney and liver**. *Toxicol Appl Pharmacol* 1980, **55**(2):245-252.

316

Woo YT, Argus MF, Arcos JC: **Tissue and Subcellular-Distribution of Dioxane-H-3 in Rat and Apparent Lack of Microsome-Catalyzed Covalent Binding in Target Tissue**. *Life Sciences* 1977, **21**(10):1447-1456.

317

Saito Y, Fukuhara A, Nishio K, Hayakawa M, Ogawa Y, Sakamoto H, Fujii K, Yoshida Y, Niki E: **Characterization of cellular uptake and distribution of coenzyme Q(10) and vitamin E in PC12 cells**. *J Nutr Biochem* 2008.

319

Ono H, Saito Y, Imai K, Kato M: **Subcellular distribution of di-(2-ethylhexyl)phthalate in rat testis**. *J Toxicol Sci* 2004, **29**(2):113-124

322

Scherer K, Abels C, Baumler W, Ackermann G, Szeimies RM: **Structure-activity relationships of three differently substituted 2,7,12,17-tetrakis-(beta-methoxyethyl) porphycene derivatives in vitro**. *Archives of Dermatological Research* 2004, **295**(12):535-541.

323

Ribou AC, Vigo J, Kohen E, Salmon JM: **Microfluorometric study of oxygen dependence of (1"-pyrene butyl)-2-rhodamine ester probe in mitochondria of living cells**. *Journal of Photochemistry and Photobiology B-Biology* 2003, **70**(2):107-115.

324

O'Malley YQ, Abdalla MY, McCormick ML, Reszka KJ, Denning GM, Britigan BE: **Subcellular localization of Pseudomonas pyocyanin cytotoxicity in human lung epithelial cells**. *American Journal of Physiology-Lung Cellular and Molecular Physiology* 2003, **284**(2):L420-L430.

325

Burger AM, Jenkins TC, Double JA, Bibby MC: **Cellular uptake, cytotoxicity and DNA-binding studies of the novel imidazoacridinone antineoplastic agent C1311**. *British Journal of Cancer* 1999, **81**(2):367-375.

326

Lansiaux A, Tanious F, Mishal Z, Dassonneville L, Kumar A, Stephens CE, Hu QY, Wilson WD, Boykin DW, Bailly C: **Distribution of furamidine analogues in tumor cells: Targeting of the nucleus or mitochondria depending on the amidine substitution**. *Cancer Research* 2002, **62**(24):7219-7229.

327

Cauchon N, Tian H, Langlois R, La Madeleine C, Martin S, Ali H, Hunting D, van Lier JE: **Structure-photodynamic activity relationships of substituted zinc trisulfophthalocyanines**. *Bioconjug Chem* 2005, **16**(1):80-89.

328

Boga C, Puggioli S, Gherpelli M, Farruggia G, Pagnotta E, Masotti L, Neyroz P: **Fluorescein conjugates of 9- and 10-hydroxystearic acids: synthetic**

329

strategies, photophysical characterization, and confocal microscopy applications. *Anal Biochem* 2004, **335**(2):196-209.

330 Liskamp RMJ, Brothman AR, Arcoleo JP, Miller OJ, Weinstein IB: **Cellular Uptake and Localization of Fluorescent Derivatives of Phorbol Ester Tumor Promoters**. *Biochemical and Biophysical Research Communications* 1985, **131**(2):920-927.

331 Londosgagliardi D, Capri M, Aubelsadron G, Maral R: **Subcellular-Localization of Some Anthracycline Derivatives in Ehrlich Ascites Tumor-Cells**. *Biochemical and Biophysical Research Communications* 1980, **97**(2):397-406.

332 Garbo GM: **Purpurins and benzochlorins as sensitizers for photodynamic therapy**. *Journal of Photochemistry and Photobiology B-Biology* 1996, **34**(2-3):109-116.

333 Berridge MV, Tan AS: **Characterization of the Cellular Reduction of 3-(4,5-Dimethylthiazol-2-Yl)-2,5-Diphenyltetrazolium Bromide (Mtt) - Subcellular-Localization, Substrate Dependence, and Involvement of Mitochondrial Electron-Transport in Mtt Reduction**. *Archives of Biochemistry and Biophysics* 1993, **303**(2):474-482.

337 Bell RG, Matschin.Jt: **Intracellular Distribution of Vitamin K in Rat**. *Biochimica Et Biophysica Acta* 1969, **184**(3):597-&.

343 Nair PP, Bucana C: **Intracellular distribution of vitamin D in rat liver**. *Biochim Biophys Acta* 1966, **124**(2):254-259.

348 Ban S, Nakagawa H, Suzuki T, Miyata N: **Novel mitochondria-localizing TEMPO derivative for measurement of cellular oxidative stress in mitochondria**. *Bioorg Med Chem Lett* 2007, **17**(7):2055-2058.

351 Ghosh SC, Auzenne E, Farquhar D, Klostergaard J: **N,N-Dimethylsphingosine-Coumarin: Synthesis, chemical characterization, and biological evaluation**. *Bioconjugate Chemistry* 2007, **18**(3):731-735.

352 Sibrian-Vazquez M, Jensen TJ, Vicente MG: **Porphyrin-retinamides: synthesis and cellular studies**. *Bioconjug Chem* 2007, **18**(4):1185-1193.

353 Li HR, Jensen TJ, Fronczek FR, Vicente MGH: **Syntheses and properties of a series of cationic water-soluble phthalocyanines**. *Journal of Medicinal Chemistry* 2008, **51**(3):502-511.

354 Sibrian-Vazquez M, Jensen TJ, Hammer RP, Vicente MG: **Peptide-mediated cell transport of water soluble porphyrin conjugates**. *J Med Chem* 2006, **49**(4):1364-1372.

355 Dickinson BC, Chang CJ: **A targetable fluorescent probe for imaging hydrogen peroxide in the mitochondria of living cells**. *Journal of the American Chemical Society* 2008, **130**(30):9638-+.

357 Amit I, Malik Z, Kessel D: **Photoproduct formation from a zinc benzochlorin iminium salt detected by fluorescence microscopy**. *Photochemistry and Photobiology* 1999, **69**(6):700-702.

358 Cappelli A, Mancini A, Sudati F, Valenti S, Anzini M, Belloli S, Moresco RM, Matarrese M, Vaghi M, Fabro A *et al*: **Synthesis and biological characterization of novel 2-quinolinecarboxamide ligands of the peripheral benzodiazepine receptors bearing technetium-99m or rhenium**. *Bioconjug Chem* 2008, **19**(6):1143-1153.

359 Sekimata K, Hatano K, Ogawa M, Abe J, Magata Y, Biggio G, Serra M, Laquintana V, Denora N, Latrofa A *et al*: **Radiosynthesis and in vivo evaluation of N-[11C]methylated imidazopyridineacetamides as PET tracers for peripheral benzodiazepine receptors**. *Nucl Med Biol* 2008, **35**(3):327-334.

362   Vin V, Leducq N, Bono F, Herbert JM: **Binding characteristics of SSR180575, a potent and selective peripheral benzodiazepine ligand**. *Biochemical and Biophysical Research Communications* 2003, **310**(3):785-790.

365   Okuyama S, Chaki S, Yoshikawa R, Ogawa S, Suzuki Y, Okubo T, Nakazato A, Nagamine M, Tomisawa K: **Neuropharmacological profile of peripheral benzodiazepine receptor agonists, DAA1097 and DAA1106**. *Life Sci* 1999, **64**(16):1455-1464.

366   Campiani G, Nacci V, Fiorini I, De Filippis MP, Garofalo A, Ciani SM, Greco G, Novellino E, Williams DC, Zisterer DM *et al*: **Synthesis, biological activity, and SARs of pyrrolobenzoxazepine derivatives, a new class of specific "peripheral-type" benzodiazepine receptor ligands**. *J Med Chem* 1996, **39**(18):3435-3450.

368   Nepomuceno MF, Mamede MED, de Macedo DV, Alves AA, Pereira-da-Silva L, Tabak M: **Antioxidant effect of dipyridamole and its derivative RA-25 in mitochondria: correlation of activity and location in the membrane**. *Biochimica Et Biophysica Acta-Biomembranes* 1999, **1418**(2):285-294.

370   Davies LP, Barlin GB, Selley ML: **New Imidazo[1,2-(B)under-Bar]Pyridazine Ligands for Peripheral-Type Benzodiazepine Receptors on Mitochondria and Monocytes**. *Life Sciences* 1995, **57**(25):Pl381-Pl386.

372   Davia K, King D, Hong YL, Swavey S: **A porphyrin-ruthenium photosensitizer as a potential photodynamic therapy agent**. *Inorganic Chemistry Communications* 2008, **11**(5):584-586.

373   Laquintana V, Denora N, Lopedota A, Suzuki H, Sawada M, Serra M, Biggio G, Latrofa A, Trapani G, Liso G: **N-benzyl-2-(6,8-dichloro-2-(4-chlorophenyl)imidazo[1,2-a]pyridin-3-yl)-N-(6-(7-nitrobenzo[c][1,2,5]oxadiazol-4-ylamino)hexyl)acetamide as a new fluorescent probe for peripheral benzodiazepine receptor and microglial cell visualization**. *Bioconjugate Chemistry* 2007, **18**(5):1397-1407.

376   Machado AHA, Braga FMP, Soares CP, Pelisson MMM, Beltrame M, Da Silva NS: **Photodynamic therapy with a new photosensitizing agent**. *Photomedicine and Laser Surgery* 2007, **25**(3):220-228.

378   Sibrian-Vazquez M, Jensen TJ, Vicente MGH: **Synthesis, characterization, and metabolic stability of porphyrin-peptide conjugates bearing bifunctional signaling sequences**. *Journal of Medicinal Chemistry* 2008, **51**(10):2915-2923.

379   Hofman JW, van Zeeland F, Turker S, Talsma H, Lambrechts SAG, Sakharov DV, Hennink WE, van Nostrum CF: **Peripheral and axial substitution of phthalocyanines with solketal groups: Synthesis and in vitro evaluation for photodynamic therapy**. *Journal of Medicinal Chemistry* 2007, **50**(7):1485-1494.

380   Liu W, Jensen TJ, Fronczek FR, Hammer RP, Smith KM, Vicente MG: **Synthesis and cellular studies of nonaggregated water-soluble phthalocyanines**. *J Med Chem* 2005, **48**(4):1033-1041.

382   Liu JY, Jiang XJ, Fong WP, Ng DK: **Synthesis, Characterization, and In Vitro Photodynamic Activity of Novel Amphiphilic Zinc(II) Phthalocyanines Bearing Oxyethylene-Rich Substituents**. *Met Based Drugs* 2008, **2008**:284691.

383   Zhou WL, Yan P, Wuskell JP, Loew LM, Antic SD: **Intracellular long-wavelength voltage-sensitive dyes dynamics of action potentials in axons and thin for studying the dendrites**. *Journal of Neuroscience Methods* 2007, **164**(2):225-239.

384 Matiukas A, Mitrea BG, Pertsov AM, Wuskell JP, Wei MD, Watras J, Millard AC, Loew LM: **New near-infrared optical probes of cardiac electrical activity**. *American Journal of Physiology-Heart and Circulatory Physiology* 2006, **290**(6):H2633-H2643.

385 Wuskell JP, Boudreau D, Wei MD, Jin L, Engl R, Chebolu R, Bullen A, Hoffacker KD, Kerimo J, Cohen LB *et al*: **Synthesis, spectra, delivery and potentiometric responses of new styryl dyes with extended spectral ranges**. *Journal of Neuroscience Methods* 2006, **151**(2):200-215.

387 Sibrian-Vazquez M, Jensen TJ, Fronczek FR, Hammer RP, Vicente MGH: **Synthesis and characterization of positively charged porphyrin-peptide conjugates**. *Bioconjugate Chemistry* 2005, **16**(4):852-863.

388 Yang YJ, Lowry M, Xu XY, Escobedo JO, Sibrian-Vazcluez M, Wong L, Schowalter CM, Jensen TJ, Fronczek FR, Warner IM *et al*: **Seminaphthofluorones are a family of water-soluble, low molecular weight, NIR-emitting fluorophores**. *Proceedings of the National Academy of Sciences of the United States of America* 2008, **105**(26):8829-8834.

393 Sibrian-Vazquez M, Jensen TJ, Vicente MGH: **Synthesis and cellular studies of PEG-functionalized meso-tetraphenylporphyrins**. *Journal of Photochemistry and Photobiology B-Biology* 2007, **86**(1):9-21.

399 Comuzzi C, Cogoi S, Overhand M, Van der Marel GA, Overkleeft HS, Xodo LE: **Synthesis and biological evaluation of new pentaphyrin macrocycles for photodynamic therapy**. *J Med Chem* 2006, **49**(1):196-204.

400 Mak NK, Kok TW, Wong RNS, Lam SW, Lau YK, Leung WN, Cheung NH, Huang DP, Yeung LL, Chang CK: **Photodynamic activities of sulfonamide derivatives of porphycene on nasopharyngeal carcinoma cells**. *Journal of Biomedical Science* 2003, **10**(4):418-429.

403 Hammer ND, Lee S, Vesper BJ, Elseth KM, Hoffman BM, Barrett AG, Radosevich JA: **Charge dependence of cellular uptake and selective antitumor activity of porphyrazines**. *J Med Chem* 2005, **48**(26):8125-8133.

405 Laville I, Figueiredo T, Loock B, Pigaglio S, Maillard P, Grierson DS, Carrez D, Croisy A, Blais J: **Synthesis, cellular internalization and photodynamic activity of glucoconjugated derivatives of tri and tetra(meta-hydroxyphenyl)chlorins**. *Bioorg Med Chem* 2003, **11**(8):1643-1652.

407 Gallagher WM, Allen LT, O'Shea C, Kenna T, Hall M, Gorman A, Killoran J, O'Shea DF: **A potent nonporphyrin class of photodynamic therapeutic agent: cellular localisation, cytotoxic potential and influence of hypoxia**. *Br J Cancer* 2005, **92**(9):1702-1710.

409 Laville I, Pigaglio S, Blais JC, Doz F, Loock B, Maillard P, Grierson DS, Blais J: **Photodynamic efficiency of diethylene glycol-linked glycoconjugated porphyrins in human retinoblastoma cells**. *J Med Chem* 2006, **49**(8):2558-2567.

410 Lee S, Vesper BJ, Zong H, Hammer ND, Elseth KM, Barrett AG, Hoffman BM, Radosevich JA: **Synthesis and Biological Analysis of Thiotetra(ethylene glycol) monomethyl Ether-Functionalized Porphyrazines: Cellular Uptake and Toxicity Studies**. *Met Based Drugs* 2008, **2008**:391418.

411 Antic S, Zecevic D: **Optical signals from neurons with internally applied voltage-sensitive dyes**. *J Neurosci* 1995, **15**(2):1392-1405.

412 Bullen A, Saggau P: **High-speed, random-access fluorescence microscopy: II. Fast quantitative measurements with voltage-sensitive dyes**. *Biophys J* 1999, **76**(4):2272-2287.

413 Obaid AL, Loew LM, Wuskell JP, Salzberg BM: **Novel naphthylstyryl-**

pyridium potentiometric dyes offer advantages for neural network analysis**. *J Neurosci Methods* 2004, **134**(2):179-190.

414 Fromherz P, Hubener G, Kuhn B, Hinner MJ: **ANNINE-6plus, a voltage-sensitive dye with good solubility, strong membrane binding and high sensitivity**. *Eur Biophys J* 2008, **37**(4):509-514.

415 Kuhn B, Fromherz P: **Anellated hemicyanine dyes in a neuron membrane: Molecular Stark effect and optical voltage recording**. *Journal of Physical Chemistry B* 2003, **107**(31):7903-7913.

417 Yang YJ, Lowry M, Schowalter CM, Fakayode SO, Escobedo JO, Xu XY, Zhang HT, Jensen TJ, Fronczek FR, Warner IM *et al*: **An organic white light-emitting fluorophore**. *Journal of the American Chemical Society* 2006, **128**(43):14081-14092.

418 Rahimipour S, Litichever-Coslovsky N, Alaluf M, Freeman D, Ehrenberg B, Weiner L, Mazur Y, Fridkin M, Koch Y: **Novel methyl helianthrones as photosensitizers: Synthesis and biological evaluation**. *Photochemistry and Photobiology* 2005, **81**(2):250-258.

421 Wang Y, Zhang Y, Yu B: **The cytotoxicity of saponins correlates with their cellular internalization**. *ChemMedChem* 2007, **2**(3):288-291.

422 Hirohara S, Obata M, Ogata S, Kajiwara K, Ohtsuki C, Tanihara M, Yano S: **Sugar-dependent aggregation of glycoconjugated chlorins and its effect on photocytotoxicity in HeLa cells**. *Journal of Photochemistry and Photobiology B-Biology* 2006, **84**(1):56-63.

423 Schweitzer D, Zhu J, Jarori G, Tanaka J, Higa T, Davisson VJ, Helquist P: **Synthesis of carbamate derivatives of iejimalides. Retention of normal antiproliferative activity and localization of binding in cancer cells**. *Bioorganic & Medicinal Chemistry* 2007, **15**(9):3208-3216.

424 Guan HJ, Liu XD, Peng WL, Cao RH, Ma Y, Chen HS, Xu AL: **beta-carboline derivatives: Novel photosensitizers that intercalate into DNA to cause direct DNA damage in photodynamic therapy**. *Biochemical and Biophysical Research Communications* 2006, **342**(3):894-901.

425 Schmitt F, Govindaswamy P, Suss-Fink G, Ang WH, Dyson PJ, Juillerat-Jeanneret L, Therrien B: **Ruthenium porphyrin compounds for photodynamic therapy of cancer**. *Journal of Medicinal Chemistry* 2008, **51**(6):1811-1816.

426 Bourre L, Simonneaux G, Ferrand Y, Thibaut S, Lajat Y, Patrice T: **Synthesis, and in vitro and in vivo evaluation of a diphenylchlorin sensitizer for photodynamic therapy**. *J Photochem Photobiol B* 2003, **69**(3):179-192.

427 Lo PC, Chan CMH, Liu JY, Fong WP, Ng DKP: **Highly photocytotoxic glucosylated silicon(IV) phthalocyanines. Effects of peripheral chloro substitution on the photophysical and photodynamic properties**. *Journal of Medicinal Chemistry* 2007, **50**(9):2100-2107.

428 Xu H, Jiang XJ, Chan EY, Fong WP, Ng DK: **Synthesis, photophysical properties and in vitro photodynamic activity of axially substituted subphthalocyanines**. *Org Biomol Chem* 2007, **5**(24):3987-3992.

429 Grichine A, Feofanov A, Karmakova T, Kazachkina N, Pecherskih E, Yakubovskaya R, Mironov A, Egret-Charlier M, Vigny P: **Influence of the substitution of 3-vinyl by 3-formyl group on the photodynamic properties of chlorin P6: Molecular, cellular and in vivo studies**. *Photochemistry and Photobiology* 2001, **73**(3):267-277.

431 Su TL, Lin CT, Chen CH, Huang HM: **Synthesis of biotinylated glyfoline for immunoelectron microscopic localization**. *Bioconjugate Chemistry* 2000,

11(2):278-281.

436 Kramer-Marek G, Serpa C, Szurko A, Widel M, Sochanik A, Snietura M, Kus P, Nunes RMD, Arnaut LG, Ratuszna A: **Spectroscopic properties and photodynamic effects of new lipophilic porphyrin derivatives: Efficacy, localisation and cell death pathways (vol 84, pg 1, 2006)**. *Journal of Photochemistry and Photobiology B-Biology* 2006, **85**(3):228-228.

437 Slaninova I, Slanina J, Taborska E: **Quaternary benzo[c]phenanthridine alkaloids--novel cell permeant and red fluorescing DNA probes**. *Cytometry A* 2007, **71**(9):700-708.

439 Kralova J, Koivukorpi J, Kejik Z, Pouckova P, Sievanen E, Kolehmainen E, Kral V: **Porphyrin-bile acid conjugates: from saccharide recognition in the solution to the selective cancer cell fluorescence detection**. *Org Biomol Chem* 2008, **6**(9):1548-1552.

442 Lo PC, Zhao B, Duan W, Fong WP, Ko WH, Ng DK: **Synthesis and in vitro photodynamic activity of mono-substituted amphiphilic zinc(II) phthalocyanines**. *Bioorg Med Chem Lett* 2007, **17**(4):1073-1077.

443 Alvarez MG, Principe F, Milanesio ME, Durantini EN, Rivarola V: **Photodynamic damages induced by a monocationic porphyrin derivative in a human carcinoma cell line**. *Int J Biochem Cell Biol* 2005, **37**(12):2504-2512.

444 Gryshuk AL, Chen Y, Potter W, Ohulchansky T, Oseroff A, Pandey RK: **In vivo stability and photodynamic efficacy of fluorinated bacteriopurpurinimides derived from bacteriochlorophyll-a**. *J Med Chem* 2006, **49**(6):1874-1881.bacteriopurpurinimides derived from bacteriochlorophyll-a

448 Lala AK: **Fluorescent and photoactivable probes in depth-dependent analysis of membranes**. *Chem Phys Lipids* 2002, **116**(1-2):177-188.

449 Lavis LD, Chao TY, Raines RT: **Fluorogenic label for biomolecular imaging**. *ACS Chem Biol* 2006, **1**(4):252-260.

452 Farruggia G, Iotti S, Prodi L, Montalti M, Zaccheroni N, Savage PB, Trapani V, Sale P, Wolf FI: **8-Hydroxyquinoline derivatives as fluorescent sensors for magnesium in living cells**. *Journal of the American Chemical Society* 2006, **128**(1):344-350.

455 Petterse.Je, Aas M: **Subcellular-Localization of Hexadecanedioic Acid Activation in Human Liver**. *Journal of Lipid Research* 1974, **15**(6):551-556.

456 Ribou AC, Vigo J, Salmon JM: **Lifetime of fluorescent pyrene butyric acid probe in single living cells for measurement of oxygen fluctuation**. *Photochem Photobiol* 2004, **80**(2):274-280.

458 Burdette SC, Walkup GK, Spingler B, Tsien RY, Lippard SJ: **Fluorescent sensors for Zn(2+) based on a fluorescein platform: synthesis, properties and intracellular distribution**. *J Am Chem Soc* 2001, **123**(32):7831-7841.

462 Salama G, Choi BR, Azour G, Lavasani M, Tumbev V, Salzberg BM, Patrick MJ, Ernst LA, Waggoner AS: **Properties of new, long-wavelength, voltage-sensitive dyes in the heart**. *J Membr Biol* 2005, **208**(2):125-140.

463 Ehrenberg B, Montana V, Wei MD, Wuskell JP, Loew LM: **Membrane-Potential Can Be Determined in Individual Cells from the Nernstian Distribution of Cationic Dyes**. *Biophysical Journal* 1988, **53**(5):785-794.

464 Grinvald A, Salzberg BM, Levram V, Hildesheim R: **Optical-Recording of Synaptic Potentials from Processes of Single Neurons Using Intracellular Potentiometric Dyes**. *Biophysical Journal* 1987, **51**(4):643-651.

465 Bouevitch O, Lewis A, Pinevsky I, Wuskell JP, Loew LM: **Probing membrane potential with nonlinear optics**. *Biophys J* 1993, **65**(2):672-679.

466   Shynkar VV, Klymchenko AS, Duportail G, Demchenko AP, Mely Y: **Two-color fluorescent probes for imaging the dipole potential of cell plasma membranes**. *Biochimica Et Biophysica Acta-Biomembranes* 2005, **1712**(2):128-136.

468   Lee PPS, Lo PC, Chan EYM, Fong WP, Ko WH, Ng DKP: **Synthesis and in vitro photodynamic activity of novel galactose-containing phthalocyanines**. *Tetrahedron Letters* 2005, **46**(9):1551-1554.

470   Camerin M, Rello S, Villanueva A, Ping XZ, Kenney ME, Rodgers MAJ, Jori G: **Photothermal sensitisation as a novel therapeutic approach for tumours: Studies at the cellular and animal level**. *European Journal of Cancer* 2005, **41**(8):1203-1212.

471   Kozikowski AP, Kotoula M, Ma D, Boujrad N, Tuckmantel W, Papadopoulos V: **Synthesis and biology of a 7-nitro-2,1,3-benzoxadiazol-4-yl derivative of 2-phenylindole-3-acetamide: a fluorescent probe for the peripheral-type benzodiazepine receptor**. *J Med Chem* 1997, **40**(16):2435-2439.

472   Lansiaux A, Dassonneville L, Facompre M, Kumar A, Stephens CE, Bajic M, Tanious F, Wilson WD, Boykin DW, Bailly C: **Distribution of furamidine analogues in tumor cells: influence of the number of positive charges**. *J Med Chem* 2002, **45**(10):1994-2002.

473   Serafim TL, Oliveira PJ, Sardao VA, Perkins E, Parke D, Holy J: **Different concentrations of berberine result in distinct cellular localization patterns and cell cycle effects in a melanoma cell line**. *Cancer Chemotherapy and Pharmacology* 2008, **61**(6):1007-1018.

474   Tarasiuk J, Stefanska B, Plodzich I, Tkaczyk-Gobis K, Seksek O, Martelli S, Garnier-Suillerot A, Borowski E: **Anthrapyridones, a novel group of antitumour non-cross resistant anthraquinone analogues. Synthesis and molecular basis of the cytotoxic activity towards K562/DOX cells**. *British Journal of Pharmacology* 2002, **135**(6):1513-1523.

475   Satz AL, White CM, Beerman TA, Bruice TC: **Double-stranded DNA binding characteristics and subcellular distribution of a minor groove binding diphenyl ether bisbenzimidazole**. *Biochemistry* 2001, **40**(21):6465-6474.

477   Lichtner RB, Rotgeri A, Bunte T, Buchmann B, Hoffmann J, Schwede W, Skuballa W, Klar U: **Subcellular distribution of epothilones in human tumor cells**. *Proc Natl Acad Sci U S A* 2001, **98**(20):11743-11748.

478   Charmantray F, Demeunynck M, Carrez D, Croisy A, Lansiaux A, Bailly C, Colson P: **4-Hydroxymethyl-3-aminoacridine derivatives as a new family of anticancer agents**. *J Med Chem* 2003, **46**(6):967-977.

479   Pavlov V, Kong Thoo Lin P, Rodilla V: **Cytotoxicity, DNA binding and localisation of novel bis-naphthalimidopropyl polyamine derivatives**. *Chem Biol Interact* 2001, **137**(1):15-24.

480   Belitsky JM, Leslie SJ, Arora PS, Beerman TA, Dervan PB: **Cellular uptake of N-methylpyrrole/N-methylimidazole polyamide-dye conjugates**. *Bioorganic & Medicinal Chemistry* 2002, **10**(10):3313-3318.

481   Wells G, Martin CRH, Howard PW, Sands ZA, Laughton CA, Tiberghien A, Woo CK, Masterson LA, Stephenson MJ, Hartley JA *et al*: **Design, synthesis, and biophysical and biological evaluation of a series of Pyrrolobenzodiazepine - Poly(N-methylpyrrole) conjugates**. *Journal of Medicinal Chemistry* 2006, **49**(18):5442-5461.

485   Mol WEM, Meijer DKF: **Hepatic Transport Mechanisms for Bivalent Organic Cations - Subcellular-Distribution and Hepatobiliary Concentration Gradients of Some Steroidal Muscle-Relaxants**. *Biochemical Pharmacology*

301

1990, **39**(2):383-390.

486 Nickols NG, Jacobs CS, Farkas ME, Dervan PB: **Improved nuclear localization of DNA-binding polyamides**. *Nucleic Acids Research* 2007, **35**(2):363-370.

488 Bickmeyer U, Grube A, Klings KW, Kock M: **Ageladine A, a pyrrole-imidazole alkaloid from marine sponges, is a pH sensitive membrane permeable dye (vol 373, pg 419, 2008)**. *Biochemical and Biophysical Research Communications* 2009, **383**(4):519-519.

492 Gogan P, Schmiedeljakob I, Chitti Y, Tycdumont S: **Fluorescence Imaging of Local Membrane Electric-Fields during the Excitation of Single Neurons in Culture**. *Biophysical Journal* 1995, **69**(2):299-310.

495 Mottram LF, Maddox E, Schwab M, Beaufils F, Peterson BR: **A concise synthesis of the Pennsylvania Green fluorophore and labeling of intracellular targets with O6-benzylguanine derivatives**. *Org Lett* 2007, **9**(19):3741-3744.

498 Mottram LF, Boonyarattanakalin S, Kovel RE, Peterson BR: **The Pennsylvania Green Fluorophore: a hybrid of Oregon Green and Tokyo Green for the construction of hydrophobic and pH-insensitive molecular probes**. *Org Lett* 2006, **8**(4):581-584.

499 Chauvin AS, Comby S, Song B, Vandevyver CD, Thomas F, Bunzli JC: **A polyoxyethylene-substituted bimetallic europium helicate for luminescent staining of living cells**. *Chemistry* 2007, **13**(34):9515-9526.

500 Galindo F, Burguete MI, Vigara L, Luis SV, Kabir N, Gavrilovic J, Russell DA: **Synthetic macrocyclic peptidomimetics as tunable pH probes for the fluorescence imaging of acidic organelles in live cells**. *Angewandte Chemie-International Edition* 2005, **44**(40):6504-6508.

502 Abbotto A, Baldini G, Beverina L, Chirico G, Collini M, D'Alfonso L, Diaspro A, Magrassi R, Nardo L, Pagani GA: **Dimethyl-pepep: a DNA probe in two-photon excitation cellular imaging**. *Biophysical Chemistry* 2005, **114**(1):35-41.

503 Allain C, Schmidt F, Lartia R, Bordeau G, Fiorini-Debuisschert C, Charra F, Tauc P, Teulade-Fichou MP: **Vinyl-pyridinium triphenylamines: Novel far-red emitters with high photostability and two-photon absorption properties for staining DNA**. *Chembiochem* 2007, **8**(4):424-433.

506 Li C, Greenwood TR, Bhujwalla ZM, Glunde K: **Synthesis and characterization of glucosamine-bound near-infrared probes for optical imaging**. *Organic Letters* 2006, **8**(17):3623-3626.

507 Beverina L, Crippa M, Landenna M, Ruffo R, Salice P, Silvestri F, Versari S, Villa A, Ciaffoni L, Collni E *et al*: **Assessment of water-soluble pi-extended squaraines as one- and two-photon singlet oxygen photosensitizers: Design, synthesis, and characterization**. *Journal of the American Chemical Society* 2008, **130**(6):1894-1902.

510 Jaffrezou JP, Chen G, Duran GE, Muller C, Bordier C, Laurent G, Sikic BI, Levade T: **Inhibition of Lysosomal Acid Sphingomyelinase by Agents Which Reverse Multidrug-Resistance**. *Biochimica Et Biophysica Acta-Molecular Cell Research* 1995, **1266**(1):1-8.

512 Van Bambeke F, Gerbaux C, Michot JM, d'Yvoire MB, Montenez JP, Tulkens PM: **Lysosomal alterations induced in cultured rat fibroblasts by long-term exposure to low concentrations of azithromycin**. *J Antimicrob Chemother* 1998, **42**(6):761-767.

513 Hjelle JT, Ruben Z: **Investigations in Intracellular Drug Storage -**

Localization of Disobutamide in Lysosomal and Nonlysosomal Vesicles. *Toxicology and Applied Pharmacology* 1989, **101**(1):70-82.

516   Dastur DK, Thakkar BK, Desai PR: **Experimental Neurotoxicity of the Anorectic Fenfluramine .1. A Fine-Structural Model for Cerebral Lysosomal Storage and Neuroglial Reaction**. *Acta Neuropathologica* 1985, **67**(1-2):142-154.

517   Bispinck F, Fischer J, Lullmann-Rauch R, Ziegenhagen MW: **Time course of the tilorone-induced lysosomal accumulation of sulphated glycosaminoglycans in cultured fibroblasts**. *Experimental and Toxicologic Pathology* 1998, **50**(4-6):411-415.

518   Bispinck F, Fischer J, Lullmann-Rauch R, von Witzendorff B: **Lysosomal glycosaminoglycan storage as induced by dicationic amphiphilic drugs: Investigation into the mechanisms underlying the slow reversibility**. *Toxicology* 1998, **128**(2):91-100.

520   Soule JC, Neale G, Peters TJ: **Functional and Biochemical Evidence of Damage to Enterocytes Induced by Triparanol - Role of Lysosomes and Effect of a Gluten-Free Diet**. *Clinical Science and Molecular Medicine* 1976, **51**(1):19-25.

521   Agoston M, Orsi F, Feher E, Hagymasi K, Orosz Z, Blazovics A, Feher J, Vereckei A: **Silymarin and vitamin E reduce amiodarone-induced lysosomal phospholipidosis in rats**. *Toxicology* 2003, **190**(3):231-241.

522   Ni-Komatsu L, Orlow SJ: **Chemical genetic screening identifies tricyclic compounds that decrease cellular melanin content**. *Journal of Investigative Dermatology* 2008, **128**(5):1236-1247.

523   Staubli W, Schweizer W, Suter J: **Some Properties of Myeloid Bodies Induced in Rat-Liver by an Antidepressant Drug (Maprotiline)**. *Experimental and Molecular Pathology* 1978, **28**(2):177-195.

527   Sherer TB, Betarbet R, Greenamyre JT: **Environment, mitochondria, and Parkinson's disease**. *Neuroscientist* 2002, **8**(3):192-197.

529   Krogstad DJ, Schlesinger PH, Gluzman IY: **Antimalarials Increase Vesicle Ph in Plasmodium-Falciparum**. *Journal of Cell Biology* 1985, **101**(6):2302-2309.

530   Glaumann H, Motakefi AM, Jansson H: **Intracellular distribution and effect of the antimalarial drug mefloquine on lysosomes of rat liver**. *Liver* 1992, **12**(4 Pt 1):183-190.

532   Li GL, Graham A, Chen YH, Dobhal MP, Morgan J, Zheng G, Kozyrev A, Oseroff A, Dougherty TJ, Pandey RK: **Synthesis, comparative photosensitizing efficacy, human serum albumin (Site II) binding ability, and intracellular localization characteristics of novel benzobacteriochlorins derived from vic-dihydroxybacteriochlorins**. *Journal of Medicinal Chemistry* 2003, **46**(25):5349-5359.

533   Houghton PJ, Sosinski J, Thakar JH, Boder GB, Grindey GB: **Characterization of the Intracellular-Distribution and Binding in Human Adenocarcinoma Cells of N-(4-Azidophenylsulfonyl)-N'-(4-Chlorophenyl)Urea (Ly219703), a Photoaffinity Analog of the Antitumor Diarylsulfonylurea Sulofenur**. *Biochemical Pharmacology* 1995, **49**(5):661-668.

534   Albert AE, Warwick GP: **The subcellular distribution of tritiated 4-dimethylaminoazobenzene and 2-methyl-4-dimethylaminoazobenzene in rat liver and spleen following a single oral administration**. *Chem Biol Interact* 1972, **5**(1):65-68.

535   Berson A, Descatoire V, Sutton A, Fau D, Maulny B, Vadrot N, Feldmann G, Berthon B, Tordjmann T, Pessayre D: **Toxicity of alpidem, a peripheral**

benzodiazepine receptor ligand, but not zolpidem, in rat hepatocytes: Role of mitochondrial permeability transition and metabolic activation. *Journal of Pharmacology and Experimental Therapeutics* 2001, **299**(2):793-800.

536 Choi CF, Huang JD, Lo PC, Fong WP, Ng DKP: **Glycosylated zinc(II) phthalocyanines as efficient photosensitisers for photodynamic therapy. Synthesis, photophysical properties and in vitro photodynamic activity**. *Organic & Biomolecular Chemistry* 2008, **6**(12):2173-2181.

537 Chen Y, Zheng X, Dobhal MP, Gryshuk A, Morgan J, Dougherty TJ, Oseroff A, Pandey RK: **Methyl pyropheophorbide-a analogues: potential fluorescent probes for the peripheral-type benzodiazepine receptor. Effect of central metal in photosensitizing efficacy**. *J Med Chem* 2005, **48**(11):3692-3695.

538 Lo PC, Fong WP, Ng DK: **Effects of peripheral chloro substitution on the photophysical properties and in vitro photodynamic activities of galactose-conjugated silicon(IV) phthalocyanines**. *ChemMedChem* 2008, **3**(7):1110-1117.

539 Phelps MA, Foraker AB, Gao W, Dalton JT, Swaan PW: **A novel rhodamine-riboflavin conjugate probe exhibits distinct fluorescence resonance energy transfer that enables riboflavin trafficking and subcellular localization studies**. *Mol Pharm* 2004, **1**(4):257-266.

540 Rancan F, Wiehe A, Nobel M, Senge MO, Omari SA, Bohm F, John M, Roder B: **Influence of substitutions on asymmetric dihydroxychlorins with regard to intracellular uptake, subcellular localization and photosensitization of Jurkat cells**. *J Photochem Photobiol B* 2005, **78**(1):17-28.

542 Yan X, Grace WK, Yoshida TM, Habbersett RC, Velappan N, Jett JH, Keller RA, Marrone BL: **Characteristics of different nucleic acid staining dyes for DNA fragment sizing by flow cytometry**. *Anal Chem* 1999, **71**(24):5470-5480.

576 Jayaraman S: **Flow cytometric determination of mitochondrial membrane potential changes during apoptosis of T lymphocytic and pancreatic beta cell lines: comparison of tetramethylrhodamineethylester (TMRE), chloromethyl-X-rosamine (H2-CMX-Ros) and MitoTracker Red 580 (MTR580)**. *J Immunol Methods* 2005, **306**(1-2):68-79.

577 Whitaker JE, Moore PL, Haugland RP: **Dihydrotetramethylrosamine: a long wavelength, fluorogenic peroxidase substrate evaluated in vitro and in a model phagocyte**. *Biochem Biophys Res Commun* 1991, **175**(2):387-393.

578 Kweon SM, Kim HJ, Lee ZW, Kim SJ, Kim SI, Paik SG, Ha KS: **Real-time measurement of intracellular reactive oxygen species using mito tracker orange (CMH(2)TMRos)**. *Bioscience Reports* 2001, **21**(3):341-352.

579 Scorrano L, Petronilli V, Colonna R, Di Lisa F, Bernardi P: **Interactions of chloromethyltetramethylrosamine (Mitotracker Orange) with isolated mitochondria and intact cells**. *Ann N Y Acad Sci* 1999, **893**:391-395.

580 Li Y, Stansbury KH, Zhu H, Trush MA: **Biochemical characterization of lucigenin (Bis-N-methylacridinium) as a chemiluminescent probe for detecting intramitochondrial superoxide anion radical production**. *Biochem Biophys Res Commun* 1999, **262**(1):80-87.

582 Galluzzi L, Zamzami N, de La Motte Rouge T, Lemaire C, Brenner C, Kroemer G: **Methods for the assessment of mitochondrial membrane permeabilization in apoptosis**. *Apoptosis* 2007, **12**(5):803-813.

583 Rashid F, Horobin RW, Williams MA: **Predicting the behaviour and selectivity of fluorescent probes for lysosomes and related structures by means of structure-activity models**. *Histochem J* 1991, **23**(10):450-459.

584 Halle A, Hornung V, Petzold GC, Stewart CR, Monks BG, Reinheckel T,

Fitzgerald KA, Latz E, Moore KJ, Golenbock DT: **The NALP3 inflammasome is involved in the innate immune response to amyloid-beta**. *Nature Immunology* 2008, **9**(8):857-865.

585 Lu W, Sun Q, Wan J, She ZJ, Jiang XG: **Cationic albumin-conjugated pegylated nanoparticles allow gene delivery into brain tumors via intravenous administration**. *Cancer Research* 2006, **66**(24):11878-11887.

586 Mironov SL, Ivannikov MV, Johansson M: **[Ca2+](i) signaling between mitochondria and endoplasmic reticulum in neurons is regulated by microtubules - From mitochondrial permeability transition pore to Ca2+-induced Ca2+ release**. *Journal of Biological Chemistry* 2005, **280**(1):715-721.

588 Pagano RE, Watanabe R, Wheatley C, Chen CS: **Use of N-[5-(5,7-dimethyl boron dipyrromethene difluoride-sphingomyelin to study membrane traffic along the endocytic pathway**. *Chemistry and Physics of Lipids* 1999, **102**(1-2):55-63.

589 Davenport L, Dale RE, Bisby RH, Cundall RB: **Transverse location of the fluorescent probe 1,6-diphenyl-1,3,5-hexatriene in model lipid bilayer membrane systems by resonance excitation energy transfer**. *Biochemistry* 1985, **24**(15):4097-4108.

590 Kaiser RD, London E: **Determination of the depth of BODIPY probes in model membranes by parallax analysis of fluorescence quenching**. *Biochim Biophys Acta* 1998, **1375**(1-2):13-22.

591 Haidekker MA, L'Heureux N, Frangos JA: **Fluid shear stress increases membrane fluidity in endothelial cells: a study with DCVJ fluorescence**. *Am J Physiol Heart Circ Physiol* 2000, **278**(4):H1401-1406.

592 Ritov VB, Banni S, Yalowich JC, Day BW, Claycamp HG, Corongiu FP, Kagan VE: **Non-random peroxidation of different classes of membrane phospholipids in live cells detected by metabolically integrated cis-parinaric acid**. *Biochim Biophys Acta* 1996, **1283**(2):127-140.

593 Lippincottschwartz J, Yuan LC, Bonifacino JS, Klausner RD: **Rapid Redistribution of Golgi Proteins into the Er in Cells Treated with Brefeldin-a - Evidence for Membrane Cycling from Golgi to Er**. *Cell* 1989, **56**(5):801-813.

594 Hempel SL, Buettner GR, O'Malley YQ, Wessels DA, Flaherty DM: **Dihydrofluorescein diacetate is superior for detecting intracellular oxidants: Comparison with 2 ',7 '-dichlorodihydrofluorescein diacetate, 5(and 6)-carboxy-2 ',7 '-dichlorodihydrofluorescein diacetate, and dihydrorhodamine 123**. *Free Radical Biology and Medicine* 1999, **27**(1-2):146-159.

595 Yu W, So PT, French T, Gratton E: **Fluorescence generalized polarization of cell membranes: a two-photon scanning microscopy approach**. *Biophys J* 1996, **70**(2):626-636.

598 Burkhardt JK, Hester S, Lapham CK, Argon Y: **The lytic granules of natural killer cells are dual-function organelles combining secretory and pre-lysosomal compartments**. *J Cell Biol* 1990, **111**(6 Pt 1):2327-2340.

600 Berns MW, Wang ZF, Dunn A, Wallace V, Venugopalan V: **Gene inactivation by multiphoton-targeted photochemistry**. *Proceedings of the National Academy of Sciences of the United States of America* 2000, **97**(17):9504-9507.

601 Qin Y, Lu M, Gong XG: **Dihydrorhodamine 123 is superior to 2,7-dichlorodihydrofluorescein diacetate and dihydrorhodamine 6G in detecting intracellular hydrogen peroxide in tumor cells**. *Cell Biology International* 2008, **32**(2):224-228.

602 Shapiro AB, Ling V: **Transport of LDS-751 from the cytoplasmic leaflet of the plasma membrane by the rhodamine-123-selective site of P-glycoprotein**. *European Journal of Biochemistry* 1998, **254**(1):181-188.

603 Barber L, Prince HM, Rossi R, Bertoncello I: **Fluoro-Gold: An alternative viability stain for multicolor flow cytometric analysis**. *Cytometry* 1999, **36**(4):349-354.

604 Makrigiorgos GM: **Detection of lipid peroxidation on erythrocytes using the excimer-forming property of a lipophilic BODIPY fluorescent dye**. *Journal of Biochemical and Biophysical Methods* 1997, **35**(1):23-35.

605 Drummen GPC, van Liebergen LCM, Op den Kamp JAF, Post JA: **C11-BODIPY581/591, an oxidation-sensitive fluorescent lipid peroxidation probe: (Micro)spectroscopic characterization and validation of methodology**. *Free Radical Biology and Medicine* 2002, **33**(4):473-490.

606 Millard PJ, Roth BL, Thi HPT, Yue ST, Haugland RP: **Development of the FUN-1 family of fluorescent probes for vacuole labeling and viability testing of yeasts**. *Applied and Environmental Microbiology* 1997, **63**(7):2897-2905.

607 Hallap T, Nagy S, Jaakma U, Johannisson A, Rodriguez-Martinez H: **Mitochondrial activity of frozen-thawed spermatozoa assessed by Mitotracker Deep Red 633**. *Theriogenology* 2005, **63**(8):2311-2322.

608 Bink K, Walch A, Feuchtinger A, Eisenmann H, Hutzler P, Hofler H, Werner M: **TO-PRO-3 is an optimal fluorescent dye for nuclear counterstaining in dual-colour FISH on paraffin sections**. *Histochemistry and Cell Biology* 2001, **115**(4):293-299.

609 Ward LD, Timasheff SN: **Cooperative Multiple Binding of Bisans and Daunomycin to Tubulin**. *Biochemistry* 1994, **33**(39):11891-11899.

611 Mukherjee S, Soe TT, Maxfield FR: **Endocytic sorting of lipid analogues differing solely in the chemistry of their hydrophobic tails**. *Journal of Cell Biology* 1999, **144**(6):1271-1284.

612 Krishna MMG, Periasamy N: **Fluorescence of organic dyes in lipid membranes: Site of solubilization and effects of viscosity and refractive index on lifetimes**. *Journal of Fluorescence* 1998, **8**(1):81-91.

613 Chiu I, Davis DM, Strominger JL: **Trafficking of spontaneously endocytosed MHC proteins**. *Proc Natl Acad Sci U S A* 1999, **96**(24):13944-13949.

615 Butler PJ, Norwich G, Weinbaum S, Chien S: **Shear stress induces a time- and position-dependent increase in endothelial cell membrane fluidity**. *American Journal of Physiology-Cell Physiology* 2001, **280**(4):C962-C969.

616 Straub M, Lodemann P, Holroyd P, Jahn R, Hell SW: **Live cell imaging by multifocal multiphoton microscopy**. *European Journal of Cell Biology* 2000, **79**(10):726-734.

617 Gidwani A, Holowka D, Baird B: **Fluorescence anisotropy measurements of lipid order in plasma membranes and lipid rafts from RBL-2H3 mast cells**. *Biochemistry* 2001, **40**(41):12422-12429.

618 Hemmrich K, Meersch M, von Heimburg D, Pallua N: **Applicability of the dyes CFSE, CM-DiI and PKH26 for tracking of human preadipocytes to evaluate adipose tissue engineering**. *Cells Tissues Organs* 2006, **184**(3-4):117-127.

620 Simard R: **Binding of Actinomycin D-3h to Heterochromatin as Studied by Quantitative High Resolution Radioautography**. *Journal of Cell Biology* 1967, **35**(3):716-&.

621 Stokke T, Steen HB: **Distinction of Leukocyte Classes Based on Chromatin-Structure-Dependent DNA-Binding of 7-Aminoactinomycin-D**. *Cytometry*

1987, **8**(6):576-583.

622 Kirschstein O, Sip M, Kittler L: **Quantitative and sequence-specific analysis of DNA-ligand interaction by means of fluorescent intercalator probes**. *Journal of Molecular Recognition* 2000, **13**(3):157-163.

623 Wistrom CA, Jones GM, Tobias PS, Sklar LA: **Fluorescence resonance energy transfer analysis of lipopolysaccharide in detergent micelles**. *Biophys J* 1996, **70**(2):988-997.

626 Pal R, Petri WA, Benyashar V, Wagner RR, Barenholz Y: **Characterization of the Fluorophore 4-Heptadecyl-7-Hydroxycoumarin - a Probe for the Headgroup Region of Lipid Bilayers and Biological-Membranes**. *Biochemistry* 1985, **24**(3):573-581.

627 Johnson ID, Kang HC, Haugland RP: **Fluorescent Membrane Probes Incorporating Dipyrrometheneboron Difluoride Fluorophores**. *Analytical Biochemistry* 1991, **198**(2):228-237.

628 Li H, Black PN, DiRusso CC: **A live-cell high-throughput screening assay for identification of fatty acid uptake inhibitors**. *Analytical Biochemistry* 2005, **336**(1):11-19.

630 Pin S, Chen HL, Lein PJ, Wang MM: **Nucleic acid binding agents exert local toxic effects on neurites via a non-nuclear mechanism**. *Journal of Neurochemistry* 2006, **96**(5):1253-1266.

631 Hoshi H, O'Brien J, Mills SL: **A novel fluorescent tracer for visualizing coupled cells in neural circuits of living tissue**. *Journal of Histochemistry & Cytochemistry* 2006, **54**(10):1169-1176.

635 Beisker W, Weller-Mewe EM, Nusse M: **Fluorescence enhancement of DNA-bound TO-PRO-3 by incorporation of bromodeoxyuridine to monitor cell cycle kinetics**. *Cytometry* 1999, **37**(3):221-229.

636 Kok JW, Babia T, Klappe K, Hoekstra D: **Fluorescent, Short-Chain C-6-Nbd-Sphingomyelin, but Not C-6-Nbd-Glucosylceramide, Is Subject to Extensive Degradation in the Plasma-Membrane - Implications for Signal-Transduction Related to Cell-Differentiation**. *Biochemical Journal* 1995, **309**:905-912.

639 Weston SA, Parish CR: **New Fluorescent Dyes for Lymphocyte Migration Studies - Analysis by Flow-Cytometry and Fluorescence Microscopy**. *Journal of Immunological Methods* 1990, **133**(1):87-97.

641 Grutzendler J, Tsai J, Gan WB: **Rapid labeling of neuronal populations by ballistic delivery of fluorescent dyes**. *Methods* 2003, **30**(1):79-85.

642 Malinin VS, Haque ME, Lentz BR: **The rate of lipid transfer during fusion depends on the structure of fluorescent lipid probes: A new chain-labeled lipid transfer probe pair**. *Biochemistry* 2001, **40**(28):8292-8299.

643 Montes LR, Lopez DJ, Sot J, Bagatolli LA, Stonehouse MJ, Vasil ML, Wu BX, Hannun YA, Goni FM, Alonso A: **Ceramide-enriched membrane domains in red blood cells and the mechanism of sphingomyelinase-induced hot-cold hemolysis**. *Biochemistry* 2008, **47**(43):11222-11230.

644 Watkins S, Geng XH, Li LH, Papworth G, Robbins PD, Drain P: **Imaging secretory vesicles by fluorescent protein insertion in propeptide rather than mature secreted peptide**. *Traffic* 2002, **3**(7):461-471.

645 Kim BG, Dai HN, McAtee M, Vicini S, Bregman BS: **Labeling of dendritic spines with the carbocyanine dye DiI for confocal microscopic imaging in lightly fixed cortical slices**. *Journal of Neuroscience Methods* 2007, **162**(1-2):237-243.

648 Lisboa S, Scherer GE, Quader H: **Localized endocytosis in tobacco pollen**

tubes: visualisation and dynamics of membrane retrieval by a fluorescent phospholipid. *Plant Cell Rep* 2008, **27**(1):21-28.

649 Leung WY, Mao F, Haugland RP, Klaubert DH: **Lipophilic sulfophenylcarbocyanine dyes: Synthesis of a new class of fluorescent cell membrane probes**. *Bioorganic & Medicinal Chemistry Letters* 1996, **6**(13):1479-1482.

650 Alba FJ, Daban JR: **Inhibition of peroxyoxalate chemiluminescence by intercalation of fluorescent acceptors between DNA bases**. *Photochemistry and Photobiology* 1999, **69**(4):405-409.

651 de Maziere AM, Hage WJ, Ubbels GA: **A method for staining of cell nuclei in Xenopus laevis embryos with cyanine dyes for whole-mount confocal laser scanning microscopy**. *J Histochem Cytochem* 1996, **44**(4):399-402.

653 Dumas D, Muller S, Gouin F, Baros F, Viriot ML, Stoltz JF: **Membrane fluidity and oxygen diffusion in cholesterol-enriched erythrocyte membrane**. *Archives of Biochemistry and Biophysics* 1997, **341**(1):34-39.

654 Lin HJ, Herman P, Lakowicz JR: **Fluorescence lifetime-resolved pH imaging of living cells**. *Cytometry Part A* 2003, **52A**(2):77-89.

655 Altan N, Chen Y, Schindler M, Simon SM: **Defective acidification in human breast tumor cells and implications for chemotherapy**. *Journal of Experimental Medicine* 1998, **187**(10):1583-1598.

657 Janas T, Yarus M: **Specific RNA binding to ordered phospholipid bilayers**. *Nucleic Acids Res* 2006, **34**(7):2128-2136.

658 Tsuboi T, Lippiat JD, Ashcroft FM, Rutter GA: **ATP-dependent interaction of the cytosolic domains of the inwardly rectifying K+ channel Kir6.2 revealed by fluorescence resonance energy transfer**. *Proc Natl Acad Sci U S A* 2004, **101**(1):76-81.

659 Ramoino P, Fronte P, Fato M, Beltrame F, Diaspro A: **Mapping cholesteryl ester analogue uptake and intracellular flow in Paramecium by confocal fluorescence microscopy**. *J Microsc* 2002, **208**(Pt 3):167-176.

660 Hwang J, Gheber LA, Margolis L, Edidin M: **Domains in cell plasma membranes investigated by near-field scanning optical microscopy**. *Biophysical Journal* 1998, **74**(5):2184-2190.

661 Simons M, Kramer EM, Macchi P, Rathke-Hartlieb S, Trotter J, Nave KA, Schulz JB: **Overexpression of the myelin proteolipid protein leads to accumulation of cholesterol and proteolipid protein in endosomes/lysosomes: implications for Pelizaeus-Merzbacher disease**. *Journal of Cell Biology* 2002, **157**(2):327-336.

662 Conti F, Fioravan.R, Malerba F, Wanke E: **Comparative Analysis of Extrinsic Fluorescence in Nerve Membranes and Lipid Bilayers**. *Biophysics of Structure and Mechanism* 1974, **1**(1):27-45.

663 Haller T, Dietl P, Deetjen P, Volkl H: **The lysosomal compartment as intracellular calcium store in MDCK cells: A possible involvement in InsP(3)-mediated Ca2+ release**. *Cell Calcium* 1996, **19**(2):157-165.

664 He W, Wang H, Hartmann LC, Cheng JX, Low PS: **In vivo quantitation of rare circulating tumor cells by multiphoton intravital flow cytometry**. *Proc Natl Acad Sci U S A* 2007, **104**(28):11760-11765.

666 Yarger DE, Patrick CB, Rapoport SI, Murphy EJ: **A continuous fluorometric assay for phospholipase A(2) activity in brain cytosol**. *J Neurosci Methods* 2000, **100**(1-2):127-133.

667 Moulton HM, Nelson MH, Hatlevig SA, Reddy MT, Iversen PL: **Cellular uptake of antisense morpholino oligomers conjugated to arginine-rich peptides**.

Bioconjug Chem 2004, **15**(2):290-299.

668 Gielen E, Vercammen J, Sykora J, Humpolickova J, vandeVen M, Benda A, Hellings N, Hof M, Engelborghs Y, Steels P *et al*: **Diffusion of sphingomyelin and myelin oligodendrocyte glycoprotein in the membrane of OLN-93 oligodendroglial cells studied by fluorescence correlation spectroscopy**. *Comptes Rendus Biologies* 2005, **328**(12):1057-1064.

670 Lee HS, Mihailoff GA: **Fluorescent double-label study of lateral reticular nucleus projections to the spinal cord and periaqueductal gray in the rat**. *Anatomical Record* 1999, **256**(1):91-98.

672 James AM, Sharpley MS, Manas ARB, Frerman FE, Hirst J, Smith RAJ, Murphy MP: **Interaction of the mitochondria-targeted antioxidant MitoQ with phospholipid bilayers and ubiquinone oxidoreductases**. *Journal of Biological Chemistry* 2007, **282**(20):14708-14718.

673 Michihara A, Toda K, Kubo T, Fujiwara Y, Akasaki K, Tsuji H: **Disruptive effect of chloroquine on lysosomes in cultured rat hepatocytes**. *Biological & Pharmaceutical Bulletin* 2005, **28**(6):947-951.

675 Kong HJ, Boontheekul T, Mooney DJ: **Quantifying the relation between adhesion ligand-receptor bond formation and cell phenotype**. *Proceedings of the National Academy of Sciences of the United States of America* 2006, **103**(49):18534-18539.

676 Thanos S: **Specific Transcellular Carbocyanine-Labeling of Rat Retinal Microglia during Injury-Induced Neuronal Degeneration**. *Neuroscience Letters* 1991, **127**(1):108-112.

677 Jagasia R, Grote P, Westermann B, Conradt B: **DRP-1-mediated mitochondrial fragmentation during EGL-1-induced cell death in C. elegans**. *Nature* 2005, **433**(7027):754-760.

678 Hoekstra D, Deboer T, Klappe K, Wilschut J: **Fluorescence Method for Measuring the Kinetics of Fusion between Biological-Membranes**. *Biochemistry* 1984, **23**(24):5675-5681.

679 Nishimura SY, Vrljic M, Klein LO, McConnell HM, Moerner WE: **Cholesterol depletion induces solid-like regions in the plasma membrane**. *Biophysical Journal* 2006, **90**(3):927-938.

680 Maier B, Gluba W, Bernier B, Turner T, Mohammad K, Guise T, Sutherland A, Thorner M, Scrable H: **Modulation of mammalian life span by the short isoform of p53**. *Genes & Development* 2004, **18**(3):306-319.

681 Laib S, Seeger S: **FRET studies of the interaction of dimeric cyanine dyes with DNA**. *Journal of Fluorescence* 2004, **14**(2):187-191.

682 Rockwell PL, Storey BT: **Kinetics of onset of mouse sperm acrosome reaction induced by solubilized zona pellucida: Fluorimetric determination of loss of pH gradient between acrosomal lumen and medium monitored by Dapoxyl (2-aminoethyl) sulfonamide and of intracellular Ca2+ changes monitored by fluo-3**. *Molecular Reproduction and Development* 2000, **55**(3):335-349.

683 Mukherjee S, Zha X, Tabas I, Maxfield FR: **Cholesterol distribution in living cells: fluorescence imaging using dehydroergosterol as a fluorescent cholesterol analog**. *Biophys J* 1998, **75**(4):1915-1925.

684 Mangiardi DA, McLaughlin-Williamson K, May KE, Messana EP, Mountain DC, Cotanche DA: **Progression of hair cell ejection and molecular markers of apoptosis in the avian cochlea following gentamicin treatment**. *Journal of Comparative Neurology* 2004, **475**(1):1-18.

685 Sutton EJ, Henning TD, Pichler BJ, Bremer C, Daldrup-Link HE: **Cell tracking**

with optical imaging. *European Radiology* 2008, **18**(10):2021-2032.

700　Ho C, Williams BW, Stubbs CD: **Analysis of cell membrane micro-heterogeneity using the fluorescence lifetime of DPH-type fluorophores**. *Biochim Biophys Acta* 1992, **1104**(2):273-282.

701　Fuchs P, Parola A, Robbins PW, Blout ER: **Fluorescence polarization and viscosities of membrane lipids of 3T3 cells**. *Proc Natl Acad Sci U S A* 1975, **72**(9):3351-3354.

702　Kuypers FA, van den Berg JJ, Schalkwijk C, Roelofsen B, Op den Kamp JA: **Parinaric acid as a sensitive fluorescent probe for the determination of lipid peroxidation**. *Biochim Biophys Acta* 1987, **921**(2):266-274.

705　Honegger UE, Roscher AA, Wiesmann UN: **Evidence for lysosomotropic action of desipramine in cultured human fibroblasts**. *J Pharmacol Exp Ther* 1983, **225**(2):436-441.

706　Walkup GK, Burdette SC, Lippard SJ, Tsien RY: **A New Cell-Permeable Fluorescent Probe for Zn2+**. *J Am Chem Soc* 2000, **122**(23):5644-5645.

708　Darzynkiewicz Z, Kapuscinski J, Carter SP, Schmid FA, Melamed MR: **Cytostatic and cytotoxic properties of pyronin Y: relation to mitochondrial localization of the dye and its interaction with RNA**. *Cancer Res* 1986, **46**(11):5760-5766.

709　Easton TG, Valinsky JE, Reich E: **Merocyanine 540 as a fluorescent probe of membranes: staining of electrically excitable cells**. *Cell* 1978, **13**(3):475-486.

711　Minier C, Moore MN: **Rhodamine B accumulation and MXR protein expression in mussel blood cells: Effects of exposure to vincristine**. *Marine Ecology-Progress Series* 1996, **142**(1-3):165-173.

712　Cooperstein SJ, Dixit PK, Lazarow A: **Studies on the Mechanism of Janus Green-B Staining of Mitochondria .4. Reduction of Janus Green-B by Isolated Cell Fractions**. *Anatomical Record* 1960, **138**(1):49-66.

713　Glunde K, Foss CA, Takagi T, Wildes F, Bhujwalla ZM: **Synthesis of 6 '-O-lissamine-rhodamine B-glucosamine as a novel probe for fluorescence imaging of lysosomes in breast tumors**. *Bioconjugate Chemistry* 2005, **16**(4):843-851.

714　Li J, Norwood DL, Mao LF, Schulz H: **Mitochondrial metabolism of valproic acid**. *Biochemistry* 1991, **30**(2):388-394.

715　Gerasimenko JV, Gerasimenko OV, Palejwala A, Tepikin AV, Petersen OH, Watson AJM: **Menadione-induced apoptosis: roles of cytosolic Ca2+ elevations and the mitochondrial permeability transition pore**. *Journal of Cell Science* 2002, **115**(3):485-497.

716　Maro B, Marty MC, Bornens M: **In vivo and in vitro effects of the mitochondrial uncoupler FCCP on microtubules**. *EMBO J* 1982, **1**(11):1347-1352.

717　Lim MLR, Minamikawa T, Nagley P: **The protonophore CCCP induces mitochondrial permeability transition without cytochrome c release in human osteosarcoma cells**. *Febs Letters* 2001, **503**(1):69-74.

718　Hruban Z: **Pulmonary changes induced by amphophilic drugs**. *Environ Health Perspect* 1976, **16**:111-118.

719　Gangalum RK, Schibler MJ, Bhat SP: **Small heat shock protein alpha B-crystallin is part of cell cycle-dependent Golgi reorganization**. *Journal of Biological Chemistry* 2004, **279**(42):43374-43377.

720　Schneckenburger H, Wagner M, Kretzschmar M, Strauss WS, Sailer R: **Laser-assisted fluorescence microscopy for measuring cell membrane**

dynamics. *Photochem Photobiol Sci* 2004, **3**(8):817-822.

721 http://www.invitrogen.com/site/us/en/home/support/Research-Tools/Image-Gallery/Image-Detail.2507.html

723 Miller CR, Clapp PJ, O'Brien DF: **Visible light-induced destabilization of endocytosed liposomes**. *Febs Letters* 2000, **467**(1):52-56.

724 Bianco F, Perrotta C, Novellino L, Francolini M, Riganti L, Menna E, Saglietti L, Schuchman EH, Furlan R, Clementi E *et al*: **Acid sphingomyelinase activity triggers microparticle release from glial cells**. *EMBO J* 2009, **28**(8):1043-1054.

725 Ducker CE, Draper JM, Xia ZP, Smith CD: **In vitro and cellular assays for palmitoyl acyltransferases using fluorescent lipidated peptides**. *Methods* 2006, **40**(2):166-170.

726 Windschiegl B, Orth A, Romer W, Berland L, Stechmann B, Bassereau P, Johannes L, Steinem C: **Lipid reorganization induced by Shiga toxin clustering on planar membranes**. *PLoS One* 2009, **4**(7):e6238.

727 Chen XC, Deng YL, Lin Y, Pang DW, Qing H, Qu F, Xie HY: **Quantum dot-labeled aptamer nanoprobes specifically targeting glioma cells**. *Nanotechnology* 2008, **19**(23).

728 Keizer K, Kuypers HGJM, Huisman AM, Dann O: **Diamidino Yellow Dihydrochloride (Dy.2hcl) - a New Fluorescent Retrograde Neuronal Tracer, Which Migrates Only Very Slowly out of the Cell**. *Experimental Brain Research* 1983, **51**(2):179-191.

729 Duvvuri M, Feng W, Mathis A, Krise JP: **A cell fractionation approach for the quantitative analysis of subcellular drug disposition.** Pharm Res 2004, 21(1):26-32.

730 Huang SS, Koh HA, Huang JS: **Suramin enters and accumulates in low pH intracellular compartments of v-sis-transformed NIH 3T3 cells.** FEBS Lett 1997, 416(3):297-301.

Invi Molecular Probes online inventory (www.invitrogen.com)

Appendix I

Chemical structures of the random dataset from DrugBank representing molecules with drug properties. Structure is presented as the Simplified Molecular Input Line Entry Specification string of the major microspecies at pH 7.4, as calculated by ChemAxon.

ID	Chemical Structure
1	P(OC1[C@@H](O[C@H](n2c3cc(C)c(cc3nc2)C)C1O)CO)(OC(CNC(=O)CC[C@]1(/C=2/NC([C@@]3(N=C([C@@H](CCC(=O)N)[C@@]3(CC(=O)N)C)\C(=C\3/N=C(\C=C\4/N=C([C@@H](CCC(=O)N)C/4(C)C)\C=2\C)[C@@H](CCC(=O)N)[C@@]/3(CC(=O)N)C)\C)C)[C@@H]1CC(=O)N)C)C)(=O)[O-]
2	O=C([O-])[C@@H]([NH3+])Cc1[nH]cnc1
3	[S+](C[C@H]1O[C@@H](n2c3ncnc(N)c3nc2)[C@H](O)[C@@H]1O)(CC[C@H]([NH3+])C(=O)[O-])C
4	O=C([O-])[C@@H]([NH3+])Cc1ccccc1
5	O=C(N)CC[C@H]([NH3+])C(=O)[O-]
6	P(OC[C@H]1O[C@@H](n2c3ncnc(N)c3nc2)[C@H](O)[C@@H]1O)(=O)([O-])[O-]
7	OC1CC(C)(C)C(\C=C\C(=C\C=C\C(=C\C=C\C=C(\C=C\C=C(\C=C\C2C(CC(O)C=C2C)(C)C)/C)/C)\C)\C)=C(C1)C
8	O=C([O-])CCC(=O)[O-]
9	O=C([O-])CC[C@H]([NH3+])C(=O)[O-]
10	O=C([O-])C[NH3+]
11	Oc1c(C=O)c(cnc1C)CO
12	s1c[n+](Cc2cnc(nc2N)C)c(C)c1CCO
13	O(C(=O)C(NC(=O)C([NH3+])CC(=O)[O-])Cc1ccccc1)C
14	[nH]1c2c(ncnc2N)nc1
15	Clc1ccc(cc1)C(CC(=O)[O-])C[NH3+]
16	O(CC(O)C[NH2+]C(C)C)c1ccc(cc1)CCC(OC)=O
17	[NH3+]C(Cc1ccccc1)(C)C
18	S1C(Cc2ccc(OCC3(Oc4c(CC3)c(C)c(O)c(C)c4C)C)cc2)C(=O)[N-]C1=O
19	O1[C@H](CC)[C@](O)(C)[C@H](O)[C@@H](C)C(=O)[C@@H](C[C@](O)(C)[C@H](O[C@@H]2O[C@@H](C[C@H]([NH+](C)C)[C@H]2O)C)[C@@H](C)[C@H](O[C@@H]2O[C@@H](C)[C@H](O)[C@](OC)(C2)C)[C@@H](C)C1=O)C
20	O(C)c1ccc(OC)cc1C(O)CNC(=O)C[NH3+]
21	O(C(=O)C(O)(C1CCCCC1)c1ccccc1)CC[N+](CC)(CC)C
22	S(=O)([O-])(=NC(=O)NC1CCC(CC1)C)c1ccc(cc1)CCNC(=O)N1CC(C)=C(CC)C1=O
23	Clc1cc2NC(N(S(=O)(=O)c2cc1S(=O)(=O)N)C)CCl
24	O1CC[NH2+]C[C@H]1[C@@H](Oc1ccccc1OCC)c1ccccc1
25	Oc1ccc(N)cc1C(=O)[O-]
26	O=C1NC(=O)[N-]C1(c1ccccc1)c1ccccc1
27	Clc1c2c(C([O-])=C3[C@H](C[C@@H]4[C@@](O)(C(=O)\C(=C(/O)\N)\C(=O)[C@H]4N(C)C)C3=O)[C@@]2(O)C)c(O)cc1
28	Clc1ccccc1C(n1ccnc1)(c1ccccc1)c1ccccc1
29	O=C([O-])C
30	S(=O)(=O)(N)c1ccc(N)cc1
31	Clc1c2CN3C(=NC(=O)[CH-]3)Nc2ccc1Cl
32	ClC(=C(c1ccc(OC)cc1)c1ccc(OC)cc1)c1ccc(OC)cc1
33	Ic1c(C(=O)[O-])c(I)c(NC(=O)C)c(I)c1NC(=O)C
34	S1[C@H]2N(C(C(=O)[O-])=C(C1)CSc1nnnn1C)C(=O)[C@@]2(OC)NC(=O)CSCC#N
35	O1[C@H](C)[C@@H](N[C@H]2C=C(CO)[C@H](O)[C@H](O)[C@H]2O)[C@H](O)[C@@H](O)[C@H]1O[C@H]1[C@H](O)[C@@H](O)[C@H](O[C@@H]1CO)O[C@H]1[C@H](O)[C@@H](O[C@@H]1CO)O
36	O1[C@@H]2[C@]34[C@H]([C@H]([NH+](CC3)C)Cc3c4c1c(O)cc3)C=C[C@@H]2O
37	O=C1N=C(Nc2n(cnc12)CCC(CO)CO)N
38	Clc1cccc(F)c1-c1noc(C)c1C(=O)N[C@H]1[C@H]2SC(C)(C)[C@@H](N2C1=O)C(=O)[O-]
39	O=C1N(C)C(=O)N(C)C(=O)C1(C(CC)C)CC=C
40	Clc1ccc(cc1S(=O)(=O)N)C1(O)NC(=O)c2c1cccc2

312

41	O=C1NC(=O)NC(=O)C1(C(CCC)C)CC		C@@](O)(CCCCC)C)[C@H]1C\C=C\CCCC(=O)[O-]
42	O=C1NC[C@H]([NH3+])C(=O)[N-][C@@H](CO)C(=O)N[C@@H](CNC(=O)C[C@@H]([NH3+])CCC[NH3+])C(=O)N\C(=C\NC(=O)N)\C(=O)NC1[C@@H]1NC(=[NH+]CC1)N	64	Clc1cc2N(c3c(Sc2cc1)cccc3)CCCN1CC[NH+](CC1)C
43	Clc1cc(Nc2ncnc3c2cc(OCCCN2CCOCC2)c(OC)c3)ccc1F	65	[NH+]1(CCC(CC1)=C1c2c(C=Cc3c1ccc3)cccc2)C
44	O1[C@](NC(=O)[C@@H]2C[C@H]3[C@H]([NH+](C2)C)Cc2c4c3cccc4[nH]c2)(C)C(=O)N2[C@@H](Cc3ccccc3)C(=O)N3[C@@H](CCC3)[C@]12O	66	S(=O)(=O)(N)c1cc2S(=O)(=O)NC(Nc2cc1C(F)(F)F)Cc1ccccc1
		67	O(C)c1cc(C)c(\C=C\C(=C\C=C\C(=C/C(=O)[O-])\C)\C)c(c)c1C
45	o1c(ccc1[N+](=O)[O-])\C=N\NC(=O)N	68	O=C1N(C)C(=O)NC(=O)C1(CC)CC
46	[NH2+](CCCC1c2c(C=Cc3c1cccc3)cccc2)C	69	s1c2c(ccc(O)c2)c(C(=O)c2ccc(OCC[NH+]3CCCCC3)cc2)c1-c1ccc(O)cc1
47	O1C(C)(C)C(=O)N(C)C1=O	70	S(=O)(=O)(N)c1ccc(-n2nc(cc2-c2ccc(cc2)C)C(F)(F)F)cc1
48	OC[C@@H](NC(=O)[C@@H]1C=C2[C@H]([NH+](C1)C)Cc1c3c2cccc3[nH]c1)CC	71	Clc1cccc(Cl)c1-c1noc(C)c1C(=O)N[C@H]1[C@H]2SC(C)(C)[C@@H](N2C1=O)C(=O)[O-]
49	Clc1ccc(cc1)C(N1CC[NH+](CC1)Cc1ccc(cc1)C(C)(C)C)c1ccccc1	72	O=C(c1ccc(cc1)C)c1n(C)c(cc1)CC(=O)[O-]
50	s1cc(nc1N)/C(=N\OC(C(=O)[O-])(C)C)/C(=O)N[C@H]1[C@@H](N(S(=O)(=O)[O-])C1=O)C	73	OC(CC[N+](CC)(CC)CC)(C1CCCCC1)c1ccccc1
		74	O=C([O-])C(CCC)CCC
51	O(CCCCC)c1ccc(cc1)-c1ccc(cc1)-c1ccc(cc1)C(=O)N[C@H]1C[C@@H](O)[C@@H](O)NC(=O)[C@H]2N(C[C@H](C)[C@@H]2O)C(=O)[C@@H](NC(=O)[C@@H](NC(=O)[C@H]2N(C[C@H](O)C2)C(=O)[C@@H](NC1=O)[C@H](O)C)[C@H](O)[C@@H](O)c1ccc(O)cc1)[C@H](O)C	75	O=C([O-])\C=C(\C=C\C=C(\C=C\C=1C(CCC=1C)(C)C)/C)/C
		76	O(C(=O)C=1C(C(C(OC)=O)=C(NC=1C)C)c1cc([N+](=O)[O-])ccc1)C(C[NH+](CCC(c1ccccc1)c1ccccc1)C)(C)C
		77	O=C1N(C)C(=O)[N-]C1(CC)c1ccccc1
		78	Clc1cc2c(Oc3c(N=C2N2CC[NH2+]CC2)cccc3)cc1
52	Oc1cc(ccc1O)[C@@H](O)C[NH3+]	79	FC1=CNC(=O)NC1=O
53	O(CC(CCC)(COC(=O)N)C)C(=O)N	80	Clc1c(cccc1Cl)-c1nnc(nc1N)N
54	S1c2c(N(c3c1cccc3)CCCN1CC[NH+](CC1)C)cc(SCC)cc2	81	S(=O)([O-])(=Nc1nc(nc(OCCO)c1Oc1ccccc1OC)-c1ncccn1)c1ccc(cc1)C(C)(C)C
55	Clc1ccccc1C1C(C(OCC)=O)=C(NC(C)=C1C(OC)=O)COCC[NH3+]	82	O(C)c1cc(ccc1OC)C[C@H]1[N@+](CCc2cc(OC)c(OC)cc12)(CCC(OCCCCOC(=O)CC[N@+]1(CCc2cc(OC)c(OC)cc2[C@H]1Cc1cc(OC)c(OC)cc1)C)=O)C
56	[nH+]1c2c(CCCC2)c(N)c2c1cccc2		
57	n1c(N)c2nc(-c3ccccc3)c(nc2nc1N)N	83	S1[C@H]2N(C(C(=O)[O-])=C(C1)C)C(=O)[C@H]2NC(=O)[C@H]([NH3+])c1ccccc1
58	Cl[C@@]12[C@H]([C@@H]3C[C@H](C)[C@](O)(C(=O)CO)[C@]3(C[C@@H]1O)C)CCC1=CC(=O)C=C[C@@]12C	84	[NH+]1(CCN(CC1)CC=Cc1ccccc1)C(c1ccccc1)c1ccccc1
59	Brc1ccc(cc1)[C@H](CC[NH+](C)C)c1nccccc1	85	O(C)c1cc2N([C@@H]3[C@@]4([C@H]5[NH+](CC=C[C@@]5(CC)[C@@H](OC(=O)C)[C@]3(O)C(OC)=O)CC4)c2cc1[C@@]1(c2[nH]c3c(c2CC[NH+]2C[C@@](O)(C[C@@H](C1)C2)CC)ccc3)C(OC)=O)C
60	Brc1ccc(OC)c(C(=O)NC[C@H]2[NH+](CCC2)CC)c1OC		
61	S1[C@H]2N([C@@H](C(=O)[O-])C1(C)C)C(=O)[C@H]2NC(=O)[C@H]([NH3+])c1ccccc1		
62	O(C(=O)[C@H](CO)c1ccccc1)C1CC2[NH+](C(C1)CC2)C		
63	O[C@H]1C[C@@H](O)[C@H](\C=C\[	86	FC(F)(F)c1cc(ccc1)CC([NH2+]CC)C

87	Clc1cccc(Cl)c1NC1=[NH+]CCN1
88	s1c(nnc1N=S(=O)([O-])c1ccc(N)cc1)C
89	S1[C@H]2N([C@@H](C(=O)[O-])C1(C)C)C(=O)[C@H]2NC(=O)C(C(=O)[O-])c1ccccc1
90	S(C(=O)[C@]1(OC(=O)CC)[C@@]2([C@H]([C@@H]3C[C@H](F)C4=CC(=O)C=C[C@]4(C)[C@@]3(F)[C@@H](O)C2)C[C@H]1C)C)CF
91	O=C(N[C@H]1C=C2[C@H](N(C1)C)Cc1c3c2cccc3[nH]c1)N(CC)CC
92	Clc1nc(C(=O)N=C(N)N)c(nc1N)N
93	Clc1cc(C(=O)NC2CC[NH+](CC2OC)CCCOc2ccc(F)cc2)c(OC)cc1N
94	Oc1cc(ccc1)[C@@H](O)[C@@H]([NH3+])C
95	Oc1cc2[C@@]34CCCC[C@@]3(O)[C@H]([NH+](CC4)CC3CCC3)Cc2cc1
96	O1c2c3c4c(c(O)c2C)C(=O)C(NC(=O)/C(=C\C=C/[C@@H](C)[C@@H](O)[C@H](C)[C@H](O)[C@H](C)[C@H](OC(=O)C)[C@H](C)[C@H](OC)\C=C/O[C@]1(C)C3=O)/C)=C1NC2(N=C14)CC[NH+](CC2)CC(C)C
97	F[C@@]12[C@H]([C@@H]3C[C@@H](O)[C@](O)(C(=O)CO)[C@]3(C[C@@H]1O)C)CCC1=CC(=O)C=C[C@@]12C
98	O=C1CC[C@@]2([C@@H]3[C@H]([C@@H]4CC[C@H](O)[C@]4(CC3)C)CCC2=C1)C
99	Clc1cc2c(NC(=O)C(N=C2c2ccccc2)C(=O)[O-])cc1
100	P(O)(=O)([O-])C(P(O)(=O)[O-])(O)CCC[NH3+]
101	Fc1ccc(cc1)Cn1c2c(nc1NC1CC[NH+](CC1)CCc1ccc(OC)cc1)cccc2
102	O(CCCC)c1ccc(cc1)C(=O)CC[NH+]1CCCCC1
103	Oc1cc2c(C[C@H]3[NH+](CC[C@]2(C)[C@H]3C)CC=C(C)C)cc1
104	Clc1cc(N2CCN(CC2)CCCN2N=C3N(C=CC=C3)C2=O)ccc1
105	O1C(CNC1=O)COc1cc(cc(c1)C)C
106	[NH3+]CCc1[nH]cnc1
107	Fc1ccc(cc1)[C@H]1N(CCO[C@H]1O[C@H](C)c1cc(cc(c1)C(F)(F)F)C(F)(F)F)CC1=NC(=O)[N-]N1
108	S1c2c(N(c3c1cccc3)C(=O)CCN1CCOCC1)cc(NC(OCC)=O)cc2
109	O1[C@H](CO)[C@@H](O)[C@H]([NH3+])[C@@H](O)[C@H]1O[C@@H]1[C@@H](O)[C@H](O[C@H]2O[C@H](C[NH3+])[C@@H](O)C[C@H]2[NH3+])[C@@H]([NH3+])C[C@H]1[NH3+]
110	Fc1cc(F)ccc1N1C=C(C(=O)[O-])C(=O)c2cc(F)c(nc12)N1C[C@@H]2[C@H](C1)C2[NH3+]
111	S1[C@H]2N(C(C(=O)[O-])=C(C1)COC(=O)C)C(=O)[C@H]2NC(=O)[C@H]([NH3+])c1ccccc1
112	Oc1cc(N(CC2=[NH+]CCN2)c2ccc(cc2)C)ccc1
113	Clc1cc(NCc2occc2)c(cc1S(=O)(=O)N)C(=O)[O-]
114	o1c(ccc1[N+](=O)[O-])\C=N/N1CC(=O)NC1=O
115	S(=O)(=O)(N(CC(C)C)C[C@@H](O)[C@@H](NC(O[C@H]1CCOC1)=O)Cc1ccccc1)c1ccc(N)cc1
116	O1[C@@H]2[C@]34CC[NH+]([C@H](Cc5c3c1c(O)cc5)[C@]4(O)CCC2=O)CC1CC1
117	O(C(C)c1c2[nH]c(C=C3N=C(C=C4N=C(C=c5[nH]c(=C2)c(C)c5C(O)C)C(C)=C4CCC(=O)[O-])C(CCC(=O)[O-])=C3C)c1C)C(C)c1c=2[nH]c(=Cc3[nH]c(\C=C\4/N=C(\C=C\5/N=C(C(=2)C(C)=C/5CCC(=O)[O-])C(CCC(=O)[O-])=C/4C)c(C)c3C(O)C)c1C
118	S1C[C@H](O[C@H]1CO)N1C=CC(=NC1=O)N
119	O(C)c1ccc(OC)cc1C(O)C([NH3+])C
120	O(C(=O)C(O)c1ccccc1)C1CC2[N+](C(C1)CC2)(C)C
121	[NH+](CC(CN1c2c(CCc3c1cccc3)cccc2)C)(C)C
122	[N+]1(CCC(CC1)=C(c1ccccc1)c1ccccc1)(C)C
123	s1c2cc(OC(F)(F)F)ccc2nc1N
124	O(Cc1ccccc1)CC(N(CC[NH+](CCN(CC(=O)[O-])CC(=O)[O-])CC(=O)[O-])CC(=O)[O-])C(=O)[O-]
125	O=C(N(O)CCCCCNC(=O)CCC(=O)N(O)CCCCC[NH3+])CCC(=O)NCCCCCN(O)C(=O)C
126	O1C2C3N(C(CC(OC(=O)C(CO)c4cccc4)C3)C12)C
127	O1CCc2c([nH]c3c2cccc3CC)C1(CC(=O)[O-])CC
128	[NH3+][C@@H]1CC1c1ccccc1
129	S([C@@H]1[NH2+][C@@H](CC1)C(=O)N(C)C)C=1[C@@H]([C@H]2N(C=1C(=O)[O-])C(=O)[C@@H]2[C@H](O)C)C
130	O=C(N[C@@H](C(C)(C)C)C(=O)NC)[C@@H]([C@H](O)C(=O)NO)CC(C)C
131	IC#CCOc1cc(Cl)c(Cl)cc1Cl
132	O=C1NCNC(=O)C1(CC)c1ccccc1
133	O(CC)c1nc2c(n1Cc1ccc(cc1)-

	c1ccccc1-c1nn[nH]n1)c(ccc2)C(=O)[O-]		C@@H](O)C[C@]1(C3C[C@@H](C)[C@@]1(C(=O)CC)C)C
134	S1CCC(c2cc(ccc12)C#Cc1ncc(cc1)C(OCC)=O)(C)C	161	O(C(=O)c1ccc(cc1)C)c1cc(ccc1OC(=O)c1ccc(cc1)C)C(O)C[NH2+]C(C)(C)C
135	Clc1c2c(cc(O)c1O)C(C[NH2+]CC2)c1ccc(O)cc1	162	s1ccc(C)c1C(=CCC[NH+]1C[C@@H](CCC1)C(=O)[O-])c1sccc1C
136	O=C1N(CCCCC(=O)C)C(=O)N(c2ncn(c12)C)C	163	S(=O)(=O)(N)Cc1noc2c1cccc2
137	O(CCC)c1ccc(cc1N)C(OCC[NH+](CC)CC)=O	164	O[C@@H]1CC(C[C@@H](O)C1)=C\C=C/1\[C@@H]2CC[C@H]([C@@H](\C=C\[C@@H](C(O)(C)C)C)C)[C@]2(CCC\1)C
138	Clc1ccc(cc1S(=O)(=O)N)C(=O)NN1c2c(CC1C)cccc2	165	S(=O)(=O)(CCn1c(ncc1[N+](=O)[O-])C)CC
139	O=C1N(N(C(=O)[C-]1CCCC)c1ccccc1)c1ccccc1	166	OCCn1c(ncc1[N+](=O)[O-])C
140	O=C(N(C1CC[NH+](CC1)CCc1ccccc1)c1ccccc1)CC	167	O=C1NN=C([C@@H](C1)C)c1ccc(NN=C(C#N)C#N)cc1
141	Oc1cc(cc(O)c1)C(O)C[NH2+]C(C)C	168	O1[C@H](CO)[C@@H](O)[C@@H](O)[C@@H]1N1C=NC(=NC1=O)N
142	O=C1c2c(N(C=C1C(=O)[O-])CC)cc(cc2)-c1ccncc1	169	S(=O)([O-])(=Nc1cc(ccc1)[C@@H](CC)C=1C(=O)C[C@](OC=1O)(CCc1ccccc1)CCC)c1ncc(cc1)C(F)(F)F
143	Oc1c(cccc1C(C)C)C(C)C		
144	s1c(nnc1S(=O)([O-])=[NH])NC(=O)C	170	[NH2+](CCCC12CCC(c3c1cccc3)c1c2cccc1)C
145	O=C1N(C)C(=O)CC1c1ccccc1	171	Oc1ccccc1C(=O)[O-]
146	O=C1CCC2=C3[C@H]([C@@H]4CC[C@@](O)(C#CC)[C@]4(C[C@@H]3c3ccc(N(C)C)cc3)C)CCC2=C1	172	O(CC(COC(=O)N)c1ccccc1)C(=O)N
		173	O(CC(O)C[NH2+]C(C)C)c1c2c([nH]cc2)ccc1
147	Clc1cc2c(NC(=O)C(O)N=C2c2ccccc2)cc1	174	O1C(C)C(NC(=O)C=2C3=Nc4c(OC3=C(C)C(=O)C=2N)c(ccc4C(=O)NC2C(OC(=O)C(N(C)C(=O)CN(C)C(=O)C3N(CCC3)C(=O)C(NC2=O)C(C)C)C(C)C)C)C(=O)NC(C(C)C)C(=O)N2C(CCC2)C(=O)N(CC(=O)N(C)C(C(C)C)C1=O)C
148	F[C@@H]1C2=CC(=O)CC[C@@]2([C@@H]2[C@H]([C@@H]3C[C@H]4OC(O[C@@]4(C(=O)CO)[C@]3(C[C@@H]2O)C)(C)C)C1)C		
149	O=C1N(C)C(=O)NC(=O)C1(CC)c1cccc1		
150	O[C@H]([C@@H]([NH2+]C)C)c1ccccc1	175	[Se]=S
151	SC([C@@H]([NH3+])C(=O)[O-])(C)C	176	O=C([O-])CN(CC[NH+](CC(=O)[O-])CC(=O)[O-])CC(=O)[O-]
152	O(CC(O)C[NH2+]C(C)C)c1ccccc1CC=C	177	OC1(CCCC1)C(C(OCC[NH+](C)C)=O)c1ccccc1
153	Oc1ccc(cc1)CC[NH2+][C@H]([C@H](O)c1ccc(O)cc1)C	178	O=C1CC[C@@H]2[C@@H]3[C@H]([C@@H]4CC[C@H](OC(=O)CCc5ccccc5)[C@]4(CC3)C)CCC2=C1
154	O(C(=O)c1ccc(NCCCC)cc1)CCOCCOCCOCCOCCOCCOCCOCCOC	179	Oc1cc(ccc1O)CC[NH3+]
		180	O(C(=O)N(CC)C)c1cc(ccc1)[C@@H]([NH+](C)C)C
155	s1c2S(=O)(=O)C(CC(NCC)c2cc1S(=O)(=O)N)C	181	O1[C@@H](C)[C@@H](O)[C@@H]([NH3+])C[C@@H]1O[C@@H]1c2c(C[C@](O)(C1)C(=O)CO)c(O)c1c(C(=O)c3c(cccc3OC)C1=O)c2O
156	Oc1cc(cc(O)c1)C(O)C[NH2+]C(C)(C)C		
157	S1c2c(cc(cc2)C(F)(F)F)C(c2c1cccc2)=CCC[NH+]1CCN(CC1)CCO	182	O=C(N)c1cc2c3C[C@H]([NH2+]C)Cc3[nH]c2cc1
158	Clc1ccc(N\C(=N\C(=[NH+]\CCCCC\[NH+]=C(\N=C(\Nc2ccc(Cl)cc2)/N)/N)\N)\N)cc1	183	O=C(Nc1c(cccc1C)C)[C@H]1[NH+](CCCC1)CCCC
159	O=C1N2C(=NC=C1c1n[n-]nn1)C(=CC=C2)C		
160	O=C1C=C2CCC3C([C@]2(C=C1)C)[		

184	O=C1N=C(Nc2n(cnc12)COC(CO)CO)N
185	S(OCCCCOS(=O)(=O)C)(=O)(=O)C
186	O=C(c1cc(ccc1)C(C(=O)[O-])C)c1ccccc1
187	Oc1cc([N+](CC)(C)C)ccc1
188	FC(F)(F)c1cc(ccc1)CCC[NH2+][C@H](C)c1c2c(ccc1)cccc2
189	Oc1c2c(C[C@@H]3C(C(=O)[C@@]4(O)[C@@H](C3)[C@H](N(C)C)C(=O)/C(=C(\O)/N)/C4=O)=C2[O-])c(N(C)C)cc1
190	O1CC2=C(C=C3N(Cc4c3nc3c(c4)c(C[NH+](C)C)c(O)cc3)C2=O)[C@@](O)(CC)C1=O
191	O(C(=O)N)C1(CCCCC1)C#C
192	S(=O)(=O)(N(CCC)CCC)c1ccc(cc1)C(=O)[O-]
193	S1c2c(N(c3c1cccc3)CCCN1CC[NH+](CC1)CCO)cc(cc2)C(=O)CC
194	O=C/1C=C(C=C\C\1=C\C=C1C=CC(C=C1)=C(N)N)C(=[NH2+])N
195	[NH3+]C12CC3(CC(C1)(CC(C3)C2)C)C
196	O1c2c3c4c(c(O)c2C)C(O)=C(NC(=O)C(=C\C=C\[C@H](C)[C@@H](O)[C@H](C)[C@@H](O)[C@H](C)[C@@H](OC(=O)C)[C@@H](C)[C@@H](OC)\C=C\O[C@]1(C)C3=O)\C(=C/NN1CCN(CC1)C)\C4=O
197	O1[C@@H](Oc2ccc3c(OC([O-])=C(NC(=O)c4cc(CC=C(C)C)c(O)cc4)C3=O)c2C)[C@H](O)[C@H](OC(=O)N)[C@@H](OC)C1(C)C
198	S(P(OCC)(OCC)=O)CC[N+](C)(C)C
199	Fc1cc2c(N(C=C(C(=O)[O-])C2=O)CC)cc1N1CC[NH2+]CC1
200	S(=O)([O-])(=NC(=O)NC1CCCCC1)c1ccc(cc1)CCNC(=O)c1ncc(nc1)C
201	S1c2c(N(c3c1cccc3)CC([NH+](C)C)C)cccc2
202	[NH2+]1CCCCC1CC(C1CCCCC1)C1CCCCC1
203	O1C(=O)C=C([C@H]2CC[C@]3(O)[C@H]4[C@@H](C[C@@H](O)[C@]23C)[C@@]2([C@@H](C[C@@H](O[C@@H]3O[C@H](C)[C@@H](O[C@@H]5O[C@H](C)[C@@H](O[C@@H]6O[C@H](C)[C@@H](O[C@@H]7O[C@@H](CO)[C@@H](O)[C@H](O)[C@H]7O)[C@@H](O)C6)[C@@H](O)C5)[C@@H](O)C3)CC2)CC4)C)[CH-]1
204	O=C([O-])CCC([NH3+])C=C
205	O(C(=O)C1(CC[NH+](CC1)CCC(C#N

	)(c1ccccc1)c1ccccc1)c1ccccc1)CC
206	O(C)c1cc(NC(CCC[NH3+])C)c2ncccc2c1
207	[N+]1(CCCC1)(CCCCC[N+]1(CCCC1)C)C
208	[NH+](Cc1c2c(ccc1)cccc2)(Cc1ccc(cc1)C(C)(C)C)C
209	FC(F)(F)c1ccc(NC(=O)c2cnoc2C)cc1
210	Oc1cc(ccc1O)[C@@H](O)C[NH2+]CCCCc1ccc(O)cc1
211	O(C)c1ccc(cc1)[C-]1C(=O)c2c(cccc2)C1=O
212	S(=O)(=O)(C[C@](O)(C(=O)Nc1cc(C(F)(F)F)c(cc1)C#N)C)c1ccc(F)cc1
213	Fc1cc2c3N(C=C(C(=O)[O-])C2=O)[C@H](COc3c1N1CCN(CC1)C)C
214	Clc1c(S(=O)(=O)N)cc(S(=O)(=O)N)cc1Cl
215	S1[C@H]2N(C(C(=O)[O-])=C(C1)\C=C\C)C(=O)[C@H]2NC(=O)[C@H]([NH3+])c1ccc(O)cc1
216	O1C(C(CC(C(O)CC(=O)c2ccc(N)cc2)C)C)C(\C=C/C=C\C=C/C=C\C=C/C(OC2O[C@H](C)[C@@H](O)[C@H]([NH3+])[C@@H]2O)CC2OC(O)(CC(O)C2C(=O)[O-])CC(O)CC(O)CC(O)CC(=O)CCCC(=O)CC1=O)C
217	Clc1cc(Cl)ccc1C(OCc1c2c(sc1)c(Cl)ccc2)Cn1ccnc1
218	Fc1ccc(cc1)[C@@]1(OCc2cc(ccc12)C#N)CCC[NH+](C)C
219	O1[C@@H](C)[C@@H](O)[C@@H]([NH3+])C[C@@H]1O[C@@H]1c2c(C[C@](O)(C1)C(=O)C)c(O)c1c(C(=O)c3c(cccc3)C1=O)c2O
220	FC(F)(F)COc1ccc(OCC(F)(F)F)cc1C(=O)NCC1[NH2+]CCCC1
221	O=C1N(CCC1)[C@H](CC)C(=O)N
222	ClCCN(N=O)C(=O)NC1CCCCC1
223	FC(F)(F)c1cc(ccc1)\C(=N/OCCCCC(=O)[O-])\c1cccnc1
224	Fc1c(N2C[C@H]([NH2+][C@H](C2)C)C)c(F)c2N(C=C(C(=O)[O-])C(=O)c2c1N)C1CC1
225	O1[C@@H](CC)[C@](O)(C)[C@H](O)[C@H](C)C(=O)[C@@H](C[C@](OC)(C)[C@H](O[C@@H]2O[C@@H](C[C@H]([NH+](C)C)[C@H]2O)C)[C@@H](C)[C@H](O[C@@H]2O[C@@H](C)[C@H](O)[C@](OC)(C2)C)[C@@H](C)C1=O)C
226	O1c2c3c4c(c([O-])c2C)c([O-])c(NC(=O)C(=C\C=C\[C@H](C)[C@@

	H](O)[C@@H](C)[C@@H](O)[C@H](C)[C@H](OC(=O)C)[C@@H](C)[C@ @H](OC)\C=C\O[C@]1(C)C3=O)c1 n2c(nc14)C=C(C=C2)C
227	O1[C@@]2([C@H](O[C@@H]1CCC) C[C@H]1[C@H]3[C@@H]([C@@]4(C(=CC(=O)C=C4)CC3)C)[C@@H](O) C[C@@]12C)C(=O)CO
228	O([C@H](C(C[C@@H]([NH+](C)C)C) (c1ccccc1)c1ccccc1)CC)C(=O)C
229	OC(CCC[NH+]1CCCCC1)(c1ccccc1)c 1ccccc1
230	O=C(N[C@@H](CC(=O)N)C(=O)N[C @H]([C@H](O)C[NH+]1CC2C(C[C@ H]1C(=O)NC(C)(C)C)CCCC2)Cc1ccc cc1)c1nc2c(cc1)cccc2
231	o1nc(cc1C)C(=O)NNCc1ccccc1
232	O1[C@@H]2C[C@H](O)[C@@]3([C @H]([C@H](OC(=O)c4ccccc4)[C@]4(O)C[C@H](OC(=O)[C@H](O)[C@@H](NC(OC(C)(C)C)=O)c5ccccc5)C(=C([C@@H](O)C3=O)C4(C)C)C)[C@]2(O C(=O)C)C1)C
233	Ic1c(C(=O)NCC(O)CO)c(I)c(N(C(=O) C)CC(O)CN(C(=O)C)c2c(I)c(C(=O)N CC(O)CO)c(I)c(C(=O)NCC(O)CO)c2I) c(I)c1C(=O)NCC(O)CO
234	Oc1ccc(N\N=C\2/C=C(C(=O)[O-])C(=O)C=C/2)cc1C(=O)[O-]
235	Fc1cc2onc(c2cc1)C1CC[NH+](CC1)C CC=1C(=O)N2C(=NC=1C)C(O)CCC2
236	Fc1cc\2c(NC(=O)/C/2=C\c2[nH]c(C)c(C(=O)NCC[NH+](CC)CC)c2C)cc1
237	S(=O)([O-])(=NC(=O)NN1CCCCCC1)c1ccc(cc1)CCNC(=O)c1noc(c1)C
238	[BiH]1OC(=O)c2c(O1)cccc2
239	Oc1c2c(ccc1)[C@@](O)([C@@H]1C(C(=O)[C@@]3(O)[C@@H](C1)[C@H](N(C)C)C(=O)/C=C(/O)\NCN1CCCC 1)/C3=O)=C2[O-])C
240	S(=O)(=O)(N(CC(C)C)C[C@@H](OP(=O)([O-])[O-])[C@@H](NC(O[C@H]1CCOC1)=O) Cc1ccccc1)c1ccc(N)cc1
241	O1[C@@H](C\C=C\C=C\[C@H](O)[C @@H](C[C@H](CC=O)[C@H](O[C@ @H]2O[C@H](C)[C@@H](O[C@@H] 3O[C@@H](C)[C@H](OC(=O)CC(C) C)[C@](O)(C3)C)[C@H]([NH+](C)C)[C@H]2O)[C@@H](OC)[C@H](OC(= O)C)CC1=O)C)C
242	O1C(CC(OC)=CC1=O)\C=C\C\=1C=C CCC=1
243	Clc1cc2NC(N(S(=O)(=O)c2cc1S(=O)(

	=O)N)C)CSCC(F)(F)F
244	S1C(SC1=C(C(=O)N)C(=O)[O-])C(=O)N[C@@]1(OC)C2SCC(CSc3n nnn3C)=C(N2C1=O)C(=O)[O-]
245	s1cccc1CC(=O)NC1(OC)C2SCC(CO C(=O)N)=C(N2C1=O)C(=O)[O-]
246	O(C(=O)C)[C@@H]1[C@@]2([C@H] ([C@H]3[C@H](CC2)[C@@]2([C@H] (C[C@H](OC(=O)C)[C@@H]([N+]4(C CCCC4)C)C2)CC3)C)[C@H]1[N+]1(CCCCC1)C)C
247	O[C@@H]([C@@H]([NH2+]C)C)c1cc ccc1
248	[NH2+](CC#C)[C@@H]1CCc2c1cccc 2
249	[Mg+]O
250	F[C@@H]1C2=CC(=O)C=C[C@@]2([C@@H]2C[C@H]([C@@H]3C[C@@ H](C)[C@](O)(C(=O)CO)[C@]3(C[C@ @H]2O)C)C1)C
251	O1[C@]2([C@@H]3C[C@H]([C@H]4[C@H]5[C@H](CC[C@]24C)[C@]2(C CC(=O)C=C2[C@H]2[C@@H]5C2)C) C3)CCC1=O
252	Fc1cc(F)ccc1N1C=C(C(=O)[O-])C(=O)c2cc(F)c(N3CC([NH2+]CC3)C)cc12
253	O=C1NC(=O)N(c2ncn(c12)C)C
254	s1cc(nc1N)/C(=C/CC(=O)[O-])/C(=O)N[C@H]1[C@H]2SCC=C(N2 C1=O)C(=O)[O-]
255	O1[C@@H](C(NH3+])[C@@H](O)[C @H](O)[C@@H]([NH3+])[C@H]1O[C @H]1[C@@H](O)[C@@H](O[C@@H]1CO)O[C@H]1[C@H](O[C@H]2O[C @@H](CO)[C@@H](O)[C@H](O)[C@H]2[NH3+])[C@@H]([NH3+])C[C@@H] ([NH3+])[C@@H]1O
256	O[C@H]1N2[C@@H]3C4[C@@H](C[C@H]2[C@@H]2N(c5c([C@@]2(C3)[C@H]4O)cccc5)C)[C@@H]1CC
257	[NH+](CCCN(C1Cc2c(C1)cccc2)c1cc ccc1)(CC)CC
258	Fc1ccc(cc1)C(N1CCN(CC1)c1nc(nc(n 1)NCC=C)NCC=C)c1ccc(F)cc1
259	s1cccc1CC[NH+]1CC(C)C(N(C(=O)C C)c2ccccc2)CC1
260	s1cccc1C(=CC([NH+](C)C)C)c1sccc1
261	[NH3+]C(Cc1c2c([nH]c1)cccc2)C
262	OC(C[NH+]1CCC(N(C(=O)CC)c2cccc c2)CC1)c1ccccc1
263	O(CC)c1ccc(cc1)Cc1nc2cc([N+](=O)[O-])ccc2n1CC[NH+](CC)CC
264	s1cccc1CC([NH+]1CCC(N(C(=O)CC) c2ccccc2)CC1)C

317

265	O=C1CC[C@@]2([C@@H]3[C@H]([C@@H]4CC[C@@](O)(C)[C@]4(CC3)C)[C@@H](CC2=C1)C)C	291	[NH+](CCCc1ccccc1)(CCCc1ccccc1)CC
266	O(C)c1ccc(cc1)CC([NH3+])C	292	O1CCN(CC1)CC1CCc2[nH]c(C)c(c2C1=O)CC
267	O1CCN(CC1)CCC(C(OCC)=O)(c1cccc1)c1ccccc1	293	[NH+](CCC(c1ccccc1)c1ncccc1)(C)C
268	O=C1C=C[C@]2([C@H](C1)CC[C@H]1[C@@H]3CC[C@H](O)[C@]3(CC[C@@H]12)C)C	294	S1c2c(N(c3c1cccc3)CCC[NH+]1CCC(CC1)CCO)cc(S(=O)(=O)N(C)C)cc2
269	O(C)c1cc(ccc1)C(CC)(CC)CNC(=O)CCCO	295	S(C)[C@H]1O[C@H]([C@H](NC(=O)C2[NH+](C[C@@H](C2)CCC)C)[C@H](O)C)[C@H](O)[C@H](O)[C@H]1O
270	Clc1cc2c(N(C)C(=O)C(OC(=O)N(C)C)N=C2c2ccccc2)cc1	296	OC[C@@H](O)[C@@H](O)[C@@H](O)[C@@H](O)CO
271	O1C(C[NH+]=C1N)c1ccccc1	297	P(OC[C@H]1O[C@@H](N2C=C(C)C(=O)NC2=O)C[C@@H]1O)(=O)([O-])[O-])
272	O[C@@H](C(C[C@H]([NH+](C)C)C)(c1ccccc1)c1ccccc1)CC	298	O1C[C@H]2O[C@@H](OC)[C@H](O)[C@@H](O)[C@H]2O[C@@]1(C(=O)[O-])C
273	O=C([O-])C1(CC[NH+](CC1)CCC(C#N)(c1ccccc1)c1ccccc1)c1ccccc1	299	OC/1=CC(=O)C(C\C\1=N\C1CC1c1ccccc1)CC([NH3+])C(=O)[O-]
274	O([C@H](C(C[C@H]([NH+](C)C)C)(c1ccccc1)c1ccccc1)CC)C(=O)C	300	[Ru+2]123N4C(=C(C=C4)CCCCCCCCC(=O)NC4C5CC6CC4CC(C5)C6)=C4N1C=CC(=C4)C)(N1C(=C4N2C=CC=C4)C=CC=C1)N1C(=C2N3C=CC=C2)C=CC=C1
275	O[C@H]1C[C@H]2[NH+]([C@H](CC2)[C@H]1C(=O)[O-])C	301	O1[N-]C(=O)C(=C1)C[C@H]([NH3+])C(=O)[O-]
276	Clc1ccccc1CC([NH3+])(C)C	302	Oc1nc(nc2[nH]nnc12)N
277	s1cccc1C(=CC([NH+](CC)CC)C)c1sccc1	303	[Hg](O)c1ccc(cc1)C(=O)[O-]
278	Clc1cc2c(NC(=O)C(N=C2c2ccccc2F)C(OCC)=O)cc1	304	O=C([O-])\C=C\C(=O)[O-]
279	[NH2+](C(Cc1ccccc1)C)CCC#N	305	O=C(NC(CC(C)C)C(=O)NC(Cc1ccccc1)C=O)C(NC(=O)NC(Cc1ccccc1)C(=O)[O-])C1NC(=[NH2+])NCC1
280	O([C@@H](C(C[C@H]([NH+](C)C)C)(c1ccccc1)c1ccccc1)CC)C(=O)C	306	O=C([O-])[C@@H]([NH3+])CCC\[NH+]=C(\N(C)C)/N
281	Clc1ccccc1C1=NCC(=O)N(c2sc(cc12)CC)C	307	O1C(CO)C(O)C(O)C(O)C1OC1C(O)C(O)C(OC1CO)O
282	O1[C@@H]2[C@]34[C@H]([C@H]([N+]([O-])(CC3)C)Cc3c4c1c(OC)cc3)C=C[C@@H]2O	308	Oc1ccc(cc1)C
283	O=C1C=C2CC[C@@H]3[C@@H]([C@]2(C=C1C=O))[C@H](O)C[C@]1([C@H]3CC[C@@]1(O)C)C	309	SCC(O)C(O)CS
284	Clc1cc2c(N(C)C(=O)CN3C2(OC(=CC3=O)C)c2ccccc2)cc1	310	P(OCC1OC(n2nc(nc2)C(=O)N)C(O)C1O)(=O)([O-])[O-]
285	Clc1cc2c(N(CC3CC3)C(=O)CN=C2c2ccccc2)cc1	311	OC(C(O)C(=O)[O-])C(=O)[O-]
286	[Zn]	312	P(O)(=O)([O-])CCCC(=O)NO
287	O=C1Nc2c(cc([N+](=O)[O-])cc2)C(=NC1)c1ccccc1	313	O=C1NC(=O)NC=2NC(=O)NC1=2
288	S(C(Sc1cc(C(C)(C)C)c(O)c(c1)C(C)(C)C)(C)C)c1cc(C(C)(C)C)c(O)c(c1)C(C)(C)C	314	O1C(COC2OC(C)C(O)C(O)C2O)C(O)C(O)C(O)C1OC1=C(Oc2c(C1=O)c(O)cc([O-])c2)c1cc(O)c(O)cc1
289	S1(=O)(=O)C2N(C(C(=O)[O-])C1(Cn1nncc1)C)C(=O)C2	315	Oc1cc(ccc1O)CC(=O)[O-]
290	S1[C@H]2N([C@@H](C(=O)[O-])C1(C)C)C(=O)[C@H]2NC(=O)[C@H](C(=O)[O-])c1ccsc1	316	Oc1cc(O)ccc1\C=C\C(=O)[O-]
		317	P(OCC(O)COC(=O)CCCCCCCCCCC)(OCC[N+](C)(C)C)(=O)[O-]
		318	P(OC(C(=O)[O-])CO)(=O)([O-])[O-]
		319	S1CC(N(S(=O)(=O)c2ccc(cc2)C)CC1)

	C(=O)NC(Cc1ccccc1)C(OCC)=O
320	O=C([O-])CCCCCC([NH3+])C([NH3+])C
321	[N+](CCCCCCCCCCCCCCCC)(C)(C)C
322	OC(C(CC(=O)[O-])C(=O)[O-])C(=O)[O-]
323	P(OCC(OC(=O)CCCCCCCCCCCCC)COC(=O)CCCCCCCCCCCCCC)(OCC[NH3+])(=O)[O-]
324	P(OC(C(=O)[O-])C)(=O)([O-])[O-]
325	ClCC([NH3+])C(=O)[O-]
326	O=C([O-])C([NH3+])C(CC)C
327	[Se]=1=C(CCC)C(=NC=1N)CCCC
328	Oc1cc2C=C(NC(=O)CCC(=O)[O-])C3N(c2cc1O)C(CCN3)C(=O)NC(C(=O)NC(CCCNC(=[NH2+])N)C(=O)NC(C(=O)NC(CCCN(O)C=O)C(=O)NC1CCCNC(=O)C(NC(=O)C(NC(=O)C(NC1=O)CCCN(O)C=O)C(O)C)C(O)C)CO)CO
329	O=C([O-])Cc1c2c(ccc1)cccc2
330	O1C(C(O)C(O)CO)C(NC(=O)C)C(O)CC1(Oc1cc2OC(=O)C=C(c2cc1)C)C(=O)[O-]
331	C1CCC(C)=C(\C=C\C(=C\C=C\C(=C\C)\C)\C)C1(C)C
332	OC(C(CO)(C)C)C(=O)NCCC(=O)[O-]
333	S(=O)(=O)(N)c1ccc(F)cc1
334	OC1C([NH3+])C=C(CC1O)CO
335	Clc1ccc(NC2=C(c3cc(Cl)ccc3)C(=O)NC2=O)cc1C(=O)[O-]
336	O=C([O-])c1cccnc1C(=O)[O-]
337	O=C([O-])C([NH3+])C=C
338	P(OC(C)C)(OCC(N)C(=O)[O-])(=O)[O-]
339	[AsH](SCC([NH3+])C(=O)[O-])O
340	n1cnc2n(nc(c2c1N)-c1ccc(cc1)C)C(C)(C)C
341	P(OCc1cnc(C)c(O)c1C[NH2+]C(CCC(=O)[O-])C(=O)[O-])(=O)([O-])[O-]
342	O(C(CCCCCCCCCCCC)CC(=O)[O-])C(=O)CCCCCCCCCCC
343	O=C(N)C(NC(=O)C([NH3+])CCCNC(N[N+](=O)[O-])=N)CC[NH3+]
344	P(=O)([O-])([O-])c1cc(ccc1P(=O)([O-])[O-])CC(NC(=O)C)C(=O)NC1CCCCc2c1cc(C(=O)N)c(OCC1CCCCC1)c2
345	FC(CC([NH3+])C(=O)[O-])CCNC(=[NH2+])C
346	O1C(O)C(O)C(O)CC1C
347	c1ccccc1CCCC
348	[CaH]OC(C(CC(=O)[O-])C(=O)[O-])C(=O)[O-]

349	O(C(Cc1ccccc1)C(\C=C(\C=C\C([NH3+])C(C(=O)[O-])C)/C)C)C
350	O1c2c(C(=O)C(O)=C1c1ccc(O)cc1)c(O)cc([O-])c2
351	O=C([O-])CCCCC(=O)[O-]
352	SC1C(O)C(O)C(S)OC1CO
353	S(OC1C(O)C(NC(=O)C)C(OC1CO)O)(=O)(=O)[O-]
354	O=C(c1[nH]c2cc(ccc2n1)C(=[NH2+])N)c1[nH]c2cc(ccc2n1)C(=[NH2+])N
355	S(CCC([NH3+])C(O)(O)c1ncccc1)C
356	S(CCC(NC(=O)C1N(CCC1)C(=O)C(NC(=O)CS)Cc1ccc(O)cc1)C(=O)N)C
357	O1C(CO)C(O)C(O)C(O)C1=O
358	O(Cc1ccccc1)C(=O)NC(C(=O)NC(C(C)C)C(=O)NC(Cc1ccccc1)CO)C
359	O=C1C2(C(=O)C(C)C)C(CCC=C(C)C)(C)C(CC1(CC=C(C)C)C(=O)C(CC=C(C)C)=C2[O-])CC=C(C)C
360	P(=O)([O-])([O-])c1cc(ccc1OCC(=O)[O-])CC(NC(=O)C)C(=O)NC1CCCCN(Cc2ccc(cc2)-c2ccccc2)C1=O
361	OC(C(O)C(O)C=O)C(O)CO
362	S(O)CC([NH3+])C(=O)[O-]
363	[Te](CC(=O)[O-])C
364	OC(C(CO)(C)C)C(=O)[O-]
365	SC[C@H](NC(=O)CC(=O)[O-])Cc1ccccc1
366	O(C(=O)c1ccc(cc1)C(=O)c1ccccc1O)C1CCC[NH2+]CC1NC(=O)c1ccc(O)cc1
367	O(C(=O)C1N(CCC1)C(=O)C(=O)C(CC)(C)C)CCCc1cccnc1
368	Clc1cc(O)ccc1
369	OB(O)CCc1ccccc1
370	s1c2S(=O)(=O)N(CC(O)c2cc1S(=O)(=O)N)c1ccc(OC)cc1
371	S(CC([NH3+])C(=O)[O-])C1NOC(=C1)C([NH3+])C(=O)[O-]
372	Nc1c2c(cc3c(c2)cccc3)ccc1
373	Oc1nc(nc2n(c[n+](c12)C)C)N
374	O[B-](O)(O)CCCCC([NH3+])C(=O)[O-]
375	Fc1cccc(N)c1C
376	s1c[n+](Cc2cnc(nc2N)C)c(C)c1CCOP(OP(=O)([O-])[O-])(=O)[O-]
377	[NH2+]1CCN(C[C@@H]1Cc1ccccc1)c1nnc(c(c1)-c1ccncc1)-c1cc2c(cc1)cccc2
378	P(OCc1cnc(C)c(O)c1C[NH2+]C(C(=O)[O-])C)(=O)([O-])[O-]
379	o1c2c(cc1C[NH+]1CC(N(CC1)CC(O)CC(Cc1ccccc1)C(=O)NC1c3c(CC1O)

319

	cccc3)C(=O)NC(C)(C)C)cccc2
380	Fc1ccc(cc1-c1onc(c1)C(=O)[O-])\C=C\COc1cccc(O)c1C(OC)=O
381	O1C(CO)C(O)C(O)C(O)C1OC1C(O)C(O)c2n(ccn2)C1CO
382	O=C(Cc1ccc(cc1)C(=[NH2+])N)C(=O)[O-]
383	Oc1c2c(Cc3c(C2=O)c(O)ccc3)ccc1CC(=O)[O-]
384	OCc1cnc(nc1N)C
385	O=C([O-])CCc1ccccc1
386	O=[N+]([O-])NC(NCCCC([NH3+])CNCC[NH3+])=N
387	S1c2c(NC(=O)C1CC(=O)NO)cccc2
388	P(OCc1cnc(C)c(O)c1C[NH2+]C1CO[N-]C1=O)(=O)([O-])[O-]
389	P(OCC(OC(=O)CCCCCCCCCCCCCC)COC(=O)CCCCCCCCCCCCCC)(OCC(O)CO)(=O)[O-]
390	[NH2+]=C(n1ncnc1)N
391	Clc1ccc(Oc2ccc(S(=O)(=O)C3(CCOCC3)CC(=O)NO)cc2)cc1
392	P(OCC(O)C(O)C(O)CO)(=O)([O-])[O-]
393	O=C1Nc2c(cccc2)C1Cc1ccc(N2CCN(CC2)C=O)cc1
394	Brc1cc(cc(-c2[nH]c3cc(ccc3n2)C(=[NH2+])N)c1[O-])C(CC(=O)[O-])C(=O)[O-]
395	S(=O)(=O)(N)c1ccc(cc1)C(=O)NCc1cccc1F
396	O=C([O-])C1([NH3+])CC1
397	[As+](c1cc(O)c(O)cc1)(c1ccccc1)(c1ccccc1)c1ccccc1
398	O=C1N(CCCCC1NC(=O)C(C(CCCO)C(=O)NO)CC(C)C)CCOC
399	s1cccc1CC(=O)NCB(O)O
400	O1C(CO)C(O)C(O)C1N1C=CC(=NC1=O)N
401	[NH3+]C(CC(C)C)C
402	[nH]1c2c(ncnc2C)nc1
403	OC1C=CC=C(C(=O)[O-])C1[NH3+]
404	P(OCCCCN1C2=C(NC(=O)NC2=O)N(CC(O)C(O)C(O)CO)C1=O)(=O)([O-])[O-]
405	S1CC(CCC(NC(=O)CCC(NC(=O)C)C(=O)NC(C(=O)NC(C(=O)[O-])C)C)=C([NH2+]C1C(NC(=O)Cc1cccc1)C(=O)[O-])C(=O)[O-]
406	[Mo-2]1(SC2=C(S1)C1Nc3c(nc(nc3O)N)NC1OC2COP(OP(OCC1OC(N2C=CC(=NC2=O)N)C(O)C1O)(=O)[O-])(=O)[O-])([OH2+])([OH2+])O

407	P(OCC1OC2([N-]C(=O)NC2=O)C(O)C1O)(=O)([O-])[O-]
408	S(CC1[NH2+]C(C(O)C1O)c1c2N=CNC(N)c2[nH]c1)C
409	O=C1C2C(Nc3c2cccc3)C2N(C1)CCCC2
410	S(=O)(=O)(Cc1ccccc1)CCC(NC(=O)C(NC(OCc1ccccc1)=O)Cc1ccccc1)CCc1ccccc1
411	OCCCCCCCO
412	S(=O)(=O)([O-])CCC[NH2+]C1CCCCC1
413	S=P([S-])(OCC(OC(=O)CCCC)COC(=O)CCCC)OCC[N+](C)(C)C
414	S(CCC(=O)C(=O)[O-])C
415	O=C(CCC(=O)[O-])C
416	S(=O)(=O)(\C=C\C(NC(=O)C(NC(=O)N1CCC(N2CCOCC2)CC1)Cc1ccccc1)CCC)c1ccccc1
417	Ic1ccccc1
418	O1C(CO)C(O)CC1N1C=CC(=O)NC1=O
419	Brc1cc(cc(Br)c1[O-])C(=O)c1c2c(oc1CC)cc(S(=O)([O-])=Nc1ccc(S(=O)(=O)N)cc1)cc2
420	O=C(CCCCC(=O)[O-])CCC(=O)[O-]
421	P(OCC(OC(=O)C)COCCCCCCCCCCCCCC)(OCC[N+](C)(C)C)(=O)[O-]
422	O=C([O-])Cc1c(c[nH]c1C[NH3+])CCC(=O)[O-]
423	O=C1N(CC=O)C(=NC1CC1C=CC(=O)C=C1)C[NH3+]
424	S(CC1OC(n2c3ncnc(N)c3nc2)C(O)C1O)C
425	O=C([O-])C([NH3+])Cc1c2c([nH]c1)cccc2N
426	O=C(N)C(NC(=O)C([NH2+]C(CCc1ccccc1)C(=O)[O-])Cc1ccccc1)CC(=O)[O-]
427	P(OC1OC(CO)C(O)C(OC(C(=O)NC(C(=O)NC(CCC(=O)[O-])C(=O)[O-])C)C)C1NC(=O)C)(OP(OCC1OC(N2C=CC(=O)NC2=O)C(O)C1O)(=O)[O-])(=O)[O-]
428	P(OC1C(O)C(OC1n1c2ncnc(N)c2nc1)COP(OP(OCC1OC(N2C=C(CC(O)C2O)C(=O)N)C(O)C1O)(=O)[O-])(=O)[O-])(=O)([O-])[O-]
429	O(C(=O)CCC(=O)[O-])C1CCC2(C3C(CCC2C1(C)C)(C)C1(C(C2CC(CCC2(CC1)C)(C(=O)[O-])C)=CC3=O)C)C
430	Clc1cc(Cl)ccc1C(=O)N(Cc1sc(cc1)-

	c1oc2c(c1)cccc2)C(Cc1ccccc1)C(=O)[O-]		cc(F)cc1
431	S1CC[NH+]=C1N	454	P(OP(OP(OCC1OC(N2C=CC(=NC2=O)N)C(O)C1O)(=O)[O-])(=O)[O-])(=O)([O-])[O-]
432	O1C(C(O)C(O)CO)C(NC(=O)C)C(O)CC1(O)C(=O)[O-]		
		455	s1c(ccc1C)C\1CC2OC(O)(C(=O)C(=O)N3C(CCCC3)C(OC(CC(=O)C(\C=C\C)/C(O)C(OC)C(=O)C(CC(\C=C/C=C\C=C/1\C)C)C)C)C(CC1CC(OC)C(O)CC1)C)=O)C(CC2)C
433	Oc1ccc(cc1)C[C@H](NC(=O)[C@@H](NC(=O)[C@@H](NC(=O)[C@H]1N(CCC1)C(=O)[C@@H](NC(=O)[C@@H](NC(=O)[C@@H](NC(=O)[C@@H](NC(=O)CNC(=O)[C@@H](NC(=O)CNC(=O)CNC(=O)CNC(=O)CNC(=O)[C@H]1N(CCC1)C(=O)[C@@H](NC(=O)[C@H]1N(CCC1)C(=O)[C@H]([NH3+])Cc1ccccc1)CCCNC(=[NH2+])N)CC(=O)N)CC(=O)[O-])Cc1ccccc1)CCC(=O)[O-])CCC(=O)[O-])[C@H](CC)C)CCC(=O)[O-])CCC(=O)[O-])C(=O)N[C@@H](CC(C)C)C(=O)[O-]		
		456	O1C2([N-]C(=O)N(O)C2=O)C(O)C(O)C(O)C1CO
		457	P(OP(OP(OCC1OC(N2C=C(C)C(=O)NC2=O)CC1O)(=O)[O-])(=O)[O-])(=O)([O-])[O-]
		458	P(OCC1OC(N2C=CC(=NC2=O)N)C(O)C1O)(=O)([O-])[O-]
434	S(=O)(=O)([O-])NC1C(O)C(OC2OC(=CC(O)C2OS(=O)(=O)[O-])C(=O)[O-])C(OC1O)CO	459	O=C([O-])CC1(C)C2([NH2+]C(C1CCC(=O)[O-])=C(C1=N\C(=C/C3=N\C(=C(/C4=NC2C(CC(=O)[O-])C4(CCC(=O)[O-])C)\C)\C(CCC(=O)[O-])C3(C)C)\C(CCC(=O)[O-])C1(CC(=O)[O-])C)C)C
435	[NH2+]=C(N)c1ccc(NCc2nc3cc(ccc3n2C)Cn2c3c(nc2C)cccc3)cc1		
436	P(OCC(N)C(=O)[O-])(OCC)(OCC)=O	460	S(=O)(CCC([NH3+])C(=O)[O-])C
437	Clc1cc2[nH]c(nc2cc1C(=[NH2+])N)-c1cccc(-c2ccccc2)c1O	461	S(CC([NH3+])C(=O)[O-])CC(=O)[O-]
		462	P(OC(C(N)C(=O)[O-])C)(=O)([O-])[O-]
438	O=C(NC(CCCNC(=O)N)C(=O)[O-])C	463	P(OC1(OC(C(O)C(O)CO)C(NC(=O)C)C(O)C1)C(=O)[O-])(OCC1OC(N2C=CC(=NC2=O)N)C(O)C1O)(=O)[O-]
439	[W-]([OH2+])(OCC1OC(n2c3ncnc(N)c3nc2)C(O)C1O)(O)O		
440	OC1C(O)Cn2c(ncc2)C1O	464	S(SCCO)CCO
441	O=C1NC(=Nc2ncc(nc12)C(O)C(O)CO)N	465	OC1(N=C(CC(C)C)C(=O)N1CC=O)C(N)C(O)C
		466	Oc1nc(nc2n(cnc12)C)N
442	Brc1c2nc3c(cccc3C(=O)NCC[NH+](C)C)c(N)c2ccc1	467	OC(Cc1ccccc1)C(=O)[O-]
		468	P(OCC(O)C(O)C(=O)C)(=O)([O-])[O-]
443	O1C2CC(O)C(O)C(O)C12CO	469	O=C(NC(CCCNC(=[NH2+])N)C(=O)[O-])CCC(=O)[O-]
444	O=C1c2c(n(C)c(CCCO)c2CO)C(=O)C=C1N1CC1		
445	[NH2+](CC)C	470	OB(O)c1ccc(cc1)\C=C\C(=O)[O-]
446	O(c1c2c(nc(nc2N)N)ccc1)c1ccc(OC)cc1	471	O(c1cccc(-c2[nH]c3cc(ccc3n2)C(=[NH2+])N)c1O)C1CCCC1
447	SCCOCCOCCOCCOCCOCCO		
448	BrCCCCCCCCCCCC(=O)[O-]	472	Oc1ccccc1CC=C
449	[NH2+]1CC2CCC1(C)C2(C)C	473	O=C(Nc1nc(ccn1)-c1n2c(nc1C)C=CC=C2)C
450	s1c(CCOP(OP(=O)([O-])[O-])(=O)[O-])c([n+](c1C(=O)C)[CH-]c1cnc(nc1N)C)C	474	S(CC)C(=[NH2+])N
		475	OCCCC[NH3+]
		476	O=C([O-])c1[nH]ccc1
451	O(C(=O)N)C1/C(=C\C(C)C(O)C(OC)CC(CC2=C(OC)C(=O)C=C(NC(=O)/C(=C\C=C/C1OC)/C)C2=O)C)/C	477	O=C(Nc1ccccc1)CCCCCC(=O)NO
		478	P(OCC(O)C(O)C(O)C(O)CO)(=O)([O-])[O-]
452	O(C(=O)CCCCCCC)CCCCCCCCCCCCCC	479	P(OC1OC(C)C(O)C(O)C1O)(=O)([O-])NC(CC(C)C)C(=O)NC(Cc1c2c([nH]c1)cccc2)C(=O)[O-]
453	S(=O)(=O)(N)c1ccc(cc1)C(=O)NCc1c		

480	[NH3+]C1NC(NC2C1CC(CC2)C[NH+]1C2C(CCCC2)CC1)N
481	Clc1cccc(Cl)c1C1=Cc2c(nc(nc2)Nc2cc(SC)ccc2)N(C)C1=O
482	O=C([O-])C([NH3+])CCCC=O
483	O(CCOCCO)CCOCCO
484	OC(C[NH3+])C
485	Clc1c(ccc(OCc2oc(cc2)C(=O)[O-])c1Cl)-c1nn(C)c(c1)C1CCN(CC1)C(=O)CNC(=O)C(NC(=[NH2+])N)CC(C)C
486	SCC(NC(=O)CCCC([NH3+])C(=O)[O-])C(=O)NC(C(C)=C)C(=O)[O-]
487	O1C2N(C(=O)C2(OC)NC(=O)C(C(=O)[O-])c2ccc(O)cc2)C(C(=O)[O-])=C(C1)C
488	P(O)(=O)([O-])CC1CC(O)(CC(O)C1O)C(=O)[O-]
489	O1C(CC=2Oc3c(c(C(=O)[O-])c(O)c([O-])c3)C(=O)C=2C1OC)C
490	O(CC1CCCCC1)c1nc(N)cc2nc[nH]c12
491	P(O)(=O)([O-])CC(OCC1OC(n2c3ncnc(N)c3nc2)C(O)C1O)=O
492	OC(C(NC(=O)C)CO)c1ccc([N+](=O)[O-])cc1
493	S(=O)(=O)(N)c1ccc(cc1)C(=O)NCc1c(F)c(F)c(F)c(F)c1F
494	O1C(CO)C(O)C(O)C(NC(=O)C)C1OC
495	[O-][N+](CCCCCCCCCC)(C)C
496	S1c2cc(O)ccc2OC(C1c1ccc(O)cc1)c1ccc(OCC([NH+]2CCCC2)C)cc1
497	s1c(ccc1CNc1[nH]c2c(n1)cccc2)-c1nc(sc1)[NH+]=C(N)N
498	Clc1cc(Cl)ccc1C(O)(CCCCC)Cn1ccnc1
499	S(=O)(=O)([O-])CCC[N+](CC)(C)C
500	O=C([O-])c1ccccc1NC(=O)C(=O)[O-]
501	P(OP(OCC1OC(n2c3N=C(NC(=O)c3nc2)N)C(O)C1O)(=O)[O-])(=O)([O-])N
502	O=C([O-])C(CCCC)CN(O)C=O
503	O1C(C)(C2C(OC)C(OC(=O)\C=C\C=C\C=C\C=C\C(=O)[O-])CCC2(O)C)C1CC=C(C)C
504	O1C(CO)C(O)C(O)C(O)C1OCCC1OC1
505	O=C(Nc1n[nH]c(c1)C1CC1)c1ccccc1
506	O=C(N)CC(=O)[O-]
507	O=C([O-])C(NC(=O)NO)Cc1ccccc1
508	O=C([O-])C([NH3+])CC(=O)[O-]
509	[Co]123[N+]4=C5C(CCC(=O)N)C(CC(=O)N)(C)C4(C4=[N+]1C(C(CCC(=O)NCC(OP(OC1C(O)C(OC1CO)n1c6c(nc1)cc(OC)cc6)(=O)[O-
510	ClCC(=O)C
511	S1CC2NC(=O)NC2C1CCCC(=O)[O-]
512	O1C(CO)C(O)C(O)C(OC2OC(CO)C(O)C(O)C2O)C1Oc1ccc(cc1)C([NH3+])C(=O)[O-]
513	O=C([O-])C(N)=C
514	OC1CC2C(C3CCC(C(CCC(=O)NCC(=O)[O-])C)C13C)C(O)CC1CC(O)CCC12C
515	O=C1NC(=NC=2NCC(NC1=2)C(O)C(O)C)N
516	S1SCC(O)C(O)C1
517	O=C(N)c1cccnc1
518	s1c(ccc1/C(=N/C(=O)C(CCc1ccccc1)CS)/C(=O)[O-])Cn1nnnc1
519	P(OC1C(O)C(OC1CO)N1C=CC(=O)NC1=O)(=O)([O-])[O-]
520	O1C(C(=O)N)C(O)C(O)C(O)C1CO
521	O1C(C(=O)[O-])C(OC)C(O)C(O)C1O
522	P(OCC(=O)[O-])(=O)([O-])[O-]
523	ONC(=[NH2+])NCCCC
524	O1C(O)C(O)C(O)C=C1C(=O)[O-]
525	P(OCC(=O)NO)(=O)([O-])[O-]
526	s1c2c(nccc2)cc1S(=O)(=O)NC1CCN(Cc2cc(ccc2O)C(=[NH2+])N)C1=O
527	O1C(CO)C(O)C(O)C1N1C=CC(=O)NC1=O
528	P(Oc1c2nc(ccc2ccc1)C#N)(=O)([O-])[O-]
529	OC(Cn1c2ncnc(N)c2nc1)C
530	O(Cc1ccccc1)C(=O)NC(Cc1ccccc1)C(=O)C[N+]#N
531	OC(CCCCCCCCCC)CC(=O)[O-]
532	C(CCCCCC)CCCCC
533	OCCCO
534	BrCC(=O)NCCC(=O)NC(C(=O)NCCc1ccc(NC(=O)C(=O)[O-])cc1)CO
535	Clc1nc(cnc1N1CCN(CC1)C)C(=O)N1CC(N(CC1)CC(O)CC(Cc1ccccc1)C(=O)NC1C(CCC1O)C)C(=O)NC(C)(C)C
536	O(C(C(=O)[O-])=C)C1=CC=CC(C(=O)[O-])C1O
537	P(OCC1OC(NC(=O)C[NH2+]CC(O)(Cc2cc3c(nc(nc3O)N)cc2)c2ccc(cc2)C(=O)NC(CCC(=O)[O-])C(=O)[O-])C(O)C1O)(=O)([O-])[O-]
538	O=C1N=C(NC=2N=CC(N(C1=2)CO)CNc1ccc(cc1)C(=O)NC(CCC(=O)[O-])C(=O)[O-])N
539	O1C(CO)C(O)C(O)C(O)C1Oc1cc(cc([

]C)(C)C4CC(=O)N)=C(C1=[N+]2C(=CC2=[N+]3C(C(CC(=O)N)(C)C2CCC(=O)N)=C5C)C(C)(C)C1CCC(=O)N)C)C

322

	N+](=O)[O-])c1)C(=O)N
540	O(C)c1cc(ccc1O)CN1C(Cc2ccccc2)C(O)CN(N(Cc2cc(OC)c(O)cc2)C1=O)Cc1ccccc1
541	O(CCO)C
542	OC(C(O)CO)CC(O)C(=O)[O-]
543	Brc1c(OCCCC(CCC(=O)[O-])C(=O)[O-])cc(cc1OC)Cc1cnc(nc1N)N
544	s1c2c(nc1C(=O)C(NC(=O)C1N(CC(O)C1)C(=O)C)CCCNC(=[NH2+])N)cccc2
545	S1C=C(NC=C(C(=O)C1c1nnn(c1)C)C(=O)[O-]
546	[PH](=O)([O-])C
547	O=C([O-])c1cc(NC(=O)C[NH3+])c(NC(=O)C)cc1
548	P(O)(=O)([O-])[O-]
549	[Fe]123[NH+]4C5=Cc6n1c(C=C1N2C(=CC=2N3C(=CC4=C(CCC(=O)[O-])C5(CC(=O)[O-])C)C(CC(=O)[O-])(C)C=2CCC(=O)[O-])C(CC(=O)[O-])=C1CCC(=O)[O-])c(CCC(=O)[O-])c6CC(=O)[O-]
550	P(OP(OCC1OC(n2c3N=C(NC(=O)c3nc2)N)C2OP(OC12)(=O)[O-])(=O)[O-])(=O)([O-])[O-]
551	S(OC1C(O)C(O)C(OC1CO)O)(=O)(=O)[O-]
552	Oc1cc(O)ccc1C(=O)[O-]
553	O1c2cc(ccc2OC1)-c1c(n[nH]c1C(=O)[O-])-c1cc(CC)c(O)cc1O
554	O=C(NCCC[NH+](C)C)c1c2[nH+]c3c(cccc3)c(N)c2ccc1
555	OC(C(O)C)(C[NH3+])C
556	P(OC1C(O)C([NH3+])C(OC1CO)O)(=O)([O-])[O-]
557	P(OC1OC(CO)C(O)C(O)C1O)(=O)([O-])[O-]
558	ClCCCN1C(=O)C2(OC1=O)CC1(C3[NH+](CCC34C2N(c2cc(OC)c(cc24)C2(CC3CC(O)(C[NH+](C3)CCc3c2[nH]c2c3cccc2)CC)C(OC)=O)C)CC=C1)CC
559	P(OCC1OC(N2C=CC(=NC2=O)N)CC1)(=O)([O-])[O-]
560	OC1C(O)C(N(Cc2cc(N)ccc2)C(O)N(Cc2cc(N)ccc2)C1Cc1ccccc1)Cc1ccccc1
561	O1C(C)C(NC2C=C(CO)C(O)C(O)C2O)C(O)C(O)C1OC1C(O)C(O)C(OC1CO)O
562	S(CCC([NH3+])C(=O)[O-])C
563	S(OCC12OC(OC1C1OS(OC1CO2)(=

	O)=O)(C)C)(=O)(=O)N
564	S(C)c1ncnc2n(cnc12)C1OC(CO)C(O)C1O
565	O=C1CC(CC(O)O)C(C)(C)C1C
566	s1c(-c2nc(ncc2)Nc2ccc(cc2)C(F)(F)F)c(nc1C)C
567	S(OCC1OC(n2c3ncnc(N)c3nc2)C(O)C1O)(=O)(=O)N
568	FC(F)(F)C([O-])([O-])C(F)(F)F
569	[Fe]123[NH+]4C5=Cc6n1c(C=C1N2C(=CC=2N3C(=CC4=C(C)C5C=C)C(C(O)=C)C=2C)C(C)=C1CCC(=O)[O-])c(CCC(=O)[O-])c6C
570	O=C([O-])C([NH3+])(C)C
571	OC(C(O)C(O)C)C(O)C=O
572	[nH]1c2c(nc1)cccc2
573	S(=O)(=O)([O-])NP(=O)(NCCCC([NH3+])C(=O)[O-])N
574	O(CCC([NH3+])C(=O)[O-])CC[NH3+]
575	S(\C(=[NH+]\CCCCCCCCCCCCCC\[NH+]=C(\SC)/N)\N)C
576	P(OCc1cnc(C)c(O)c1C[NH2+]C(CCC)C(=O)[O-])(=O)([O-])[O-]
577	[Hg]c1ccc(S(=O)(=O)[O-])cc1
578	S(C)c1cc(Nc2ncnc3c2cc(OC)c(OC)c3)ccc1
579	[NH3+]C1CCCCC1
580	OC1(CCC2C3C(=C4C(=CC(=O)CC4)CC3)C=CC12C)C
581	S(=O)(=O)([O-])CC(NC(=O)CCC([NH3+])C(=O)[O-])C(=O)NCC(=O)[O-]
582	[nH+]1c2c(CCCC2)c(NCCn2nncc2CCCCCC[n+]2c3cc(N)ccc3c3c(cc(N)cc3)c2-c2ccccc2)c2c1cccc2
583	Clc1sc(Cl)cc1-c1nc(ncc1)N
584	P(OCCCN1C2=C(NC(=O)NC2=O)N(CC(O)C(O)C(O)CO)C1=O)(=O)([O-])[O-]
585	OC(CCCC)C=C
586	Oc1nc[nH]c2-c1nnc2
587	S(=O)(=O)(N)c1ccc(cc1)C(=O)NCc1cc(F)ccc1F
588	O=C([O-])CN(CC(=O)[O-])CC(=O)[O-]
589	P(OCC(O)C(O)C(O)C(=O)[O-])(=O)([O-])[O-]
590	O1CCN(CC1)CCOc1c2c(cccc2)c(NC(=O)Nc2n(nc(c2)C(C)(C)C)-c2ccc(cc2)C)cc1
591	S(=O)(=O)(n1ncc(c1)-c1c2cc(ccc2ccc1OC)C(=[NH2+])N)C
592	O1CCCC1C(=O)[O-]

593	P(=O)([O-])([O-])C1([NH3+])CC1	624	SCC([NH3+])C(=O)[O-]
594	O=C[CH-]C=O	625	O1C(COC(=O)c2cc(O)c(O)c(O)c2)C(OC(=O)c2cc(O)c(O)c(O)c2)C(OC(=O)c2cc(O)c(O)c(O)c2)C(OC(=O)c2cc(O)c(O)c(O)c2)C1OC(=O)c1cc(O)c(O)c(O)c1
595	O(c1ccc(NC(=O)c2cc([N+](=O)[O-])ccc2)cc1NC(=O)c1cc([N+](=O)[O-])ccc1)c1cc(C(=O)[O-])c(cc1)C(=O)[O-]		
596	Fc1ccc(cc1)C=1CC[NH+](CC=1)CCCC=1NC(=O)c2c(N=1)c(ccc2)C	626	O1C(C)C(OC2OC(C)C(OC3OC(C)C(=O)CC3)C(O)C2)C([NH+](C)C)CC1OC1CC(O)(CC)C(O)c2c1c(O)c1c(c2)C(=O)c2c(C1=O)c(O)ccc2
597	S(=O)(=O)(NC(CC(=O)[O-])C(=O)NC(Cc1ccc(cc1)C(=[NH2+])N)C(=O)N1CCCCC1)c1c(C)c(C)c(OC)cc1C		
		627	O=C(CC(C)C)C(=O)[O-]
		628	OC(C(O)C(=O)[O-])CC(=O)C(=O)[O-]
598	s1ccnc1C(CC)C	629	O=C([O-])C(n1nnc(c1)C[NH3+])CC(C)C
599	O=C([O-])C([NH3+])CC(=O)[O-]		
600	Fc1[nH]c(N)c-2nc(nc-2n1)Cc1cc(OC)ccc1OC	630	[nH]1cncc1-c1ccccc1
		631	Oc1ccccc1
601	[N+](C)(C)(C)C	632	O=C(Nc1cc(Nc2nc(ccn2)-c2cccnc2)c(cc1)C)c1ccc(cc1)CN1CC[NH+](CC1)C
602	P(OC1OC(CO)C(O)C1O)(=O)([O-])[O-]		
603	OCCCC([NH3+])C(=O)[O-]	633	s1c2S(=O)(=O)N(C(=Cc2c1S(=O)(=O)N)CN1CCOCC1)c1cc(O)ccc1
604	OC1C(O)C(O)C(O)C(O)C1O		
605	P(Oc1ccccc1C=O)(OCC1CCCCC1)(=O)[O-]	634	O1C(CO)C(=O)C(O)C1n1c2ncnc(N)c2nc1
		635	OC(C(O)CO)CO
606	O1[N-]C(=O)C([NH3+])C1	636	P(OCC1OC(n2c3ncnc(N)c3nc2)C(O)C1O)(OP(OP(OP(OP(OCC1OC(N2C=C(C)C(=O)NC2=O)CC1O)(=O)[O-])(=O)[O-])(=O)[O-])(=O)[O-])(=O)[O-]
607	O1CCOB1OCCCNC(=[NH2+])N		
608	s1c2c(nc1SCCCS(=O)(=O)[O-])cccc2		
609	O1C(C(O)C(O)C(O)C1CO)c1[nH]c2cc(ccc2n1)C		
		637	O1CC(O)C(O)C=C1C(=O)[O-]
610	O=C([O-])C([NH3+])CCCC(=O)[O-]	638	Oc1cc(O)ccc1C(=O)\C=C\c1ccc(O)cc1
611	P(O)(=O)([O-])CCN(O)C=O		
612	Ic1c2cc(sc2ccc1)C(=[NH2+])N	639	P(OCc1cnc(C)c(O)c1C[NH2+]C(\C=C\OCC[NH3+])C(=O)[O-])(=O)([O-])[O-]
613	OB(O)c1ccc(cc1)C(=O)[O-]		
614	P(OCC1OC(n2c3ncnc(N)c3nc2)C(O)C1O)(=O)([O-])CP(O)(=O)[O-]	640	SCC(NC(=O)CCC([NH3+])C(=O)[O-])C(=O)NCC(=O)NCCC[NH2+]CCCC[NH3+]
615	[Cu]123[Cu]45[Cu]1[S+2]24[Cu]35	641	S(=O)(=O)([O-])CC[NH2+]C1CCCCC1
616	O1C(C(=O)[O-])C(O)C(O)C(O)C1O		
617	Oc1c(cccc1-c1[nH]c2c(c1)cc(cc2)C(=[NH2+])N)-c1ccccc1	642	S(SCC(NC(=O)CCC([NH3+])C(=O)[O-])C(=O)NCC(=O)[O-])CC(NC(=O)CCC([NH3+])C(=O)[O-])C(=O)NCC(=O)[O-]
618	O1C(CO)C(O)C(O)C1n1c2ncnc(N)c2cc1	643	Brc1cc(cc(Br)c1[O-])C(=O)c1c2c(oc1CC)cc(S(=O)(=O)Nc1ccc(S(=O)([O-])=Nc3sccn3)cc1)cc2
619	S(CCNC(=O)CCNC(=O)[C@]1(O)[C@H](OP(OP(OC[C@H]2O[C@@H](n3c4ncnc(N)c4nc3)[C@@H](O)[C@@H]2OP(=O)([O-])[O-])(=O)[O-])(=O)[O-])C1(C)C)C(=O)\C=C\c1cc(OC)c(O)c(OC)c1		
		644	o1nc(O)c(CC([NH3+])C(=O)[O-])c1C(C)(C)C
		645	O1CC2N(C3=C(N=C(NC3=O)N)NC2)C1=O
		646	O1C(CO)C(O)C(O)C(O)C1OCCCCCC
620	S(CCC(SSCCO)CCCCC(=O)[O-])C[NH3+]	647	O=C([O-])c1cc(NC(N)N)c(NC(=O)C)cc1
621	O1C(OC2OC(CO)C(O)C(O)C2O)(CO)C(O)C(O)C1COC(=O)CCCCCCC	648	P(OC1C(OP(=O)([O-])[O-])C(OP(=O)([O-])[O-
622	O=C1NC(=Nc2ncc(nc12)CO)N		
623	P(OCC1OC(n2c3c(nc2)ncnc3)C(O)C1O)(=O)([O-])[O-]		

	])C(O)C(OP(=O)([O-])[O-])C1OP(=O)([O-])[O-])(=O)([O-])[O-]
649	Brc1nc2c(ncnc2N)n1C1OC(COP(=O)([O-])[O-])C(O)C1O
650	[As](SCC([NH3+])C(=O)[O-])(=O)([O-])[O-]
651	O=C([O-])C1N(CCC1)C(=O)C
652	SCCC(=O)N1CCc2c([nH]c3c2cccc3)C1
653	S(OCC1OC(n2c3ncnc(N)c3nc2)C(O)C1O)(=O)([O-])=NC(=O)C(N)C
654	Oc1ccc(cc1)C[C@H]([NH3+])C(=O)N
655	O=C(N(O)C(C)C)C(=O)[O-]
656	OC1CCC(NC(=O)C(OC)C(O)C(O)C(O)\C=C\C(C)(C)C)C(=O)NC1
657	P(OC1OC(CO)C(O)C(O)C1NC(=O)C)(OP(OCC1OC(N2C=CC(=O)NC2=O)C(O)C1O)(=O)[O-])(=O)[O-]
658	[N+](CC)#C
659	O=C([O-])CCc1ccc(cc1)C
660	O=C1CN(CC1NC(=O)C(NC(OCc1ccccc1)=O)CC(C)C)C(=O)C(NC(OCc1ccccc1)=O)CC(C)C
661	SCC(NC(=O)CCC([NH3+])C(=O)[O-])C(=O)[O-]
662	OC1C([NH2+]CC1O)CO
663	s1c[n+](Cc2cnc(nc2N)C)c(C)c1CCOP(=O)([O-])[O-]
664	O1C(C(O)C(O)CO)C(NC(=O)C)C(NC(=[NH2+])N)CC1C(=O)[O-]
665	OC(C([NH3+])Cc1ccccc1)C(=O)NC(CC(C)C)C(=O)[O-]
666	O=C([O-])C(CC([NH3+])C(=O)[O-])C
667	P(OCc1cnc(C)c(O)c1C[NH2+]CC(OP(=O)([O-])[O-])C)(=O)([O-])[O-]
668	O1C(C)C([NH3+])C(O)C(O)C1O
669	S(=O)([O-])C(C(N\C=C\C=O)C(=O)[O-])(Cn1nncc1)C
670	P(OC1CC(OC1CO)N1C=CC(=O)NC1=O)(=O)([O-])[O-]
671	S1CC(CC(OC)=O)=C(NC1C(NC(=O)Cc1sccc1)C=O)C(=O)[O-]
672	O1[C@H](CN(CC[C@H]([NH3+])C(=O)[O-])C)[C@@H](O)[C@@H](O)[C@@H]1n1c2ncnc(N)c2nc1
673	O=C1NC(=O)NC=C1C
674	O1c2c(C(=O)CC1c1ccc(O)cc1)c(O)cc(O)c2
675	O=C(NC(CCc1ccccc1)CCC(=O)[O-])CCCCCCc1ccccc1
676	O=C(NC)CCC([NH3+])C(=O)[O-]
677	S(=O)(=O)([O-])c1cc2c(c(O)c1\N=N\c1ccccc1S(=O)(

	=O)[O-])c(Nc1nc(nc(n1)N)N)cc(S(=O)(=O)[O-])c2
678	Brc1ccc(cc1)-c1n(nc(c1)C(F)(F)F)-c1ccc(S(=O)(=O)N)cc1
679	O1C2([N-]C(=O)N(C)C2=O)C(O)C(O)C(O)C1CO
680	P(=O)([O-])([O-])C(F)(F)c1ccc(cc1)CC(NC(=O)C(NC(=O)c1ccccc1)CCC(=O)[O-])C(=O)NC(Cc1ccc(cc1)C(P(=O)([O-])[O-])(F)F)C(=O)N
681	P(OCC(O)CO)(OCC[NH3+])(=O)[O-]
682	P(OC1OC(CO)C(O)C(O)C1F)(OP(OC1OC(N2C=CC(=O)NC2=O)C(O)C1O)(=O)[O-])(=O)[O-]
683	Fc1cc2nc([nH]c2cc1C(=[NH2+])N)-c1cccc(OCC(C)C)c1O
684	SCP(O)(=O)[O-]
685	[nH]1c2c(ncnc2N)cc1
686	[se]1c2c([nH]cc2CC([NH3+])C(=O)[O-])cc1
687	O=C1NC(=O)NC=C1C#C
688	P(Oc1c2NCCCc2ccc1)(=O)([O-])[O-]
689	P(OCC1OC(n2c3ncnc(N)c3nc2)C(O)C1O)(OP(OCC1OC([n+]2cc(ccc2)C(=O)N)C(O)C1O)(=O)[O-])(=O)[O-]
690	O(Cc1ccccc1)C(=O)NC(CCCNC(N)N)C(=O)NC(C(=O)C)C
691	O=C1C2CC(C1)CC2
692	P(OC1C(O)C(O)C(O)C(O)C1O)(=O)([O-])[O-]
693	P(OCC(O)C(O)C(O)CNc1ccccc1C(=O)[O-])(=O)([O-])[O-]
694	S1C2N(C(C(=O)[O-])C1(C)C)C(=O)C2NC(=O)CCCC([NH3+])C(=O)[O-]
695	O(CCOCCOCCOCCOCC)CCOCCOCCOCCO
696	C1CCCCC1
697	[NH2+](CCCC[NH3+])CCC[NH3+]
698	Clc1cc(cc(Cl)c1)CNC(=O)c1cc(-n2nc3c(nc(nc3O)N)n2)ccc1
699	OCC(n1cc(nc1)C(=O)N)CCc1c2c(ccc1)cccc2
700	P(=O)([O-])([O-])C([NH2+]Cc1ccccc1)c1ccccc1
701	Oc1ccc(N2N(C(=O)[C-](CCCC)C2=O)c2ccccc2)cc1
702	O=C([O-])C([NH3+])CCCC([NH3+])C(=O)[O-]
703	P(=O)([O-])([O-])C(F)(F)c1ccc(cc1)CC(NC(=O)C)C(=O)NC1CCCCN(Cc2ccc(cc2)-

325

	c2ccccc2)C1=O
704	Ic1cc(cc(I)c1Oc1cc(I)c(O)cc1)CC(=O)[O-]
705	O=C1CCC2C3C(CCC12C)C1(C(CC(=O)CC1)CC3)C
706	O1C(/C(=C/C2CC(OC)C(Oc3cc4c(n(cc4)C)cc3)CC2)/C)C(C)C(O)CC(=O)C(\C=C(\C)/C(O)C(CC(OC)C2OC(O)(C(=O)C(=O)N3C(CCCC3)C1=O)C(CC2OC)C)CC
707	Oc1ccc(cc1)-c1cc2c3c(ccc2nc1)ccnc3
708	P(=O)([O-])([O-])C(=O)Nc1ccc(cc1)CC
709	P(OCc1c[n+]([O-])c(C)c(O)c1C=O)(=O)([O-])[O-]
710	Ic1ccccc1CS
711	P(O)(=O)([O-])CC(=O)NO
712	O=C(NC(CCCC[NH3+])C(=O)Nc1ccccc1)C(CCCC)CNNCC(CCCC)C(=O)NC(CCCC[NH3+])C(=O)Nc1ccccc1
713	S1C(C)(C)C(NC1C(NC(=O)C([NH3+])c1ccc(O)cc1)C=O)C(=O)[O-]
714	S(=O)(=O)([O-])CC([NH3+])C(=O)[O-]
715	O(CC(=O)C(C)C)c1nc(nc2nc[nH]c12)N
716	S(OC1C(OC2OC(C(=O)[O-])C(OC3OC(COS(=O)(=O)[O-])C(OC)C(OC)C3OS(=O)(=O)[O-])C(OC)C2OC)C(OC(OC2C(OC)C(OS(=O)(=O)[O-])C(OC2C(=O)[O-])OC2C(OS(=O)(=O)[O-])C(OS(=O)(=O)[O-])C(OC2COS(=O)(=O)[O-])OC)C1OS(=O)(=O)[O-])COS(=O)(=O)[O-])(=O)(=O)[O-]
717	P(OCC1OC(N2C(=O)[CH-]C(=O)NC2=O)C(O)C1O)(=O)([O-])[O-]
718	O1C(=O)C=C(C2CCC3(O)C4C(CC(O)C23C)C2(C(CC(O)CC2)CC4)C)[CH-]1
719	[Hg+]C
720	O=C(NC1CCCCC1)NCCCCCCCCCC
721	S(Cc1ccc([N+](=O)[O-])cc1)CC(NC(=O)CCC([NH3+])C(=O)[O-])C(=O)NCC(=O)[O-]
722	OCCC(=O)[O-]
723	S(OCC([NH3+])C(=O)[O-])(=O)(=O)CCCCCCCCCCCCCCC
724	S=C(Nc1ccccc1)N
725	O(C)c1ccc(OC)cc1Cc1cnc2nc(nc(N)c2c1C)N
726	O=C1NC(=NC(NC)=C1[N+](=O)[O-])N

727	OCC[NH+](CC(=O)[O-])CCO
728	C(CCCCCCC)CCCCCCC
729	O1CC(O)C(O)C(O)C1OC1CCNC(=O)C1O
730	O=C([O-])/C(/N)=C/C
731	P(OC1OC(C)C(O)C(O)C1O)(OP(OC1OC(N2C=C(C)C(=O)NC2=O)CC1O)(=O)[O-])(=O)[O-]
732	Clc1ccc(cc1)C(=O)[O-]
733	S1C2OC(CO)C(O)C(O)C2N=C1C
734	OCC([NH3+])(CO)CO
735	SC(CCCC(=O)[O-])CCS
736	O(C)c1cc(OO)ccc1O
737	O1C(CO)C(O)CC(O)C1OCCCCCC
738	O=C([O-])C([NH3+])CCC=O
739	Clc1cc(Cl)ccc1Oc1ccc(OC(C(=O)[O-])C)cc1
740	O=C(N)CCCCCCC\C=C\CCCCCCCC
741	n1ccn(C)c1C
742	S(CCC([NH3+])C(=O)[O-])C(F)(F)F
743	O=C([O-])C([NH3+])CCCNC(=O)[O-]
744	FC(F)(F)c1ccc(NC(=O)C(C(O)C)C#N)cc1
745	O(CCCCCCOc1ccc(cc1)C(=[NH2+])N)c1ccc(cc1)C(=[NH2+])N
746	O=CC(N)Cc1[nH]cnc1
747	P(OCCCN1C2=C(NC(=O)NC2=O)N(CC(O)C(O)C(O)CO)C1=O)(=O)([O-])[O-]
748	P(OC(O)C(N)C(=O)[O-])(=O)([O-])[O-]
749	P(OCC[N+](C)(C)C)(=O)([O-])CCC(OC(=O)CCCCC)COC(=O)CCCC
750	o1c(nnc1C(C)(C)C)C(=O)C1[NH2+]CCC1
751	O=C([O-])CCCCCCCCC
752	[Cu+2](O)(O)(n1ccnc1)(n1ccnc1)(n1cnc1)n1ccnc1
753	O=C
754	O(c1cc(ccc1OC)C1(CCC(CC1)C(=O)[O-])C#N)C1CCCC1
755	O1C(CC(OC)C(CCC(=O)C(C(OC)C\C=C\N(CO)C)C)C)C(CC\C=C/c2occ(n2)-c2occ(n2)-c2occ(n2)C(OC)C(C)C(=O)CC(O)CC(O)CC1=O)C
756	SC1OC(CO)C(O)C(O)C1O
757	OC1CCC2C3C(CCC12C)c1c(CC3CCCCCCCCC(=O)N(CCCC)C)cc(O)cc1
758	SCC(O)CO
759	Clc1cc2[nH]c(cc2cc1C(=[NH2+])N)-c1cccc(-c2ccccc2)c1O
760	O1C(CO)C(O)C(O)C1OC1C(O)C(OC

	C1O)O	785	S1C(O)c2c(OC1N)cccc2
761	O1C(C)C(O)CCC1O	786	P(OCCCN1C2=C(NC(=O)NC2=O)N(CC(O)C(O)C(O)CO)C1=O)(=O)([O-])[O-]
762	[Ru+2]123(N4C(=C(C=C4)CCCCCCCCC(=O)NC4C5CC6CC4CC(C5)C6)=C4N1C=CC(=C4)C)(N1C(=C4N2C=CC=C4)C=CC=C1)N1C(=C2N3C=CC=C2)C=CC=C1		
		787	[Hg]c1ccc(cc1)C(=O)[O-]
		788	S(OC1COC(=CC1O)C(=O)[O-])(=O)(=O)[O-]
763	s1c2ncccc2cc1C(=[NH2+])N	789	S(Cc1ccccc1)CC(NC(=O)C(NC(=O)N1CCOCC1)Cc1ccccc1)C=O
764	s1cccc1SCC(C(CC(C)C)C(=O)NC(Cc1ccccc1)C(=O)NC)C(=O)NO		
		790	[NH+](CCC=C(C)C)(C)[C@H]1CCC(=CC1)C
765	OC1CCC2C3C(CCC12C)C1(C(CC(O)CC1)CC3)C	791	O1C(CO)C(O)C(O)C(O)C1O
766	O=C(Cc1ccccc1)C(=O)[O-]	792	O1C(C(O)C(O)CO)C(NC(=O)C)C(O)C=C1C(=O)[O-]
767	P(OCC1OC(n2c3c(nc2)ncnc3N)C(O)C1O)(=O)([O-])[O-]		
		793	O=C(NCC([NH3+])C(=O)[O-])c1ccccc1
768	O=C([O-])C([NH3+])CCCN\C(=[NH+]\CC=C)\N	794	O=C([O-])CCC(C)C
		795	P(OCC(N)Cc1[nH]cnc1)(=O)([O-])[O-]
769	Oc1ccc(cc1)CCC(=O)[O-]	796	P(O)(=O)([O-])CCCC
770	O=C([O-])C(=O)[O-]	797	O=C([O-])c1cc2c([nH]cc2)cc1NC(=O)C(=O)[O-]
771	O=C1NC(=NC=2NCC(NC1=2)C(O)C(O)C)N		
772	Oc1ccc(NC(=O)\C=C(\C=C\C=C(\C=C\C=2C(CCCC=2C)(C)C)/C)/C)cc1	798	P(=O)([O-])([O-])c1cc(ccc1OCC(=O)[O-])CC(NC(=O)C)C(=O)NC(C)c1cc(C(=O)N)c(OCC2CCCC2)cc1
773	OC1CCC2C3C(CCC12C)C1(C(CC(O)CC1)CC3)C	799	Brc1ccc(OCCCON2C(N=C([NH+]=C2N)N)(C)C)cc1
774	Clc1c2OC3c4c(C5=CC=CC35OC3OC(C)(C)C([NH+](C)C)C(O)C3O)cc(cc4)C(OC(=O)c3cc(OC)cc4OC(=C)C(=O)Nc34)COC(=O)CC([NH3+])c(cc2O)c1	800	O(C)c1cc(ccc1)-c1[nH]c2c(n1)cccc2C(=O)N
		801	O1C(C[NH+](CC1C)CCCCCCCCNC=O)C
		802	P(OC1OC(C(=O)[O-])C(O)C(O)C1O)(OP(OCC1OC(n2c3N=C(NC(=O)c3nc2)N)C(O)C1O)(=O)[O-])(=O)[O-]
775	[Zn]123[N+]4=C5C=c6n1c(=CC1=[N+]2C(=Cc2n3c(C=C4C(C=C)=C5C)c(C)c2C=C)C(C)=C1CCC(=O)[O-])c(CCC(=O)[O-])c6C		
		803	S(S)CCNC(=O)CCNC(=O)C(O)C(COP(OP(OCC1OC(n2c3ncnc(N)c3nc2)C(O)C1OP(=O)([O-])[O-])(=O)[O-])(C)C
776	S1C2N(C(=O)C2NC(=O)CCCC([NH3+])C(=O)[O-])C(C(=O)[O-])=C(C1)C		
777	Oc1ccc(cc1)CCCCCCC		
778	P(OCC[N+](C)(C)C)(=O)([O-])[O-]	804	O=C([O-])C([NH3+])(CC(C)C)C
779	SC(Cc1ccccc1)C(=O)NC(Cc1ccccc1)C(=O)NC(Cc1ccc(O)cc1)C(=O)[O-]	805	OC(C(CC(=O)[O-])C(=O)[O-])(C(=O)[O-])C
		806	O=C(C(C)C)C(=O)[O-]
780	[S-]\C(=[NH+]\CCCC([NH3+])C(=O)[O-])\N	807	OC(C([NH3+])Cc1ccccc1)C(=O)N1CCCC1C(=O)N1CCCC1C(=O)NC(C(=O)N)C
781	O(O)C1(N=C2N(C=C(NC2CC2CCCC2)c2ccc(O)cc2)C1=O)Cc1ccc(O)cc1		
		808	OCCC(=O)C
782	P1(OC(CO)(C)C(O)COP(O1)(=O)[O-])(=O)[O-]	809	O1C(CO)C(O)C(O)C(O)C1OC1C(O)C(O)C(O)NC1CO
783	Brc1nc2c(ncnc2N)n1C1OC(COP(OP(OCC2OC([n+]3cc(ccc3)C(=O)N)C(O)C2O)(=O)[O-])(=O)[O-])C(O)C1OP(=O)([O-])[O-]		
		810	P(OC1OC(CO)C(F)C(O)C1O)(OP(OCC1OC(N2C=CC(=O)NC2=O)C(O)C1O)(=O)[O-])(=O)[O-]
784	Clc1c2OC(=O)C(NC(=O)c3cc(CC=C(C)C)c(O)cc3)=C([O-])c2ccc1OC1OC(C)(C)C(OC)C(OC(=O)c2[nH]c(cc2)C)C1O		
		811	O(C(=O)CO)\N=C(/C1(CC1)c1cc2nc(n(c2cc1)C)CNc1ccc(cc1)C(=[NH2+])N)

	\c1ncccc1)CC
812	S(CCNC(=O)CCNC(=O)C(O)C(COP(OP(OCC1OC(n2c3ncnc(N)c3nc2)C(O)C1OP(=O)([O-])[O-])(=O)[O-])(=O)[O-])(C)C)C(=O)\C=C\c1ccc(N(C)C)cc1
813	O=C1NC(=O)NC(NCC(O)C(O)C(O)CO)=C1N=O
814	O(C)c1cc2[nH]cnc2cc1
815	Clc1ccc(cc1)C1N(C(=O)N2CC[NH2+]CC2)C(=NC1c1ccc(Cl)cc1)c1ccc(OC)cc1OC(C)C
816	Ic1cc(cc(I)c1[O-])CC(NC(=O)C)C(=O)NC(C(O)C)C(=O)[O-]
817	O1[N-]C(=O)C2=C1CCCC=C2C[C@H]([NH3+])C(=O)[O-]
818	S(CC(NC(=O)CCC([NH3+])C(=O)[O-])C(=O)NCC(=O)[O-])CO
819	O=C(N)CC
820	O=C([O-])[C@]([NH3+])(CC)C
821	S(=O)(=O)(N)c1ccc(cc1)C(=O)NCc1cc(F)cc1F
822	O=C([O-])C
823	S(CC(NC(=O)CCC([NH3+])C(=O)[O-])C(=O)NCC(=O)[O-])C1c2c(-c3c(cccc3)C1O)cccc2
824	P(OCC1OC(n2c3ncnc(N)c3nc2)C(O)C1O)(OC(=O)C(N)Cc1[nH]cnc1)(=O)[O-]
825	O=C([O-])C(=N)C
826	O=C(NC1CCCCC1)NCCCc1ccccc1
827	Brc1cc(cc(-c2[nH]c3c(c2)cc(cc3)C(=[NH2+])N)c1O)C
828	O=C([O-])C([NH3+])C#C
829	[V](O[V](O)O)(O[V](O)O)(O)O
830	O=C([O-])CCCCCCC\C=C\CCCCCCCC
831	O=C([O-])CCC([NH3+])CC
832	OCCC([NH3+])(CCO)CCO
833	S(=O)(=O)(NC(Cc1cc(ccc1)C(=[NH2+])N)C(=O)N1CCCCC1C(=O)[O-])c1cc2c(cc1)cccc2
834	Oc1c2c(ccc1[C@@H](CC)C)cc1c(C(=O)C[C@@H](C1)[C@H](OC)C(=O)[C@@H](O)[C@H](O)C)c2O
835	O1C(CO)C(OC2OC(CO)C(O)C(O)C2O)C(O)C(O)C1OC1C(O)C(O)C(OC1CO)O
836	O=C(N)c1cc(N2CC2)c([N+](=O)[O-])cc1[N+](=O)[O-]
837	O=C([O-])CCCCCCC\C=C\CCCCC
838	OC1CC(O)C\C(=C\C=C\2/C3CCC(C(\C=C\C=C\C(O)(CC)CC)C)C3(CCC/2)

	C)\C1=C
839	Oc1nc(nc2c1cc(cc2)CC(C(=O)[O-])c1ccc(cc1)C(=O)NC(CCC(=O)[O-])C(=O)[O-])N
840	Clc1c2c(CCC[NH2+]C2)ccc1Cl
841	P(OCC(O)C(O)C(O)C(=O)CO)(=O)([O-])[O-]
842	SCCCNC(=O)C(NC(=O)CNC(=O)C(NC(=[NH2+])N)C1CCCCC1)C
843	ClC=1CCC2N(C(=O)C2NC(=O)C([NH3+])c2ccccc2)C=1C(=O)[O-]
844	O=C(CCC([NH3+])C(=O)[O-])C
845	S1C(\C=C(\C=C)/)(C)C([O-])=C(C)C1=O
846	O1C(C(=O)[O-])C(OC)C(O)C(O)C1O
847	Oc1cc2c(CCC2[NH2+]CC#C)cc1
848	S=C1NC(C(C(OCC)=O)=C(N1)C)c1cc(O)ccc1
849	O(CCOCCOC)CCOCCO
850	Clc1ccc(NC(=O)Nc2ccc(cc2)C(=[NH2+])N)cc1
851	S(CC([NH3+])C(=O)[O-])CC(=O)[O-]
852	O=C([O-])C=O
853	O=C([O-])CCCC
854	OC1C(O)CC(C=C1[O-])C(=O)[O-]
855	OC(CO)C
856	O=C1N[C@@H](CCCC(=O)[O-])C(=O)N[C@@H](CCC\N=C(\NC(=O)C)/N)C(=O)N2[C@H](CCC2)C(=O)N[C@H]2C[C@@H](O)N([C@H]1Cc1[nH]cnc1)C2=O
857	O=C([O-])C\C(=C\C(=O)[O-])\C(=O)[O-]
858	O(C(C)(C)C)C(=O)NC(Cc1ccccc1)C(=O)CC(Cc1ccccc1)C(=O)NC(CCC(=O)N)C(=O)NC(Cc1ccccc1)C(=O)N
859	P(OC1OC(CO)C(O)C(O)C1O)(OP(OCC1OC(N2C=CC(=O)NC2=O)C(O)C1O)(=O)[O-])(=O)[O-]
860	O=C/1NC(=N\C\1=C\1/CCNC(=O)c2[nH]ccc/12)N
861	O=C1NC(=NC=2NCC(N(C1=2)C)CNc1ccc(cc1)C(=O)NC(CCC(=O)[O-])C(=O)[O-])N
862	OC(CC(=O)[O-])(CC(=O)[O-])C
863	O=CN(C(C)c1ccccc1)C
864	OC[C@@H]([NH3+])C(C)C
865	O=C([O-])C([NH3+])CCC=O
866	O=C1NC(=NC=2NCC(=NC1=2)C(O)C(O)C)N
867	S(=O)(=O)(NC(CC#CCOC)C(=O)[O-])c1ccc(cc1)-c1ccc(OC)cc1
868	[Co]123n4c5C=c6n1c(=Cc1n2c(C=c2n3c(=Cc4c(C)c5CCC(=O)[O-

	])c(CCC(=O)[O-])c2C)c(CCC(=O)[O-])c1C)c(CCC(=O)[O-])c6C
869	O(C(=O)C(Cc1cc(ccc1)C(=[NH2+])N)C(NC(=O)c1ccc(cc1)-c1cc(ccc1)C[NH3+])C)C
870	O=C1N2C(CCC2)C(=O)NC1CCC[NH+]=C(N)N
871	[As+](c1ccccc1)(c1ccccc1)(c1ccccc1)c1ccccc1
872	Fc1cc(ccc1O)C[C@H]([NH3+])C(=O)[O-]
873	O1C(CO)C(O)C(O)C1n1c2ncncc2nc1
874	[Hg](I)I
875	Fc1cc(F)ccc1CO
876	P(OCC1OC2([N-]C(=O)N(CCCC(N(O)CO)C(=O)[O-])C2=O)C(O)C1O)(=O)([O-])[O-]
877	O=C([O-])CCc1c2[nH]c(Cc3[nH]c(Cc4[nH]c(Cc5[nH]c(C2)c(CCC(=O)[O-])c5C)c(C)c4CCC(=O)[O-])c(C)c3CCC(=O)[O-])c1C
878	Oc1c(cccc1O)C(=O)N
879	OC[C@@H](O)[C@@H](O)CO
880	[PH](OC(C)C)(OC(C)C)=O
881	[Mo+9]([O-])([O-])[O-]
882	S(C(=O)CC(=O)[O-])CCNC(=O)CCNC(=O)C(O)C(COP(OP(OCC1OC(n2c3ncnc(N)c3nc2)C(O)C1OP(=O)([O-])O-])(=O)O-])(=O)[O-])(C)C
883	O1C(C(O)CO)C(O)C(O)C(O)C1O
884	[nH]1c2c(cccc2)cc1
885	Oc1ccc(cc1N)C
886	O=C(N)C([NH3+])Cc1c2c([nH]c1)cccc2
887	O=C([O-])C(C([NH3+])C(=O)[O-])C
888	O=C([O-])C(CC(=O)[O-])CC(=O)[O-]
889	O1[C@H](CO)[C@@H](O)[C@H](O)[C@@H](O)C1=O
890	P(OCC1OC(n2c3N=CNC(=O)c3nc2)C(O)C1O)(=O)([O-])[O-]
891	O1C(CO)C(O)C(O)C1n1c[nH+]cc1N
892	O(Cc1ccccc1)C=O
893	O=C(N)c1cc(cc(c1)C(=O)[O-])-c1ccc(cc1)-c1ccccc1
894	OC(CC(=O)[O-])CC(=O)[O-]
895	O1C[C@H]2O[C@@H](O)[C@@H](O)[C@@H](O)[C@@H]2O[C@]1(C(=O)[O-])C
896	Clc1ccc(C(=O)[O-])c(N)c1O
897	Ic1c2c(ncnc2N)n(c1)[C@@H]1O[C@H](CO)[C@@H](O)[C@H]1O
898	o1cc(cc1)C(=O)N[C@@H](C(C)C)C(=

	O)N[C@@H](C(C)C)C(=O)N[C@@H](CC(C)C)C(=O)N[C@H](\C=C\C(OCC)=O)C[C@@H]1CCNC1=O
899	[nH+]1c2c(CCCC2)c(NCCCCCCCCNc2c3c([nH+]cc2)cccc3)c2c1cccc2
900	[nH+]1c2c(CCCC2)c(NCCCCCCCC[NH3+])c2c1cccc2
901	O1[C@@H]2[C@H](NC1=O)c1c(cccc1)[C@@H]2C1=CN[C@@](Cc2ccccc2)(C[C@H](O)[C@@H](NC(OCCOCC)=O)Cc2ccccc2)C1=O
902	O1[C@H]2N3C=CC(=O)N=C3O[C@H]2[C@H](O)[C@H]1CO
903	O1[C@@H]2[C@H](N=C1N(C)C)[C@@H](O)[C@H](O[C@@H]1O[C@H](CO)[C@@H](O[C@@H]3O[C@H](CO)[C@@H](O)[C@@H](O)[C@H]3NC(=O)C)[C@@H](O)[C@H]1NC(=O)C)[C@H]2CO
904	[NH2+](CCCNCCC[NH2+]CC)CCC
905	BrCCCCCCO
906	O=C([O-])[C@@H]([NH3+])Cc1ccc(cc1)-c1ccccc1
907	OB(O)[C@H](NC(=O)[C@@H](NC(=O)CC[C@H](NC(OC(C)(C)C)=O)C(=O)[O-])CCCCNC(OCc1ccccc1)=O)C
908	Clc1cc(ccc1Cl)-c1c([nH+]c(nc1N)N)C
909	O(CCC[C@H]1C[C@](O)(C[C@@H](O)[C@@H]1O)C(=O)[O-])c1ccccc1
910	S(\C(=N/OS(=O)(=O)[O-])\Cc1ccccc1)[C@@H]1C[C@H](CO)[C@@H](O)[C@H](O)[C@H]1O
911	S(O[C@H]1[C@@H](O)[C@H](O[C@@H](OC[C@H](NC(=O)CCCCCCCCCCC\C=C/CCCCCCCC)[C@H](O)\C=C\CCCCCCCCCCCCC)[C@@H]1O)CO)(=O)(=O)[O-]
912	O=C1N[C@@H](C)C(=O)N[C@@H](CCC(C[C@@H]([C@@H](OC)Cc2ccccc2)C)C)[C@@H](C)C(=O)\N=C(/CCC(=O)N(C)[C@@H](C)C(=O)N[C@H](C)C(=O)N[C@@H](CC(C)C)C(=O)N[C@@H](C(=O)[O-])[C@@H]1C)\C(=O)[O-]
913	S(=O)(=O)(NCCCC[C@H]([NH3+])C(=O)[O-])c1c2c(ccc1)c(N(C)C)ccc2
914	O1[C@H](CO)[C@@H](O)[C@H](O[C@@H]2O[C@H](CO)[C@H](O)[C@H](O)[C@H]2O[C@@H]2O[C@@H](C)[C@H](O)[C@@H](O)[C@@H]2O)[C@@H](N[C@@H](O)C)[C@@H]1O
915	O1[C@H](CO)[C@H](O)[C@H](O)[C@@H](O)[C@@H]1OCCCCCCCCC(

	OC)=O	938	o1cncc1-c1ccc(NC(=O)Nc2cc(ccc2)CNC(O[C@H]2CCOC2)=O)cc1OC
916	O[C@H]1C[C@H]2[NH+]([C@H](CC2)[C@H]1C(OC)=O)C		
917	Brc1cc(ccc1O)C1(OC(=O)c2c3c1cccc3c(Cl)cc2)c1cc(Br)c(O)cc1	939	Brc1cc2N=CN(CC(=O)CC3[NH2+]CCC[C@H]3O)C(=O)c2cc1Cl
918	S(=O)([O-])(=Nc1nn[nH]n1)c1cc2c(Oc3c(cccc3)C2=O)cc1	940	Clc1ccccc1-c1nc(sc1)NC(=O)c1n(c2c(c1)cccc2)CC(=O)[O-]
919	S(C[C@H](NC(=O)CC[C@H]([NH3+])C(=O)[O-])C(=O)NCC(=O)[O-])C	941	O1c2n(CCC1)c1c(cccc1)c2C(=O)NCC1CC[NH+](CC1)CCCC
920	S(=O)(=O)(N1CCC[NH2+]CC1)c1c2c(ccc1)C(=O)NC=C2	942	O1[C@H](CO)[C@@H](O)[C@H](O)[C@@H](O)C1n1c2cc(O)ccc2c2c3c(c4c5c([nH]c4c12)cc(O)cc5)C(=O)N(NC(CO)CO)C3=O
921	Ic1c(C(=O)[O-])c(I)cc(I)c1NC(=O)CCCCC(=O)Nc1c(I)c(C(=O)[O-])c(I)cc1I	943	O(C)c1nc(O[C@H](C(OC)(c2ccccc2)c2ccccc2)C(=O)[O-])nc(OC)c1
922	s1cc(nc1C)CN1CCN([C@@H](C(C)C)C(=O)N[C@H]([C@H](O)CN(S(=O)(=O)c2ccc(cc2)\C=N\[O-])CC(C)C)Cc2ccccc2)C1=O	944	O1c2c3c(OC(=O)C=C3CCC)c3c(O[C@H](C)[C@@H](C)[C@@H]3O)c2C=CC1(C)C
923	P(OC[C@@H](OC(=O)CCCCCCC\C=C/CCCCCC)COC(=O)CCCCCCC\C=C/CCCCCCC)(=O)([O-])[O-]	945	O[C@@H]1CC(C[C@@H](O)C1=C=C\C=C/1[C@@H]2CC[C@H]([C@H](CC)C)[C@]2(CCC\1)C
924	Clc1cc(Nc2ccccc2C(=O)[O-])cc(Cl)c1OOO	946	S1SCC(NC(=O)C(NC(=O)C(NC(=O)C(NC(=O)C(NC(=O)C([NH3+])Cc2ccccc2)C1)Cc1ccc(O)cc1)Cc1c2c([nH]c1)cccc2)CCCC[NH3+])C(C)C)C(=O)NC(Cc1c2c([nH]c1)cccc2)C(=O)N
925	O=C1N=C(NC=2NC[C@@H](N(C1=2)C)CNc1ccc(cc1)C(=O)N[C@@H](CCC(=O)[O-])C(=O)[O-])N		
926	O1[C@H]2[C@H](OC[C@H]2Oc2ccc(cc2)C(=[NH2+])N)[C@@H](Oc2cc(ccc2)C(=[NH2+])N)C1	947	O=C(N(CC)CC)[C@@]1(C[C@@H]1C[NH3+])c1ccccc1
927	O[C@@H]1CC(C[C@@H](O)C1)=C\C=C/1\C2CC[C@H]([C@@H](CC#CC(O)(C)C)C)[C@]2(CCC\1)C	948	O(CCC)c1cc2[nH]c(nc2cc1)NC(OC)=O
		949	Clc1c(OC)c(ccc1N)C(=O)NC1C2CCC[NH+](C2)CC1
928	s1c2c(nc1)C([O-])=C(CCCCCCCCCC)C(=O)C2=O	950	O(C)c1cc(ccc1OC)C(=O)NCc1ccc(OCC[NH+](C)C)cc1
929	S(=O)(=O)([O-])Nc1n(nc(c1)-c1ccccc1)C	951	ClC(Cl)=CC1C(C)(C)C1C(OCc1cc(Oc2ccccc2)ccc1)=O
930	O1C(C)C(NC(=O)c2ncccc2O)C(=O)NC(CC)C(=O)N2C(CCC2)C(=O)N(C)C(Cc2ccccc2)C(=O)N2C(CC(=O)CC2)C(=O)NC(c2ccccc2)C1=O	952	O=C(Nc1cc2c(cc1)C(CCC2(C)C)(C)C)c1ccc(cc1)C(=O)[O-]
931	Oc1c2c(ccc1)C(=O)c1c(C2=O)c(O)ccc1	953	O1[C@H](CO)[C@@H](O)[C@@H](O)[C@@H]1n1c2ncnc(N[C@@H]3CCOC3)c2nc1
932	O=C(NNC(C)C)c1ccncc1	954	Clc1cc(ccc1)C1=CC(=O)N(c2c1cc(cc2)[C@]([NH3+])(c1ccc(Cl)cc1)c1n(cnc1)C)C
933	O=C(NNCCC(=O)NCc1ccccc1)c1ccnccc1		
934	[NH+](=C(\[NH+]=C(N)N)/N)/CCCC	955	O=C1N=C(N)C2N1C2
935	Brc1ccc(cc1)C(=CC[NH+](C)C)c1cccnc1	956	O1[C@H](C(=O)NCC(O)C(O)[C@@H]1n1c2nc(nc(N)c2nc1)C#CCC1CC(CC1)C(OC)=O
936	O(C(=O)CC)[C@@H]1[C@@]2([C@H]([C@H]3[C@H](CC2)[C@@]2([C@H](C[C@H](OC(=O)C)[C@@H]([NH+]4CCCCC4)C2)CC3)C)C[C@@H]1[N+]1(CCCCC1)CC=C)C	957	Fc1ccccc1-c1onc(n1)-c1cc(ccc1)C(=O)[O-]
		958	ClC(=NOC[C@H](O)C[NH+]1CCCCC1)c1ccc[n+]([O-])c1
937	[NH2+]=C(N)N1CCc2c(C1)cccc2	959	O1[C@@H]2[C@]34CC[NH+]([C@H]

	(Cc5c3c1c(O)cc5)[C@]4(O)CCC2=O)CC1CC1	979	O1[C@@H]2[C@]34CC[NH+]([C@H](Cc5c3c1c(O)cc5)[C@]4(O)CCC2=O)CC1CC1
960	[Mo-2]([SH2+])[SH2+]		
961	S1[C@H]2[C@@H]3N([C@H](c4c2c(OC(=O)C)c(c2OCOc24)C)COC(=O)[C@@]2(NCCc4cc(O)c(OC)cc24)C1)[C@@H](O)[C@H]1[NH+]([C@@H]3c2c(cc(C)c(OC)c2O)C1)C	980	O1[C@@H]2[C@]34CC[NH+]([C@H](Cc5c3c1c(O)cc5)[C@]4(O)CC[C@@H]2O)CC1CCC1
		981	Clc1cc(ccc1C1CCCCC1)\C=C/C[NH+](CC)C1CCCCC1
962	O1c2c3c(cccc3O[C@@H]3O[C@H](C)[C@H](O)[C@@](O)(C)[C@H]3O[C@H]3O[C@H](C)[C@H](O)[C@H](OC)[C@H]3[NH3+])c(O)c3c2-c2c(c(ccc2OC3=O)C)C1=O	982	S(SCCNC(=O)CC[NH3+])CCNC(=O)CC[NH3+]
		983	S(O[C@@H]1CC2=CC[C@H]3[C@@H]4CCC(=O)[C@]4(CC[C@@H]3[C@]2(CC1)C)C)(=O)(=O)[O-]
963	O=C(C[C@@H]1[NH+](C)[C@@H](CCC1)C[C@H](O)c1ccccc1)c1ccccc1		
964	FC(F)(F)Oc1ccc(cc1)CO[C@H]1Cn2cc([N+](=O)[O-])nc2OC1	984	[Si](CCc1c2c(nc3c1cccc3)C=1N(C2)C(=O)C2=C(C=1)[C@@](O)(CC)C(OC2)=O)(C)(C)C
965	FC(F)(F)C1=CC(=O)Nc2c1cc(N1[C@@H](CC[C@@H]1[C@@H](O)C(F)(F)F)C)cc2	985	O=C(N(C1CC[NH+](CC1)CCc1ccccc1)c1ccccc1)CC
		986	O=C(N)c1cc2c(nc1)cccc2
		987	O(C(=O)C(=O)C)CC
966	O1[C@@H]2C[C@H](O)[C@@]3([C@H]([C@H](OC(=O)c4ccccc4)[C@]4(O)C[C@H](OC(=O)[C@H](O)[C@@H](NC(=O)c5ccccc5)c5ccccc5)C(=C([C@H](OC(=O)C)C3=O)C4(C)C)[C@]2(OC(=O)C)C1)C	988	[NH3+]CCc1[nH]cnc1
		989	o1c2c(cc1C(=O)N[C@H]1C3CC[NH+](CC3)[C@H]1Cc1cccnc1)cccc2
		990	OC[C@H](Nc1nc(NCc2ccccc2)c2ncn(c2n1)C(C)C)CC
967	Brc1cc(F)c(Nc2ncnc3c2cc(OC)c(OCC2CC[NH+](CC2)C)c3)cc1		
968	s1cc(nc1-c1cc(OCC)c(OCC)cc1)-c1nc(ccc1)C(=O)[O-]	991	s1cccc1C[C@H](NC(=O)CNC(=O)C1N(C[C@H](O)C1)C(=O)C1N(CCC1)C(=O)C(NC(=O)[C@H]([NH3+])CCC[NH+]=C(N)N)CCC[NH+]=C(N)N)C(=O)N[C@H](C(=O)N1Cc2c(CC1C(=O)N1[C@@H]3[C@H](CC1C(=O)N[C@@H](CCC[NH+]=C(N)N)C(=O)[O-])CCCC3)cccc2)CO
969	Brc1cc(F)c(cc1)CN1C(=O)[C@@]2(n3c(ccc3)C1=O)CC(=O)NC2=O		
970	O=C1C[C@@H](O)[C@H](\C=C\CC(O)(CCCC)C)[C@H]1CCCCCCC(OC)=O		
971	[NH3+]CCc1[nH]cnc1	992	FC(F)(F)COc1ccccc1OCC[NH2+][C@@H](Cc1cc(c2N(CCc2c1)CCCO)C(=O)N)C
972	[Cl+]([O-])[O-]		
973	Clc1cc(Nc2ncnc3c2cc(NC(=O)C=C)c(OCCCN2CCOCC2)c3)ccc1F	993	S([C@H]1C[C@H]([NH2+]C1)CNS(=O)(=O)N)C=1[C@@H]([C@H]2N(C=1C(=O)[O-])C(=O)[C@@H]2[C@H](O)C)C
974	O(CCOCCOCCOC)c1cc2=NC=C3N=C(C=c4[nH]c(=CC5=NC(=CN=c2cc1OCCOCCOCCOC)C(C)=C5CCCO)c(CC)c4CC)C(CCCO)=C3C		
		994	Clc1cc2c(N(CCC[C@H]2O)C(=O)c2cc(NC(=O)c3ccccc3C)cc2C)cc1
975	ClC(Cl)C(OC1(CC[C@H]2[C@H]3[C@@H]([C@@]4(C(=CC(=O)C=C4)CC3C)[C@@H](O)C[C@]12C)C(OCC)=O)=O	995	Clc1cc2C3C(c4c(Oc2cc1)cccc4)CN(C3)C
		996	F\C=C\1/[C@H](O)[C@H](O[C@H]/1N1C=CC(=NC1=O)N)CO
976	ClC12C(C3CC(C)C(O)(C(=O)CO)C3(CC1O)C)CCC1=CC(=O)C=CC12C	997	o1cccc1CNC(=O)c1ccccc1N(C(=O)COc1ccccc1)C
977	O(CCC[NH+]1CCCCC1)c1cc2ncnc(N3CCN(CC3)C(=O)Nc3ccc(OC(C)C)cc3)c2cc1OC	998	S(Oc1ccc(cc1)CCOc1ccc(cc1)C[C@H](OCC)C(=O)[O-])(=O)(=O)C
		999	O[C@H]1[C@@H](C(NC(=O)C)C(CC)CC)[C@H]([NH+]=C(N)N)C[C@@H]1C(=O)[O-]
978	O=C(N[C@@H](Cc1c2c([nH]c1)cccc2)C(=O)[O-])CC[C@@H]([NH3+])C(=O)[O-]	1000	Fc1ccc(cc1)CNc1[nH+]c(N)c(NC(OCC)=O)cc1

Chemical structures of the random sample from PubChem database representing small organic compounds without drug related properties and without subcellular localization information. Structure is presented as the Simplified Molecular Input Line Entry Specification string of the major microspecies at pH 7.4, as calculated by ChemAxon.

ID	Chemical Structure
1	O1[C@](O[C@H]2O[C@H](CO)[C@@H](O)[C@H](O)[C@H]2O)(CO)[C@@H](O)[C@H](O)[C@H]1CO
2	O1c2cc(ccc2OC1)C=CC(=O)[O-]
3	OCC(=O)[O-]
4	Fc1cc2c(N(C=C(C(=O)[O-])C2=O)C2CC2)c(OC)c1N1CC2C([NH2+]CCC2)C1
5	O=C1CC[C@@H]2[C@@H]3[C@H]([C@@H]4CC[C@@](O)(C#C)[C@]4(CC3)CC)CCC2=C1
6	S(=O)(=O)([O-])CC12CCC(CC1=O)C2(C)C
7	O=C1N(CC(=O)Nc2ccccc2)C(=O)N(C)C1=O
8	[NH+](N)=C(N)N
9	O1C2C34C(C([NH+](CC3)C)Cc3c4c1c(OCC)cc3)C=CC2O
10	P1(OC2C(O1)C(OC2CO)n1c2ncnc(N)c2nc1)(=O)[O-]
11	S=C([S-])N(C)C
12	ONc1cc2Cc3c(-c2cc1)cccc3
13	C(CCCCCCCCC)CCCCCCCCC
14	FC(F)(F)C(=O)CCCCCCCCCCCCCCC
15	N(=N\c1ccc(N(C)C)cc1)/c1cc(ccc1)C
16	S(=O)(=O)(C(CC(=O)c1cccccc1)c1ccccc1)c1ccc(N)cc1
17	n1cn(nc1)Cc1cccccc1
18	[N+](CCCC)(CCC)(CCC)CCC
19	ClCCOC(=O)Cc1cccccc1
20	[n+]12c(-c3[n+](CC1)cccc3)cccc2
21	[NH2+]1CCCC1C
22	ClC(Cl)C(=O)Nc1ccc(cc1)C
23	O1C2=CC(=[N+](CC)CC)C=CC2=C(c2c1cc(N(CC)CC)cc2)c1ccccc1C(=O)[O-]
24	FC(F)(F)C(=O)CCCC=CCC=CCC=CCC=CCCCCC
25	S(=O)(=O)(NCC(O)CNC(=O)C(CC(C)C)c1cc(ccc1)-c1ccccc1)c1ncccc1
26	S=C([S-])OC1CCCCC1
27	O=CNCC
28	O=C(N)C(CC[N+](CC)(C)C)(c1cccccc1)c1ccccc1
29	O1C(OC2OC3C(OC(OC4C(O)C(O)C([

	NH3+])CC4[NH3+])C([NH3+])C3C(O)C2[NH2+])C)C)C(O)C(O)C([NH3+])C1CO
30	BrC(F)(F)C(F)(F)C(F)(F)C(F)(F)C(F)(F)C(F)(F)C(F)(F)C(F)(F)C(F)(F)C(F)(F)F
31	O(CCCCCCCC)c1ccc(N)cc1CO
32	Clc1cc(Cl)ccc1OCCCC(=O)[O-]
33	O=C1N(Cc2n(-c3c1cc(N=[N+]=[N-])cc3)cnc2C(OCC)=O)C
34	O=C(NCc1ccccc1)C
35	o1nc(cc1CC[NH+](CC)CC)-c1ccc(OC)cc1
36	S(P(=S)(OC)OC)CC(=O)NCCOC
37	S(OCC)(OCC)(=O)=O
38	OC1CC(O)C(CC=CCCCC(OC(C)C)=O)C1CCC(=O)CCCCCCC
39	O=CCCC
40	Brc1cc(ccc1)C(=O)[O-]
41	SCC[NH2+]CCC(=O)N
42	S=P(N1CCCCCC1)(N1CC1)N1CC1
43	OCCN(CCO)c1ccc(\N=N\c2ccccc2)cc1
44	Fc1ccc(cc1)C(O)CCC[NH+]1CCN(CC1)c1ccccc1OC
45	O(C(=O)C(OCC)(c1cccccc1)c1cccccc1)C1CC[NH+](CC1)CC
46	O=C([O-])C([NH3+])CCC(=O)[O-]
47	O1c2c(C=C(c3cccnc3)C1=O)cccc2
48	S1c2c(N(c3c1cccc3)CCC[NH+]1CCN(CC1)CCOC(=O)CCCCCCCCC)cc(cc2)C(F)(F)F
49	O(C(=O)C1(CCCCC1)C1CCCCC1)CC[NH+]1CCCCC1
50	O=C1CCCC1C1CCCC1
51	Clc1cc2[nH]c3c(cc(OC)cc3)c(NC(CCN(CCCl)CCCl)C)c2cc1
52	O1C2CCC1C(C(=O)[O-])C2C(=O)[O-]
53	O=C1CC[C@@]2([C@@H]3[C@H]([C@@H]4CC[C@H](OC(=O)CCCCCC)[C@]4(CC3)C)CCC2=C1)C
54	S(C)c1nc(nc(n1)NCC)NC(C)(C)C
55	O(C(=O)C(C)C)C1CCC([NH+]2CCCCC2)CC1
56	Clc1ccc(cc1)Cn1c2c(nc1C[NH+]1CCCC1)cccc2
57	O=C([N-]c1nc(nc(n1)[N-

	]C(=O)c1ccccc1)[N-]C(=O)c1ccccc1)c1ccccc1
58	ICCCCCCCCCCC
59	O(CC)C(=O)N(N=O)CC
60	O1c2cc(O)cc3c2c(c2c(C(C3(O)C3(O)c4cc(O)cc5OC(C(c6c(C3c3ccc(O)cc3)c(O)cc(O)c6)c45)c3ccc(O)cc3)c3ccc(O)cc3)c(O)cc(O)c2)C1c1ccc(O)cc1
61	O(C)c1ccccc1-c1ccccc1
62	O(C)c1ccc(cc1O)C=O
63	OC(C(O)C(=O)[O-])C(O)CO
64	[NH2+](C(C)C)C(C)C
65	P(Oc1c2c(ccc1)cccc2)(=O)([O-])[O-]
66	S(=O)([O-])c1ccc(cc1)C
67	P(OCC1OC(n2c[nH+]c(C(=O)[O-])c2N)C(O)C1O)(=O)([O-])[O-]
68	C(CCCCCCC)CCCCCC=C
69	[N+](CCN(C1CCCCC1)c1ccccc1)(C)(C)C
70	[NH2+](CCc1ccccc1)CCc1ccccc1
71	S(=O)(=O)(N)c1cc(ccc1C)C(O)C[NH2+]CCOc1ccccc1OC
72	O=C1NCC(=O)NC1CC(C)C
73	O1c2c(C3=C(CCC(C3)C)C1(C)C)c(O)cc(c2)CCCCCC
74	O=C1CCCCC1C(=O)C
75	O=C(N(CC)CC)c1c2CCCCCc2nc2c1cccc2
76	ClC(Cl)(F)C(F)(F)F
77	O(C(OCC)CC)CC
78	ONc1c2c(ccc1)cccc2
79	ClC(C)=C=O
80	O(CC(O)C)c1c2c(cccc2)c(cc1)C(=O)C
81	O=C(Cc1ccccc1)CC(=O)C
82	S(=O)(=O)([O-])c1c2c(cccc2Nc2ccccc2)ccc1
83	O=C([O-])CC(=O)[O-]
84	Oc1ccccc1C(=O)[O-]
85	S(=O)(=O)([O-])c1cc2c(cc1)c([N+](=O)[O-])cc([N+](=O)[O-])c2[O-]
86	[NH2+](C[C@]1(C2CCc3cc(ccc3[C@]2(CCC1)C)C(C)C)C)CC[NH2+]C[C@]1(C2CCc3cc(ccc3[C@]2(CCC1)C)C(C)C)C
87	ON=CN
88	ClC(S)=O
89	O=C1c2c(NC1=O)c(ccc2)C
90	O=[N+]([O-])c1ccccc1
91	P(F)(=O)([O-])[O-]
92	OC1CCC2C3C(CCC12C)C1(C(=CC(=O)CC1)C[C@H]3C)C
93	S=C=Nc1ccc(cc1)C#N
94	O1C(C(CCC12OC1CC=C(C)C(OC3OC

	(C)C(O)C(OC)C3)C(C=CC=C3COC4CC(=CC(C34O)C(OC(C2)C1)=O)C)C)C)C1CCCC1
95	O(C)c1c(OC)cc(cc1OC)C(=O)N1CCN(CC1)CC(OC(=O)c1cc(OC)c(OC)c(OC)c1)C
96	BrCc1ccccc1Cl
97	[NH3+]C1CCCCC1
98	ClC(F)(F)C(F)F
99	O1c2c(C=CC1=O)ccc(OC)c2CC=C(C)C
100	O1C(C)C(O)C([NH3+])CC1OC1CC(O)(Cc2c1c(O)c1c(C(=O)c3c(C1=O)c(OC)ccc3)c2O)C(=O)CO
101	O1CC[NH+](CC1)C(CC(C(=O)CC)(c1ccccc1)c1ccccc1)C
102	o1c(nc(CCOc2ccc(cc2)CC(Nc2ccccc2C(=O)c2ccccc2)C(=O)[O-])c1C)-c1ccccc1
103	ClCCCCO
104	O(C(=O)C=C(NC(C(=O)[O-])c1ccccc1)C)CC
105	Ic1c(C(=O)[O-])c(I)c(NC(=O)C)c(I)c1N(C(=O)C)C
106	S(=O)(=O)(N(C(CCC)C)CC(=O)NO)c1cc(OC)cc1
107	ClCCCCC
108	FC(F)(F)c1cc(OCCC[NH+]2CCC3(CCCCC3)CC2)ccc1
109	S1C(C)(C)C(NC1C(NC(=O)Cc1ccccc1)C(=O)NCc1ccccc1)C(=O)NC(Cc1ccccc1)C(O)CC(=O)NCc1[nH]c2c(n1)cccc2
110	S1(=O)(=O)CCC=C1
111	N#CCC(C)C
112	C(CC(C)=C)(C)(C)C
113	Clc1cc2[nH+]c3c(cc(OC)cc3)c(NC(CCC[NH+](CC)CC)C)c2cc1
114	o1c(ccc1[N+](=O)[O-])C=O
115	O=C(CCCCCCC(=O)NO)c1ccc(N2CCN(CC2)c2ccccc2)cc1
116	[As](c1ccccc1)(c1ccccc1)c1ccccc1
117	C(CCC=C)CC=C
118	S1CCSC1=S
119	O=C([O-])C([NH3+])Cc1[nH]cnc1
120	[n+]1(ccccc1)CCCCCCCCCCCCCCCC
121	[nH]1nccc1
122	S(C(C)C)C
123	O=C1N(CC(=O)N)C(=O)N(CC(=O)N)C(=O)N1CC(=O)N
124	O(Cc1ccccc1)C(=O)C(CC)(C[NH+](C)C)c1ccccc1
125	P(OCC(O)C(O)C(O)CN1C=2NC(=O)NC(=O)C=2Nc2cc(C)c(cc12)C)(=O)([O-])[O-]

333

126	O(C)c1c([N+](=O)[O-])cc([N+](=O)[O-])cc1[N+](=O)[O-]	162	Clc1ccc(NC=O)cc1
127	O=C(NN=C1CCCC1)c1ccc([N+](=O)[O-])cc1	163	Clc1cc(ccc1)C(=O)C([NH2+]C(CO)(C)C)C
128	O=C1NC(=O)NC1(C)C1CCCCC1	164	C1c2c(-c3c1cccc3)cc1c(c2)cccc1
129	[N+](#C)c1ccc(cc1)C	165	ON
130	O=C1N(CCCC)C(=O)N(c2ncn(c12)CC(=O)C)CCCC	166	O(C)c1cc(C(N(CC(=O)[O-])CC(=O)[O-])CN(CC(=O)[O-])CC(=O)[O-])c([N+](=O)[O-])cc1OC
131	O(CCC)c1cc(N)ccc1C(OCC[NH+](CC)CC)=O	167	O=C1N(CCC1)CCCCC[N+](C)(C)C
132	Oc1cc(C(=O)[O-])c([N+](=O)[O-])cc1	168	O=C([O-])CN(CC[NH+](CCN(CC(=O)[O-])CC(=O)[O-])CC(=O)[O-])CC(=O)[O-]
133	O(C)c1ccc(N=O)cc1	169	O=CCCC=C
134	OCC[NH+](CCCC)CCO	170	[Ca+2]
135	O=C1CC[C@@]2([C@@H]3[C@H]([C@@H]4CC[C@](OC(=O)C)(C(=O)C)[C@]4(CC3)C)C=C(C2=C1)C)C	171	O(CC)c1ccc(cc1)C(OCC[NH+](CC)CC)=O
136	O=C(NCCCCCNC(=O)CCN1CC1)CCN1CC1	172	O1C(C(N=C1C)(C(OC)=O)C(OC)=O)c1ccoc1
137	S=C=Nc1cc(N=C=S)ccc1C	173	O(C)c1ccccc1N1C2=NC(NC(=C2N=C1)C(=O)N)(C)C
138	[As](Cl)(c1ccccc1)c1ccccc1	174	S(=O)(=O)(N)N1CCN(CC1)C=1C(=O)N=C(NC=1N)C
139	Oc1c2NC(=CC(=O)c2ccc1)C(=O)[O-]	175	O=C1[N-]C(=O)C2(C3CCC(C=C3)C12C#N)C#N
140	n1c(nc(nc1N(C)C)N)N(C)C	176	O(C)c1cc(ccc1OC)C\N=C\NC(=C(N)C#N)C#N
141	OC(CC(=O)[O-])(CCO)C	177	[S+]1(CCCC1)Cc1oc(cc1)C[S+]1CCCC1
142	O=C1N=C(NC(=N1)CC)c1ccccc1	178	S(=O)(=O)(NN=Cc1ccccc1)c1ccc(cc1)C=C1NC(=O)NC1=O
143	P(OCC)(OCC)(OP(OC)OC)=O	179	O=C1C(CCC1=CC=Cc1ccccc1)CNc1ccccc1
144	O1C(C(O)C(O)C(O)C1CO)c1c([O-])c(O)c2c(c1O)C(=O)c1c(cc(O)c(C(=O)[O-])c1C)C2=O	180	O(C(C)(C)C)C(=O)NC(=O)N(CC[NH+]1CCCC1)C
145	O1c2c3C4(C1CC(O)C=C4)CC[NH+](Cc3ccc2OC)C	181	O=C1N2N(Cc3c(C2)cccc3)C=C1
146	n1c(ncnc1CC)CC	182	O(C)C1=CC(=O)c2c(C1=O)c(O)ccc2O
147	S(=O)(=O)(N1CCCC1COC)c1cc2c(NC(=O)C2=O)cc1	183	Brc1ccc(cc1)-c1nc(sc1)NNC=1SC(=Cc2cc(OC)c(OC)c(OC)c2)C(=O)N=1
148	Nc1ccc(cc1)CCCCCCCCCCCC	184	Oc1cc2CCC3C4CC[C@H](O)[C@]4(CCC3c2cc1C=C(C)C)C
149	Ic1cc(cc(C(=O)Nc2cc(Cl)c(cc2)C(=[NH2+])N)c1O)C	185	OC1[C@@H](O)CN(OCc2ccccc2)C[C@H]1O
150	[n+]1(c2c(cccc2)c(N)c2c1cccc2)C	186	O=C([O-])c1nc2c(nc1Nc1ccc(cc1)C(=O)[O-])cccc2
151	O(CCCCCC)c1ccc(cc1)-c1c2c([n+](c3c1cccc3)C)cccc2	187	s1cc(cc1)[C-](C(=O)c1occc1)CC(=O)c1occc1
152	O(CC[NH+]1CCCC1)c1ccc(cc1)-c1[nH]c2c(cccc2)c1-c1ccccc1	188	O=C([O-])C(N(CC(=O)[O-])CC(=O)[O-])c1ccccc1
153	OC(C([NH2+]C)C)c1ccc(N)cc1	189	Brc1ccccc1S(=O)(=O)c1ccccc1NC
154	O=C([O-])CCC1C=2[NH2+]C(=CC3NC(=CC4[NH2+]C(C=C5NC(C=2)=C(CCC(=O)[O-])C5C)C(C)C4C=C)C(C)C3C=C)C1C	190	Clc1cc(SSc2cc(Cl)c(cc2S(=O)([O-])=Nc2[nH]c3cccnc3n2)C(=O)Nc2ccccc2)c(S(=O)([O-])=Nc2[nH]c3cccnc3n2)cc1C(=O)Nc1cc
155	O=C(N(CC)CC)N		
156	O=C(Nc1c2c(c3c(c1)cccc3)cccc2)C		
157	O1CCN(CC1)CC#N		
158	S(OOS(=O)(=O)[O-])(=O)(=O)[O-]		
159	FC(F)(F)c1cc(\N=N\c2ccc(N(C)C)cc2)ccc1		
160	O(C)c1ccc([N+](=O)[O-])cc1		
161	O=C1N=C(Nc2ncc(nc12)C(O)C(O)C)N		

	ccc1		ccccc1)=O
191	O1c2c(C34C1C[NH+](C(C3)CCC4)C)c ccc2O	219	OCc1ncn(c1)C(c1ccccc1)(c1ccccc1)c1 ccccc1
192	Brc1sc(Br)c2c1C(=O)[C@@H](Br)[C@@H]2[NH3+]	220	ClCC1c2c(N(S(=O)(=O)c3[nH]c4c(cc(OC)cc4)c3)C1)cc(N)cc2
193	O(C(C)(C)C)C(=O)NCCCCC([NH3+])C(=O)N	221	O1[C@@H]2C34C5(C6C(C2(OC)C=C5)C(=O)NNC6=O)C([NH+](CC3)C)Cc2c4c1c(OC)cc2
194	O=C1c2c(CC13Cc1cc(ccc1C3)C)cccc2	222	O=C1NC(=NC(=O)[CH-]1)NN1C(=NC(=Cc2ccccc2)C1=O)c1ccccc1
195	Brc1c2c(cccc2)c(OCc2ccccc2)cc1		
196	O=C1C(CCCC1=C)CCC(CCOC)=C	223	ClCCCSc1ccccc1NC(=O)C=Cc1ccccc1
197	O(C)c1cc2CCc3c(n(c4c3cc(OC)cc4)CC[NH+]3CCCCC3)-c2cc1	224	S(=O)(=O)(c1ccc(NC(=O)c2ccccc2SC(=O)CCCC[n+]2ccccc2)cc1)c1ccc(NS(=O)(=O)Cc2ccccc2[N+](=O)[O-])cc1
198	S(=O)(=O)(N1CC(CN(S(=O)(=O)c2ccc(cc2)C)CCC[NH+](CCC1)CC(CC)C)=C)c1ccc(cc1)C	225	[S-]c1cc2c(NC(=CC2=O)c2ccccc2)cc1
		226	O=C1NN=C(N1N=Cc1ccncc1)C
199	O1[C@@H]2C3C(=C(C[C@H](OC(=O)c4ccccc4)C2[C@H](C)C1=O)C)C(=O)C=C3C	227	O(C(=O)[O-])C12C(CCCC1)C(=O)C1C2CCCC1
		228	OC(CNC(=O)Nc1ccccc1)C[NH+](C)C
200	Clc1cc(SC(C(=O)[O-])c2ccccc2)c(S(=O)([O-])=Nc2nc(nc(n2)N)N(C)C)cc1C	229	O(C(C(=O)NC(NC(=O)C)Cc1ccccc1)C
		230	O=C1N(c2c(cccc2)C(N=[N+]=[N-])=C1)c1ccccc1
201	s1cccc1C(=O)N(C(=O)N1CCCCC1)c1ccccc1		
202	BrC(C(Cl)(C)C)CC\C(=C\C)\CBr	231	Clc1cc(ccc1Cl)C=C1C(=O)C([P+](c2ccccc2)(c2ccccc2)c2ccccc2)=C([O-])C([P+](c2ccccc2)(c2ccccc2)c2ccccc2)=C1O
203	s1c2N(c3ccccc3)C(=S)N(CC(OCC)=O)C(=O)c2nc1SC		
204	O=C1n2c3c(nc2[N-]N=C1)cccc3	232	O=C([O-])C([NH2+]CC#C)Cc1ccccc1
205	O(C)c1cc(Nc2nc(nc(n2)NNC(=O)Cc2ccccc2)NNC(=O)c2ccncc2)ccc1	233	S1CC2N(C1)C(=O)c1c(N=C2NCC(OCC)=O)cccc1
206	Clc1cc([S-])c(S(=O)(=O)NC=2NCCCN=2)cc1C	234	S1SCCC(=O)N[C@H](C(OC)=O)C1(C)C
		235	S1c2c(C(=Nc3c1cccc3)N)c(F)ccc2
207	P(OC(C)C)(OC(C)C)(=O)C(N(C(=[NH+]C=1OC(OCC)=NC(N=1)(C(F)(F)F)C(F)(F)N)C)C(C)C	236	ClC(Cl)(P(=O)(CC)CC)C(O)C(C)(C)C
		237	O1[C@@H](C)[C@](CC12CC[NH+](CC2)C)(C(=O)C)c1ccccc1
208	IC(C(=O)c1ccccc1)=C1CCCC1C	238	O=C(NCC([N+](=O)[O-])(CNC(=O)c1ccccc1)C)c1ccccc1
209	Clc1cc([S-])c(S(=O)([O-])=Nc2nc([nH]n2)N)cc1C		
210	s1cccc1C(=O)N1CCc2c(C1)cccc2	239	O1CC2Cc3c(cc4OCOc4c3)C1(C2CO)c1cc(OC)c(OC)c(OC)c1
211	O1[C@@H]2[C@]34C5([C@H]([NH+](CC3)C)Cc3c4c1c(OC)cc3)CC(C(O)(C)C)C2(OC)CC5	240	O1C(CCC1N1C=CC(=NC1=O)N)(CO)C
		241	Fc1ccc(cc1)C(=O)CCC[NH+]1CCC2(Oc3c(cccc3)C(=O)N2)CC1
212	O(C(OC)CNC(=O)C(NC(=O)C=Cc1ccccc1)C)C	242	Clc1cc(ccc1)COc1ccc(cc1)C=CC(=O)N(O)C
213	O=C1c2c(N(c3ncccc13)CC[NH+](CC)CC)ccc1c2n(nc1)CC[NH+](CC)CC	243	O1[C@@H]2[C@@H](C[C@@H](O)[C@@]1(CCC=C(CCC[C@H](C)[C@@H]2O)C)C)C1(CC1)C(OC)=O
214	Clc1cc(NC)c(cc1)C(=O)N1CCC[C@H]1CO	244	O1C[C@@H](O)[C@H](n2c3ncnc(N)c3nc2)[C@@H]1C(OC)OC
215	O=C1N2N(C3CCC2CC3)C(=O)N1c1ccccc1	245	Clc1ccc(cc1)CC1=NNC(=O)N1n1c(ccc1C)C
216	O=C1C=C2C=C(NC=C2C=C1[O-])C(=O)Nc1ccccc1		
217	O=C1N(C(=O)C=2C(NNC=2N)=C1C#N)c1ccccc1	246	Oc1c(cccc1O)C(=O)NCCN(CCNC(=O)c1cccc(O)c1O)CCNC(=O)c1cccc(O)c1
218	O(Cc1ccccc1)c1ccc(nc1)CC(N)C(OCc1		

	O
247	O=C1c2c(CC1Cc1cc(ccc1C(OC)=O)C)c(ccc2)C
248	O1C(CO)C(O)C(O)C(OC2OCC(O)(COC(=O)C(=CCCC(CCO)C)C)C2O)C1O[C@@H]1OC=C(C2C1[C@@](O)(CC2)C)C(=O)[O-]
249	OC[C@H]1C[C@H](CC1)Cn1nnc2c1nc(nc2N)N
250	O=C1N(N(C(=O)C)C(=O)C)C(=NN1C(=O)C)Cc1ccc(cc1)C
251	O1c2c(cc(cc2\C=N\c2ccccc2O)C)C=CC12Oc1c(cccc1)C(=O)N2C
252	O1C(C(O)C(O)C1CO)c1oc(O[C@@H]2CC[C@H]2C(C)C)nn1
253	O(c1ccc(cc1)C1(O)CC[NH+](CC1C(=O)c1ccc(Oc2ccc(cc2)C)cc1)CC)c1ccc(cc1)C
254	S(CCOCN1C(Cc2ccccc2)=C(CC)C(=O)NC1=O)c1ccccc1
255	O=C(NN=C(C)c1ncccc1)NN=C(C)c1ncccc1
256	S1(=O)(=O)C(=Cc2cc(Oc3ccccc3)ccc2)C(=O)N(C1c1ccccc1)c1ccc(OC)cc1
257	O=C1N(C(=O)C2C1C1CC(CCC1c1c2[nH]c2c1cccc2)C(C)(C)C)c1ccc([N+](=O)[O-])cc1
258	O(C)c1c(OC)cc(cc1OC)C=Nc1ncccc1
259	S(=O)(=O)(N)c1cc(S(=O)(=O)N)ccc1[N-]C(=O)N=S(=O)([O-])c1ccc(cc1)C
260	O(CC(=O)[O-])c1cc(nc2c1cc(OC)cc2)-c1ccccc1
261	O(C)c1cc(\N=N\N2CCCC2)ccc1
262	O=C(Nc1c2c(ccc1)cccc2)NCCCCCC[NH2+]Cc1c2c(ccc1)cccc2
263	O1C2=C(CC1C(C)=C)C(=O)c1c(cccc1O)C2=O
264	O(Cc1ccccc1)c1cc(cc(O)c1)CCNC(=O)CCc1cc(O)c(O)cc1
265	O=C(NC(CCC(=O)NCCCCCCCCCC)C(=O)NCCCCCCCCCCC)c1ccc(N(Cc2nc3c(nc(nc3N)N)nc2)C)cc1
266	s1c2c(cc1C(=O)C)C(=O)c1c(cc(cc1)C(=O)C)C2=O
267	S(C12C=CC(OC1=O)CC12CCOC1=O)c1ccc(cc1)C
268	O1OC(OC)CCC1CO
269	S(=O)(Nc1ccccc1)c1ccccc1OC
270	[n+]1(c2c(ccc3c2nccc3)ccc1)C
271	S(c1cc(C#N)c(N)cc1)c1cc(C#N)c(N)cc1
272	O=C1N(N2C(=NNC2=O)c2ccccc2)C(=O)C=C1
273	S(=O)([O-])(=Nc1cc(OC)ccc1OC)c1cc2c(N=CN(

	NC(=O)CNc3cc(OC)ccc3OC)C2=O)cc1
274	O1[C@@H]2C[C@H](ON3O[C@H]([C@@H](C23)C1=O)C(OCC)=O)OC1CCCC1(c1ccccc1)c1ccccc1
275	Oc1ccc(cc1)CC(NC(=O)C(NC(=O)C)CO)C(=O)NCC(=O)N
276	Brc1c(-c2cc(OC)c(OC)cc2)c(Br)[nH]c1C(OCC)=O
277	O=C1c2c(CCCC1=Cc1ccccc1)cccc2
278	O=C1N(C)C(=O)N([N-]1)c1c(cc(cc1C)C)C
279	O1CCOC12C1CCC(C)(C2OCC(C)(C)C1(C)C
280	O(C)c1cc(ccc1OC)C(=Cc1cc(OC)c(OC)cc1)C(OCC=C)=O
281	O1[C@@H]2[C@@H](O[C@H](C2)[C@@]2(OCC[C@H](C)[C@@H]2O)O)C=CC(=C[C@H](C[C@]2(O[C@H]([C@]34O[C@](CC3)(C[C@H](O4)[C@@H]3O[C@](CC3=O)(C)[C@@H](O)[C@@H]3O[C@@]4(O[C@H](CCC4)[C@H](C)C1=O)CC3)CO)CC2)C)C)C
282	O=C1c2c3c(cccc3cc3c2ccccc3)C1=NNC(=O)c1ccc(cc1)C
283	S(C(=O)CCCC[n+]1ccccc1)c1ccccc1C(=O)Nc1ccc(S(=O)([O-])=Nc2oc(C)c(n2)C)cc1
284	O=C1n2c(nc3cc(ccc23)Cc2cc3nc-4n(c3cc2)C(=O)c2c3c(ccc2)c(N)ccc3-4)-c2c3c1cccc3c(N)cc2
285	OC=1N(CC(OCC)=O)[CH-]C(=O)C=1C1=CC(=O)N(C1)CC(OCC)=O
286	O1C2c3c(OCC2(O)Cc2cc(OC)ccc12)cc(OC)cc3
287	O(C)c1c2c(cc(c1)C)c(cc(-c1cc(c3c(c1O)c(OC)cc(c3)C)-c1c3c([C@H]([NH+](C)[C@@H](C3)C)C)c(O)cc1O)c2O)-c1c2c(C([NH2+][C@@H](C2)C)C)c(O)cc1O
288	O(C(=O)C1N(CCC1)C(=O)C(NC(OC(C)(C)C)=O)CC(C)C)Cc1ccccc1
289	S(C1OC(COC(=O)C)C(OC(=O)C)C(OC(=O)C)C1OC(=O)C)C1=NC(=Cc2ccc(cc2)C)C(=O)N1CC=C
290	Clc1cc2c(NC(=C(C(OCC)=O)C2=O)c2ccccc2)cc1
291	O1CC[NH+](CC1)C1CCCC2c3c(cccc3)[C@]12O
292	O(C(=O)C)C=1C(=O)C2(C(CCC(C)C(OC(=O)C)CCC(=CCCC(=CC2)C)C)C=1C(COC(=O)C)C)C
293	Clc1ccc(Nc2sc(C(=O)c3occc3)c(n2)N)c

	c1		(C)C2=O)c2ccccc2)CC1
294	Clc1ccc(NC=2n3c(nc4cc(C)c(cc34)C)C(C#N)=C(C=2)c2ccccc2)cc1	322	O1C(CO)C(O)C(O)C(O)C1OC1C(O)C(O)C(OC1O[C@H]1CC[C@]2([C@@H](CC[C@@]3([C@@H]2CC=C2[C@@H]4CC(CC[C@]4(CC[C@]23C)C(=O)[O-])(C)C)C)C)C1(C)C)CO
295	Clc1ccc(cc1)CNC(=O)c1cc2sccc2nc1C(F)(F)F		
296	O1c2cc(OC)c3c(O[C@H](C)[C@@H](C)C3=O)c2C=CC1(C)C	323	Oc1ccc(O)cc1C=Cc1ccc(cc1)C(OC)=O
297	OC=1N(c2c(cccc2)C(=O)C=1C(=O)NCC[NH+](C)C)C	324	O\1c2c(ccc(O)c2)C(=O)/C/1=N/c1ccccc1
298	S(=O)(=O)(N(CC=C)c1cc(OC)c2[nH]cc(c2c1[N+](=O)[O-])C)C	325	S=C1N(C(=O)C(=O)N1C1CCCCC1)C1CCCCC1
299	O=C1NC(=O)NC(NN(C)C)=C1	326	O(C)c1ccc(N2C(=O)C(CC2=O)C2CC(CCC2=O)C(C)(C)C)cc1
300	s1ccc(C)c1C=NNc1sc2c(n1)cccc2	327	O1c2c(C(=CC1=O)C)c(OC)cc(OC)c2
301	O(CC[NH+](C)C)c1ccc(cc1)-c1n2c(C=CC=C2)c(C(=O)C)c1-c1ccccc1	328	OC12C(CCCCC1O)[C@]1(OC(=O)C)C2CCCCC1
302	O1c2c(OCC1C[NH+]1CCC3(N(CN(C(C)C)C)C3=O)c3ccccc3)CC1)cccc2	329	O=C1N2N(CCCCC2)C=C1
		330	O(C)c1cc2c3NCCN(c4c3c(nc2cc1)c([N+](=O)[O-])cc4)CC[NH+](C)C
303	S(=O)([O-])(=Nc1noc(c1)C)c1ccc(Nc2c3c([nH+]c4c2cccc4)c(ccc3)C(=O)Nc2ccc(NC(=O)C)cc2)cc1	331	Brc1cc(cc(Br)c1N)-c1sc2c(n1)cccc2
		332	O=C(NC1CCCCC1)c1ccc(N(Cc2nc3c(nc(nc3N)N)nc2)C)cc1
304	Oc1ccc(cc1)C=CC(C=C)(C)C	333	O(CC(\N=C\c1cccnc1)=NNC(=O)c1ccncc1)c1ccc(OC)cc1
305	O1c2c(cccc2)C(=C(Oc2ccccc2)C1=O)c1ccc(O)cc1		
306	O1c2c(C(=O)[C@H](C)C1C)c(O)cc1OC(CCc12)(C)C	334	[Si](O[C@H]([C@@H](NC(=O)c1ccccc1)c1ccccc1)C(OC(c1ccc(OC)cc1)c1ccc(OC)cc1)=O)(C(C)(C)C)(C)C
307	S1(OCCOS(=O)(=O)C1CN1C(=O)c2c(cccc2)C1=O)(=O)=O		
308	O1C[C@@H](NC1=O)COc1ccc(cc1)C=O	335	O=C1C=C2C=C(NC=C2C=C1[O-])C(OC)=O
309	S1C=2N(N=C1N)C(=O)c1c(N=2)cccc1	336	Oc1cc(ccc1O)C=C(C(=O)NCCCCCCCNC(=O)C(=Cc1cc(O)c(O)cc1)C#N)C#N
310	S1CC2OC(n3c4ncnc(N)c4nc3)C(O)C2(O)CC1		
		337	s1c2c(cc1C1(NC(=O)C)CCCCCC1)cccc2
311	Brc1cnc(Oc2ccc([N-]C(=O)NC(=O)c3ccccc3NC(=O)C[NH3+])cc2C)nc1	338	O(C(=O)C(=CC(OC)=O)c1c2-c(cc(ccc2C)C(C)C)c(c1)C)C
312	O=C1N=C(NC(=C1)C)NNC(C#N)c1ccc(N(C)C)cc1	339	OC1(C2C(C(C1)c1ccccc1)C(=O)c1c(NC2=O)cccc1)c1ccccc1
313	S1C(c2c([NH+]=C1N)n(nc2C)C(=O)Cc1ccccc1)c1cc(OC)ccc1	340	Oc1ccc(O)cc1CC=C(CCC=C(CCC=C(CCC=C(CCC=C(CCC=C(CCC=C(C)C)C)C)C)C)C)C
314	O=C(Nc1cc2c(cc1)cccc2)Nn1cnnc1		
315	O=C1N=C(Nc2nc[nH]c12)Nc1cc(CO)c(cc1)C	341	Clc1ccc(cc1)C=1N=C(c2n(C=1)c1c(n2)cccc1)C=Cc1sccc1
316	O=C1N(Cc2nnn(c2)COCCOC(=O)C)C(=O)N(C=C1C)C(=CC(OCC)=O)C(OCC)=O	342	S=C1N(CCC1c1c(c[nH]c1C([O-])=C[N+]#N)C(OCC)=O)CC
317	Clc1cc(NC=2OCCN=2)c(OC)cc1OC	343	S(=O)(=O)(N(N=CC(OC(=O)C)C(OC(=O)C)C(OC(=O)C)C(OC(=O)C)COC(=O)C)C(=O)C)c1ccc(cc1)C=C1NC(=O)NC1=O
318	O=C1N2[C@@H](Cc3c([nH]c4c3cccc4)C2CC(C)C)C(=O)NC1COC(C)(C)C		
319	O1c2c(cc3OCOc3c2)C(C(C)C1[NH+](C)CC)c1cccc(OC)c1OC	344	Fc1ccc(cc1)C1(OC(=O)c2c1cccc2)c1ccc(cc1O)C
320	s1nc(N2CCCC2)c(C(OCC)=O)c1Nc1ccccc1	345	S(=O)([C@@H]([C@@H](Nc1ccc(OC)cc1)C(F)(F)F)c1ccccc1)c1ccc(cc1)C
321	s1cc(c2c1cccc2)CC[NH+]1CCC2(N(CN	346	O=C1C(=O)N(C(=O)[C-]1C(=O)C)c1cccc(C)c1C

337

347	P1(OC(CN1C(C)(C)C)(C)C)(=O)C(CC)C=O	375	O=C1N(CC(=O)N2c3c(cccc3)[C@@H](CC2(C)C)C)C(=O)CC1
348	O=C1CCC2(CC1C(OC)=O)Cc1c(cccc1)C2=O	376	O=C1NC(C)=C(C(OCCC(C)C)=O)[C@H](N1)c1ccc(cc1)C
349	[nH]1cc(c2c1cccc2)-c1ncc(nc1)-c1c2c([nH]c1)cccc2	377	S=C(Nc1cc(F)ccc1)NCc1ncccc1
350	S1C=2N(N=C1SCc1ccccc1)C(=O)C=C(N=2)C	378	Clc1ccccc1C=NN1CCN(CC1)c1ccc(cc1)C
351	S1C23C(CC14N(CCc1c4[nH]c4c1cccc4)C2=O)CCCC3	379	O=C(N[C@H]1CCCC[C@H]1C)c1ccc([N+](=O)[O-])cc1
352	s1c2[n+](nc1N)c(n(n2)Cc1ccccc1)C	380	Clc1ccc2c(NC(C)=C(CN3CC[NH+](CC3)C)C2=O)c1C
353	O=C1c2cc(ccc2CC1Cc1ccccc1C(=O)[O-])C	381	S(=O)(=O)(Nc1ccccc1C#N)c1ccccc1
354	ClC=1C=CC2=NC3=NC(=O)NC(=C3C(NCC[NH2+]CCO)=C2C=1)C	382	O1CCN(CC1)c1ccccc1NC(=O)c1ccccc1
355	Oc1ccc(cc1)C[C@H](N=C1[C@@H]2C[C@@]([N+](=O)[O-])(C)[C@@]1(O)CCC2)C(OCC)=O	383	O=C1NC(C)=C(C(OC(C)C)=O)[C@@H](N1)c1ccccc1
356	O=C1N=C(N)C=CN1COCCOCc1cc(cc1C)C	384	O(C)c1ccc(cc1)C(=O)NNC1=Nc2c3c1cccc3ccc2
357	O=C1NC(=O)NC(\N=N\c2cc(C)c(cc2)C)=C1	385	O=C1N(N(C)C(C)=C1NC(OCc1ccccc1)=O)c1ccccc1
358	O=C(N(CCn1c(ncc1[N+](=O)[O-])C)C)CCCn1ccnc1[N+](=O)[O-]	386	O=C(N)C1CC[NH+](CC1)CCC(=O)Nc1cc2CCCc2cc1
359	O=C1N(c2cccc(C)c2C)C(=O)C2C1C1CC(CCC1c1c2[nH]c2c1cccc2)C(C)(C)C	387	O1C(=CC(=Cc2cc([N+](=O)[O-])ccc2)C1=O)c1ccccc1
360	S1C2N(c3c(C2=NN(C)C1=N)cccc3)C(=O)C	388	O1c2cc(ccc2OC1)C1[NH2+]CCc2c1cc(OC)c(OC)c2
361	s1ccc(c1-c1sccc1)-c1sccc1	389	Clc1ccc(cc1N)-c1oc2c(n1)cc(cc2)C
362	O=C1C=C2NC(=O)C(=CC=C[C@H](OC)[C@H](OC(=O)N)C(=C[C@@H](C)[C@@H](OC(=O)CC[NH+](C)C)[C@H](OC)C[C@@H](CC(=C1NCC=C)C2=O)C)C)C	390	S(Cc1ccc(cc1)C)c1nnc(n1N)-c1ccccc1
		391	O1CCN(CC1)C(=O)c1cc2c(cc1O)cccc2
363	O=C1c2c(CC1=Cc1ccccc1C(OC)=O)c1CCCc1cc2	392	O(CCC(C)C)c1ccc(cc1)[C@]1(NC(=O)NC1=O)C
		393	Brc1cc(OCC(Oc2ccccc2C)=O)ccc1
364	[I+](C=1C(=O)NC(=NC=1[O-])N)c1ccccc1	394	s1cccc1S(=O)(=O)N1c2c(CCC1)cccc2O
365	OC1(N=C(c2c(-n3c1ccc3)cccc2)c1ccccc1)CC	395	S\1c2c(N(CCO)/C/1=C\c1[n+](cccc1)C)cccc2
366	O=C(N)C=1NC(N=C2N(C=NC=12)Cc1ccccc1)(C)C	396	s1c2N(CN(Cc2c(C)c1C)CC=C)C(=O)c1ccccc1
367	O=C1CCC(N(C(=O)c2ccccc2)CCCC)c2c1[nH]c1c2cccc1	397	S1CC(=O)Nc2cc(ccc12)C(=O)N1CCOCC1
368	[n+]1(c2c(cccc2)c(N(C)C)cc1C)CCCCCCCCC[n+]1c2c(cccc2)c(N(C)C)cc1C	398	Clc1ccc([N+](=O)[O-])cc1N1C(=O)[C@H]2[C@H]([C@H]3O[C@@H]2C=C3)C1=O
		399	O1CC[C@@](CC1(C)C)(Cc1ccccc1)CCN1C(=O)CCC1=O
369	Fc1ccc(cc1)C(CC1OCCO1)C[NH+]1CC2(N(C)C(=O)N(C)C2=O)CC1	400	O=C(Nc1ccccc1)c1ccc(cc1)C
370	Clc1ccccc1C1=COc2c(ccc(F)c2)C1=O	401	S(=O)(=O)(NCc1ccc(cc1)C)c1cc(OC)c(OC)cc1
371	Clc1cc2N=C(N(C(=O)c2cc1)c1scc(n1)C)C	402	S(Cc1ccc(cc1)C(OC)=O)c1nncn1C
372	O(CC)c1ccc(N\C=C(/C#N)\c2[nH]c3c(n2)cccc3)cc1	403	O1CCC[C@H]1COC(=O)[C@@H]1CC=CC[C@H]1C(=O)Nc1ccccc1
373	Clc1c(cccc1Cl)\C=C(/C(=S)N)\C#N	404	O(C)c1cc(N2C(=O)CN=C2Nc2nc(cc(n2)C)C)ccc1OC
374	s1c2c(nc1NC(=O)\C=C\c1c3c(ccc1)ccc3)cccc2		

405	O=C1N2C(=Nc3c1cccc3)[C@@H](c1c(C2)cccc1)Cc1ccccc1
406	O=C(C)c1cc(NC(=O)\C(=C\c2ccc(cc2)C(C)C)\C#N)ccc1
407	O=C1NCCC[C@@H]1C(=O)NC[C@H](O)CO
408	O1c2n[nH]c(c2[C@H](C(C#N)=C1N)c1ccc(OC(C)C)cc1)C
409	O([C@H](C(=O)NN=C1CC[NH+](CC1)C)c1ccccc1)C
410	S=C(NC(=O)c1occc1)[N-]c1ccc(N(C)C)cc1
411	O(C[C@@H]1CCC=CC1)C[C@H](O)Cn1c2c(nc1CC)cccc2
412	Brc1cc(ccc1)[C@H]1SC[C@@H](N1)C(=O)[O-]
413	Clc1ccc(cc1)CSc1nc2c(cc1)cccc2
414	O(c1ccccc1C=CC(=O)[O-])c1ccccc1
415	O(CC)C(=O)Nc1ccccc1C(=O)N1CCCCC1
416	O=C(NC1CCCCC1)N1c2c(cc(cc2)C)[C@H](CC1(C)C)C
417	O(C)c1ccccc1C=CC(=O)Nc1cc(cc(c1)C)C
418	O(C(=C(C#N)C#N)c1ccccc1)C
419	O=C1c2c(cccc2)C(=O)C1=C(Nc1ccccc1C)C#N
420	o1c2c(nc1-c1cc(N)ccc1)cc(cc2)CC
421	O=C(N[C@@H](C(=O)N)C#N)C
422	o1cccc1C(O[C@H]1CCC[NH+](C1)C)=O
423	O(C)c1ccccc1C(=O)NC1CC([NH2+]C(C1)(C)C)(C)C
424	O=C1NC(C(C(OC)=O)=C(N1)C)c1cc([N+](=O)[O-])c([O-])cc1
425	[nH+]1c2c(n(CC[NH+](C)C)c1N)cccc2
426	ON=Cc1c(n(nc1C)-c1ccccc1)C
427	O(C)c1ccccc1Nc1c2cc(ccc2ncc1C(OC)=O)C
428	s1ccnc1NC(=O)c1cc(OC)cc(OC)c1
429	Clc1cccc(Cl)c1C1=CC(=O)N(C)C1CCCCC1
430	s1c(N=CC2C(=O)CCCC2=O)c(cc1C)C(OCC)=O
431	O=C1N2N=C(n3nc(cc3C)C)c3c(C2=Nc2c1cccc2)cccc3
432	O1[C@@]2(O)c3c(cccc3)C(=O)[C@]2(O)C(C(OCC)=O)=C1C
433	O(C)c1cc(ccc1OC)C=NNC(=O)c1n[nH]c2c1CCCC2
434	S=C1NC(=O)/C(/N1)=C\c1ccccc1OC
435	o1c(ccc1COc1cc2c(cc1)cccc2)C(=O)NN
436	s1cccc1[C@](O)(C(=O)NNc1ccc(cc1)C)c1ccccc1
437	Fc1cc(ccc1)C=1OC(=O)/C(/N=1)=C\c1c2c(ccc1)cccc2
438	O(C)c1cc(ccc1OC)C(=O)CC(=O)c1ccccc1O
439	Brc1ccc(cc1)C(=O)CSc1nc([nH]n1)CC
440	O1c2c(C=C(C(=O)Nc3ccccc3OC)C1=O)cc(OC)cc2
441	Brc1cc(C)c(OC(=O)c2cc(OC)ccc2)c(c1)C
442	S(=O)(=O)(N)c1cc2[C@@H]3[C@@H](CC=C3)[C@H](Nc2cc1)C(C)C
443	s1c2c(CC[C@@H](C2)C)c(C(OC)=O)c1NC(=O)COC
444	s1cccc1-c1[nH]nc2OC(N)=C(C#N)[C@@H](c12)c1ccccc1F
445	O=C(NN=CC(C)C)c1ccc(N(C)C)cc1
446	O(C)c1cc2c(cc1OC)CCN(C(=O)c1ccccc1)[C@H]2C
447	O(CC(=O)c1ccc(O)cc1O)c1cc2c(cc1)cccc2
448	S(=O)(=O)(N)c1ccc(cc1)CCNC(=S)Nc1ccccc1
449	S(C)C=1NC(=O)[C@@H](C(OC)=O)[C@H](C=1C#N)c1ccccc1C
450	FC(F)(F)COc1ccc(OCC(F)(F)F)cc1
451	O1c2c(ccc(OC(C(=O)NC3CCCCC3)C)c2)C(=CC1=O)C
452	s1c2cc(ccc2nc1NC(=O)c1occc1)C
453	Brc1ccc(N2C(=O)[C@H](NCc3occc3)CC2=O)cc1
454	S=C1NC(=O)C(OC2=NNC(=O)C=C2)=C(N1)C
455	Fc1ccc(NC(=O)[C@@H](Oc2ccccc2)CC)cc1[N+](=O)[O-]
456	Brc1cc2c(ncnc2N[C@H](C(C)C)C(=O)[O-])cc1
457	Brc1c(nc(nc1OC)N(C(=O)C)CC=C)C
458	S=C(Nc1cc(ccc1)C(OC)=O)NNC
459	Fc1cc(NC(=O)c2nccnc2)ccc1
460	N1c2c(N[C@@H](CC(C)=C)[C@@H]1CC(C)=C)cccc2
461	O=C(Nc1ccc(cc1)CCC)\C=C\C(=O)[O-]
462	O=C([O-])/C=C(\C=C\c1c2c([nH]c1)cccc2)/C
463	Clc1cc(Cl)ccc1O[C@@H](C(=O)NC1CCCC1)C
464	O(C)c1cc(ccc1OC)C=NN1CCN(CC1)c1ncccc1
465	O1C=C\C(=N/c2ccc(cc2C)C)\c2cc(ccc12)C
466	O=C1NC(=O)N(c2nc(n(c12)CCC(C)C)N(C)C)C

339

467	O(C)c1cc(ccc1OC)C(=O)NNC=1CC(CC(=O)C=1)(C)C	497	Clc1ccc(N2CC[NH+](CC2)C2C3CC4CC2CC(C3)C4)cc1
468	o1c2c(nc1-c1ccc(N)cc1)cc(cc2)CC	498	O(C)c1cc(OC)ccc1CN1CCN(CC1)C(=O)c1cccnc1
469	O(C(=O)CN1C(=O)c2c(cccc2)C1=O)c1ccccc1OC	499	Clc1cc(NS(=O)(=O)c2ccccc2C)cc(Cl)c1[O-]
470	O(C)c1ccc(cc1C)C[NH2+]C1C2CC3CC1CC(C2)C3	500	Clc1cc2sc(nc2cc1)NN
471	S=C1N[C@H](C=2CCc3c(cc(OC)cc3)C=2N1)c1ccc(F)cc1	501	Clc1cc2nccc(OC(=O)N3CCOCC3)c2cc1
472	Clc1c(cc(OCC(=O)Nc2sc(nn2)C)cc1C)C	502	Fc1cc(ccc1)CC[NH2+][C@@H]1CC(=O)N(C1=O)c1ccc(cc1)C
473	Clc1ccccc1[C@@H]1NC(=O)Cc2cc(OC)c(OC)cc12	503	S=C1NC(=O)/C(/N1)=C\c1ccc(cc1)CC
474	O(C)c1cc(OC)ccc1\C=N\CC1(CCCC1)c1ccccc1	504	Brc1ccc(cc1)-c1oc(SC)nn1
475	O=C(N)c1n(ncc1\N=C\c1ccc([N+](=O)[O-])cc1)C	505	S(CC(=O)c1ccc([N+](=O)[O-])cc1)c1oc(nn1)-c1ccncc1
476	S(=O)(=O)(N)c1ccc(NC(=O)C=C(C)C)cc1	506	Clc1cc(ccc1Cl)-c1nc(sc1)NC(=O)C1CC1
477	Fc1ccccc1CC(NC(=O)C)C(=O)[O-]	507	ClC(=CCSc1nc2N(C)C(=O)NC(=O)c2n1C)C
478	O(C)c1ccc(Nc2cc([nH+]c3c2cc(cc3)C(OC)=O)C)cc1	508	O1C[C@H]1CN1C(=O)c2c(cc3c(c2)C(=O)N(C[C@H]2OC2)C3=O)C1=O
479	[NH+]1(CCN(N=Cc2ccc(cc2)C)CC1)Cc1ccccc1	509	S1c2c(N=C(C[C@H]1c1ccc(OC)cc1)c1ccccc1)cccc2
480	O(CC(=O)NC(C)c1ccccc1)c1cc(C)c(cc1)C(C)C	510	S=C1NN=C(N1N=C(C)c1ccc(F)cc1)CC
481	O=C(NC1CCCCC1)N1c2c(cc(cc2)C)[C@@H](CC1(C)C)C	511	O=C1NC(C)=C(C(=O)C)C([C@H]1C#N)c1cc([N+](=O)[O-])ccc1
482	Clc1ccc(cc1)C(=O)Nc1cc2nc(oc2cc1)-c1ccccc1	512	O(CC(=O)Nc1cc(O)ccc1)c1ccc(cc1)C
483	O=C1N=C(NC(=C1)C)NCC[NH+](C)C	513	O=C(NC1(CCCC1)CCC)c1ccccc1
484	S(=O)(=O)(CC)c1cc(O)c(NC(=O)c2ccccc2)cc1	514	O=C1NC(=O)N(c2nc(n(c12)CCC(C)C)N1CC[NH2+]CC1)C
485	Clc1cc(NC(=O)COc2ccccc2C(C)(C)C)ccc1OC	515	Fc1cc2cc([nH]c2cc1)C(=O)N
486	O1c2c(C=C(C(Oc3ccccc3OCC)=O)C1=O)cccc2	516	S(C)C=1NC(=O)[C@H](C(OC)=O)[C@@H](C=1C#N)c1ccccc1OC
487	S(=O)(=O)(Nc1ccc(cc1)C(OC)=O)\C=C\c1ccccc1	517	O(C)c1ccc(cc1)C=1C(C#N)=C(n2c(nc3c2cccc3)C=1C#N)N
488	O=C1C[C@@]2(CC[C@@]1(C)C2(C)C)C(=O)NCC	518	o1c2cc(ccc2nc1-c1cc(N)cc(N)c1)C
489	O(CC(=O)Nc1ccc(OC(C)C)cc1)c1ccccc1[N+](=O)[O-]	519	Fc1ccc(cc1)-c1c2C[C@H](CCc2nc(N)c1C#N)C
490	Clc1ccc(cc1)C(=NNC(=O)COc1ccc(cc1)C)C	520	O1C=C\C(=N/c2ccccc2)\c2cc(ccc12)C
491	FC(F)(F)c1nc2c(n1CC(OCC)=O)cccc2	521	O=C1N(C)C(=NN=C1)NCC[NH+](C)C
492	FC1=CN(CCC(=O)[O-])C(=O)NC1=O	522	Clc1ccc(S(=O)(=O)Nc2ccccc2CO)cc1
493	S(CC(=O)Nc1c2c(ccc1)cccc2)c1n2c(nn1)C=CC=C2	523	Clc1ccc(cc1)C=NN1C(=O)c2c(cccc2)C1=O
494	S=C(Nc1cc(cc(c1)C)C)N	524	[nH]1c2c(cccc2)c(-c2c3c(ncc2)cccc3)c1C
495	Clc1ccccc1[C@H]1NC(=O)N(C)C(C)=C1C(OCC)=O	525	O(C)c1ccccc1-n1cnc(N)c1C(OC)=O
496	S(=O)(CCC(=O)[O-])c1ccccc1C(=O)[O-]	526	Clc1ccc(NC(=O)CCC(=O)Nc2ccc(Cl)cc2)cc1
		527	[nH]1nc(C)c(-c2c(n[nH]c2C)C)c1C
		528	Clc1cc(ccc1)C=NNC(=O)c1nc2n(n1)C(=CC(=N2)C)C
		529	O=C(NN=C(C)c1cc(N)ccc1)c1cc([N+](=O)[O-])ccc1
		530	S=C(NC(=O)c1ccccc1)[N-

	]c1ccccc1C(=O)N
531	Brc1cc(ccc1OC)C[NH2+]Cc1ccccc1OC
532	Clc1cc(NC(=O)c2nsnc2)c(OC)cc1OC
533	Clc1ccccc1NCN1C(=O)[C@H]2[C@@H](CC=CC2)C1=O
534	Clc1ccccc1-c1nnc(SCc2ccccc2F)n1N
535	s1c2C[C@@H](CCc2c2c1N=CN(CC(=O)N(CC)CC)C2=O)C
536	Clc1cc(NC(=O)\C(=C\c2oc(cc2)C)\C#N)ccc1
537	Clc1cc(cc(Cl)c1)C(=O)Nc1sc2c(n1)c(cc2)C
538	O(C(=O)c1nc(NC[C@@H](O)C)c2c(n1)cccc2)CC
539	o1c(ccc1C)[C@H]1NC(=O)NC(C)=C1C(OC(C)C)=O
540	Clc1ccc(S(=O)(=O)Nc2cc(ccc2)CC)cc1
541	s1c(C(OCC)=O)c(nc1NC(=O)C=Cc1occc1)C
542	O(CC)c1ccc(N2C(=O)[C@H]3[C@H]([C@@H]4C=C[C@H]3C4)C2=O)cc1
543	s1cc(c2c1N=CN([C@@H](C(=O)[O-])C)C2=O)-c1ccccc1
544	s1c2N=CNC(=O)c2c(C)c1C(OCc1cccc1)=O
545	Clc1cc(Cl)ccc1OCC(=O)Nc1nn(nn1)CC
546	Clc1cc(-c2onc(n2)-c2ccccc2C)c(OC)cc1
547	s1c(nnc1Nc1ccc(cc1)C(=O)C)-c1ccncc1
548	O(C)c1ccccc1NCC(=O)NN=C1CCCC1
549	Fc1cc2c(N(C=C(C(=O)[O-])C2=O)C2CC2)c(OC)c1N1C[C@H]([NH2+]CC1)C
550	O(C)c1cc(OC)c(O)cc1C=C[N+](=O)[O-]
551	S=C(NC(=O)c1c(OC)cccc1OC)[N-]c1ccccc1
552	Fc1cc(F)ccc1NC(=O)NCc1cccnc1
553	S=C(NC(=O)CCC)[N-]c1ccc(cc1)-c1oc2cccnc2n1
554	O(C(=O)/C(=C/c1c2c(n(c1)C)cccc2)/C#N)C
555	Clc1cc(ccc1Cl)C(=O)Nc1c2c(nccc2)ccc1
556	O=C1Nc2c(N[C@H]1CC(=O)Nc1c3c(ccc1)cccc3)cccc2
557	S(=O)(=O)(Nc1ccc(cc1)C(=O)Nc1ccccc1C)C
558	Clc1cc(Cl)ccc1COc1ccc(cc1)C(=O)CC
559	Brc1ccc(SCC(=O)N2CCC(CC2)C)cc1
560	O(C(C)C)c1ccccc1C=NNC(=O)c1cc(NC(=O)C)ccc1
561	O(C)c1ccc(OC)cc1C=NNC(=O)c1cc(NC(=O)C)ccc1

562	Clc1cccc(NC(=S)Nc2ccc(N(CC)CC)cc2)c1C
563	S=C(Nc1cc(ccc1)C(=O)C)N(Cc1cn(nc1C)CC)C
564	o1c(ccc1C)C=C(C#N)c1ccc(cc1)C
565	O=C(Nc1cc(ccc1C)C)C=Cc1ccc(cc1)C
566	o1cccc1C(=O)Nc1cc(NC(=O)CCC)c(OC)cc1
567	S(Cc1ccc(cc1)C(=O)NC1CCCC1)c1ccc(cc1)C
568	Clc1c2nc(sc2ccc1)NC(=O)c1oc2c(c1)cccc2
569	Clc1ccccc1-c1oc(nn1)C
570	s1c(N2C(=O)[C@H]3[C@H]([C@@H]4C=C[C@H]3C4)C2=O)c(cc1C)C(OCC)=O
571	S(=O)(=O)(Nc1ccccc1C(=O)N)c1ccc(cc1)C
572	Clc1ccccc1OCC(=O)NN=Cc1ccccc1OC
573	O1CCN(CC1)c1ccc(NC(=O)CC(C)C)cc1
574	O(CC(=O)NC(C)(C)C)c1ccc(cc1C)C
575	O1CCC[C@H]1CNc1nc(nc2c1cccc2)Nc1cc(cc(c1)C)C
576	O(C(=O)[C@@H](C(=O)Nc1ncccn1)C1CCCCC1)C
577	O1c2cc(C=C(C#N)c3ccc(cc3)C)c(OC)cc2OC1
578	Clc1cc2nc(sc2cc1OC)NC(=O)c1ccc(cc1)CC
579	S=C(NC(=O)c1ccc(cc1C)C)[N-]c1ccccc1
580	O=C/1N(c2c(cccc2)\C\1=C/c1cc([nH]c1C)C)c1ccccc1
581	S=C(NC1CC1)NCc1cc(OC)ccc1
582	s1c2N3C(=NNC3=S)N(CC=C)C(=O)c2c(C)c1C
583	S(=O)(=O)(N1CCCCC1)c1c2c(ccc1)ccc2
584	Fc1ccccc1[C@@H]1Nc2c(cccc2)C(=O)N1Cc1occc1
585	Clc1cc(ccc1Cl)CN(S(=O)(=O)C)c1ccccc1
586	O=Cc1c2c(n(c1)CC(=O)N1CCc3c(C1)cccc3)cccc2
587	s1cccc1C(=O)Nc1cc2nc(oc2cc1)-c1cc(C)c(cc1)C
588	Fc1ccc(cc1)CNC(=O)[C@H](Oc1ccccc1)CC
589	O1CCC[C@@H]1[C@@H](NC(=O)Nc1ccc(cc1)C(OCC)=O)C
590	s1c2cc(OC)ccc2nc1NC(=O)c1ccc(cc1C)C
591	S=C(NC(=O)C(C)(C)C)[N-]c1ccc(cc1)-

341

	c1oc(cc1)CO		cc1
592	Fc1cc(NC(=O)Nc2ccc(OCC)cc2)ccc1C	622	Clc1ccccc1C(=O)Nc1cc(NC(=O)C(C)C)ccc1
593	FC(F)C=1n2ncc(c2N=C(C=1)C)C(=O)Nc1ccc(cc1C)C	623	O=C(N)c1cc(N)c(N2CCC(CC2)C)cc1
594	O(C)c1ccc(cc1)CC(=O)NN=Cc1cccnc1	624	s1c2cc(NC(=O)C)ccc2nc1NC(=O)c1ccc(cc1)CC
595	o1cccc1C(=O)Nc1c2c(ccc1)C(=O)N(C2=O)c1ccccc1	625	Clc1cc([N-]C(=S)NC(=O)c2ccc(cc2C)C)ccc1
596	S(CC(=O)Nc1ccc(F)cc1)c1nc(c2CCCCc2n1)C	626	Clc1cccc(NC(=O)CCC)c1N1CCOCC1
597	S=C(NC1C2CC3CC1CC(C2)C3)NC(=O)c1cc(OC)ccc1	627	Clc1cccc(F)c1CC(=O)Nc1cc(Cl)c(Cl)cc1
598	O1C([O-])=C(CC=2C(=O)C=C(OC=2O)C)C(=O)C=C1C	628	o1cccc1CNC(=O)[C@H](C#N)c1ccccc1
599	s1c2CCCCc2nc1NC(=O)CSCc1ccccc1	629	o1c(C)c(cc1C)C=C(C#N)C#N
600	Clc1ccc(Cl)cc1C(=O)Nc1ccc(cc1)C(=O)N	630	O=C(NN=Cc1ccc(cc1)C#N)CNc1ccc(c1C)C
601	Clc1ccc(cc1)C(=O)NNC(=O)c1ccc(OCC(C)C)cc1	631	o1c(ccc1C)C(=O)C[C@@]1(O)c2c(N(CCC)C1=O)cccc2
602	o1cccc1\C=C\C(=O)Nc1cc(ccc1OC)C	632	Clc1cc(ccc1C(=O)NNC(=O)c1ccncc1)C
603	S=C(NC1CCCC1)N[C@@H](C)c1cc(OC)c(OC)cc1	633	Fc1ccc([N+](=O)[O-])cc1NC(=O)c1ccc(cc1)-c1ccccc1
604	O=C(Nc1cc(NC(=O)CC)ccc1)c1cccc([N+](=O)[O-])c1C	634	S1C(=Cc2cccnc2)C(=O)N=C1Nc1ccccc1C
605	Clc1cc(Cl)ccc1COc1ccc(cc1OCC)C[NH3+]	635	Clc1ccc(cc1)C(=O)Nc1ccc(N)cc1OC
606	Clc1cc(C)c(S(=O)(=O)N2C[C@H](CCC2)C)cc1C	636	Clc1cc(ccc1Cl)C(OCc1cc(ccc1)C(OC)=O)=O
607	O(CC(=O)N1CCCC1)c1c2c(ccc1)cccc2	637	s1cccc1S(=O)(=O)NC(=S)NC1CCCCC1
608	S(Cc1ccc(cc1)C(C)(C)C)c1nnnn1C1CCCCC1	638	O=C/1N(c2c(cccc2)\C\1=C/c1ccc(N(C)C)cc1)c1ccccc1
609	O=C(NN=Cc1ccc(N(CC)CC)cc1)Cn1cc[nH+]c1C	639	O(CC(=O)NN=Cc1cc(ccc1)C)c1cc2c(c1)cccc2
610	O=C(NN=Cc1cc(ccc1)C)c1ccccc1C(=O)[O-]	640	O(CC)C(=O)/C(=C/c1cc2c(cc1)cccc2)/C#N
611	S(Cc1oc2c(cc(OC)cc2)c1C(OCC)=O)c1ccccc1	641	S(Cc1ccccc1C)CC(=O)[O-]
612	O(C)c1ccccc1CNc1nc2c(n1C(C)C)cccc2	642	S(=O)(=O)(N1CCC(CC1)C(=O)NN)c1c(cc(cc1C)C)C
613	n1cnc2n(ncc2c1NCc1ccccc1)-c1cc(ccc1)C	643	S=C1NC(C(C(=O)C)=C(N1)C)c1cc(OC)c(O)cc1
614	O=C(NCC(C)C)C=Cc1ccc(cc1)C	644	O=C(NC(C)c1[nH]c2c(n1)cccc2)C1CC1
615	o1c(ccc1COc1ccc(cc1)CCC)C(OC)=O	645	S(C)c1nnc(n1C)COc1c2nc(ccc2ccc1)C
616	O(C)c1ccc(cc1)[C@H](NC(=O)[C@H](C)c1ccccc1)C	646	S=C(NCc1ncccc1)NCCc1cc(OC)c(OC)cc1
617	s1c2c(nc1NC(=O)c1oc([N+](=O)[O-])cc1)c(OC)cc(OC)c2	647	Clc1cc(Cl)ccc1NC(=O)Nc1nccc(c1)C
618	S(CC(=O)Nc1ccccc1C)CC(=O)Nc1ccc(cc1)CC	648	S1c2n(N=C1c1ccc(NC(=O)Cc3ccccc3)cc1)c(nn2)C
619	Clc1ccc([N-]C(=S)NC(=O)c2cc(ccc2)C)cc1C(=O)[O-]	649	S(CC(=O)NC1CCCC1)c1nnc(n1C)C1CCCC1
620	O=C(CC(=O)Nc1ccc(N(C)C)cc1)C	650	Fc1ccccc1C(=O)N(CC1=Cc2cc(ccc2NC1=O)C)CC
621	O([C@H](CC)C(=O)Nc1ccccc1C)c1ccc	651	O=C1N(C)C(=O)N(c2n(cnc12)CC(=O)Nc1nccc(c1)C)C
		652	S(CC(=O)NC(C)C)c1nnc(n1C1CCCCC

	1)C
653	O(Cc1ccccc1)c1ccc(NC(=O)Nc2ccc(OC)cc2)cc1
654	s1c2c(nc1SCC(=O)N(CC)c1ccccc1)cccc2
655	Brc1ccc(NC(=O)c2noc(c2)-c2ccccc2)cc1
656	Brc1cc(NC(=O)CC)ccc1OC
657	o1cccc1\C=C\C(=O)Nc1cc(ccc1)C
658	Clc1ccc(cc1)C=[N+]([O-])c1ccc(cc1)C
659	S=C(Nc1cc(ccc1)C)NNC(=S)NCc1ccccc1
660	Fc1cc2c3N([C@H](CCc3c1)C)C(O)=C(C(=O)NCC[NH+](C)C)C2=O
661	O(CC(=O)Nc1cccc(C)c1C)c1c(cccc1C)C
662	Clc1ccccc1NC(=O)[C@@H](Oc1cc(Cl)ccc1)C
663	Fc1ccc(cc1)\C=N\c1ccc(cc1)C(=O)[O-]
664	O(CC)c1ccccc1C=NNC(=O)c1cc(NC(=O)C)ccc1
665	O(C)c1cc(OC)c([N+](=O)[O-])cc1\C=C(/C#N)\c1ccc(cc1)C#N
666	S(=O)(=O)(Nc1cc(O)c(cc1)C(=O)[O-])c1ccc(F)cc1
667	O(C)c1ccccc1NCC(=O)NN=Cc1cc(OC)c(OC)cc1
668	O=C(C)c1cc(NC(=O)Nc2cn(nc2C(=O)N)CC)ccc1
669	Clc1ccccc1OCC(=O)NN=Cc1cc(OC)ccc1
670	Clc1cc(Cl)ccc1C(=O)Nc1ccc(N)cc1C
671	o1c(C)c(cc1C(OC)=O)CC(=O)c1c(O)cc(O)cc1O
672	s1c2CCCCc2c2c1nc(SC)nc2N1CCCC1
673	O(C)c1c(OC)c(OC)ccc1C=CC(=O)N1CCC1
674	Clc1cc2NC(=O)/C(/c2cc1)=C/c1cc(n(c1C)-c1ccccc1)C
675	Clc1ccc(OCC(=O)NN=Cc2cc(O)c(OC)cc2)cc1
676	Clc1ccccc1C=CC(=O)N1CCN(CC1)c1ccccc1
677	Fc1ccc(cc1)COc1cc(ccc1)C[NH2+]C1CCC1
678	S(=O)(=O)(n1c2cc(C)c(cc2nc1)C)N1CCOCC1
679	O=C1N(C)C(=O)N(c2n(cnc12)CC(=O)NC1CCCCC1)C
680	Clc1cccc(F)c1COc1ccc(NC(=O)C)cc1
681	O(CC(=O)NNC(=O)c1n[nH]c(c1)C)c1cc(ccc1)C
682	n1c2c(n([C@@H](CC)C)c1CC)cccc2
683	Brc1ccc(cc1)C[NH2+]CC(C)C
684	Fc1cc(F)ccc1\N=C\c1cc(oc1C)C
685	S(=O)(=O)(N1CCCCC1)c1ccc(\N=C\c2oc(cc2)C)cc1
686	s1cccc1CC(=O)NN=Cc1cc(OC)c(OC)cc1
687	O=C(Nc1ccc(cc1)C)C(=Cc1ccc(cc1)C#N)C#N
688	O(C(=O)c1ccccc1)c1ccc(cc1)-c1nc2n(c1)C=CC=C2
689	O1c2cc(\C=C(/C#N)\c3ccc(cc3)C)c(OC)cc2OC1
690	s1c(ccc1C)C=NNC(=O)CNc1ccccc1C
691	s1cccc1-c1n(C(C)C)c(cc1)CCC(=O)[O-]
692	O1c2cc(C=NNC(=O)c3cccnc3)c([N+](=O)[O-])cc2OC1
693	S(CC(=O)Nc1cc(F)ccc1)c1ccccc1
694	Clc1cccc(F)c1Cn1c2c(nc1C(O)C)cccc2
695	Clc1cc(ccc1C(=O)N1CCN(CC1)c1cc(Cl)ccc1)C
696	O=C1CC(Cc2nc(ncc12)NC(=O)Nc1cccc1)(C)C
697	Clc1cc(C(=O)Nc2ccccc2C)c(O)cc1
698	Brc1ccc(OCC(=O)N2CCc3c2cccc3)cc1C
699	Clc1ccc(Cl)cc1C(=O)Nc1ccccc1C(F)(F)F
700	S(=O)([O-])(=Nc1cc(ccc1)C(=O)C)c1cc(ccc1OC)C
701	Clc1ccc(Cl)cc1C(=O)NC
702	O(C)c1c2c(C[C@H]3N(C2)CCc2cc(OC)c(OC)cc23)ccc1OC
703	Brc1ccc(OCC(=O)N2CCN(CC2)C=O)cc1C
704	Brc1c2c(ccc1)c(ccc2)C(=O)[N-]c1cnn(nn1)CC
705	Clc1cc2nc(sc2cc1OC)NC(=O)c1sccc1
706	S(\C(=C\c1ccc(OCC(C)C)cc1)\C(=O)[O-])c1nc([nH]n1)C
707	s1c2nc(nc(N[C@H]([C@H](CC)C)C(=O)[O-])c2cc1CC)C
708	Clc1ccc(cc1NC(=O)Cc1ccc(cc1)C)C(F)(F)F
709	Clc1ccc(Cl)cc1\N=C\c1ccc(F)cc1
710	Clc1ccc(Cl)cc1-c1onc(n1)-c1ccc(cc1)C
711	n1c2c(n(CC)c1-c1ccc(cc1)C)cccc2
712	S=C(NC[C@@H]1OCCC1)N[C@H](C)c1cc(OC)ccc1OC
713	S=C(Nc1cc(OC)c(OC)cc1)NCCc1ccc(F)cc1
714	s1cccc1C=NNC(=O)c1ccccc1C
715	Fc1ccccc1CNC(=O)Nc1cc2OCOc2cc1

716	Clc1ccccc1OCC(=O)NN=Cc1cc(OC)c(OC)cc1	746	Brc1ccc(-n2c3CC(CC(=O)c3cc2C)(C)C)cc1
717	S=C(NC1C2CC3CC1CC(C2)C3)NC(=O)c1ccc(cc1C)C	747	O(C)c1ccccc1NCC(=O)NN=Cc1cc2c(cc1)cccc2
718	Oc1ccc(\N=C\c2n(ccc2)-c2cc3c(cc2)cccc3)cc1	748	S(=O)(=O)(N1[C@@H](CCC1=O)C(=O)N)c1ccc(cc1)C
719	Brc1ccc(NC(=O)CC2(CCCC2)CC(=O)[O-])cc1	749	O(Cc1c2c(ccc1)cccc2)c1ccc(cc1OC)C=NNC(=O)N
720	s1ccc(C)c1CNc1cc2OCOc2cc1	750	s1cccc1CC(=O)NN=C(Cc1ccc(OC)cc1)C
721	O[C@@H](C)c1nc2c(n1Cc1ccc(cc1)C(C)C)cccc2	751	S(Cc1ccc(cc1)C#N)c1nnc(n1CC)-c1ccncc1
722	FC(F)(F)[C@]1(O)N(N=C(C1)CC)C(=O)[C@H](O)c1ccccc1	752	Clc1ccc(OCC(=O)c2cc3CCCCc3cc2)cc1
723	Fc1c(Oc2cc(O)ccc2)c(F)c(F)nc1N1CCCCC1	753	s1c2cc(NC(=O)C)ccc2nc1[N-]C(=S)NC(=O)CCC
724	O=C(Nc1c(cc(cc1C)C)C)\C=C\c1ccccc1	754	O=C(NN=C1CCCC1)CNc1ccccc1C
725	O=C(Nc1c2ncccc2ccc1)c1ccc(cc1)C	755	ClC=1C[C@@H]2[C@@H](CC=1)C(=O)N(c1[nH]ncc1)C2=O
726	n1c2cc(\N=C\c3ccccc3)ccc2n(c1)C1CCCC1	756	O=C([O-])c1cc(N2Cc3cc(C)c(cc3C2)C)ccc1
727	s1c(nnc1SCC(=O)NCc1ccc(cc1)C)NC(=O)C	757	O(CC(=O)N)c1ccc(cc1)C=NNC(=O)c1cc(N(C)C)ccc1
728	S(=O)(=O)(N[C@@H](C(=O)NCc1ccccc1OC)C)c1ccccc1	758	S1c2n(ncn2)C(=O)[C@@H]1CC(=O)Nc1ccc(OC)cc1
729	Fc1cc2c3ncnc(N4CC[NH+](CC4)CCO)c3[nH]c2cc1	759	O(C(C)C)c1ccc(cc1)C(=O)Nc1ccc(NC(=O)CC)cc1
730	S=C1NN=C(N1N=Cc1ccc(OC)cc1)c1ncccc1	760	O(C)c1c(OC)c(OC)ccc1C=CC(=O)Nc1cc(ccc1C)C
731	O(CC(=O)Nc1c(cc(cc1C)C)C)c1ccc(cc1)-c1ccccc1	761	FC(F)Oc1ccccc1NC(=O)c1ccc(cc1)-c1ccccc1
732	Clc1cc(ccc1)C(=O)Nc1ccc(N2CC[NH+](CC2)C)cc1	762	Clc1ccccc1C=CC(=O)N1CCC(CC1)C(OCC)=O
733	O=C(Cn1cc(c2c1cccc2)C=O)c1cc([N+](=O)[O-])ccc1	763	S([C@H](C(=O)N1CCN(CC1)c1ccccc1)C)c1ccc(cc1)C
734	S(C(=Cc1cc(O)c(OC)cc1)C(=O)[O-])c1nc([nH]n1)C	764	Clc1cc2c(OC(=O)C=C2C)cc1OCc1cc(cc(c1)C)C
735	O1[C@H](CN(C[C@@H]1C)C(=O)Nc1ccc(cc1)C(OCC)=O)C	765	o1c(C)c(cc1C)\C=C(/C#N)\c1ccccc1
736	O(CC(=O)NC(C)(C)C)c1ccc(cc1)CNc1nn[nH]n1	766	s1cccc1C(=NNC(=O)CSc1nc2c(n1C)ccc2)C
737	Brc1ccc(OCC(=O)Nc2ccc(cc2)CC)cc1C	767	Clc1cc(N2C(c3cc(OCC)ccc3NC2=O)=C)ccc1
738	O1CCOc2c1cc(NC(=O)[C@H](Oc1cccc1)CC)cc2	768	S=C(Nc1ccc(cc1)[C@H](CC)C)[N-]c1cn(nc1C(=O)N)CC
739	O[C@@H](Cn1c2CCCCc2c2cc(ccc12)C)C[NH2+]Cc1ccccc1	769	O1c2cc(ccc2OC1)C(=O)Nc1c2c3c(CCc3ccc2)cc1
740	s1ccc(NC(=O)Nc2cc(OC)c(OC)cc2)c1C(OC)=O	770	S(=O)(=O)(N1CCCC1)c1ccc(NC(=O)c2ccccc2)cc1
741	Fc1cccc(F)c1NC(=O)\C=C\c1occc1	771	O=C(Nc1ccccc1[C@@H](CC)C)c1cc(cc(c1)C)C
742	s1c(nnc1SCC(=O)Nc1cc(ccc1F)C)C	772	O(C)c1cc2c(nc(nc2C)NC=2NC(=O)[C@@H](N=2)CC(=O)[O-])cc1
743	s1ccc(C)c1C=NN1C(=NNC1=S)c1cc(OC)ccc1	773	O1C(C)=C(C(=O)Nc2ccc(OCC)cc2)C(=CC1=O)C
744	o1cccc1\C=C\C(=O)Nc1ccc(cc1)CC		
745	s1c2C[C@@H](CCc2c2c1NC(NC2=O)c1ccc(OC)cc1)C	774	Fc1ccc(cc1)-

344

	c1n(CC(C)C)c(cc1)CCC(=O)[O-]
775	O(C(=O)\C=C\c1ccccc1)c1cc(C)c(cc1)C
776	s1nc2c(n1)cccc2NC(=O)c1c(noc1C)-c1ccccc1
777	O1CCC[C@H]1CNC(=O)c1cc(NC(=O)C(CC)CC)ccc1
778	o1c(nc(C#N)c1N1CCCCC1)-c1ccc(cc1)C
779	S=C(NC(=O)C=Cc1ccc(OC)cc1)[N-]c1ccc(cc1O)C
780	Clc1cc(O[C@H](C(=O)NCCc2ccccc2)C)ccc1
781	S=C(Nc1ccc(N(CC)CC)cc1)NCc1ccc(F)cc1
782	O1C=C(CCC1)C[NH+]1CC2=C(NC(=NC2=O)N)CC1
783	Clc1sc(cn1)CN1CCc2nc(ncc2C1)-c1ccccc1
784	Brc1cncc([N+](=O)[O-])c1NC(C)C
785	S(C)C1=NC(=O)C2=C(N1)CCN(C2)Cc1cc(C)c(F)nc1
786	O=C1N=C(NC2=C1CN(CC2)Cc1[nH]c(cn1)C)C
787	O(CC)c1cc(ccc1)-c1ncc(cc1)CN1CC2=C(NC(=NC2=O)C2CCCCC2)CC1
788	O(CC(O)C[NH2+]C(C)C)c1ccc(cc1OC)C[NH2+]C(C)(C)C
789	O(C)c1cc(ccc1OC)-c1nn(c2ncnc(N)c12)C[C@@H](CO)C
790	[NH+]1(CCc2nc(ncc2C1)-c1ccc(N)cc1)Cc1n(ccc1)-c1cc(ccc1)C#N
791	O=C1N=C(NC2=C1C[NH+](CC2)Cc1ccc(C)c1C)C1=NCCCC1
792	Clc1cc(ccc1Cl)Cn1cccc1CN1CC2=C(NC(=NC2=O)C(C)(C)C)CC1
793	s1c2ncccc2c(-c2cc(F)ccc2)c1S(=O)(=O)c1cc(F)c(OC)cc1
794	O1c2c(cccc2)C(=O)C(CN2CCc3nc(ncc3C2)C)=C1N
795	O=C1N=C(NC2=C1CN(CC2)Cc1cnn(c1C)-c1ccccc1C)c1ccncc1
796	S(C)C1=NC(=O)C2=C(N1)CC[NH+](C2)Cc1c2cc(ccc2nc2c1cccc2)C
797	O(C)c1n(nc(C)c1CN1CCc2nc(ncc2C1)C1CC1)C
798	Clc1ccc(Cl)cc1-c1oc(cc1)CN1CC2=C(NC(=NC2=O)C(C)C)CC1
799	S(C)C1=NC(=O)C2=C(N1)CCN(C2)Cc1c(n[nH]c1C)C
800	FC(F)(F)c1ccc(cc1)-

	c1nc2CC[NH+](Cc2cn1)Cc1c2c([nH]c1)cccc2OCc1ccccc1
801	O=C([O-])C[C@H](C[C@H]([NH3+])C(=O)[O-])C(=O)[O-]
802	Clc1cc2c(OC(N)=C(CN3CCc4nc(ncc4C3)-c3ccc(cc3)C(F)(F)F)C2=O)cc1
803	Brc1cc(cnc1)C[NH+]1CC2=C(NC(=S)NC2=O)CC1
804	Clc1ccc(cc1)-c1nc(ccc1)CN1CC2=C(NC(=S)N=C2)CC1
805	O=C1N=C(NC2=C1CN(CC2)Cc1cccnc1NC(=O)C(C)(C)C)C1CC1
806	O(CC1CCN(C1)C(OC(C)(C)C)=O)c1cc(N(C)C)ccc1
807	s1cccc1-c1ncc(cc1)C[NH+]1CCc2nc(ncc2C1)-c1ccncc1
808	Clc1ccccc1-c1ncc(cc1)C[NH+]1CCc2nc(ncc2C1)-c1cccnc1
809	Brc1nc(ccc1)CN1CCc2nc(SC)ncc2C1
810	Clc1sc(cc1)CN1CCc2nc(ncc2C1)N
811	Clc1cccc(C)c1C[NH+]1C[C@@H](O)CCC1
812	O=C1N=C(NC2=C1C[NH+](CC2)Cc1[nH]c(cc1C)C)CCC
813	Clc1ccc(cc1-c1nc(Cl)ncc1)C(=O)C
814	Fc1ccc(cc1)C(OC(=O)c1ccc([N+](=O)[O-])cc1)C(=O)NCC(OCC)=O
815	S(=O)(=O)(C)C1=NC(=O)C2=C(N1)CCN(C2)Cc1n(nc(c1)C)C
816	O1CC(=Cc2c1cccc2)CN1CC2=C(NC(=NC2=O)c2ccccc2)CC1
817	Brc1cc(cc(Br)c1)-c1ncc(cc1)CN1CC2=C(NC(=NC2=O)C(C)C)CC1
818	Clc1cc(Cl)ccc1-c1oc(cc1)CN1CC2=C(NC(=NC2=O)c2ccccc2)CC1
819	O1CC[NH+](CC1)C1CCN(CC1)c1ccc(nc1)NC1=CC(=CN(C)C1=O)c1cccc(NC(=O)c2ccc(cc2)C(C)(C)C)c1C
820	Brc1c2c(sc1C[NH+]1CCc3nc(ncc3C1)-c1cccnc1)cccc2
821	FC(F)(F)c1ccc(cc1)C1=NC(=O)C2=C(N1)CCN(C2)Cc1nccnc1
822	s1cnc(C)c1C[NH+]1CCc2nc(ncc2C1)-c1ccc(cc1)C(F)(F)F
823	Fc1cc(F)ccc1-c1ncc(cc1)C[NH+]1CCc2nc(ncc2C1)N
824	Clc1ncc(Cl)cc1CN1CC2=C(NC(=NC2=O)CCC)CC1
825	Brc1cc2c([nH]cc2CN2CC3=C(NC(=NC

	3=O)C3=NCCCC3)CC2)cc1
826	S(=O)(=O)([O-])c1oc(cc1)CN1CCc2nc(ncc2C1)-c1cncnc1
827	o1c(ccc1C)-c1nn(cc1CN1CC2=C(NC(=NC2=O)c2cc(N)cc2)CC1)-c1ccccc1
828	Brc1oc(cc1)CN1CC2=C(NC(=NC2=O)c2sccc2)CC1
829	o1nc(cc1-c1ccccc1)CN1CCc2nc(ncc2C1)C1CCCCC1
830	O(C)c1ccc(cc1)-c1nc(ccc1)CN1CC2=C(NC(=NC2=O)C2CC2)CC1
831	Fc1ccc(-n2nc(C)c(c2)C[NH+]2CCc3nc(ncc3C2)C2=NCCCC2)cc1
832	Oc1c2nc(ccc2ccc1)CN1CC2=C(NC(=NC2=O)c2cncnc2)CC1
833	S(c1oc(cc1)CN1CCc2nc(ncc2C1)C(F)(F)F)c1[nH]c2c(n1)cccc2
834	o1c(ccc1C[NH+]1CCc2nc(ncc2C1)-c1ccncc1)C1CC1C
835	s1cc(cc1)-c1oc(cc1)CN1CCc2nc(ncc2C1)C(C)C
836	s1cccc1-c1nc2CC[NH+](Cc2cn1)Cc1ccc(nc1)-c1cc(OC)c(OC)cc1
837	Clc1nc([nH]c1CN1CC2=C(NC(=NC2=O)c2ccc(Cl)cc2)CC1)CCCC
838	s1c(cnc1N)CN1CC2=C(NC(=NC2=O)c2cncnc2)CC1
839	O1c2cc(OC)ccc2C[C@H](O)C1c1cc([N+](=O)[O-])ccc1
840	ClC=1c2cc(Cl)ccc2OC(=O)C=1CN1CC2=C(NC(=NC2=O)c2ccc(cc2)C(F)(F)F)CC1
841	FC(F)(F)c1cc(ccc1)CNC(=O)C(=Cc1cc(O)c(O)cc1)C#N
842	FC(F)(F)c1ccc(cc1)-c1nc2CC[NH+](Cc2cn1)Cc1c2cc(OC)ccc2n(c1)C
843	OC1CCC[NH+](C1)Cc1cccc(C)c1C
844	S(c1oc(cc1)CN1CCc2nc(ncc2C1)C1=NCCCC1)c1[nH]c2cc(ccc2n1)C
845	s1cnc(-c2ccccc2)c1C[NH+]1CCc2nc(ncc2C1)C1CCCCC1
846	Clc1cc(C)c(OC2C[NH2+]C2)cc1
847	Brc1ccc(cc1)-c1oc(cc1)CN1CC2=C(NC(=NC2=O)c2cncnc2)CC1
848	S(=O)(=O)(C)C1=NC(=O)C2=C(N1)CCN(C2)Cc1cccnc1OCC1CC1

849	[NH+]1(CCc2nc(ncc2C1)-c1ccncc1)Cc1[nH]cnc1
850	Clc1nc(N2CCN(CC2)C(=O)NC)ccn1
851	Clc1nc2c(cc1C[NH+]1CC3=C(NC(=S)NC3=O)CC1)cccc2C
852	O=[N+]([O-])c1cc(ccc1NCc1ccc([N+](=O)[O-])cc1)C#N
853	Clc1cc(ccc1C)-c1ncc(cn1)C(OCC)=O
854	Brc1cc2[nH]cc(c2cc1)C[NH+]1CC2=C(NC(SC)=NC2=O)CC1
855	FC(F)(F)c1ccccc1C1CCC[NH2+]C1
856	Fc1ccc(OC)cc1CN1C[C@H]([NH3+])CC1
857	S(C)c1[nH]c(c(n1)-c1cc(ncc1)NCC(CC)C)-c1ccc(F)cc1
858	Clc1cc(cnc1)CN1CC2=C(NC(=NC2=O)c2ccc(N)cc2)CC1
859	Clc1ccncc1CN1CCc2nc(ncc2C1)C1=NCCCC1
860	O(C)c1ncc(cc1)C[NH+]1CCc2nc(ncc2C1)-c1ccc(N)cc1
861	Fc1cc(cnc1OC)CN1CC2=C(NC(=NC2=O)c2occc2)CC1
862	Clc1ncccc(c1)C(=O)NCc1ccccc1C
863	ClC=1c2c(OC(=O)C=1CN1CCc3nc(ncc3C1)-c1sccc1)cccc2
864	Fc1cc(ccc1)-c1[nH]ncc1CN1CC2=C(NC(=NC2=O)C(C)C)CC1
865	ClC=1c2cc(F)ccc2OCC=1CN1CCc2nc(ncc2C1)-c1ccncc1
866	O=[N+]([O-])c1cc([N+](=O)[O-])ccc1NCCC1CC[NH2+]CC1
867	S(C)c1nc2CCN(Cc2cn1)Cc1occn1
868	Clc1ncnc2nc([nH]c12)-c1sccc1
869	FC(F)(F)c1ccc(cc1)C1=NC(=O)C2=C(N1)CCN(C2)Cc1cnccc1C
870	[NH+]1(CCc2nc(ncc2C1)-c1ccncc1)Cc1cn[nH]c1
871	Fc1cc(C)c(cc1)C[NH+]1C[C@@H](O)CC1
872	[Si](C(C)C)(C(C)C)(C(C)C)c1oc(cn1)CN1CCc2nc(ncc2C1)N
873	O=C1N=C(NC2=C1CN(CC2)Cc1[nH]c(cn1)C)N
874	[Si](C\C(=C/CC\C=C(/C[Si](C)(C)C)\C)\C)(C)(C)C
875	Fc1cccnc1CN1CCc2nc(ncc2C1)C1=NCCCC1
876	Clc1ncnc(c1)-c1ccc(OC(F)(F)F)cc1
877	s1ccc(C)c1C[NH+]1CC2=C(NC(=NC2=O)C(C)(C)C)CC1
878	S(C)C1=NC(=O)C2=C(N1)CC[NH+](C2)Cc1cc(n(c1C)-c1ccccc1)C

879	Brc1cc(F)c(OC2CN(C2)C(OC(C)(C)C)=O)cc1	900	[NH+]1(CCc2nc(ncc2C1)N)Cc1c2c(n(c1)CC=C)cccc2
880	FC(F)(F)Oc1ccc(cc1)-c1ncc(cc1)C[NH+]1CCc2nc(ncc2C1)-c1cccnc1	901	O(\N=C/1\Cc2c(CC\1[NH3+])cccc2)CCCc1ccccc1
881	Fc1cc(CN2CCc3nc(ncc3C2)C(C)(C)C)c(OC)nc1	902	FC(F)(F)c1ccc(cc1)C1=NC(=O)C2=C(N1)CCN(C2)Cc1nc2c(cc1)cccc2O
882	S(=O)(=O)([O-])c1oc(cc1)CN1CC2=C(NC(=NC2=O)C2CCCCC2)CC1	903	O=C1N=C(NC2=C1CN(CC2)Cc1[nH]c([nH]c1)C)C1CC1
883	O(C)c1c2[C@H]3C=4C5=NC(C=4[C@@H](c2c(OC)cc1)CC3)=Cc1[nH]c(C=c2[nH]c(=CC3=NC(C=4[C@H]6c7c([C@@H](C3=4)CC6)c(OC)ccc7OC)=C5)c3[C@H]4c5c([C@H](CC4)c23)c(OC)ccc5OC)c2[C@H]3c4c([C@H](CC3)c12)c(OC)ccc4OC	904	S(=O)(=O)(C)c1nc2CCN(Cc2cn1)CC=1COc2c(C=1)cccc2
		905	S=C1NC(=O)C2=C(N1)CC[NH+](C2)Cc1c(n(nc1C)C)C
		906	O=C1N=C(NC2=C1CN(CC2)Cc1nc2c(n1CCC)cccc2)C(C)C
884	S(C)c1nc2CC[NH+](Cc2cn1)Cc1[nH]c2c(c1)cccc2	907	[NH+]1(CCc2nc(ncc2C1)C1CCCCC1)Cc1nc2nccccc2cc1
885	Fc1ccc(cc1)-c1c(-c2ccc(F)cc2)c(n(C(C)C)c1CC[C@@H](O)C[C@@H](O)CC(=O)[O-])C(=O)Nc1ccccc1	908	OC[C@H](C[C@H]([NH3+])C(=O)[O-])C(=O)[O-]
		909	s1c(C[NH+]2CCc3nc(ncc3C2)-c2ccc(N)cc2)c(nc1C)-c1ccccc1
886	Clc1ccc(cc1)C1=NC(=O)C2=C(N1)CC[NH+](C2)CC=1C2CC(CC=1)C2(C)C	910	s1c(ccc1C[NH+]1CC2=C(NC(=NC2=O)c2cncnc2)CC1)-c1ccccc1OC
887	FC(F)(F)c1cc([N+](=O)[O-])c(NCc2ccccc2C)cc1	911	O=C1N=C(NC2=C1CN(CC2)Cc1cn(nc1-c1ccncc1)-c1ccccc1)N
888	Fc1cc\2c(NC(=O)/C/2=C\c2[nH]c(C)c(C(=O)N[C@H]3CCN(N(C)C)C34C(=O)C4=O)c2C)cc1	912	[nH]1c(C)c(nc1CN1CCc2nc(ncc2C1)C1=NCCCC1)C
		913	o1cccc1-c1nc2CC[NH+](Cc2cn1)Cc1nc[nH]c1C
889	O=C1Nc2cc(\N=C/3\N=C(N4NC=C(CCCC1)C4=N\3)Nc1cc(ccc1)C(=O)N(CC[NH+](C)C)C)ccc2	914	Clc1cccc(C[NH+]2CC(O)CCC2)c1F
		915	[NH+]1(CCc2nc(ncc2C1)N)Cc1cncnc1
890	O=C([O-])[C@@H]1CCC[NH+](C1)Cc1ccc(cc1)C	916	Oc1c(CN2CC3=C(NC(=NC3=O)C3CCCCC3)CC2)c(cnc1C)CO
891	Fc1cc2[nH]cc(c2cc1)C[NH+]1CCc2nc(ncc2C1)-c1cccnc1	917	O=[N+]([O-])c1cc(ccc1NCCC1CC[NH2+]CC1)C#N
892	Clc1nc(ccc1)C(=O)NCc1cc([N+](=O)[O-])ccc1	918	S(CC)c1ccc(cc1)-c1ncc(cc1)CN1CC2=C(NC(=NC2=O)c2ccncc2)CC1
893	FC(F)(F)c1nc2CC[NH+](Cc2cn1)Cc1c2c(n(c1)CC=C)cccc2	919	Clc1ccc(cc1)-c1nc2CC[NH+](Cc2cn1)Cc1cn[nH]c1-c1ccc(OC)cc1
894	n1cnc2n(nc(c2c1N)-c1cc2c(cc1)cccc2)CC	920	Fc1ncc(cc1)CN1CC2=C(NC(=NC2=O)CCC)CC1
895	Clc1ccc(cc1)-c1nc2CC[NH+](Cc2cn1)Cc1c2c(ncc1)cccc2	921	FC(F)(F)c1ccc(cc1)-c1nc2CC[NH+](Cc2cn1)Cc1cn(nc1C)C
896	Fc1c(cccc1O[C@H]1C[C@H](NC1)C(OC)=O)C(F)(F)F	922	Fc1ccc(cc1)-c1nc(C(=O)N([C@@H](C)c2ccccc2)C)c(n1CC[C@@H](O)C[C@@H](O)CC(=O)[O-])C(C)C
897	Brc1cnccc1C[NH+]1CCc2nc(ncc2C1)-c1ccc(Cl)cc1	923	Clc1cc(ccc1Cl)-c1ncc(cc1)C[NH+]1CCc2nc(ncc2C1)CC
898	O1c2c(OCC1(OC)C=1NCCN=1)cccc2-c1ccccc1	924	S(=O)(=O)(C)C1=NC(=O)C2=C(N1)CCN(C2)Cc1ccc(F)nc1
899	S(=O)(=O)(C)C1=NC(=O)C2=C(N1)CCN(C2)Cc1c(cc(OC)cc1OC)C	925	Fc1ccccc1[C@H]([C@@H]([NH+](C)C)C1CCCCC1)CC[NH+]1CCN(CC1)c1cc

	ccc1OC
926	S=C1NC(=O)C2=C(N1)CC[NH+](C2)Cc1oc(cc1)C
927	Clc1ccc(cc1)-c1sc(cn1)CN1CCc2nc(ncc2C1)C
928	s1cccc1-c1nn(cc1C[NH+]1CCc2nc(ncc2C1)C(F)(F)F)-c1ccccc1
929	O=C1N=C(NC2=C1CN(CC2)Cc1n[nH]c(c1)C)c1ccc(N)cc1
930	S=C1NC(=O)C2=C(N1)CC[NH+](C2)Cc1n(nc(c1)C)C
931	[nH]1c2cc(ccc2cc1)-c1nn(c2ncnc(N)c12)C
932	Fc1ccc(F)cc1N1N=C(C(=O)C)C(C1)(CCN1[C@H]2C[C@H](OC2)C1)c1ccccc1
933	FC(F)(F)c1ccc(cc1)-c1nc2CCN(Cc2cn1)Cc1cccnc1OC
934	Clc1cc(cnc1OC)B(O)O
935	Fc1ccc(F)cc1C1=NN(C(=O)NCC)C(C1)(CCCCO)c1ccccc1
936	Clc1ccc(Cl)cc1-c1oc(cc1)C[NH+]1CCc2nc(ncc2C1)-c1cncnc1
937	Clc1cncc(Cl)c1C[NH+]1CCc2nc(ncc2C1)C(C)C
938	s1cccc1-c1[nH]ncc1C[NH+]1CCc2nc(ncc2C1)-c1sccc1
939	Brc1c2c(sc1C[NH+]1CCc3nc(ncc3C1)C1CC1)cccc2
940	Clc1ncc(cc1)C(=O)NCc1cccnc1
941	Clc1n(nc(C)c1C[NH+]1CCc2nc(ncc2C1)-c1sccc1)-c1ccccc1
942	S=C1NC2=C(CN(CC2)Cc2nc3ncccc3c2)C=N1
943	O=C([O-])[C@H]1CCC[NH+](C1)Cc1cc([N+](=O)[O-])ccc1
944	O(C(C)(C)C)C(=O)Nc1nc(ccc1)C(O)c1ccccc1
945	Clc1cc(ccc1OC)-c1oc(cc1)CN1CC2=C(NC(=NC2=O)C2CCCCC2)CC1
946	Clc1nc2cc(ccc2cc1C[NH+]1CC2=C(NC(=NC2=O)CCC)CC1)C
947	FC(F)(F)c1ccc(cc1)C1=NC(=O)C2=C(N1)CCN(C2)Cc1cnn(CC)c1C
948	Brc1cc(sc1)CN1CCc2nc(ncc2C1)-c1occc1
949	Clc1nc(ncc1C(C)C)C(C)C
950	Clc1nc(ccn1)-c1ccc(cc1)C(C)(C)C
951	O=C1N=C(NC2=C1CN(CC2)Cc1nc(ccc1)-c1cc([N+](=O)[O-])ccc1)c1cccnc1

952	S(CC[C@H](NC(=O)[C@@H](NC(=O)[C@@H](NC(=O)[C@@H](NC(=O)[C@H]([NH3+])CS)CCC[NH+]=C(N)N)[C@H](CC)C)CCC[NH+]=C(N)N)C(=O)N[C@H](C(=O)NC(C(=O)NCC(=O)N[C@H](C(=O)[O-])CS)C)CO)C
953	o1c(C)c(cc1CN1CCc2nc(ncc2C1)C(C)(C)C)C
954	Clc1ccc(cc1F)C[NH+]1CC(CCC1)C(=O)[O-]
955	S(C)c1nc2CC[NH+](Cc2cn1)Cc1[nH]c(cc1C)C
956	S=C1NC(=O)C2=C(N1)CC[NH+](C2)Cc1ccc(nc1)-c1ccccc1C(F)(F)F
957	o1c(ccc1C[NH+]1CCc2nc(ncc2C1)-c1cccnc1)-c1cc([N+](=O)[O-])ccc1
958	FC(F)(F)Oc1cc(ccc1)-c1ncc(cc1)C[NH+]1CCc2nc(ncc2C1)C1=NCCCC1
959	s1cccc1C1=NC(=O)C2=C(N1)CCN(C2)Cc1nc(sc1)C
960	Clc1cccc(F)c1CN1C[C@H]([NH3+])CC1
961	Brc1cnc(Cl)nc1Nc1ccc(OC)cc1
962	n1c2c(cc(cc2)-c2nn(c3ncnc(N)c23)C(C)C)ccc1N
963	Brc1cc2c(OC(=O)C(CN3CCc4nc(ncc4C3)CCC)=C2Cl)cc1
964	O(C)c1cc(cnc1)C[NH+]1CCc2nc(ncc2C1)N
965	O(c1ncccc1CN1CC2=C(NC(=NC2=O)c2cncnc2)CC1)C1CCCCC1
966	Clc1ccc(cc1)-c1nc2CC[NH+](Cc2cn1)Cc1ccc(OC2CCC2)nc1
967	o1c(ccc1C[NH+]1CC2=C(NC(=NC2=O)c2ccccc2)CC1)-c1ccccc1
968	O(CC1CC1)c1ncccc1CN1CCc2nc(ncc2C1)-c1ccc(N)cc1
969	Fc1ccccc1[C@H]([C@@H](NC(=O)N(C)C)C1CCCCC1)CC[NH+]1CCN(CC1)c1ccccc1OC
970	FC(F)(F)c1ccc(cc1)-c1nc2CC[NH+](Cc2cn1)Cc1ncn(c1)C
971	P(OC[C@H]1O[C@@H](n2c3ncnc(N)c3nc2)[C@H](O)[C@@H]1OC(=O)C/1=CCCC\C\1=N/C)(OP(OP(O)(=O)[O-])(=O)[O-])(=O)[O-]
972	S(C)C1=NC(=O)C2=C(N1)CCN(C2)Cc1c(noc1C)C
973	O=C1N=CC=C(NCc2ncccc2)C1c1[nH]c2c(n1)c(cc(-n1ccnc1)c2)C
974	Brc1cc(sc1)CN1CCc2nc(ncc2C1)-c1ccc(N)cc1
975	Fc1cc([N+](=O)[O-

	])c2OC=C(CN3CCc4nc(ncc4C3)-c3cncnc3)C(=O)c2c1
976	S(c1oc(cc1)CN1CCc2nc(ncc2C1)-c1occc1)c1[nH]c2cc(ccc2n1)C
977	O1[C@]2(O[C@@H](CC(=C2)C)[C@@H](\C=C\[C@@H]2O[C@@]3(O[C@@H]4[C@H](O[C@H]([C@@H](O)C[C@H](C)[C@H]5O[C@]6(OCCCC6)CC[C@H]5C)C(=C)[C@H]4O)CC3)CC2)C)[C@H](O)CC[C@H]1C[C@@](O)(C(=O)[O-])C
978	s1c2ncccc2cc1C[NH+]1CC2=C(NC(=NC2=O)c2ccccc2)CC1
979	Clc1cc(ccc1)C=1Nc2c(cc(OC)cc2)C(=

	O)C=1
980	Clc1ccc(cc1)-c1sc(cn1)C[NH+]1CC2=C(NC(=S)N=C2)CC1
981	Fc1ccc(cc1)-c1ccc(Oc2cc(C)c(\[NH+]=C\N(CC)C)cc2C)cc1
982	Clc1ncc(cc1)CN1CC2=C(NC(=NC2=O)C(F)(F)F)CC1

Appendix K

Matlab code for cellular parameters used in T and R models for studying lysosomotropic behavior. This also is the Matlab code of numerical solution for coupled ordinary differential equation. All explanations come after the symbol '%'.

```matlab
% The R-Model

% Clear the memory
clear

% Constant
T = 310.15;                         % temperature (37centigrade)
R = 8.314;                          % universal gas constant
F = 96484.56;                       % faraday constant
La = 0;                                  % lipid fraction in apical compartment
Lc = 0;                                  % lipid fraction in cytosol
Lm = 0;                                  % lipid fraction in mitochondria
Ll = 0;                                  % lipid fraction in lysosomes
Lb = 0;                                  % lipid fraction in basolateral compartment
Wa = 1-La;                          % water fraction in apical compartment
Wc = 1-Lc;                          % water fraction in cytosol
Wm = 1-Lm;                          % water fraction in mitochondria
Wl = 1-Ll;                          % water fraction in lysosomes
Wb = 1-Lb;                          % water fraction in basolateral compartment
gamma_na = 1;           % activity coefficient of neutral molecules in apical compartment
gamma_da = 1;           % activity coefficient of ionic molecules in apical compartment
gamma_nc = 1.23026877;      % activity coefficient of neutral molecules in cytosol
gamma_dc = 0.73799822;      % activity coefficient of ionic molecules in cytosol
gamma_nm = 1.23026877;      % activity coefficient of neutral molecules in mitochondria
gamma_dm = 0.73799822;      % activity coefficient of ionic molecules in mitochondria
gamma_nl = 1.23026877;       % activity coefficient of neutral molecules in lysosomes
gamma_dl = 0.73799822;       % activity coefficient of ionic molecules in lysosomes
gamma_nb = 1;                    % activity coefficient of neutral molecules in basolateral
gamma_db = 1;                    % activity coefficient of ionic molecules in basolateral
```

```
    Ca = 1 ;                                        % apical initical drug concentration (mM)

    % areas and volumes (m^2, m^3)
    % epithelium is considered as a square with the lengh of 10^(-5)m.
    % mitochondria and lysosomes are considered as spheres with the diameter of 10^(-6)m
    Aa = 50*10^(-10) ;                     % the apical membrane surface area
    Aaa = 20*10^(-10) ;                    % the monolayer area
    Am = 100*3.14*10^(-12);            % the mitochondrial membrane surface area
    Al = 100*3.14*10^(-12);            % the lysosomal membrane surface area
    Ab = 10^(-10);                        % the basolateral membrane surface area
    Vc = 10*10^(-15);                     % the cytosolic volume
    Vm = 100*5.24*10^(-19);            % the mitochondrial volume, 100 mitochondria
    Vl = 100*5.24*10^(-19);            % the lysosomal volume, 100 lysosomes
    Vb = 4.7*10^(-3);                     % the volume of basolateral compartment

    % Membrane potential (units in 'Voltage')
    Ea = -0.0093 ;                        % apical membrane potential
    Em = -0.15 ;                          % mitochondrial membrane potential
    El = 0.01 ;                           % lysosomal membrane potential
    Eb = 0.0119 ;                         % basolateral membrane potential

    % pH values
    pHa = 5.5 ;                           % pH value in apical compartment
    pHc = 7.0 ;                           % pH value in cytosol
    pHm = 8.0 ;                           % pH value in mitochondria
    pHl = 5.0 ;                           % pH value in lysosomes
    pHb = 7.4 ;                           % pH value in basolateral compartment

    % read drug properties from files
    [DrugName,pKaall,logPnall,logPdall, ZNall] = textread('Molecules.txt',
    '%s %f %f %f %f','commentstyle','matlab');

    % The calculated results are saved in this file 'MoleculesR.dat'
```

```matlab
len = length(pKaall) ;
fid1 = fopen('MoleculesR.dat','w');
str1 = ' Name --------------- pKa ----- logP_n ---logP_d---Cc(mM)-----Cm(mM)-------Clyso(mM)------
-Peff(cm/sec) ' ;
fprintf(fid1,'%s\n',str1) ;

% liposomal approximation for logP_n and logP_d
for n = 1:len
    if ( abs(ZNall(n)-1) <= 10^(-6) )
        logP_nlipT(n) = 0.33*logPnall(n)+2.2 ;
        logP_dlipT(n) = 0.37*logPdall(n)+2 ;
    end
    if ( abs(ZNall(n)+1) <= 10^(-6) )
        logP_nlipT(n) = 0.37*logPnall(n)+2.2 ;
        logP_dlipT(n) = 0.33*logPdall(n)+2.6 ;
    end
    if ( abs(ZNall(n)-0) <= 10^(-5) )
        logP_nlipT(n) = 0.33*logPnall(n)+2.2 ;
        logP_dlipT(n) = 0.33*logPdall(n)+2.2 ;
    end
end

% Get the first two decimals.
logP_nlip = round(logP_nlipT*100)/100 ;
logP_dlip = round(logP_dlipT*100)/100 ;

% solve differential equations

for n = 1:len
    pKa = pKaall(n);
    logP_n = logP_nlip(n) ;
    logP_d = logP_dlip(n) ;
    z = ZNall(n) ;
    i = -sign(z) ;
```

```
Na = ((z)*(Ea)*F)/(R*T);
Nm = ((z)*(Em)*F)/(R*T);
Nl = ((z)*(El)*F)/(R*T);
Nb = ((z)*(-Eb)*F)/(R*T);


Pn = 10^(logP_n-6.7);
Pd = 10^(logP_d-6.7);
Kn_a = La*1.22*10^(logP_n);
Kd_a = La*1.22*10^(logP_d);
Kn_c = Lc*1.22*10^(logP_n);
Kd_c = Lc*1.22*10^(logP_d);
Kn_m = Lm*1.22*10^(logP_n);
Kd_m = Lm*1.22*10^(logP_d);
Kn_l = Ll*1.22*10^(logP_n);
Kd_l = Ll*1.22*10^(logP_d);
Kn_b = Lb*1.22*10^(logP_n);
Kd_b = Lb*1.22*10^(logP_d);


fn_a = 1/(Wa/gamma_na+Kn_a/gamma_na+Wa*10^(i*(pHa-pKa))/gamma_da...
       +Kd_a*10^(i*(pHa-pKa))/gamma_da);
fd_a = fn_a*10^(i*(pHa-pKa));
fn_c = 1/(Wc/gamma_nc+Kn_c/gamma_nc+Wc*10^(i*(pHc-pKa))/gamma_dc...
       +Kd_c*10^(i*(pHc-pKa))/gamma_dc);
fd_c = fn_c*10^(i*(pHc-pKa));
fn_m = 1/(Wm/gamma_nm+Kn_m/gamma_nm+Wm*10^(i*(pHm-pKa))/gamma_dm...
       +Kd_m*10^(i*(pHm-pKa))/gamma_dm);
fd_m = fn_m*10^(i*(pHm-pKa));
fn_l = 1/(Wl/gamma_nl+Kn_l/gamma_nl+Wl*10^(i*(pHl-pKa))/gamma_dl...
       +Kd_l*10^(i*(pHl-pKa))/gamma_dl);
fd_l = fn_l*10^(i*(pHl-pKa));
fn_b = 1/(Wb/gamma_nb+Kn_b/gamma_nb+Wb*10^(i*(pHb-pKa))/gamma_db...
        +Kd_b*10^(i*(pHb-pKa))/gamma_db);
fd_b = fn_b*10^(i*(pHb-pKa));
```

```
k11 = -(Aa/Vc)*Pn*fn_c-(Aa/Vc)*Pd*Na*fd_c*exp(Na)/(exp(Na)-1)...
       -(Am/Vc)*Pn*fn_c-(Am/Vc)*Pd*Nm*fd_c/(exp(Nm)-1)...
       -(Al/Vc)*Pn*fn_c-(Al/Vc)*Pd*Nl*fd_c/(exp(Nl)-1)...
       -(Ab/Vc)*Pn*fn_c-(Ab/Vc)*Pd*Nb*fd_c/(exp(Nb)-1) ;

k12 = (Am/Vc)*Pn*fn_m+(Am/Vc)*Pd*Nm*fd_m*exp(Nm)/(exp(Nm)-1) ;
k13 = (Al/Vc)*Pn*fn_l+(Al/Vc)*Pd*Nl*fd_l*exp(Nl)/(exp(Nl)-1) ;
k14 = (Ab/Vc)*Pn*fn_b+(Ab/Vc)*Pd*Nb*fd_b*exp(Nb)/(exp(Nb)-1) ;
S1 = (Aa/Vc)*Ca*(Pn*fn_a+Pd*Na*fd_a/(exp(Na)-1)) ;

k21 = (Am/Vm)*Pn*fn_c+(Am/Vm)*Pd*Nm*fd_c/(exp(Nm)-1) ;
k22 = -(Am/Vm)*Pn*fn_m-(Am/Vm)*Pd*Nm*fd_m*exp(Nm)/(exp(Nm)-1) ;
k23 = 0 ;
k24 = 0 ;
S2 = 0 ;

k31 = (Al/Vl)*Pn*fn_c+(Al/Vl)*Pd*Nl*fd_c/(exp(Nl)-1) ;
k32 = 0 ;
k33 = -(Al/Vl)*Pn*fn_l-(Al/Vl)*Pd*Nl*fd_l*exp(Nl)/(exp(Nl)-1) ;
k34 = 0 ;
S3 = 0 ;

k41 = (Ab/Vb)*Pn*fn_c+(Ab/Vb)*Pd*Nb*fd_c/(exp(Nb)-1) ;
k42 = 0 ;
k43 = 0 ;
k44 = -(Ab/Vb)*Pn*fn_b-(Ab/Vb)*Pd*Nb*fd_b*exp(Nb)/(exp(Nb)-1) ;
S4 = 0 ;

A = [k11, k12, k13, k14; k21, k22, k23, k24; k31, k32, k33, k34; k41, k42, k43, k44] ;
G = [S1, S2, S3, S4]' ;
RR = [0,0,0,0]' ;          % initial conditions: at t = 0, Ccyto=0; Cmito=0; Clyso=0; Cbaso=0
t = 10^6 ;                 % the time point at which intracellular / subcellular …
                           %concentrations were calculated
```

```
    % Solve the system.
    [V,E] = eig(A);
    E = diag(E);
    H = inv(V)*G;
    B = V \ RR;
    C = B + H./E;
    Z = -(H./E) + exp(t * E).*C ;
    Y = real(V * Z);
    Y = Y';
    Peff = Y(4)*Vb*10^8/(t*Aaa*Ca);
    NA = [pKa, logP_n, logP_d, Y(1),Y(2),Y(3), Peff];
    str = DrugName{n};
    fprintf(fid1,'%s\t %12.2f %12.2f %12.2f %12.4f %12.4f  %12.4f %12.4f\n',str, NA') ;
end
    fclose(fid1);


% The T-Model
clear

% Constant
T = 310.15 ;                              % Temperature
R = 8.314 ;                               % Universal gas constant
F = 96484.56 ;                            % Faraday constant
Lo = 0 ;                                      % Lipid fraction in apical compartment
Lc = 0 ;                                      % Lipid fraction in cytosol
Lm = 0 ;                                      % Lipid fraction in mitochondria
Ll = 0 ;                                      % Lipid fraction in lysosomes
Wo = 1-Lo ;                               % Water fraction in apical compartment
Wc = 1-Lc ;                               % Water fraction in cytosol
Wm = 1-Lm ;                               % Water fraction in mitochondria
Wl = 1-Ll ;                               % Water fraction in lysosomes
gamma_no = 1;                         % activity coefficient of neutral molecules out of the cells
```

```matlab
gamma_do = 1;                         % activity coefficient of ionic molecules out of the cells
gamma_nc = 1.23026877;        % activity coefficient of neutral molecules in cytosol
gamma_dc = 0.73799822;        % activity coefficient of ionic molecules in cytosol
gamma_nm = 1.23026877;        % activity coefficient of neutral molecules in mitochondria
gamma_dm = 0.73799822;        % activity coefficient of ionic molecules in mitochondria
gamma_nl = 1.23026877;        % activity coefficient of neutral molecules in lysosomes
gamma_dl = 0.73799822;        % activity coefficient of ionic molecules in lysosomes

% areas and volumes (units in m^2 and m^3 respectively)
Ac = 3.14*10^(-10) ;          % the suface area of a floating-cell, 10 um (10^-5m) diameter
Vc = 5.24*10^(-16) ;          % the cytosolic volume
Am = 30*4*pi*(1*10^(-6))^2 ;          % the mitochondrial membrane surface area
Vm = 30*(4/3)*pi*(1*10^(-6))^3 ;      % the mitochondrial volume
Al = 20*4*pi*(0.5*10^(-6))^2 ;        % the lysosomal membrane surface area
Vl = 20*(4/3)*pi*(0.5*10^(-6))^3 ;    % the lysosomal volume, 20 lysosomes

% membrane potential (units in 'Voltage')
Ec = -0.06 ;                          % the plasma membrane potential
Em = -0.15 ;                          % the mitochondrial membrane potential
El = 0.01 ;                           % the lysosomal membrane potential

% pH values
pHo = 7.4 ;                           % the extracellular pH value
pHc = 7 ;                             % the cytosolic pH
pHm = 8 ;                             % the mitochondrial pH
pHl = 5 ;                             % the lysosomal pH

Co = 1 ;                              % the extracellular drug concentration, unit in mM

% Read drug properties from files
[DrugName,pKaall,logPnall,logPdall, ZNall] = textread('Molecules.txt',
'%s %f %f %f %f','commentstyle','matlab');

% The calculated results are saved in this file 'MoleculesT.dat'
```

```
len = length(pKaall) ;
fid1 = fopen('MoleculesT.dat','w');
str1 = ' Name --------------- pKa ----- logP_n ---logP_d---Cc(mM)-----Cm(mM)-------Clyso(mM) ' ;
fprintf(fid1,'%s\n',str1) ;

% liposomal approximation for logP_n and logP_d
for n = 1:len
    if ( abs(ZNall(n)-1) <= 10^(-6) )
        logP_nlipT(n) = 0.33*logPnall(n)+2.2 ;
        logP_dlipT(n) = 0.37*logPdall(n)+2 ;
    end
    if ( abs(ZNall(n)+1) <= 10^(-6) )
        logP_nlipT(n) = 0.37*logPnall(n)+2.2 ;
        logP_dlipT(n) = 0.33*logPdall(n)+2.6 ;
    end
    if ( abs(ZNall(n)-0) <= 10^(-5) )
        logP_nlipT(n) = 0.33*logPnall(n)+2.2 ;
        logP_dlipT(n) = 0.33*logPdall(n)+2.2 ;
    end
end

% Get the first two decimals
logP_nlip = round(logP_nlipT*100)/100 ;
logP_dlip = round(logP_dlipT*100)/100 ;

% solve differential equations
for n = 1:len
    pKa = pKaall(n);
    logP_n = logP_nlip(n) ;
    logP_d = logP_dlip(n) ;
    z = ZNall(n) ;
    i = -sign(z) ;
    Nc = ((z)*(Ec)*F)/(R*T);
    Nm = ((z)*(Em)*F)/(R*T);
```

```
Nl = ((z)*(El)*F)/(R*T);


Pn = 10^(logP_n-6.7) ;
Pd = 10^(logP_d-6.7) ;
Kn_o = Lo*1.22*10^(logP_n) ;
Kd_o = Lo*1.22*10^(logP_d) ;
Kn_c = Lc*1.22*10^(logP_n) ;
Kd_c = Lc*1.22*10^(logP_d) ;
Kn_m = Lm*1.22*10^(logP_n) ;
Kd_m = Lm*1.22*10^(logP_d) ;
Kn_l = Ll*1.22*10^(logP_n) ;
Kd_l = Ll*1.22*10^(logP_d) ;


fn_o = 1/(Wo/gamma_no+Kn_o/gamma_no+Wo*10^(i*(pHo-pKa))/gamma_do...
       +Kd_o*10^(i*(pHo-pKa))/gamma_do) ;
fd_o = fn_o*10^(i*(pHo-pKa)) ;
fn_c = 1/(Wc/gamma_nc+Kn_c/gamma_nc+Wc*10^(i*(pHc-pKa))/gamma_dc...
       +Kd_c*10^(i*(pHc-pKa))/gamma_dc) ;
fd_c = fn_c*10^(i*(pHc-pKa)) ;
fn_m = 1/(Wm/gamma_nm+Kn_m/gamma_nm+Wm*10^(i*(pHm-pKa))/gamma_dm...
       +Kd_m*10^(i*(pHm-pKa))/gamma_dm) ;
fd_m = fn_m*10^(i*(pHm-pKa)) ;
fn_l = 1/(Wl/gamma_nl+Kn_l/gamma_nl+Wl*10^(i*(pHl-pKa))/gamma_dl...
       +Kd_l*10^(i*(pHl-pKa))/gamma_dl) ;
fd_l = fn_l*10^(i*(pHl-pKa)) ;


k11 = -(Ac/Vc)*Pn*fn_c-(Ac/Vc)*Pd*Nc*fd_c*exp(Nc)/(exp(Nc)-1)...
       -(Am/Vc)*Pn*fn_c-(Am/Vc)*Pd*Nm*fd_c/(exp(Nm)-1)...
       -(Al/Vc)*Pn*fn_c-(Al/Vc)*Pd*Nl*fd_c/(exp(Nl)-1);


k12 = (Am/Vc)*Pn*fn_m+(Am/Vc)*Pd*Nm*fd_m*exp(Nm)/(exp(Nm)-1) ;
k13 = (Al/Vc)*Pn*fn_l+(Al/Vc)*Pd*Nl*fd_l*exp(Nl)/(exp(Nl)-1) ;
S1 = (Ac/Vc)*Co*(Pn*fn_o+Pd*Nc*fd_o/(exp(Nc)-1)) ;
```

```
k21 = (Am/Vm)*Pn*fn_c+(Am/Vm)*Pd*Nm*fd_c/(exp(Nm)-1) ;
k22 = -(Am/Vm)*Pn*fn_m-(Am/Vm)*Pd*Nm*fd_m*exp(Nm)/(exp(Nm)-1) ;
k23 = 0 ;
S2 = 0 ;

k31 = (Al/Vl)*Pn*fn_c+(Al/Vl)*Pd*Nl*fd_c/(exp(Nl)-1) ;
k32 = 0 ;
k33 = -(Al/Vl)*Pn*fn_l-(Al/Vl)*Pd*Nl*fd_l*exp(Nl)/(exp(Nl)-1) ;
S3 = 0;

A = [k11, k12, k13; k21, k22, k23; k31, k32, k33];
G = [S1, S2, S3]' ;
RR = [0,0,0]' ;
t = 1000000 ;

[V,E] = eig(A) ;
E = diag(E) ;
H = inv(V)*G ;
B = V \ RR ;
C = B + H./E ;
Z = -(H./E) + exp(t * E).*C ;
Y = real(V * Z) ;
Y = Y' ;
NA = [pKa, logP_n, logP_d, Y] ;

str = DrugName{n};
fprintf(fid1,'%s\t %12.2f %12.2f %12.2f %12.4f %12.4f  %12.4f\n',str, NA') ;
end
  fclose(fid1);
```

Appendix L

MATLAB® code and R code for the Monte Carlos simulation of phospholipidosis effect on chloroquine intracellular accumulation. To simulate CQ uptake in MDCK cells with the assumption of lysosomal swelling and CQ binding to cellular lipid fractions, save Code_S1 and Code_S2 as .m files. To simulate CQ uptake in without binding, in Code_S1, use $\log P_{n,d1,d2}$ instead of $\log P_{n,d1,d2\_cell}$ in calculated sorption coefficients ($K_{n,d1,d2}$) in each compartment. To simulate CQ uptake without volume expansion, in Code_S2, substitute A_slope_Gr and V_slope_Gr (rate of change in lysosomal area or volume) to an array of 0s. MATLAB® R2009b was used to code the programs; higher versions MATLAB® should be able to run the files. Code_S3.txt was copied into R 2.8.1 program to plot Monte Carlos simulation of CQ uptake. To generate green or blue histograms when simulating uptake without binding or swelling, substitute code "col="black"" or "col="white"" to "col="green"" or "col="blue"" in the "hist" and "lines" command.

1) Code _S1. m

```
% The following section is to simulate the intracellular
% concentration of CQ in MDCK cells with volume expansion in acidic
% compartment and binding of CQ to cellular membrane structures.
% Smiles: CCN(CC)CCCC(C)NC1=C2C=CC(=CC2=NC=C1)Cl.OP(=O)(O)O.OP(=O)(O)O
% MDCK cells on 24well plates, 2cm^2 bottom, assuming 60*10^4 cell/well

% Clear the memory
clear
clc

global V_l_initial A_l_initial V_c_initial A_a V_m A_m V_a i
global Pn Pd1 Pd2
global Nd1_a Nd1_m Nd1_l Nd2_a Nd2_m Nd2_l
global fn_a fn_c fn_l fn_m
global fd1_a fd1_c fd1_l fd1_m
global fd2_a fd2_c fd2_l fd2_m

% Constant
T = 310.15 ;                    % temperature
```

```matlab
R = 8.314 ;                      % Universal gas constant
F = 96484.56 ;                   % Faraday constant

% Group conditions: 1-4, CQ treatments (25, 50, 100, 200 uM); 5-8, CQ/Suc.
% treatments (25, 50, 100, 200 uM); and 9-12, CQ/Baf. treatments (25, 50,
% 100, 200 uM).

C_aGr = [0.025, 0.050, 0.100, 0.200, 0.025, 0.050, 0.100, 0.200, 0.025,...
    0.050, 0.100, 0.200] ;        % Apical initial drug concentration (mM)
V_cGr_a = [1452, 1752, 1616, 1314, 2761, 2572, 2391, 2630, 1491, 1437,...
    1512, 1608] ;                   % cell volume, lower bound (um^3)
V_cGr_b = [1874, 1922, 2042, 1916, 3250, 3535, 3516, 3904, 1989, 1961,...
    2022, 1945] ;                   % cell volume, upper bound (um^3)
pH_lGr_a = [4.88, 5.22, 5.45, 5.20, 5.51, 5.73, 6.09, 6.25, 5.26, 5.05,...
    5.64, 5.48] ;                   % pH in lysosome, lower bound
pH_lGr_b = [5.84, 5.80, 6.17, 6.76, 6.31, 6.43, 6.81, 7.21, 5.84, 6.33,...
    6.12, 7.04] ;                   % pH in lysosome, upper bound
pH_cGr_a = [7.29, 7.34, 7.28, 7.27, 7.34, 7.34, 7.34, 7.32, 7.33, 7.32,...
    7.29, 7.10] ;                   % cytosolic pH, lower bound
pH_cGr_b = [7.43, 7.38, 7.42, 7.33, 7.40, 7.38, 7.40, 7.38, 7.43, 7.38,...
    7.39, 7.24] ;                   % cytosolic pH, upper bound
A_l_initial_Gr_a = [111.5, 111.5, 111.5, 111.5, 517.5, 517.5, 517.5,...
    517.5, 111.5, 111.5, 111.5, 111.5] ;
    % initial lysosomal membrane area, lower bound
A_l_initial_Gr_b = [335.0, 335.0, 335.0, 335.0, 899.7, 899.7, 899.7,...
    899.7, 335.0, 335.0, 335.0, 335.0] ;
    % initial lysosomal membrane area, upper bound
V_l_initial_Gr_a = [8.8, 8.8, 8.8, 8.8, 54.9, 54.9, 54.9, 54.9, 8.8,...
    8.8, 8.8, 8.8] ; % initial lysosomal volume, lower bound
V_l_initial_Gr_b = [32.4, 32.4, 32.4, 32.4, 128.0, 128.0, 128.0, 128.0,...
    32.4, 32.4, 32.4, 32.4] ; % initial lysosomal volume, upper bound

rand('seed',2010);
```

```matlab
for i = 1:1:12
    for round = 1:1:10000

C_a = C_aGr(i);                                 % extracellular concentration
cellNo = (50+20*rand())*10^4;                   % cell number per well

% Drug information -- ChemAxon calculation including logPn, pKa1, and pKa2
pKa1 = 9.96+0.25-0.5*rand() ;   % higher pKa
pKa2 = 7.47+0.25-0.5*rand() ;   % lower pKa
z1 = 1 ;                        % electric charge
z2 = 2 ;                        % electric charge
i1 = sign(z1) ;
i2 = sign(z2) ;
logPn = 3.93+0.25-0.5*rand() ;
    % logarithm of octanol/water partition coefficient for neutral species
logPd1 = 0.43+0.25-0.5*rand() ;
    % logarithm of octanol/water partition coefficient for +1 ion species
logPd2 = -0.91+0.25-0.5*rand() ;
    % logarithm of octanol/water partition coefficient for +2 ion species

logPn_cell = 1.70+rand()*(1.83-1.70) ;
logPd1_cell = 1.70+rand()*(1.83-1.70) ;
logPd2_cell = 1.70+rand()*(1.83-1.70) ;
    % logarithm of cellular partition coefficient for all three species

Pn = 10^(logPn-6.7) ;           % membrane permeability for neutral species
Pd1 = 10^(logPd1-6.7) ;         % membrane permeability for +1 ion species
Pd2 = 10^(logPd2-6.7) ;         % membrane permeability for +2 ion species

% pH values
pH_a = 7.4+0.1*rand() ;                          % pH in apical compartment
pH_c = pH_cGr_a(i)+(pH_cGr_b(i)-pH_cGr_a(i))*rand() ; % pH in cytosol
pH_l = pH_lGr_a(i)+(pH_lGr_b(i)-pH_lGr_a(i))*rand() ; % pH in lysosomes
pH_m = 8.0;                                      % pH in mitochondria
```

```matlab
% lipid fractions
L_l = 0.025+0.05*rand() ;           % lipid fraction in lysosomes
L_c = 0.05 ;            % lipid fraction in cytosol
L_m = 0.05 ;                        % lipid fraction in mitochondria

% Areas and volumes (units in m^2 and m^3)
A_a = 100*10^(-10) ;                % apical membrane surface area
A_l_initial = 10^(-12)*(A_l_initial_Gr_a(i)+(A_l_initial_Gr_b(i)...
    -A_l_initial_Gr_a(i))*rand()) ;  % lysosomal membrane surface area
A_m = 250*7.85*10^(-13) ;           % mitochondrial membrane surface area
V_a = 0.5*10^(-6)/cellNo ;          % extracellular drug solution volume
V_c_initial = 10^(-18)*(V_cGr_a(i)+(V_cGr_b(i)-V_cGr_a(i))*rand()) ;
                                    % initial cytosolic volume
V_l_initial = 10^(-18)*(V_l_initial_Gr_a(i)+(V_l_initial_Gr_b(i)...
    -V_l_initial_Gr_a(i))*rand()) ;  % lysosomal volume
V_m = 250*6.55*10^(-20);            % mitochondrial volume

% Membrane potential (units in 'Voltage')
E_a = -0.009 ;                      % membrane potential of apical membrane
E_l = +0.01-0.005+0.01*rand() ;  % membrane potential of lysosomal membrane
E_m = -0.16 ;                       % membrane potential of mitochondrial membrane

% Apical Compartment
fn_a = 1/(1+10^(i1*(pKa1-pH_a))+10^(i1*(pKa1-pH_a)+i2*(pKa2-pH_a))) ;
% ratio of the activity of neutral species and
% total molecular concentration in apical compartment
fd2_a = fn_a*10^(i1*(pKa1-pH_a)+i2*(pKa2-pH_a)) ;
% ratio of the activity of +1 ion species and
% total molecular concentration in apical compartment
fd1_a = fn_a*10^(i1*(pKa1-pH_a)) ;
% ratio of the activity of +2 ion species and
% total molecular concentration in apical compartment
Nd2_a = z2*E_a*F/(R*T) ;
```

```matlab
Nd1_a = z1*E_a*F/(R*T) ;

% Cytoplasm
W_c = 1-L_c ;           % water fraction in cytosol
Is_c = 0.3 ;            % ionic strength in cytosol (mol)
gamman_c = 10^(0.3*Is_c) ;
                        % activity coefficient of neutral molecules in cytosol
gammad1_c = 10^(-0.5*z1*z1*(sqrt(Is_c)/(1+sqrt(Is_c))-0.3*Is_c)) ;
                        % activity coefficient of monovalent base in cytosol
gammad2_c = 10^(-0.5*z2*z2*(sqrt(Is_c)/(1+sqrt(Is_c))-0.3*Is_c)) ;
                        % activity coefficient of bivalent base in cytosol
Kn_c = L_c*1.22*10^(logPn_cell) ;
                        % sorption coefficient for neutral species in cytosol
Kd1_c = L_c*1.22*10^(logPd1_cell) ;
                        % sorption coefficient for +1 ion species in cytosol
Kd2_c = L_c*1.22*10^(logPd2_cell) ;
                        % sorption coefficient for +2 ion species in cytosol
an_c = 1/(1+10^(i1*(pKa1-pH_c))+10^(i1*(pKa1-pH_c)+i2*(pKa2-pH_c))) ;
                        % activity of neutral species in cytosol
ad2_c = an_c*10^(i1*(pKa1-pH_c)+i2*(pKa2-pH_c)) ;
                        % activity of +1 ion species in cytosol
ad1_c = an_c*10^(i1*(pKa1-pH_c)) ;
                        % activity of +2 ion species in cytosol
Dd2_c = ad2_c/an_c ;
Dd1_c = ad1_c/an_c ;
fn_c = 1/(W_c/gamman_c+Kn_c/gamman_c+Dd2_c*W_c/gammad2_c...
    +Dd2_c*Kd2_c/gammad2_c+Dd1_c*W_c/gammad1_c+Dd1_c*Kd1_c/gammad1_c) ;
% ratio of the activity of neutral species and
% total molecular concentration in cytosol
fd2_c = fn_c*Dd2_c ;
% ratio of the activity of +1 ion species and
% total molecular concentration in cytosol
fd1_c = fn_c*Dd1_c ;
% ratio of the activity of +2 ion species and
```

```matlab
% total molecular concentration in cytosol

% Mitochondria
W_m = 1-L_m ;           % water fraction in mitochondria
Is_m = 0.3 ;            % ionic strength in mitochondria (mol)
Nd2_m = z2*E_m*F/(R*T) ;
Nd1_m = z1*E_m*F/(R*T) ;
gamman_m = 10^(0.3*Is_m) ;
                % activity coefficient of neutral molecules in mitochondria
gammad1_m = 10^(-0.5*z1*z1*(sqrt(Is_m)/(1+sqrt(Is_m))-0.3*Is_m)) ;
                % activity coefficient of +1 ion molecules in mitochondria
gammad2_m = 10^(-0.5*z2*z2*(sqrt(Is_m)/(1+sqrt(Is_m))-0.3*Is_m)) ;
                % activity coefficient of +2 ion molecules in mitochondria
Kn_m = L_m*1.22*10^(logPn_cell) ;
                % sorption coefficient for neutral species in mitochondria
Kd1_m = L_m*1.22*10^(logPd1_cell) ;
                % sorption coefficient for +1 ion species in mitochondria
Kd2_m = L_m*1.22*10^(logPd2_cell) ;
                % sorption coefficient for +2 ion species in mitochondria
an_m = 1/(1+10^(i1*(pKa1-pH_m))+10^(i1*(pKa1-pH_m)+i2*(pKa2-pH_m))) ;
                % activity of neutral species in mitochondria
ad2_m = an_m*10^(i1*(pKa1-pH_m)+i2*(pKa2-pH_m)) ;
                % activity of +1 ion species in mitochondria
ad1_m = an_m*10^(i1*(pKa1-pH_m)) ;
                % activity of +2 ion species in mitochondria
Dd2_m = ad2_m/an_m ;
Dd1_m = ad1_m/an_m ;
fn_m = 1/(W_m/gamman_m+Kn_m/gamman_m+Dd2_m*W_m/gammad2_m...
    +Dd2_m*Kd2_m/gammad2_m+Dd1_m*W_m/gammad1_m+Dd1_m*Kd1_m/gammad1_m ) ;
% ratio of the activity of neutral species and
% total molecular concentration in mitochondria
fd2_m = fn_m*Dd2_m ;
% ratio of the activity of +1 ion species and
% total molecular concentration in mitochondria
```

```matlab
fd1_m = fn_m*Dd1_m ;
% ratio of the activity of +2 ion species and
% total molecular concentration in mitochondria

% lysosomes
W_l = 1-L_l ;                   % water fraction in lysosomes
Is_l = 0.2 + 0.2 * rand() ;     % ionic strength in lysosomes (mol)
Nd2_l = z2*E_l*F/(R*T) ;
Nd1_l = z1*E_l*F/(R*T) ;
gamman_l = 10^(0.3*Is_l) ;
                   % activity coefficient of neutral molecules in lysosomes
gammad1_l = 10^(-0.5*z1*z1*(sqrt(Is_l)/(1+sqrt(Is_l))-0.3*Is_l));
                   % activity coefficient of +1 ion molecules in lysosomes
gammad2_l = 10^(-0.5*z2*z2*(sqrt(Is_l)/(1+sqrt(Is_l))-0.3*Is_l));
                   % activity coefficient of +2 ion molecules in lysosomes
Kn_l = L_l*1.22*10^(logPn_cell) ;
                   % sorption coefficient for neutral species in lysosomes
Kd1_l = L_l*1.22*10^(logPd1_cell) ;
                   % sorption coefficient for +1 ion species in lysosomes
Kd2_l = L_l*1.22*10^(logPd2_cell) ;
                   % sorption coefficient for +2 ion species in lysosomes
an_l = 1/(1+10^(i1*(pKa1-pH_l))+10^(i1*(pKa1-pH_l)+i2*(pKa2-pH_l))) ;
                   % activity of neutral species in lysosomes
ad2_l = an_l*10^(i1*(pKa1-pH_l)+i2*(pKa2-pH_l)) ;
                   % activity of +1 ion species in lysosomes
ad1_l = an_l*10^(i1*(pKa1-pH_l)) ;
                   % activity of +2 ion species in lysosomes
Dd2_l = ad2_l/an_l ;
Dd1_l = ad1_l/an_l ;
fn_l = 1/(W_l/gamman_l+Kn_l/gamman_l+Dd2_l*W_l/gammad2_l...
    +Dd2_l*Kd2_l/gammad2_l+Dd1_l*W_l/gammad1_l+Dd1_l*Kd1_l/gammad1_l ) ;
% ratio of the activity of neutral species and
% total molecular concentration in lysosomes
fd2_l = fn_l*Dd2_l ;
```

```matlab
% ratio of the activity of +1 ion species and
% total molecular concentration in lysosomes
fd1_l = fn_l*Dd1_l ;
% ratio of the activity of +2 ion species and
% total molecular concentration in lysosomes


% Solve the differential equation system:
% Given a system of linear ODE's expressed in matrix form:
% Y' = AY+G with initial conditions Y(0) = [0 0 0 1 1 C_a]'

time = 14400;
Y0 = [0 0 0 1 1 C_a]';
[TI,Y] = ode15s(@Code_S2,[0,time],Y0);
[a,b]=size(Y);
Mass_cell = Y(a,1)*(V_c_initial-V_l_initial*Y(a,4))*10^12+...
    (Y(a,2)*V_m+Y(a,3)*V_l_initial*Y(a,4))*10^12 ;
    % intracellular mass (pmol/cell)
Mass_all = Y(a,1)*(V_c_initial-V_l_initial*Y(a,4))*cellNo*10^9+...
    (Y(a,2)*V_m+Y(a,3)*V_l_initial*Y(a,4)+Y(a,6)*V_a)*cellNo*10^9 ;
    % total mass (nmol)
N = [i, round, C_a, Y(a,1), Y(a,2), Y(a,3), Y(a,4), Y(a,5), Y(a,6),...
    Mass_cell, Mass_all];
if mod(i,4)==1
    fid = fopen('Monte25.dat','a');
elseif mod(i,4)==2
    fid = fopen('Monte50.dat','a');
elseif mod(i,4)==3
    fid = fopen('Monte100.dat','a');
else fid = fopen('Monte200.dat','a');
end
fprintf(fid,'%+12.0f %+12.0f %+12.2f %+12.6f %+12.6f %+12.6f %+12.6f %+12.6f %+12.6f %+12.6f %+12.6f\n', N);
fclose(fid);
```

```matlab
    clear Y TI;

        end
end
```

2) Code_S2.

```matlab
% The following section is the function called by Code_S1.m to simulate
% intracellular concentration of CQ in MDCK cells with volume expansion in
% acidic compartment and binding of CQ to cellular membrane structures.

function [dCR] = Code_S2(t,CR)

global V_l_initial A_l_initial V_c_initial A_a V_m A_m V_a i
global Pn Pd1 Pd2
global Nd1_a Nd1_m Nd1_l Nd2_a Nd2_m Nd2_l
global fn_a fn_c fn_l fn_m
global fd1_a fd1_c fd1_l fd1_m
global fd2_a fd2_c fd2_l fd2_m

% Solve the differential equation system for each drug:
% Given a system of linear ODE's expressed in matrix form:
% Y' = AY+G with initial conditions Y(0) = [0 0 0 1 1 C_a]'

A_slope_Gr = [237.75, 464.69, 246.37, 161.42, 339.03, 549.90, 624.23,...
    206.23, 0.00, 0.00, 0.00, 0.00] ; % rate of change in lyso surface area
V_slope_Gr = [68.77, 106.88, 66.07, 45.08, 121.37, 227.24, 266.29,...
    127.33, 0.00, 0.00, 0.00, 0.00] ; % rate of change in lyso volume
V_slope_base = [20.6, 20.6, 20.6, 20.6, 91.42, 91.42, 91.42, 91.42,...
    20.6, 20.6, 20.6, 20.6] ; % initial lysosomal volume (um^3)
A_slope_base = [223.26, 223.26, 223.26, 223.26, 708.61, 708.61, 708.61,...
    708.61, 223.26, 223.26, 223.26, 223.26] ;
    % initial lysosomal surface area (um^2)
```

```
V_l = V_l_initial*CR(4) ;
A_l = A_l_initial*CR(5) ;
V_c = V_c_initial-V_l ;

k11 = -(A_a/V_c)*Pn*fn_c...
      -(A_a/V_c)*Pd1*Nd1_a*fd1_c*exp(Nd1_a)/(exp(Nd1_a)-1)...
      -(A_a/V_c)*Pd2*Nd2_a*fd2_c*exp(Nd2_a)/(exp(Nd2_a)-1)...
      -(A_m/V_c)*Pn*fn_c-(A_m/V_c)*Pd1*Nd1_m*fd1_c/(exp(Nd1_m)-1)...
      -(A_m/V_c)*Pd2*Nd2_m*fd2_c/(exp(Nd2_m)-1)...
      -(A_l/V_c)*Pn*fn_c-(A_l/V_c)*Pd1*Nd1_l*fd1_c/(exp(Nd1_l)-1)...
      -(A_l/V_c)*Pd2*Nd2_l*fd2_c/(exp(Nd2_l)-1) ;
k12 = (A_m/V_c)*Pn*fn_m+(A_m/V_c)*Pd1*Nd1_m*fd1_m*exp(Nd1_m)/...
      (exp(Nd1_m)-1)+(A_m/V_c)*Pd2*Nd2_m*fd2_m*exp(Nd2_m)/(exp(Nd2_m)-1) ;
k13 = (A_l/V_c)*Pn*fn_l+(A_l/V_c)*Pd1*Nd1_l*fd1_l*exp(Nd1_l)/...
      (exp(Nd1_l)-1)+(A_l/V_c)*Pd2*Nd2_l*fd2_l*exp(Nd2_l)/(exp(Nd2_l)-1) ;
k16 = (A_a/V_c)*Pn*fn_a+(A_a/V_c)*Pd1*Nd1_a*fd1_a/...
      (exp(Nd1_a)-1)+(A_a/V_c)*Pd2*Nd2_a*fd2_a/(exp(Nd2_a)-1) ;


k21 = (A_m/V_m)*Pn*fn_c+(A_m/V_m)*Pd1*Nd1_m*fd1_c/(exp(Nd1_m)-1)...
      +(A_m/V_m)*Pd2*Nd2_m*fd2_c/(exp(Nd2_m)-1) ;
k22 = -(A_m/V_m)*Pn*fn_m-(A_m/V_m)*Pd1*Nd1_m*fd1_m*exp(Nd1_m)/...
      (exp(Nd1_m)-1)-(A_m/V_m)*Pd2*Nd2_m*fd2_m*exp(Nd2_m)/(exp(Nd2_m)-1) ;

S4 = V_slope_Gr(i)/V_slope_base(i)/3600 ;
S5 = A_slope_Gr(i)/A_slope_base(i)/3600 ;

k31 = (A_l/V_l)*Pn*fn_c+(A_l/V_l)*Pd1*Nd1_l*fd1_c/(exp(Nd1_l)-1)...
      +(A_l/V_l)*Pd2*Nd2_l*fd2_c/(exp(Nd2_l)-1) ;
k33 = -(A_l/V_l)*Pn*fn_l-(A_l/V_l)*Pd1*Nd1_l*fd1_l*exp(Nd1_l)/...
      (exp(Nd1_l)-1)-(A_l/V_l)*Pd2*Nd2_l*fd2_l*exp(Nd2_l)/(exp(Nd2_l)-1)...
      -S4/CR(4) ;

k61 = (A_a/V_a)*Pn*fn_c+(A_a/V_a)*Pd1*Nd1_a*fd1_c*exp(Nd1_a)...
      /(exp(Nd1_a)-1)+(A_a/V_a)*Pd2*Nd2_a*fd2_c*exp(Nd2_a)/(exp(Nd2_a)-1) ;
```

```
k66 = -(A_a/V_a)*Pn*fn_a-(A_a/V_a)*Pd1*Nd1_a*fd1_a/...
    (exp(Nd1_a)-1)-(A_a/V_a)*Pd2*Nd2_a*fd2_a/(exp(Nd2_a)-1) ;

% CR = [0,0,0,1,1, C_a];
dCR(1) = k11*CR(1)+k12*CR(2)+k13*CR(3)+ k16*CR(6);
dCR(2) = k21*CR(1)+k22*CR(2);
dCR(3) = k31*CR(1)+k33*CR(3);
dCR(4) = S4;
dCR(5) = S5;
dCR(6) = k61*CR(1)+k66*CR(6);


dCR = [dCR(1),dCR(2),dCR(3),dCR(4),dCR(5), dCR(6)]' ;


end
```

3) Code_S3.txt

```
#---Remove extra top margin:
par(mar=c(3,3,1,1))   # Trim margin around plot [b,l,t,r]
par(tcl=0.35)   # Switch tick marks to insides of axes
par(mgp=c(1.5,0.2,0))   # Set margin lines; default c(3,1,0) [title,labels,line]
par(xaxs="r",yaxs="r")   # Extend axis limits by 4% ("i" does no extension)
par(lwd=1)
par(mfrow=c(4,3))

## 25uM

IntraMass_exp= 0.0052
IntraMass_exp_std = 0.0015
IntraMass_expS = 0.0062
IntraMass_exp_stdS = 0.001
IntraMass_expB = 0.0020
IntraMass_exp_stdB = 0.0014
```

```
file <- "Monte25.dat"
Data <- read.table(file,header=F)

Data.IntraMass <- log(Data[1:10000,10], base=10)
Data.IntraMassS <- log(Data[10001:20000,10], base=10)
Data.IntraMassB <- log(Data[20001:30000,10], base=10)

Histo <- hist(Data.IntraMass, freq=T, breaks=c(-125:0)/25, axes=TRUE, main="", xlim=c(-4,-1),
ylim=c(0,1500), col="white")
axTicks(1)
axTicks(2)
axis(1, lwd = 4.5)
axis(2, lwd = 4.5)
lines(Histo$mids, Histo$counts, lwd=4.5, col="black")
abline(v=log10(IntraMass_exp), col="red", lty=1, lwd=3)
abline(v=log10(IntraMass_exp+IntraMass_exp_std), col="red", lty=2, lwd=3)
abline(v=log10(IntraMass_exp-IntraMass_exp_std), col="red", lty=2, lwd=3)

Histo <- hist(Data.IntraMassS, freq=T, breaks=c(-125:0)/25, axes=TRUE, main="", xlim=c(-4,-1),
ylim=c(0,1500), col="white")
axTicks(1)
axTicks(2)
axis(1, lwd = 4.5)
axis(2, lwd = 4.5)
lines(Histo$mids, Histo$counts, lwd=4.5, col="black")
abline(v=log10(IntraMass_expS), col="red", lty=1, lwd=3)
abline(v=log10(IntraMass_expS+IntraMass_exp_stdS), col="red", lty=2, lwd=3)
abline(v=log10(IntraMass_expS-IntraMass_exp_stdS), col="red", lty=2, lwd=3)

Histo <- hist(Data.IntraMassB, freq=T, breaks=c(-125:0)/25, axes=TRUE, main="", xlim=c(-4,-1),
ylim=c(0,1500), col="white")
axTicks(1)
axTicks(2)
```

```
axis(1, lwd = 4.5)
axis(2, lwd = 4.5)
lines(Histo$mids, Histo$counts, lwd=4.5, col="black")
abline(v=log10(IntraMass_expB), col="red", lty=1, lwd=3)
abline(v=log10(IntraMass_expB+IntraMass_exp_stdB), col="red", lty=2, lwd=3)
abline(v=log10(IntraMass_expB-IntraMass_exp_stdB), col="red", lty=2, lwd=3)


## 50uM

IntraMass_exp= 0.0108
IntraMass_exp_std = 0.0004
IntraMass_expS = 0.0170
IntraMass_exp_stdS = 0.0044
IntraMass_expB= 0.0034
IntraMass_exp_stdB = 0.0012

file <- "Monte50.dat"
Data <- read.table(file,header=F)

Data.IntraMass <- log(Data[1:10000,10], base=10)
Data.IntraMassS <- log(Data[10001:20001,10], base=10)
Data.IntraMassB <- log(Data[20001:30000,10], base=10)

Histo <- hist(Data.IntraMass, freq=T, breaks=c(-125:0)/25, axes=TRUE, main="", xlim=c(-4,-1),
ylim=c(0,1500), col="white")
axTicks(1)
axTicks(2)
axis(1, lwd = 4.5)
axis(2, lwd = 4.5)
lines(Histo$mids, Histo$counts, lwd=4.5, col="black")
abline(v=log10(IntraMass_exp), col="red", lty=1, lwd=3)
abline(v=log10(IntraMass_exp+IntraMass_exp_std), col="red", lty=2, lwd=3)
abline(v=log10(IntraMass_exp-IntraMass_exp_std), col="red", lty=2, lwd=3)
```

```
Histo <- hist(Data.IntraMassS, freq=T, breaks=c(-125:0)/25, axes=TRUE, main="", xlim=c(-4,-1),
ylim=c(0,1500), col="white")
axTicks(1)
axTicks(2)
axis(1, lwd = 4.5)
axis(2, lwd = 4.5)
lines(Histo$mids, Histo$counts, lwd=4.5, col="black")
abline(v=log10(IntraMass_expS), col="red", lty=1, lwd=3)
abline(v=log10(IntraMass_expS+IntraMass_exp_stdS), col="red", lty=2, lwd=3)
abline(v=log10(IntraMass_expS-IntraMass_exp_stdS), col="red", lty=2, lwd=3)

Histo <- hist(Data.IntraMassB, freq=T, breaks=c(-125:0)/25, axes=TRUE, main="", xlim=c(-4,-1),
ylim=c(0,1500), col="white")
axTicks(1)
axTicks(2)
axis(1, lwd = 4.5)
axis(2, lwd = 4.5)
lines(Histo$mids, Histo$counts, lwd=4.5, col="black")
abline(v=log10(IntraMass_expB), col="red", lty=1, lwd=3)
abline(v=log10(IntraMass_expB+IntraMass_exp_stdB), col="red", lty=2, lwd=3)
abline(v=log10(IntraMass_expB-IntraMass_exp_stdB), col="red", lty=2, lwd=3)

## 100uM

IntraMass_exp= 0.0153
IntraMass_exp_std = 0.0019
IntraMass_expS = 0.0216
IntraMass_exp_stdS = 0.0057
IntraMass_expB= 0.0048
IntraMass_exp_stdB = 0.0012

file <- "Monte100.dat"
Data <- read.table(file,header=F)
```

```
Data.IntraMass <- log(Data[1:10000,10], base=10)
Data.IntraMassS <- log(Data[10001:20000,10], base=10)
Data.IntraMassB <- log(Data[20001:30000,10], base=10)

Histo <- hist(Data.IntraMass, freq=T, breaks=c(-125:0)/25, axes=TRUE, main="", xlim=c(-4,-1),
ylim=c(0,1500), col="white")
axTicks(1)
axTicks(2)
axis(1, lwd = 4.5)
axis(2, lwd = 4.5)
lines(Histo$mids, Histo$counts, lwd=4.5, col="black")
abline(v=log10(IntraMass_exp), col="red", lty=1, lwd=3)
abline(v=log10(IntraMass_exp+IntraMass_exp_std), col="red", lty=2, lwd=3)
abline(v=log10(IntraMass_exp-IntraMass_exp_std), col="red", lty=2, lwd=3)

Histo <- hist(Data.IntraMassS, freq=T, breaks=c(-125:0)/25, axes=TRUE, main="", xlim=c(-4,-1),
ylim=c(0,1500), col="white")
axTicks(1)
axTicks(2)
axis(1, lwd = 4.5)
axis(2, lwd = 4.5)
lines(Histo$mids, Histo$counts, lwd=4.5, col="black")
abline(v=log10(IntraMass_expS), col="red", lty=1, lwd=3)
abline(v=log10(IntraMass_expS+IntraMass_exp_stdS), col="red", lty=2, lwd=3)
abline(v=log10(IntraMass_expS-IntraMass_exp_stdS), col="red", lty=2, lwd=3)

Histo <- hist(Data.IntraMassB, freq=T, breaks=c(-125:0)/25, axes=TRUE, main="", xlim=c(-4,-1),
ylim=c(0,1500), col="white")
axTicks(1)
axTicks(2)
axis(1, lwd = 4.5)
axis(2, lwd = 4.5)
lines(Histo$mids, Histo$counts, lwd=4.5, col="black")
abline(v=log10(IntraMass_expB), col="red", lty=1, lwd=3)
```

```
abline(v=log10(IntraMass_expB+IntraMass_exp_stdB), col="red", lty=2, lwd=3)
abline(v=log10(IntraMass_expB-IntraMass_exp_stdB), col="red", lty=2, lwd=3)

## 200uM

IntraMass_exp= 0.0110
IntraMass_exp_std = 0.0013
IntraMass_expS = 0.0191
IntraMass_exp_stdS = 0.0047
IntraMass_expB= 0.0056
IntraMass_exp_stdB = 0.0003

file <- "Monte200.dat"
Data <- read.table(file,header=F)

Data.IntraMass <- log(Data[1:10000,10], base=10)
Data.IntraMassS <- log(Data[10001:20000,10], base=10)
Data.IntraMassB <- log(Data[20001:30000,10], base=10)

Histo <- hist(Data.IntraMass, freq=T, breaks=c(-125:0)/25, axes=TRUE, main="", xlim=c(-4,-1),
ylim=c(0,1500), col="white")
axTicks(1)
axTicks(2)
axis(1, lwd = 4.5)
axis(2, lwd = 4.5)
lines(Histo$mids, Histo$counts, lwd=4.5, col="black")
abline(v=log10(IntraMass_exp), col="red", lty=1, lwd=3)
abline(v=log10(IntraMass_exp+IntraMass_exp_std), col="red", lty=2, lwd=3)
abline(v=log10(IntraMass_exp-IntraMass_exp_std), col="red", lty=2, lwd=3)

Histo <- hist(Data.IntraMassS, freq=T, breaks=c(-125:0)/25, axes=TRUE, main="", xlim=c(-4,-1),
ylim=c(0,1500), col="white")
axTicks(1)
axTicks(2)
```

```
axis(1, lwd = 4.5)
axis(2, lwd = 4.5)
lines(Histo$mids, Histo$counts, lwd=4.5, col="black")
abline(v=log10(IntraMass_expS), col="red", lty=1, lwd=3)
abline(v=log10(IntraMass_expS+IntraMass_exp_stdS), col="red", lty=2, lwd=3)
abline(v=log10(IntraMass_expS-IntraMass_exp_stdS), col="red", lty=2, lwd=3)

Histo <- hist(Data.IntraMassB, freq=T, breaks=c(-125:0)/25, axes=TRUE, main="", xlim=c(-4,-1),
ylim=c(0,1500), col="white")
axTicks(1)
axTicks(2)
axis(1, lwd = 4.5)
axis(2, lwd = 4.5)
lines(Histo$mids, Histo$counts, lwd=4.5, col="black")
abline(v=log10(IntraMass_expB), col="red", lty=1, lwd=3)
abline(v=log10(IntraMass_expB+IntraMass_exp_stdB), col="red", lty=2, lwd=3)
abline(v=log10(IntraMass_expB-IntraMass_exp_stdB), col="red", lty=2, lwd=3)
```